nature

THE INTERNATIONAL WEEKLY JOURNAL OF SCIENCE

AVALANCHE OSCILLATOR

Microcrystal plasticity opens window to the world of large complex systems, jammed solids and earthquakes PAGE 517

US ELECTION

THE ONES TO WATCH

Science at stake in key state votes

PAGE 453

RESOURCES

A FLOTATION TOO FAR

Why a market for water spells trouble

PAGE 469

REVIEWS SPECIAL

AUTUMN BOOKS

From fractals to food, via planets and pseudoscience

PAGE 474

NATURE.COM/NATURE

25 October 2012 £10

Vol. 490, No. 7421

9 770028 083095 43

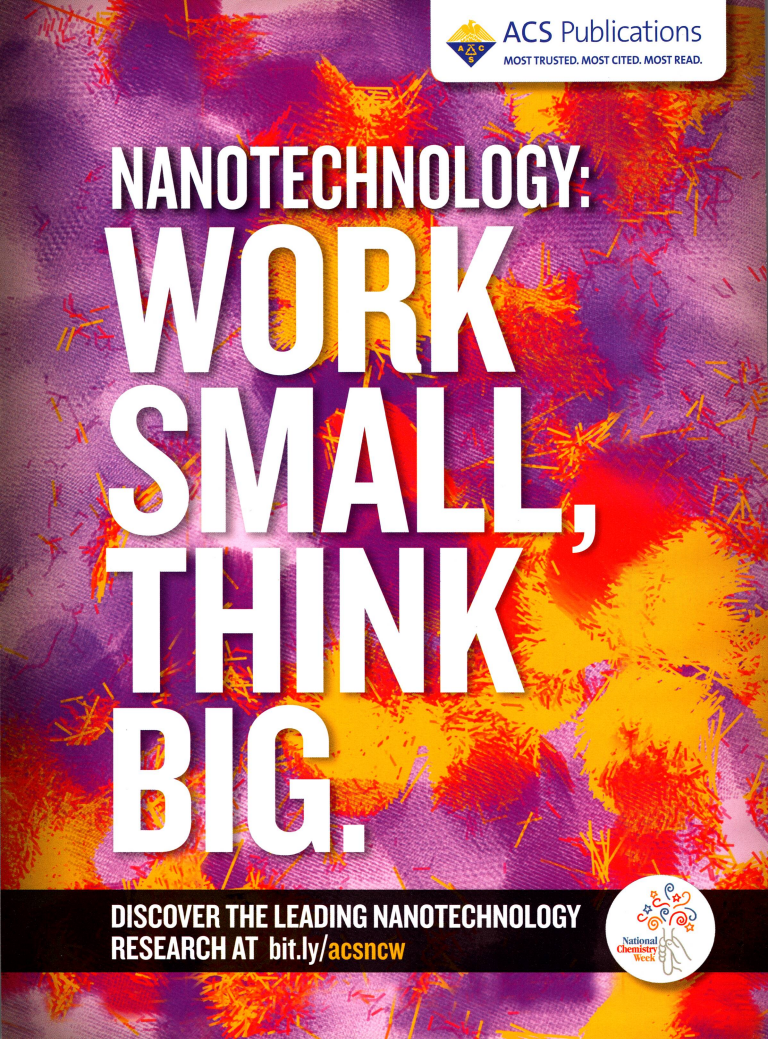
ACS Publications
MOST TRUSTED. MOST CITED. MOST READ.
NANOTECHNOLOGY:
WORK SMALL, THINK BIG.
DISCOVER THE LEADING NANOTECHNOLOGY RESEARCH AT bit.ly/acsncw
National Chemistry Week

nature OUTLOOK

Published in the 11 October issue of *Nature* and available free online for six months

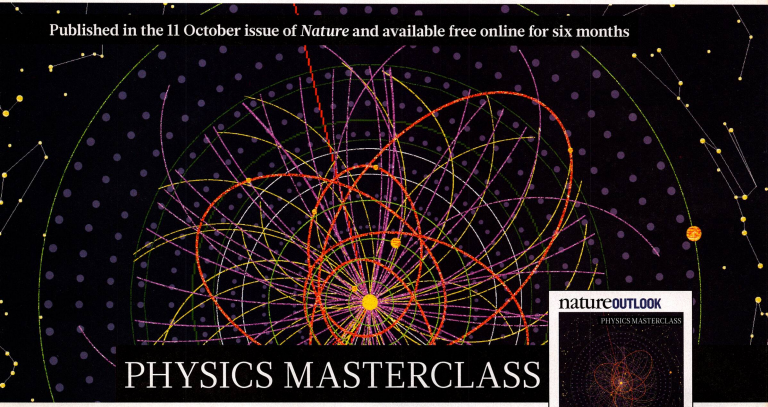

PHYSICS MASTERCLASS

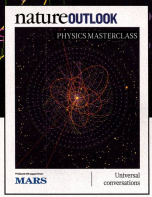

From subatomic particles to cosmic-scale phenomena, *Nature Outlook: Physics Masterclass* uses the Lindau Nobel Laureate Meeting 2012 to launch an examination of some of the biggest breakthroughs in physics — including conversations between physics laureates and the young researchers who hope to emulate them.

Access the Outlook free online for six months.
nature.com/nature/outlook/masterclass_2012

Scan this tag to access the Outlook on your smartphone

Supported by: MARS

If you would be interested in partnering with *Nature* on a similar project please contact: sponsorship@nature.com

nature publishing group npg

MiSeq. Next-generation sequencing for all you seek.

You want amazing accuracy and performance on your benchtop. Illumina delivers—yet again. The MiSeq Personal Sequencer is the only fully integrated, truly end-to-end benchtop solution around. It's just one more example of why Illumina solutions generate a remarkable 90% of all the world's sequencing data. Discover what's possible.

www.illumina.com/iseek

illumina®

CONTENTS

25 October 2012 / Vol 490 / Issue No 7421

THIS WEEK

EDITORIALS

445 US ELECTION
A vote for science
Barack Obama and the Democrats are the better bet for research

446 RESEARCH FUNDING
Banish cronyism
The contempt for peer review means heads should roll at Texas cancer institute

446 ITALY
Shock and law
Scientists should protest over the guilty verdict in the L'Aquila trial

WORLD VIEW

447 **Throw off the cloak of invisibility**
Athene Donald
To secure a higher profile for women in science, contributions must be honoured

RESEARCH HIGHLIGHTS

448 SELECTIONS FROM THE SCIENTIFIC LITERATURE
Moving statues on Easter Island / Rats and eggs / Carbon clock refined / Cutting the glare from white LEDs

SEVEN DAYS

450 THE NEWS IN BRIEF
Iconic ibis shot / Early reports suggest no life in Lake Vostok / Brazil's forest code makes it into law, finally / Guilty verdict in L'Aquila trial / Lithium-ion battery maker goes bust

CAREERS

571 WORK EXPERIENCE
Stepping stones
Internships can kick start a career, though rarely in the host organization

573 CAREER BRIEFS

NATUREJOBS ADVERTISING FEATURE
Spotlight on postgraduate opportunities.

NEWS IN FOCUS

453 US ELECTION
Where Romney and Obama stand on research

456 BIOSAFETY
Researchers up in arms over proposal to reclassify flu virus as high risk

457 TECHNOLOGY
Marblar website aims to crowdsource new uses for inventions

458 GEOENGINEERING
Outcry over iron-seeding project in Canadian waters

459 PEER REVIEW
Texas cancer institute seeks a fresh start after resignations

FEATURES

462 TOXICOLOGY
The learning curve
Small doses of some chemicals may be more harmful than previously thought

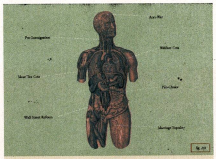

NEUROSCIENCE
Body politic
How your biological make-up might influence the way you vote PAGE 466

COMMENT

469 FINANCE
Wall Street's thirst for water
Frederick Kaufman
Stop the commodities market for water

472 PHYSICS
Why symmetry matters
Mario Livio
Reflections on the guiding light of modern physics

AUTUMN BOOKS

474 ENVIRONMENTAL SCIENCES
Divided we save
Peter Kareiva

476 MATHEMATICS
A fractal life
Mark Buchanan

476 NEW IN PAPERBACK

477 MEDICAL HISTORY
Stemming the red tide
Stefan H E Kaufmann

479 PLANETARY SCIENCE
The search for Earth's twin
Sara Seager

480 PSEUDOSCIENCE
A fringe too far
David Morrison

481 NEUROSCIENCE
Encounters with the nonexistent
Dominic Ffytche

483 FOOD SECURITY
Growing trouble
Calestous Juma

484 BIOTECHNOLOGY
Random harvest
Ian Wilmut

CORRESPONDENCE

487 Research in Canada / Cooperative spirit / Beit fellowships / A return to the Moon? / The problem with bureaucracy

OBITUARY

488 **Louise Johnson (1940–2012)**
Mark Sansom

FUTURES

576 **Glass future**
Deborah Walker

Abgent: your partner in Neurosciences antibodies.

Neurosciences are impacted by a multitude of cellular processes and mechanisms, from apoptosis, autophagy, cell signaling, and cell differentiation to protein modifications. Antibodies have become a predominant tool for the study of Neurosciences, from biochemistry assays to analyzing the dynamics of individual nerve cells and their molecular constituents. With unsurpassed production capabilities and flexibility, Abgent is proud to be your partner in Neurosciences antibodies for areas including:

- **Neurodegenerative diseases** *[Alzheimer's, Parkinson's...]*
- **Neurotransmitters**
- **Synaptogenesis**
- **Neurogenesis**

Visit our website at **www.abgent.com** for more information on Abgent's Neurosciences line of products and learn more about our EVALUATION SIZE program that allows you to order a sample size of our antibodies for a fraction of the cost.

© 2012 ABGENT. All rights reserved. It's all about New, is a trademark of ABGENT. For Research Use Only. Not For Use In Diagnostic Procedures. ABG-00134-0912

It's all about New
Unsurpassed Development Capabilities

ABGENT, A WUXI APPTEC COMPANY, IS AN INTERNATIONALLY RECOGNIZED ANTIBODY MANUFACTURER OFFERING OVER 18,000 HIGH-QUALITY OFF-THE-SHELF ANTIBODIES. UNSURPASSED DEVELOPMENT CAPABILITIES AND FLEXIBILITY ENABLE ABGENT TO DEVELOP OVER 5,000 NEW ANTIBODIES PER YEAR.

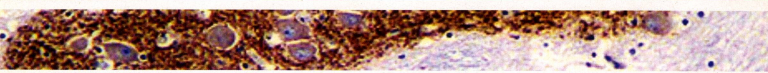

www.abgent.com

WuXi AppTec | ABGENT a WuXi AppTec company

CONTENTS

25 October 2012 / Vol 490 / Issue No 7421

RESEARCH

NEW ONLINE

489 Papers published this week at nature.com

NEWS & VIEWS

490 CANCER
Destiny from density
Reduction in CD36 expression leads to higher mammographic density
Victoria L Seewaldt

491 EARTH SCIENCE
Signs of instability
Destabilization of gas hydrates off the east coast of America
Juergen Mienert SEE LETTER P.527

492 STRUCTURAL BIOLOGY
Snapshot of an activated peptide receptor
Structure of a G-protein-coupled receptor bound to a peptide agonist
Felix Hausch & Florian Holsboer
SEE ARTICLE P.508

493 GENETICS
The inner life of proteins
Epistasis is the main factor regulating protein evolution
Günter P Wagner SEE LETTER P.535

494 COSMOLOGY
Infrared light from wandering stars
New insight into the cosmic infrared background radiation
Andrea Ferrara SEE LETTER P.514

ARTICLES

497 PLANT GENOMICS **A map of rice genome variation reveals the origin of cultivated rice**
X Huang et al.

502 IMMUNOLOGY **Compensatory dendritic cell development mediated by BATF–IRF interactions**
R Tussiwand et al.

508 STRUCTURAL BIOLOGY **Structure of the agonist-bound neurotensin receptor**
J F White et al. SEE N&V P.492

LETTERS

514 ASTRONOMY **Near-infrared background anisotropies from diffuse intrahalo light of galaxies**
A Cooray et al. SEE N&V P.494

517 PHYSICS **Quasi-periodic events in crystal plasticity and the self-organized avalanche oscillator**
S Papanikolaou et al..

522 ORGANIC CHEMISTRY **Forming all-carbon quaternary stereogenic centres in acyclic systems from alkynes**
Y Minko, M Pasco, L Lercher, M Botoshansky & I Marek

527 CLIMATE SCIENCE **Recent changes to the Gulf Stream causing widespread gas hydrate destabilization**
B J Phrampus & M J Hornbach
SEE N&V P.491

531 EARTH SCIENCE **The origin of the terrestrial noble-gas signature**
S S Shcheka & H Keppler

535 EVOLUTION **Epistasis as the primary factor in molecular evolution**
M S Breen, C Kemena, P K Vlasov, C Notredame & F A Kondrashov
SEE N&V P.493

539 IMMUNOLOGY **Phosphorylation of NLRC4 is critical for inflammasome activation**
Y Qu et al.

543 IMMUNOLOGY **BATF–JUN is critical for IRF4-mediated transcription in T cells**
P Li et al.

ON THE COVER

Stress relief

A nickel microcrystal array under compression, a model for intermittent phenomena where coexisting slow relaxations compete to minimize local internal stress. Such systems include complex networks during relaxation, jammed solids and earthquake faults.

PAGE 517

ARRAY: DENNIS M. DIMIDUK / FAULT: D K LYNCH / USGS

547 CANCER **Mitochondrial defect drives non-autonomous tumour progression through Hippo signalling in *Drosophila***
S Ohsawa et al.

552 NEUROSCIENCE **Black mamba venom peptides target acid-sensing ion channels to abolish pain**
S Diochot et al.

556 MOLECULAR BIOLOGY **Structure-based prediction of protein–protein interactions on a genome-wide scale**
Q C Zhang et al.

561 IMMUNOLOGY **Clonal allelic predetermination of immunoglobulin-κ rearrangement**
M Farago et al.

566 STRUCTURAL BIOLOGY **Crystal structure of the multidrug transporter P-glycoprotein from *Caenorhabditis elegans***
M S Jin, M L Oldham, Q Zhang & J Chen

570 CORRIGENDUM **Neutralizing antibodies derived from the B cells of 1918 influenza pandemic survivors**
X Yu et al.

570 CORRIGENDUM **RNA sequencing of pancreatic circulating tumour cells implicates WNT signalling in metastasis**
M Yu et al.

570 CORRIGENDUM **High-performance bulk thermoelectrics with all-scale hierarchical architectures**
K Biswas et al.

STRUCTURAL BIOLOGY

Close couple

The structure of a GPCR, neurotensin, bound to a peptide agonist. PAGE 508

nature

25 October 2012 / Vol 490 / Issue No. 7421

EDITORIAL

LONDON, MUNICH, WASHINGTON DC, NEW YORK, BOSTON, PARIS, SAN FRANCISCO, TOKYO nature@nature.com

EDITOR-IN-CHIEF: Philip Campbell

EXECUTIVE EDITOR: Nick Campbell

PUBLISHING EXECUTIVE EDITOR: Maxine Clarke **EXECUTIVE EDITOR:** Véronique Kiermer

CHIEF MAGAZINE EDITOR: Tim Appenzeller

THIS WEEK/NEWS/FEATURES: Alison Abbott, David Adam, Ananyo Bhattacharya, Geoff Brumfiel, Declan Butler, Ewen Callaway, Erika Check Hayden, Daniel Cressey, David Cyranoski, Natasha Gilbert, Eric Hand, Heidi Ledford, Corie Lok, Brendan Maher, Emma Marris, Richard Monastersky, Brian Owens, Helen Pearson, Mark Peplow, Eugenie Samuel Reich, Ivan Semeniuk, Quirin Schiermeier, Jeff Tollefson, Richard Van Noorden, Meredith Wadman, M Mitchell Waldrop **COMMENT:** Sara Abdulla, Joanne Baker, Rosalind Cotter, Barbara Kiser, Alison McCook, Lucy Odling-Smee, Sarah Tomlin **NATURE PODCAST/VIDEO:** Adam Rutherford, Thea Cunningham, Kerri Smith, Charlotte Stoddart **NEWS AND VIEWS:** Sadaf Shadan, Ana Lopes, Andrew Mitchinson, Cesar Sanchez, Marian Turner **RESEARCH:** Ritu Dhand, Karl Ziemelis, Francesca Cesari, I-han Chou, Tanguy Chouard, Rosamund Daw, Alex Eccleston, Angela Eggleston, Joshua Finkelstein, Henry Gee, Patrick Goymer, Noah Gray, Marie-Thérèse Heemels, Magdalena Helmer, Karen Howell, Claudia Lupp, Barbara Marte, Andrew Mitchinson, Juliane Mössinger, Deepa Nath, Wayne Peng, Leslie Sage, Magdalena Skipper, Clare Thomas, Maria Trojkovska, John VanDecar, Liesbeth Venema, Ursula Weiss, Michael White **INSIGHTS/REVIEWS/PERSPECTIVES:** Ursula Weiss **CAREERS:** Gene Russo, Karen Kaplan **TECHNOLOGY FEATURES:** Vivien Marx **FILTURES:** Colin Sullivan **SUPPLEMENTS:** Herb Brody, Michelle Grayson, Tony Scully **SUBEDITORS:** Colin Sullivan, Mary Abraham, Sarah Archibald, Nicola Bailey, Nicolas Fanget, Isobel Flanagan, Paul Fletcher, Anne Haggart, Sasha Lewis, Dinah Loon, Louisa Lyon, Anna Novitzky, Yukie Ozawa, Katherine Perry, David Price, Jenny Rooke, David Winters, Anna York **PRODUCTION:** Jenny Henderson, Leonora Dawson-Bowling, Dan Foley, Stewart Fraser, Susan Gray, Simon Gribbin, Hazel Mayhew, James McQuat, Emilia Oviss, Yvonne Strong, Robert Sullivan, Roberta Tarran, Charles Wenz **ART AND DESIGN:** Kelly Buckheit Krause, Wesley Fernandes, Madeline Hutchinson, Barbara Izdebska, Paul Jackman, Jasiek Krzyzstofiak, Aninthea Lewis, Chris Ryan, Nik Spencer, Claire Welsh, Mark Wood **JAPAN EDITION:** Eiji Matsuda, Mika Ishida, Mitsuyo Utsugi, Sayaka Ayame **PRESS OFFICE:** Ruth Francis, Neda Afsarmanesh, Lisa Boucher, Rachel Twinn, Rebecca Walton **ADMINISTRATION:** Paul Sng, Liz Bankes, Roseann Campbell, Peter Cary, Ffion Cleverley, Dana Coles, Faye Fornasier, Ashlee Gagui, Peter Hewitt, Caroline McLean, Anastasia Panoutsou, Kenneth Simpson, Michelle Viscuso, Diane Yorke

PUBLISHING

LONDON feedback@nature.com

MANAGING DIRECTOR & PUBLISHER: Steven Inchcoombe

ASSOCIATE PUBLISHER: Arash Hejazi

PUBLISHING PROJECT MANAGERS: Claudia Desay, Christian Manco

TOKYO feedback@natureasia.com

REGIONAL MANAGING DIRECTOR — ASIA-PACIFIC: David Swinbanks

DIRECTOR — ASIA-PACIFIC: Antoine E Bocquet

OPERATIONS DIRECTOR — ASIA-PACIFIC: Hiroshi Minemura

DISPLAY ADVERTISING, SPONSORSHIP & NATUREJOBS

GLOBAL HEAD: Andrew Douglas a.douglas@nature.com

DISPLAY ADVERTISING AND SPONSORSHIP

GLOBAL HEAD: Gerard Preston g.preston@nature.com

ASSISTANT SPONSORSHIP MANAGER: Reya Silao Tel: +44 (0)20 7843 4977 (r.silao@nature.com)

EUROPE/REST OF WORLD display@nature.com Tel +44 (0)20 7843 4960

GERMANY/SWITZERLAND/AUSTRIA: Sabine Hugi-Fürst Tel: +41 52761 3386

UK/IRELAND/SCANDINAVIA/SPAIN/PORTUGAL: Evelina Robo Hakansson Tel: +44 (0)20 7843 4079

FRANCE/BELGIUM/THE NETHERLANDS/LUXEMBOURG/ITALY/OTHER EUROPE: Nicola Wright Tel: +44 (0)20 7843 4959

NORTH AMERICA display@natureny.com

NEW ENGLAND/ EASTERN CANADA: Sheila Reardon Tel: +1 617 494 4900

NEW YORK/MID-ATLANTIC/SOUTHEAST: Jim Breault Tel: +1 212 726 9334

MIDWEST: Mike Rossi Tel: +1 212 726 9255

WEST COAST/ WESTERN CANADA: George Lui Tel: +1 415 781 3804

WEST COAST NORTH: Kayla McCutchan Tel: +1 415 403 9038

ASIA-PACIFIC display@natureasia.com

ASIA-PACIFIC HEAD: Kate Yoneyama

JAPAN: Ken Mikami Tel: +81 3 3267 8765

GREATER CHINA/SINGAPORE: Gloria To Tel: +852 2811 7191

INDIA: Vikas Chawla Tel: +91 124 288 1057

SPONSORSHIP

BUSINESS DEVELOPMENT MANAGER: David Bagshaw Tel: +1 212 726 9215

BUSINESS DEVELOPMENT MANAGER: Patrick Murphy Tel: +1 617 475 9216

NATUREJOBS naturejobs@nature.com

EUROPEAN HEAD OFFICE, LONDON: Tel: +44 (0)20 7843 4961

EUROPEAN SALES MANAGER: Nils Moeller (n.moeller@nature.com) **BUSINESS DEVELOPMENT MANAGER, MIDDLE EAST:** Jon Giuliani (j.giuliani@nature.com) **ADVERTISING PRODUCTION MANAGER:** Stephen Russell **NATUREJOBS ONLINE PRODUCTION:** Dennis Chu

US HEAD OFFICE, NEW YORK: naturejobs@natureny.com **US SALES MANAGER:** Ken Finnegan

JAPAN HEAD OFFICE, TOKYO: Tel: +81 3 3267 8765 **ASIA-PACIFIC HEAD:** Kate Yoneyama

ASIA-PACIFIC SALES & BUSINESS DEVELOPMENT MANAGER: Yuki Fujiwara **BUSINESS DEVELOPMENT MANAGER, GREATER CHINA, SINGAPORE:** Gloria To Tel: +852 2811 7191

INDIA: Vikas Chawla Tel: +91 1242881057 (v.chawla@nature.com)

MARKETING & SUBSCRIPTIONS

USA/CANADA/LATIN AMERICA subscriptions@us.nature.com

Tel: (USA/Canada)+1 866 363 7860; (outside USA/Canada) +1 212 726 9223

MARKETING: Sara Girard **FULFILMENT:** Karen Dawson

JAPAN/CHINA/KOREA subscriptions@natureasia.com

Tel: +81 3 3267 8751 **MARKETING:** Sachiyo Ikeda **FULFILMENT:** Masayo Tanaka

EUROPE/REST OF WORLD subscriptions@nature.com

Tel: +44 (0)1256 329242

MARKETING: Elena Woodstock, Marcus Parker, Hannah Phipps **FULFILMENT:** Jean Burrows

INDIA npgindia@nature.com

Tel: +91 124 2881053/54

HEAD OF BUSINESS DEVELOPMENT, INDIA: Debashish Brahmachari **MARKETING:** Harpal Singh Gill

ANNUAL SUBSCRIPTIONS (UK/Europe, including post and packing)

FULL RATE: £1,400

PERSONAL RATES: UK £135; Europe €209; Rest of World £210

STUDENT RATES: UK £79; Europe €122; Rest of World £125

Individual rates apply to payments by personal cheque or credit card. Back issues: £20.00.

ANNUAL SUBSCRIPTIONS (USA, including post and packing)

INSTITUTIONAL/CORPORATE RATE: $2,730 ; **PERSONAL RATE:** $199; **STUDENT RATE:** $99;

POSTDOC RATE: $119

Printed in USA. Individual rates available only to subscribers paying by personal check or credit card. Orders for student/postdoc subscriptions must be accompanied by a copy of student ID. Rates apply to USA, Canada, Mexico/Central & South America. Add 7% GST tax in Canada (Canadian GST number 140911595). **BACK ISSUES:** US$20.00.

ANNUAL SUBSCRIPTIONS (Asia, including post and packing)

JAPAN: 年間購読料金： *Nature* のみ 437,800 円 +21,890 円 (消費税) =459,690 円 (合計)
Nature + *Nature Digest* 466,550 円 +23,328 円 (消費税) =489,878 (合計)
お問い合わせ 日本出版貿易株式会社 国内営業 1 部
〒101-0064 東京都千代田区猿楽町 1-2-1 Tel: 03-3292-3767 Fax: 03-3292-8766
個人/学生購読について
NPG タイチャー アジア パシフィック フルフィルメント & カスタマーサービス
〒162-0843 東京都新宿区市谷田町2-37 千代田ビル Tel: 03-3267-8759 Fax: 03-3267-8752

CHINA: www.natureasia.com/cn/subscribe; **KOREA:** www.natureasia.com/korea/subscribe

NATURE ONLINE WWW.NATURE.COM/NATURE

CHIEF TECHNOLOGY OFFICER: Howard Ratner **ASSOCIATE DIRECTOR, NATURE.COM:** Daniel Pollock

PLATFORM DEVELOPMENT: Jeremy Macdonald **WEB PRODUCTION:** Alexander Thurrell, Deborah Anthony **WEB DESIGN:** Juan-Carlos Sobrino, Luke Stavenhagen **PLATFORM INTERFACES:** Amanda Ward

SITE LICENCES, FULFILMENT & CUSTOMER SERVICES

SITE LICENCES: npg.nature.com/libraries feedback@nature.com

CHIEF OPERATIONS OFFICER: John Carroll **ASSOCIATE DIRECTOR OF OPERATIONS:** Dominic Pettit

CUSTOMER SERVICE: Liz Davidson **ORDER PROCESSING OPERATIONS:** Steve Poulter

NATURE PUBLISHING GROUP OFFICES

LONDON: The Macmillan Building, 4 Crinan Street, London N1 9XW Tel: +44 (0)20 7833 4000 Fax: +44 (0)20 7843 4596/7

BASINGSTOKE: Nature Publishing Group, Subscriptions, Brunel Road, Basingstoke, Hants RG21 6XS, UK Tel: +44 (0)1256 329242

WASHINGTON DC: 968 National Press Building, 529 14th St NW, Washington DC 20045-1938 Tel: +1 202 737 2355

NEW YORK: 75 Varick St, 9th Floor, New York, NY 10013-1917 Tel: +1 212 726 9200

BOSTON: 25 First Street, Suite 104, Cambridge, MA 02141 Tel: +1 617 475 9275

SAN FRANCISCO: 225 Bush Street, Suite 1453, San Francisco, CA 94104 Tel: +1 415 403 9002

MUNICH: Nymphenburger Strasse 14, D-80335 München Tel: +49 89 549057-13

PARIS: Moulin de Malicorne, Sainte Maure de Touraine, Paris 37800 Tel: +33 2 47 35 72 15

TOKYO: Chiyoda Building, 2-37 Ichigayatamachi, Shinjuku-ku, Tokyo 162-0843 Tel: +81 3 3267 8751

INDIA: Nature Publishing Group, 3A, 4th Floor, DLF Corporate Park, Gurgaon 122002 Tel: +91 124 2881053/54

Nature® (ISSN 0028-0836) is published by Nature Publishing Group, a division of Macmillan Publishers Ltd (The Macmillan Building, 4 Crinan Street, London N19XW). Registered as a newspaper at the British Post Office. North and South American orders to subscriptions@nature.com (Tel: +1 866 363 7860). Other orders to subscriptions@nature.com (Tel. +44 (0)1256 329242; Fax +44 (0)1256 812358). Authorization to photocopy material for internal or personal use, or internal or personal use of specific clients, is granted by *Nature* to libraries and others registered with the Copyright Clearance Center (CCC) Transactional Reporting Service, provided the relevant copyright fee is paid direct to CCC, 222 Rosewood Drive, Danvers MA 01923, USA. Identification code for *Nature*: 0028-0836/03. CPC PUB AGREEMENT #40032744. In the US, *Nature* (ISSN 0028-0836) is published weekly on Thursday, except the last week in December by Nature Publishing Group, 75 Varick St, 9th Fl, New York NY 10013-1917, USA. US Periodicals postage paid at New York NY, and additional mailing post offices. US POSTMASTER: send address changes to *Nature*, Subscription Dept, 75 Varick St, 9th Fl, New York NY 10013-1917, USA. Published in Japan by NPG Nature Asia-Pacific, Chiyoda Building, 2-37 Ichigayatamachi, Shinjuku-ku, Tokyo 162-0843, Japan.

© 2012 Macmillan Publishers Limited. All rights reserved.

THIS WEEK

EDITORIALS

EARTHQUAKE Shockwaves as Italian seismologists get six years in prison **p.446**

WORLD VIEW Women scientists are given the Wikipedia treatment **p.447**

CONTEMPT Prey familiarity breeds indifference in black rats **p.448**

A vote for science

In support for science and environmental issues, Barack Obama and the Democrats have a clear advantage over Mitt Romney and the Republican Party.

When Americans vote for their next president in early November, they will select not just one man to occupy the White House, but also the thousands of party members who will sweep into Washington DC. Those appointees from the president's political party will help to set priorities in science funding, negotiate international treaties and decide whether to create new regulations — or ignore existing ones.

This is important to consider when evaluating the two candidates because the challenger to President Barack Obama, Republican Mitt Romney, has not offered specific plans to manage the roughly US$65 billion of funding that goes to non-military research and development each year. The past positions of the candidates and the records of their own political parties make it clear that Obama and the Democrats offer important advantages for science over Romney and the Republicans.

Budget proposals show the clearest differences. During his term, Obama has consistently supported strategic spending increases for science, with his most recent budget proposal calling for a 5% boost that targets physical sciences. Although some have been unhappy with the details — in particular the decision to forgo a funding increase for the US National Institutes of Health — Obama's science portfolio has fared remarkably well during the financial crisis.

Romney has voiced his support for science and said that he would make federally funded research a budget priority, but he has offered no specific details. Given Romney's pledge to reduce overall federal spending and to lower taxes, some scientists worry that key research agencies would experience sharp budget cuts. Last week, 68 Nobel science laureates said as much in an open letter of support for Obama. A Romney budget, the letter said, would "devastate a long tradition of support for public research and investment in science at a time when this country's future depends, as never before, on innovation".

DOLLAR DRAIN

It is notable that Romney chose Paul Ryan, a congressman from Wisconsin, as his vice-presidential nominee. Ryan this year offered a long-term budget plan that would slash spending for civilian research and development.

The two parties diverge in past support for key areas of research. In 2009, Obama reversed an executive order by former president George W. Bush that had restricted government-supported research on human embryonic stem cells. Romney's position on the topic remains unclear, although his shift over the past few years towards more conservative policies on abortion has worried supporters of human embryonic stem-cell research. To back such work, he would have to cross the hard line established by his own party. In August, Republicans issued a political platform that said: "We oppose federal funding of embryonic stem cell research." And Ryan voted several times as a congressman to curtail federal funding in this area.

Similar strong differences can be seen in positions on climate-change research and policies. When he took office, Obama reversed a trend of declining support for the US climate-research portfolio, and he wants a further 5.6% increase in 2013. He authorized the EPA to set limits on greenhouse-gas emissions from cars. And Obama's team has engaged in the United Nations' climate negotiations to the extent possible given congressional constraints. The administration has taken a leadership role in the Montreal Protocol to protect the ozone layer, as well as in the Climate and Clean Air Coalition, an international effort launched in February to reduce pollutants such as methane, black carbon and tropospheric ozone, which warm Earth's surface.

"Romney's plans do not bode well for US science or its international partners."

Romney has diverged with many in his party by acknowledging that humans have helped to warm the planet, but he has exaggerated the disagreements among climate scientists. According to Romney: "There remains a lack of scientific consensus on the issue — on the extent of the warming, the extent of the human contribution, and the severity of the risk — and I believe we must support continued debate and investigation within the scientific community." He has campaigned against international climate agreements and last month told the television programme *Meet the Press* that "I'm not in this race to slow the rise of the oceans or to heal the planet".

His running mate has gone further to challenge climate scientists. After the release of e-mails in 2009 from the University of East Anglia in Norwich, UK, Ryan wrote: "These e-mails from leading climatologists make clear efforts to use statistical tricks to distort their findings and intentionally mislead the public on the issue of climate change." He also joined nearly all Republicans in the House of Representatives in 2011 to try to prevent any US funding of the Intergovernmental Panel on Climate Change. Romney and Ryan have vowed to roll back some of Obama's climate policies and would strip the EPA of its power to regulate greenhouse gases.

They have also promised to cut back sharply on new regulations and to require Congress to approve any major ones, which would effectively block agencies from setting important new rules. That requirement is so limiting that it will probably not come to pass, but it has helped to foster extreme views about government that could keep science agencies from carrying out their missions should Republicans sweep the November elections.

Over the past four years, Obama has demonstrated strong support for science and innovation, as well as policies that flow from research. Romney has not offered many details of his plans for science, but those he has released — and the recent record of his party — do not bode well for US science or its international partners. ■

Banish cronyism

A Texas cancer-research fund needs big fixes to restore badly eroded trust.

What a window into reality one misdirected e-mail can provide. Jimmy Mansour, head of the governing board at the Cancer Prevention and Research Institute of Texas (CPRIT) in Austin, mistakenly hit 'reply all' on a missive he sent last week, celebrating the resignations of many of the institute's scientific peer reviewers. The e-mail, first publicized by the *Houston Chronicle*, makes clear that Mansour, an accountant, lawyer and telecommunications entrepreneur, views scientists and scientific review with breathtaking disdain. "Better to get them all out of the way now," Mansour wrote following yet another of the letters of resignation tendered to the CPRIT in recent weeks by at least 29 of the institute's first-rate scientific reviewers. The letters were written in solidarity with the very public departure from the CPRIT of Nobel laureate Alfred Gilman, who until two weeks ago was the institute's chief scientific officer.

Gilman had given up on a review process that he labelled as corrupted by cronyism and unduly influenced by "really evil" political appointees on the CPRIT's governing board, motivated by regional Texas rivalries and personal interest. For instance, several grants to scientists at the University of Texas Southwestern Medical Center at Dallas, easily the best biomedical research institution in the state, were shelved by CPRIT leaders early this year despite strong endorsement from scientific reviewers. At the same time, a business-incubator grant was speedily awarded without scientific review: US$18 million went to the University of Texas MD Anderson Cancer Center and $2 million to Rice University, both in Houston. After Gilman and the chairs of all eight of the CPRIT's scientific-review panels complained, the incubator grant was pulled back, and the institute said that a scientific-review panel and commercial reviewers would all need to agree that it passed muster. It hired a compliance officer and, in August funded the shelved grants.

An outside observer could have been forgiven for surmising that with these last three actions, the institute was mending its ways and beginning a new chapter. But then, as we report on page 459, came Mansour's e-mail, written to CPRIT executive director William Gimson on 14 October, two days after Gilman's departure.

The exodus of scientific reviewers "gives us the prime opportunity to announce a new regime", wrote Mansour. "There will be a number of Texas Institutions who will be ecstatic." If the CPRIT concentrates on positive messaging at a conference this week, he added, "Gilman and the regime of the old guard (of research) will get the message" that the institute is moving forward. Forward towards what? His words give little confidence that the goal is a process that will judge science purely on its merits.

"The CPRIT's leadership must change at the very highest levels."

Mansour would make an almost comic villain were the stakes not so high. He is responsible for the $3 billion that more than 60% of voting Texans approved in 2007 to fight cancer over ten years; his term at the head of the governing board does not expire until 2015.

Yet it is clear that, if the institute hopes to recruit independent peer reviewers of the calibre that have just departed in droves, its leadership must change at the very highest levels. Mansour's removal is essential; at least one ethicist has suggested that Gimson should go as well. Such housecleaning is also the only way to begin rebuilding the trust of the Texas public, which has every right to expect that the $2 billion as yet unspent by the CPRIT be awarded through unimpeachable peer review. After all, when they voted five years ago, Texans authorized the state to borrow $3 billion "for research in Texas to find the causes of and cures for cancer". They did not vote for awards to bypass scientific scrutiny, for cronyism or for the equal distribution of grants between Texas institutions, regardless of the quality of proposed projects.

Happily, the citizens of the state still have some leverage. A vote of the state legislature is required every year to issue the annual $300 million in funding that supports the CPRIT. Texans should insist that their state politicians make future funding contingent on a serious clean-up, and on the re-implementation of top-calibre peer review for every single project that the CPRIT funds. ■

Shock and law

The Italian system's contempt for its scientists is made plain by the guilty verdict in L'Aquila.

"I'm not crazy. I know they can't predict earthquakes," the Italian public prosecutor Fabio Picuti told *Nature* last year. He was speaking as the manslaughter trial began in the ruined town of L'Aquila of six scientists and one government official for their alleged role in the deaths of 309 people in the quake of April 2009 (see *Nature* **477**, 264–269; 2011). On Monday evening, the seven were found guilty and sentenced to six years in prison (see *Nature* http://doi.org/jkp; 2012). The verdict is perverse and the sentence ludicrous. Already some scientists have responded with warnings about the chilling effect on their ability to serve in public risk assessments.

Even Picuti was surprised. He had requested a prison term of four years. "We'll have to read the judge's motivations to understand why," he said. Under Italian law, judge Marco Billi has up to three months to reveal his reasoning.

Despite the way the verdict has been portrayed in the media as an attack on science, it is important to note that the seven were not on trial for failing to predict the earthquake. As members of an official risk commission, they had all participated in a meeting held in L'Aquila on 31 March 2009, during which they were asked to assess the risk of a major earthquake in view of the many tremors that had hit the city in the previous months, and responded by saying that the earthquake risk was clearly raised but that it was not possible to offer a detailed prediction. The meeting was unusually quick, and was followed by a press conference at which the Civil Protection Department and local authorities reassured the population, stating that minor shocks did not increase the risk of a major one.

According to the prosecutor, such reassurances led 29 victims who would otherwise have left L'Aquila in the following days to change their minds and decide to stay; they died when their homes collapsed. The prosecutor thus reasoned that the "inadequate" risk assessment of the expert panel led to scientifically incorrect messages being given to the public, which contributed to a higher death count.

The seven — Bernardo De Bernardinis, Enzo Boschi, Giulio Selvaggi, Franco Barberi, Claudio Eva, Mauro Dolce and Gian Michele Calvi — are appealing against the verdict. They will remain free until the appeals process is finished, which could take years.

That provides an opportunity. There will be time enough to ponder the wider implications of the verdict, but for now all efforts should be channelled into protest, both at the severity of the sentence and at scientists being criminalized for the way their opinions were communicated. Science has little political clout in Italy and the trial proceeded in an absence of informed public debate that would have been unthinkable in most European countries or in the United States. Billi should promptly explain his decision, and the scientific community should promptly challenge it. ■

NATURE.COM
To comment online, click on Editorials at:
go.nature.com/xhunqv

Biometra
An Analytik Jena Company

Competence in Electrophoresis

Versatile Systems for Scientific Laboratories

Agarose Gel Electrophoresis
Compact-Line

- Easy to use design

PAGE Electrophoresis and Blotting
Eco-Line

- Modular Tank System for mini and maxi gels

PAGE Electrophoresis
Minigel Family

- Leak-free systems for native and SDS gels

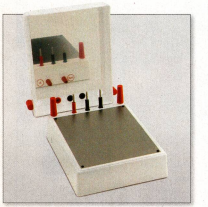

Semi-Dry Blotting Systems
Fastblots

- Rapid and high efficient transfer

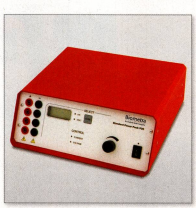

Power Packs
P25/P25T

- Universal for electrophoresis and blotting

Pulsed Field Gel Electrophoresis
Rotaphor System 6.0

- Separation of large DNA molecules up to 8 MB

www.biometra.com
+49 551 50686-0 · info@biometra.com

Innovation · Advancement · Development
Quality Products Made in Germany

UC RIVERSIDE
UNIVERSITY OF CALIFORNIA

LIVING THE PROMISE

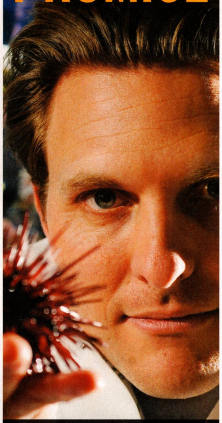

Breakthrough Research

Inspired by nature:
By studying sea urchins, corals and snails, UCR engineers learn to synthesize new materials like lightweight armor and flexible ceramics.

Explore more impacts >
promise.ucr.edu

CUSTOM MONOCLONAL ANTIBODIES
Rat mAb ◦ Mouse mAb ◦ Ascites

CUSTOM PROTEIN EXPRESSION
HEK293 ◦ Baculovirus ◦ *E. coli*

Superior Quality • Unrivaled Expertise
www.promab.com
1.866.339.0871 | info@promab.com
ProMab Biotechnologies, Inc.

nature jobs

Read our Postdoc articles and news in the **News and Comment** section of **naturejobs.com**

- Helpful advice
- Real life experiences
- Follow the highs and lows of postdoc life

High impact science
for the Arabic community

nature
الطبيعة العربية

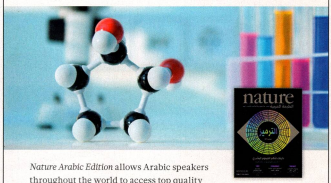

Nature Arabic Edition allows Arabic speakers throughout the world to access top quality science news and comment from *Nature*, as well as summaries of all the research papers from the leading multidisciplinary journal. Content is freely available online every week, with limited monthly copies available in print.

Access *Nature Arabic Edition* online and apply for your free subscription

arabicedition.nature.com

In partnership with:

مدينة الملك عبدالعزيز للعلوم والتقنية KACST

nature publishing group npg

R. TAYLOR/WWW.TAYLOR-PHOTO.CO.UK

Throw off the cloak of invisibility

Improving Wikipedia entries for notable women scientists should be only the start for a higher profile for women in science, says **Athene Donald**.

Take a look at Wikipedia this week and you will find that something has changed. The online reference tool now includes an entry for Eleanor Maguire, the cognitive neuroscientist at University College London who showed that the brains of London's taxi drivers change as the drivers develop their knowledge of the city's streets. And Louise Johnson, a molecular biophysicist at the University of Oxford, UK, from 1990 until her death last month, now has a longer entry more worthy of her achievements. The changes are welcome, but overdue.

Around this summer's Olympic and Paralympic Games I heard much discussion, some rather surprised, about the excitement and excellence of women's sports. Suddenly, people realized that women could excel at everything from football to cycling, from rowing to boxing — and be thrilling to watch. Despite years of work to address sexism, women in science tend to be the equivalent poor relation. Although we are known to lurk in there somewhere, on occasion women are still seen as add-ons who need to be patted on their pretty little heads, not always taken seriously and disadvantaged in pay and in other resources.

Indeed, a study published last month in the *Proceedings of the National Academy of Sciences* showed that for identical CVs submitted under a male or female name, the women were rated as significantly less competent and hireable than men — irrespective of the sex of the evaluator — and there were notable differences in the salary recommended (C. A. Moss-Racusin *et al. Proc. Natl Acad. Sci. USA* http://dx.doi.org/10.1073/pnas.1211286109; 2012). Unconscious bias is still prevalent, even if overt discrimination is rare.

Following on from a successful 'Edit-a-thon' earlier this year in collaboration with the Smithsonian Institute in the United States, last Friday Wikipedia held a similar event in conjunction with the Royal Society in London, to improve poor entries for some notable women scientists.

The Royal Society's library made its extensive resources available, to help to ensure that the new and improved entries are not only comprehensive but also accurate, something not always guaranteed on the Internet. This has to be a step in the right direction. But it is only one small step; there is a great deal of work to be done to ensure that female scientists and their important contributions are recognized appropriately, both on Wikipedia and more generally.

The latest Edit-a-thon was timed to tie in with Ada Lovelace Day. Lovelace is often remembered just as the daughter of the poet Byron, rather than as a mathematician who made important contributions to the field that would become computer science, including what could be considered the first computer program, to be used in conjunction with Charles Babbage's 'difference engine'. She does, at least, have a comprehensive Wikipedia entry.

By raising the profile of some women scientists and by training editors to be sensitive to the fact that such women are under-represented (in both number and length of entry) on Wikipedia, we can hope for a steady improvement in how women scientists are portrayed. Young aspiring scientists are very likely to use Wikipedia to gather information about past and present scientists. To help them to see what life might be like if they did pursue a career in science, we need realistic entries that provide valuable insight about living as well as dead scientists.

I sincerely hope that this edit-a-thon will encourage more people to overhaul the online portfolio of women scientists' entries. The number of female Fellows of the Royal Society is small, although growing, so it should be a reasonable aspiration for us in the United Kingdom to give each one a decent write-up. I'll put my hand up and admit that as one such female fellow, I do have a rudimentary entry, although it is not particularly informative or inspiring in its current state.

But we fellows are just one tiny band of largely academic scientists. We need entries for more women scientists, and for technologists too, with handsome photographs and some context for their work and lives. I have a long-standing interest in this issue. I sit on the Royal Society's Equality and Diversity Network and I chair the Athena Forum, a national group dedicated to improve the progression of women in science, technology and medicine. And I blog.

DESPITE YEARS OF WORK TO ADDRESS SEXISM, WOMEN IN SCIENCE TEND TO BE THE POOR RELATION.

We must continue to raise the profile of women in science, and remind people — as we did with the Olympic sports — that women's contributions are every bit as important as men's.

We need to do this for a variety of reasons. First, to inspire young women currently considering their options at school; second, to provide role models for women already studying science but uncertain whether they should pursue it further; and third, for simple natural justice. Women have, throughout the centuries, made contributions to the scientific endeavour. Historically, their opportunities were dire and their numbers small. Today the situation is very different, but this is still not a problem solved. ■

➲ NATURE.COM
Discuss this article online at:
go.nature.com/qofi9m

Athene Donald *is a professor of physics at the University of Cambridge, UK.*
e-mail: amd3@cam.ac.uk

RESEARCH HIGHLIGHTS

Selections from the scientific literature

BIOCHEMISTRY

EPO made from scratch

The hormone that triggers red blood cell production, erythropoietin (EPO), is often given to patients undergoing treatment for kidney failure or cancer. A team at the Sloan-Kettering Institute for Cancer Research in New York city has devised a method to synthesize a pure form of this complex protein from scratch.

Samuel Danishefsky and his colleagues built the protein, which until now could be made only in cell culture, by piecing together four glycopeptides that they had assembled in the lab. The researchers then folded the amino-acid chain into the final protein and used mass spectroscopy to verify the structure. Umbilical-cord blood-progenitor cells that were cultured with the synthetic molecule formed red blood cells.

Angew. Chem. Int. Edn. **http://dx.doi.org/10.1002/anie.201206090 (2012)**

ECOLOGY

Protecting prey with their odours

Exposing wild black rats to the smell of bird prey seems to put them off prey that is introduced later on — a strategy that could prove useful in species conservation.

To simulate bird nesting odours, Catherine Price and Peter Banks at the University of Sydney, Australia, placed feathers and faeces from quail (*Coturnix coturnix japonica*) in the habitat of the wild black rat (*Rattus rattus*; **pictured**). Seven days later, the researchers introduced artificial nests containing quail eggs. In areas where rats had been pre-exposed to the nesting odours, quail-egg survival was 62% greater than in areas where rats and eggs were introduced simultaneously.

The authors suggest that, during the pre-exposure period, the rats learned to ignore the odour cues because they were not associated with an egg reward.

Proc. Natl Acad. Sci. USA **http://dx.doi.org/10.1073/pnas.1210981109 (2012)**

B. BLAND/NATURE PL

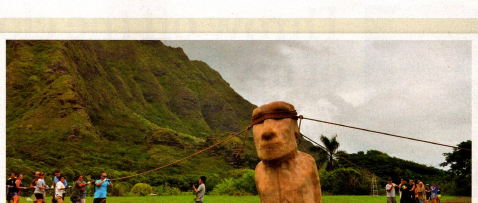

T. L. HUNT

ARCHAEOLOGY

How to move a 4-tonne statue

The Polynesian settlers of Easter Island may have transported their gigantic statues by slowly rocking them from side to side to make them 'walk'.

Nearly 1,000 statues litter the island, with the largest weighing about 74 tonnes and standing more than 10 metres tall. Some archaeologists propose that the statues, or moai, were transported from the quarry in a horizontal position on top of logs. However, Carl Lipo at California State University, Long Beach, and his team say that evidence points instead to an upright mode of transportation. Broken moai that were found along roads sloping upwards mostly lay on their backs, whereas those discovered on downwards sloping roads tended to be lying face down.

The researchers built a 3-metre-high concrete scale model, which they say has the same physical properties as a moai. Using three hemp ropes, a team of 18 people was able to move the statue 100 metres in 40 minutes (pictured). However, others are sceptical of the findings, saying that the shape of the model is inaccurate.

J. Archaeol. Sci. **http://dx.doi.org/10.1016/j.jas.2012.09.029 (2012)**

For a longer story on this research, see go.nature.com/1qoups

PLANETARY SCIENCE

Moon spun off from Earth

A catastrophic collision between Earth and another body probably created the Moon. Computer models predict that the Moon was derived from the impacting body, and yet Earth and the Moon are chemically almost identical. Two new models show how this scenario could arise if Earth was spinning faster at the point of impact than it does today.

One model, by Robin Canup of the Southwest Research Institute in Boulder, Colorado, suggests that if the impactor was larger than previous models have allowed — perhaps even Earth-sized — a collision could create a planet and a disk of Moon-forming material, both with the same composition and made from the impactor and its target.

Meanwhile, Matija Ćuk and Sarah Stewart at Harvard University in Cambridge, Massachusetts, show that if Earth used to spin faster than it does today, even a small, fast impactor could cause Earth

to shake off a disk of material that could subsequently form the Moon.
Science **http://dx.doi.org/10.1126/science.1226073; http://dx.doi.org/10.1126/science.1225542 (2012)**

BIOMATERIALS

Super-reflective fish skin

Three species of silvery fish seem to have found a way around a law of physics that governs the reflection of light.

The skin of the Atlantic herring (*Clupea harengus*), European sardine (*Sardina pilchardus*; **pictured**) and sprat (*Spratus spratus*) is made up of alternating layers of cytoplasm and highly reflective crystals of guanine — a molecule that is also found in DNA and RNA. Nicholas Roberts and his colleagues at the University of Bristol, UK, report that the fishes' skin can reflect light without polarizing it, even when the light hits the reflectors at angles that would normally result in fully polarized reflections. The skin contains a mixture of two types of guanine crystal with different optical properties — when the two are present in a specific ratio, this mixture prevents polarization and maintains high reflectivity.

These reflectors help the fish to camouflage themselves by matching the light environment of the open ocean, say the authors. Moreover, the principles at work in these fish could have applications in optical devices such as light-emitting diodes.
Nature Photon. **http://dx.doi.org/10.1038/nphoton.2012.260 (2012)**
For a longer story on this research, see go.nature.com/ndcqjt

P. FENN GALLERY/GETTY

CANCER

Targeting a vicious cycle

Cancer cells proliferate by sending the cell cycle into overdrive, but early attempts to target the cell cycle with drugs were marred by problems with toxicity. Now two groups show that shutting down cell-cycle proteins called D-type cyclins seems to stop tumour growth without affecting normal tissue.

Piotr Sicinski and his colleagues at the Dana-Farber Cancer Institute in Boston, Massachusetts, engineered mice in which the production of cyclin D1 can be switched on and off. Loss of the protein had no apparent effect on healthy adult mice, but halted the growth of mammary tumours in mice that were also genetically predisposed to developing breast cancer.

Sicinski's team, and Iannis Aifantis at the New York University School of Medicine and his colleagues, showed independently that loss of cyclin D3 either triggered the death of tumour cells, or prevented their growth, in mouse models and human cell lines of an aggressive form of leukaemia. Inhibiting downstream proteins called cyclin-D associated kinases also killed tumour cells.
Cancer Cell *22*, **438–451; 452–465 (2012)**

ARCHAEOLOGY

A more accurate carbon clock

Determining the age of fossils and other ancient objects could become more accurate, thanks to measurements of radioactive carbon-14 from a lake in Japan.

Radiocarbon dating is based on the steady decay rate of carbon-14 in samples, and archaeologists calibrate this carbon clock by comparing the known ages of tree rings with their carbon ages. But the tree-ring carbon record goes back only about 14,000 years, and less reliable marine records have been used to fill the gap. Christopher Ramsey at the University of Oxford, UK, and his colleagues extracted roughly 70-metre-long core samples from the bed of Lake Suigetsu. By counting the number of distinct sediment layers in the core — two layers have formed every summer and winter over the past 52,000 years — the team was able to compare the ages of the layers with their carbon-dated ages.

The more accurate carbon-14 record could help archaeologists to fine-tune the dates of key events, such as the coexistence of humans and Neanderthals.
Science 338, **370–374 (2012)**
For a longer story on this research, see go.nature.com/pbv6ey

PHOTONICS

White LEDs without glare

A new luminescent material reduces the glare of white light-emitting diodes (LEDs) and could make them more practical for home lighting.

A team led by Hisayoshi Daicho of Koito Manufacturing in Shizuoka, Japan, designed the material, which consists of chlorosilicates that have been implanted with europium ions. The phosphor absorbs violet light and re-emits it in a yellow shade. The researchers combined this phosphor with a blue one and then added a violet LED to create a system that emits white light with a uniform hue (**pictured**) and no glare.
Nature Commun. **http://dx.doi.org/10.1038/ncomms2138 (2012)**

COMMUNITY CHOICE
The most viewed papers in science

GEOSCIENCE

Sudden rupture in deadly earthquake

HIGHLY READ on www.agu.org 15 Oct–21 Oct

A brutal secondary rupture may have been responsible for much of the devastation caused by the Wenchuan earthquake, which killed more than 69,000 people in Sichuan province, China, on 12 May 2008.

A team led by Guohong Zhang of the China Earthquake Administration in Beijing used ground-acceleration data from a national network of earthquake-monitoring stations to reconstruct the spread of the 7.9-magnitude quake. Records from 26 local stations indicate that the main slip area — a high-friction patch of fault located 25 to 50 kilometres from the epicentre — resisted the seismic stress building up around it for about 30 seconds. The slip area then failed catastrophically in a sudden 12.5-metre jolt.

Researchers have long hypothesized that an initial quake can trigger secondary ruptures. The study shows that this is a realistic scenario, the team concludes.
Geophys. Res. Lett. **http://dx.doi.org/10.1029/2012GL052516 (2012)**

➲ **NATURE.COM**
For the latest research published by *Nature* visit:
www.nature.com/latestresearch

SEVEN DAYS *The news in brief*

POLICY

Biodiversity cash

Wealthy nations have agreed to double their support to developing countries for protecting biodiversity, to reach about US$10 billion annually by 2015. The pledge was made at the United Nations Convention on Biological Diversity in Hyderabad, India, which ended on 20 October. The host country said that it would contribute $50 million over two years for conservation.

Egg freezing is safe

Egg freezing is no longer an 'experimental' procedure, says the American Society for Reproductive Medicine in Birmingham, Alabama, which issued new guidelines for the controversial practice on 22 October. That change in policy is expected to accelerate the growth of clinics that offer to freeze the eggs of women who face fertility-damaging treatment or who wish to delay having a baby. See go.nature.com/ugsflc for more.

Biofuels rethink

The European Commission launched an overhaul of its biofuels policies on 17 October, after criticism that the rules have contributed to rising food prices and concerns that biofuels may produce greater greenhouse-gas emissions than fossil fuels (see *Nature* http://doi.org/bmssn7; 2011). The proposals retain a target that 10% of transport fuels should come from renewable sources by 2020 — but set a 5% cap on food-based biofuels. See go.nature.com/xhgytb for more.

Forest-code veto

President Dilma Rousseff once more exercised her veto before finally signing off the long-delayed revision of Brazil's forest code into law on 17 October. She rejected nine provisions that, among other things, would have removed forest protection along rivers and slopes, and would have allowed lawbreakers to receive a blanket amnesty. The country's National Congress initially passed a bill to roll back forest protection in April, and Rousseff then used her veto powers to alter that version and send it back to lawmakers.

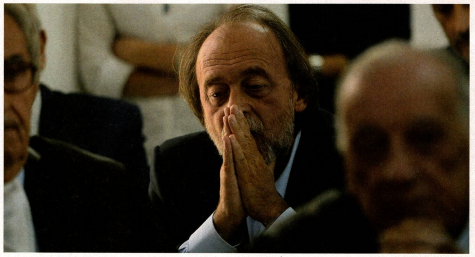

F. MONTEFORTE/AFP/GETTY

Manslaughter verdict rocks seismology

After a 13-month trial, six scientists and former government official Bernardo De Bernardinis (**pictured**) have been found guilty of manslaughter because of the way that they assessed and communicated risk before the earthquake that hit the Italian city of L'Aquila in April 2009, killing 309 people. The seven men were each sentenced to six years in prison, and must pay compensation to the victims' families, although the defendants will appeal the verdict. At the 22 October hearing, a prosecutor said that the men's reassurances led to the wrong messages being given to the public, which added to the death count. See page 446 and go.nature.com/5orvaa for more.

Badger cull stalled

The British government on 23 October delayed a controversial cull of badgers (*Meles meles*) that has provoked years of heated debate among researchers, farmers and politicians. The cull was scheduled to start imminently as part of efforts to control bovine tuberculosis, which badgers can transmit to cattle (see *Nature* **490**, 317–318; 2012) — but it will now take place no sooner than next summer. See go.nature.com/aizbax for more.

India GM concerns

Prospects for growing genetically modified (GM) food crops in India receded further when a panel of scientists called for a moratorium on all field trials in a report issued on 17 October. The five-member panel had been appointed by India's Supreme Court in May in response to a petition from anti-GM protesters. Its conclusions echo an August parliamentary report, but go further, calling for a re-examination of biosafety data on GM crops already approved for field trials. See go.nature.com/kovfrc for more.

BUSINESS

Stem-cell bid

Tom Okarma and Michael West, former chief executives of biotechnology firm Geron, sent the company's shareholders a letter bidding for its stem-cell assets on 18 October. Geron, based in Menlo Park, California, spent more than a decade developing a spinal-cord-injury treatment derived from human embryonic stem cells and performed early clinical testing in 2010. But John Scarlett, the company's current chief executive, shut down the programme last November, saying that Geron's cancer

WALDRAPTEAM

therapeutics are a better investment. See go.nature.com/tihbe6 for more.

Diet-pill concern

Europe's drug regulators have recommended against approving a diet pill recently cleared for sale in the United States. The European Medicines Agency's Committee for Medicinal Products for Human Use said that it was concerned about cardiovascular and nervous-system side effects for the obesity drug made by Vivus of Mountain View, California. Vivus says that it will appeal the 18 October opinion.

Battery bankruptcy

A123 Systems, a leading US manufacturer of lithium-ion batteries for electric vehicles, filed for bankruptcy on 16 October. The firm, based in Waltham, Massachusetts, had been backed by a US$249-million grant from the US Department of Energy. Founded in 2001, it was a spin-off from work at the Massachusetts Institute of Technology in Cambridge. See go.nature.com/mkqsbc for more.

PEOPLE

EU health fracas

Europe's health commissioner, John Dalli, has left his role amid fallout from a corruption investigation. The European Commission said on 16 October that Dalli resigned after the European Union (EU) anti-fraud office, OLAF, looked into legislation on tobacco regulation. According to the commission, a tobacco company complained that a third party had suggested using contacts with Dalli to influence the proposed legislation. Dalli denies the allegations. See go.nature.com/zqplrx for more.

RESEARCH

Vostok lifeless?

No native microbes were found by an early analysis of the ice on the drill used by a Russian team to penetrate Lake Vostok, a body of water buried deep under Antarctica's ice, in February. The top layer of the lake seems to be lifeless, according to "very preliminary results" presented by Sergey Bulat of the Petersburg Nuclear Physics Institute in Gatchina, Russia, at the 12th European Workshop on Astrobiology in Stockholm on 16 October. See go.nature.com/cpe12m for more.

Iconic ibis shot

A bird that had been hand-reared by researchers as part of a project to save a rare species of ibis was killed by poachers in Italy on 13 October. Goja (**pictured**), a northern bald

ibis (*Geronticus eremita*), had been trained to migrate from a breeding area in Germany to wintering grounds in Italy and was the first bird in the project to fly back unaided to Germany in summer 2011. The bird has been extinct in the wild in Europe for nearly 400 years. See go.nature.com/4buekb for more.

UK animal research

A poll released on 19 October by Ipsos Mori suggests that 63% of people in the United Kingdom support animal experimentation where there is no alternative — a drop from 73% in 2010. Only 43% think that UK rules on animal experimentation are well enforced, down from 56% two years ago. In response, medical charities, drug firms and 15 universities issued a declaration affirming that their research involves animals only where other avenues are not possible, and said that they would develop transparency principles to win over the public to the need for animal research. See go.nature.com/lspaam for more.

Chimp haven

The US National Institutes of Health (NIH) said on 17 October that it will send 20 chimpanzees to permanent retirement in a federally funded sanctuary by August 2013 — double the number it announced last month. The animals are among 110 NIH-owned chimpanzees that the agency is removing from the New Iberia Research Center in Lafayette, Louisiana. Officials at the 80-hectare Chimp Haven sanctuary in Keithville, Louisiana, say that they would like to accommodate all the animals, but need an extra US$2.55 million to build the necessary structures.

EVENTS

Phones and tumours

Italy's highest civil court has stated that mobile phones can cause brain tumours — to the dismay of medical experts who say no study has proven a clear causal link between health risks and mobile-phone use. In a 12 October decision made public last week, the court ruled in favour of a commerce manager who claimed his tumour was a consequence of the heavy phone usage demanded by his job. See go.nature.com/bg6zly for more.

SOURCE: WHO

TREND WATCH

New cases of tuberculosis (TB) fell by 2.2% between 2010 and 2011, the World Health Organization said in its annual report on the disease. But some 3.7% of new TB cases are now multi-drug resistant. In some countries in eastern Europe and central Asia, multi-drug resistance occurs in more than 20% of cases (see chart). Because of incorrect diagnoses and a shortage of data in some places, even this is probably an underestimate. See go.nature.com/pytbbu for more.

DRUG-RESISTANT TB SPREADS IN EASTERN EUROPE

In seven former Soviet countries, a fifth or more of new tuberculosis cases are now multi-drug resistant.

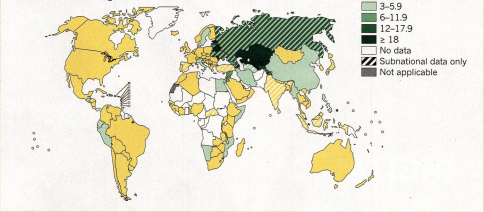

"There's a way to do it better — **find it.**"

Thomas Edison

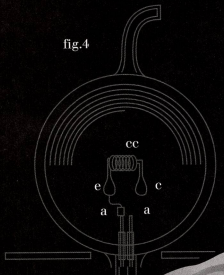

ReadCube is a better way to **read**, **search**, **organize** and **find** your research literature.

Digital Science – **software that understands science**.

DIGITAL science

www.digital-science.com

readcube

www.readcube.com

NEWS IN FOCUS

BIOSECURITY Tighter shackles loom for SARS and H5N1 research **p.456**

ENVIRONMENT Iron-dumping project unleashes a sea of troubles **p.458**

BIOMEDICINE Resignations expose tensions at Texas cancer institute **p.459**

NEUROSCIENCE In political choices, does the body rule the mind? **p.466**

S. LOEB/AFP/GETTY

President Barack Obama (left) and presidential candidate Mitt Romney often take opposing stances on government's role in science and innovation.

POLITICS

High stakes for US science

As the election nears, the opinions of the presidential candidates diverge over research.

BY JEFF TOLLEFSON AND HEIDI LEDFORD

Science rarely takes the stage in US presidential campaigns. But as President Barack Obama and Republican challenger Mitt Romney make their final bids for votes on 6 November, their sharply contrasting visions of the size and proper role of government have profound implications for science.

In the face of a sluggish economy and competition from countries such as China, "we've got to make sure that we've got the best science and research in the world", Obama said during his second debate with Romney, on 16 October. Romney, previously a business executive and the former governor of Massachusetts, responded with a refrain that has become a centrepiece of his campaign: "Government does not create jobs." The exchange captures differences that could directly affect a wide range of science-related matters for years to come, including research funding, energy development, environmental regulation and public health (see 'In their own words').

In his campaign rhetoric and in the policy decisions made during his first term as president (see *Nature* **487**, 414–415; 2012), Obama has kept science near the centre of his economic plan for the United States. He has defended investment in education and in basic and applied research as essential — especially during times of austerity. By contrast, Romney has emphasized the need to scale back government and rein in the trillion-dollar deficits that have marked Obama's first term. Romney's campaign affirms the federal government's importance in funding basic research, but asserts that commercial innovation belongs squarely in the private sector.

"These are really important signals," says David Victor, a public-policy expert at the University of California, San Diego. "It certainly does not appear that a Romney administration is going to put spending on research and development and education at the centre of their priorities, whereas Obama has made science and education an important part of his agenda."

For research advocates, Obama's stance puts him at a clear advantage. Despite generally tight budgets across federal granting agencies in recent years, "Obama has a strong track record" of investing in science, says Abby Benson, president of the Science Coalition, a non-profit organization based in Washington DC that represents 50 US research universities. ▶

NATURE.COM
Visit *Nature*'s election special:
www.nature.com/election2012

IN THEIR OWN WORDS

Barack Obama (blue) and Mitt Romney (red) speak about science issues on the campaign trail.

CLIMATE

"Climate change is one of the biggest issues ... we have to meet this challenge by driving smart policies that lead to greater growth in clean energy generation and result in a range of economic and social benefits."

"I oppose steps like a carbon tax or a cap-and-trade system ... Economic growth and technological innovation, not economy-suppressing regulation, is the key to environmental protection."

The bottom line: Romney opposes all climate regulations. Obama used regulatory powers to push through energy and climate regulations, and subsidies for low-carbon energy technology.

EDUCATION

"Now I want to hire another hundred thousand new math and science teachers and create two million more slots in our community colleges so that people can get trained for the jobs that are out there right now."

"I propose we grade our schools so parents ... can take their child to a school that's being more successful. I don't want to cut our commitment to education, I want to make it more effective and efficient."

The bottom line: Obama often emphasizes science education. Romney focuses on streamlining the federal role in education while encouraging school choice and voucher programmes.

ENERGY

"I have supported an all-of-the-above energy approach that will allow us to take control of our energy future, one where we safely and responsibly develop America's many energy resources."

"A crucial component of my plan ... is to dramatically increase domestic energy production and partner closely with Canada and Mexico to achieve North American energy independence by 2020."

The bottom line: Romney and Obama have tussled over who supports fossil fuels the most. The difference is that Obama continues to push to develop renewable sources for the long term.

INNOVATION

"I am committed to doubling funding for key research agencies to support scientists and entrepreneurs, so that we can preserve America's place as the world leader in innovation."

"The promotion of innovation will begin on Day One, with efforts to simplify the corporate tax code, reform job retraining programmes, reduce regulatory burdens, and protect American intellectual property."

The bottom line: Obama deployed stimulus money to commercialize new technologies. Romney supports basic research, but leaves innovation and commercialization to the private sector.

REGULATION

"Smart rules can save lives and keep us safe, but there are some regulations that don't make sense and cost too much."

"We must reduce the power of unaccountable regulators by requiring that all major regulations receive congressional approval and by imposing a regulatory cap that prevents the addition of new regulatory costs."

The bottom line: Romney would slow or stop regulation where possible. Obama moved to reduce unnecessary regulatory burdens, but also used regulatory powers to further his agenda.

SPACE

"Our goal is the capacity for people to work and learn and operate and live safely beyond the Earth for extended periods of time, ultimately in ways that are more sustainable and even indefinite."

"America has enjoyed a half-century of leadership in space, but now that leadership is eroding ... I will bring together all the stakeholders ... and define the pathway forward."

The bottom line: Under Obama, NASA has drifted into budgetary and mission limbo. Romney has underscored the problem but offers few specifics about what he would change.

STEM CELLS

"We will vigorously support scientists who pursue this research. And we will aim for America to lead the world in the discoveries it one day may yield."

"I have a deep concern about curing disease ... but I will not create new embryos through cloning or through embryo farming, because that would be creating life for the purpose of destroying it."

The bottom line: Obama repealed limits on federal funding of stem-cell research. Romney has not specified his stance, but his religious views may stand in opposition to current policy.

▶ "Romney has talked about it, but we don't know how that will translate into policy."

On other issues, both candidates have shifted with the times. As governor of Massachusetts, Romney ushered in a 'climate protection plan' in 2004 that sought to reduce greenhouse-gas emissions while fostering a transition to cleaner energy sources. But one year later, he baulked at joining the Regional Greenhouse Gas Initiative, a cap-and-trade system covering carbon emissions from utilities in the northeastern part of the United States. This year, on the campaign trail, Romney has frequently pointed out that 'global warming' is not 'America warming', meaning that the United States should not take action — and increase costs on US manufacturers and businesses — while carbon emissions are accelerating in China and India. Romney has said that he would work to reverse greenhouse-gas regulations instituted by the US Environmental Protection Agency under Obama.

CLIMATE SWINGS

For his part, after watching climate legislation wither in Congress in 2010, Obama has focused on increasing fossil-fuel energy production as well as boosting renewables. Much to the dismay of environmentalists, the Obama administration has supported shale-gas development and opened up new territory in the Arctic to drilling. Oil and natural-gas output are on the rise in the United States, which has translated into less reliance on foreign oil and a reduction in greenhouse-gas emissions as electric utilities switch from coal to natural gas.

Roger Pielke Jr, an environmental-policy expert at the University of Colorado, Boulder, says that Obama has been pushed so far towards the right by political realities in Washington that the core of his energy policy looks a lot like Romney's. "There are plenty of people who like Obama because of what he believes," Pielke says, "but if you are a policy pragmatist, what really matters is not what people feel in their heart, but what their actual policies are."

Nonetheless, Romney has vowed to make clear turns away from current energy policy. He has said that he would reverse a century of public policy and turn the management of federal lands over to individual states to hasten energy production. He has also repeatedly questioned the wisdom of subsidies for renewable energy production. In particular, Romney has made it clear that he would end the kind of public–private ventures that resulted in government loans to the California solar energy firm Solyndra, which filed for bankruptcy last year despite US$535 million in federal loan guarantees.

Obama and Romney both say that they would bolster the scientific workforce through easier immigration policies for foreign-born graduates of university science and mathematics programmes. Yet Mary Woolley, president of the advocacy group Research!America, based in Alexandria, Virginia, frets that neither

OTHER VOTES TO WATCH

During the US elections on 6 November, all 435 seats in the House, 33 seats in the Senate and 11 state governorships will be contested. In many cases, the outcomes could affect science-related policies.

BALLOT MEASURES

- **Agriculture** California could become the first state to require labelling of genetically modified (GM) foods, and a North Dakota measure could make planting GM crops a constitutional right.
- **Energy** A Michigan measure would require 25% of electricity sold in the state to come from renewable sources. A California vote could divert more state taxes to green energy.
- **Marijuana** Arkansas, Massachusetts and Montana will vote on allowing or expanding marijuana for medical use. Colorado, Oregon and Washington may opt to legalize it altogether.
- **Wildlife** Pre-empting challenges by animal-rights advocates, Idaho, Kentucky, Nebraska and Wyoming will vote on constitutional guarantees for hunting and fishing in those states.

TIGHT RACES
(D, Democrat; R, Republican)

1. **California (10th District)** Jeff Denham (R), who voted against greenhouse-gas regulation, faces former astronaut Jose Hernández (D).
2. **Florida (Senate)** Two-term Senator Bill Nelson (D), a strong supporter of NASA, battles a challenge from Connie Mack IV (R).
3. **Missouri (Senate)** Claire McCaskill (D), a stem-cell champion, duels Todd Akin (R), who supports right-to-life for human embryos.
4. **Montana (Senate)** Denny Rehberg (R), tough on NIH officials during his tenure in the House, wants Jon Tester's (D) Senate seat.
5. **Washington (Governor)** Jay Inslee (D), outspoken on climate, clean energy and environmental legislation, is aiming to lead the state.

campaign has been specific enough about its commitment to biomedical research. "I think that's concerning," she says. "Experience shows that candidates who don't talk about an issue before they are elected are unlikely to be champions of that issue after they are in office."

DOLLARS AND CELLS

Although Obama has a proven track record of support for biomedicine — he allocated $10.4 billion in economic stimulus funds to the National Institutes of Health (NIH) in 2009 — he has flatlined the agency's funding in his latest budget request. Romney's pledge to tighten government purse strings while boosting defence spending could force cuts to the NIH and to regulatory agencies such as the Food and Drug Administration, says Woolley.

Supporters of research that uses human embryonic stem (ES) cells are particularly nervous about what actions Romney might take if he becomes president. Under Obama's executive order of March 2009, which overturned restrictions imposed by the preceding George W. Bush administration, the number of human ES cell lines available to federally funded researchers has soared from around 20 to 182. Some fear that those gains may be frozen or even lost with Romney in the White House.

Romney's statements about stem cells during the 2012 campaign have been vague enough to leave his policy intentions unclear, and the Romney campaign did not respond to *Nature*'s requests for clarification on the issue. But in 2011, Romney's running mate, Paul Ryan, co-sponsored a bill that would guarantee every fertilized embryo the right to life. That, combined with policy statements from the Republican platform and the tone of Romney's recent comments about abortion, "does not give us much reason to think he would support stem-cell research as president", says Sean Tipton, vice-president of communications for the Coalition for the Advancement of Medical Research in Washington DC, an umbrella group that supports government funding of research on human ES cells.

Whoever wins the election on 6 November will inherit both a sputtering economic recovery and severe spending constraints. A combative and nearly evenly divided Congress could hamper new policy initiatives regardless of who is president, which means that tight races for the House and Senate will have significance beyond their local districts (see 'Other votes to watch'). For US researchers, then, the future will depend not only on who wins the vote, but also on who can carry the momentum of an election victory into cooperative action across the political spectrum. ■ SEE EDITORIAL P.445

Additional reporting by **Helen Shen** *and* **Meredith Wadman**.

MORE ONLINE

LISTEN

The beluga whale that had something to say
go.nature.com/1jlyhg

READ

- Brain scans during sleep can decode visual content of dreams
go.nature.com/5tfa34
- Fossil scars capture dinosaur headbutts go.nature.com/cqpcaj
- Core sample sends carbon clock farther back in time go.nature.com/pbv6ey

WATCH

The buzz about pesticides go.nature.com/ubtfix

M. TAUBER/BLEND IMAGES/GETTY

INFECTIOUS DISEASE

Viral research faces clampdown

US biosecurity concerns could harm collaboration.

BY DECLAN BUTLER

Federal health agencies in the United States have acted to tighten security surrounding research on two deadly pathogens. The move is intended to enhance public safety, but some fear that it may hamper research in the United States and abroad.

Earlier this month, US health agencies added the SARS virus to its list of select agents — pathogens and toxins that it deems to have the "potential to pose a severe threat to public health and safety". In addition, the agencies last week opened a public consultation about whether they should designate strains of H5N1 avian influenza virus that are transmissible between mammals as 'Tier 1' select agents — a newly created class subject to the strictest levels of biosecurity. The consultation comes after the Intragovernmental Select Agents and Toxins Technical Advisory Committee advised the agencies that the virus could "potentially overwhelm the health care system".

The listing of the SARS virus as a select agent — along with two recently discovered haemorrhagic-fever viruses, Lujo and Chapare — means that dozens of US labs holding the virus have until 3 April to either upgrade the biosecurity of their labs or destroy or transfer their stocks. The US government estimates that 38 of the labs — 10 academic, 22 commercial and 6 government labs — do not currently have the extra biosecurity measures required to carry out select-agent research, including stricter lab-access rules and vetting of staff.

Shinji Makino, a SARS researcher at the University of Texas Medical Branch in Galveston, whose biosafety-level-3 (BSL-3) lab is one of the 38 affected, is "disappointed" by the move. His university owns the BSL-4 Galveston National Laboratory, which has the highest biosafety containment rating and so is select-agent compliant, and Makino is now seeking lab space there to continue his research.

The restrictions could interfere with sharing the virus or reagents between labs based in the United States or overseas, warns Michael Buchmeier, deputy director of the Pacific Southwest Center of Excellence for Biodefense and Emerging Infectious Diseases at the University of California, Irvine. "The threat of criminal prosecution and severe penalties will have a chilling effect on the kinds of collaborative efforts that have characterized SARS work up until now," he says.

For H5N1 researchers, the proposal to add mammalian-transmissible forms of the virus to the Tier 1 list is the latest twist in a year-long international storm that erupted over experiments by Ron Fouchier at the Erasmus Medical Center in Rotterdam, the Netherlands, and Yoshihiro Kawaoka at the University of Wisconsin–Madison. Critics have questioned the benefits of the work, which showed that a few genetic tweaks allowed the avian virus to spread easily in ferrets, an animal model used for research into human flu. They say that if this virus escaped from a lab it might cause a pandemic in humans. In the face of these concerns, flu researchers agreed last January to a self-imposed moratorium on such work, which has yet to be lifted.

"We need as many labs to do research as possible, as H5N1 remains a direct threat to animal and public health."

The US Department of Agriculture already lists H5N1 as a select agent on the basis of the risks to animal health. But labs handling Tier 1 select agents must take security precautions that go beyond the already stringent requirements for handling select agents. These include instituting extra physical barriers, video surveillance and stricter staff vetting and monitoring.

The Tier 1 subset of select agents was created following the FBI's conclusion that a government scientist, Bruce Ivins, was responsible for the anthrax mailing attacks in 2001. It became effective on 5 October and includes the pathogens responsible for smallpox, Ebola, anthrax, foot-and-mouth disease and rinderpest (see 'Top tier').

The Department of Health and Human Services and the Centers for Disease Control and Prevention proposed adding some forms of H5N1 to the list on 18 October, and the public, as well as scientists, have 60 days to respond. If the extra restrictions are imposed, they are likely to influence the way the research is regulated globally, because the United States is the largest funder of flu work.

Not before time, claim the critics. Mammalian-transmissible H5N1 viruses definitely meet all the stated criteria for a Tier 1 select agent, given their potential deadliness, the lack of immunity in humans and the absence of sufficient drugs or vaccines to cope with a pandemic, says Richard Ebright, a molecular biologist and biodefence expert at Rutgers University in Piscataway, New Jersey.

But Fouchier argues that by creating a burden that would keep all but a few labs from working on the virus, listing H5N1 as a Tier 1 agent could ultimately make the world less secure. "We need as many labs to do research as possible, as this virus remains a direct threat to animal and public health," he says. "Restricting the research on this pathogen will not increase global safety and security; it will make things worse." ■

TOP TIER

The US Federal Select Agent Program this month created a new subset of 13 'Tier 1' disease agents or toxins considered to be exceptional threats to security. Some forms of H5N1 may be added to the list.

Agent	Type	Danger
Botulinum neurotoxin	Toxin	One of the most potent neurotoxins known
Ebola virus	Virus	Ebola haemorrhagic fever
Francisella tularensis	Bacterium	Tularaemia. Found in many animals, in particular rabbits
Marburg virus	Virus	Marburg haemorrhagic fever
Botulinum-neurotoxin-producing species of *Clostridium*	Bacterium	Toxin causes botulism food poisoning
Variola major virus	Virus	Most common form of smallpox
Variola minor virus	Virus	Rarer and less lethal form of smallpox
Yersinia pestis	Bacterium	Pneumonic and bubonic plague
Bacillus anthracis	Bacterium	Anthrax
Burkholderia mallei	Bacterium	Glanders in humans and horses
Burkholderia pseudomallei	Bacterium	Melioidosis
Foot-and-mouth disease virus	Virus	Foot-and-mouth disease
Rinderpest virus	Virus	Rinderpest

TECHNOLOGY

Website pitches solutions in search of problems

Marblar aims to help scientists turn discoveries into innovative applications.

BY RICHARD VAN NOORDEN

In this age of social media, innovators eager to develop high-tech products are tapping into the wisdom of crowds to solve problems, with crowdsourcing sites such as Innocentive and Kaggle offering cash prizes for answers to science or data questions. The launch this week of a site called Marblar (www.marblar.com) is turning this model on its head.

Marblar gives scientists a space to tout solutions that have yet to find their problem. Members, who can come from any background, are invited to publicly discuss potential uses for patented discoveries made in research laboratories that as yet may not have led to real-world applications.

Sites that help to match up technology developers with potential investors — such as Yet2.com, iBridgeNetwork.org and ninesigma.com — do so in private. By contrast, every suggestion at Marblar is posted on a public forum alongside video interviews with the scientists and explanations of their work. Website visitors suggest applications and vote them up and down, and the scientists behind the discovery are encouraged to take part in the discussion. Popular suggestions are recognized with a points system (denoted by marbles — hence the name) and, in some cases, small cash prizes.

The venture has attracted £371,000 (US$600,000) of backing from IP Group, a technology-investment firm based in London. The site charges listing fees and gets prizes sponsored; if it takes off, it may offer recruitment services, or even get a small slice of royalties from spin-off companies.

The website is the brainchild of entrepreneur and biochemistry doctoral student Dan Perez at the University of Oxford, UK. Perez argues that scientists seeking commercial use for their work don't consult widely enough. "So much science lies fallow because people pursue the wrong avenues," he says, noting that the search often stops at the door of the university technology-transfer office, where inventions are pushed towards a few narrow applications that may not bear fruit. Marblar, he hopes, will throw that consultation process open to the world.

"The idea addresses an important problem," says George Whitesides, a famously inventive chemist at Harvard University in Cambridge, Massachusetts, who is not involved with the company. "There is all manner of really interesting science that has not been exploited." However, he points out that the cost of turning an idea into a practical product is the biggest barrier to commercialization. Furthermore, the best applications are likely to have found backers already. "Having said that, what this kind of idea might do is to stimulate thinking about really new and unconventional types of applications and products," he says.

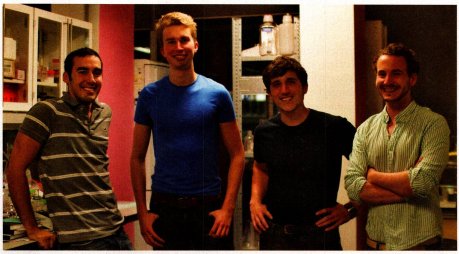

MARBLAR

Team Marblar: (from left) Mehmet Fidanboylu, Gabriel Mecklenburg, Daniel Perez and Tom von Erlach hope that their website will open fresh pathways to success for inventions.

"Marblar is trying to open up questions about what you do with inventions."

Perez says that Marblar users will initially be discussing more than 30 technologies offered by UK and US universities and research-funding agencies. These include optical tweezers that can deform and manipulate nanoparticles; a device that can transmit multiple data signals through power lines; and a way of bringing molecules inside cells by hitching them to antibodies attached to cell-invading viruses.

So will Marblar work? "Like all these things, the idea depends on the people involved more than anything else — and Dan is quite persuasive," says Graham Richards, a former head of chemistry at the University of Oxford, who has founded numerous spin-off firms and now sits on the board of IP Group.

Successful technology transfer depends on wide networking with the right people, adds Richards. Perez is well connected: in June 2011 he founded an industry discussion forum for young scientists, which has now become the Oxbridge Biotech Roundtable, and to which Marblar's three other young founders also belong.

Marblar has already had a trial run, using work by chemist Tom Brown from the University of Southampton, UK, which involves a method to chemically join DNA and RNA together without using biological enzymes. The pilot was fairly successful, says Adam Irvine, who works in the university's technology-transfer office. "I was sceptical that much would come back from this," he says. "So it was interesting for me to see that we could get useful ideas."

Contributors to Marblar are made aware that they are effectively giving up their ideas for free by discussing them in public, but Perez notes that beyond the rewards the site provides, there may be a future for winning entries. For example, the architect of the top suggestion in Marblar's pilot challenge is now in talks with the inventor to start a company to develop drugs that bind to RNA.

"It's very difficult to measure how successful crowdsourcing websites have been — of course, they will all trumpet successes for clients," says Michael Hill-King, who leads knowledge-transfer schemes at King's College London. But, he says, "Marblar is trying to open up questions about what you do with inventions — and I hope it will cause some waves". ■

➲ **NATURE.COM**
Read more about Daniel Perez and Marblar:
go.nature.com/6anjmf

GEOENGINEERING

Ocean-fertilization project off Canada sparks furore

Bid to boost salmon stocks relied on hotly debated science and dubious carbon credits.

BY JEFF TOLLEFSON

When a chartered fishing boat strewed 100 tonnes of iron sulphate into the ocean off western Canada last July, the goal was to supercharge the marine ecosystem. The iron was meant to fertilize plankton, boost salmon populations and sequester carbon. Whether the ocean responded as hoped is not clear, but the project has touched off an explosion on land, angering scientists, embarrassing a village of indigenous people and enraging opponents of geoengineering.

The first reports about the project, which appeared in British newspaper *The Guardian* on 15 October, presented it as a rogue geoengineering scheme — the largest in history — in "blatant violation" of international treaties. Critics suggested that Russ George, a US entrepreneur, had persuaded the Haida Nation village of Old Massett on the Queen Charlotte Islands to fund the project by promising that it would be possible to sell carbon credits for the carbon dioxide taken up by phytoplankton.

The reality was much more complex, and it underscores the combustible politics and uncertain science of geoengineering.

Contacted by *Nature*, George lashed out at the media and "radical environmentalists" for manufacturing a "racist" story about a maverick geoengineer taking advantage of naïve natives. "This was their work and their project," he says. "It is not the result of them being too stupid to know better."

It is now clear that Old Massett, a fishing village of fewer than 1,000 people, embraced the project in hopes of restoring dwindling salmon runs by boosting phytoplankton and, in turn, the entire marine food web. Villagers voted in February 2011 to lend Can$2.5 million (US$2.5 million) to the Haida Salmon Restoration Corporation (HSRC) to fertilize the ocean, says John Disney, head of the Old Massett-based corporation and economic-development officer for the village. George, who previously headed Planktos, a firm based in San Francisco, California, that had sought to commercialize ocean fertilization using iron, signed on as chief scientist after the HSRC approached him, says Disney. The company planned to repay the village for its loan by selling carbon credits to companies seeking to offset their greenhouse-gas emissions, he adds.

HSRC

Workers on a Haida Salmon Restoration Corporation boat release iron sulphate into the Pacific Ocean.

"We created life where there wasn't life," says Disney, adding that the fertilization fed a phytoplankton bloom of some 10,000 square kilometres, which attracted fish, birds and whales (see 'Sowing controversy'). "The only difference between what we've done and what everybody else has done is that we've taken it up a notch."

In fact, the Old Massett scheme dumped five times more iron than previous fertilization experiments. And no scientists outside the project have seen data that might show whether it worked as advertised. "I'm not going to condemn it offhand, but this is just not the way to do this experiment," says Victor Smetacek, a marine biologist with the Alfred Wegener Institute for Polar and Marine Research in Bremerhaven, Germany. "It's quite sophisticated science, and it would have been good if scientists had carried it out."

The project was also on uncertain legal grounds. Ocean fertilization is restricted by a voluntary international moratorium on geoengineering, as well as a treaty on ocean pollution. Both agreements include exemptions for research, and the treaty calls on national environment agencies to regulate experiments. Officials from Environment Canada say that the agency warned project leaders in May that ocean fertilization would require a permit.

"Environment Canada did not approve this non-scientific event," environment minister Peter Kent told Parliament on 18 October. "Enforcement officers are now investigating." The Canadian National Research Council gave nearly Can$70,000 in funding to the HSRC, and the US National Oceanic and Atmospheric Administration provided 20 buoys to help to monitor water conditions. But officials at those agencies say they were never informed of the ocean-fertilization project, and they thought that the work involved salmon ecology.

Jason Blackstock, a geoengineering expert at the University of Oxford, UK, says that the situation highlights the grey area between geoengineering to alter global climate, and local actions with other goals such as boosting salmon stocks or seeding clouds for weather modification. "This has the potential to become a ubiquitous

SOWING CONTROVERSY

A company backed by a Canadian indigenous group has attempted to fertilize a region of the Pacific Ocean important for salmon stocks.

problem," says Blackstock.

The ETC Group, an advocacy organization based in Ottawa that has led a global drive against geoengineering, has suggested that George misrepresented the project's potential to generate carbon credits. Documents from the Old Massett website imply that in raising funds, project leaders stressed the potential for easy carbon credits. One document, tied to a 2011 loan application, showed that bank managers were wary of the HSRC's claims that the market for such carbon offsets was proven and that "retail outlets and banks in Germany are begging for the product".

In fact, carbon credits from iron-fertilization projects cannot be offered on formal markets such as the European emissions trading system, although willing buyers might be found outside those markets. And whether iron fertilization actually sequesters carbon is uncertain. A study[1] by Smetacek published in July — based on analysis of an experiment in 2004 — found that at least half of the carbon taken up by the iron-fertilized plankton was buried after they sank to the bottom of the sea. But other studies[2] have found that carbon in the blooms remains in the active biological cycle and is not sequestered at all.

George says that the bankers were ultimately satisfied, and that carbon credits are no more than a possible source of future funding, if the science supports them. But in an initial interview, Disney repeatedly said that the company needs to sell the carbon credits quickly to repay its loan from the community. "Being the guy who sold this to the community, I bloody well better come up with the money," he said. Disney later backed off his emphasis on carbon credits and stressed that he stands by George.

It is unclear whether the project will restore the salmon. A bumper run of sockeye salmon (*Oncorhynchus nerka*) in 2010 came two years after a volcanic eruption in Alaska sent a layer of iron-rich ash over the ocean, fertilizing a plankton bloom[3]. But many scientists remain sceptical.

Whether the Haida experiment worked won't be known for two years, when the youngest of the salmon feeding in the ocean today return home to spawn. John Nightingale, president of the Vancouver Aquarium in Canada, says that will be a chance to glean some science from the project. The work may have lacked scientific rigour, he says, but the HSRC has now agreed to make all of its data available to scientists. It has "done something unique", Nightingale says. "I want the maximum information, the maximum analysis, the maximum debate." ■

1. Smetacek, V. *et al. Nature* **487,** 313–319 (2012).
2. Boyd, P. W. *et al. Nature* **407,** 695–702 (2000).
3. Jones, N. *Nature* http://dx.doi.org/10.1038/news.2010.572 (2010).

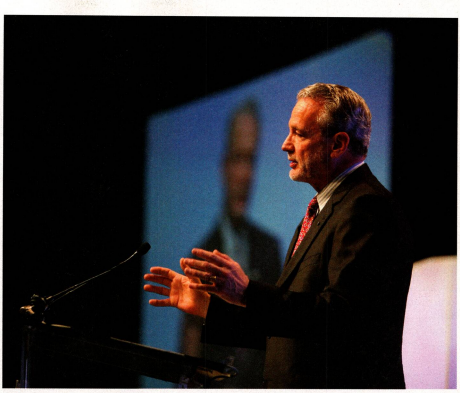

IHK-STRATEGIES

William Gimson of the Cancer Prevention and Research Institute of Texas is on the hunt for a chief scientist.

PEER REVIEW

Texas cancer fund seeks fresh start

Critics question whether institute has resolved conflicts between commercial and scientific goals.

BY MONYA BAKER

It must be hard filling a position when the last person in the job was a Nobel laureate who quit in protest over a disregard for peer review, and whose departure triggered an avalanche of other resignations. Nevertheless, the Cancer Prevention and Research Institute of Texas (CPRIT) is confident that it will announce a chief scientific officer to replace Alfred Gilman, who departed on 12 October, by the end of the year. But institute watchers suspect that even an ideal candidate might not be able to dispel the science community's unease about the CPRIT's attempt to simultaneously support basic research and nurture companies.

"I can't think of a better example than this one of how a potential conflict of interest can undermine an institution," says Paul Root Wolpe, a bioethicist at Emory University in Atlanta, Georgia.

The Austin-based CPRIT was created in 2007 when Texas voters agreed to a US$3-billion initiative that would spend $300 million a year to advance basic research, reduce cancer rates and nurture Texas companies. Since then, the state agency has awarded 427 grants totalling more than $750 million, with $574 million designated for scientific research and the rest for commercialization and prevention. Its funding of innovative research has won accolades.

Controversy erupted in May after Gilman, who won the 1994 medicine Nobel, tendered his resignation in a strongly worded letter criticizing a $20-million commercial 'incubator' grant that had been awarded without scientific review. Much of the grant was slated for a group led by Lynda Chin at the University of Texas MD Anderson Cancer Center in Houston, where Chin's husband, Ronald DePinho, is president. CPRIT internal correspondence that was subsequently made public through freedom-of-information rules ▶

➲ NATURE.COM
Read an interview with a former CPRIT scientific reviewer:
go.nature.com/rxa4y1

▶ suggests that the grant criteria were tailored to improve Chin's eligibility (see *Nature* **486**, 169–170; 2012). At the same time as the incubator grant was awarded, a set of grants recommended for approval by the CPRIT's scientific council stalled.

Gilman said that he would remain with the CPRIT until the autumn. Over the summer, the contentious $20-million grant was withdrawn for 're-review', and provisions were made for scientific review of all commercial grants. The previously sidelined grants were approved (as were all grants recommended by reviewers), and a compliance officer was hired to prevent submission irregularities.

But the measures to uphold peer review have not won over the CPRIT's critics, and many scientific reviewers, including at least seven of the eight heads of the institute's external scientific review panels, decided to depart along with Gilman. Their resignation letters accused the CPRIT of "hucksterism" and of having "dishonored" the system of peer review. They also complained of unusual circumstances faced by reviewers evaluating commercial proposals, saying that CPRIT staff sent them additional information and invited them to revise unfavourable scores. The resignation letters said that concerns they expressed were ignored, and Gilman himself suggests that CPRIT officials have been biding their time, "waiting for me to get out of the way".

An e-mail from Jimmy Mansour, a Texas businessman who heads the CPRIT's governing board, to his fellow committee members said that he looked forward to the appointment of MD Anderson's provost, Raymond DuBois, in Gilman's place. "Gilman is gone and so is his influence," Mansour wrote last week in an e-mail made public by the *Houston Chronicle* on 18 October. Mansour later told *Nature* that Gilman's peer-review system was a "cornerstone" of funding decisions. DuBois, for his part, says that he has not accepted a position at the CPRIT and is instead taking up a role at Arizona State University in Tucson.

"I can't think of a better example than this one of how a potential conflict of interest can undermine an institution."

William Gimson, the CPRIT's executive director, agrees that there were "process problems" with the grants, but denies more serious underlying issues. The concerns "mostly boil down to the natural conflict that exists between our scientific and commercialization portfolios", he says.

Such conflicts can undermine an institution, says Hamilton Moses at Alerion Advisors, a consulting firm for research institutes in North Garden, Virginia. "There are very few examples I can think of where adequate review has occurred when there has been an economic-development agenda."

Wolpe says that the CPRIT needs to take explicit action to restore trust between its overseers and its scientific reviewers. "The quickest way they can come back is through the resignation of the director," he says, a move that would signal a commitment to change. "Barring that, they need to put in a fully independent external review of their processes and procedures. And they need to announce very clear remedial measures." Gimson says that he has no plans to resign and that concerns about scientific integrity are unfounded.

Garnet Coleman, a member of the Texas House of Representatives, believes that the CPRIT's problems originated with the legislation that created the institute, which he says lacks appropriate internal safeguards and oversight by the legislature. "It was like somebody didn't know how to write the creation of a state agency, but they did anyway," he says. "We need to take the rules, fix them and put them in statute." He hopes to introduce a new measure next year.

Gilman, now retired, says that if the CPRIT cannot fund the best science, "I would personally rather see the money not spent and go back to the taxpayers". ■ SEE EDITORIAL P.446

SCIENCE FROM CHICAGO

Underwater Eden
Saving the Last Coral Wilderness on Earth
Edited by GREGORY S. STONE and DAVID OBURA
Cloth $40.00

The Last Walk
Reflections on Our Pets at the End of Their Lives
JESSICA PIERCE
Cloth $26.00

A World in One Cubic Foot
Portraits of Biodiversity
DAVID LIITTSCHWAGER
With a Foreword by E. O. Wilson
Cloth $45.00

The Pseudoscience Wars
Immanuel Velikovsky and the Birth of the Modern Fringe
MICHAEL D. GORDIN
Cloth $29.00

Wild Hope
On the Front Lines of Conservation Success
ANDREW BALMFORD
Cloth $26.00

Nature All Around Us
A Guide to Urban Ecology
Edited by BEATRIX BEISNER, CHRISTIAN MESSIER, and LUC-ALAIN GIRALDEAU
Paper $18.00

The Evolution of Primate Societies
Edited by JOHN C. MITANI, JOSEP CALL, PETER M. KAPPELER, RYNE A. PALOMBIT, and JOAN B. SILK
Paper $50.00

The University of Chicago Press
www.press.uchicago.edu

eppendorf

EPPENDORF AWARD FOR YOUNG EUROPEAN INVESTIGATORS

Winner 2012
Elizabeth Murchison,
United Kingdom

APPLICATION DEADLINE
15 JANUARY 2013

Call for Entries!

Eppendorf Award 2013 for Young European Investigators
Since 1995 the Eppendorf Young Investigator Award is granted annually to European researchers not older than 35 years. It acknowledges outstanding contributions to biomedical research in Europe based on methods of molecular biology, including novel analytical concepts. The winner is selected by an independent expert committee chaired by Reinhard Jahn (Max Planck Institute for Biophysical Chemistry, Göttingen, Germany).

Selection criteria
1. Ability to work independently
2. Creativity
3. Successful practical application of research approach
4. Significance of research results for the field of medicine
5. Achievement of candidate in relation to his/her age

You could be next to receive
> a prize money of 15,000 Euro
> an invitation to the prize ceremony at the EMBL Advanced Training Centre in Heidelberg on 6 June 2013
> an invitation to visit Eppendorf AG in Hamburg
> coverage of your work by Nature in print and in a podcast

Apply online at www.eppendorf.com/award/application

The Eppendorf Award is presented in partnership with
nature

Eppendorf® is a registered trademark of Eppendorf AG. All rights reserved, incl. graphics and images. Copyright ©2012 by Eppendorf AG.

THE LEARNING CURVE

Researchers say that some chemicals have unexpected and potent effects at very low doses — but regulators aren't convinced.

BY DAN FAGIN

Near the end of an adventurous life spent wandering the fortress towns of central Europe, clashing with bloodletters and other tradition-bound healers of the day, the irascible sixteenth-century physician Paracelsus wrote a defence of his unorthodox use of mercury, opium and other potentially dangerous medicines. "All things are poison, and nothing is without poison: the dose alone makes a thing not poison," he wrote. Centuries later, after many of his once-radical ideas found wide acceptance, Paracelsus's pronouncement would be distilled into a pithy phrase that became foundational dogma for the modern science of toxicology: "the dose makes the poison."

The contemporary interpretation of Paracelsus's famous declaration, for which he is often called the father of toxicology, is that dose and effect move together in a predictably linear fashion, and that lower exposures to a hazardous compound will therefore always generate lower risks. This idea is not just a philosophical abstraction; it is the core assumption underlying the system of chemical-safety testing that arose in the mid-twentieth century. Risk assessors typically look for adverse effects of a compound over a range of high doses and, from there, extrapolate downwards to establish health standards — always assuming, like Paracelsus, that chemicals toxic at high doses are much less risky at lower, real-world levels.

But what if the Paracelsian presumption is wrong? What if, for a large and potent class of compounds, lower doses pose higher risks? A growing number of academic researchers are making just such a claim for endocrine disrupters, a large group of synthetic chemicals able to interact with cellular hormone receptors. These compounds, which range from the common weed killer atrazine and the plasticizer bisphenol A (BPA) to the antibacterial agent triclosan (used in cleansers) and the vineyard fungicide vinclozolin, don't play by the usual rules of toxicology. On the basis of conventional high-dose testing, regulators have set maximum acceptable levels for each of them that assume all doses below that level are safe. But academic researchers who have studied a wider range of doses, including very low ones found in the everyday environment, say that their experiments usually do not generate the tidy, familiar 'ski-slope' dose-response graphs of classic toxicology. Instead, most endocrine disrupters have 'non-monotonic' dose-response curves, meaning that their slopes change at least once from negative to positive, or vice versa, forming 'U' shapes, inverted 'U's or even stranger shapes that resemble undulating Chinese dragons (see 'Curious curves').

"We're seeing that for every one of these compounds we test, there will be a non-monotonic response — every one!" says Frederick vom Saal, a neurobiologist at the University of Missouri-Columbia, who has been sounding the alarm about endocrine disrupters since the 1970s. "Low doses of endocrine disrupters act in ways that are totally unpredicted by the traditional approaches of toxicology." Vom Saal and his colleagues believe that very low doses of these compounds in the environment are contributing to a wide range of human health problems — including obesity, diabetes, cancer, cardiovascular disease, and infertility and other disorders related to sexual development.

Many toxicologists, however, are not convinced — especially those in industry or government who have spent their careers deeply involved in traditional risk assessment. Although they acknowledge that endocrine disrupters have unusual toxicological quirks, they say that the work of vom Saal and like-minded researchers is still insufficiently replicated, too reliant on unvalidated assays and too focused on end points such as organ weight, precancerous growths and changes in the activity of genes and proteins, which may not pose significant health threats. "If we're going to take this seriously, we need to have some evidence of a real phenomenon that happens not just in the hands of one researcher and one test, something repeatable that can stand up to scientific scrutiny about how it could lead to real health effects we want to avoid," says Lorenz Rhomberg, a toxicologist at the environmental-consulting firm Gradient in Cambridge, Massachusetts. Rhomberg also serves as a consultant on endocrine disrupters to the American Chemistry Council, an association of chemical manufacturers.

"IF WE'RE GOING TO TAKE THIS SERIOUSLY, WE NEED TO HAVE SOME EVIDENCE OF A REAL PHENOMENON."

Vom Saal and his colleagues counter that this is precisely the type of systematic evidence they can now provide, thanks to a boom in endocrine-disrupter research. The most comprehensive review yet of the field[1], published in March, included more than 600 studies — almost half of them published within the past five years — and found credible evidence of non-monotonic responses with low-dose health effects in 18 endocrine disrupters, including BPA, atrazine and vinclozolin. "We kept hearing from our critics that there aren't enough examples to prove this phenomenon is real, so we took that as a challenge," says Laura Vandenberg, a postdoctoral fellow at Tufts University in Medford, Massachusetts, and the lead author of the review.

Government officials in Europe and the United States are paying attention. "I find the Vandenberg review to be quite compelling and quite convincing," says Linda Birnbaum, director of the US National Institute of Environmental Health Sciences (NIEHS) in Research Triangle Park, North Carolina. In an April editorial in the NIEHS-published journal *Environmental Health Perspectives*, Birnbaum argued that "it is time to start the conversation" about incorporating low doses and non-monotonic relationships into regulatory decisions[2]. At a European Commission scientific conference on endocrine disrupters this June in Brussels, delegates failed to reach a consensus on the importance of non-monotonicity at low doses but they did agree that existing regulations need to be stricter, according to Björn Hansen, who heads the chemicals unit at the commission's Directorate-General for Environment in Brussels. In the United States, meanwhile, the Environmental Protection Agency (EPA) and the Food and Drug Administration (FDA) are showing a new willingness to at least discuss the issue — although they say that major regulatory revisions are not on the table for now.

Big changes are unlikely, some observers suggest, as long as the field remains so polarized. "There is a very large divide out there between the risk assessors and the endocrine scientists," says Thomas Neltner, who studies chemical food additives at the non-profit Pew Health Group in Washington DC, which has been trying to arrange a rapprochement through a series of scientific meetings. "Our feeling is that the two sides have been talking past each other."

EARLY SIGNS

For as long as there has been controversy over the effects of endocrine disrupters, vom Saal has been at the centre of it. Lean and intense, the 67-year-old native New Yorker is an amateur pilot who flies his Cessna to scientific conferences and is not shy about tangling with his critics wherever he lands. As a postdoctoral fellow at the University of Texas at Austin in the 1970s, vom Saal was startled to discover that subtle variations in sex-hormone levels in the womb could have life-long effects on mice. A female mouse positioned between two males in the uterus would later, as an adult, display significantly more 'masculine' characteristics, such as aggression, than would a female surrounded prenatally by other females, vom Saal found[3]. The apparent cause: a minuscule amount of extra testosterone released by the neighbouring male fetuses.

Experimenting first with natural hormones and the synthetic oestrogen diethylstilbestrol (DES), vom Saal found that male mice exposed prenatally to very low levels of DES developed heavier prostates than unexposed mice — making them more vulnerable later in life to prostate disease, including cancer. Strangely, however, he found that higher doses of DES did not trigger the same effect[4]. It was one of the first non-monotonic dose-response curves mapped for an endocrine disrupter. Since then, vom Saal and his Missouri colleague Wade Welshons have identified similar non-monotonic responses from a variety of endocrine disrupters, most notably BPA[5], a ubiquitous ingredient of polycarbonate plastics and epoxy coatings, including in food packaging.

Vom Saal's early work helped to generate a torrent of international interest in BPA, including an ultimately successful campaign by activists in the United States, Canada and some European countries to halt its use in baby bottles and toddlers' sippy cups. It also helped to inspire a legion of researchers to look for — and often find — other endocrine-related effects in animals exposed to very low levels of BPA and other hormone mimics. At Tufts, for example, cell biologist Ana Soto won notoriety for discovering that early exposure to BPA can alter the development of mammary glands in mice and rats, spurring the growth of oestrogen receptors and leading to precancerous growths and non-invasive cancers[6]. In Spain, another cell biologist, Angel Nadal of Miguel Hernández University in Elche, exposed human

pancreatic cells to BPA and mapped non-monotonic relationships between dose levels and altered glucose metabolism, a key risk factor for diabetes and obesity[7]. Epidemiologists jumped into the fray, too. They found associations between urine BPA levels and obesity in children[8], and linked other endocrine disrupters to incidence of diabetes[9].

Their studies, and many others, depict a weird world of endocrine disruption that is as different from traditional toxicology as quantum mechanics is from the staid clockwork of Newtonian physics. When even minuscule quantities of BPA and other disrupters interact with hormone receptors at crucial moments in development — activating, jamming, hijacking or otherwise messing with their normal function — they can give rise to strange-looking experimental results, especially when other hormones are thrown into the mix.

At the University of Illinois at Chicago, for example, reproductive physiologist Gail Prins implants prostate-like glands, grown from human stem cells and mixed with mouse tissue, into young mice, and then feeds some of them very low doses of BPA. As the mice age, Prins also gives them low doses of oestradiol, a naturally occurring hormone that becomes more potent in human males as they age and is a known risk factor for prostate cancer. Between 35% and 40% of the mice fed BPA plus oestradiol have developed prostate cancer, compared with 10% of the mice that were given oestradiol only. Her working theory is that BPA binds with oestrogen receptors in prostate stem cells, reprogramming genes in ways that leave the cells more sensitive to oestradiol later on. "What's remarkable," she says, "is that we're working with very low doses that are definitely within the range of normal human exposure." She plans to publish her results in early 2013, as soon as she has collected more data.

The interplay of these types of receptor mechanisms can generate bizarre dose-response relationships, many of which are still being mapped out. Earlier this month, vom Saal's group at Missouri published the first full non-monotonic dose-response curve for the widely used plastics ingredient known as DEHP, or di(2-ethylhexyl) phthalate[10]. The Missouri team subjected 78 pregnant mice to an extremely wide range of DEHP doses — from 0.5 micrograms per kilogram of body weight per day all the way up to 500,000 micrograms. They found that the animals' testosterone levels rose or fell in surprising ways, altering sexual development depending on the dose received. For male offspring, for example, the dose-response curve looked something like the profile of a craggy mountain. Serum levels of testosterone rose between the 0 and 0.5 microgram dose levels, then fell slightly at 1, rose again through 5 and 500 before declining again at 50,000 and plunging at the 500,000-microgram dose level. The highest dose, in fact, was virtually identical to the results for unexposed controls. Seeking to deflect another potential line of attack from his critics, vom Saal conducted a 'goodness of fit' statistical analysis confirming that a non-monotonic curve best fits his data.

> "LOW DOSES OF ENDOCRINE DISRUPTERS ACT IN WAYS THAT ARE TOTALLY UNPREDICTED BY THE TRADITIONAL APPROACHES OF TOXICOLOGY."

The biochemical mechanism behind the strange DEHP curve is unknown — vom Saal says that it awaits further study — but researchers have worked out the specific causes of other non-monotonic curves. One of the best understood examples involves not a pollutant, but a drug: the chemotherapy agent tamoxifen, which binds to oestrogen receptors in breast cells and has a dose-response curve shaped like an upside-down U. Very low doses have little effect on cancer cells, but as the drug builds up in breast tissue it actually stimulates tumour growth, triggering a painful 'flare' period for patients. When tamoxifen levels grow high enough to occupy most of the available oestrogen receptors, the effect reverses and the drug begins to inhibit the cancer cells' growth. "All of this is very well known to endocrinologists," says Thomas Zoeller of the University of Massachusetts Amherst, who studies the effects of endocrine disrupters on the thyroid. "Non-monotonic dose-response is a fact of life."

A turning point was a 2009 scientific statement by the Endocrine Society in Chevy Chase, Maryland, the first in its 95-year history. It called endocrine disrupters a "significant concern to public health"; endorsed stricter regulations; acknowledged non-monotonic responses; and declared that "even infinitesimally low levels of exposure — indeed, any level of exposure at all — may cause endocrine or reproductive abnormalities"[11]. Seven other scientific bodies then joined the Endocrine Society in a letter of concern published last year in *Science*[12]. "That's as mainstream as you can get. It really changed the nature of the game," says another long-time researcher in the field, molecular biologist Bruce Blumberg of the University of California, Irvine.

PUT TO THE TEST

Critics, however, say that the mere existence of non-monotonic responses and low-dose effects is not the point. What matters is the extent of the health concerns they raise. "There is non-monotonicity, but the question is, is it toxicologically relevant?" asks Jason Aungst, a supervisory toxicologist with the FDA's Center for Food Safety and Applied Nutrition in Silver Spring, Maryland. He and a senior toxicologist at the EPA, Earl Gray, argue that the low-dose health effects identified in studies by vom Saal, Soto and others are still relatively rare and have not been conclusively linked to major health problems. Low-dose effects that are more clearly harmful, such as organ deformities, are usually monotonic, and can be identified under current regulatory testing protocols, according to Gray. "You could never say that non-monotonicity doesn't happen, but as far as its relevance to risk assessment, we really haven't seen it in the high-quality studies," he says.

The schism in the field is in part a result of the different types of tests that academic researchers and risk assessors carry out. Many of the private testing labs hired by manufacturers seeking regulatory approval for new products are not equipped to do the radioimmunoassay analyses required to measure extremely low chemical concentrations. Nor do private labs typically look for the complex biochemical changes, such as alterations in protein levels, that are now part of the standard tool kit of researchers such as Zoeller, Soto and vom Saal. Instead, agency-mandated guideline tests are standardized; involve simpler assays that are easier to replicate; use higher numbers of test animals; and generally seek to identify more obvious health problems, such as acute toxicity, cancer and physical deformities. "We do validated studies, the basic researchers don't," says Rochelle Tyl, a developmental toxicologist at RTI International, a firm in Research Triangle Park that conducts research for clients such as regulatory agencies and chemical manufacturers. "That doesn't mean they're wrong, it just means they're doing work that hasn't been validated."

Yet even when government and industry-hired scientists look for low-dose effects, they often don't find them. For example, Tyl[13] (who conducted her studies for two industry groups) and Gray[14] have each tested BPA at very low doses without finding the potent developmental effects identified by vom Saal, Prins and others. Vom Saal and his allies counter that the Tyl and Gray studies were insensitive to low-dose effects because their positive-control animals, which were

CURIOUS CURVES

Researchers have found that many endocrine-disrupting chemicals do not generate the standard monotonic dose-response curves seen for other types of compound.

MONOTONIC CURVE

In some cases, dose and response increase together. The plant oestrogen genistein, for instance, causes the mouse uterus to increase in weight.

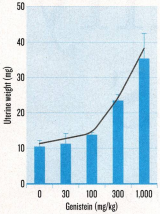

SOURCE: Ohto, R. *et al. J. Toxicol. Sci.* **37**, 879–889 (2012)

NON-MONOTONIC CURVES

Mice exposed to moderate doses of bisphenol A develop the largest tumours. Moderate and high doses are thought to induce tumour-cell proliferation, but high doses also trigger cell death.

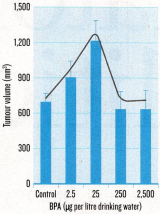

SOURCE: Jenkins, S. *et al. Environ. Health Perspect.* **119**, 1604–1609 (2011)

The oestrogen mimic *p*-nonylphenol stimulates the ERK cell-signalling pathway at low and high doses. Interactions with hormone receptors and other membrane proteins explain the complex shape of the curve.

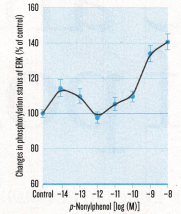

SOURCE: Bulayeva, N. N. & Watson, C. S. *Environ. Health Perspect.* **112**, 1481–1487 (2004)

Above a certain dose, the herbicide atrazine causes the larynx muscle to shrink in male frogs. But the effect does not increase at higher doses.

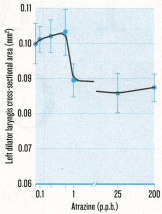

SOURCE: Hayes, T. A. *et al. Proc. Natl Acad. Sci. USA* **99**, 5476–5480 (2002).

given oestradiol alone, received doses that were much too high. The dispute has been harsh and public, playing out at conferences and in a seemingly endless series of sharply worded journal articles, rebuttals, counter-rebuttals and counter-counter-rebuttals. The arguments became so heated that Tyl stopped doing BPA work. "I gave up BPA when it ceased to be scientific and became personal," she says. "It became flag-waving and it became political."

Largely because of the Tyl and Gray studies, neither the FDA nor the EPA have altered their risk assessments for BPA. The FDA still says that BPA has no adverse effects at levels below 50 milligrams per kilogram of body weight per day — a level that vom Saal contends should actually be two million times lower, at 25 nanograms. Both agencies, however, are now cooperating on a much larger study designed to settle the dispute. The newly launched US$20-million study, led by the NIEHS and the FDA's National Center for Toxicological Research, is the most ambitious effort ever to look for non-monotonic dose-response curves that include very low doses. Last month, researchers began hand-feeding BPA to about a thousand rats at five dose levels ranging from 2.5 micrograms per kilogram of body weight up to 25,000 micrograms, plus two positive-control groups (which received much lower oestradiol doses than either Tyl or Gray used) and an unexposed control group. Vom Saal, Zoeller and other academics will be participating in the tissue analysis, allowing them to look for an array of health effects, such as metabolic changes in the prostate and mammary glands, that go well beyond those in standard regulatory protocols.

But with the results of the BPA mega-study not expected for at least five years, a major rewriting of chemical regulations to take non-monotonic low-dose effects into account still seems distant. The European Commission has to meet a self-imposed deadline of December 2013 to draft the first governmental criteria defining endocrine disruption, but without a scientific consensus on the issue the criteria may end up addressing only high-dose effects, predicts Andreas Kortenkamp, a toxicologist at Brunel University in Uxbridge, UK, who has been advising the European Commission. In the United States, meanwhile, the EPA and FDA have convened a joint working group to review the evidence accumulating in the peer-reviewed literature, but "not only is the jury still out, the jury hasn't even had a chance to look at the evidence yet", says Rita Schoeny, a senior science adviser at the EPA in Washington DC.

Some veterans of the field have decided not to wait, and are collaborating on what amounts to an effort to bypass the regulatory system. They have written a paper[15], scheduled to be published in January in the journal *Green Chemistry*, that gives industrial chemists detailed advice on how to screen newly synthesized compounds for endocrine-related effects, how to test at very low doses and how to look for non-monotonic dose-response curves. The paper, and a companion website, are aimed at trying to head off potentially harmful endocrine disrupters before they reach the marketplace.

An ancillary benefit, vom Saal hopes, will be to increase the pressure on regulatory agencies to curb exposures to compounds already on the market. "We're saying that if you care about developing a safe chemical, here's what you should do," says vom Saal. "Who could argue with that?" ■

Dan Fagin *is a science journalism professor at New York University and the author of* Toms River: A Story of Science and Salvation *(Bantam Books), to be published in March 2013.*

1. Vandenberg, L. N. *et al. Endocr. Rev.* **33,** 378–445 (2012).
2. Birnbaum, L. S. *Environ. Health Persp.* **120,** 143–144 (2012).
3. vom Saal, F. S. & Bronson, F. H. *Biol. Reprod.* **19,** 842–853 (1978).
4. vom Saal, F. S. *et al. Proc. Natl Acad. Sci. USA* **94,** 2056–2061 (1997).
5. Welshons, W. V., Nagel, S. C., Thayer, K. A., Judy, B. M. & vom Saal, F. S. *Toxicol. Indust. Health* **15,** 12–25 (1999).
6. Murray, T. J., Maffini, M. V., Ucci, A. A., Sonnenschein, C. & Soto, A. M. *Reprod. Toxicol.* **23,** 383B–3390 (2007).
7. Alonso-Magdalena, P., Morimoto, S., Ripoll, C., Fuentes, E. & Nadal, A. *Environ. Health Perspect.* **114,** 106–112 (2006).
8. Trasande, L., Attina, T. M. & Blustein, J. *J. Am. Med. Assoc.* **308,** 1113–1121 (2012).
9. Lee, D. H. *et al. Environ. Health Persp.* **118,** 1235–1242 (2010).
10. Do, R. P., Stahlhut, R. W., Ponzi, D., vom Saal, F. S. & Taylor, J. A. *Reprod. Toxicol.* http://dx.doi.org/10.1016/j.reprotox.2012.09.006 (2012).
11. Diamanti-Kandarakis, E. *et al. Endocr. Rev.* **30**, 293–342 (2009).
12. American Society of Human Genetics *et al. Science* **331,** 1136 (2011).
13. Tyl, R. W. *et al. Toxicol. Sci.* **104,** 362–384 (2008).
14. Ryan, B. C., Hotchkiss, A. K., Crofton, K. M. & Gray, L. E. *Jr Toxicol. Sci.* **114,** 133–148 (2010).
15. Schug, T. T., O'Brien, K. P & Myers, J. P. *Green Chem.* (in the press).

The anatomy of politics

From genes to hormone levels, biology may help to shape political behaviour.

BY LIZZIE BUCHEN

A popular political advertisement from early this summer begins with US President Barack Obama addressing a crowd of moon-eyed supporters. Suddenly, the screen goes dark to a crescendo of minor chords. Phrases such as "Fear and Loathing", "Nauseating" and "Divide and Conquer" flash onto the screen, along with video clips of commentators complaining that Obama has used scare tactics to manipulate voters. In the final scene, the iconic poster from Obama's 2008 election campaign appears, the word HOPE transforming into FEAR as it bursts into flames.

The advertisement, produced by the conservative organization American Crossroads in Washington DC, is typical of those that have come to dominate the US airwaves and YouTube in preparation for next month's presidential election. Emerging from both the right and the left, these commercials increasingly resemble horror films as they seek to sway voters by triggering basic emotions such as fear, anger and disgust.

That strategy fits with emerging scientific evidence about how people acquire their political beliefs. In the past, political scientists agreed that social forces — most importantly, parents and the childhood environment — strongly influenced whether people became conservative or liberal, and whether they voted or engaged in politics at all. "We now know that it is probably not the whole story," says John Jost, a psychologist at New York University.

An increasing number of studies suggest that biology can exert a significant influence on political beliefs and behaviours. Biological factors including genes, hormone levels and neurotransmitter systems may partly shape people's attitudes on political issues such as welfare, immigration, same-sex marriage and war. And shrewd politicians might be able to take advantage of those biological levers through clever advertisements aimed at voters' primal emotions.

Many of the studies linking biology to politics remain controversial and unreplicated. But the overall body of evidence is growing and might alter how people think about their own and others' political attitudes.

"People are proud of their political beliefs," says John Hibbing, a political scientist at the University of Nebraska–Lincoln. "We tend to think they're the result of some rational responses to the world around us." But in fact, a combination of genes and early experiences may predispose people to perceive and respond to political issues in certain ways. Recognizing that could help the public and politicians to develop more respect for those with opposing viewpoints.

"I'd like to see people have a little less chutzpah about their political beliefs, and understand that some people experience the world differently," says Hibbing.

INNATE IDEOLOGY

The past few decades have seen a wave of research connecting genes to disorders such as schizophrenia, depression and alcoholism, and to complex outcomes such as sexual orientation and how far people progress in education. But until the past decade, this trend largely passed by the field of political science. Modern politics seemed too divorced from basic human biology, too recent an innovation in human evolutionary history, to be influenced by genetic material.

In 1986, Nicholas Martin and his colleagues published a study[1] suggesting that genes could exert a pull on attitudes concerning topics such as abortion, immigration, the death penalty and pacifism. Martin, a geneticist now at the Queensland Institute of Medical Research in Brisbane, Australia, used a classic behavioural-genetics technique: comparing genetically identical twins with fraternal twins of the same sex (who share only 50% of genes on average). The identical twins had similar political beliefs more often than fraternal twins did. Because twins tend to grow up in the same family environments, Martin's team suggested that genes made the difference, and that they have a significant role in helping to shape attitudes on social issues.

Although Martin's study had obvious implications for political science, researchers in that field ignored the work. The eugenics movement in the early part of the twentieth century and Nazi theories about the biology of human differences had made political scientists extremely wary

➲ **NATURE.COM**
To listen to a podcast about biology and politics, visit:
go.nature.com/kfockd

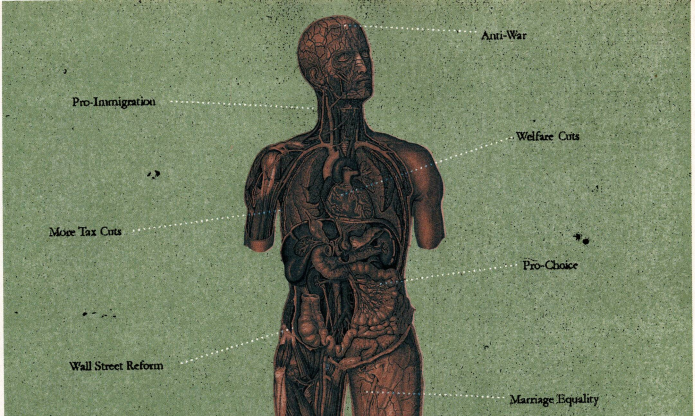

fig. 201

OLIVER MUNDAY

about topics that examined genetic differences among people.

The publication "was like a stone down a well", says Martin. "There was absolutely no reaction. It just lay there for 20 years."

But in the early 2000s, Hibbing and John Alford, a political scientist at Rice University in Houston, Texas, learned about Martin's work. They reanalysed his data and incorporated similar data from a study[2] of attitudes among US twins. In 2005, Hibbing and Alford published[3] findings nearly identical to those earlier studies — showing strong correlations between genetics and political views. These finally caught the attention of political scientists.

It wasn't the kind of attention that Alford and Hibbing were hoping for, however. "They thought we were crazy," says Hibbing.

But a few researchers, mainly in the United States, were intrigued enough to follow up with further work. James Fowler, a political scientist at the University of California, San Diego, used the twin method to show[4] that voter turnout and political participation also had a genetic component. Peter Hatemi, a political scientist at Pennsylvania State University in University Park, found results similar to Alford and Hibbing's using twins from Australia, Denmark, Sweden and the United States, although the work has not yet been published.

TROUBLE WITH TWINS

The twin studies were far from definitive, in large part because such research cannot completely control for environmental factors. Compared with fraternal twins, genetically identical twins are more likely to have the same friends and to maintain regular contact as adults. Furthermore, parents, friends and teachers often treat identical twins more equally than fraternal twins. All of that makes it hard to unpack how much genes and environment each contribute to the shared political attitudes of identical twins.

> "I would like to see people have a little less chutzpah about their political beliefs."

A few attempts have been made to tease apart the various influences. In one study[5], Hatemi found that identical twins who do not spend much time together are still more concordant than are fraternal twins who do, suggesting that genetic factors do matter. But the twin studies continue to face strong opposition. "I'm very sceptical about estimating heritability from twin studies," says Laura Stoker, a political scientist at the University of California, Berkeley. "The entire framework is built with a tonne of assumptions."

Twin studies also offer no insight into how the genome can nudge people to lean left or right on various political issues. For that, researchers have started exploring candidate genes. Genes involved with the olfactory system and the neurotransmitters glutamate, dopamine and serotonin have all been linked to behaviours such as voter turnout[6] and ideology[7], although these findings have come under scrutiny and are yet to be independently replicated.

Jeremy Freese, a sociologist at Northwestern University in Evanston, Illinois, says that such studies have found "implausibly large" effects from individual genes. "What's been revealed over the past few years is just how vulnerable the candidate-gene approach is," he says.

Part of the problem, says Freese, is that studies linking specific genes to political behaviours have usually been published in political-science journals, rather than scientific journals, so editors and reviewers may not have picked up on some deficiencies in the studies. "The reviewers have not been familiar with the replication problems that exist," says Freese.

Christopher Dawes, a political scientist at New York University, acknowledges complications in some of his own studies of specific genes and says that more illuminating results might come from molecular techniques such as genome-wide association studies, which scan the genomes of large numbers of people, looking for sequences linked to a behaviour or trait. But researchers in this area are only just beginning

to use such resource-intensive strategies.

"We're starting to better appreciate the limitations of the data and techniques," says Dawes.

If other complex behaviours and traits are any indication, the answer is not going to be simple. Even for traits known to have a very large genetic component, such as height, the evidence points to the influence of thousands of genes, each applying a feather-light force. So it seems unlikely that a small number of genes can push someone towards being a liberal activist, a social conservative or a libertarian.

Many researchers have come to the conclusion that it is premature to focus on the genetics of politics. "It doesn't make sense to go after the most difficult part of the puzzle," says Alford.

An easier approach is to investigate the pathways that might connect genes with political behaviours and attitudes. One connection that has been suggested is personality. US conservatives may not seem to have much in common with Iraqi or Italian conservatives, but many political psychologists agree that political ideology can be narrowed down to one basic personality trait: openness to change. Liberals tend to be more accepting of social change than conservatives. Some studies[8] suggest that liberals tolerate more ambiguity and uncertainty, whereas conservatives are more decisive, conscientious and attracted to order.

Theoretically, a person who is open to change might be more likely to favour gay marriage, immigration and other policies that alter society and are traditionally linked to liberal politics in the United States; personalities leaning towards order and the status quo might support a strong military force to protect a country, policies that clamp down on immigration and bans on same-sex marriage. But some researchers baulk at such simple links between personality and ideology. Evan Charney, a political scientist at Duke University in Durham, North Carolina, points out that conservatives sometimes embrace change, such as proposals in the United States to alter the tax code and welfare system. He also says that he and most people in his field are liberals — an imbalance that could bias how they interpret connections between personality and politics.

> "If people spend most of their lives focusing on negative rather than positive, they're probably going to have a different way of experiencing the world."

VISCERAL REACTIONS

Some researchers have sought to move beyond personality studies to evaluate how participants' physiological reactions can influence how they interpret and respond to political issues. In 2008, Alford, Hibbing, Hatemi and others measured how people reacted to threatening images and sudden, loud noises[9]. People who blinked harder and showed heightened sensitivity — as gauged by their skin conductance — were more likely to favour gun rights, capital punishment and the war in Iraq than were those who showed less sensitivity.

In another study[10], Hibbing showed subjects a series of emotionally charged images, including a spider on a man's face, a maggot-infested wound, a cute rabbit and a happy child. People who described themselves as conservatives tended to respond more strongly when looking at the negative images than at the positive images, whereas liberals reacted more to the positive pictures. Conservatives also stared at the negative images longer than liberals did, which Hibbing connects to the idea that conservatives are more likely to confront fearful or disgusting situations, making them more disposed to support a strong military and harsh sanctions for criminals.

Some researchers are exploring whether hormone systems play a part in political attitudes. A few studies, for example, have looked at connections between people's prejudices and their levels of oxytocin — the feel-good hormone linked to empathy and bonding with loved ones. In one experiment[11], Dutch participants who had taken puffs of oxytocin responded more favourably to Dutch people than to foreigners, suggesting a bias towards their own group.

Hatemi and Rose McDermott, a political scientist at Brown University in Providence, Rhode Island, are currently investigating whether other hormones, such as testosterone and cortisol, have any connections with ideology. Many of the hormone studies done so far have come under attack, because they often rely on small samples and the reported effects are sometimes weak.

Given the research so far, Hibbing remains "agnostic" about whether genes or environmental factors such as parental guidance influence political behaviour the most. Either way, he says, it is difficult to change someone's mind about political issues because their reactions are rooted in their physiology.

"If people spend most of their lives focusing on negative rather than positive, they're probably going to have a different way of experiencing the world than those who do the opposite," says Hibbing. So people on the right are unlikely to be reached by arguments that seem rational to the left, or vice versa.

But tapping into emotions might prove more successful. After the terrorist attacks in the United States on 11 September 2001, New Yorkers who had been directly exposed to the trauma of the events experienced a 'conservative shift', expressing views that were more patriotic, more supportive of the military and more religious than they had before[12]. Disgust, too, can shift attitudes. One study[13] suggested that people exhibit more conservative views when reminded of impurity — for example, by the proximity of a bottle of hand sanitizer, a sign reminding them to clean their hands or a foul smell.

Does that mean that negative political adverts, designed to invoke fear and disgust, could actually change people's views? Alford says that these commercials are targeted more at mobilizing favourable voters — and demobilizing the opposition. "People who run political campaigns know that it's all about turnout," says Alford. "It's not about changing hearts and minds; it's about changing who shows up on election day."

Regardless of whether biology shapes political choice, it may affect a person's likelihood of voting in the first place. In an as-yet unpublished study, Hibbing has found that people with high levels of the stress hormone cortisol are much less likely to vote than are demographically similar people who have lower cortisol levels. Hibbing is currently working to find a way to ease voting for these 'stressed' people, perhaps through options such as postal voting.

Alford says that the biggest impact of all this research may be to make political discourse more civil and accepting of differences. "It would be nice if political science made dinner tables a little more humane," he says. ■

Lizzie Buchen *is a freelance writer living in San Francisco, California.*

1. Martin, N. G. *et al. Proc. Natl Acad. Sci. USA* **83,** 4364–4368 (1986).
2. Lake, R. I., Eaves, L. J., Maes, H. H., Heath, A. C. & Martin, N. G. *Behav. Genet.* **30,** 223–233 (2000).
3. Alford, J. R., Funk, C. L. & Hibbing, J. R. *Am. Polit. Sci. Rev.* **99,** 153–167 (2005).
4. Fowler, J. H., Baker, L. A. & Dawes, C. T. *Am. Polit. Sci. Rev.* **102,** 233–248 (2008).
5. Smith, K. *et al. Am. J. Polit. Sci.* **56,** 17–33 (2012).
6. Fowler, J. H. & Dawes, C. T. *J. Polit.* **70,** 579–594 (2008).
7. Settle, J. E., Dawes, C. T., Christakis, N. A. & Fowler, J. H. *J. Polit.* **72,** 1189–1198 (2010).
8. Carney, D. R., Jost, J. T., Gosling, S. D. & Potter, J. *Polit. Psychol.* **29,** 807–840 (2008).
9. Oxley, D. R. *et al. Science* **321,** 1667–1670 (2008).
10. Dodd, M. D. *et al. Phil. Trans. R. Soc. B* **367,** 640–649 (2012).
11. De Dreu, C. K. W., Greer, L. L., Van Kleef, G. A., Shalvi, S. & Handgraaf, M. J. J. *Proc. Natl Acad. Sci. USA* **108,** 1262–1266 (2011).
12. Bonanno, G. A. & Jost, J. T. *Basic Appl. Soc. Psychol.* **28,** 311–323 (2006).
13. Helzer, E. G. & Pizarro, D. A. *Psychol. Sci.* **22,** 517–522 (2011).

COMMENT

PHYSICS In praise of symmetry, our guide through nature's labyrinth **p.472**

AUTUMN BOOKS Reviews special, from exoplanets to hallucinations **p.474**

AUTUMN BOOKS Pinker, Dawkins, Krauss and more in paperback highlights **p.476**

OBITUARY Louise Johnson, structural-biology pioneer, remembered **p.488**

M. OSTERGAARD/PANOS

A girl drinks water drawn from a river in Ethiopia, where some 49 million people lack access to safe water.

Wall Street's thirst for water

Moves towards a global water commodities market must be stopped. It will push the price of food far beyond the peaks of the past five years, warns **Frederick Kaufman**.

Early last year, I published an article in *Foreign Policy* that explained how Wall Street profits from hunger. I traced the history of financial markets in food and noted how the prices of maize (corn), soya, rice and wheat had broken records three times in the past five years[1]. I examined the impacts of climate change and biofuel mandates on the grain futures markets, and argued that a global food-pricing system that once benefited farmers, bakers and consumers had been undermined by financial derivatives created by investment banks.

These commodity index funds effectively destroyed the traditional 'price discovery' function of the grain futures exchanges in Chicago, Kansas City and Minneapolis, and turned these markets into profit engines for banks and hedge funds while driving up the price of our daily bread[2].

Although regulation of global food derivatives has been promised, years have passed and nothing has materialized. In Washington DC, abuses of commodity markets and other fiddles resulted in 30,000 pages of new regulations: the Dodd–Frank Wall Street Reform and Consumer Protection Act of 2010. Predictably, implementation of these laws has been challenged in court and stalled. Even if the regulations make it beyond the Beltway, there will be plenty of room for exceptions for the biggest banks.

Therefore, it is wise to consider what global resource will be the next financial derivative. What could be more catastrophic than betting on the world's food supply? What about our water?

Speculators can already bet on snow, wind and rain through weather-related futures contracts bought and sold on the Chicago Mercantile Exchange. The market value of weather grew by 20% from 2010 to 2011. ▶

But the sector remains small — a paltry US$11.8 billion. Still, weather futures indicate how restless Wall Street has become to transform Mother Nature into the mother of all casinos.

Some environmentalists argue that putting a price on fresh water may be our best bet to save the planet's supply. The more it costs, the less we will waste. In fact, the financialization of precious resources underlies the Economics of Ecosystems and Biodiversity (TEEB), an international initiative hosted by the United Nations Environment Programme and supported by the European Commission, Germany, the United Kingdom, the Netherlands, Norway, Sweden and Japan. TEEB aims to calculate the worth of ecosystems down to the last trillion dollars, riyals or renminbi. And then there is the PES movement — payment for ecosystem (or environmental) services, which refers to such things as the air we breathe and the water we drink. Among the many supporters of this concept are the World Bank and the UN Food and Agriculture Organization. As TEEB's 2010 report for business puts it: "Modern society's predominant focus on market-delivered components of well-being, and our almost total dependence on market prices to indicate value, means that we generally do not measure or manage economic values exchanged other than through markets."

Wall Street's success in cashing in on the food bubble, Washington's inability to regulate global derivatives and the push to commodify nature through TEEB and PES converged into a single focus this summer, when drought descended on the United States. With it came a slew of doom-laden social, environmental and economic predictions: there will be 3 billion "water-stressed" people on Earth by 2035; water shortages will become chronic, wildfires will be pervasive, monsoons will be even more unpredictable; and snow run-offs will radically decrease owing to increasingly sultry winters.

At the same time, water is becoming essential to a widening variety of industries, from hydroelectric power and fracking to beer brewing and semiconductor manufacturing. Hydrologists warn that water tables are dropping across Asia. Political scientists predict squabbles over the ownership and use of Himalayan rivers, and every water-well driller in Nebraska knows that the Ogallala aquifer under parts of the midwestern United States is declining at an alarming rate.

The implications are dire: the destruction of aquatic ecosystems, the extinction of innumerable species and the risk of regional and international conflicts — the much-dreaded 'water wars' of the twenty-first century. What will Egypt do when Ethiopia dams the Blue Nile? What will happen when Yemen becomes the first country to run out of water? The short answer: nothing good.

CASHING IN

Investors of all stripes adore the apocalyptic vibe. Within the interstices of violence and chaos there will be money to be made. These days, the biggest profits do not come from buying or selling actual things (such as houses or wheat or cars), but from the manipulation of ethereal concepts like risk and collateralized debt. Wealth flows from financial instruments that are one step away from reality.

Investing in a water index is now more popular than ever. There are more than 100 indices[2] that track and measure the value of stocks of companies in water-related businesses, such as utilities, sewage treatment and desalination. Several offer healthy returns (see go.nature.com/zrl4qo).

As a result, the World Bank and the International Monetary Fund — both always on the lookout for market-based security for the billions of dollars of credit they extend — have been pushing countries to privatize their resources. These include the lakes, streams and reservoirs of Argentina, Bolivia, Ghana, Mexico, Malaysia, Nigeria and the Philippines (see, for example, go.nature.com/iuwp8m). What better guarantee of prosperity than a rush of multinationals determined to generate revenues from something no one can manage without?

So this summer, as cornfields from Ukraine to Kansas withered, as bacon shortages made headlines and dairymen fed candy to their cows, a new message congealed: the world's next great commodity will not be gold or grain or oil. It will be water. Useable water. Although collecting stakes in indices of publicly traded companies is nice, and water certainly generates predictable profits, wouldn't it be more efficient if it could be translated into a cash equivalent? Perhaps, plotted the hedgers and speculators, there should be a commodity market in water, as there is for gold and grain — a futures exchange in which assurances to deliver or accept water on some specified future date can be traded like cash.

"Within the interstices of violence and chaos there will be money to be made."

In certain respects, water is a likely candidate for a futures contract on a commodity exchange. First, it meets the requirement of fungibility — the commodity pumped from one lake or river or stream is pretty much the same as that collected from an iceberg, extracted from an aquifer, or collected in a rain barrel. And water will soon meet the second requirement of commoditization: it is becoming increasingly liquid, as in convertible to cash. Most obviously, water is global. River-basin management is as hot a topic for the Volta as it is for the Senegal[4]. From a money perspective, there is no difference if the river is Spain's Guadalquivir, the French Rhone, the Niger or the Sacramento in California.

Financial forecasters perceive that much like traditionally traded commodities — precious metals, for example — the useable water of the future will be so scarce as to need to be mined, processed, packaged and, most importantly, moved around the world. And they know that the demand will not go away. That is the thrust of the thinking behind a global water futures market.

HIGH STAKES

The year 1996 marked a Rubicon in the history of water and money. The water from California's Westlands irrigates an estimated $1-billion-worth of food a year; at 2,000 square kilometres, it is the largest agricultural water district in the United States. In 1996, the district introduced an electronic bulletin board for farmers to buy and sell their rights to Westlands' water from their home computers. Trading water rights from a laptop is now a given, just as commodities that once could be bought and sold only on the trading floors of Chicago or Kansas City are now routinely trafficked by mathematics PhDs at hedge funds in Connecticut. If and when water becomes an exchange-traded derivative, it will join Brent crude, jet fuel, and soya bean oil — and be traded any time, anywhere, by anyone.

Making money come out of the tap means that fresh water must be given a price anywhere it is traded — a global price that can be arbitraged across the continents. Those in Mumbai or midtown Manhattan who understand the increasing value of water in the world economy will speculate on this undervalued 'asset', and their investments will drive up the cost everywhere[5]. A water calamity in China or India — and the food inflation, political instability and humanitarian crisis that will surely follow — will reverberate in price spikes from London to Sydney. This is how bankers will profit.

Economists have begun to model a global water-based futures market featuring financial puts, calls, shorts, longs, exchange-traded funds, indices of indices, options piled on top of options, and all sorts of opportunity for over-the-counter swaps. Flood-insurance companies will certainly want to buy stakes that could mitigate their financial risk. In fact, every corporation that conducts its business in a flood plain, anywhere, would probably participate. Farmers will want to hedge their bets that it will or will not rain, as will frackers and fishermen. As for the speculators, we know who they will be.

C. ALSPAUGH

A woman in Jamam refugee camp in South Sudan holds up a container of water from a makeshift well.

Currently, no one is trading water futures, but it won't take much to spark the market into life. When the state of Texas tallied up to $10 billion in economic losses due to the recent drought, academics set about theorizing how the water of the Rio Grande might be indexed for a futures market[6]. After the floods in Thailand last year caused economic losses totalling $46 billion, Thailand's Securities and Exchange Commission studied the possibility of financial derivatives indexed to rainfall and dams[7]. The semiconductor manufacturer Intel might have been interested — the mud and muck that reportedly halted its chip-making operation in Thailand cost the company up to $1 billion.

A truly global trade in water futures will have to wait until the financiers come up with a universally adopted measure of water stress. Until then, water futures markets will emerge as local phenomena based on local concerns. For example, in drought-riddled Australia, every element of an indexed futures market is ready to go on the Sydney Futures Exchange (see go.nature.com/u7hdas). In the Medinipur and Tumkur districts in West Bengal and Karnataka in India, where the monsoon has become less and less predictable, a south Asian water futures exchange has been conceptualized, to be traded on the Delhi Stock Exchange[8].

Futures trading will extend from the most pristine rivers to the barely legal effluvia of solid-waste plants. Commodity theorists in Switzerland have taken the first steps in setting up markets that will trade in water futures derived from sewage. The team calls its concept an ethical water futures market (see go.nature.com/dq6fm4). In my view, it is a financial platform to sell treated water to the highest bidder.

In all of these cases, the futures contracts will emerge from valuations of relative water scarcity or plenitude based on an index of water levels in dams, average precipitation or other indicators and predictors. Ultimately, the financial instrument will have the same basic structure as the index funds which brought unprecedented levels of speculation to the global grain market, increasing the volatility in prices — volatility that futures exchanges were originally meant to blunt. After all, if the natural-gas industry can pay more for water than soya farmers, then the gas drillers will get the water and the soya will not.

PRICED OUT

The reverberations of a global water futures market can hardly be imagined. This much is clear: a water betting game will leave crops thirsting and push the global price of food far beyond the peaks of the past five years.

The good news is that, unlike the failed attempts to regulate the derivatives markets in food, something can still be done in the case of water. There are plenty of examples of valuing water outside the realm of pure commodification. One of the best examples has been developed in the Ruhr basin in Germany[4]. This riverine resource is managed not by the invisible hand of the market, but by a policy-creating body called the Ruhr Association. Cities, counties, industries and enterprises in the region are represented by associates and delegates. A total of 543 stakeholders negotiate water-abstraction fees and pollution charges. The politics may be messy, but it works. Unfortunately, that is the way with democracy.

There is no easy panacea for the world's water needs, least of all the global derivatives business, which has proved that it is not to be trusted with mortgage-backed securities, much less our most precious resource. There is no need to initiate a futures market in water only to create yet more financial madness that seems to resist all attempts at regulation. This time around, let the business stop before it starts. ■

Frederick Kaufman *is a professor at the Graduate School of Journalism, City University of New York, New York 10018, USA. He is author of* Bet the Farm: How Food Stopped Being Food *(Wiley, 2012).*

1. Kaufman, F. *Foreign Policy* 27 April 2011.
2. Lagi, M., Bar-Yam, Y., Bertrand, K. Z. & Bar-Yam, Y. Preprint at http://arxiv.org/abs/1109.4859 (2011).
3. Moya, E. *The Guardian* 8 August 2010.
4. Global Water Partnership & International Network of Basin Organizations *A Handbook for Integrated Water Resources Management in Basins* (GWP/INBO; 2009); available at http://go.nature.com/huzxcf.
5. Keim, B. *Wired Science* 6 March 2012.
6. Brookshire, D. S., Gupta, H. V. & Matthews, O. P. (eds) *Water Policy in New Mexico* (RFF Press Water Policy Series, 2011)
7. Nguyen, A. *Bloomberg* 14 December 2011; available at http://go.nature.com/dwndzp.
8. Ghosh, N. *Commodity Vision* **4**, 8–18 (2010).

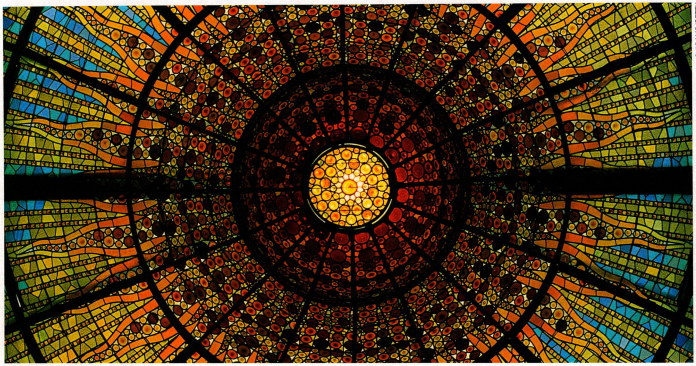

S. ADAMS/GETTY

Symmetries feature in the stained-glass ceiling of the Palace of Catalan Music in Barcelona, Spain.

Why symmetry matters

Mario Livio celebrates the guiding light for modern physics.

Symmetries lie at the heart of the laws of nature. Early scientific giants such as Galileo Galilei, René Descartes and Isaac Newton did not speak in those terms, but symmetries were implicit in their ideas of a comprehensive framework of the Universe. And symmetries lie explicitly at the basis of modern physics, from general relativity to quantum field theory.

To a physicist, symmetry is a broader concept than the reflective form of butterfly wings, or the rotational similarity of a triangular roundabout sign. In physics, to be symmetrical is to be immune to possible changes. Symmetry represents those stubborn cores that remain unaltered even under transformations that could change them.

Sometimes symmetries break down. The announcement on 4 July that two teams at the Large Hadron Collider (LHC) at CERN, Europe's particle-physics laboratory near Geneva, Switzerland, had discovered a Higgs-like boson marked the end of a heroic quest to confirm a 'symmetry-breaking' mechanism. That such a process endows particles with mass was suggested in 1964 by theoretical physicist Peter Higgs and two other groups (Robert Brout and François Englert; and Gerald Guralnik, Carl Hagen and Tom Kibble).

If the new boson is confirmed as the long-sought Higgs, our faith in symmetry as a core concept in physics will be cemented. Further tests of symmetry's power as a guide to physical laws will follow, in the quantum realm and through concepts such as supersymmetry. But what is symmetry and how is it broken?

THE LAWS OF NATURE

Universal laws are symmetric under translation in space and time — they don't change from place to place or from today to tomorrow. As astronomers know, hydrogen atoms billions of light years away are subject to the same physics as on Earth. Because physics has no preferred direction, natural laws are also symmetric under rotation. Whether we measure orientation with respect to the farthest quasar or the nearest coffee shop, the rules are the same.

Such symmetries are true of Newton's laws of gravity and motion, which he applied in the seventeenth century to falling apples, ocean tides, the Moon and planetary orbits. They are also true of those laws' twentieth-century successors: Albert Einstein's special and general theories of relativity, with their revolutionary ideas about the constancy of the speed of light, the equivalence of acceleration and gravity, and the warping of space-time by masses.

Imposing symmetry on all frames of reference was Einstein's motivation for developing relativity theory. He wanted to find a way of describing the laws of nature that would look the same to all observers, whether at rest, moving at a constant velocity or accelerating.

In looking for symmetries, Einstein was following in the footsteps of James Clerk Maxwell, a physicist who died the same year Einstein was born, in 1879. Purely for mathematical balance, Maxwell added to equations describing electromagnetism an extra term that related electrical currents to a resulting magnetic field. In doing so, he unified all electric and magnetic phenomena then known, as well as the laws of optics.

INTERNAL SYMMETRIES

The symmetries that give rise to the Higgs boson are different. They originate in the probabilistic world of quantum physics — 'internal symmetries' reflect the robustness of universal laws to changes in the identity of some elementary particles. Just as a particle's position may be uncertain according to quantum rules, so may its identity. Some types of particles are thus

interchangeable within the equations.

Electrons and neutrinos can be swapped without altering the laws of nature. This symmetry is central to the 'electroweak theory', developed in the 1960s by physicists Steven Weinberg, Sheldon Glashow and Abdus Salam. The theory unifies electromagnetism with the weak nuclear force, which is responsible for some radioactive decays (such as a neutron to a proton) and underlies nuclear reactions in stars. The Higgs boson has a role in breaking the symmetry of weak interactions.

The strong nuclear force, which acts among quarks to make up protons and neutrons, and binds protons and neutrons to form atomic nuclei, is also subject to symmetries. The laws of physics are blind, for instance, to exchanges of up quarks and down quarks (protons are made of two up quarks and one down quark).

The standard model of particle physics combines the electroweak theory with quantum chromodynamics, the theory of strong interactions within the nucleus. The model's great achievement is that it unifies three of the four known forces through which particles interact (gravity stubbornly continues to resist unification).

Internal symmetries are local, or independent of the locations of particles. Quarks (or electrons and neutrinos) at different points in space and time may be exchanged without consequence. Fields, with their associated gauge bosons, mediate these remote interactions. The electromagnetic interaction is carried by the photon. In electroweak theory, the photon is joined by the three carriers of the weak nuclear force: W^+, W^- and Z^0 particles. Gluons shepherd the strong force between quarks.

The symmetries associated with a given fundamental force act on all associated elementary particles, not just the force mediators. The same electroweak symmetry that treats the W^+, W^- and Z^0 particles as equivalent, for instance, applies to the electron and neutrino. The symmetry requirement dictates which particles and interactions are necessary for a given theory.

Yet the cosmos does not always manifest perfect symmetry. The equations describing the electroweak interaction, for example, are symmetrical. They do not change when a photon is swapped with a W or Z particle. But the solutions to these equations — the particles themselves — are not identical. The photon is massless, and the W and Z particles are about 100 times heavier than a proton. The symmetry of the governing equations is somehow lost, or broken, in physical reality.

BROKEN SYMMETRIES

The concept of spontaneous symmetry-breaking allows physicists to preserve a symmetric theory while confronting puzzling observations.

In the 1930s, the Jewish–Russian physicist Lev Landau realized that phase transitions are accompanied by a loss of symmetry. Take magnetic materials. When hot iron is cooled below its Curie temperature (around 770 °C), it acquires bulk magnetism. Its internal magnetic fields, pointing in random directions when hot, collectively settle on one orientation. The symmetry is broken. The equations describing the magnetic field within the iron are symmetric — they have no preferred orientation. It is the physical state of the iron that changes.

Higgs and his colleagues realized in 1964 that symmetry-breaking could be applied to particle physics. They proposed that a fraction of a second after the Big Bang, as the Universe expanded and cooled, it went through a dramatic phase transition (see 'Fundamental forces'). The internal symmetry of the weak interactions, which held true at very high energies, broke when the Universe's energy dropped below some threshold.

FUNDAMENTAL FORCES

After the Big Bang, the four forces divided as the cooling Universe underwent phase transitions. The Higgs boson broke the symmetry between the electromagnetic and weak nuclear forces.

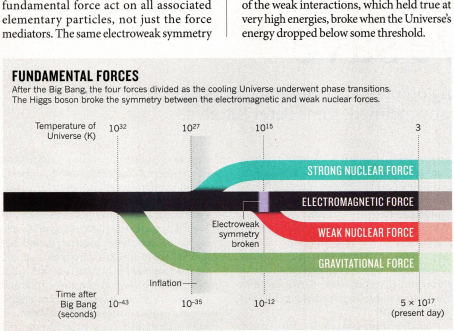

The mechanism by which it did so (the Higgs mechanism) involves a quantum field (the Higgs field), which has a non-zero value associated with every point in space. The Higgs particle is a ripple, a parcel of energy, in the Higgs field.

The Higgs field tugs on W and Z particles, restricting their communication of the weak force to an extremely short range (less than about one-ten-thousand-trillionth of a centimetre). In other words, it gives the W and Z particles inertia, or mass. In similar fashion, the molasses-like Higgs field gives mass to other fundamental particles, such as electrons and quarks.

Because the vacuum does not carry electrical charge, the photon travels unhindered. So the photon remains massless and can render the electromagnetic force over long distances.

So far, the particle discovered in July at the LHC looks a lot like the Higgs boson. More tests are needed to prove it. First, the experimentalists must determine the quantum spin of the new boson (the Higgs is predicted to have no spin). Second, they need to measure the rates at which it decays into other particles and compare those to theoretical expectations. Even if the boson passes these tests, symmetry and its breaking do not leave centre stage.

One of the major steps beyond the standard model involves supersymmetry — the idea that each particle we know has a not-yet-discovered superpartner, with a spin removed by half a quantum-mechanical unit. Supersymmetry is manifestly broken; otherwise the superpartners would have had the same masses and charges as the known particles and would have been detected already. A broken supersymmetry opens the door to a host of other potential bizarre processes, such as an electron transforming into a muon.

There are no signs as yet from the LHC of supersymmetric particles, but this could change. Although the simplest versions of supersymmetry seem to have been ruled out, no one knows what to expect when the LHC increases its energy in two years.

Of course, the ultimate goal remains an all-embracing theory that will unify gravity with the other interactions. We still do not know if the underlying principle of such a theory is symmetry, but a confirmation of the newfound boson as the Higgs will show, once again, that symmetry is a guiding light through nature's labyrinth. ■

Mario Livio *is an astrophysicist at the Space Telescope Science Institute, Baltimore, Maryland 21218, USA. He is author of* The Equation That Couldn't Be Solved: How Mathematical Genius Discovered the Language of Symmetry *(Simon & Schuster, 2005).*
e-mail: mlivio@stsci.edu

AUTUMN BOOKS

ILLUSTRATIONS BY SPENCER WILSON

ENVIRONMENTAL SCIENCES

Divided we save

An expanded model for heading off planetary tipping points offers much to both optimists and the apocalyptically inclined, finds **Peter Kareiva**.

Pessimism usually seems smarter than optimism. The pessimist is the ant in Aesop's fable: the realistic, sage, cautionary voice. The optimist is the grasshopper: the naive, un-analytical fool. Thomas Malthus was perhaps the most famous pessimistic intellectual, writing in his 1798 *An Essay on the Principle of Population*: "The power of population is so superior to the power of the earth to produce subsistence for man, that premature death must in some shape or other visit the human race."

The latest contribution to this grand apocalyptic tradition is *Bankrupting Nature*. But, unlike previous pessimistic assessments of tipping points for humanity and Earth, this book by Johan Rockström, head of the Stockholm Resilience Centre, and Anders Wijkman, a former member of the European Parliament, combines a critique of political and economic systems with an assessment of global ecology. It is an extension of the influential planetary-boundaries idea that Rockström and colleagues first published in *Nature* in 2009.

Many scientists and scholars have issued warnings about impending famine and environmental decimation, only to witness a relentless improvement in the human condition; but that is no reason to dismiss this book. First, the framing of limits in the past has primed important discussions and motivated change. Second, the ten planetary boundaries that Wijkman and Rockström have set out are not grounded in human thresholds, but are based on ecological, biogeochemical and atmospheric processes such as ocean acidification, biodiversity loss and freshwater use. Most importantly, no one can dispute that

human impacts on the planet are greater than ever — and still increasing, as the population grows and developing nations aspire to North American levels of consumption.

And the stakes are high. If one mistakenly warns of a doom that is not really around the corner, the cost might be slower economic growth. But if one fails to see the true apocalypse on the horizon, the consequences could be calamitous. For this reason, *Bankrupting Nature* deserves our attention.

The book's arguments are familiar, but rarely have they been gathered together in one place to clarify the links between politics, economics and ecology. Wijkman and Rockström lay out the dangers inherent in ignoring the planet's boundaries, and focus on renewable resources as an energy solution. They make a clarion call for transforming our economic system, replacing the outdated economic indicator of gross domestic product with broader human-welfare metrics such as Chilean economist Manfred Max-Neef's model and its incorporation of human needs, from freedom to creativity.

There are strengths and weaknesses in each of these discussions. Wind and solar power, the featured renewables, are really only an electricity solution. That leaves out many of our energy demands. And there is still a need to be as critical of problems with the transmission, storage and land footprints of renewable alternatives as we have learned to be with fossil fuels.

Regarding a new economics, the book spins several nice stories, but is light on analytical policy options. Take the authors' championing of a 'circular' economy, based on service, virtual assets and re-use as opposed to ever-expanding consumption of raw materials or a no-growth economy. What about the server farms that store and deliver all our information? These are energy hogs full of metals such as copper and silver, which must be extracted through often-damaging mining processes. Even recycling is not always environmentally benign.

Unlike many 'limits to growth' proclamations, however, Wijkman and Rockström's book makes the useful distinction between global and local perspectives. So although the nitrogen cycle is globally disrupted by excessive fertilization, additional fertilizer is still a good idea for depleted soils in Africa. Recovery, restoration and resilience might have been included, as in many cases, restoration remains possible even where boundaries have been locally exceeded and ecosystems have collapsed.

Bankrupting Nature: Denying Our Planetary Boundaries
ANDERS WIJKMAN, JOHAN ROCKSTRÖM
Routledge: 2012. 208 pp. £24.99, $44.95

It has to be said that the boundary framing does not lend itself to policy actions. For example, we need, however roughly, to estimate the likelihood of people suffering severe impacts from climate disruption, and then to analyse the costs and benefits of different actions that could influence the carbon dioxide emissions trajectory. It is the relative effectiveness of natural gas at replacing coal that is the central question — not the planetary boundary for CO_2.

The authors sensibly sidestep the boundary model in discussing population growth, which they emphasize is the ultimate driver of many environmental problems. Instead, they focus on planetary opportunities: proven ways of reducing population, such as modest investments in family planning, economic opportunities for women and education of young girls. Similarly, in the developed world, we can modify consumption using modern marketing, education and pricing incentives. Approaching CO_2, acidification, nitrogen and the many other planetary boundaries in the same way would have been useful.

However the approaches are shaped, Wijkman and Rockström remind that action is imperative to stave off crisis. But a crisis of what magnitude? They warn of a coming apocalypse triggered by climate disruption and resource scarcity, drawing on Gwynne Dyer's book *Climate Wars* (Random House, 2008), with its scenarios of civil wars, conflicts between nations and collapsed governments. Earth does face severe environmental challenges, but these are a far cry from impending collapse. And although Rockström points to the risk of science being drawn into the political process, modern environmental science is all about examining trade-offs between choices in energy, resource use, infrastructure and waste disposal.

The ideas in this book are interesting and often inspiring, and, to some extent, the future of sustainability depends on wrestling them to the ground. In doing so, it is key to recognize that some scientists are optimists and others pessimists. To progress, this debate about limits and tipping points needs to be recast as a series of testable hypotheses about resource extraction, land and water use, and energy portfolios, addressable by models and data.

Some say that innovation, technology and new partnerships between business and conservation hold the answers to a bright future. Others argue that slower growth, happiness indicators and strong regulatory constraints are the only way to avert the apocalypse. It is premature to predict who will win the debate — the grasshopper or the ant. ■

Peter Kareiva *is chief scientist at The Nature Conservancy in Arlington, Virginia. e-mail: pkareiva@tnc.org*

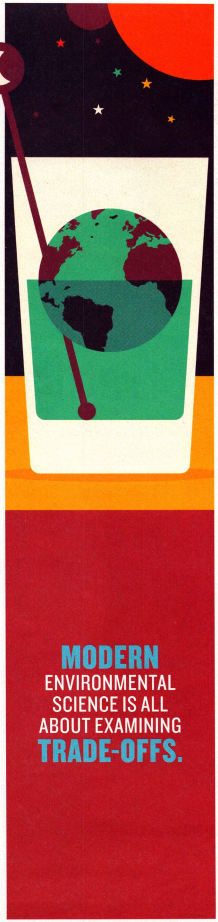

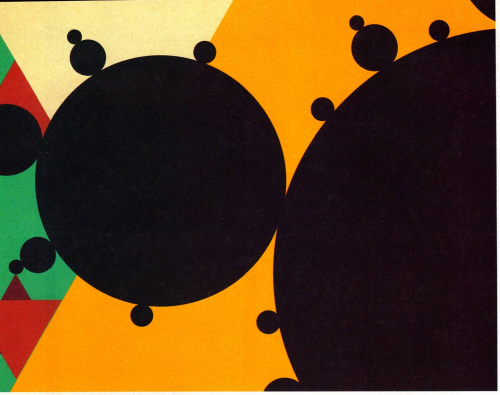

MATHEMATICS

A fractal life

Mark Buchanan enjoys the quirky memoir of a mathematical rebel — the late Benoît Mandelbrot.

At the start of *The Fractalist* is a photograph dated June 1930. In a Jewish family's apartment in Warsaw, four Polish mathematicians are hosting a meal for an honoured guest — French mathematician Jacques Hadamard. Somewhere in the same house, although not pictured, would have been a six-year-old named Benoît. The family's surname was Mandelbrot.

A hugely productive theorist of geometry and roughness, and the "father of fractals", Benoît Mandelbrot died aged 85 on 14 October 2010. *The Fractalist* is his posthumously published autobiography, polished with help from his former assistant and colleagues.

A collection of poignant vignettes, the memoir paints Mandelbrot as an intellectual individualist who created his own field. He was reputedly a prickly character, self-important and quick to take offence. Traces of his strong opinions come through, but they are overwhelmed by warm and delightful reminiscences of family and colleagues.

Mandelbrot explains that in that 1930 photo are several of the most important people in his life. Key among them is his mathematician uncle, Szolem. The first in the family to attend university, Szolem Mandelbrot had travelled to Paris to study mathematics under Hadamard, and went on to hold the same chair at the Collège de France as Henri Poincaré. He was Mandelbrot's informal mentor, and linked the family to international science.

In 1936, as European civilization began to dissolve, Mandelbrot's "lucid and decisive" parents took the family to Paris to join Szolem. Benoît recalls learning about the history and architecture of the city during long walks. When the war started, the family fled occupied Paris for rural Tulle in the unoccupied Limousin region.

Danger was never far away, and in 1943, the family went into hiding and the parents and children split up. Posing as apprentice tool-makers, Benoît and his cousin Leon aroused suspicion and were arrested by the police, who were seeking the culprits of a bombing. Days of anguish followed before a helpful official intervened on their behalf.

The Fractalist: Memoir of a Scientific Maverick
BENOÎT MANDELBROT
Pantheon; 2012. 352 pp. $30

Through such kindnesses, and the determination of his parents, Mandelbrot survived the war. Back in Paris, his mathematical skill gained him entrance to the prestigious École Polytechnique. This would have guaranteed him a comfortable career in France, but Mandelbrot never settled for the safe option.

In one vignette, Mandelbrot recalls a "life-altering verbal lashing from Szolem". It was 1952 and Mandelbrot, aged 28, was back in Paris after studying fluid dynamics and aircraft design at the California Institute of Technology in Pasadena. He hadn't chosen a topic for his PhD, and Szolem berated him for excessive book learning and preparation to be a "well-trained monkey".

Szolem suggested pursuing quadratic dynamics, the sometimes complex behaviour of mathematical functions when iterated — plug in a number, take the result and plug that back in again, endlessly. Mandelbrot looked into the topic, then dropped it. But the lashing had an effect. Soon, Szolem pointed Mandelbrot to the linguist George Zipf, who had found a scaling law in the relative frequency of word use that seemed to be universal across languages. "Silly stuff only you can like" was Szolem's view. Benoît, to the alarm of his professors, chose it as his thesis topic — and so set a course to revolutionize science.

Mandelbrot's insight that the apparently random might harbour hidden order broadened over his postdoc positions at the Massachusetts Institute of Technology (MIT) in Cambridge; Princeton University in New

NEW IN PAPERBACK

Highlights from this season's releases

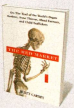

The Red Market: On the Trail of the World's Organ Brokers, Bone Thieves, Blood Farmers, and Child Traffickers
Scott M. Carney (William Morrow, 2012; $14.99)
From illegal adoptions to a bag of tibias used to make flutes on the Indo-Bhutanese border, Scott Carney explores the illegal trade in human bodies and body parts. His investigation into this shadowy realm exposes a system that exploits donors, benefits middlemen and puts a price on our very existence. (See Laura Spinney's review: *Nature* **474,** 156–158; 2011.)

Jersey; and the University of Geneva in Switzerland. In 1958, he began a 35-year career at the IBM Research Center in Yorktown Heights, New York.

His work on market fluctuations in the 1960s could have revolutionized financial economics if the field's equilibrium-focused ideology hadn't pushed it aside for 30 years. Perceiving parallels in everything from fractured surfaces to stock-market movements, Mandelbrot coined the term fractals and did more than anyone to make it possible to talk about natural roughness and disorder in a precise, scientific way.

In 1979, he returned to Szolem's suggestion of quadratic dynamics. Within a year, his explorations of functional iterations led him to discover the Mandelbrot set — an astonishing pattern of infinite richness produced by simple rules. This launched a whole branch of mathematics.

Much of what makes *The Fractalist* fun to read is Mandelbrot's scattered recollection of encounters with luminaries. At MIT he discussed linguistics with the young Noam Chomsky and argued with anthropologist Margaret Mead. Robert Oppenheimer liked his ideas, and Mandelbrot worked with the famed psychologist Jean Piaget in Geneva and computing pioneer John von Neumann at Princeton.

Mandelbrot recalls how after one of his lectures, a famous mathematician objected, saying he had made "absolutely no sense at all". Oppenheimer and von Neumann sprang into action, explaining points that even Mandelbrot hadn't noticed. The meeting, he remembers, "went from abysmally low to unforgettably high". His appreciation of friends, music and quirky mathematics colours every page of *The Fractalist*. Mandelbrot's odd habits explain why he was so original: he avoided work involving direct competition with others, and naturally worked in the gaps between fields, in blind spots.

"A youthful decision set me on a maverick's lonely ride," he writes. "Its consequences took a long time to develop." ■

Mark Buchanan *is a physicist and writer based in France. His latest book is* The Social Atom.
e-mail: buchanan.mark@gmail.com

MEDICAL HISTORY

Stemming the red tide

Lab luminaries jostle with consumptive cultural icons in a vivid history of tuberculosis, finds **Stefan H. E. Kaufmann.**

Tuberculosis has killed more people than all wars combined, and was a leading cause of death in many Western megacities as recently as the 1950s. Historically, tuberculosis (TB) was hothoused in overcrowded European and US cities: at the start of the twentieth century in New York and Berlin, it killed 40% of people aged 25–40. Yet TB was in decline until the late twentieth century, when the HIV/AIDS epidemic in sub-Saharan Africa triggered a resurgence. Now, it is the number one cause of death among people with HIV, and the incidence of multi-drug-resistant strains is rising.

But the story goes beyond the medical. TB's long history, wide spread and lethality irrevocably link it to social and cultural history, as Helen Bynum reveals in her gripping history of the disease and its impacts, *Spitting Blood*.

Bynum kicks off with the case of George Orwell, which encapsulates the progression of TB and its impact on culture. In 1949, when Orwell published *Nineteen Eighty-Four*, he was in the late stages of the disease, which arguably influenced his novel's dystopian tone; he died a year later. Bynum goes on to expertly turn the many facets of TB to the light, from biology to medicine and socio-economics. She ends with a brief account of why it has not been eradicated.

TB is caused by *Mycobacterium tuberculosis*, a bacterium that probably evolved from an environmental microbe to a human pathogen. The signs of 'consumption' or phthisis — pulmonary TB, triggered by aerosol infection of the lung — are coughing and spitting of blood. Before the nineteenth century, another common form was scrofulosis, in which the lymph nodes became pus-filled and ulcerated. It usually arises from ingesting bacteria, so the increasing eradication of bovine TB and the sterilization of milk have radically reduced its incidence. Pott's disease, a third, rare form, affects the bones.

Phthisis and scrofulosis were known in antiquity. But it was not until the late Renaissance that anatomists came to recognize TB lesions, and spotted similarities between the manifestations of the disease.

TB began to gain cultural cachet as artists succumbed. The death at 25 of English Romantic poet John Keats (a trained surgeon) did much to glamorize the disease. In Rome in 1820, Keats "vomited near two cupfuls of blood"; he died a few months later. Anne Brontë and, possibly, her sister Emily succumbed at 29 and 30. Consumption became linked to the punishment and redemption of a bohemian life, as with the courtesan Violetta in Giuseppe Verdi's 1853 opera *La Traviata*.

Meanwhile, as Bynum shows, the medical disease began to emerge, and "consumption became tuberculosis". Louis Pasteur provided the first evidence that microbes caused certain diseases. Robert Koch showed that TB was infectious, and demonstrated that a single pathogen was responsible for its different forms. At the time, clinicians tried to treat the disease using the 'pneumothorax' method, collapsing the lung by inserting needles into the pleural cavity, in the hope that pressure on the lung would lead to a cure. But the unveiling of TB as a bacteriological disease paved the way for effective drugs, diagnostics and a vaccine.

Spitting Blood: The History of Tuberculosis
HELEN BYNUM
Oxford Univ. Press: 2012. 352 pp. £16.99, $34.95

In the second half of the nineteenth century, efforts to control public spitting began. Dispensaries were set up, then sanatoriums for the rich, the first in Germany in the 1860s. Working-class sanatoriums emerged courtesy ▶

Knocking on Heaven's Door
Lisa Randall (Ecco, 2012; $16.99)
What can CERN's Large Hadron Collider (LHC) reveal about the make-up of the Universe? Particle physicist Lisa Randall explains, alternating details of the LHC's inner workings with more general musings on the philosophy of science. (See Joseph Silk's review: *Nature* **477**, 30–31; 2011.)

Survivors: The Animals and Plants that Time Has Left Behind
Richard Fortey (Harper, 2012; £9.99)
Palaeontologist Richard Fortey narrates the history of life by looking not to the long-extinct, but to organisms that have survived, almost unchanged, for millions of years. These survivors, he says, speak to us of pivotal evolutionary events.

of national-insurance programmes and philanthropy. People with joint and bone TB, often children, underwent orthopaedic treatments, such as wearing shells and jackets that left just face and ears exposed.

In 1921, as Bynum reveals, Albert Calmette and Camille Guérin devised the first breakthrough: the vaccine bacille Calmette–Guérin (BCG). Twenty years later, Albert Schatz and Selman Waksman discovered the second: the TB drug streptomycin. Intensive research spawned others, and the 1950s saw the first broad-scale fight against TB, with mass X-ray screening and drug therapy. But although national TB-control programmes sprang up, interrupted treatments and poor patient compliance led to drug resistance, notably in regions of conflict and asylum camps. From the beginning, resistance against single drugs was noted, and clinical trials spearheaded by the UK Medical Research Council revealed that multi-drug therapy was essential for preventing the development of drug-resistant strains.

A rigorous multi-drug treatment programme led by the World Health Organization (WHO) effectively defeated non-resistant TB, but about 50 million people currently harbour multi-drug-resistant tubercle bacilli. Of these, nearly half a million develop the disease each year. With around 15 million people co-infected with HIV and tubercle bacilli, and nearly 1 million active TB cases a year among people with HIV, we are seeing a perfect storm. If Bynum's book has a weakness, it is that it lacks an outlook on how the WHO's goal to eliminate TB by 2050 could be achieved.

Spitting Blood provides impressive insight into TB as a medical and social disease. Meanwhile, photographer James Nachtwey's gallery of people with drug-resistant TB (www.xdrtb.org) complements this work on a disease that is still very much with us. In 2009, London alone harboured nearly 3,500 TB cases: an almost 50% increase over the preceding decade. ■

Stefan H. E. Kaufmann *is director of the department of immunology at the Max Planck Institute for Infection Biology in Berlin.*
e-mail: kaufmann@mpiib-berlin.mpg.de

A More Perfect Heaven: How Copernicus Revolutionised the Cosmos
Dava Sobel (Bloomsbury, 2012; £8.99)
Mixing drama with history, Dava Sobel offers a biography of Copernicus with a twist, working in a two-act play in which a student convinces him to publish his revolutionary work. (See Owen Gingerich's review: *Nature* **477**, 276–277; 2011.)

Margaret Sanger: A Life of Passion
Jean H. Baker (Hill and Wang, 2012; $17.00)
Margaret Sanger emerges as a daring and determined character in historian Jean Baker's vivid life. Sanger's fervent belief that women should be able to limit the size of their families led to the development of the contraceptive pill. (See W. F. Bynum's review: *Nature* **478**, 318; 2011.)

PLANETARY SCIENCE

The search for Earth's twin

Sara Seager enjoys a frank and vivid account of planet hunting.

People have pondered the existence of Earth-like worlds beyond our Solar System for millennia. In 1995, the first exoplanet was spotted, orbiting a Sun-like star. Fewer than two decades later, hundreds of planets and thousands of candidates are known. Yet the sheer variety of exoplanet masses, sizes and orbits indicates that close copies of the Solar System are rare.

In *Mirror Earth*, science writer Michael Lemonick relates astronomers' abiding interest in sister worlds, from ancient Greece — where Aristotle surmised that there is only one world, Earth — to today, and beyond. Spotting a small, light and faint planet near its massive, bright host star is difficult and requires abstruse techniques. Lemonick sets out these methods — radial velocity, transits, microlensing, direct imaging, astrometry and pulsar timing — with impressive clarity.

NASA's Kepler space telescope is rightly a focus of the book. The Kepler mission's goal is to establish how common Earth-size planets in Earth-like orbits about Sun-like stars are. But, as Lemonick is careful to spell out, these will not necessarily be Earth 'twins' — planets with water oceans, continents and thin atmospheres conducive to life.

Knowing a planet's size doesn't tell us whether it is habitable. Venus, for example, is about the same size as Earth but not at all Earth-like. A thick carbon dioxide atmosphere causes greenhouse heating of the surface to temperatures exceeding 700 kelvin, hot enough to melt lead.

The Kepler telescope, launched in March 2009 and trailing Earth as the planet orbits the Sun, is making astonishing discoveries. One is that 'mini-Neptunes' — planets a few times Earth's diameter and a little smaller than Neptune — are many times more common than larger 'Jupiters', planets about 11 times the size of Earth. There are hints that smaller planets may be even more numerous. This tantalizing finding could imply that rocky planets (thought to reach no more than 1.75 times Earth's size) outnumber their gas-rich cousins.

Kepler has also vastly increased our knowledge of the variety of planetary systems. These include single planets orbiting two suns and dozens of multiple-planet systems, some in surprisingly compact orbits. The book covers the zoo of planetary types thought to exist, as well as theories of planet formation, conditions for habitability and the origin of life.

Lemonick describes Kepler's rocky road from conception to launch, including how its technical feasibility was repeatedly challenged, leading to the proposal being rejected by NASA several times. And he discusses the implication of the recent realization that most Sun-like stars are more variable than our Sun. That means Kepler must scour them for twice as long to pick out the signature dimming of passing planets, doubling the time it will take to reach the census goal.

KNOWING A PLANET'S SIZE DOESN'T TELL US WHETHER IT IS HABITABLE.

Finding exoplanets is an art as well as a science, and Lemonick gives examples to demonstrate how hard it can be to tease a weak signal out of data. "It's my Rembrandt," declared exoplanet hunter Paul Butler of his computer code — six years in the making — that cracked the puzzle of how to measure the precise motion of a star caused by an orbiting planet. Controversy invariably follows about which detections are robust, and Lemonick captures some of those lively exchanges with quotes and stories.

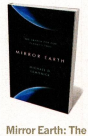

Mirror Earth: The Search for Our Planet's Twin
MICHAEL D. LEMONICK
Walker: 2012. 304 pp. $26, £19.99

Lemonick provides a brutally honest character exposition of well-known exoplaneteers. He details Geoff Marcy's feelings of being, in Marcy's words, "an impostor" early in his career owing to a severe lack of confidence that plagues many young scientists, and Debra Fischer's unusual route into astrophysics via nursing.

One intriguing thread in the book is the tension between scientists and journalists. Exoplanet discoveries are ripe for misinterpretation and exaggeration. The media and the public want an exciting story even when there is none, and it is easy for a scientist to get caught up in the hype. Lemonick describes how one astronomer felt he was induced by a journalist to say that "the chances for life" were "100 percent" on a new planet, the very existence of which is now challenged.

Mirror Earth captures the excitement of planet hunting and the ups and downs of discovery. Yet today, the quest for an Earth twin remains just out of reach. To identify a truly Earth-like world will require a more sophisticated space telescope than Kepler, to look for water and signs of life. Lemonick speculates on how that might happen. It may take decades to see how the story really unfolds. Stay tuned. ■

Sara Seager *is a professor of planetary science and a professor of physics at the Massachusetts Institute of Technology in Cambridge.*
e-mail: seager@mit.edu

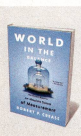

World in the Balance: The Historic Quest for an Absolute System of Measurement
Robert P. Crease (W. W. Norton, 2012; $17.95)
From weighing out food to telling the time, we have long sought to measure experience. Robert Crease traces the origins of such rules, which now seem "part of the contour of things". (See Andrew Robinson's review: *Nature* **478**, 32–33; 2011.)

The Abacus and the Cross
Nancy Marie Brown (Basic Books, 2012; $16.99)
The idea that anti-scientific superstition defined the Middle Ages is challenged by science writer Nancy Marie Brown in this life of 'Scientist Pope' Gerbert of Aurillac. Gerbert devised early forms of the computer and the planetarium, and his teaching helped spread science through Europe.

PSEUDOSCIENCE

A fringe too far

David Morrison finds contemporary echoes in a history of 'science wars', from Velikovsky to Lysenko and beyond.

From creationism and climate-change denial to cold fusion, pseudoscience pervades the media, often drowning out real science. Michael Gordin's scholarly and highly readable *The Pseudoscience Wars* uses Immanuel Velikovsky's 'cosmic catastrophe' theory — once a hugely influential recasting of ancient history — as the organizing principle for a discussion of modern pseudoscience and "science wars". The book also covers Lysenkoism and young-Earth geology in depth.

Gordin, a science historian, asserts that scientists apply the label of pseudoscience — which he defines as "doctrines that are non-science but pretend to be, or aspire to be, or are simply mistaken for scientific" — only to ideas whose public appeal makes them seem threatening. His goal is to examine how scientists try to deal with the issue of 'outsiders' and understand their thinking, and what light the Velikovsky phenomenon sheds on that.

For much of the past half-century, Velikovsky's big idea both enjoyed public popularity and drew the opprobrium of scientists. A Russian immigrant to the United States, Velikovsky was a psychiatrist by training, yet thought of himself as a historian who used the insights of psychoanalysis to interpret the myths of early civilizations. He collected and correlated myths from the first and second millennia BC, many dealing with catastrophes such as the Egyptian plagues described in the Bible's Old Testament. Eventually, he began to propose cosmic events that could explain things that happened in the myths.

By the late 1940s, Velikovsky had convinced himself that Earth had nearly collided with Venus and Mars between 2000 and 800 BC. This grand synthesis was published in 1950 as *Worlds in Collision*, followed by several further books and dozens of articles. In spite of scathing criticism from other scientists, he never wavered from his conviction: a few weeks before his death in 1979, he said: "No one has disproved *Worlds in Collision*."

The Pseudoscience Wars: Immanuel Velikovsky and the Birth of the Modern Fringe
MICHAEL D. GORDIN
University of Chicago Press: 2012. 304 pp. £18.50, $29

The book became a best-seller. But Velikovsky wanted to be recognized as a bona fide scholar. He was stung by harsh reviews, including pressure from prominent scientists that resulted in the book being dropped by Macmillan (which publishes this journal), then the main publisher of science textbooks in the United States, and transferred to the trade publisher Doubleday.

Velikovsky sought scientific legitimacy by courting individual scientists, especially Albert Einstein, who, like Velikovsky, lived in Princeton, New Jersey. Gordin discusses these efforts and the mainly hostile reactions to them. Scientists recognized that Velikovsky's planetary collisions, and his suggestion that electromagnetism rather than gravitation dominated planetary motions, were (in Einstein's term) "crazy". Velikovsky was simply not speaking the same language as the scientific community, yet his books were received uncritically by many of the public.

If the story had ended there, he would quickly have retreated into oblivion. But in the 1970s, Velikovsky became a symbol of the US counterculture. His reissued books hit the best-seller lists again; students invited him to speak on college campuses, and he acquired a group of enthusiastic disciples.

This assault from a crank baffled the scientific community. Gordin adds context

How Old Is the Universe?
David A. Weintraub (Princeton Univ. Press, 2012; $22.95)
Astronomers do not believe the Universe is 13.7 billion years old, writes David Weintraub; they know it. But how? Weintraub chronicles centuries of scientists' painstaking work gauging the ages of planets and stars to arrive at the answer.

Our Magnetic Earth: The Science of Geomagnetism
Ronald T. Merrill (Univ. Chicago Press, 2012; $17.00)
Earth scientist Ronald Merrill draws together topics relating to geomagnetism, from mammals using the magnetic field for sensing to what magnetized rocks reveal about Earth's history.

with the tale of the agronomist and pseudoscientist Trofim Lysenko, whose theory of heredity, supported by Joseph Stalin, came close to destroying the science of genetics in the Soviet Union. One reason scientists so strongly opposed Velikovsky was the recent, chilling memory of Lysenkoism.

There are fascinating and alarming parallels between these outsider narratives and Christian creationists' use of pseudoscientific arguments to lend legitimacy to their cause. Henry Morris and John Whitcomb's 1961 publication *The Genesis Flood* (Presbyterian and Reformed Publishing) became the foundation of the 'creation science' movement. Like Velikovsky, these authors postulated a catastrophic history of Earth, reinterpreting all geology in terms of a single universal flood, as described in chapters 6–11 of Genesis. They based their conclusions solely on a literal interpretation of scripture, and rejected Velikovsky's naturalist explanations.

Pseudoscience that has the support of organized religion or economic interests tends to survive much longer than the work of a lone eccentric such as Velikovsky. In his final pages, Gordin touches on a new phase of pseudoscience, practised by a few rogue scientists themselves. Climate-change denialism is the prime example, in which a handful of researchers, allied with an effective public-relations machine, are publicly challenging the scientific consensus that global warming is real and is attributable mainly to human consumption of fossil fuels. Deniers' questioning of the climate data and their attacks on the integrity and motivations of the scientists involved was exemplified by the e-mail-hacking 'climategate' scandal of 2009. This is perhaps the greatest threat from pseudoscience today.

Velikovsky and Lysenko may be largely forgotten, but other forms of pseudoscience are flourishing — among both the public and many politicians. Gordin's historical analysis of pseudoscience remains disturbingly relevant. ■

David Morrison *is the director of the Carl Sagan Center for Study of Life in the Universe in Mountain View, California. e-mail: dmorrison@seti.org*

NEUROSCIENCE

Encounters with the nonexistent

Dominic ffytche contemplates Oliver Sacks' journey through the past and future science of hallucinations.

Oliver Sacks' *Hallucinations* opens with something of an apology. The neurologist explains that his book will not focus on cutting-edge brain-imaging studies of what happens during a hallucination or what predisposes individuals to having them; rather, it will concentrate on first-person accounts, with the aim of understanding what it is like to hallucinate. It is as if Sacks worries that such an approach is insufficiently scientific, in an era of functional and structural neuroimaging.

Such concerns are unfounded. Imaging studies have made significant contributions to the field, but it is still Sacks' clinical territory — where the listening, archiving and recognition of repeated patterns of symptoms takes place — that sets the research agenda.

Hallucinations
OLIVER SACKS
Picador/Knopf: 2012. 336/352 pp. £18.99/$26.95

By analogy to eighteenth-century catalogues of flora and fauna from different corners of the world, Sacks structures his book as a 'natural history' of hallucinations. Chapter by chapter, he describes the various clinical and physiological settings in which people have hallucinations. They might ▸

The Collapse of Mechanism and the Rise of Sensibility
Stephen Gaukroger (Oxford Univ. Press, 2012; £25)
Historian of philosophy Stephen Gaukroger charts how a sensory view of nature coincided with the novel's rise in 1680–1760. (See George Rousseau's review: *Nature* **470**, 462–463; 2011.)

A Universe from Nothing: Why There Is Something Rather than Nothing
Lawrence M. Krauss (Simon & Schuster, 2012; £8.99)
The current thinking on multiverses, dark energy and what is meant by 'nothing' is unpicked by theoretical physicist Lawrence Krauss. (See Caleb Scharf's review: *Nature* **481**, 440; 2012.)

see indecipherable writing, or miniature costumed figures (visual hallucinations); smell dill pickles (olfactory hallucinations); or hear incessant renditions of the song *White Christmas* (musical auditory hallucinations).

Using descriptions from his patients, correspondents and published accounts, Sacks covers areas as diverse as eye disease, stroke, drugs (in poignant revelations from his own past) and bereavement, as well as bizarre perceptual experiences that defy simple classification. Such classificatory dilemmas include the case of Sarah, who saw herself from the ceiling of an operating theatre (in an 'out of body' experience); and Ellen, whose brother's profile remained fixed in her vision for days (visual perseveration). What all such experiences share is that the perceived object either isn't there or differs in some way from how others would perceive it.

In the neurology clinic, hallucinations tend to be visual; in the psychiatric clinic, the overwhelming majority are auditory — specifically, voices. Sacks writes from a neurologist's perspective, so his catalogue of visual phenomena and other neurological symptoms is comprehensive and scholarly. Hallucinated voices and other manifestations of schizophrenia and bipolar disorder he mentions only in passing. They require, he suggests, a book of their own.

Hallucinations gives Sacks the opportunity to explore an area new to him: the paranormal. Before the twentieth century, hallucinations were often seen as belonging to the domain of spiritualism, ghost hunting, telepathy, crystal gazing and divination. The most detailed survey of hallucinations ever undertaken remains the International Census of Waking Hallucinations in the Sane, conducted in the 1890s for the Society for Psychical Research in London, to uncover evidence for communication from the dead.

Chapter titles such as 'Phantoms, Shadows, and Sensory Ghosts' and 'The Haunted Mind' remind us of these metaphysical probings. Hallucinations and other anomalous brain experiences, Sacks suggests, lie behind psychical and paranormal phenomena, as well as fairy-tale and folklore descriptions of devils, witches, elves and leprechauns (or, more recently, alien encounters).

Sacks' book comes at a time of exciting developments in hallucination science. A key challenge to progress at present is the question of whether all types of hallucination are caused by the same brain mechanism, or by several distinct ones. In Sacks' natural-history terms, are hallucinations a single species of symptom or a family of species? It seems probable that the answer is a mixture of the two. Although they are very different, hallucinations originating in eye disease, hearing loss, amputation, sensory deprivation or stroke might be considered a single species because, for each, loss of input to the brain triggers a sequence of neurophysiological changes that results in spontaneous neural firing and hallucinations.

A KEY CHALLENGE IS WHETHER ALL TYPES OF HALLUCINATION ARE CAUSED BY THE SAME BRAIN MECHANISM.

Another cause of hallucinations, which might be considered a second species, is faulty efference signals. These signals come from the motor system and spread throughout the brain to inform it of impending movement or action. In current psychiatric accounts of hallucinations, faulty efference signals are thought to cause a failure to recognize thoughts, actions or inner speech as originating with oneself, so that they are perceived as spoken or controlled by others.

Other hallucination theories are based on knowledge stored in the brain that influences what we perceive through expectation or preoccupation. Sacks tells us of Marion, for example, who while grieving the loss of her husband, heard and saw him greeting her as she returned home — a 'top-down' influence that might be considered a third species of hallucination.

Current research is seeking to establish whether these apparently different species can be reconciled in a single overarching mechanism. Whatever the outcome, future classificatory schemes of hallucinations and related phenomena are likely to be very different from those we have now.

Hallucinations also take us to the edge of our understanding of perceptual consciousness by hinting at brain functions and processes that we did not even know were there. There is nothing in our models of object vision that explains Rosalie's descriptions, in *Hallucinations*, of silent multitudes in elaborate Eastern dress, or Marlon seeing his home, in reality ordered and tidy, as a world of chaotic dilapidation. It is observations such as these, derived from the consulting room, that challenge the neuroscience of perception — and Sacks is leading the way. ■

Dominic ffytche *is Clinical Senior Lecturer in Old Age Psychiatry at King's College London. He specializes in visual hallucinations and related visual perceptual disorders.*
e-mail: dominic.ffytche@kcl.ac.uk

The Better Angels of Our Nature: Why Violence Has Decreased
Steven Pinker (Penguin, 2012; $20)
We are becoming less violent thanks to societal evolution, avers psychologist Steven Pinker, citing significant evidence showing that warfare and murder rates are falling. (See Martin Daly's review: *Nature* **478,** 453–454; 2011.)

In Other Worlds: SF and the Human Imagination
Margaret Atwood (Virago, 2012; £9.99)
The creator of dystopian worlds in *Oryx and Crake* and *The Year of the Flood* looks to her own work and that of authors such as Kazuo Ishiguro and H. G. Wells in a collection of essays exploring science fiction. (See Q&A: *Nature* **478,** 35; 2011.)

FOOD SECURITY

Growing trouble

Calestous Juma assesses a call for policy to feed the world at a time of squeezed production and soaring prices.

We forget that part of the impetus behind the Arab Spring was the food price spikes of 2007–8. As, globally, we continue to deal with the political and diplomatic ramifications of that, another price spike is projected — this time as a result of serious recent drought in the United States, Latin America and South Asia.

These events are key to assessing the policy relevance of environmental analyst Lester Brown's *Full Planet, Empty Plates*. Brown's message is that the deteriorating world food situation has far-reaching geopolitical ramifications that demand urgent policy action. Saving civilization, says Brown, needs to be a contact sport, "not a spectator sport".

The book offers some general indication of how that saving might happen — not least through galvanizing the international community. And it stresses the global and systematic nature of the challenges. But the book is silent on the urgent need for an institutional response that matches the magnitude of the problem.

Brown argues that the biggest threat to global stability is the potential for food crises in developing countries. That risk is exacerbated by population growth: some 219,000 people are joining the dinner table every night. Meanwhile, the rise in affluence is driving up demand for grain-intensive livestock and poultry products — at a time when nearly one-third of US grain output is being diverted from food to fuel for cars. These challenges are compounded by degradation of farmlands, water scarcity, climate change and the fact that grain yields are starting to plateau.

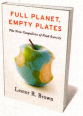

Full Planet, Empty Plates: The New Geopolitics of Food Scarcity
LESTER BROWN
W. W. Norton: 2012
160 pp. $27.95, £20

According to Brown, the overall effect of these dynamics is a dangerous transition from a time of plenty to one of food scarcity. The result is a global rush for land, and "a new geopolitics of food". Brown avers: "Food is the new oil. Land is the new gold." Yet the newness of this thesis is overstated: food has always been a geopolitical issue. The green revolution of the 1960s and 1970s, for example, was inspired by geopolitical considerations; one being the possibility of popular uprisings following famines in countries such as India and Mexico, as was well documented by John Perkins in *Geopolitics and the Green Revolution* (Oxford University Press, 1997).

How does Brown envisage tackling the dilemmas? He asserts that conventional supply-oriented policy measures such as offering farmers financial incentives and higher price support are simply not enough. Measures of demand form the centrepiece of the book's policy response. They include stabilizing the global population, eradicating poverty, reducing meat consumption and changing biofuels policies by curtailing the growth of the industry and switching to electric vehicles.

On the face of it, Brown's proposals seem sensible. However, the book focuses on what needs to be done, but provides very little indication of how such policies might be implemented. As a result, there are few new insights on how the world can avert the "food breakdown". Although poverty eradication is a desirable goal, so far it has remained elusive, and there are no new ideas here on tackling it.

Probably the weakest aspect of *Full Planet, Empty Plates* is its failure to clearly outline the institutional mechanisms through which to address the challenge. So far, the world has tried to deal with the issue largely through international bodies such as the United Nations. Their efficacy is now in question, but there is no discussion of alternatives. And the solutions Brown cites derive from national efforts. What works for one country may not work for all.

For example, he alludes to efforts by organizations including the World Bank and the United Nations Food and Agriculture ▶

Is That a Fish in Your Ear? The Amazing Adventure of Translation
David Bellos (Particular Books, 2012; £8.99)
Culture, nationalism and semantics all feature as translator David Bellos gives both a history of the shifting meaning of translation and practical insight into the complexity it involves. (See Ellen Bialystok's review: *Nature* **477,** 536; 2011.)

The Quest: Energy, Security, and the Remaking of the Modern World
Daniel Yergin (Penguin, 2012; $20)
Oil pools at the centre of Daniel Yergin's analysis of the challenge to supply the world with energy. Also focal is his belief that the energy question should be integral to foreign policy. (See Vaclav Smil's review: *Nature* **477,** 403; 2011.)

Organization to work out principles for governing land acquisitions in developing countries. This has emerged as one of the most controversial aspects of African agriculture, with most of the land deals concentrated in countries such as Ethiopia, Ghana, Liberia, Madagascar, Mozambique, South Sudan and Zambia.

These are relatively poor countries that need enhanced capability in resource management. Simply offering new guidelines won't do it. Ethiopia, for example, has a long-term vision to modernize its agriculture, but Brown offers little indication of how such countries could play a part.

There have been previous predictions of food crises. A variety of creative responses — especially those made possible by advances in science and technology — helped to forestall disaster and buy the international community time. The green revolution, by introducing inputs such as fertilizer and high-yielding crop varieties, boosted food production. Brown ignores technology, however, even though almost all of the measures he proposes — from the management of population to the expansion of prosperity and switching of energy sources — require the marshalling of human ingenuity.

The green revolution offers another important insight: Latin America and Asia responded to the food crises by expanding local food-production capacity. A global network of agricultural research institutes was created under the Consultative Group on International Agricultural Research (CGIAR) to promote such capacity. The CGIAR is probably the most important geopolitical innovation ever created in response to food crises. The world will need to either strengthen it or offer an alternative.

Full Planet, Empty Plates is a call to arms against the wolf at the door. Admitting the presence of a wolf is one thing; designing an attack strategy is another. For that, we need to turn elsewhere. ■

Calestous Juma *is professor of the practice of international development at Harvard Kennedy School, Cambridge, Massachusetts, USA.*
e-mail: calestous_juma@harvard.edu

BIOTECHNOLOGY

Random harvest

Ian Wilmut assesses a critique of how genomics, bioethics and neuroscience are meeting their potential.

The subtitle of this book — *Bioscience's Promethean Promises* — led me to expect I would be reading about the harm caused by biomedical research. Instead, I found a scathing account of the failure of recent projects in biology to provide significant new knowledge.

In *Genes, Cells and Brains*, their fifth book together, sociologist Hilary Rose and her husband, neuroscientist Steven Rose, consider in detail several disciplines that have become fashionable during the past 30 years. These include genomics, experiments on animals, biobanks, regenerative medicine and neuroscience. The duo also reviews mechanisms of evolution and informatics.

The authors introduce each theme with a historical account of its scientific, ethical and sociological background, according to their views. Anyone who has read *Love, Power and Knowledge: Towards a Feminist Transformation of the Sciences* (Polity, 1994) by Hilary Rose and *Alas Poor Darwin: Arguments Against Evolutionary Psychology* (Jonathan Cape, 2000), edited by both authors, will know broadly what to expect from their socialist and feminist perspectives. So there is criticism of modern academics being encouraged to patent their research or becoming involved in commercializing their work, and of pre-implantation genetic diagnosis. Whether or not you agree with the Roses' perspectives, they provide thought-provoking and interesting contrasts to the secular, neo-liberal view that predominates at present.

The authors describe why, in many cases, they believe that misunderstandings about the underlying biology inevitably led to projects failing to achieve their aims. In their view, for example, the gene-centric view of biology exaggerates the probability of finding linkages between genes and disease. They also forcefully criticize today's free-market capitalist global economy, suggesting that the undesirable social environment it creates often leads to inappropriate organization of bioscience projects, with, for example, serious risks of personal data being released into the public domain.

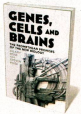

Genes, Cells and Brains: Bioscience's Promethean Promises
HILARY ROSE AND STEVEN ROSE
Verso: 2012. 336 pp. £20, $26.95

They address their criticisms particularly at the genome-wide association studies of human inherited disease that have sprung up since the human genome was first sequenced. In such studies, the genomes of populations in a community are analysed in a search for evidence that a specific form of a gene (allele) is associated with a high risk of the person having a serious illness. So far, these projects have failed to fulfil the unrealistic expectations that were raised by publicity from the research community.

But Will the Planet Notice? How Smart Economics Can Save the World
Gernot Wagner (Hill and Wang, 2012; $16)
You can avoid meat, plastic bags and air miles, writes economist Gernot Wagner, but individual choices have no effect on the planet. Harnessing market forces to incentivize green behaviour is the key to confronting climate chaos, he argues.

Alone Together: Why We Expect More from Technology and Less from Each Other
Sherry Turkle (Basic Books, 2012; $16.99)
Computers are changing the way we interact, warns social scientist Sherry Turkle, leading us to view digital connections as a substitute for intimacy. Many people are 'always online'; others have never known life without computers.

I must declare an interest: I am a member of the group that the Roses hold largely responsible for the failure of the "New Biology" to provide important new knowledge. I am a 68-year-old Caucasian male who has worked in biotechnology for the past 30 years; I am also one of the inventors named on several patents. At one point I was an employee and shareholder of Geron in Menlo Park, California, a biopharmaceutical company that is criticized in one section of the book.

The authors repeatedly raise two general concerns about biotechnology. They criticize the extent to which many biologists, adopting a gene-centric view, attribute aspects of human behaviour — including sexuality, an inclination to shoplift and altruism — to the influence of specific genes. They make the point that humans and fruitflies have a very similar number of genes, but very different levels of complexity, with the implication that genes cannot account for everything.

In this context, it is surprising to see so little mention of the apparent role of the different populations of RNA molecules in generating complex functions. Reports of the ENCODE project, which is providing the first detailed map of these regulators, were published in September. However, the general concept that non-coding RNA sequences have a vital regulatory function is more than a decade old (J. S. Mattick *EMBO Rep.* **2,** 986–991; 2001).

The authors' second beef is that commercialization now so dominates science that it distorts research management and priorities. They assert, for example, that successive British governments have supported research with human embryonic stem cells because of the potential for wealth creation. To those of us involved in the research, these unique cells should be thoroughly investigated because of the potential to treat debilitating degenerative diseases for which there is currently no treatment.

Without wishing to ignore their charge, I would balance the discussion by mentioning the private sector's very large investment in biotechnology. The authors surely do not imagine that governments would provide such funding if private investment ceased?

What of their overall comments about genomics? No doubt many of those who were involved in the research are as disappointed as the authors by the limited clinical benefit so far. Experience shows that it is difficult to predict the outcome of research and that it is hard to estimate the use that can be made of new knowledge. However, thousands of academic and clinical laboratories are making daily use of information about the human genome and of the methods that have been developed during the past decade for measuring gene expression in a small sample of cells.

I share the authors' disappointment at the rate of progress. But I am convinced that, in time, these fields will provide treatments for diseases such as motor neuron disease, multiple sclerosis, Parkinson's disease, diabetes and some forms of heart disease — eventually having a beneficial effect comparable to the revolutionary control of infectious diseases achieved during the past century. Sadly for those currently afflicted, it seems that it will take several decades for this to happen. ■

Ian Wilmut *is professor emeritus in the University of Edinburgh's Medical Research Council Centre for Regenerative Medicine, of which he was the founding director. e-mail: iwilmut@staffmail.ed.ac.uk*

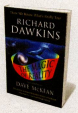

The Magic of Reality

Richard Dawkins and Dave McKean (Doubleday, 2012; £19.99)

In this edition of his illustrated bestseller for young people, eminent biologist Richard Dawkins aims to reveal scientific truth as more magical than myth, while Dave McKean's photoreal images viscerally evoke the wonder.

The Fair Society

Peter Corning (Univ. Chicago Press, 2012; $17)

A sense of fairness is innate in humans, argues Peter Corning. He cites examples such as public outcry at discrimination cases and divorce-court wrangling as evidence that society is underpinned by notions of reciprocity, justice and what is fair.

Principles of Biology

by nature EDUCATION

Bringing biology to life

To learn more about *Principles of Biology*, the first interactive textbook from Nature Education, visit **www.nature.com/principles**

nature publishing group npg

Correspondence

Reallocate funds to boost performance

Last month's report by the Council of Canadian Academies, prepared at the government's request, reveals that Canada's research output and impact rank seventh and sixth in the world, respectively (see go.nature.com/pyvwlk). Shouldn't the country be performing better, given its sustained investment in research and development (R&D)?

Gross domestic expenditure on R&D by the government and higher-education sectors was 0.77% of gross domestic product (GDP) in 2008 and has been maintained throughout the global financial crisis (0.79% in 2010). Although Canada performs well given its small population, its GDP is relatively high because of natural-resource exports, so these figures may be underestimates. Its 2008 R&D investments exceeded those of Japan and of every European Union member except Finland and France (see go.nature.com/59dg8f).

Canadian academia can improve returns on this public investment. Stimulating competition and responsibility for delivering research output and impact would support the government's commitment to fiscal accountability. For example, it could assess researchers every 5–10 years and reallocate a small amount of existing public funding to the highest performers. These measures could bring Canada in line with other developed countries, such as the United Kingdom and Australia.

Andrew J. Tanentzap *York University, Toronto, Canada.*
atanzap@yorku.ca

Social insight rings true 125 years on

David Rand and colleagues pose the question: "Are we intuitively cooperative, with reflection upon the logic of self-interest causing us to rein in our cooperative urges and instead act selfishly?" (*Nature* **489,** 427–430; 2012). In answering affirmatively, they confirm an observation made 125 years ago by the Republican Senator for California, Leland Stanford.

Stanford had introduced a bill to foster worker cooperatives in 1886, and was interviewed by *The Cincinnati Enquirer*. When Stanford broached the issue of women's rights, the reporter asked him, "Do you not think women will go off on sentimental issues if they undertake the business of government and break up the organizations by which men work out large ends?" Stanford replied, "Oh! It is not sentiment that we have to fear so much as we suppose. A man's sentiments are generally just and right, while it is second selfish thought which makes him trim and adopt some other view. The best reforms are worked out when sentiment operates, as it does in women, with the indignation of righteousness." (See go.nature.com/i6b91d.)

Stanford's discernment of rapid, pro-social sentiment and slower, selfish calculation is but one part of a larger body of thought on the potentials for cooperation in the economy, which we may find worth revisiting today.

Lee Altenberg *Maui, Hawaii, USA.*
altenber@hawaii.edu

Beit fellowships forge a Nobel link

The Beit Memorial Fellowship scheme, the first specifically to support young UK medical researchers, has made a remarkable contribution to British biomedical science over the past 100 years. John Gurdon's Nobel prize this year (see go.nature.com/yo3cxf) is the seventh to be awarded to a former Beit fellow.

Other Nobel laureates who once held Beit fellowships were Alexander Todd (chemistry, 1957), Fred Sanger (chemistry, 1958 and 1980), Macfarlane Burnet (physiology or medicine, 1960), Bernard Katz (physiology or medicine, 1970) and Tim Hunt (physiology or medicine, 2001). Some 10% of Beit fellows have gone on to become fellows of the Royal Society, including Marjory Stephenson (1914 Beit fellowship), who became one of the first two female Royal Society fellows in 1945.

The scheme merged with the Wellcome Trust Intermediate Fellowship in 2009 to create the Wellcome–Beit Prize Fellowships (see go.nature.com/i2tofa).

Andrew McMichael *Weatherall Institute of Molecular Medicine, University of Oxford, UK.*
andrew.mcmichael@imm.ox.ac.uk
Cyril Chantler *UCL Partners Academic Health Science Partnership, London.*

Timely reminder to return to the Moon

The death of astronaut Neil Armstrong (see *Nature* **489,** 368; 2012) reminds us that, 43 years after he set foot on the Moon, the satellite is still a hot target.

It is the best and most accessible place in the Solar System for robotic and human assets to address fundamentally important scientific questions while expanding our technological capabilities. Most of the Moon remains unexplored: we have never been to its far side, or to its polar regions.

In the last year of his life, Armstrong told a committee appointed by the US Congress that the larger human-exploration goals lie beyond low Earth orbit, namely: "Luna, the lunar Lagrangian points, Mars and its natural satellites, and near-Earth objects including meteoroids, comets and asteroids". He went on: "Last year I testified to this committee on the rationale for selecting Luna and its environs as the preferred initial option for America's exploration beyond Earth orbit. All that I have learned in the past year has just reinforced that opinion."

Let's hear and act on those words. Rather than exploring new options, we should begin building the hardware, selecting the landing sites, training the crews and planning the details of missions that take us to the Moon and a future of new discoveries.

David A. Kring *Universities Space Research Association, Lunar and Planetary Institute, Houston, Texas, USA.*
kring@lpi.usra.edu
Jack O. Burns *University of Colorado Boulder, Colorado, USA.*
D. Ben J. Bussey *Johns Hopkins University Applied Physics Laboratory, Laurel, Maryland, USA.*
Competing financial interests declared; see go.nature.com/4exu7l.

Bureaucracy bypass let research flourish

The remarkable success of the UK Laboratory of Molecular Biology in Cambridge (W. Bynum *Nature* **490,** 31–32; 2012) might be explained in the words of Max Perutz. When asked what makes creative research, he would say: "No politics, no committees, no referees, just talented highly motivated people" (G. Radda *Nature Med.* **8,** 205; 2002).

Four of the greatest discoveries of the twentieth century — the structure of the atom, quantum mechanics, the theory of relativity and the structure of DNA — were made without project reviewers or grant-giving agencies (B. Gal-Or *Cosmology, Physics, and Philosophy* p. 493; Springer, 1983).

Min-Liang Wong *College of Veterinary Medicine, National Chung-Hsing University, Taichung, Taiwan.*
mlwong@dragon.nchu.edu.tw

Louise Johnson

(1940–2012)

Biophysicist who helped to establish the field of structural biology.

Louise Johnson transformed our understanding of how complex enzymes and other proteins work. By combining her in-depth knowledge of X-ray crystallography with a long-standing interest in biochemistry, she helped to launch structural biology as a new discipline.

Johnson, who died on 25 September, was born on 26 September 1940 in Worcester, UK. She attended Wimbledon High School for Girls in London and then completed a degree in physics at University College London.

In 1962, Johnson started a PhD at London's Royal Institution — working under David Phillips, a pioneer of protein crystallography. There she contributed to studies on lysozyme, an enzyme that is abundant in various substances, such as tears and egg whites, and which breaks down the cell walls of bacteria. Even at this early stage in her career, Johnson was not interested in just working out structures, but wanted to use an understanding of structure to uncover fundamental biochemical mechanisms.

By firing X-rays at the crystallized protein and studying the angles and intensities of the diffracted beams, Phillips established lysozyme's structure in 1965. This was the second protein structure to be solved by X-ray crystallography (the first was myoglobin, found in muscle). Johnson's contribution was to work out what lysozyme looked like when it was bound to *N*-acetyl-glucosamine, a component of bacterial cell walls. Johnson and Phillips's work led to the first structural evidence that a substrate slots into an enzyme, much as a key fits into a lock.

After her PhD, Johnson spent a year at Yale University in New Haven, Connecticut, where she worked as a postdoc with biophysicist Fred Richards. Here she uncovered the structure of the enzyme ribonuclease S, showing that X-ray crystallography could be applied to proteins that were more complex than lysozyme. In 1967, she returned to the United Kingdom and rejoined Phillips in the Laboratory of Molecular Biophysics at the University of Oxford.

I first encountered Johnson about ten years later. I was a first-year undergraduate at Oxford studying biochemistry, and my tutor sent me to her to learn the basics of how protein structures are determined. Instead of providing me with a standard textbook description, Johnson threw me in at the deep end. I was soon working through Fourier transforms — mathematical descriptions of what happens when X-rays are scattered by protein molecules.

A.K. PURKISS, WELLCOME IMAGES

In 1990, Johnson was made the David Phillips Professor of Molecular Biophysics, and she remained in this post until her retirement. By this time, the Laboratory of Molecular Biophysics had become part of Oxford's biochemistry department.

From 2003, Johnson combined her position at Oxford with leading the development of the UK national synchrotron, the Diamond Light Source near Didcot. The largest science facility to have been built in the country for more than 40 years, the synchrotron produces beams of light that can be used to investigate the structure and properties of materials including proteins. I recall accompanying her (both of us wearing hard hats and boots) as she showed me the nascent facility with evident pride.

Johnson's many achievements included establishing the structure of a large and complex enzyme called glycogen phosphorylase. Present in muscle, this enzyme turns inert glycogen into the sugar needed to power physical activity. Johnson showed how the addition or removal of phosphate groups from the protein regulates its activity. (Phosphorylation has since turned out to be a key form of regulation in all sorts of cellular processes.) She subsequently carried out a set of groundbreaking studies on proteins that have key roles in the regulation of cell division.

In all this work, Johnson demonstrated that X-ray crystallography could reveal detailed catalytic and regulatory mechanisms, and can potentially unmask how large proteins work as complex biochemical machines. Her 1976 book *Protein Crystallography* (co-authored with Tom Blundell) was for many years the classic textbook on the topic.

Johnson received many honours in recognition of her work, including being made a fellow of the British Royal Society in 1990 and a foreign associate of the US National Academy of Sciences in 2011.

Louise was very supportive of young scientists, particularly women. Married, with two children, to physicist and Nobel laureate Abdus Salam, she understood the challenges of juggling a scientific career with looking after a family. A quiet and kind person, she directed her students and fellow researchers carefully but gently. The harshest comment I remember receiving from her — on my hastily written grant proposal — was "perhaps a little nebulous". She was a source of inspiration to all around her, and will be greatly missed. ■

Mark Sansom *is the David Phillips Professor of Molecular Biophysics in the Department of Biochemistry, University of Oxford, Oxford OX1 3QU, UK. He was Louise Johnson's graduate student from 1979 to 1983.*
e-mail: mark.sansom@bioch.ox.ac.uk

RESEARCH

NEW ONLINE

Papers published this week at Nature.com/nature

NEWS & VIEWS CD36 protein is a possible target in some breast cancers **p.490**

LETTER Mysterious infrared emissions tracked to stars lost by colliding galaxies **p.514**

LETTER Changes in the Gulf Stream are releasing sea-bed methane **p.527**

PUBLISHED 21 OCTOBER 2012

STRUCTURAL BIOLOGY

CXCR1 structure in a membrane

G-protein coupled receptors (GPCRs) are ubiquitous membrane proteins that transduce chemical signals from the outside of a cell, and many of them are drug targets. Sang Ho Park *et al.* now present a new nuclear magnetic resonance spectroscopy method for the study of membrane proteins in phospholipid bilayers and use it to determine the structure of human CXCR1, a high-affinity GPCR for interleukin-8, a major mediator of immune and inflammatory responses.

Structure of the chemokine receptor CXCR1 in phospholipid bilayers
S H Park *et al.*
doi:10.1038/nature11580

ECOLOGY

Pesticides knock bees off course

Neonicotinoid pesticides are thought to be factors in current bee declines. Richard Gill *et al.* show a direct link between exposure to neonicotinoid and pyrethroid pesticides and behaviour in individual worker bumblebees, as well as the consequent impacts on colony fitness. The pesticides reduce the effectiveness of foraging, which compromises brood care and colony productivity.

Combined pesticide exposure severely affects individual- and colony-level traits in bees
R J Gill *et al.*
doi:10.1038/nature11585

Bumblebees and pesticides
J L Osborne
doi:10.1038/nature11637

BIOCHEMISTRY

A bimodular mechanism of calcium control in eukaryotes
H Tidow *et al.*
doi:10.1038/nature11539

Structural insight into the type-II mitochondrial NADH dehydrogenases
Y Feng *et al.*
doi:10.1038/nature11541

Structure and mechanism of a bacterial sodium-dependent dicarboxylate transporter
R Mancusso *et al.*
doi:10.1038/nature11542

IMMUNOLOGY

BTB-ZF factors recruit the E3 ligase cullin 3 to regulate lymphoid effector programs
R Mathew *et al.*
doi:10.1038/nature11548

CLIMATE SCIENCE

Lower satellite-gravimetry estimates of Antarctic sea-level contribution
M A King *et al.*
doi:10.1038/nature11621

PUBLISHED 24 OCTOBER 2012

GEOLOGY

Down-river effect of climate change

Brady Foreman *et al.* provide insight into the response of fluvial systems to climate change. They found that the nature of fluvial deposition in the Piceance Creek in western Colorado shifted during the Palaeocene/Eocene thermal maximum, a global warming event that took place about 56 million years ago. They interpret the change as a sudden reorganization of river systems in response to the profound changes in climate. The palaeo-landscape was slow to recover, with the change in run-off regime recorded in fluvial patterns until long after the end of the warming event.

Fluvial response to abrupt global warming at the Palaeocene/Eocene boundary
B Z Foreman *et al.*
doi:10.1038/nature11513

MICROBIOLOGY

Live-wire sea-bed bacteria

Multicellular organisms face a major challenge: supplying every cell with food and oxygen. Christian Pfeffer *et al.* now reports a surprising solution, arrived at by multicellular filamentous Desulfobulbaceae bacteria several centimetres long living in marine sediments in Aarhus Bay, Denmark. These organisms can act as electric cables, transporting electrons from sulphides generated in organic matter in deep, anoxic sediments to the oxygen available in the surface layers. The concept of a living microcable raises a host of possibilities for future research — and technological application.

Filamentous bacteria transport electrons over centimetre distances
C Pfeffer *et al.*
doi:10.1038/nature11586

Bacterial power cords
G Reguera
doi:10.1038/nature11638

GENE THERAPY

Mitochondrial gene replacement

Mutations in mitochondrial DNA (mtDNA) cause various human diseases. Inheritance is from the mother because all zygotic mitochondria come from the oocyte. Shoukhrat Mitalipov and colleagues previously reported proof-of-concept replacement of mtDNA through chromosome spindle transfer in macaque oocytes. They now extend the technology to human oocytes. They also report on the health of a three-year old macaque born from an mtDNA-replaced oocyte. This work suggests that replacement therapy for mtDNA disorders could become a reality.

Towards germline gene therapy of inherited mitochondrial diseases
M Tachibana *et al.*
doi: 10.1038/nature11647

CANCER

Pancreatic cancer genomes reveal aberrations in axon guidance pathway genes
A V Biankin *et al.*
doi:10.1038/nature11547

VIROLOGY

Resurrection of endogenous retroviruses in antibody-deficient mice
G R Young *et al.*
doi:10.1038/nature11599

HIV therapy by a combination of broadly neutralizing antibodies in humanized mice
F Klein *et al.*
doi:10.1038/nature11604

EVOLUTION

The genomic landscape of species divergence in *Ficedula* flycatchers
H Ellegren *et al.*
doi:10.1038/nature11584

MOLECULAR BIOLOGY

Direct imaging of RecA nucleation and growth on single molecules of SSB-coated ssDNA
J C Bell *et al.*
doi:10.1038/nature11598

A glimpse of molecular competition
S T Lovett
doi:10.1038/nature11639

The TEL patch of telomere protein TPP1 mediates telomerase recruitment and processivity
J Nandakumar *et al.*
doi:10.1038/nature11648

CANCER

Destiny from density

The identification of a signalling protein that regulates the accumulation of fat and connective tissue in breasts may help to explain why high mammographic density is linked to breast-cancer risk. It may also provide a marker for predicting this risk.

VICTORIA L. SEEWALDT

Our ability to evaluate the lifetime risk of breast cancer in women who have a family history of breast and ovarian cancer was revolutionized by the identification[1] of the breast-cancer-associated genes *BRCA1* and *BRCA2*. But although this was a landmark discovery, it has not translated into improvements in the assessment of breast-cancer risk in the general population[2], because more than 95% of women who develop breast cancer do not have a *BRCA*-gene mutation[3]. So the search for biomarkers to predict the risk in these women remains a goal for many biologists, clinicians and epidemiologists.

Over the past decade, increased mammographic density — thought to result primarily from an increased proportion of breast collagen content relative to fat-tissue content[4,5] — has emerged as a non-genetic marker of breast-cancer risk[6]. However, the biological mechanism that relates tissue density to tumour development is poorly defined. Writing in *Cancer Discovery*, DeFilippis *et al.*[7] now provide a link between mammographic density and cellular signalling during the initiation of breast cancer.

The human breast is composed of many cell types, including connective-tissue (stromal) cells, fat cells (adipocytes), cells that make up blood vessels (endothelial cells) and immune cells. Collectively, these cells make up the microenvironment of the breast[8]. Over the past five years, it has been increasingly recognized that this microenvironment, including the relative proportions of different types of cell and therefore the tissue density, may have a major role in the initiation and progression of breast cancer[9,10]. One indication of this role is the epidemiological link between mammographic density and cancer risk: Caucasian women with high mammographic density have a two- to sixfold increase in lifetime risk of developing breast cancer[6]. Another indication is the physical change in the breast microenvironment that is seen in the initial stages of breast-tumour formation. This is described as a desmoplastic reaction, which is characterized by the recruitment and activation of stromal cells and results in increased collagen deposition in the breast — and therefore increased mammographic density[11].

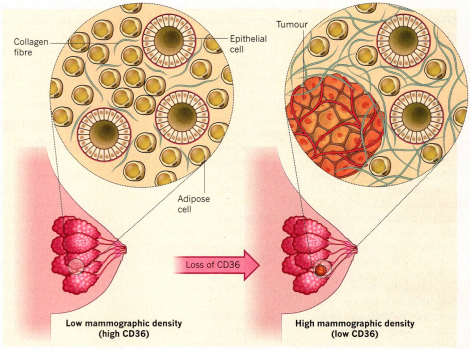

Figure 1 | Regulating the breast microenvironment. The main tissue types in human breasts are adipose (fat) tissue and stromal (connective) tissue, which contains collagen. The ratio of fat to collagen determines the mammographic density of the breast, with density increasing as the relative amount of fat tissue falls. High mammographic density is a known risk factor for breast cancer, and mammographic density also increases as a breast tumour forms. DeFilippis *et al.*[7] have found that expression of the cell-signalling protein CD36 is lower in several types of cell taken from breasts that have high mammographic density, whether or not cancer is present. They also show that a reduction in CD36 expression leads to increased collagen deposition and decreased fat accumulation in the breast.

The increased density is measured by a general increase in X-ray absorbance and is therefore relatively inexpensive and easy to measure. But we have little understanding of what determines increased density and how this is linked to increased cancer risk and the initiation of tumour formation[4,6]. The situation is complicated by the complex relationships between mammographic density, breast-cancer risk, ageing, obesity and race. For example, mammographic density typically declines with age[12], but, because breast cancer is an age-related disease, this means that, paradoxically, a woman's breast-cancer risk will increase with age while her mammographic density declines.

DeFilippis and colleagues have helped to unravel this story by revealing that expression of a single molecule, CD36, is necessary and sufficient to regulate two key features of mammographic density: the number of adipocytes in the breast and the amount of collagen deposited in the breast tissue. The authors show that expression of CD36 is lower in breast-tissue cells of women with high mammographic density — in women with or without breast cancer — than in cells from breasts with normal density (Fig. 1). CD36 is an integral membrane protein found in many cell types, and it is already known to regulate several basic cellular processes governing how cells interact and grow, including the differentiation of adipocytes, the growth of new blood vessels (angiogenesis) and immune signalling[13]. Now it seems that an influence on mammographic density can be added to this list.

To establish how CD36 expression exerts its effects on breast-tissue density, the authors modulated CD36 expression *in vitro* in cells

taken from healthy human breast tissue. They found that reducing CD36 expression led to a decrease in the total number of fat cells and an increase in the amount of collagen deposited in the extracellular matrix around the cells; higher CD36 expression increased the number of fat cells (Fig. 1). The researchers also observed lower fat accumulation and greater collagen accumulation in the mammary glands of mice lacking the *Cd36* gene. These findings indicate that inhibition of this protein is sufficient to recapitulate some of the key events that lead to higher mammographic density and initiation of breast cancer.

Not only do these findings provide a mechanistic link between cell-signalling pathways and mammographic density, they are also a convincing indication that loss of CD36 may be an early event in breast carcinogenesis. Although mammographic density is used as a surrogate marker of breast-cancer risk in the general population, it is an imprecise indicator. It gives little insight into the biology of why a woman might develop breast cancer, and it is confounded by paradoxes, such as the increase in density but decrease in risk if a woman exercises, or the decrease in density but increase in risk as a woman ages. By demonstrating that CD36 links the biology of breast density with the biology of breast-cancer initiation, DeFilipis and colleagues have provided information that may help to make density a more useful marker of risk. Finally, their results also raise the possibility that CD36 could be pharmacologically targeted in attempts to prevent breast cancer in the majority of women who (fortunately) lack a *BRCA* mutation. ■

Victoria L. Seewaldt *is in the Department of Medicine, Duke University, Durham, North Carolina 27710, USA.*
e-mail: seewa001@mc.duke.edu

1. King, M.-C. *et al. Science* **302,** 643–646 (2003).
2. John, E. M. *et al. J. Am. Med. Assoc.* **298,** 2869–2876 (2007).
3. Shih, H. A. *et al. J. Clin. Oncol.* **27,** 994–999 (2002).
4. Arendt, L. M., Rudnick, J. A., Keller, P. J. & Kuperwasser, C. *Semin. Cell Dev. Biol.* **21,** 11–18 (2010).
5. Conklin, M. W. *et al. Am. J. Pathol.* **178,** 1221–1232 (2011).
6. Boyd, N. F. *et al. N. Engl. J. Med.* **356,** 227–236 (2007).
7. DeFilippis, R. A. *et al. Cancer Discov.* **2,** 826–839 (2012).
8. Maller, O., Martinson, H. & Schedin, P. J. *Mammary Gland Biol. Neoplasia* **15,** 301–318 (2010).
9. Place, A. E., Huh, S. J. & Polyak, K. *Breast Cancer Res.* **13,** 227 (2011).
10. Nakasone, E. S. *et al. Cancer Cell* **21,** 488–503 (2012).
11. Walker, R. A. *Breast Cancer Res.* **3,** 143–145 (2001).
12. Lehman, C. D. *et al. Cancer* **103,** 1898–1905 (2005).
13. Silverstein, R. L. & Febbraio, M. *Sci. Signal.* **2,** re3 (2009).

EARTH SCIENCE

Signs of instability

The finding that pools of gas hydrates — compounds that trap natural gas emissions — in ocean sediments are deeper than expected implies that the hydrates are destabilizing, and might release gigatonnes of methane. SEE LETTER P.527

JUERGEN MIENERT

Methane hydrate is an ice-like substance that exists at low temperatures and high pressures, and which fills the pore space of sediments in the seabed and sub-seabed. Increases in sea temperature could destabilize methane hydrate, releasing methane gas into the ocean and possibly into the atmosphere — where, if released in sufficient quantities, it would act as a potent greenhouse gas and thus contribute to global warming. On page 527 of this issue, Phrampus and Hornbach[1] report a combination of seismic data and thermal models that suggests that changes in the Gulf Stream are rapidly destabilizing methane hydrate along the North American continental margin — the zone of ocean floor where the deep ocean meets the shallow continental shelves, and which marks the transition between continental and oceanic crust.

Methane hydrates are found within a region of sediments known as the gas-hydrate stability zone (GHSZ). The depth of the GHSZ varies mainly with pressure (which depends on water depth); with the composition of the natural gas trapped in the hydrates (which depends on whether the gas is produced by microbes at shallow depths or by thermal processes at greater depths); with the temperature gradient beneath the seabed; and with the water temperature at the seabed. If the deep gas reservoirs in continental margins are leaking, they may contribute methane to the shallower gas-hydrate reservoir system.

One of the most pressing issues in climate change is the relationship between ocean warming and methane escape from the seabed[2–5] (Fig. 1). The extent to which such methane venting is connected to the thawing of methane-hydrate reservoirs is the crux of this issue, but also of two big, related stories involving methane in the environment: the large-scale collapse of continental slopes (steep inclines at the edge of continental shelves) and the increasing methane levels in the atmosphere. For example, some areas of the ocean margins along the east coast of the United States[6] and the Norwegian Arctic[7] have cracked, and seem to be susceptible to future slope failures. This, in turn, may enable mechanisms to develop that allow the rapid transfer of methane from sub-seabed gas-hydrate deposits into the upper ocean and the atmosphere, which would add to greenhouse-gas emissions. Such destabilization in the

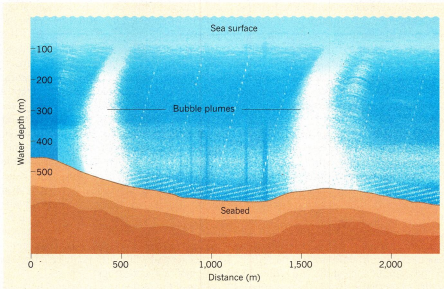

Figure 1 | Bubbling up. Hydrocarbon gas, including methane, seeps from sub-seabed reservoirs and forms plumes of bubbles. The graphic shows two plumes in the Gulf of Mexico as an east–west trace, based on echo-sounding data[10]. Phrampus and Hornbach[1] report that changes in the Gulf Stream could trigger the release of gigatonnes of methane from ocean sediments off the east coast of America. (Figure adapted from ref. 10.)

methane-hydrate reservoirs and continental slope may occur at intermediate depths along upper continental margins, down to approximately 1,000 metres below sea level.

Phrampus and Hornbach's paper adds to the scientific debate concerning the risk of substantial, rapid methane emissions in the future, and will certainly draw considerable attention to the cracked continental slope of the east coast of North America. The authors' seismic data reveal that the GHSZ in this region is deeper than predicted from models based on current ocean temperatures, indicating that transient processes for methane-hydrate melting are occurring in the sub-seabed. The researchers rule out several factors that could explain this observation, such as changes of sea level, increases in the contribution of thermogenic gas from deep hydrocarbon reservoirs, increased sedimentation rates and lower heat flow in the sub-seabed. Instead, they conclude that the discrepancy was probably caused solely by warming of the ocean at intermediate depths over the past few thousand years, the heat from which has not yet fully penetrated the seabed, and so has yet to affect the depth of the GHSZ.

Phrampus and Hornbach argue that the required warming can be explained by changes in the temperature or path of the Gulf Stream within the past 5,000 years or so. Extrapolating from their data, they estimate that these changes will ultimately warm the western North Atlantic margin by as much as 8 °C, and will trigger the destabilization of 2.5 gigatonnes of methane hydrate. What's more, taking into account changes observed in the Arctic environment[4,8] that could also cause methane-hydrate destabilization, the authors suggest that this quantity may represent only a fraction of the methane hydrate that is currently destabilizing around the world. However, the extent of global destabilization is difficult to determine exactly, because estimates of the temperatures of ocean water at intermediate depths on glacial–interglacial timescales of several thousand years suggest that ocean warming may be different between oceans[9].

Whether the destabilization of gigatonnes of methane hydrate from the east coast of North America would adversely affect climate in the future depends on how rapid temperature changes associated with the Gulf Stream will affect approximately 10,000 square kilometres of the US eastern continental margin, an area prone to submarine landslides. More broadly, the big unknowns regarding this century's ocean-temperature shifts are to what extent, and how rapidly, such shifts will reduce the stability of methane hydrate in ocean margins. It may (hopefully) turn out to be the case that intermittent increases in ocean temperature along methane-hydrated regions are not enough to increase ocean acidification and — if methane is released from the ocean — the level of carbon in the atmosphere.

Phrampus and Hornbach's GHSZ mapping may provide a timely lesson about how the conditions of the sea floor down to a depth of about 1,000 metres below sea level can change from favouring methane-hydrate formation to favouring methane-hydrate melting. It shows that we must use seismic records as indicators of past conditions affecting ocean methane hydrates, and also suggests that real-time, long-term recording of anticipated sea-floor releases of gigatonnes of methane are needed to provide the ultimate proof that a warming Gulf Stream is causing methane-hydrate melting. ■

Juergen Mienert *is in the Department of Geology, University of Tromsø, NO-9037 Tromsø, Norway.*
e-mail: jurgen.mienert@uit.no

1. Phrampus, B. J. & Hornbach, M. J. *Nature* **490,** 527–530 (2012).
2. Zachos, J. C. *et al. Science* **308,** 1611–1615 (2005).
3. Westbrook, G. K. *et al. Geophys. Res. Lett.* **36,** L15608 (2009).
4. Biastoch, A. *et al. Geophys. Res. Lett.* **38,** L08602 (2011).
5. Ferré, B., Mienert, J. & Feseker, T. *J. Geophys. Res.* http://dx.doi.org/10.1029/2012JC008300 (2012).
6. Driscoll, N. W., Weissel, J. K. & Goff, J. A. *Geology* **28,** 407–410 (2000).
7. Mienert, J. *et al. Int. J. Earth Sci.* **99,** 207–225 (2010).
8. Shakhova, N., Semiletov, I. & Panteleev, G. *Geophys. Res. Lett.* **32,** L09601 (2005).
9. Cronin, T. M. *et al. Nature Geosci.* **5,** 631–634 (2012).
10. Solomon, E. A., Kastner, M., MacDonald, I. R. & Leifer, I. *Nature Geosci.* **2,** 561–565 (2009).

STRUCTURAL BIOLOGY

Snapshot of an activated peptide receptor

Developing therapeutic drugs that target peptide receptors is challenging. The structure of one of these G-protein–coupled receptors, NTS1, activated and bound to a peptide, provides an excellent starting point. SEE ARTICLE P.508

FELIX HAUSCH & FLORIAN HOLSBOER

Some peptides act as chemical signals between cells, controlling mood, behaviour, stress responses, blood pressure, digestion and cancer progression[1]. They typically interact with receptor proteins at the cell surface — for example, with the G-protein-coupled receptors (GPCRs) that pass the message on to G proteins inside the cells to induce specific cellular responses. Pharmacological activation of peptide-recognizing GPCRs could thus enable improved therapies to be produced for diseases that involve these receptors. Unfortunately, drug development for these receptors is notoriously difficult, in part owing to the lack of structural information about how the peptide binds or how the receptor is activated. On page 508 of this issue, White *et al.*[2] present the structure of a typical peptide-interacting GPCR (called neurotensin receptor 1), bound to an activating peptide. This work gives the first insight into the mechanisms by which this class of receptor is turned on and will substantially facilitate the design of candidate drugs*.

One of the difficulties associated with the discovery of drugs that act on peptide-recognizing GPCRs is that peptides often bind to their target proteins through multiple hydrogen bonds or electrostatic interactions — something that is difficult to replicate in synthetic molecules while maintaining their drug-like properties. Moreover, unlike cytoplasmic proteins, GPCRs are inserted in the cell membrane and are therefore unstable in the aqueous solutions used for the crystallographic techniques that are commonly needed for structure-based drug design.

White and colleagues' structure of the peptide-activated neurotensin receptor 1 (NTS1) is the latest result of a technological revolution that GPCR biochemistry has witnessed in recent years[3–6]. It was made possible by several methodological breakthroughs, such as the engineering of GPCRs to create receptors that are more stable than their natural counterparts (by changing specific amino acids or by fusion with other stabilizing proteins), as well as the development of specific conditions for crystallizing membrane proteins (lipidic cubic phase methods).

The overall protein architecture of NTS1 is expected to be representative of the large and, so far, structurally unexplored β-subgroup of GPCRs. More importantly, the structure clarifies how peptide agonists (that is, activators) interact with GPCRs. Until now, peptide agonists had been thought to bind to the extracellular side of their GPCRs, but any further details were unclear. White *et al.* show that a neurotensin analogue (a peptide similar

*This article and the paper under discussion[2] were published online on 10 October 2012.

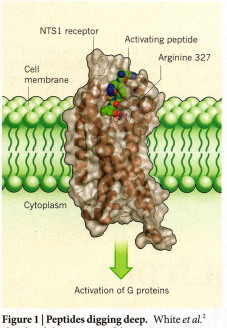

Figure 1 | Peptides digging deep. White *et al.*[2] elucidated the structure of the NTS1 protein (a G-protein-coupled receptor that is inserted in the cell membrane) bound to an activating peptide. The protein's backbone is shown in dark brown, whereas its surface is indicated as a grey transparent envelope. Arginine 327 is a key residue for activation of the receptor. Some amino-acid residues (from arginine 328 to glutamate 337) have been omitted to allow a better view of the peptide. Carbon, oxygen and nitrogen atoms are green, red and blue, respectively, in the peptide. The cytoplasmic part of the receptor passes the activation signal to G proteins, which in turn trigger cellular responses.

to neurotensin, NTS1's natural substrate) penetrates deeply into the interior of the receptor like a nail (Fig. 1), albeit not as deeply as non-peptidic agonists do in the GPCRs to which they bind.

Because agonist binding activates GPCRs by inducing changes in the receptors' conformation, a credible structure of an activated state is essential for the design of drug-like agonists. This seems to have been achieved for NTS1, as judged on the basis of previous biochemical studies and plausible comparisons with other activated GPCRs. However, a touch of ambiguity in the NTS1 structure is the poor resolution of the carboxy-terminal end of the bound peptide, which is precisely the part of the agonist that seems to be most important for activation of the receptor.

How does neurotensin turn its receptor on? The authors observe several intriguing interactions between amino-acid residues at the receptor's cytoplasmic face; such interactions might have a role in the activation mechanism. This hypothesis can now be tested straightforwardly by altering those residues by making specific mutations in the NTS1-encoding gene. Although the structure clearly shows how NTS1 binds to the peptide on the receptor's extracellular side, how this is translated into the observed active-like conformation at the cytoplasmic face is less clear. It is possible that neurotensin pulls on certain residues on NTS1 (such as arginine 327, see Fig. 1), as happens during the activation of another GPCR, the β2-adrenergic receptor[7–11]. However, the full details of NTS1 activation might be revealed only by a direct comparison of White and colleagues' structure with an inactive-like state — for example, that of NTS1 in complex with an antagonist, a molecule that locks the receptor into an inactive conformation. The structure of such an inactive state is now eagerly awaited.

In summary, the presented NTS1 structure gives an immediate guideline for the design of improved agonists. The neurotensin analogue binds in a concave pocket and establishes mainly hydrophobic contacts with the receptor, rather than extensive hydrogen bonds or electrostatic interactions — characteristics that drug discoverers like to see. If this knowledge can indeed be translated into potent NTS1 agonists (ideally, small non-peptide molecules), White and colleagues' work could be the beginning of the end for the 'poor druggability' mantra commonly associated with peptide-interacting GPCRs. And, because of neurotensin's role as a neurotransmitter in the brain, it might eventually lead to new treatment options for mental disorders such as schizophrenia[1]. ■

Felix Hausch *and* **Florian Holsboer** *are at the Max-Planck Institute of Psychiatry, 80804 Munich, Germany.*
e-mails: hausch@mpipsykl.mpg.de; holsboer@mpipsykl.mpg.de

1. Griebel, G. & Holsboer, F. *Nature Rev. Drug Discov.* **11,** 462–478 (2012).
2. White, J. F. *et al. Nature* **490,** 508–513 (2012).
3. Granier, S. *et al. Nature* **485,** 400–404 (2012).
4. Manglik, A. *et al. Nature* **485,** 321–326 (2012).
5. Thompson, A. A. *et al. Nature* **485,** 395–399 (2012).
6. Wu, H. *et al. Nature* **485,** 327–332 (2012).
7. Hausch, F. *Angew. Chem. Int. Edn Engl.* **47,** 3314–3316 (2008).
8. Rasmussen, S. G. F. *et al. Nature* **469,** 175–180 (2011).
9. Rosenbaum, D. M. *et al. Science* **318,** 1266–1273 (2007).
10. Warne, T. *et al. Nature* **469,** 241–244 (2011).
11. Warne, T. *et al. Nature* **454,** 486–491 (2008).

GENETICS

The inner life of proteins

A quantitative analysis shows that epistasis — the fact that genetic background determines whether a mutation is beneficial, deleterious or inconsequential — is the main factor regulating evolution at the level of proteins. SEE LETTER P.535

GÜNTER P. WAGNER

There is a long-standing controversy in evolutionary biology about the relative importance of 'internal' versus 'external' factors in determining the rate and outcomes of evolution. Is evolution primarily determined by ecology and the environment, or do an organism's own functional and developmental features make a substantial contribution? Now, at least at the level of proteins, it seems we have an answer. On page 535 of this issue, Breen *et al.*[1] present a rigorous statistical analysis of protein sequences that suggests that functional interactions among amino acids are a major determinant of protein-sequence evolution.

Most people are familiar with the principle of adaptive evolution, which underlies Charles Darwin and Alfred Russel Wallace's theories of natural selection. This model describes how organisms change in response to biotic or abiotic variations in their environment — familiar examples include the large body size and white fur of the polar bear, where the body size helps to retain heat and the fur colour provides camouflage. In fact, responses to environmental conditions have been so successful in explaining biological diversity that it became tempting to see adaptation as the only factor determining evolutionary outcomes and patterns. In its extreme, this view leads to what philosophers call the functionalist interpretation of life — the idea that the function of body parts explains their existence and structure.

However, evolutionary biologists know that factors internal to organisms also contribute to biological diversity. Darwin himself discussed the 'law of correlated growth', which states that size changes in various body parts do not occur independently of each other but are subject to limitations that result from the integrated nature of development and growth. In contemporary language, these factors are considered constraints that arise from functional or developmental interdependencies between parts of the organism.

Fundamentally, these constraints manifest themselves as interactions between genes.

Here, a key concept is epistasis, the term used to describe the context dependency of mutation effects — in other words, that the genetic background on which a mutation occurs determines whether the mutation has any effect and, if so, whether it is beneficial or deleterious. A frequently observed manifestation of epistasis occurs between the sex-determining factors (in mammals, the X and Y chromosomes) and some disease risk factors. For instance, in men the ε3/ε2 genotype at the gene encoding the protein ApoE leads to an earlier onset of coronary artery disease, compared to the ε3/ε3 genotype[2]. But in women, no such effect is observed.

In evolutionary theory, however, epistasis has a curious status. One of the pillars of population genetics is the 'fundamental theorem' of natural selection, which says that the response to selection, and thus the process of adaptation, depends only on the context-independent (additive) genetic effects that exist in a population; according to this theory, although epistasis exists, it is simply noise in an otherwise fairly deterministic process[3]. This hypothesis is widely misunderstood, even by many population geneticists, as saying that epistasis is insignificant. Breen and colleagues' results provide a convincing demonstration to the contrary, demonstrating that epistasis is the primary factor affecting the evolution of proteins.

"Amino-acid substitutions will persist, on an evolutionarily relevant timescale, only when the 'correct' amino acids are present elsewhere in the protein."

The authors used an ingenious approach to test how epistatic interdependencies among the amino-acid residues of a protein contribute to the rate at which that protein evolves. They studied the amino-acid sequences of 16 proteins for which sequence information was available, in public databases, for at least 1,000 species. From this analysis they estimated that, on average, each position in a protein accepts around eight alternative amino-acid residues. They then reasoned that, if these alternative amino-acid residues are equally acceptable in the protein, regardless of the amino-acid composition of the rest of the protein — in other words, without epistasis — then the rate of amino-acid evolution should be about 60% of the neutral rate (the rate that would occur if all amino acids were acceptable).

However, they found instead that the rate of protein evolution is only 5% of the neutral rate. After excluding several potential sources of error that could influence this statistic, they conclude that interdependency among different amino-acid residues in a protein is the major factor determining its rate of evolution. This means that, in the vast majority of cases, amino-acid substitutions will persist, on an evolutionarily relevant timescale, only when the 'correct' amino acid, or amino acids, are present elsewhere in the protein.

It follows that internal constraints — not only internal to the organism but internal to each protein — are the dominant factor in determining the rate of protein evolution. If that is true at the level of individual proteins, then it is likely also to be true at the level of the organism. Thus, Breen and colleagues have provided convincing evidence that epistasis should be considered alongside adaptation as a key player in evolution. ■

Günter P. Wagner *is in the Department of Ecology and Evolutionary Biology, and at the Yale Systems Biology Institute, Yale University, New Haven, Connecticut 06477, USA.*
e-mail: gunter.wagner@yale.edu

1. Breen, M. S., Kemena, C., Vlasov, P. K., Notredame, C. & Kondrashov, F. A. *Nature* **490,** 535–538 (2012).
2. Templeton, A. R. in *Epistasis and the Evolutionary Process* (eds Wolf, J. B., Brodie, E. D. III & Wade, M. J.) 41–57 (Oxford Univ. Press, 2000).
3. Fisher, R. A. *The Genetical Theory of Natural Selection* (Clarendon, 1930).

COSMOLOGY

Infrared light from wandering stars

An explanation has been proposed for the observed excess of cosmic light at infrared wavelengths. It invokes stars that are cast into the dark-matter haloes of their parent galaxies during powerful galaxy collisions. SEE LETTER P.514

ANDREA FERRARA

Ever since the collective infrared light from cosmic sources was found[1] to exceed the expected emissions from known galaxies, researchers have considered[2–6] whether the excess might comprise radiation from distant stars and galaxies too faint to be detected individually. However, on page 514 of this issue, Cooray *et al.*[7] suggest instead that the excess signal could be provided largely by nearby stars that were stripped from the main body of their parent galaxies during collisions.

According to the standard Big Bang model, cosmic structures originated from tiny lumps of unseen dark matter in the early Universe that grew large enough to collect the normal (baryonic) matter from which stars eventually formed. On theoretical grounds[8], it is believed that the first stars were 10–100 times more massive than the Sun, because their parent gas clumps would have been poor in metals (elements other than hydrogen and helium), enabling them to avoid fragmentation into smaller clumps.

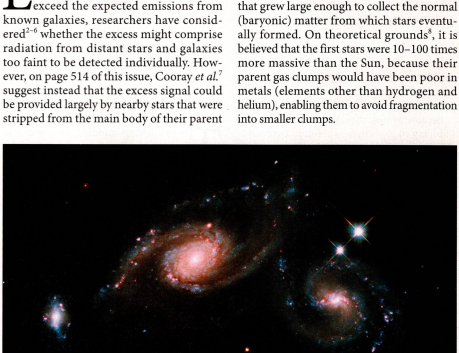

M. LIVIO/HUBBLE HERITAGE TEAM (STSCI/AURA)/ESA/NASA

Figure 1 | Galaxy collision. Cooray *et al.*[7] propose that the observed large-scale excess of cosmic infrared background radiation could be produced by stars that were thrown into the outer reaches of their parent galaxies during galaxy collisions such as the one shown here.

Searching for the first stars and, more generally, for the first generations of galaxies that might have hosted them, is a primary function for many current and future telescopes. Knowledge of the first stars would shed light on our origins, and allow researchers to refine the Big Bang model. Over the past decade, we have witnessed remarkable progress in the discovery of ever more distant galaxies, with the record-holder updated almost monthly. Deep images from the Hubble Space Telescope's infrared camera WFC3 — which has exquisite sensitivity and a relatively wide field of view — routinely reveal[9,10] candidate galaxies at early cosmic epochs. And, whenever possible, these candidates are subsequently confirmed using spectroscopic observations.

However, there is evidence to suggest that the observed early-epoch galaxies alone could not have provided the radiation that was required to 'reionize' hydrogen atoms, an event that was complete by about 1 billion years after the Big Bang[11,12]. It is therefore possible that astronomers are observing only the most luminous objects in an underlying population of faint galaxies.

How can this hypothesis be tested? This is where the collective infrared light from cosmic sources, or the cosmic infrared background (CIB), comes in. Measurements of the CIB intensity, or more precisely its fluctuations, could potentially be used to detect the combined emissions from a population of faint galaxies. Even after removal of the infrared light from known galaxies, the CIB intensity is not perfectly uniform across the sky: it shows fluctuations in different directions of about 10% around the mean, indicating that the underlying sources of the signal gather into clusters. The degree to which these sources cluster as a function of their angular separation on the sky is encoded in a mathematical quantity known as the angular power spectrum. However, the CIB intensity is contaminated by sunlight reflected by local interplanetary dust in the Solar System — the zodiacal light. The detection of a faint-galaxy population from CIB fluctuation measurements is therefore dependent on the accurate subtraction of this light.

Previous high-resolution infrared images taken with the Spitzer Space Telescope[13,14] and the AKARI satellite[15] have made it possible to measure such fluctuations and to subtract the contribution of the zodiacal light reliably. These observations have revealed that the angular power spectrum, and thus the clustering strength, increases towards large angular distances on the sky, up to one degree. This increase cannot be accounted for solely by the light produced by known galaxies[16].

In their study, Cooray *et al.* analyse recent deep images from Spitzer and detect the same increase in clustering strength. What's more, they demonstrate that the increase cannot be explained by either of two existing hypotheses — one based on a contribution from a population of faint, distant galaxies during the cosmic 'reionization' epoch[17–20], and another that invokes dwarf galaxies at intermediate distances from Earth. Intriguingly, however, the shape of the power spectrum is consistent with the distant-galaxy hypothesis.

What, then, is producing these large-scale CIB fluctuations? Cooray and colleagues propose that the source of this signal is light from intrahalo stars of known galaxies — that is, stars that have been stripped from the main body of their parent galaxies and cast into the galaxies' dark-matter haloes during galaxy collisions (Fig. 1). As interesting and plausible as it is, this explanation is based heavily on the poorly understood abundance and spectral energy distribution of intrahalo stars. In contrast to the distant-galaxy hypothesis, this model also predicts fluctuations induced by intrahalo stars in the visible part of the electromagnetic spectrum, in which the light from the first galaxies is blanketed by intervening intergalactic neutral hydrogen.

It will be interesting to see whether the authors' proposal stands up to scrutiny. However, the most exciting endeavour will be to isolate the CIB signal produced by the faint, reionizing galaxies and thereby make them amenable to study. Because this signal is buried under the putative signal of the intrahalo stars, it will be necessary to accurately remove this 'foreground' before that goal can be attained. ■

Andrea Ferrara *is in the Classe di Scienze, Scuola Normale Superiore, Pisa 56126, Italy. e-mail: andrea.ferrara@sns.it*

1. Matsumoto, T. *et al.* in *ISO Surveys of a Dusty Universe* Vol. 548 (eds Lemke, D., Stickel, M. & Wilke, K.) (Springer, 2000).
2. Salvaterra, R. & Ferrara, A. *Mon. Not. R. Astron. Soc.* **339,** 973–982 (2003).
3. Santos, M. R., Bromm, V. & Kamionkowski, M. *Mon. Not. R. Astron. Soc.* **336,** 1082–1092 (2002).
4. Madau, P. & Silk, J. *Mon. Not. R. Astron. Soc.* **359,** L37–L41 (2005).
5. Kashlinsky, A. *Astrophys. J.* **633,** L5–L8 (2005).
6. Fernandez, E. R. & Komatsu, E. *Astrophys. J.* **646,** 703–718 (2006).
7. Cooray, A. *et al. Nature* **490,** 514–516 (2012).
8. Greif, T. H. *et al. Mon. Not. R. Astron. Soc.* **424,** 399–415 (2012).
9. Bouwens, R. J. *et al. Astrophys. J.* **752,** L5 (2012).
10. McLure, R. J. *et al. Mon. Not. R. Astron. Soc.* **418,** 2074–2105 (2011).
11. Mitra, S., Choudhury, T. R. & Ferrara, A. *Mon. Not. R. Astron. Soc.* **419,** 1480–1488 (2012).
12. Finkelstein, S. L. *et al.* Preprint at http://arXiv.org/abs/1206.0735 (2012).
13. Kashlinsky, A., Arendt, R. G., Mather, J. & Moseley, S. H. *Nature* **438,** 45–50 (2005).
14. Kashlinsky, A. *et al. Astrophys. J.* **753,** 63 (2012).
15. Matsumoto, T. *et al. Astrophys. J.* **742,** 124 (2011).
16. Helgason, K., Ricotti, M. & Kashlinsky, A. *Astrophys. J.* **752,** 113 (2012).
17. Salvaterra, R. & Ferrara, A. *Mon. Not. R. Astron. Soc.* **367,** L11–L15 (2006).
18. Cooray, A. *et al.* Preprint at http://arXiv.org/abs/1205.2316 (2012).
19. Fernandez, E. R., Iliev, I. T., Komatsu, E. & Shapiro, P. R. *Astrophys. J.* **750,** 20 (2012).
20. Yue, B., Ferrara, A., Salvaterra, R. & Chen, X. Preprint at http://arXiv.org/abs/1208.6234 (2012).

50 Years Ago

Nuclear explosions in space produce negligible effects on the Earth, for example, a distinctly decreased intensity of fall-out; they produce more significant perturbations of the upper atmosphere, but these are very temporary (measured in hours). It is in near-space itself where very noticeable effects can be produced which can last for many months because of the presence of the Earth's magnetic field. It is evident that weapons tests in space can have important scientific by-products. The most interesting are the creation of a thin shell of 2-MeV fission electrons . . . as well as the creation of a thick belt of low-energy protons from fusion neutrons. It will probably be desirable to monitor these artificial radiation belts with quite sophisticated energy-resolving detectors, to suppress the naturally trapped radiation, as well as the much larger changes (of factors of 10–100 and even higher) produced by such natural events as solar flares and magnetic storms.
From *Nature* 27 October 1962

100 Years Ago

American naturalists are delighted by the announcement that Mrs. Russell Sage, widow of the late well-known Wall Street financier, has purchased Marsh Island, off the coast of Louisiana, in order to make it a perpetual bird sanctuary … The island in question is about 75,000 acres in extent. It is a sylvan labyrinth affording shelter and food to hundreds of thousands of wild birds which resort to it in winter when the northern lakes and streams are locked fast under ice. For this reason it has been the great killing ground for the markets of New Orleans, St. Louis, Cincinnati, and Chicago, no fewer than seventy market gunners being regularly employed there every winter.
From *Nature* 24 October 1912

ACS Catalysis

The Best in Biocatalysis >>>

Editor-in-Chief:
Christopher W. Jones
Georgia Institute of Technology

Associate Editor:
Huimin Zhao
University of Illinois at Urbana-Champaign

HIGHLIGHTS IN BIOCATALYSIS

REVIEWS

ω-Transaminases for the Production of Optically Pure Amines and Unnatural Amino Acids
Sam Mathew and Hyungdon Yun
DOI: 10.1021/cs300116n

Tuning P450 Enzymes as Oxidation Catalysts
Rudi Fasan
DOI: 10.1021/cs300001x

LETTERS

Light-Driven, Quantum Dot-Mediated Regeneration of FMN To Drive Reduction of Ketoisophorone by Old Yellow Enzyme
Tarak Nath Burai, Aram Joel Panay, Haiming Zhu, Tianquan Lian, and Stefan Lutz
DOI: 10.1021/cs300085h

Harnessing Protein Symmetry for Enzyme Design
Bigna Wörsdörfer, Lisa M. Henning, Richard Obexer, and Donald Hilvert
DOI: 10.1021/cs300076t

ARTICLES

Computational Evidence for the Catalytic Mechanism of Human Glutathione S-Transferase A3-3: A QM/MM Investigation
Matteo Calvaresi, Marco Stenta, Marco Garavelli, Piero Altoé, and Andrea Bottoni
DOI: 10.1021/cs200369b

Dynamic Kinetic Resolution Process Employing Haloalkane Dehalogenase
Alja Westerbeek, Wiktor Szymański, Ben L. Feringa, and Dick B. Janssen
DOI: 10.1021/cs2003565

For the latest high-impact research in all fields of catalysis, go to: pubs.acs.org/catalysis

ACS Publications
MOST TRUSTED. MOST CITED. MOST READ.

ARTICLE

doi:10.1038/nature11532

A map of rice genome variation reveals the origin of cultivated rice

Xuehui Huang[1]*, Nori Kurata[2]*, Xinghua Wei[3]*, Zi-Xuan Wang[1,2]*, Ahong Wang[1], Qiang Zhao[1], Yan Zhao[1], Kunyan Liu[1], Hengyun Lu[1], Wenjun Li[1], Yunli Guo[1], Yiqi Lu[1], Congcong Zhou[1], Danlin Fan[1], Qijun Weng[1], Chuanrang Zhu[1], Tao Huang[1], Lei Zhang[1], Yongchun Wang[1], Lei Feng[4], Hiroyasu Furuumi[2], Takahiko Kubo[2], Toshie Miyabayashi[2], Xiaoping Yuan[3], Qun Xu[3], Guojun Dong[3], Qilin Zhan[1], Canyang Li[1], Asao Fujiyama[2], Atsushi Toyoda[2], Tingting Lu[1], Qi Feng[1], Qian Qian[3], Jiayang Li[4] & Bin Han[1,5]

Crop domestications are long-term selection experiments that have greatly advanced human civilization. The domestication of cultivated rice (*Oryza sativa* L.) ranks as one of the most important developments in history. However, its origins and domestication processes are controversial and have long been debated. Here we generate genome sequences from 446 geographically diverse accessions of the wild rice species *Oryza rufipogon*, the immediate ancestral progenitor of cultivated rice, and from 1,083 cultivated *indica* and *japonica* varieties to construct a comprehensive map of rice genome variation. In the search for signatures of selection, we identify 55 selective sweeps that have occurred during domestication. In-depth analyses of the domestication sweeps and genome-wide patterns reveal that *Oryza sativa japonica* rice was first domesticated from a specific population of *O. rufipogon* around the middle area of the Pearl River in southern China, and that *Oryza sativa indica* rice was subsequently developed from crosses between *japonica* rice and local wild rice as the initial cultivars spread into South East and South Asia. The domestication-associated traits are analysed through high-resolution genetic mapping. This study provides an important resource for rice breeding and an effective genomics approach for crop domestication research.

Cultivated rice (*Oryza sativa* L.), which is grown worldwide and is one of the most important cereals for human nutrition, is considered to have been domesticated from wild rice (*Oryza rufipogon*) thousands of years ago[1–4]. The differences between *O. sativa* and *O. rufipogon* are reflected in a wide range of morphological and physiological traits[5–9]. Despite the fact that rice is a major cereal and a model system for plant biology, the evolutionary origins and domestication processes of cultivated rice have long been debated. The puzzles about rice domestication include: (1) where the geographic origin of cultivated rice was, (2) which types of *O. rufipogon* served as its direct wild progenitor, and (3) whether the two subspecies of cultivated rice, *indica* and *japonica*, are derived from a single or multiple domestications.

A wide range of genetic and archaeological studies have been carried out to examine the phylogenetic relationships of rice, and investigate the demographic history of rice domestication[10–19]. Molecular phylogenetic analyses indicated that *indica* and *japonica* originated independently[3,10,20]. However, the well-characterized domestication genes in rice were found to be fixed in both subspecies with the same alleles, thus supporting a single domestication origin[6–9,16]. Recently, a demographic analysis of single-nucleotide polymorphisms (SNPs) detected from 630 gene fragments suggested a single domestication origin of rice[17]. Meanwhile, population genetics analyses of genome-wide data of cultivated and wild rice have tended to suggest that *indica* and *japonica* genomes generally appear to be of independent origin[18,19], but many genomic segments bearing domestication alleles may have originated only once[18]. Despite these advances, wider sampling with population-scale whole-genome sequencing is needed to shed greater light on the evolutionary history of rice domestication. An in-depth investigation of the haplotype structure near the domestication sites will be critical for evaluating the direction of introgression. The specific ancestral population and the subsequent demographic event are yet to be identified.

Moreover, a comprehensive map of rice genome variation will facilitate genetic mapping of complex traits in rice. We recently collected diverse rice cultivars for sequencing, and carried out genome-wide association studies (GWAS) for many agronomic traits in cultivated rice[21,22]. Here we sequenced and analysed the genomes of 446 *O. rufipogon* accessions to investigate the phylogenetic relationships between cultivated and wild rice and identify the signatures of selection in rice domestication. This research also provides a robust foundation that will enable rice breeders to effectively exploit diverse genetic resources for rice improvement.

Analysis of wild rice populations

The strategy of this study is briefly described in Supplementary Fig. 1. The genus *Oryza* consists of 23 species[23,24], and the wild rice *O. rufipogon* is believed to be the immediate progenitor of the cultivated rice *O. sativa* (Supplementary Fig. 2 and Supplementary Table 1). From large collections of wild rice germplasm maintained in China and Japan, we selected 446 diverse *O. rufipogon* accessions including both perennial and annual (also called as *Oryza nivara*) forms from Asia and Oceania, spanning the native geographic range of the species (Supplementary Tables 2 and 3). We sequenced these accessions with twofold genome coverage. After aligning the reads against the rice reference genome sequence, we identified a total of 5,037,497 non-singleton SNPs. Based on the SNP data, the sequence diversity (π) of *O. rufipogon*

[1]National Center for Gene Research, Institute of Plant Physiology and Ecology, Shanghai Institutes for Biological Sciences, Chinese Academy of Sciences, Shanghai 200233, China. [2]Plant Genetics Laboratory and Comparative Genomics Laboratory, National Institute of Genetics, Mishima, Shizuoka 411-8540, Japan. [3]State Key Laboratory of Rice Biology, China National Rice Research Institute, Chinese Academy of Agricultural Sciences, Hangzhou 310006, China. [4]National Center for Plant Gene Research, State Key Laboratory of Plant Genomics, Institute of Genetics and Developmental Biology, Chinese Academy of Sciences, Beijing 100101, China. [5]Beijing Institute of Genomics, Chinese Academy of Sciences, Beijing 100029, China.
*These authors contributed equally to this work.

was estimated at ~0.003, which is higher than that in *O. sativa*—the sequence diversity is 0.0024 for *O. sativa*, and 0.0016 and 0.0006 for *indica* and *japonica*, respectively[21]. Approximately 82% of SNPs (minor allele frequency > 0.05) segregating in *O. rufipogon* also segregate in *O. sativa* (Supplementary Table 4). This observation is consistent with previous suggestions that part of the genetic diversity in the progenitor would be lost because only a limited number of individuals were used during domestication[11,25].

We investigated the population structure of the *O. rufipogon* accessions. On the basis of the neighbour-joining tree, as well as principal-component analysis (PCA), we classified the *O. rufipogon* species into three types, simply designated as Or-I, Or-II and Or-III in this study (Fig. 1a and Supplementary Fig. 3). We found that the rice population structure strongly correlated with geographic distribution ($r^2 = 0.2$ between the first principal component and the longitude, and $r^2 = 0.3$ between the second principal component and the latitude)[26]. Interestingly, the *O. rufipogon* accessions sampled from southern China mostly belong to the Or-III type (Fig. 1b and Supplementary Fig. 4). The level of population differentiation, F_{ST}, was estimated at 0.18 among the groups of *O. rufipogon*, which is much lower than that of *O. sativa* (~0.55 on average[21]). The differentiation was not evenly distributed across the rice genome (Supplementary Fig. 5). We scanned the whole genome for highly differentiated loci and found 68 loci with $F_{ST} > 0.3$, which covered ~3% of the complete rice genome (Supplementary Table 5). Of these loci, we found several known genes or quantitative trait loci (QTLs) that included *DPL2* (hybrid incompatibility[27]) (Fig. 1c), *OsSOC1* and *Ghd7* (flowering time[28–30]) and *qCTS12* (cold tolerance[31]), all of which have been reported to be closely related to *indica–japonica* differentiation in rice. Hence, the highly differentiated loci can provide important clues for searching the genes involved in local adaptation.

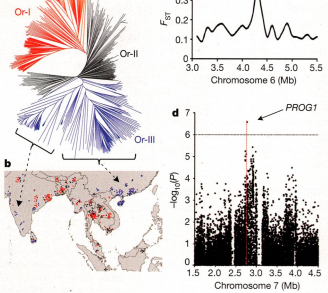

Figure 1 | Genetic structure and association analysis in the wild rice population. a, Neighbour-joining tree of 446 *O. rufipogon* accessions, which was calculated from ~5 million SNPs, identifies the three groups of Or-I (red), Or-II (grey) and Or-III (blue). **b**, Geographic origins of wild rice accessions. **c**, The level of genetic differentiation (F_{ST}) in *O. rufipogon* population around the *DPL2* gene that underlies *indica–japonica* hybrid incompatibility in rice. **d**, Regional Manhattan plots of GWAS for tiller angle in *O. rufipogon* population identify a known gene, *PROG1*, using a compressed mixed linear model. The genome-wide significance threshold (1×10^{-6}) and the position of the peak SNP are indicated by a horizontal dash-dot line and a vertical red line, respectively.

Because *O. rufipogon* is an out-crossing species, it was expected to have a relatively high decay rate of linkage disequilibrium. We found that the decay rate of linkage disequilibrium in *O. rufipogon*, expressed as r^2, dropped to half of its maximum value at ~20 kilobases (kb) on average (Supplementary Fig. 6), which is much more rapid than that in *O. sativa* (~123 kb and ~167 kb in *indica* and *japonica*, respectively)[21]. To perform GWAS in *O. rufipogon*, we used the *k*-nearest neighbour algorithm for data imputation (Supplementary Table 6), and phenotyped the *O. rufipogon* population for two traits, leaf sheath colour and tiller angle. The strongest associations for sheath colour and tiller angle were found to be just around the known loci *OsC1*, for colouration[32], and *PROG1*, for prostrate growth[7,8] (Fig. 1d and Supplementary Figs 7–9). Through computational simulations we predicted that the mapping resolution of GWAS in *O. rufipogon* was approximately three times greater than that in *O. sativa* on average (Supplementary Figs 10–12). Hence, the wild rice population and accompanying comprehensive sequence resource should be of great utility for directly dissecting agronomic traits in rice.

Phylogenetic relationships of rice

We used whole-genome sequencing data for a large panel of accessions containing 446 *O. rufipogon* accessions and 1,083 *O. sativa* varieties to explore their phylogenetic relationships. The 1,083 diverse *O. sativa* varieties were collected throughout the world and sequenced with one-fold genome coverage (Supplementary Table 7). Of these, 950 genomes had previously been reported[21,22], and the remaining 133 genomes, including many representative varieties (for example, *aromatic* rice), were sequenced and first reported in this study. A total of 7,970,359 non-singleton SNPs were identified from the 1,529 genome sequences. To determine the ancestral states of the SNPs, the close relatives of *O. rufipogon* and *O. sativa* were also sequenced with a total of approximately 50-fold genome coverage (Supplementary Table 8). Using genome sequences of these outgroups, we were able to identify the ancestral states of 6,119,311 SNPs out of the approximately 8 million SNPs (77%).

We used the genotype data set of the ~8 million SNP sites from 1,529 genomes to infer genome-wide relationships. Both the phylogenetic tree and the PCA plots indicate that *O. sativa indica* and *japonica* are descended from Or-I and Or-III, respectively (Fig. 2a and Supplementary Fig. 13). We then investigated the detailed relationship between *indica* and Or-I and that between *japonica* and Or-III separately (Supplementary Figs 14–16). The level of genetic differentiation between *indica* and Or-I was modest ($F_{ST} = 0.17$), and *indica* contains approximately 75% of the genetic diversity in Or-I (Fig. 2b). A small number of *indica* and Or-I accessions seemed to be intermediate between cultivated and wild rice (Fig. 2a). In contrast, the *japonica* groups (*temperate japonica*, *tropical japonica* and *aromatic*) were all clustered together, and had descended from wild rice in southern China (sub-clade Or-IIIa). There was an obvious genetic distinction between *japonica* and Or-IIIa (Fig. 2a), which had a relatively high level of population differentiation ($F_{ST} = 0.36$). We found that only approximately 33% of the genetic diversity of Or-III persisted in *japonica* (Fig. 2b). The strong genetic bottleneck indicates that a small effective population from Or-III was used for domesticating *japonica* cultivars.

On the basis of our SNP data, most sequence variants observed between *indica* and *japonica*, which were estimated to have diverged hundreds of thousands of years ago[20], already existed in the progenitor gene pools. However, the differentiation was enhanced during domestication, with F_{ST} expanding from 0.18 in *O. rufipogon* to 0.55 in *O. sativa* (Fig. 2b). The high level of genetic differentiation between *indica* and *japonica* has resulted from a combination of the modest differentiation present within their ancestor population and the recent domestication bottleneck (Fig. 2c). For example, at the causal SNP site for *GS3* (a major QTL for grain shape[33,34]), the null allele mainly existed in the wild rice populations in the Guangxi and Guangdong provinces of southern China. This allele rapidly extended to become the major

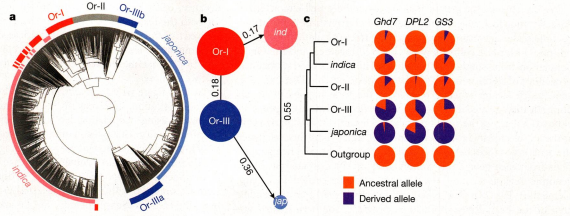

Figure 2 | Genome-wide relationship between cultivated rice and its wild progenitor. **a**, Phylogenetic tree of the full population (446 *O. rufipogon* accessions and 1,083 *O. sativa* varieties) calculated from ~8 million SNPs in *O. rufipogon* and *O. sativa*. The double-layer rings indicate *O. rufipogon* (outer ring: Or-I, Or-II and Or-III are coloured in red, grey and blue, respectively) and *O. sativa* (inner ring: *indica* and *japonica* subspecies are in pink and sky blue, respectively). **b**, Illustration of genetic diversity and population differentiation in *O. rufipogon* and *O. sativa*. The size of the circles represents the level of genetic diversity (π) of the groups, and the F_{ST} values between the groups are indicated. *ind*, *indica*; *jap*, *japonica*. **c**, The spectrum of allele frequencies at the causal polymorphisms of *Ghd7*, *DPL2* and *GS3*.

allele (~98%) in the *japonica* population, thus generating a distinct phenotypic difference between *indica* and *japonica*. We screened all SNPs that were highly differentiated in frequency between *indica* and *japonica*, and found a total of 213,188 *indica*–*japonica*-differentiated SNPs. With regard to the differentiated SNPs, the differences present within the *O. rufipogon*, the domestication bottleneck in *japonica* and in *indica* were estimated to contribute ~50%, ~40% and ~10% of total alterations in allele frequency, respectively (Supplementary Fig. 17).

We examined the ancestral states of *indica*–*japonica*-fixed SNPs, and found that 55% of SNPs of the ancestral alleles are fixed in *indica* and the other 45% are fixed in *japonica*. The dN/dS ratio (dN, number of non-synonymous substitutions per non-synonymous site; dS, number of synonymous substitutions per synonymous site) of the SNPs was calculated to be 0.34, which was almost equal to the average level of the total SNPs. In contrast, for the 9,595 SNPs that were fixed between *O. rufipogon* and *O. sativa*, the ancestral alleles of 93.3% SNPs are identical to *O. rufipogon*, indicating that *O. rufipogon* has retained more ancestral states than *O. sativa*, which also further supported our conclusion that *O. rufipogon* is likely to be the ancestral progenitor of *O. sativa*. The dN/dS ratio of the fixed SNPs between *O. rufipogon* and *O. sativa* is calculated to be 1.04, indicating positive selection during domestication ($P < 0.001$, chi-square test).

Screens and annotation of domestication loci

Selective signatures from domestication include a reduction in nucleotide diversity and altered allele frequency in the domestication loci[19,25]. We measured the ratio of the genetic diversity in wild rice to that in cultivated rice (π_w/π_c) across the rice genome, and determined the cutoff on the basis of permutation tests (Supplementary Information section 2). We performed whole-genome screening in *indica*, *japonica* and the full population using the diversity ratios (Fig. 3 and Supplementary Figs 18–20). In total we identified 60 loci in *indica*, 62 in *japonica* and 55 in the full population (Supplementary Tables 9–11). We noticed that many loci with strong signals of selection were nearly identical in both *indica* and *japonica* where F_{ST} between *indica* and *japonica* was extremely low, indicating that introduction of traits during domestication has in many cases involved introgression events. We noted that most well-characterized domestication genes, including *Bh4* (hull colour[9]), *PROG1* (tiller angle[7,8]), *sh4* (seed shattering[5,6]), *qSW5* (grain width[35]) and *OsC1* (leaf sheath colour and apiculus colour[33]), were among the 55 loci detected in the full population (Fig. 3). Another three well-characterized domestication genes, *qSH1* for seed shattering[36], *Waxy* for grain quality[37] and *Rc* for pericarp colour[38,39], which showed strong selection signals in the *japonica* panel, were not fully shared in the *indica* population.

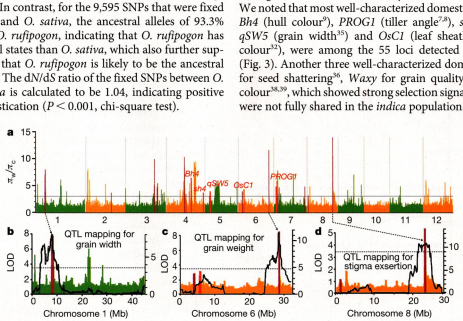

Figure 3 | Whole-genome screening and functional annotations of domestication sweeps. **a**, Whole-genome screening of domestication sweeps in the full population of *O. rufipogon* and *O. sativa*. The values of π_w/π_c are plotted against the position on each chromosome. The horizontal dashed line indicates the genome-wide threshold of selection signals ($\pi_w/\pi_c > 3$). **b**–**d**, A large-scale high-resolution mapping for fifteen domestication-related traits was performed in an *O. rufipogon* × *O. sativa* population. The domestication sweeps overlapped with characterized domestication-related QTLs are shown in dark red, and the loci with known causal genes are shown in red. Among them, three strong selective sweeps were found to be associated with grain width (**b**), grain weight (**c**) and exserted stigma (**d**), respectively. In **b**–**d**, the likelihood of odds (LOD) values from the composite interval mapping method are plotted against position on the rice chromosomes. Grey horizontal dashed line indicates the threshold (LOD > 3.5).

We investigated the genetic patterns around the well-characterized domestication loci, which were quite different from those at the whole-genome scale. According to phylogenetic trees calculated from SNPs on these loci, most cultivars were clustered together, and the Or-III population from southern China tended to be the closest ancestral progenitor of all the cultivars (Supplementary Fig. 21). These patterns were much clearer when expanded to the total regions of the 55 domestication-related loci (Fig. 4a). The *indica* cultivars were generally close to Or-I across the genome, but were closer to Or-IIIa than to Or-I at the 55 selected loci (Supplementary Fig. 22). We further calculated the genetic distances between cultivated rice and the wild rice populations from each geographic sampling region through analysis of the genomic regions around the 55 domestication-related loci (Supplementary Fig. 23). Our genetic approach showed that the middle area of the Pearl River in Guangxi province, southern China, was probably the place of the first development of cultivated rice (Fig. 4b–d), although an archaeological finding had identified the Lower Yangtze region in eastern China as one of the centres of rice cultivation[14,15]. These results suggest a model in which *japonica* was first domesticated from Or-III in southern China, and was subsequently crossed to local wild rice in South East Asia and South Asia, thus generating *indica* after many cross-differentiation-selection cycles (Fig. 4e). Furthermore, we performed computational simulations to generate *in silico* data sets under various demographic scenarios (Supplementary Fig. 24), using the forward simulator SFS_CODE[40] (Supplementary Information section 5). We calculated the genetic distances of *indica* and *japonica* with different clades of *O. rufipogon* for both the real and simulated data (Supplementary Fig. 25), which showed that there were significant differences between the real data and the simulated ones in all the scenarios except for the model proposed here ($P < 0.01$, rank sum test), providing further support for the model that we propose.

To investigate why these chromosomal loci were selected during rice domestication, QTL mapping of domestication-related traits was performed using a population that was developed from a cross between *O. sativa indica* Guanghui-4 and *O. rufipogon* (Or-IIIa accession W1943). Using a sequencing-based genotyping method[41], we sequenced 271 lines in the population with 0.5× coverage for each, and constructed an ultra-dense genotype map. A total of 15 domestication-related traits were phenotyped, with 58 QTLs detected using a composite interval mapping method (Supplementary Fig. 26 and Supplementary Tables 12, 13). For ten QTLs for which causal genes have been reported, almost all the peak signals were within 200 kb from the known genes, indicating that a high mapping resolution was achieved (Supplementary Fig. 27).

Of the 58 QTLs detected, 32 QTLs were located within domestication sweeps (Fig. 3b–d and Supplementary Figs 28–30). The overlap of the QTLs for domestication traits with domestication sweeps is very significant ($P < 0.001$, chi-square test). Among them, the QTLs for traits like exserted stigma (controlling mating system) and grain size (controlling output yield) show stronger signals than those for shattering (*sh4*) and plant architecture (*PROG1*). Mating systems have been proposed to have a fundamental part in crop domestication[42,43]. We identified three major loci and two minor loci responsible for exserted stigma, and found that all the five QTLs were located within domestication sweeps.

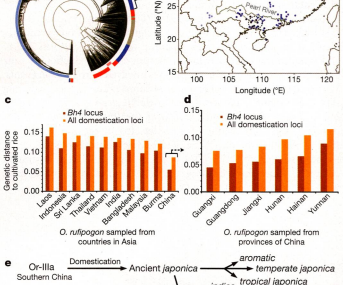

Figure 4 | Genetic and geographic origins of rice domestication. **a**, Phylogenetic tree of 446 *O. rufipogon* accessions and 1,083 *O. sativa* varieties calculated from SNPs in the overall regions of the 55 major domestication sweeps. **b**, Geographic locations of 62 *O. rufipogon* accessions, whose phylogenetic positions during domestication are indicated. Colour index represents the average of the genetic distance of *O. rufipogon* accessions to all cultivated rice accessions. Two major rivers in southern China are labelled in grey in the map. **c**, The average distance of *O. rufipogon* accessions from different countries to all cultivars. The distance was estimated by simple matching distance of SNPs around the *Bh4* locus or all SNPs within the 55 domestication sweeps. **d**, The average distance of *O. rufipogon* accessions from different provinces in southern China to all cultivars. **e**, Schematics of the origin of cultivated rice. The *aus* and *aromatic* rice are minor groups of rice accessions with small geographic distributions.

Identification of domestication-associated variants

Characterization of domestication-associated genes and their genetic variation relies on high-quality genome sequences of both the cultivated species and its immediate progenitor[44,45]. Hence, we further sequenced the *O. rufipogon* accession W1943 with 100-fold genome coverage and carried out *de novo* genome assembly. The total length of the assembly is 406 megabases (Mb) and the N50 length of the initial contigs was 16 kb. After aligning the assembly against the reference genome of cultivated rice, we identified 2,621,077 SNPs, 619,132 small indels and 140,075 structural variants of large size (Supplementary Table 14). We examined the sequence variants for their potential effects on protein coding, and identified a total of 128,010 non-synonymous SNPs and 49,236 sequence variants with large effect. Moreover, we surveyed the allele information at all the polymorphic sites across all rice accessions, and constructed a comprehensive sequence-variant frequency spectrum map.

We investigated the patterns of sequence polymorphism to detect variants that affect gene coding and have differential frequency in different populations. For the domestication loci with well-characterized genes, this approach allowed us to narrow down the causative polymorphism to a limited number of sequence variants (Supplementary Figs 31–34). For the domestication loci for which known genes have not yet been identified, we found a total of 273 novel functional variants within 204 genes that showed high differentiation in allele frequencies between cultivated and wild rice (Supplementary Table 15). Moreover, we identified 305 sequence variants in the promoter regions with a differential frequency between cultivated and wild rice (Supplementary Table 16), and 1,120 functional variants that were fixed in either *japonica* or *indica* panel (Supplementary Tables 17 and 18).

Discussion

Our study has provided new insights into how and where rice was likely to be domesticated, and we have identified a set of domestication sweeps and putative causal genes. Such endeavours will be enhanced by continuing improvements in assembly and annotation of wild rice

genome sequences, generation of functional genomics data sets of wild rice[46], advances in mapping of rice domestication traits[47], and biological follow-up of the putative causal genes. The understanding of past domestication, including the selections on critical traits and the recent rapid speciation, will further guide future breeding efforts[48]. Moreover, the great diversity in the wild rice populations, which have much more natural allelic variation than domesticated rice, will further facilitate breeding to modify crops in the post-domestication era.

METHODS SUMMARY

The cultivated and wild rice accessions were all from large collections of rice accessions preserved at the China National Rice Research Institute in Hangzhou, China, and the National Institute of Genetics in Mishima, Japan. The DNA samples were sequenced on the Illumina Genome Analyzer IIx or HiSeq2000.

Full Methods and any associated references are available in the online version of the paper.

Received 18 January; accepted 20 August 2012.
Published online 3 October 2012.

1. Oka, H. I. *Origin of cultivated rice.* (Japan Scientific Societies Press, 1988).
2. Khush, G. S. Origin, dispersal, cultivation and variation of rice. *Plant Mol. Biol.* **35,** 25–34 (1997).
3. Cheng, C. *et al.* Polyphyletic origin of cultivated rice: based on the interspersion pattern of SINEs. *Mol. Biol. Evol.* **20,** 67–75 (2003).
4. Fuller, D. Q. *et al.* Consiliience of genetics and archaeobotany in the entangled history of rice. *Archaeol. Anthropol. Sci.* **2,** 115–131 (2010).
5. Li, C., Zhou, A. & Sang, T. Genetic analysis of rice domestication syndrome with the wild annual species, *Oryza nivara*. *New Phytol.* **170,** 185–194 (2006).
6. Li, C., Zhou, A. & Sang, T. Rice domestication by reducing shattering. *Science* **311,** 1936–1939 (2006).
7. Jin, J. *et al.* Genetic control of rice plant architecture under domestication. *Nature Genet.* **40,** 1365–1369 (2008).
8. Tan, L. *et al.* Control of a key transition from prostrate to erect growth in rice domestication. *Nature Genet.* **40,** 1360–1364 (2008).
9. Zhu, B. F. *et al.* Genetic control of a transition from black to straw-white seed hull in rice domestication. *Plant Physiol.* **155,** 1301–1311 (2011).
10. Londo, J. P., Chiang, Y. C., Hung, K. H., Chiang, T. Y. & Schaal, B. A. Phylogeography of Asian wild rice, *Oryza rufipogon*, reveals multiple independent domestications of cultivated rice, *Oryza sativa*. *Proc. Natl Acad. Sci. USA* **103,** 9578–9583 (2006).
11. Caicedo, A. L. *et al.* Genome-wide patterns of nucleotide polymorphism in domesticated rice. *PLoS Genet.* **3,** e163 (2007).
12. Kovach, M. J., Sweeney, M. T. & McCouch, S. R. New insights into the history of rice domestication. *Trends Genet.* **23,** 578–587 (2007).
13. Sang, T. & Ge, S. The puzzle of rice domestication. *J. Integr. Plant Biol.* **49,** 760–768 (2007).
14. Zong, Y. *et al.* Fire and flood management of coastal swamp enabled first rice paddy cultivation in east China. *Nature* **449,** 459–462 (2007).
15. Fuller, D. Q. *et al.* The domestication process and domestication rate in rice: spikelet bases from the Lower Yangtze. *Science* **323,** 1607–1610 (2009).
16. Zhang, L. B. *et al.* Selection on grain shattering genes and rates of rice domestication. *New Phytol.* **184,** 708–720 (2009).
17. Molina, J. *et al.* Molecular evidence for a single evolutionary origin of domesticated rice. *Proc. Natl Acad. Sci. USA* **108,** 8351–8356 (2011).
18. He, Z. *et al.* Two evolutionary histories in the genome of rice: the roles of domestication genes. *PLoS Genet.* **7,** e1002100 (2011).
19. Xu, X. *et al.* Resequencing 50 accessions of cultivated and wild rice yields markers for identifying agronomically important genes. *Nature Biotechnol.* **30,** 105–111 (2012).
20. Ma, J. & Bennetzen, J. L. Rapid recent growth and divergence of rice nuclear genomes. *Proc. Natl Acad. Sci. USA* **101,** 12404–12410 (2004).
21. Huang, X. *et al.* Genome-wide association studies of 14 agronomic traits in rice landraces. *Nature Genet.* **42,** 961–967 (2010).
22. Huang, X. *et al.* Genome-wide association study of flowering time and grain yield traits in a worldwide collection of rice germplasm. *Nature Genet.* **44,** 32–39 (2012).
23. Ge, S., Sang, T., Lu, B. R. & Hong, D. Y. Phylogeny of rice genomes with emphasis on origins of allotetraploid species. *Proc. Natl Acad. Sci. USA* **96,** 14400–14405 (1999).
24. Vaughan, D. A., Morishima, H. & Kadowaki, K. Diversity in the *Oryza* genus. *Curr. Opin. Plant Biol.* **6,** 139–146 (2003).
25. Doebley, J. F., Gaut, B. S. & Smith, B. D. The molecular genetics of crop domestication. *Cell* **127,** 1309–1321 (2006).
26. Novembre, J. & Stephens, M. Interpreting principal component analyses of spatial population genetic variation. *Nature Genet.* **40,** 646–649 (2008).
27. Mizuta, Y., Harushima, Y. & Kurata, N. Rice pollen hybrid incompatibility caused by reciprocal gene loss of duplicated genes. *Proc. Natl Acad. Sci. USA* **107,** 20417–20422 (2010).
28. Tadege, M. *et al.* Reciprocal control of flowering time by *OsSOC1* in transgenic *Arabidopsis* and by *FLC* in transgenic rice. *Plant Biotechnol. J.* **1,** 361–369 (2003).
29. Wang, L. *et al.* Mapping 49 quantitative trait loci at high resolution through sequencing-based genotyping of rice recombinant inbred lines. *Theor. Appl. Genet.* **122,** 327–340 (2011).
30. Xue, W. *et al.* Natural variation in *Ghd7* is an important regulator of heading date and yield potential in rice. *Nature Genet.* **40,** 761–767 (2008).
31. Andaya, V. C. & Tai, T. H. Fine mapping of the *qCTS12* locus, a major QTL for seedling cold tolerance in rice. *Theor. Appl. Genet.* **113,** 467–475 (2006).
32. Saitoh, K., Onishi, K., Mikami, I., Thidar, K. & Sano, Y. Allelic diversification at the *C* (*OsC1*) locus of wild and cultivated rice: nucleotide changes associated with phenotypes. *Genetics* **168,** 997–1007 (2004).
33. Fan, C. *et al. GS3*, a major QTL for grain length and weight and minor QTL for grain width and thickness in rice, encodes a putative transmembrane protein. *Theor. Appl. Genet.* **112,** 1164–1171 (2006).
34. Takano-Kai, N. *et al.* Evolutionary history of *GS3*, a gene conferring grain length in rice. *Genetics* **182,** 1323–1334 (2009).
35. Shomura, A. *et al.* Deletion in a gene associated with grain size increased yields during rice domestication. *Nature Genet.* **40,** 1023–1028 (2008).
36. Konishi, S. *et al.* An SNP caused loss of seed shattering during rice domestication. *Science* **312,** 1392–1396 (2006).
37. Wang, Z. Y. *et al.* The amylose content in rice endosperm is related to the post-transcriptional regulation of the *waxy* gene. *Plant J.* **7,** 613–622 (1995).
38. Sweeney, M. T., Thomson, M. J., Pfeil, B. E. & McCouch, S. Caught red-handed: Rc encodes a basic helix-loop-helix protein conditioning red pericarp in rice. *Plant Cell* **18,** 283–294 (2006).
39. Sweeney, M. T. *et al.* Global dissemination of a single mutation conferring white pericarp in rice. *PLoS Genet.* **3,** e133 (2007).
40. Hernandez, R. D. A flexible forward simulator for populations subjects to selection and demography. *Bioinformatics* **24,** 2786–2787 (2008).
41. Huang, X. *et al.* High-throughput genotyping by whole-genome resequencing. *Genome Res.* **19,** 1068–1076 (2009).
42. Chen, K. Y., Cong, B., Wing, R., Vrebalov, J. & Tanksley, S. D. Changes in regulation of a transcription factor lead to autogamy in cultivated tomatoes. *Science* **318,** 643–645 (2007).
43. Riesenberg, L. H. & Blackman, B. K. Speciation genes in plants. *Ann. Bot.* **106,** 439–455 (2010).
44. Gan, X. *et al.* Multiple reference genomes and transcriptomes for *Arabidopsis thaliana*. *Nature* **477,** 419–423 (2011).
45. Schneeberger, K. *et al.* Reference-guided assembly of four diverse *Arabidopsis thaliana* genomes. *Proc. Natl Acad. Sci. USA* **108,** 10249–10254 (2011).
46. Lu, T. *et al.* Collection and comparative analysis of 1888 full-length cDNAs from wild rice *Oryza rufipogon* Griff. W1943. *DNA Res.* **15,** 285–295 (2008).
47. Tang, H., Sezen, U. & Paterson, A. H. Domestication and plant genomes. *Curr. Opin. Plant Biol.* **13,** 160–166 (2010).
48. Morrell, P. L., Buckler, E. S. & Ross-Ibarra, J. Crop genomics: advances and applications. *Nature Rev. Genet.* **13,** 85–96 (2012).

Supplementary Information is available in the online version of the paper.

Acknowledgements We thank the China National Rice Research Institute for providing all cultivated rice germplasm and Chinese wild rice accessions. The rest of the wild rice accessions were distributed from the Rice Collection of National Institute of Genetics jointly supported by the National Bioresource Project, MEXT, and Systems Functional Genetics Project of the Transdisciplinary Research Integration Center, ROIS, Japan. We thank Z. Ning, Y. Minobe and A. Osbourn for their advice and assistance in this work. This work was supported by the Ministry of Science and Technology of China (2011CB100205, 2012AA10A302 and 2012AA10A304), the Ministry of Agriculture of China (2011ZX08009-002 and 2011ZX08001-004), the National Natural Science Foundation of China (31121063) and the Chinese Academy of Sciences (to B.H.).

Author Contributions B.H. conceived the project and its components. X.H. and B.H. designed studies and contributed to the original concept of the project. X.W., X.Y. and Q.X. contributed the collection of rice cultivars and Chinese wild rice accessions. N.K., H.F., T.K., T.M., A.F. and A.T. contributed the collection of other wild rice accessions and analysed geographical distributions of wild rice. Z.-X.W., A.W., Y.W., L.F., Qilin Z., C.L., G.D. and Q.Q. contributed in phenotyping of rice. Z.-X.W., A.W. and L.F. contributed in phenotyping of the backcross inbred line population and genetic mapping of domestication-related traits. W.L., Y.G., Y.L., C.Z., D.F., Q.W. and Q.F. performed the genome sequencing. X.H., Y.Z., K.L., C.Z., T.H., L.Z. and T.L. performed genome data analysis. Qiang Z. and H.L. performed *de novo* genome assembly. X.H. performed evolutionary study and genome annotation. X.H., Y.Z. and K.L. performed GWAS, population genetics, and statistical analyses. J.L. contributed to functional analyses. X.H. and B.H. analysed whole data and wrote the paper.

Author Information DNA sequencing data are deposited in the European Nucleotide Archive (http://www.ebi.ac.uk/ena/) under accession numbers ERP001143, ERP000729 and ERP000106. *De novo* assembly and genome annotation of wild rice W1943, the genotype dataset of 1,529 rice accessions and the imputed dataset of 446 *O. rufipogon* accessions for GWAS are available at the Rice Haplotype Map Project database (http://www.ncgr.ac.cn/RiceHap3). Reprints and permissions information is available at www.nature.com/reprints. This paper is distributed under the terms of the Creative Commons Attribution-Non-Commercial-Share-Alike license, and the online version of the paper is freely available to all readers. The authors declare no competing financial interests. Readers are welcome to comment on the online version of the paper. Correspondence and requests for materials should be addressed to B.H. (bhan@ncgr.ac.cn).

ARTICLE

doi:10.1038/nature11531

Compensatory dendritic cell development mediated by BATF–IRF interactions

Roxane Tussiwand[1]*, Wan-Ling Lee[1]*, Theresa L. Murphy[1]*, Mona Mashayekhi[1], Wumesh KC[1], Jörn C. Albring[1], Ansuman T. Satpathy[1], Jeffrey A. Rotondo[1], Brian T. Edelson[1], Nicole M. Kretzer[1], Xiaodi Wu[1], Leslie A. Weiss[2], Elke Glasmacher[3], Peng Li[4], Wei Liao[4], Michael Behnke[2], Samuel S. K. Lam[1], Cora T. Aurthur[1], Warren J. Leonard[4], Harinder Singh[3], Christina L. Stallings[2], L. David Sibley[2], Robert D. Schreiber[1] & Kenneth M. Murphy[1,5]

The AP1 transcription factor *Batf3* is required for homeostatic development of CD8α$^+$ classical dendritic cells that prime CD8 T-cell responses against intracellular pathogens. Here we identify an alternative, *Batf3*-independent pathway in mice for CD8α$^+$ dendritic cell development operating during infection with intracellular pathogens and mediated by the cytokines interleukin (IL)-12 and interferon-γ. This alternative pathway results from molecular compensation for *Batf3* provided by the related AP1 factors *Batf*, which also functions in T and B cells, and *Batf2* induced by cytokines in response to infection. Reciprocally, physiological compensation between *Batf* and *Batf3* also occurs in T cells for expression of IL-10 and CTLA4. Compensation among BATF factors is based on the shared capacity of their leucine zipper domains to interact with non-AP1 factors such as IRF4 and IRF8 to mediate cooperative gene activation. Conceivably, manipulating this alternative pathway of dendritic cell development could be of value in augmenting immune responses to vaccines.

BATF[1] and BATF3 are activator protein 1 (AP1)[2] transcription factors[3,4] with immune-specific functions[5–8]. *Batf* is required for development of T-helper cells producing IL-17 (T_H17) and follicular helper T (T_{FH}) cells[5], and class-switch recombination (CSR) in B cells[6,9]. *Batf3* is required for development of CD8α$^+$ classical dendritic cells (cDCs) and related CD103$^+$ dendritic cells[8] that cross-present antigens to CD8 T cells[7] and produce IL-12 in response to pathogens[10].

We recently recognized a heterozygous phenotype for *Batf3* of 50% fewer CX3CR1$^-$CD8α$^+$ cDCs in *Batf3*$^{+/-}$ mice[11], indicating that levels of BATF3 are limiting for CD8α$^+$ dendritic cell development under homeostatic conditions. While analysing *Toxoplasma gondii* infection in *Batf3*$^{-/-}$ mice, we observed evidence indicating *Batf3*-independent CD8α$^+$ cDC development[10] based on apparent priming of pathogen-specific CD8 T cells in *Batf3*$^{-/-}$ mice treated with IL-12. Here we report a *Batf3*-independent pathway of CD8α$^+$ cDC development that functions physiologically during infection by intracellular pathogens and describe its molecular basis, which involves compensatory BATF factors.

Pathogens and IL-12 restore CD8α$^+$ cDCs in *Batf3*$^{-/-}$ mice

IL-12 administration to *Batf3*$^{-/-}$ mice before infection with type II Prugniaud (Pru) *T. gondii* reversed their susceptibility by inducing interferon (IFN)-γ production not only from natural killer (NK) cells but also from CD8 T cells[10], indicating potentially restored cross-priming. To test this idea, we infected *Batf3*$^{-/-}$ mice with the attenuated[12] RHΔ*ku80*Δ*rop5* strain of *T. gondii* and examined CD8α$^+$ cDCs (Supplementary Fig. 1a). Notably, CD8α$^+$ cDCs reappeared in spleens of *Batf3*$^{-/-}$ mice by day 10 after infection. Infection by *Listeria monocytogenes* also restored CD8α$^+$ cDC production in *Batf3*$^{-/-}$ mice (Supplementary Fig. 1b). Aerosol-mediated infection with *Mycobacterium tuberculosis* caused a progressive restoration of CD8α$^+$ cDCs in *Batf3*$^{-/-}$ mice and expanded CD8α$^+$ cDCs in wild-type mice (Fig. 1a). *Mycobacterium tuberculosis* infection of *Batf3*$^{-/-}$ mice restored the missing lung-resident CD103$^+$ cDCs (DEC205$^+$CD24$^+$CD4$^-$SIRP-α$^-$CD11b$^-$)[8,13] (Supplementary Fig. 1c). *Batf3*$^{-/-}$ mice showed no difference in survival to *M. tuberculosis* infection compared to wild-type mice (Supplementary Fig. 1d), suggesting that the initial lack of CD8α$^+$ cDCs and peripheral CD103$^+$ cDCs was not sufficient for lethality with *M. tuberculosis*. Because IL-12 is important in control of *M. tuberculosis*[14], we measured serum IL-12 levels in *M. tuberculosis*-infected wild-type and *Batf3*$^{-/-}$ mice (Fig. 1b). IL-12 levels were reduced in *Batf3*$^{-/-}$ mice in the first 3 weeks, but increased after 6 weeks to approximately 50% of *M. tuberculosis*-infected wild-type mice.

We found that IL-12 administration restored CD8α$^+$ cDC production in all backgrounds of *Batf3*$^{-/-}$ mice (Fig. 1c and Supplementary Fig. 2a). Restored CD8α$^+$ cDCs were functional for cross-presentation[7,15,16] (Fig. 2a and Supplementary Fig. 2b). Purified splenic CD8α$^+$ and CD4$^+$ cDCs from wild-type or *Batf3*$^{-/-}$ mice, treated with vehicle or IL-12, were tested for cross-presentation. As a control, OT-I T cells proliferated in response to wild-type CD8α$^+$ dendritic cells, but not CD4$^+$ dendritic cells, co-cultured with ovalbumin-loaded cells with or without IL-12 treatment (Fig. 2a). Importantly, OT-I T cells proliferated similarly in response to IL-12-induced *Batf3*$^{-/-}$ CD8α$^+$ dendritic cells, but not *Batf3*$^{-/-}$ CD4$^+$ dendritic cells, as to wild-type CD8α$^+$ cDCs. The CD8α$^+$ cDCs restored by IL-12 administration in *Batf3*$^{-/-}$ mice showed a gene expression profile that was more similar to wild-type CD8α$^+$ dendritic cells than to CD4$^+$ cDCs (Supplementary Fig. 2c). A total of 1,855 genes differed more than fourfold in expression between IL-12-induced CD8α$^+$ cDCs and CD4$^+$ cDCs within *Batf3*$^{-/-}$ mice. However, in comparing IL-12-induced CD8α$^+$ cDCs in *Batf3*$^{-/-}$ mice with the rare CD8α$^+$ cDCs from *Batf3*$^{-/-}$ C57BL/6 mice, or with CD8α$^+$ cDCs in wild-type mice, there were only 34 and 206 genes, respectively, differing more than fourfold in expression.

[1]Department of Pathology and Immunology, Washington University School of Medicine, 660 South Euclid Avenue, St Louis, Missouri 63110, USA. [2]Department of Molecular Microbiology, Washington University School of Medicine, St Louis, Missouri 63110, USA. [3]Department of Discovery Immunology, Genentech, Inc., 1 DNA Way, South San Francisco, California 94080, USA. [4]Laboratory of Molecular Immunology and Immunology Center, National Heart, Lung, and Blood Institute, National Institutes of Health, Bethesda, Maryland 20892-1674, USA. [5]Howard Hughes Medical Institute, Washington University School of Medicine, 660 South Euclid Avenue, St Louis, Missouri 63110, USA.
*These authors contributed equally to this work.

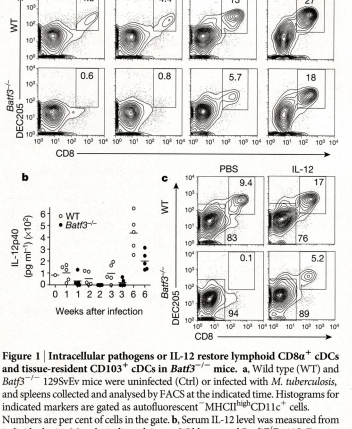

Figure 1 | Intracellular pathogens or IL-12 restore lymphoid CD8α$^+$ cDCs and tissue-resident CD103$^+$ cDCs in *Batf3*$^{-/-}$ mice. a, Wild type (WT) and *Batf3*$^{-/-}$ 129SvEv mice were uninfected (Ctrl) or infected with *M. tuberculosis*, and spleens collected and analysed by FACS at the indicated time. Histograms for indicated markers are gated as autofluorescent$^-$MHCII^{high}CD11c$^+$ cells. Numbers are per cent of cells in the gate. **b**, Serum IL-12 level was measured from individual mice (**a**) at the indicated time. **c**, Wild-type and *Batf3*$^{-/-}$ 129SvEv mice were treated with vehicle (PBS) or IL-12 and analysed by FACS after 3 days as in **a**.

The IL-12-induced restoration of CD8α$^+$ cDCs in *Batf3*$^{-/-}$ mice was dependent on IFN-γ *in vivo* (Supplementary Fig. 2d). With administration of control antibody, IL-12 induced a threefold increase in CD8α$^+$ cDCs in wild-type mice and restored CD8α$^+$ cDC production in *Batf3*$^{-/-}$ mice. Both effects were blocked by anti-IFN-γ antibody. IL-12 induced IFN-γ production from NK cells but not T cells (Supplementary Fig. 2e), and IL-12 treatment was able to restore CD8α$^+$ cDCs in *Rag2*$^{-/-}$*Batf3*$^{-/-}$ mice (Supplementary Fig. 2f), indicating that T cells and B cells are not required for this effect.

Batf3$^{-/-}$ mice fail to reject highly immunogenic H31m1 and D42m1 fibrosarcomas[2]. However, *Batf3*$^{-/-}$ mice pre-treated with IL-12 either fully rejected or showed reduced growth of these fibrosarcomas (Fig. 2b and Supplementary Fig. 2g). Rejection was not simply due to NK cell activation, as IL-12 treatment failed to alter tumour growth in *Rag2*$^{-/-}$ mice. Notably, IL-12-treated *Batf3*$^{-/-}$ mice re-established priming of CD8 T cells capable of infiltrating tumours similar to wild-type mice (Fig. 2c). Mice with the inactivating IRF8 R249C mutation[17–19] failed to restore CD8α$^+$ cDCs upon IL-12 administration (Supplementary Fig. 3a), indicating that restoration requires functional IRF8 protein. Furthermore, these mice were highly susceptible to infection by aerosol-administered *M. tuberculosis*[20] (Supplementary Fig. 3b), indicating that *Batf3*$^{-/-}$ mice may resist *M. tuberculosis* infection by restoration of CD8α$^+$ cDCs. Thus, physiological *Batf3*-independent development of CD8α$^+$ cDCs is induced by pathogens, mediated by IL-12 and IFN-γ.

Batf, *Batf2* and *Batf3* cross-compensate

We next investigated whether *Batf* could replace *Batf3* for *in vitro* cDC development[7,21] (Fig. 3a). CD103$^+$SIRP-α$^-$ cDCs do not develop in Flt3L-treated *Batf3*$^{-/-}$ bone marrow cultures. Retroviral expression of *Batf3* into *Batf3*$^{-/-}$ bone marrow progenitors restored CD103$^+$ cDC development. Notably, *Batf* expression fully and cell-intrinsically restored CD103$^+$SIRP-α$^-$ cDC development, whereas *Fos* was inactive (Supplementary Fig. 3c). CD103$^+$ cDCs restored by *Batf* and *Batf3* expression *in vitro* were functional, showing features of mature CD103$^+$ cDCs, including loss of SIRP-α and CD11b expression, upregulation of CD24, and selective production of IL-12 in response to *T. gondii* antigen (Supplementary Fig. 3c, d). Reciprocally, *Batf3* but not *Fos* restored cell-intrinsic IL-17a production by *Batf*$^{-/-}$ T cells and CSR in *Batf*$^{-/-}$ B cells (Supplementary Fig. 3e, f). Thus, *Batf* and *Batf3* can molecularly cross-compensate for several distinct lineage-specific functions, activities not shared by *Fos*.

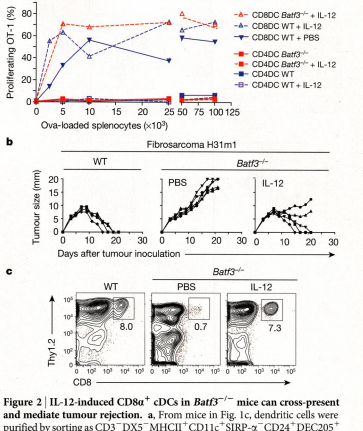

Figure 2 | IL-12-induced CD8α$^+$ cDCs in *Batf3*$^{-/-}$ mice can cross-present and mediate tumour rejection. a, From mice in Fig. 1c, dendritic cells were purified by sorting as CD3$^-$DX5$^-$MHCII$^+$CD11c$^+$SIRP-α$^-$CD24$^+$DEC205$^+$ dendritic cells (CD8DC) and CD3$^-$DX5$^-$MHCII$^+$CD11c$^+$SIRP-α$^+$CD24$^-$DEC205$^-$ dendritic cells (CD4DC) and assayed for cross-presentation[7]. OT-I proliferation in response to cDCs mixed with the indicated number of MHC-class-I-deficient ovalbumin (Ova)-loaded splenocytes is shown. **b**, Wild-type or *Batf3*$^{-/-}$ mice treated with vehicle (PBS) or with IL-12 were inoculated with 1×10^6 H31m1 fibrosarcomas. Tumour size in individual mice is shown. **c**, Mice in **b** were analysed by FACS 11 days after H31m1 inoculation for CD8 T-cell infiltration into tumours[2].

We also identified *in vivo* compensation between *Batf* and *Batf3* in dendritic cells. On the 129SvEv and BALB/c backgrounds, *Batf3*$^{-/-}$ mice completely lack CD8α$^+$ cDCs (Fig. 3b and Supplementary Fig. 2a). In contrast, C57BL/6 *Batf3*$^{-/-}$ mice retain a 3–7% population of CD8α$^+$ cDCs[19,22] in spleen and unexpectedly retain a completely normal population of CD8α$^+$ cDCs in skin-draining inguinal lymph nodes (ILNs) (Fig. 3b). These CD8α$^+$ cDCs are functional, as C57BL/6 *Batf3*$^{-/-}$ mice showed robust priming of CD8 T cells against herpes simplex virus (HSV) infection in the footpad, whereas 129SvEv *Batf3*$^{-/-}$ mice, lacking CD8α$^+$ cDCs in ILNs, did not (Supplementary Fig. 3g). However, C57BL/6 *Batf*$^{-/-}$*Batf3*$^{-/-}$ mice lack CD8α$^+$ dendritic cells in ILNs and fail to prime T cells against HSV. Thus, retention of functional CD8α$^+$ cDCs in ILNs of C57BL/6 *Batf3*$^{-/-}$ mice is *Batf*-dependent.

Batf and *Batf3* also compensate in expression of genes by T cells. IL-4 and IL-10 production was not substantially affected in either *Batf*$^{-/-}$ or *Batf3*$^{-/-}$ T_H2 cells (Fig. 3c and Supplementary Fig. 3i–k). However, IL-10 is reduced at least eightfold in *Batf*$^{-/-}$*Batf3*$^{-/-}$ T_H2

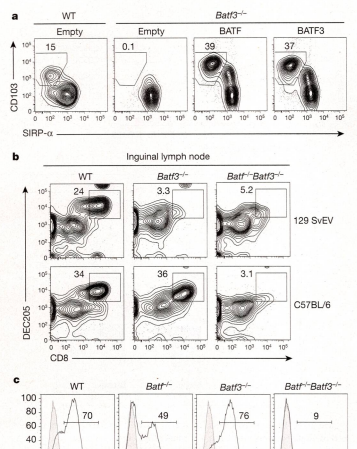

Figure 3 | *Batf* compensates for CD8α$^+$ cDC development in *Batf3*$^{-/-}$ mice. a, Wild-type or *Batf3*$^{-/-}$ bone marrow cells were infected with GFP-RV[35] (empty) or retrovirus expressing the indicated cDNA and cultured with Flt3L[7]. Histograms for the indicated markers are for B220$^-$CD11c$^+$ cells on day 10. Numbers are the per cent of cells in the gate. **b**, Inguinal lymph nodes from wild-type, *Batf3*$^{-/-}$ or *Batf*$^{-/-}$*Batf3*$^{-/-}$ mice on 129SvEv or C57BL/6 backgrounds were analysed by FACS. Shown are histograms for DEC205 and CD8α. **c**, CD4 T cells of the indicated genotype were differentiated twice under T_H2 conditions[9] and analysed by FACS for intracellular IL-10.

cells. Also, expression of the inhibitory receptor CTLA4 is partially reduced in *Batf*$^{-/-}$ T_H2 cells but reduced threefold further in *Batf*$^{-/-}$*Batf3*$^{-/-}$ T_H2 cells. In contrast, IFN-γ production by T_H1 cells is unaffected by loss of *Batf*, *Batf3* or both.

We asked whether IL-12-induced restoration of CD8α$^+$ cDCs in *Batf3*$^{-/-}$ mice was due to compensation by *Batf* (Supplementary Fig. 3h). Restoration of splenic CD8α$^+$ cDCs in IL-12-treated *Batf*$^{-/-}$*Batf3*$^{-/-}$ mice was reduced to 5% from 11% in IL-12-treated *Batf3*$^{-/-}$ mice. Whereas *Batf* seems to be responsible for roughly half of the IL-12-induced restoration of CD8α$^+$ cDCs in *Batf3*$^{-/-}$ mice, some residual compensation remained in *Batf*$^{-/-}$*Batf3*$^{-/-}$ mice. We asked if a third factor might compensate for *Batf* and *Batf3*. *Batf2* (also called *SARI*)[23] is closely related to *Batf* and *Batf3* and is induced by lipopolysaccharide (LPS) and IFN-γ in macrophages and CD103$^+$ dendritic cell populations (Supplementary Fig. 4a–c). We found that *Batf2* was induced by IFN-γ in wild-type and *Batf3*$^{-/-}$ dendritic cells derived from Flt3L-cultured bone marrow (Supplementary Fig. 4d, e) and *in vivo* by IL-12 in dendritic cells in *Batf3*$^{-/-}$ mice (Supplementary Fig. 4f). Induction of *Batf2* by IFN-γ in cDCs made it a potential candidate to mediate IFN-γ-dependent compensation for *Batf3*.

We generated *Batf2*$^{-/-}$ mice by targeting exons 1 and 2, eliminating BATF2 protein expression (Supplementary Fig. 5). *Batf2*$^{-/-}$ mice had normal development of NK, T and B cells, pDCs, neutrophils, resting cDCs, and peritoneal, liver and lung macrophages (Supplementary Fig. 6a–c). However, *Batf2*$^{-/-}$ mice displayed significantly decreased survival after infection by *T. gondii* (Pru) (Fig. 4a), although parasite burden and serum cytokine levels were similar to wild-type mice (Supplementary Fig. 7a, b). Notably, *Batf2*$^{-/-}$ mice showed significantly decreased numbers of lung-resident CD103$^+$CD11b$^-$ dendritic cells and CD103$^-$CD11b$^-$ macrophages after infection (Fig. 4b and Supplementary Fig. 7c). These changes were specific, as there were no differences in other myeloid subsets (Supplementary Fig. 7d, e). Thus, *Batf2* has a role in maintaining numbers of *Batf3*-dependent CD103$^+$ dendritic cells in the lung after infection with *T. gondii*.

We next investigated whether *Batf2* could compensate for dendritic cell defects in *Batf3*$^{-/-}$ mice and for T and B cell defects in *Batf*$^{-/-}$ mice (Fig. 4c and Supplementary Fig. 8a, b). Like *Batf*, retroviral expression of *Batf2* restored development of CD103$^+$SIRP-α$^-$ dendritic cells in Flt3L-treated *Batf3*$^{-/-}$ bone marrow. Unlike *Batf* and *Batf3*, expression of *Batf2* did not restore T_H17 development in *Batf*$^{-/-}$ T cells and only weakly restored CSR in *Batf*$^{-/-}$ B cells. Thus, *Batf2* selectively compensates for *Batf* and *Batf3* in cDCs but not in T or B cells. We next

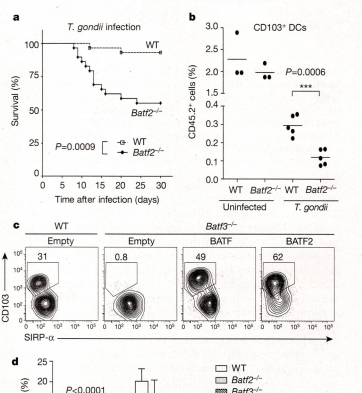

Figure 4 | *Batf2* compensates for *Batf3* in CD8α$^+$ and CD103$^+$ cDC development during *T. gondii* infection. a, Wild-type and *Batf2*$^{-/-}$ mice were infected with *T. gondii* and monitored for survival. $n = 29$ for wild-type (dashed line) and *Batf2*$^{-/-}$ (solid line) mice. **b**, Shown are percentages of lung CD103$^+$ dendritic cells of total CD45.2$^+$ cells for uninfected and infected (*T. gondii*) wild-type or *Batf2*$^{-/-}$ mice on day 10. $n = 5$ from one of three experiments. **c**, Wild-type or *Batf3*$^{-/-}$ bone marrow cells were infected with the indicated retrovirus, cultured with Flt3L and analysed by FACS on day 10. **d**, Groups of five mice each of the indicated genotypes were treated with vehicle (PBS) or IL-12 and analysed by FACS after 3 days. Shown are percentages and s.e.m. of CD8α$^+$ cDCs as a total of splenic cDCs.

examined *in vivo* IL-12-induced restoration of CD8α$^+$ cDCs in *Batf2*$^{-/-}$, *Batf3*$^{-/-}$ and *Batf2*$^{-/-}$*Batf3*$^{-/-}$ mice (Fig. 4d and Supplementary Fig. 8c). IL-12 treatment restored CD8α$^+$ cDCs from ≤1% to >5% of total cDCs in *Batf3*$^{-/-}$ mice, but this was significantly reduced to ~2% in *Batf2*$^{-/-}$*Batf3*$^{-/-}$ mice. This suggests that *Batf2* is responsible for roughly half of IL-12-induced CD8α$^+$ cDC restoration in *Batf3*$^{-/-}$ mice. We found similar results with *in vitro* CD103$^+$ cDC development. Whereas granulocyte–macrophage colony-stimulating factor (GM–CSF) restored only CD103 and not DEC205 expression in Flt3L-treated *Batf3*$^{-/-}$ bone marrow cultures[19], adding IFN-γ with GM–CSF restored DEC205$^+$CD103$^+$CD11b$^-$ dendritic cells (Supplementary Fig. 8d, e). We used this system to analyse compensation between *Batf*, *Batf2* and *Batf3* (Supplementary Fig. 8d, e). Relative to wild-type bone marrow, CD103$^+$DEC205$^+$CD11b$^-$ cDCs were partially reduced in *Batf*$^{-/-}$, *Batf2*$^{-/-}$ and *Batf3*$^{-/-}$ singly deficient bone marrow, but were reduced to an even greater extent in both *Batf*$^{-/-}$*Batf3*$^{-/-}$ and *Batf2*$^{-/-}$*Batf3*$^{-/-}$ bone marrow relative to all single-deficient bone marrow cultures. Collectively, these results suggest that *Batf* and *Batf2* both act in the cytokine-dependent rescue of CD8α$^+$ cDC development in *Batf3*$^{-/-}$ mice.

The BATF LZ domain interacts with IRF4 and IRF8

To understand BATF cross-compensation, we analysed chimaeric proteins containing fused domains of BATF, BATF2 and FOS (Supplementary Fig. 9). FOS inactivity could result from inhibitory actions of amino- and carboxy-terminal domains missing in BATF and BATF3 (Fig. 5a). However, removing these domains from FOS (Δ5′FOSΔ3′) or fusing the BATF DNA-binding domain (DBD) with the FOS leucine zipper (LZ) (BBRFFΔ3′) failed to restore CD103$^+$ cDC development (Fig. 5a), T_H17 development or CSR activity (Supplementary Fig. 10a, b). However, fusing the BATF LZ with the FOS DBD (Δ5′FFQBB) fully restored CD103$^+$ cDC development in Flt3L-treated *Batf3*$^{-/-}$ bone marrow cultures, fully restored CSR in *Batf*$^{-/-}$ B cells and exhibited 20% of wild-type activity for restoring IL-17 production. Furthermore, BATF with a C-terminal GFP (BATF–GFP) or FOS (BBBF) domain had >40% of wild-type BATF activity in all three assays (Supplementary Fig. 11). Thus, the LZ domain, not the DBD, determines BATF specificity.

Removing the BATF2 C-terminal domain (BATF2 DM) allowed for full restoration of CD103$^+$ cDC development, but led to only partial restoration of CSR activity (~15%), and no restoration of T_H17 development (Supplementary Fig. 10c–h). Fusing the BATF DBD with the BATF2 LZ (B1HB2 DM) allowed for approximately 50% of wild-type BATF activity for CSR and T_H17 development in *Batf*$^{-/-}$ B and T cells. Fusing the BATF2 DBD with BATF LZ (B2QB1) allowed for 50% of wild-type BATF activity in CD103$^+$ cDC development, but provided less than 5% wild-type BATF activity in T_H17 development. Thus, the BATF2 DBD restricts activity in T and B cells, but its LZ functions for all BATF lineage-specific activities.

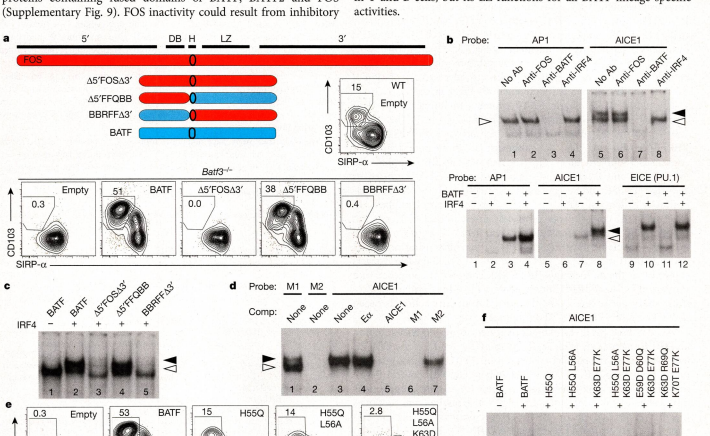

Figure 5 | BATF leucine zipper interactions with non-AP1 factors mediate lineage-specific actions. a, Structures of chimaeric proteins are shown below a diagram of FOS. DNA binding domain (DB), hinge (H), leucine zipper (LZ), N (5′) and C termini (3′) are indicated. Flt3L-treated wild-type or *Batf3*$^{-/-}$ bone marrow cells infected with the indicated retrovirus were analysed after 10 days. **b**, 293T cells expressing both *Batf* and *Irf4* (upper panel) or *Batf* and *Irf4* as indicated (lower panel) were analysed by EMSA with the indicated probes and antibodies **c**, 293T cells expressing IRF4 (+) and the indicated BATF chimaera were analysed by EMSA with the AICE1 probe. **d**, B cells were analysed by EMSA with the indicated probe and competitor oligonucleotides (comp). **e**, *Batf3*$^{-/-}$ bone marrow cells infected with the indicated BATF retroviruses encoding BATF were analysed as in **a**. **f**, 293T cells expressing the indicated BATF mutants were analysed by EMSA with the AICE1 probe.

A recent study[24] proposed that IRF4 and BATF may interact. Correspondence between the phenotypes of *Batf*$^{-/-}$ with *Irf4*$^{-/-}$ mice, lacking T_H17 development and CSR, and *Batf3*$^{-/-}$ with *Irf8*$^{-/-}$ mice, lacking CD8α$^+$ cDC development (Supplementary Fig. 12)[5–7,25–28], suggested that BATF and BATF3 may cooperate with both IRF4 and IRF8. Furthermore, ChIP-seq analysis of BATF and IRF4 revealed coincident binding to composite AP1 and IRF motifs[29,30]. By analogy with the ETS–IRF composite elements (EICE)[31], the AP1–IRF composite elements are designated as AICE[29,30]. Recalling the FOS LZ interaction with NF-AT that mediates cooperative binding to *Il2* regulatory regions[32], we therefore asked whether the BATF LZ interacted with non-AP1 factors, including IRF4.

Electrophoretic mobility shift assays (EMSAs) demonstrated interactions between BATF and both IRF4 and IRF8 (Fig. 5 and Supplementary Figs 13 and 14). The BATF–JUN complex that formed on an AP1 consensus probe[12] was unchanged by addition of IRF4 or IRF8. Its abundance was increased by additional JUNB (Supplementary Fig. 13a). However, using an AICE from the *Ctla4* locus, a slower mobility complex formed with addition of either *Irf4* or *Irf8*, which required the IRF consensus element (Fig. 5b and Supplementary Fig. 13b). This BATF–JUN–IRF4 complex required both BATF and IRF protein, and IRF4 was unable to bind the AICE1 probe without BATF (Fig. 5b). In contrast, IRF4 was able to bind to an ETS–IRF consensus element[33] (EICE) in the presence of PU.1 independently of BATF (Fig. 5b). The BATF–JUN–IRF4 complex had similar mobility to the FOS–JUN complex in activated cells, but could be distinguished by antibody supershifts (Supplementary Fig. 13c). Spatial constraints on the BATF–IRF4 interaction are suggested by lack of BATF–IRF4 complex formation on the AICE2 probe with reversed orientation of the AP1 and IRF elements (Supplementary Fig. 13a, c).

The ability of chimaeric BATF proteins to interact with IRF4 correlated with their functional activity (Fig. 5c). The active Δ5′FFQBB interacted with IRF4, but the inactive Δ5′FOSA3′ and BBRFFΔ3′ did not (Fig. 5c), although all three bound an AP1 consensus (Supplementary Fig. 13d). A BATF–IRF complex also formed in B and T cells, requiring both the IRF and AP1 consensus elements (Fig. 5d and Supplementary Fig. 14c), and involved contribution by endogenous IRF4 and IRF8 (Supplementary Fig. 14a, b, d). The BATF–IRF complex was completely absent in *Batf*$^{-/-}$ B cells, but was partially retained in single-deficient *Irf4*$^{-/-}$ or *Irf8*$^{-/-}$ B cell extracts (Supplementary Fig. 14a, b). Supershifts using anti-IRF4 and anti-IRF8 antibodies in *Irf4*$^{-/-}$ or *Irf8*$^{-/-}$ B cell nuclear extracts showed that the endogenous BATF–IRF complex is composed of a mixture of IRF4 and IRF8 (Supplementary Fig. 14b). Similarly, supershifts of primary T_H17 cells demonstrate an interaction between BATF and both IRF4 and IRF8 (Supplementary Fig. 14d).

We identified BATF LZ mutations which abrogated both function and IRF4 interactions (Fig. 5e, f). Positions b, c and f of the FOS LZ face away from the parallel coiled-coil of the JUN LZ and mediate interactions with NF-AT[32] (Supplementary Fig. 9d). Several BATF mutations in these positions had no effect on activity (Supplementary Table 1 and Supplementary Fig. 9c). However, four residues together controlled nearly all BATF-specific activity (Fig. 5e and Supplementary 15). BATF(L56A), BATF(K63D) and BATF(E77K) showed no reduction in CD103$^+$ cDC development, and retained >60% of wild-type BATF activity in CSR. In contrast, BATF(H55Q) activity was reduced by nearly 70% (Fig. 5e). Double mutants BATF(K63D/E77K) and BATF(H55Q/L56A) were reduced by 50% and 75%, but quadruple mutant BATF(H55Q/L56A/K63D/E77K) had less than 10% of wild-type BATF activity in CD103$^+$ cDC development (Fig. 5e). This loss of activity was specific, as two other quadruple mutants—BATF(E59Q/D60Q/K63D/E77K) and BATF(K63D/R69Q/K70D/E77K)—maintained >50% of wild-type BATF activity (Supplementary Fig. 15c, d). A similar pattern was seen for CSR in *Batf*$^{-/-}$ B cells (Supplementary Fig. 15b). The activity of these mutants correlated with IRF4 interaction (Fig. 5f). Wild-type BATF and functional mutant BATF(K63D/E77K), and both functional quadruple mutants, formed a complex with IRF4, whereas the less active BATF(H55Q) and BATF(H55Q/L56A), and the completely inactive BATF(H55Q/L56A/K63D/E77K), did not, although all were stably expressed and could bind an AP1 site (Supplementary 13e, f).

Discussion

We have uncovered a cytokine-driven pathway for expansion of functional CD8α$^+$ cDCs occurring physiologically during infection by intracellular pathogens. This pathway relies on functional compensation for *Batf3* provided by *Batf* and *Batf2* through a shared specificity defined by the BATF LZ domain to support CD8α$^+$ cDC and T_H17 development, and CSR in B cells. This compensatory pathway of CD8α$^+$ cDC development may provide a basis for augmenting therapeutic immune responses. The basis of this shared specificity is the LZ interaction with non-AP1 factors, including IRF4 and IRF8, extending the repertoire of AP1 interactions beyond the recognized association of FOS with NF-AT[32]. The ability of both BATF and BATF3 to support both IRF4- and IRF8-dependent lineage activities implies that the specificity for gene activation is determined largely by the IRF factors. An important next step will be to determine how regulatory elements discriminate between these distinct complexes.

METHODS SUMMARY

Mice. *Batf*$^{-/-}$, *Batf2*$^{-/-}$ and *Batf3*$^{-/-}$ mice and intercrosses were bred in our specific pathogen-free animal facility according to institutional guidelines. *Irf8*$^{-/-}$ mice from the European Mutant Mouse Archive and BXH2/TyJ mice from The Jackson Laboratory were maintained on the C57BL/6 background. Germline-deleted *Irf4*$^{-/-}$ mice were produced from crossing B6.129S1-*Irf4*^{tm1Rdf}/J mice obtained from The Jackson Laboratory with a CMV-Cre deleter strain on the C57BL/6 background. Experiments were in accordance with procedures approved by the AAALAC accredited Animal Studies Committee of Washington University in St Louis.

***In vivo* IL-12 treatment.** Recombinant murine IL-12 (Peprotech and Pfizer) was suspended in pyrogen-free saline at 2.5 μg ml^{-1}. Mice were injected intraperitoneally with 0.5 μg of IL-12 two times 3 days before analysis. For tumour transplantation and tumour collection experiments, mice were treated on days 4, 3 and 1 before tumour inoculation and 24 h after tumour inoculation.

Full Methods and any associated references are available in the online version of the paper.

Received 31 May; accepted 31 August 2012.
Published online 19 September 2012.

1. Dorsey, M. J. *et al.* B-ATF: a novel human bZIP protein that associates with members of the AP-1 transcription factor family. *Oncogene* **11,** 2255–2265 (1995).
2. Wagner, E. F. & Eferl, R. Fos/AP-1 proteins in bone and the immune system. *Immunol. Rev.* **208,** 126–140 (2005).
3. Williams, K. L. *et al.* Characterization of murine BATF: a negative regulator of activator protein-1 activity in the thymus. *Eur. J. Immunol.* **31,** 1620–1627 (2001).
4. Echlin, D. R., Tae, H. J., Mitin, N. & Taparowsky, E. J. B-ATF functions as a negative regulator of AP-1 mediated transcription and blocks cellular transformation by Ras and Fos. *Oncogene* **19,** 1752–1763 (2000).
5. Schraml, B. U. *et al.* The AP-1 transcription factor Batf controls T_H17 differentiation. *Nature* **460,** 405–409 (2009).
6. Ise, W. *et al.* The transcription factor BATF controls the global regulators of class-switch recombination in both B cells and T cells. *Nature Immunol.* **12,** 536–543 (2011).
7. Hildner, K. *et al.* Batf3 deficiency reveals a critical role for CD8α$^+$ dendritic cells in cytotoxic T cell immunity. *Science* **322,** 1097–1100 (2008).
8. Edelson, B. T. *et al.* Peripheral CD103$^+$ dendritic cells form a unified subset developmentally related to CD8α$^+$ conventional dendritic cells. *J. Exp. Med.* **207,** 823–836 (2010).
9. Betz, B. C. *et al.* Batf coordinates multiple aspects of B and T cell function required for normal antibody responses. *J. Exp. Med.* **207,** 933–942 (2010).
10. Mashayekhi, M. *et al.* CD8α$^+$ dendritic cells are the critical source of interleukin-12 that controls acute infection by *Toxoplasma gondii* tachyzoites. *Immunity* **35,** 249–259 (2011).
11. Bar-On, L. *et al.* CX3CR1$^+$ CD8α$^+$ dendritic cells are a steady-state population related to plasmacytoid dendritic cells. *Proc. Natl Acad. Sci. USA* **107,** 14745–14750 (2010).

12. Behnke, M. S. *et al.* Virulence differences in *Toxoplasma* mediated by amplification of a family of polymorphic pseudokinases. *Proc. Natl Acad. Sci. USA* **108,** 9631–9636 (2011).
13. Ginhoux, F. *et al.* The origin and development of nonlymphoid tissue $CD103^+$ DCs. *J. Exp. Med.* **206,** 3115–3130 (2009).
14. Modlin, R. L. & Barnes, P. F. Il12 and the human immune response to mycobacteria. *Res. Immunol.* **146,** 526–531 (1995).
15. den Haan, J. M., Lehar, S. M. & Bevan, M. J. $CD8^+$ but not $CD8^-$ dendritic cells cross-prime cytotoxic T cells *in vivo*. *J. Exp. Med.* **192,** 1685–1696 (2000).
16. Wilson, N. S. *et al.* Systemic activation of dendritic cells by Toll-like receptor ligands or malaria infection impairs cross-presentation and antiviral immunity. *Nature Immunol.* **7,** 165–172 (2006).
17. Aliberti, J. *et al.* Essential role for ICSBP in the *in vivo* development of murine $CD8\alpha^+$ dendritic cells. *Blood* **101,** 305–310 (2003).
18. Tailor, P., Tamura, T., Morse, H. C. & Ozato, K. The BXH2 mutation in IRF8 differentially impairs dendritic cell subset development in the mouse. *Blood* **111,** 1942–1945 (2008).
19. Edelson, B. T. *et al.* Batf3-dependent $CD11b^{low/-}$ peripheral dendritic cells are GM-CSF-independent and are not required for Th cell priming after subcutaneous immunization. *PLoS ONE* **6,** e25660 (2011).
20. Marquis, J. F., Lacourse, R., Ryan, L., North, R. J. & Gros, P. Disseminated and rapidly fatal tuberculosis in mice bearing a defective allele at IFN regulatory factor 8. *J. Immunol.* **182,** 3008–3015 (2009).
21. Jackson, J. T. *et al.* Id2 expression delineates differential checkpoints in the genetic program of $CD8\alpha^+$ and $CD103^+$ dendritic cell lineages. *EMBO J.* **30,** 2690–2704 (2011).
22. Edelson, B. T. *et al.* $CD8\alpha^+$ dendritic cells are an obligate cellular entry point for productive infection by *Listeria monocytogenes*. *Immunity* **35,** 236–248 (2011).
23. Su, Z. Z. *et al.* Cloning and characterization of SARI (suppressor of AP-1, regulated by IFN). *Proc. Natl Acad. Sci. USA* **105,** 20906–20911 (2008).
24. Ravasi, T. *et al.* An atlas of combinatorial transcriptional regulation in mouse and man. *Cell* **140,** 744–752 (2010).
25. Brüstle, A. *et al.* The development of inflammatory T_H17 cells requires interferon-regulatory factor 4. *Nature Immunol.* **8,** 958–966 (2007).
26. Klein, U. *et al.* Transcription factor IRF4 controls plasma cell differentiation and class-switch recombination. *Nature Immunol.* **7,** 773–782 (2006).
27. Tamura, T. & Ozato, K. ICSBP/IRF-8: its regulatory roles in the development of myeloid cells. *J. Interferon Cytokine Res.* **22,** 145–152 (2002).
28. Sciammas, R. *et al.* Graded expression of interferon regulatory factor-4 coordinates isotype switching with plasma cell differentiation. *Immunity* **25,** 225–236 (2006).
29. Glasmacher, E. *et al.* A genomic regulatory element that directs assembly and function of immune-specific AP-1-IRF complexes. *Science.* (in the press).
30. Li, P. *et al.* BATF–JUN is critical for IRF4-mediated transcription in T cells. *Nature* http://dx.doi.org/10.1038/nature11530 (19 September 2012).
31. Brass, A. L., Zhu, A. Q. & Singh, H. Assembly requirements of PU.1-Pip (IRF-4) activator complexes: inhibiting function *in vivo* using fused dimers. *EMBO J.* **18,** 977–991 (1999).
32. Chen, L., Glover, J. N., Hogan, P. G., Rao, A. & Harrison, S. C. Structure of the DNA-binding domains from NFAT, Fos and Jun bound specifically to DNA. *Nature* **392,** 42–48 (1998).
33. Eisenbeis, C. F., Singh, H. & Storb, U. Pip, a novel IRF family member, is a lymphoid-specific, PU.1-dependent transcriptional activator. *Genes Dev.* **9,** 1377–1387 (1995).
34. Heng, T. S. & Painter, M. W. The Immunological Genome Project: networks of gene expression in immune cells. *Nature Immunol.* **9,** 1091–1094 (2008).
35. Ranganath, S. *et al.* GATA-3-dependent enhancer activity in IL-4 gene regulation. *J. Immunol.* **161,** 3822–3826 (1998).

Supplementary Information is available in the online version of the paper.

Acknowledgements This work was supported by the Howard Hughes Medical Institute, National Institutes of Health (AI076427-02) and Department of Defense (W81XWH-09-1-0185) (K.M.M.), the American Heart Association (12PRE8610005) (A.T.S.), German Research Foundation (AL 1038/1-1) (J.C.A), American Society of Hematology Scholar Award and Burroughs Welcome Fund Career Award for Medical Scientists (B.T.E.), and Cancer Research Institute predoctoral fellowship (W.-L.L.). We thank the ImmGen consortium[34]. M. White for blastocyst injections and generation of mouse chimaeras, the Alvin J. Siteman Cancer Center at Washington University School of Medicine for use of the Center for Biomedical Informatics and Multiplex Gene Analysis Genechip Core Facility. The Siteman Cancer Center is supported in part by the NCI Cancer Center Support Grant P30 CA91842. IL-12 was a gift from Pfizer.

Author Contributions R.T., W.-L.L., T.L.M. and M.M. performed experiments with *Batf*$^{-/-}$, *Batf2*$^{-/-}$, *Batf3*$^{-/-}$ and double-knockout mice; T.L.M. made and analysed all BATF mutants; J.A.R. aided with EMSAs; W.K.C., J.C.A. and A.T.S. were involved with microarray analysis and generation of mutant mice. J.C.A. was involved in generating of *Batf2*$^{-/-}$ mice. B.T.E. was involved with *L. monocytogenes* analysis; N.M.K was involved with cross-presentation analysis. X.W. was involved with bioinformatic analysis; L.A.W. and C.L.S. were involved with *M. tuberculosis* infection; E.G. and H.S. helped to identify EMSA probes; P.L., W.L. and W.J.L. performed ChIP-seq and helped to identify EMSA probes; M.B. and L.D.S. aided with *T. gondii* infections; S.S.K.L., C.T.A. and R.D.S. aided with tumour models. H.S. and W.J.L. provided helpful discussions. K.M.M. directed the work and wrote the manuscript. All authors discussed the results and contributed to the manuscript.

Author Information All original microarray data have been deposited in NCBI's Gene Expression Omnibus under accession number GSE40647. Reprints and permissions information is available at www.nature.com/reprints. The authors declare no competing financial interests. Readers are welcome to comment on the online version of the paper. Correspondence and requests for materials should be addressed to K.M.M. (kmurphy@wustl.edu).

ARTICLE

doi:10.1038/nature11558

Structure of the agonist-bound neurotensin receptor

Jim F. White[1], Nicholas Noinaj[2], Yoko Shibata[3]†, James Love[4]†, Brian Kloss[4], Feng Xu[1]†, Jelena Gvozdenovic-Jeremic[1]†, Priyanka Shah[1], Joseph Shiloach[5], Christopher G. Tate[3] & Reinhard Grisshammer[1]

Neurotensin (NTS) is a 13-amino-acid peptide that functions as both a neurotransmitter and a hormone through the activation of the neurotensin receptor NTSR1, a G-protein-coupled receptor (GPCR). In the brain, NTS modulates the activity of dopaminergic systems, opioid-independent analgesia, and the inhibition of food intake; in the gut, NTS regulates a range of digestive processes. Here we present the structure at 2.8 Å resolution of *Rattus norvegicus* NTSR1 in an active-like state, bound to NTS_{8-13}, the carboxy-terminal portion of NTS responsible for agonist-induced activation of the receptor. The peptide agonist binds to NTSR1 in an extended conformation nearly perpendicular to the membrane plane, with the C terminus oriented towards the receptor core. Our findings provide, to our knowledge, the first insight into the binding mode of a peptide agonist to a GPCR and may support the development of non-peptide ligands that could be useful in the treatment of neurological disorders, cancer and obesity.

Neurotensin (NTS) is a short peptide that is found in the nervous system and in peripheral tissues[1]. NTS shows a wide range of biological activities and has important roles in Parkinson's disease and the pathogenesis of schizophrenia, the modulation of dopamine neurotransmission, hypothermia, antinociception, and in promoting the growth of cancer cells[2–4]. Three neurotensin receptors have been identified. NTSR1 (ref. 7) and NTSR2 (ref. 8) belong to the class A GPCR family, whereas NTSR3 (also called SORT1) is a member of the sortilin family with a single transmembrane domain[9]. Most of the known effects of NTS are mediated through NTSR1 (ref. 5), which signals preferentially via the G_q protein. Many aspects of ligand binding to NTSR1 have been addressed by mutagenesis and modelling[10–12] but the details of ligand binding remain poorly understood at the molecular level. This has limited the rational design of compounds targeting NTSR1 for therapeutic purposes[2] in the absence of structural information on NTSR1 in complex with agonist or antagonist.

Recent progress in elucidating GPCR structures in complex with either small-molecule antagonists, agonists, or in complex with a heterotrimeric G protein has provided detailed molecular insights into GPCR function (reviewed in refs 13–15). However, most receptor structures are of GPCRs belonging to the α group of class A (ref. 16), which characteristically bind small endogenous agonists deep within the transmembrane core. NTSR1 belongs to a large family of peptide receptors in the β group of class A GPCRs[16] (Supplementary Fig. 1) that includes receptors for substance P, cholecystokinin, neuropeptide Y, endothelin and oxytocin. These peptide receptors bind agonists of a wide range of sizes, from a few amino acid residues to over 60. Current structural information on peptide receptors is limited to representatives of the γ group of class A GPCRs[16], namely the opioid receptors[17–20] and a chemokine receptor[21], all bound to non-peptidic drug-like antagonists. The CXCR4 receptor has also been crystallized in the presence of a cyclic peptide antagonist[21]. Although the structural understanding of peptide receptors has advanced, structures of peptide GPCRs from the β group have not yet been reported. In addition, no structures have been presented of a GPCR bound to a peptide agonist and only the structures of rhodopsin[22,23] and the adenosine A_{2A} receptor ($A_{2A}R$)[24] have been determined bound to endogenous agonists. Here we present the crystal structure of *Rattus norvegicus* NTSR1 from the β GPCR subfamily bound to the C-terminal portion (NTS_{8-13}) of the endogenous agonist NTS.

Structure determination of the agonist-bound NTSR1

Wild-type NTSR1 is unstable in detergent solution and hence is a difficult target for structural studies, particularly in the agonist-bound state which is generally thought to be less stable than the antagonist-bound state[25]. The first step was therefore to stabilize NTSR1 using the strategy of conformational thermostabilization[26]. Previous work had generated a thermostable mutant of NTSR1, but the purified receptor was found to be unsuitable for crystallization, possibly because the receptor contained mutations that were selected in the unliganded state[27]. NTSR1 was therefore thermostabilized in the presence of the agonist NTS through the inclusion of six stabilizing mutations (mutant NTSR1-GW5; $A86L^{1.54}$, $E166A^{3.49}$, $G215A^{ECL2}$, $L310A^{6.37}$, $F358A^{7.42}$ and $V360A^{7.44}$, where superscripts are the Ballesteros–Weinstein numbers[28]) (Supplementary Fig. 2 and Supplementary Table 1). Pharmacological characterization of NTSR1-GW5 (Supplementary Fig. 3, Supplementary Table 2 and Supplementary Discussion) showed that the affinity for the agonist NTS was similar to that of the wild-type receptor, but that the apparent affinity for the neutral antagonist SR48692 and the sensitivity to Na^+ ions was lower. In G protein coupling assays, NTSR1-GW5 did not catalyse nucleotide exchange at $G\alpha_q$ in response to NTS (Supplementary Fig. 3), indicating that the stabilizing mutations may have limited the ability to propagate the agonist-induced conformational change at the ligand-binding

[1]Membrane Protein Structure Function Unit, National Institute of Neurological Disorders and Stroke, National Institutes of Health, Department of Health and Human Services, Rockville, Maryland 20852, USA. [2]Laboratory of Molecular Biology, National Institute of Diabetes and Digestive and Kidney Diseases, National Institutes of Health, Department of Health and Human Services, Bethesda, Maryland 20892, USA. [3]MRC Laboratory of Molecular Biology, Hills Road, Cambridge CB2 0QH, UK. [4]Protein Production Facility of the New York Consortium on Membrane Protein Structure, New York Structural Biology Center, New York, New York 10027, USA. [5]Biotechnology Core Lab, National Institute of Diabetes and Digestive and Kidney Diseases, National Institutes of Health, Department of Health and Human Services, Bethesda, Maryland 20892, USA. †Present addresses: Medimmune, Milstein Building, Granta Park, Cambridge CB21 6GH, UK (Y.S.); Albert Einstein College of Medicine, Price Center, New York, New York 10461, USA (J.L.); College of Pharmacy, State Key Laboratory of Medicinal Chemical Biology and Tianjin Key Laboratory of Molecular Drug Research, Nankai University, Tianjin 300071, China (F.X.); National Human Genome Research Institute, National Institutes of Health, Department of Health and Human Services, Bethesda, Maryland 20892, USA (J.G.-J.).

pocket to the re-arrangement of the intracellular face of the receptor required for G protein binding and activation.

For crystallization of NTSR1-GW5, T4 lysozyme (T4L) was engineered into intracellular loop 3 (ICL3) to improve the probability of obtaining well-diffracting crystals[29]. NTSR1-GW5-T4L was expressed in insect cells using the baculovirus expression system, solubilized and purified in lauryl maltose neopentyl glycol and crystallized using the lipidic cubic phase methodology[30]. Diffraction data were collected to 2.8 Å resolution from a single crystal and used to determine the structure by molecular replacement (Supplementary Table 3, Supplementary Fig. 4 and Supplementary Fig. 5). The final model of NTSR1-GW5-T4L, refined to R/R_{free} values of 0.23/0.28, includes 454 residues, 2 HEPES molecules, 23 H_2O molecules and the agonist ligand NTS_{8-13}.

Overall structure of NTSR1–GW5–T4L

The receptor core has seven transmembrane helices (TM1–TM7) (Fig. 1 and Supplementary Fig. 6), as expected, but there was no density corresponding to amphipathic helix 8 at the C terminus of the receptor. Helix 8 has been observed in all GPCR structures except for the chemokine receptor CXCR4 (ref. 21), so the absence of helix 8 in the structure of NTSR1-GW5-T4L could be because either NTSR1 *in vivo* does not possess helix 8 or this is the result of a crystallization artefact. On the intracellular side, TM7 is elongated by three helical turns beyond the conserved $NP^{7.50}XXY^{7.53}$ motif, whereas other GPCRs have only one helical turn. This extension of TM7 is associated with the intracellular end of TM6 through hydrogen bonds between the side chain atoms of N375 and Q378 to the backbone carbonyl oxygen of $A302^{6.29}$ (Supplementary Fig. 7).

Of the intracellular loops in NTSR1, ICL1 was disordered (K93–Q96), ICL3 was disrupted through insertion of T4L, and only ICL2 showed density for a structural element, a short π-helix (Fig. 1). ICL2 is thought to be important for G protein coupling, and the short helix in NTSR1 is similar to those observed in identical positions in both the inactive state[31] and in active states[32,33] of β-adrenergic receptors (βARs). In the β_1-adrenergic receptor (β_1AR)[31], the helix in ICL2 is stabilized by the interaction of a tyrosine residue in the middle of the helix that forms a hydrogen bond with the aspartate residue of the conserved $D/ER^{3.50}Y$ sequence in TM3. In NTSR1, K178 in the middle of the π-helix in ICL2 may perform a similar function, although its side chain is disordered, probably because the stabilizing mutation $E166A^{3.49}$ prevents the formation of the salt bridge. The extracellular surface of NTSR1 is composed of three short extracellular loops (ECL1, ECL2 and ECL3) and the N-terminal residues N52–D60 that extend across the receptor to form one side of the ligand-binding pocket (see below). The longest loop is ECL2, which contains two short antiparallel β-strands that are linked to TM3 by a disulphide bond between the conserved residues $C142^{3.25}$ and $C225^{ECL2}$. These β-strands are characteristic of all the peptide GPCR structures determined so far.

NTSR1-GW5-T4L contains six thermostabilizing mutations and none of these residues is in the NTS binding pocket (Fig. 1). Three of these mutations may directly affect the equilibrium between inactive and active states of NTSR1. The mutation $F358A^{7.42}$ is located at the kink in TM7, with the alanine side chain pointing into the receptor core, and the F358A mutant is known to be constitutively active[34]. The mutation $E166A^{3.49}$ is in the conserved $D/ER^{3.50}Y$ motif in TM3 and will prevent the formation of the intrahelical salt bridge with $R167^{3.50}$, thus facilitating the transition to the active state[35,36] by allowing $R167^{3.50}$ to interact with $N257^{5.58}$. The R167–N257 interaction may be promoted by the $L310A^{6.37}$ mutation through decreasing the size of the side chain. The reasons for the thermostabilizing effect of the $A86L^{1.54}$, $V360A^{7.44}$ and $G215A^{ECL2}$ mutations are not obvious, although it is interesting that an alanine residue[37] is found in human NTSR1 (Supplementary Fig. 8) at the position equivalent to G215 in rat NTSR1.

NTSR1–GW5 is in an active-like conformation

Upon agonist binding, a GPCR undergoes conformational changes that ultimately allow binding and activation of a G protein at the

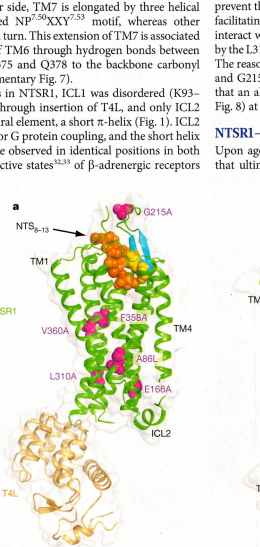

Figure 1 | Overview of the NTSR1 structure bound to the peptide agonist NTS_{8-13}. **a**–**c**, Cartoon representation of NTSR1-GW5-T4L; side view (**a**), extracellular view (**b**), intracellular view (**c**). Space-filling models are used to depict the agonist NTS_{8-13} (orange), the side chains of thermostabilizing mutations (purple) and the disulphide bond (yellow) between the conserved residues C142 and C225. Also shown are the β-hairpin in extracellular loop 2 (blue–green) and the π-helix in intracellular loop 2 (ICL2). T4L has been omitted from the intracellular view for clarity.

intracellular surface of the receptor. Agonist-induced conformational changes in the ligand-binding pocket are largely receptor specific and thought to be relatively small, leading to larger conformational changes in the intracellular half of the receptor[13]. There are no reported structures of NTSR1 in an inactive conformation, so we are unable to discuss agonist-specific conformational changes in the ligand-binding pocket. However, it is possible to compare the NTSR1 structure to the inactive and active conformations of rhodopsin and β_2AR. This allows an assessment of the overall conformation of NTSR1 and, in addition, the rotamer conformations of mechanistically important residues that show characteristic interactions depending on whether the receptor is in an inactive or active state. These comparisons indicate that NTSR1 is in an active-like state.

One of the major conformational changes occurring during the transition from the inactive to an active state is an outward tilt of TM6 at the intracellular face of the GPCR. The extent of movement of TM6 upon activation is 6 Å for rhodopsin and 11–14 Å for β_2AR^{32}, with TM6 of NTSR1 in a position similar to that seen for the active states of rhodopsin[22,38] (Fig. 2). The distance between the Cα atoms of $R^{3.50}$ and $E^{6.30}$ change upon activation from 9 Å to 15 Å in rhodopsin[22,39], and from 11 Å to 19 Å in $\beta_2AR^{32,40}$. The equivalent distance in NTSR1 is 14 Å.

Other features of NTSR1 are also remarkably similar to those found in the active conformations of rhodopsin and β_2AR. In inactive receptor conformations, $R^{3.50}$ of the D/ERY motif forms an intrahelical salt bridge with $D/E^{3.49}$, which is, for example, present in the inactive structure of the nociceptin/orphanin FQ receptor (NOP)[19] (Fig. 3), which is the closest structural homologue of NTSR1 among peptide receptors. Upon activation, the $D/E^{3.49}$-$R^{3.50}$ salt bridge is broken and $R^{3.50}$ re-orients to form an interhelical hydrogen bond with the conserved tyrosine residue $Y^{5.58}$, linking TM3 and TM5 (ref. 13). In NTSR1, the $R167^{3.50}$ side chain is hydrogen bonded to $N257^{5.58}$ that interacts with the conserved residue $S164^{3.47}$ (Fig. 3), stabilizing TM5 in an active-like orientation[35]. In addition, $Y369^{7.53}$ of the highly conserved $NP^{7.50}XXY^{7.53}$ motif occupies space within the helical bundle as seen for $Y^{7.53}$ in the active states of rhodopsin and β_2AR (Fig. 3). In contrast to the active rhodopsin and β_2AR, $Y369^{7.53}$ in NTSR1 does not pack against $R167^{3.50}$, suggesting that $N257^{5.58}$ has a greater contribution to the active state stabilization than $Y369^{7.53}$ (ref. 35).

Comparison of the NTSR1 structure with rhodopsin and β_2AR suggests that it is in an active-like state, indicating that it may couple effectively to G proteins. NTSR1-GW5-T4L, as expected, does not couple to G protein (Supplementary Fig. 3), because T4L replaces most of ICL3, which is essential for G protein binding, and sterically blocks access to the intracellular surface of the receptor. Surprisingly, NTSR1-GW5 that contains the wild-type ICL3 also does not catalyse nucleotide exchange at $G\alpha_q$ in response to NTS (Supplementary Fig. 3). This may be a consequence of the extended region of TM7 on the intracellular surface forming an interhelical contact with TM6 (Supplementary Fig. 7). This appears to occlude the cavity at the intracellular face of the receptor where the C-terminal portion of the Gα protein binds to fully active receptors[22,23,32,38]. Thus, although the structure of NTSR1 contains many features of an active receptor it is possible that the intracellular surface of the receptor does not represent the structure of fully active NTSR1.

The NTS_{8-13} binding site

NTSR1-GW5-T4L was co-crystallized with NTS_{8-13}, which has higher potency and efficacy than full-length NTS[10,41], although it does not exist *in vivo*. NTSR1 also binds the NTS-related hexapeptide neuromedin N, which is produced along with NTS during proteolytic processing of the proNTS precursor[5]. The amino acid sequence of neuromedin N (KIPYIL) is similar to NTS_{8-13} (RRPYIL). Potent NTS analogues that can cross the blood–brain barrier (for example, derivatives of RKPWLL) can also be synthesized (see ref. 5). The similarity of these agonists to NTS_{8-13} indicates that they all bind in a similar manner. There is charge complementarity between NTS_{8-13} and its binding pocket, with the positive-charged arginine side chains of NTS_{8-13} adjacent to the electronegative rim of the binding site, and the C terminus of NTS_{8-13} is predicted to form a salt bridge with $R327^{6.54}$ (Fig. 4 and Supplementary Table 4). There are also extensive van der Waals interactions between NTS_{8-13} and the receptor along with hydrogen bonds and a salt bridge (Supplementary Table 4, Supplementary Table 5 and Supplementary Fig. 9). It is striking that only three out of eight hydrogen bonds are made between the side chains of NTS_{8-13} and the receptor, with the bulk of receptor–ligand contacts being van der Waals interactions.

The ligand binding pocket for NTS_{8-13} is composed of amino acid residues in the N terminus, the three extracellular loops (ECL1–ECL3) and six transmembrane α-helices (TM2–TM7), with the greatest number of ligand–receptor contacts from residues in ECL2, ECL3, TM6 and TM7 (Supplementary Table 5). The binding pocket is wide open on the extracellular surface of NTSR1 (Fig. 4 and Supplementary Fig. 10) with density for NTS_{8-13} clearly discernable from a difference electron density map (Supplementary Fig. 11), but we believe that radiation damage during data collection has resulted in reduced density for the C-terminal carboxylate group (Supplementary Fig. 12). The extended conformation of NTS_{8-13} in the crystal structure is in good

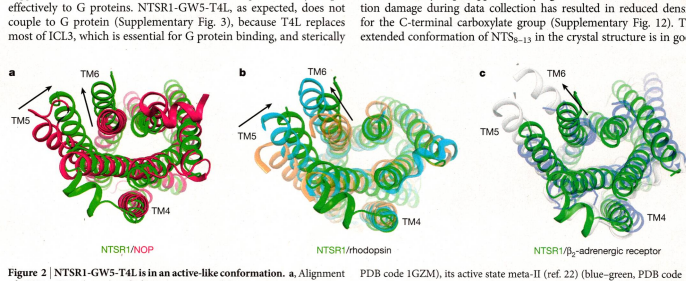

Figure 2 | NTSR1-GW5-T4L is in an active-like conformation. a, Alignment of NTSR1-GW5 (green) with the inactive state of the nociceptin receptor (NOP)[19] (red; Protein Data Bank (PDB) code 4EA3). NTSR1 was most similar to NOP (root mean squared deviation = 2.1 Å for Cα atoms in the TM domains) upon alignment of the TM domains of NTSR1 with other peptide receptors[17–21]. **b**, Alignment of the inactive state of rhodopsin[38] (light brown, PDB code 1GZM), its active state meta-II (ref. 22) (blue–green, PDB code 3PQR) and NTSR1-GW5 (green). **c**, Alignment of the inactive state of β_2AR[40] (pale mauve, PDB code 2RH1) and its active state[32] (pale grey, PDB code 3SN6) and NTSR1-GW5 (green). All views are from the intracellular surface. The arrows indicate the apparent displacement of TM5 and TM6 of NTSR1-GW5 relative to the corresponding helix positions in the inactive receptor structures.

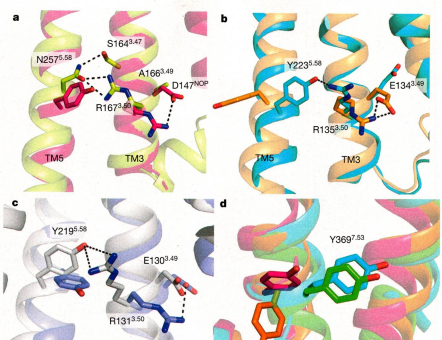

Figure 3 | The conserved D/ERY and NPXXY motifs in NTSR1-GW5. **a**, Comparison of the side-chain orientations of $R^{3.50}$ and $Y/N^{5.58}$ of NTSR1-GW5 and the inactive nociceptin receptor (NOP)[19] (PDB code 4EA3). NTSR1-GW5 residues (R167, N257, labelled) are in green; corresponding NOP residues (R148, Y235, unlabelled) are in red. $D147^{3.49}$ of NOP and $A166^{3.49}$ of NTSR1 are also shown. **b**, In an inactive GPCR, $R^{3.50}$ interacts with $E^{3.49}$ as shown here for rhodopsin[19] (pale brown, PDB code 1GZM). This salt bridge is broken upon activation, allowing $R^{3.50}$ to contact residue $Y/N^{5.58}$, as depicted for active rhodopsin (ref. 22) (blue–green, PDB code 3PQR) (residues E134, R135 and Y223). **c**, The same comparison for inactive β_2AR^{40} (pale mauve, PDB code 2RH1) and active β_2AR^{32} (pale grey, PDB code 3SN6) (residues E130, R131 and Y219). **d**, $Y369^{7.53}$ of NTSR1 (green) occupies space as seen for $Y306^{7.53}$ in active rhodopsin (blue–green; PDB code 3PQR). The orientation of $Y306^{7.53}$ in the inactive rhodopsin (pale brown; PDB code 1GZM) and the inactive NOP (red; PDB code 4EA3) is shown for comparison.

agreement with that of NTS_{8-13} bound to wild-type NTSR1 analysed by solid-state NMR[42] (Supplementary Fig. 13). The overall shape of the NTSR1 ligand-binding pocket is narrower than that observed in the other peptide receptors[17–21] due to an inward shift of the extracellular regions of TM2 and TM6 (Supplementary Fig. 14), probably as a result of the pronounced kink in TM2 at $A120^{2.57}$ and a change in tilt of TM6. At the extracellular surface, the NTS_{8-13} binding pocket is partially capped by the ECL2 β-hairpin and the proximal end of the receptor N terminus. NTSR1 has been subjected to extensive site-directed mutagenesis studies to define ligand–receptor interactions

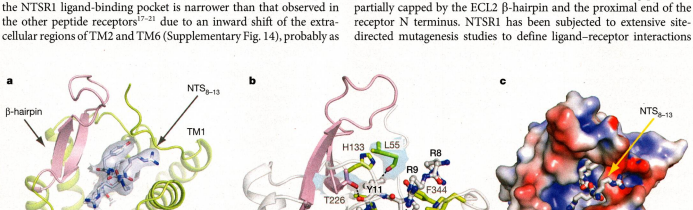

Figure 4 | The NTSR1 agonist binding pocket. All views are from the extracellular side, with NTS_{8-13} shown as a stick model. **a**, Cartoon representation of the ligand-binding pocket with the ECL2 β-hairpin (pink). The quality of the electron density of NTS_{8-13} is depicted as blue isosurface ($2F_o - F_c$ map contoured at 1σ). **b**, Key NTSR1 residues (green residues with grey labels) in contact with the peptide ligand (grey residues with bold black labels). Hydrogen bonds and salt bridges are indicated by dashed lines (black). The electron density maps of selected NTSR1 residues (L55, Y146, T226, R327) are shown as blue isosurface ($2F_o - F_c$ map contoured at 1σ). **c**, The charge complementarity between NTS_{8-13} and its binding pocket is depicted with the NTSR1 surface coloured according to its electrostatic potential ($-4\ kT\ e^{-1}$ to $+4\ kT\ e^{-1}$; red, negative; blue, positive). The positively charged arginine side chains of the ligand face the electronegative rim of the binding pocket, whereas the negatively charged carboxylate of L13 resides in an electropositive environment. See also Supplementary Information.

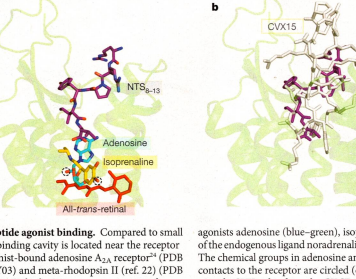

Figure 5 | A new paradigm for peptide agonist binding. Compared to small endogenous agonists, the NTS_{8-13} binding cavity is located near the receptor surface. **a**, The structures of the agonist-bound adenosine A_{2A} receptor[24] (PDB code 2YDO), β_1AR[25] (PDB code 2Y03) and meta-rhodopsin II (ref. 22) (PDB code 3PQR) were aligned in PyMOL. Only the cartoon representation for NTSR1-GW5 is shown (pale green) with NTS_{8-13} depicted in purple. The agonists adenosine (blue–green), isoprenaline (yellow; an isopropyl derivative of the endogenous ligand noradrenaline) and all-*trans*-retinal (red) are labelled. The chemical groups in adenosine and isoprenaline that make agonist-specific contacts to the receptor are circled (dashed line). **b**, The cyclic antagonist peptide CVX15 binds to the CXCR4 receptor[13] (grey; PDB code 3OE0) in a similar fashion to NTS_{8-13} (purple) in NTSR1-GW5 (pale green cartoon).

(see Supplementary Discussion) and there is excellent agreement between those data and the structure of NTSR1.

There is a striking difference between the binding mode of NTS_{8-13} in NTSR1 with the binding of agonists in rhodopsin, β_1AR and $A_{2A}R$ (Fig. 5). The agonist-specific interactions made by isoprenaline in β_1AR (ref. 43) and adenosine in $A_{2A}R$ (ref. 24) all occur at a similar depth in the receptor with respect to the extracellular surface as retinal in rhodopsin[22,23]. In contrast, NTS_{8-13} does not penetrate the receptor as deeply, with the C terminus of NTS_{8-13} over 5 Å closer to the extracellular surface than the hydroxyl groups in isoprenaline and adenosine that are characteristic of agonists for βARs and $A_{2A}R$. This indicates that the mode of activation of NTSR1 is subtly different from these receptors. Structures of NTSR1 in the inactive state will be necessary to gain a better understanding of how peptide agonists activate GPCRs.

METHODS SUMMARY

The stabilized NTSR1 mutant with T4 lysozyme replacing most of intracellular loop 3 was expressed in insect cells and purified by cobalt affinity chromatography. It was crystallized in lipidic cubic phase. Diffraction data were collected at the GM/CA-CAT beamline of the Advanced Photon Source at the Argonne National Laboratory. The structure was solved by molecular replacement using data from a single crystal.

Full Methods and any associated references are available in the online version of the paper.

Received 26 June; accepted 11 September 2012.
Published online 10 October 2012.

1. Carraway, R. & Leeman, S. E. The isolation of a new hypotensive peptide, neurotensin, from bovine hypothalami. *J. Biol. Chem.* **248,** 6854–6861 (1973).
2. Bissette, G., Nemeroff, C. B., Loosen, P. T., Prange, A. J. Jr & Lipton, M. A. Hypothermia and intolerance to cold induced by intracisternal administration of the hypothalamic peptide neurotensin. *Nature* **262,** 607–609 (1976).
3. Carraway, R. E. & Plona, A. M. Involvement of neurotensin in cancer growth: evidence, mechanisms and development of diagnostic tools. *Peptides* **27,** 2445–2460 (2006).
4. Griebel, G. & Holsboer, F. Neuropeptide receptor ligands as drugs for psychiatric diseases: the end of the beginning? *Nature Rev. Drug Discov.* **11,** 462–478 (2012).
5. Kitabgi, P. Targeting neurotensin receptors with agonists and antagonists for therapeutic purposes. *Curr. Opin. Drug Discov. Devel.* **5,** 764–776 (2002).
6. Schimpff, R.-M. *et al.* Increased plasma neurotensin concentrations in patients with Parkinson's disease. *J. Neurol. Neurosurg. Psychiatry* **70,** 784–786 (2001).
7. Tanaka, K., Masu, M. & Nakanishi, S. Structure and functional expression of the cloned rat neurotensin receptor. *Neuron* **4,** 847–854 (1990).
8. Chalon, P. *et al.* Molecular cloning of a levocabastine-sensitive neurotensin binding site. *FEBS Lett.* **386,** 91–94 (1996).
9. Mazella, J. Sortilin/neurotensin receptor-3: a new tool to investigate neurotensin signaling and cellular trafficking? *Cell. Signal.* **13,** 1–6 (2001).
10. Barroso, S. *et al.* Identification of residues involved in neurotensin binding and modeling of the agonist binding site in neurotensin receptor 1. *J. Biol. Chem.* **275,** 328–336 (2000).
11. Härterich, S., Koschatzky, S., Einsiedel, J. & Gmeiner, P. Novel insights into GPCR-peptide interactions: mutations in extracellular loop 1, ligand backbone methylations and molecular modeling of neurotensin receptor 1. *Bioorg. Med. Chem.* **16,** 9359–9368 (2008).
12. Pang, Y. P., Cusack, B., Groshan, K. & Richelson, E. Proposed ligand binding site of the transmembrane receptor for neurotensin$_{8-13}$. *J. Biol. Chem.* **271,** 15060–15068 (1996).
13. Deupi, X. & Standfuss, J. Structural insights into agonist-induced activation of G-protein-coupled receptors. *Curr. Opin. Struct. Biol.* **21,** 541–551 (2011).
14. Katritch, V., Cherezov, V. & Stevens, R. C. Diversity and modularity of G protein-coupled receptor structures. *Trends Pharmacol. Sci.* **33,** 17–27 (2012).
15. Lebon, G., Warne, T. & Tate, C. G. Agonist-bound structures of G protein-coupled receptors. *Curr. Opin. Struct. Biol.* **22,** 1–9 (2012).
16. Fredriksson, R., Lagerstrom, M. C., Lundin, L. G. & Schioth, H. B. The G-protein-coupled receptors in the human genome form five main families. Phylogenetic analysis, paralogon groups, and fingerprints. *Mol. Pharmacol.* **63,** 1256–1272 (2003).
17. Granier, S. *et al.* Structure of the δ-opioid receptor bound to naltrindole. *Nature* **485,** 400–404 (2012).
18. Manglik, A. *et al.* Crystal structure of the μ-opioid receptor bound to a morphinan antagonist. *Nature* **485,** 321–326 (2012).
19. Thompson, A. A. *et al.* Structure of the nociceptin/orphanin FQ receptor in complex with a peptide mimetic. *Nature* **485,** 395–399 (2012).
20. Wu, H. *et al.* Structure of the human κ-opioid receptor in complex with JDTic. *Nature* **485,** 327–332 (2012).
21. Wu, B. *et al.* Structures of the CXCR4 chemokine GPCR with small-molecule and cyclic peptide antagonists. *Science* **330,** 1066–1071 (2010).
22. Choe, H. W. *et al.* Crystal structure of metarhodopsin II. *Nature* **471,** 651–655 (2011).
23. Standfuss, J. *et al.* The structural basis of agonist-induced activation in constitutively active rhodopsin. *Nature* **471,** 656–660 (2011).
24. Lebon, G. *et al.* Agonist-bound adenosine A_{2A} receptor structures reveal common features of GPCR activation. *Nature* **474,** 521–525 (2011).
25. Gether, U. *et al.* Structural instability of a constitutively active G protein-coupled receptor. Agonist-independent activation due to conformational flexibility. *J. Biol. Chem.* **272,** 2587–2590 (1997).
26. Tate, C. G. A crystal clear solution for determining GPCR structures. *Trends Biochem. Sci.* **37,** 343–352 (2012).
27. Shibata, Y. *et al.* Thermostabilization of the neurotensin receptor NTS1. *J. Mol. Biol.* **390,** 262–277 (2009).
28. Ballesteros, J. A. & Weinstein, H. Integrated methods for the construction of three-dimensional models and computational probing of structure-function relations in G protein-coupled receptors. *Methods Neurosci.* **25,** 366–428 (1995).
29. Rosenbaum, D. M. *et al.* GPCR engineering yields high-resolution structural insights into β2-adrenergic receptor function. *Science* **318,** 1266–1273 (2007).
30. Caffrey, M. & Cherezov, V. Crystallizing membrane proteins using lipidic mesophases. *Nature Protocols* **4,** 706–731 (2009).
31. Warne, T. *et al.* Structure of a β1-adrenergic G-protein-coupled receptor. *Nature* **454,** 486–491 (2008).
32. Rasmussen, S. G. *et al.* Crystal structure of the β2 adrenergic receptor-Gs protein complex. *Nature* **477,** 549–555 (2011).

33. Rasmussen, S. G. *et al.* Structure of a nanobody-stabilized active state of the β_2 adrenoceptor. *Nature* **469,** 175–180 (2011).
34. Barroso, S., Richard, F., Nicolas-Etheve, D., Kitabgi, P. & Labbe-Jullie, C. Constitutive activation of the neurotensin receptor 1 by mutation of Phe358 in helix seven. *Br. J. Pharmacol.* **135,** 997–1002 (2002).
35. Goncalves, J. A. *et al.* Highly conserved tyrosine stabilizes the active state of rhodopsin. *Proc. Natl Acad. Sci. USA* **107,** 19861–19866 (2010).
36. Vogel, R. *et al.* Functional role of the "ionic lock"—an interhelical hydrogen-bond network in family A heptahelical receptors. *J. Mol. Biol.* **380,** 648–655 (2008).
37. Vita, N. *et al.* Cloning and expression of a complementary DNA encoding a high affinity human neurotensin receptor. *FEBS Lett.* **317,** 139–142 (1993).
38. Scheerer, P. *et al.* Crystal structure of opsin in its G-protein-interacting conformation. *Nature* **455,** 497–502 (2008).
39. Li, J., Edwards, P. C., Burghammer, M., Villa, C. & Schertler, G. F. Structure of bovine rhodopsin in a trigonal crystal form. *J. Mol. Biol.* **343,** 1409–1438 (2004).
40. Cherezov, V. *et al.* High-resolution crystal structure of an engineered human β_2-adrenergic G protein-coupled receptor. *Science* **318,** 1258–1265 (2007).
41. Henry, J. A., Horwell, D. C., Meecham, K. G. & Rees, D. C. A structure-affinity study of the amino acid side-chains in neurotensin: N and C terminal deletions and Ala-scan. *Bioorg. Med. Chem. Lett.* **3,** 949–952 (1993).
42. Luca, S. *et al.* The conformation of neurotensin bound to its G protein-coupled receptor. *Proc. Natl Acad. Sci. USA* **100,** 10706–10711 (2003).
43. Warne, T. *et al.* The structural basis for agonist and partial agonist action on a β_1-adrenergic receptor. *Nature* **469,** 241–244 (2011).

Supplementary Information is available in the online version of the paper.

Acknowledgements This research was supported by the Intramural Research Program of the National Institutes of Health (J.F.W., J.G.-J., P.S. and R.G.: National Institute of Neurological Disorders and Stroke; N.N. and J.S.: National Institute of Diabetes and Digestive and Kidney Diseases) and a joint grant from Pfizer Global Research and Development and the MRCT Development Gap Fund in addition to core funding from the UK Medical Research Council MRC U105197215 (Y.S., C.G.T.). The Protein Production Facility of the New York Consortium on Membrane Protein Structure was supported by the National Institutes of Health grant U54GM075026 (J.L., B.K.). We acknowledge the NIH Roadmap grant P50 GM073197 for technology development (to R. C. Stevens) for visitor support at The Scripps Research Institute. We thank the staff at the General Medicine and Cancer Institute's Collaborative Access Team (GM/CA-CAT) beamline at the Advanced Photon Source, Argonne National Laboratory for their assistance during data collection. Use of the Advanced Photon Source was supported by the US Department of Energy, Basic Energy Sciences, Office of Science, under contract No. DE-AC02-06CH11357.

Author Contributions J.F.W. characterized various NTSR1 constructs by ligand binding and G protein assays, tested NTSR1 mutants for stability, and purified NTSR1 for crystallization. N.N. collected diffraction data and solved the structure. Y.S. performed alanine scanning mutagenesis and tested NTSR1 mutants for stability, and C.G.T. was responsible for the mutagenesis strategy. J.L. and B.K. explored and performed the automation of alanine scanning mutagenesis. F.X. performed crystallization experiments and stability tests. J.G.-J. and P.S. did alanine scanning and molecular biology on NTSR1. J.S. performed large-scale fermentation. R.G. performed crystallization experiments, assisted with data collection and was responsible for the overall project strategy. The manuscript was written by R.G. and C.G.T.

Author Information Coordinates and structure factors for NTSR1-GW5-T4L are deposited in the Protein Data Bank under accession code 4GRV. Reprints and permissions information is available at www.nature.com/reprints. The authors declare no competing financial interests. Readers are welcome to comment on the online version of the paper. Correspondence and requests for materials should be addressed to R.G. (rkgriss@helix.nih.gov).

LETTER

doi:10.1038/nature11474

Near-infrared background anisotropies from diffuse intrahalo light of galaxies

Asantha Cooray[1], Joseph Smidt[1], Francesco De Bernardis[1], Yan Gong[1], Daniel Stern[2], Matthew L. N. Ashby[3], Peter R. Eisenhardt[2], Christopher C. Frazer[1], Anthony H. Gonzalez[4], Christopher S. Kochanek[5], Szymon Kozłowski[5,6] & Edward L. Wright[7]

Unresolved anisotropies of the cosmic near-infrared background radiation are expected to have contributions from the earliest galaxies during the epoch of reionization[1–5] and from faint, dwarf galaxies at intermediate redshifts[6,7]. Previous measurements[8–12] were unable to pinpoint conclusively the dominant origin because they did not sample spatial scales that were sufficiently large to distinguish between these two possibilities. Here we report a measurement of the anisotropy power spectrum from subarcminute to one-degree angular scales, and find the clustering amplitude to be larger than predicted by the models based on the two existing explanations. As the shot-noise level of the power spectrum is consistent with that expected from faint galaxies, a new source population on the sky is not necessary to explain the observations. However, a physical mechanism that increases the clustering amplitude is needed. Motivated by recent results related to the extended stellar light profile in dark-matter haloes[13–15], we consider the possibility that the fluctuations originate from intrahalo stars of all galaxies. We find that the measured power spectrum can be explained by an intrahalo light fraction of 0.07 to 0.2 per cent relative to the total luminosity in dark-matter haloes of 10^9 to 10^{12} solar masses at redshifts of about 1 to 4.

To distinguish between the two interpretations of the near-infrared anisotropy power spectrum, we have analysed imaging data from the Spitzer Deep, Wide-Field Survey (SDWFS)[16]. This survey covers 10.5 square degrees on the sky with the IRAC instrument in its four bands between 3.6 and 8 μm. We focus on the data at 3.6 and 4.5 μm, as the confusion from zodiacal light limits extragalactic background studies at 5 and 8 μm (ref. 8). The data were taken in four separate epochs between 2004 and 2008, and observations were conducted in ways to minimize the systematic errors associated with anisotropy measurements. In particular, the four different epochs were observed at different roll angles of the instrument so that the measurements are robust against detector artefacts, persistence resulting from saturated bright stars, and variations in the bias level. The SDWFS mapping strategy was also optimized to facilitate self-calibration[17] of the data by maximizing inter-pixel correlations.

To limit the influence of bright stars and galaxies, including extended sources, in our anisotropy measurements, we mask all sources that are detected either in the combined SDWFS data or in the ancillary multi-band optical and near-infrared data[18]. The effects of assembling ('mosaicing') individual detector frames, pixelization of the maps, and the detected-source mask are captured by the map-making transfer function (Supplementary Information). We compute the transfer function and its uncertainty with a large set of sky simulations. The point-spread function (PSF) and its uncertainty were determined by measuring and modelling the PSF of stars in different subregions of the image and computing the variance of the differences between the modelled PSFs.

The power spectrum measurements at 3.6 and 4.5 μm show a clear excess above the shot-noise level (Fig. 1). The shot noise dominates the anisotropy power spectrum at subarcminute angular scales corresponding to angular multipole moment $\ell > 10^5$. Such a shot noise is expected from the small-scale Poisson behaviour of the spatial distribution of sources on the sky. The clustering amplitude we measure at $\ell \approx 10^4$ is fully consistent with existing measurements of the anisotropy power spectrum with IRAC in deeper, but smaller-area, fields[8,9,12]. At angular scales of tens of arcseconds, corresponding to $\ell > 5 \times 10^4$, our shot-noise level is higher than that of a recent measurement by a factor of about 2 because deeper data allow more of the fainter sources to be individually detected and masked[12]. Nevertheless, we independently confirm the near-infrared background anisotropies at angular scales larger than a few arcminutes at the previously reported amplitude[12].

The near-infrared anisotropies have been previously interpreted as either due to spatial clustering of primordial galaxies responsible for cosmic reionization[8] or due to faint, dwarf galaxies at low redshifts that fall below the individual source detection threshold of Spitzer images[6,7,9]. Figure 1 shows that the measured fluctuations in SDWFS are well above both these interpretations. The power spectrum predictions for galaxies at redshifts $z > 6$ rely on a combination of analytical calculations[19] and numerical simulations[20] of reionization. If we force the $z > 6$ galaxy model to fit the power spectrum data, then the integrated intensity of $z > 6$ galaxies is about 2 nW m^{-2} sr^{-1} at 3.6 μm (ref. 19). To reach such a high intensity, these galaxies must be very efficient in converting baryons to stars[20]. In fact, the required star-formation rate conflicts with the measured metal abundance at $z > 4$, the measured X-ray background when compared to X-rays from stellar end products such as black holes, and the measured luminosity functions of bright Lyman-dropout galaxies[21]. Unless a significant revision of our current understanding of $z > 6$ galaxy statistics is made, it is unlikely that the measured anisotropy power spectrum is dominated by the primordial galaxies.

A large compilation of multi-wavelength luminosity functions and galaxy number counts[7] allow predictions to be made for the intensity fluctuations due to low-redshift, faint galaxies. The measured luminosity-function slope at the faint end is used to extrapolate to the fainter galaxies that are undetected in the Spitzer images. An increase in the faint-end slope above the measured values does not increase the clustering amplitude on the angular scales of interest without modifying the shot-noise level. Although the clustering amplitude is smaller than the measurements, the prediction related to faint, dwarf galaxies[7] shows that they generate a shot-noise level consistent with the measured small-scale anisotropy power spectrum (Fig. 1). At angular scales of a few tens of arcminutes, the measurements are such that the clustering amplitude is a factor of about 6 to 10 above the prediction. Although this difference suggests that a new model to explain the anisotropy power spectrum is clearly needed, the consistency with the shot-noise level is

[1]Department of Physics and Astronomy, University of California, Irvine, California 92697, USA. [2]Jet Propulsion Laboratory, California Institute of Technology, Pasadena, California 91109, USA. [3]Harvard-Smithsonian Center for Astrophysics, 60 Garden Street, Cambridge, Massachusetts 02138, USA. [4]Department of Astronomy, University of Florida, Gainesville, Florida 32611, USA. [5]Department of Astronomy, The Ohio State University, Columbus, Ohio 43210, USA. [6]Warsaw University Observatory, Aleje Ujazdowskie 4, 00-478 Warszawa, Poland. [7]Department of Physics and Astronomy, University of California, Los Angeles, California 90095, USA.

such that we do not need to invoke a new population of point sources on the sky to explain the observations.

While keeping the shot-noise level the same, the measurements can be explained by any physical effect that boosts the two-halo term of the halo model of galaxy clustering[22]. One possibility is to increase the halo masses of the faint, dwarf galaxies so that their clustering amplitude is increased with a corresponding increase in their large-scale bias factor[22].

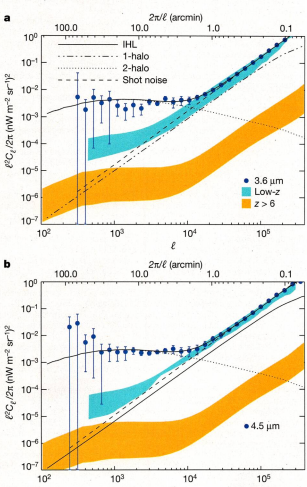

Figure 1 | The angular power spectrum of the unresolved near-infrared background. Shown is the total power spectrum $\ell^2 C_\ell/2\pi$ of SDWFS at 3.6 μm (**a**) and 4.5 μm (**b**) as a function of the multipole moment ℓ. The corresponding angular scale $2\pi/\ell$ is listed on the upper x axis in units of arcminutes. SDWFS imaging data were taken on the same field at four separate epochs in January 2004, August 2007, February 2008 and March 2008. Each epoch of data, taken over 7 to 10 days, includes 4,300–4,900 IRAC frames that were combined to make mosaics using the self-calibration algorithm[17]. The total integration time is 6 min per pixel. These individual frames were first visually inspected and cleaned of artefacts such as asteroidal trails and hot pixels. Through cross-correlations between sum and difference maps between epochs, we make independent measurements of the sky signal and noise. The final power spectrum (filled circles) is the average of the multi-epoch cross-correlation data under the assumption that the instrumental noise is not correlated between epochs. The two shaded regions show the expected contribution from $z > 6$ galaxies[16] (blue) and low-redshift galaxies[7] (yellow) based on two model predictions in the literature. The lines shows a diffuse IHL model where we show the signal in terms of the total (solid), one (dashed-dotted) and two (dotted) halo terms. The dashed line is the best-fit shot-noise signal that dominates the anisotropies at small angular scales. In **a** and **b**, the error bars are 1σ uncertainties in the power spectrum. They are determined by propagating the errors from the beam measurement into the power spectrum, while the simulations, based out of noise measurements, were used to obtain instrumental and sky variance. The quadratic sum of these errors and the map-making transfer function uncertainty constitutes the final error estimate.

The required modification needed to explain the fluctuation data is, however, ruled out by the measured number counts and the redshift distribution[7]. Because intensity anisotropies are measured, another option is to introduce a luminosity component to the dark-matter haloes that remain unmasked when the hosted bright galactic disks are masked as part of the analysis. Such a possibility exists in the literature in the form of diffuse halo stars in the extended stellar profile of galaxies out to distances of 100 kpc (ref. 23). In our anisotropy measurements, we mask the faintest detected galaxies to 3–4 arcsec, which removes the light from the bulges and disks of those galaxies. To remove the diffuse light component, we would have to mask to a radius greater than 10 arcsec around each galaxy. The surface density of galaxies down to AB-magnitude $m_{AB} < 22$ at 3.6 μm is such that we expect 2 to 3 galaxies within a circle of radius 10 arcsec. Thus masks which successfully remove the diffuse component leave no pixels on the map from which to measure the anisotropy power spectrum.

Existing studies discuss this extended emission in terms of the diffuse intrahalo light (IHL)[15], explained as originating in tidally stripped stars produced during galaxy mergers and collisions. The fraction of stripped stars is expected to be a function of the halo mass, with more massive haloes containing a larger fraction of the diffuse halo emission[13,14,24]. On galaxy cluster scales, the diffuse intracluster light[25,26] is a significant

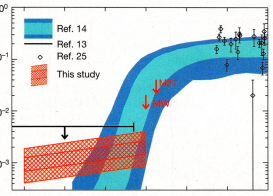

Figure 2 | The IHL fraction from diffuse stars as a function of the halo mass. The dark and light blue shaded regions show the 95% and 68% range of intrahalo light fraction f_{IHL} relative to the total luminosity of the dark-matter haloes as a function of the halo mass M from an analytical prediction[14], valid for $f_{IHL} > 4 \times 10^{-4}$ and $M > 5 \times 10^{10}\,M_\odot$ and at $z = 0$. We show the case where dark matter subhaloes on orbits passing within a critical radius of the host halo centre contribute their light to the central galaxy rather than to the diffuse component. We also show a prediction where f_{IHL} is constant[13], due to dwarf galaxies that are completely destroyed, with a value of ~0.005 when $M \lesssim 5 \times 10^{11}\,M_\odot$ (solid line fixed at $f_{IHL} = 5 \times 10^{-3}$). The downward arrow indicates the possibility that the constant f_{IHL} value for low-mass haloes may be smaller at higher redshifts. The red and orange hatched regions at the bottom of the plot are the preferred 68% and 95% confidence level range, respectively, on f_{IHL} from our analysis of the SDWFS near-infrared anisotropy power spectrum. The mass range is determined by the minimum and maximum halo masses consistent with the halo model fit that includes the IHL component. Both the mass and f_{IHL} ranges are valid over the broad redshift interval from $z = 1$ to 4 over which the anisotropy signal is generated. We do not find a significant halo mass dependence on the IHL fraction, with the mass-dependent power-law having a value of 0.09 ± 0.01 between 10^9 and $10^{12}\,M_\odot$ (see Supplementary Information section 9), consistent with the possibility that f_{IHL} is mass independent[13] when $M \lesssim 5 \times 10^{11}\,M_\odot$. Our model requires the total luminosity/halo-mass relation to evolve with redshift as $(1+z)^{1.2 \pm 0.1}$. This luminosity evolution with redshift can also be absorbed into the evolution of $f_{IHL}(M)$ with redshift. For reference, we also show measurements (open diamonds) and 1σ errors of the intracluster light[26], the galaxy group and cluster analogue for IHL when $M > 5 \times 10^{13}\,M_\odot$. At halo masses around $10^{12}\,M_\odot$ we show (red arrows) the 95% confidence level upper limit on f_{IHL} estimated for Milky Way[29] and Andromeda (M31)[30].

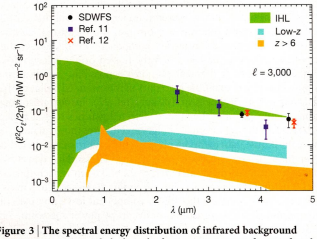

Figure 3 | The spectral energy distribution of infrared background anisotropies. Data symbols show the frequency spectrum of near-infrared and optical background anisotropies as a function of the wavelength. We show the r.m.s. fluctuation amplitude at $\ell = 3{,}000$, corresponding to fluctuations at 6-arcminute angular scales; our measurements (black filled circle) and the existing measurements in the literature (purple filled squares, ref. 11; red crosses, ref. 12) are presented at the same angular scales. Error bars are the 1σ uncertainties directly propagated to a r.m.s. fluctuation amplitude from the power spectrum errors. We do not show the measurements at 1.6 and 1.1 μm (ref. 10) as they do not probe fluctuations on scales greater than 2 arcmin on the sky due to the narrow field of view of the observations. The shaded regions are predictions for the IHL taking a variety of spectral energy distributions for the stripped stars (green), $z > 6$ galaxies (yellow) and low-redshift galaxies below the detection level of masking (blue).

fraction of the total luminosity of the cluster. We describe the intensity anisotropy power spectrum from the IHL by modifying the standard galaxy clustering predictions[22] to include a profile for the diffuse stars in haloes (see Supplementary Information section 8). If the clustering excess in near-infrared anisotropy power spectrum is due to IHL, then we find that measured anisotropies can be described with haloes in the mass range of 10^9 to 10^{12} solar masses ($M_\odot$). Averaged over this mass range, we find an IHL fraction relative to the total luminosity $f_{\rm IHL}$ of 0.07–0.2% at a 68% confidence level (Fig. 2). The implied fraction is consistent with the theoretical expectation that the IHL level is small for low-mass haloes, but differences also exist with current theory predictions[13,14], especially in terms of the power-law slope of the halo mass dependence.

If this new interpretation involving IHL is the correct description of measured infrared background anisotropies, we find that the IHL in all dark-matter haloes that we are probing contribute 0.75 ± 0.25 nW m^{-2} sr^{-1} to the total intensity at 3.6 μm. This intensity can be compared to the r.m.s. fluctuations of about 0.1 nW m^{-2} sr^{-1} at an angular scale of a few arcminutes (see Fig. 3). The IHL fluctuation signal varies spatially at a level of 10–15% of its integrated intensity and below 1% of the total background intensity of 13.3 ± 2.8 nW m^{-2} sr^{-1} at 3.6 μm (ref. 27). As the spectral energy distribution of IHL is mostly unknown, we make use of a variety of spectral energy distributions (SEDs) from B- to K-type stellar spectral templates and find an order of magnitude variation at wavelengths of ~1 μm (Fig. 3). In all these cases, we predict the existence of optical background light fluctuations. They will have a similar power spectrum shape and will be fully correlated with fluctuations at 3.6 μm. Furthermore, the near-infrared anisotropies we have measured should be correlated with the submillimetre anisotropies[28], especially if there is diffuse and extended dust associated with galaxies. These form future tests that can be used to improve our understanding of the content and nature of IHL in distant dark-matter haloes.

Received 5 June; accepted 15 August 2012.

1. Santos, M. R., Bromm, V. & Kamionkowski, M. The contribution of the first stars to the cosmic infrared background. *Mon. Not. R. Astron. Soc.* **336,** 1082–1092 (2002).
2. Salvaterra, R. & Ferrara, A. The imprint of the cosmic dark ages on the near-infrared background. *Mon. Not. R. Astron. Soc.* **339,** 973–982 (2003).
3. Cooray, A., Bock, J. J., Keating, B., Lange, A. E. & Matsumoto, T. First star signature in infrared background anisotropies. *Astrophys. J.* **606,** 611–624 (2004).
4. Kashlinsky, A., Arendt, R., Gardner, J. P., Mather, J. C. & Moseley, S. H. Detecting population III stars through observations of near-infrared cosmic infrared background anisotropies. *Astrophys. J.* **608,** 1–9 (2004).
5. Fernandez, E. R., Komatsu, E., Iliev, I. T. & Shapiro, P. R. The cosmic near-infrared background II: fluctuations. *Astrophys. J.* **710,** 1089–1110 (2010).
6. Chary, R., Cooray, A. & Sullivan, I. Contribution to unresolved infrared fluctuations from dwarf galaxies at redshifts of 2–3. *Astrophys. J.* **681,** 53–57 (2008).
7. Helgason, K., Ricotti, M. & Kashlinsky, A. Reconstructing the near-IR background fluctuations from known galaxy populations using multiband measurements of luminosity functions. *Astrophys. J.* **752,** 113 (2012).
8. Kashlinsky, A., Arendt, R. G., Mather, J. & Moseley, S. H. Tracing the first stars with fluctuations of the cosmic infrared background. *Nature* **438,** 45–50 (2005).
9. Cooray, A. *et al.* IR background anisotropies in Spitzer GOODS images and constraints on first galaxies. *Astrophys. J.* **659,** L91–L94 (2007).
10. Thompson, R., Eisenstein, D., Fan, X., Rieke, M. & Kennicutt, R. C. Evidence for a z 8 origin of the source-subtracted near-infrared background. *Astrophys. J.* **666,** 658–662 (2007).
11. Matsumoto, T. *et al.* AKARI observation of the fluctuation of the near-infrared background. *Astrophys. J.* **742,** 124 (2011).
12. Kashlinsky, A. *et al.* New measurements of the cosmic infrared background fluctuations in deep Spitzer/IRAC survey data and their cosmological implications. *Astrophys. J.* **753,** 63 (2012).
13. Purcell, C. W., Bullock, J. S. & Zentner, A. R. Shredded galaxies as the source of diffuse intrahalo light on varying scales. *Astrophys. J.* **666,** 20–33 (2007).
14. Purcell, C. W., Bullock, J. S. & Zentner, A. R. The metallicity of diffuse intrahalo light. *Mon. Not. R. Astron. Soc.* **391,** 550–558 (2008).
15. Conroy, C., Wechsler, R. H. & Kravtsov, A. V. The hierarchical build-up of massive galaxies and the intracluster light to z=1. *Astrophys. J.* **668,** 826–838 (2007).
16. Ashby, M. L. N. *et al.* The Spitzer Deep, Wide-field Survey. *Astrophys. J.* **701,** 428–453 (2009).
17. Arendt, R. G., Fixsen, D. J. & Moseley, S. H. Dithering strategies for efficient self-calibration of imaging arrays. *Astrophys. J.* **536,** 508–512 (2000).
18. Jannuzi, B. T. & Dey, A. in *Photometric Redshifts and the Detection of High Redshift Galaxies* (eds Weymann, R., Storrie-Lombardi, L., Sawicki, M. & Brunner, R.) 111–116 (ASP Conf. Ser. Vol. 191, Astron. Soc. Pacif., 1999).
19. Cooray, A., Gong, Y., Smidt, J. & Santos, M. G. The near-IR background intensity and anisotropies during the epoch of reionization. *Astrophys. J.* **756,** 92 (2012).
20. Fernandez, E. R., Iliev, I. T., Komatsu, E. & Shapiro, P. R. The cosmic near infrared background. III. Fluctuations, reionization, and the effects of minimum mass and self-regulation. *Astrophys. J.* **750,** 20 (2012).
21. Madau, P. & Silk, J. Population III and the near-infrared background excess. *Mon. Not. R. Astron. Soc.* **359,** L37–L41 (2005).
22. Cooray, A. & Sheth, R. Halo models of large scale structure. *Phys. Rep.* **372,** 1–129 (2002).
23. Tal, T. & van Dokkum, P. The faint stellar halos of massive red galaxies from stacks of more than 42000 SDSS LRG images. *Astrophys. J.* **731,** 89 (2011).
24. Lin, Y. & Mohr, J. J. K-band properties of galaxy clusters and groups: brightest cluster galaxies and intracluster light. *Astrophys. J.* **617,** 879–895 (2004).
25. Rudick, C. S., Mihos, J. C., Frey, L. H. & McBride, C. K. Tidal streams of intracluster light. *Astrophys. J.* **699,** 1518–1529 (2009).
26. Gonzalez, A. H., Zabludoff, A. I. & Zaritsky, D. Intracluster light in nearby galaxy clusters: relationship to the halos of brightest cluster galaxies. *Astrophys. J.* **618,** 195–213 (2005).
27. Levenson, L. R., Wright, E. L. & Johnson, B. D. DIRBE minus 2MASS: confirming the CIRB in 40 new regions at 2.2 and 3.5 microns. *Astrophys. J.* **666,** 34–44 (2007).
28. Amblard, A. *et al.* Submillimetre galaxies reside in dark matter haloes with masses greater than 3×10^{11} solar masses. *Nature* **470,** 510–512 (2011).
29. Carollo, D. *et al.* Structure and kinematics of the stellar halos and thick disks of the Milky Way based on calibration stars from Sloan Digital Sky Survey DR7. *Astrophys. J.* **712,** 692–727 (2010).
30. Courteau, S. *et al.* The luminosity profile and structural parameters of the Andromeda Galaxy. *Astrophys. J.* **739,** 20 (2011).

Supplementary Information is available in the online version of the paper.

Acknowledgements We acknowledge support from NSF CAREER (to A.C.), NASA ADAP and an award from JPL/Caltech. We thank R. Arendt for sharing his IRAC self-calibration code. We thank J. Bock and M. Zemcov for their contributions to the SDWFS project. This work is based on observations made with the Spitzer Space Telescope. This work also made use of data products provided by the NOAO Deep Wide-Field Survey. A.C. thanks the Aspen Center for Physics for hospitality.

Author Contributions A.C. planned the study, developed the IHL model, supervised the research work of J.S., F.D.B., C.C.F. and Y.G., and wrote the draft version of this paper. J.S. and C.C.F. performed the power spectrum measurements and F.D.B. interpreted those measurements with a halo model for the IHL. Y.G. developed a model for the high-redshift galaxies. All other co-authors contributed extensively and equally by their varied contributions to the SDWFS project (led by D.S. as the Principal Investigator), planning of SDWFS observations, analysis of SDWFS data, and by commenting on this manuscript as part of an internal review process.

Author Information Reprints and permissions information is available at www.nature.com/reprints. The authors declare no competing financial interests. Readers are welcome to comment on the online version of the paper. Correspondence and requests for materials should be addressed to A.C. (acooray@uci.edu).

LETTER

doi:10.1038/nature11568

Quasi-periodic events in crystal plasticity and the self-organized avalanche oscillator

Stefanos Papanikolaou[1], Dennis M. Dimiduk[2], Woosong Choi[3], James P. Sethna[3], Michael D. Uchic[2], Christopher F. Woodward[2] & Stefano Zapperi[4,5]

When external stresses in a system—physical, social or virtual—are relieved through impulsive events, it is natural to focus on the attributes of these avalanches[1,2]. However, during the quiescent periods between them[3], stresses may be relieved through competing processes, such as slowly flowing water between earthquakes[4] or thermally activated dislocation flow[5] between plastic bursts in crystals[6–8]. Such smooth responses can in turn have marked effects on the avalanche properties[9]. Here we report an experimental investigation of slowly compressed nickel microcrystals, covering three orders of magnitude in nominal strain rate, in which we observe unconventional quasi-periodic avalanche bursts and higher critical exponents as the strain rate is decreased. Our experiments are faithfully reproduced by analytic and computational dislocation avalanche modelling[10,11] that we have extended to incorporate dislocation relaxation, revealing the emergence of the self-organized avalanche oscillator: a novel critical state exhibiting oscillatory approaches towards a depinning critical point[12]. This theory suggests that whenever avalanches compete with slow relaxation—in settings ranging from crystal microplasticity to earthquakes—dynamical quasi-periodic scale invariance ought to emerge.

Physical systems under slowly increasing stress may respond through abrupt events. Such jumps in observable quantities are abundant, being found in systems ranging from complex social networks to earthquakes. Even though these avalanches appear randomly sized and randomly placed, the statistical properties of avalanches are universal, falling into well understood non-equilibrium universality classes. The main unifying concept is the depinning of an interface under an external field. An implicit assumption underlying this concept is that all other coexisting physical processes are either too fast, and thus average out, or too slow, rendering a static approximation valid. However, the latter assumption is not always true if the slow processes rearrange the pinning landscape at rates comparable to the external field driving rates. For as the fast avalanches are scale-invariant, the whole time series, including the waiting intervals between the fast events, is also scale-invariant. It is within the waiting intervals that a slow restructuring of the pinning field can thrive and alter universal predictions.

Although intermittent plastic flow is well known[13], only recently was it shown as being statistically akin to universal mean-field avalanche behaviour in the quasi-static limit. Investigations of the phenomenon have used a wide variety of techniques, including acoustic emission from deforming ice[6], high-resolution extensometry of tensile strained copper[14], and microcrystal compression tests for face-centred cubic and body-centred cubic crystals[15]. However, most of these single-crystal studies covered only a narrow range of nominal high strain rates. Preliminary evidence that suggests a more complex physical picture was discussed in ref. 16, where a rate dependence of the cumulative strain event size distributions was observed. Interesting rate effects have also been observed in materials with solute atoms, typically polycrystalline, that display the Portevin-Le Chatelier (PLC) effect[17–19]. The PLC avalanche distribution exponents show no evidence of strain-rate dependence (although strain dependence is shown), whereas PLC at lower rates turns into similar-size localized slip excitations and chaotic behaviour[20], distinctly different from the physical behaviour observed in ref. 16. Instead, the PLC avalanche behaviour is more consistent with the phenomenology of theories of avalanches with weakening effects[21]. In the experiments we report here, single nickel microcrystals of comparatively large dimensions, having diameters between 18 and 30 μm, were uniaxially compressed[15]. By controlling the applied external stress to maintain a nominal strain rate and by detecting slip with extremely sensitive extensometry, we track crystal displacements in time. In order to study the rate dependence, we perform our experiments at three different nominal strain rates ($10^{-4}\,s^{-1}$, $10^{-5}\,s^{-1}$, $10^{-6}\,s^{-1}$). For each sample, the time series of the displacement time derivative is filtered using optimal Wiener filtering methods adapted for avalanche time series[22], and avalanche events are appropriately defined without using thresholding.

As deformation proceeds in the microcrystals, the dislocation ensemble evolves at different timescales. The most apparent activity is associated with fast glide processes, which produce stochastic plastic bursts. Concurrently and between these events, other less observable processes (Fig. 1) contribute to collective slower relaxations. Like glide, these too are thermally activated processes accessible at these high levels of stress, but have different activation barriers: for example, the viscoelastic response of the dislocation forests after fast avalanche strain bursts, the localized dislocation climb motion in directions other than the glide plane under high local stresses, and also the cross-slip processes of dislocations shifting between glide planes. They all compete to minimize the far-field stress while changing the local stress landscape and bypassing the fast glide process. They affect dislocation slip, but at a slower rate than avalanche glide[23]. In our experiments, we classify as 'slow relaxation' all the deformation that does not belong to avalanches of the scaling regime. Using this definition, the slow relaxation fraction increases drastically at the two slowest strain rates. Thus, rate dependence of the avalanche size distribution (Fig. 2c) occurs when the nominal strain-rate becomes comparable to the rate of the slow relaxation processes (Fig. 1). Although the exact mechanisms are unknown, one localized reorganization mechanism possible at these large local stresses and low temperatures (0.17 times the melting temperature, ~300 K)[23] could be tied to newly discovered unconventionally large cross-slip rates calculated for similar conditions to our experiments[24]. Regardless of the possible types of relaxation mechanisms, we focus on the experimental fact that relaxation and driving rates become comparable. We model phenomenologically the slow relaxation in an intuitive manner, and then show a posteriori that our results are independent of the particular form of relaxation dynamics (see Supplementary Information).

The slip event sizes S, labelled by their beginning time, display a striking dependence on the driving rate. After we smooth the time

[1]Department of Mechanical Engineering and Materials Science and Department of Physics, Yale University, New Haven, Connecticut 06520-8286, USA. [2]Air Force Research Laboratory, Materials and Manufacturing Directorate, AFRL/RXCM, Wright-Patterson AFB, Ohio 45433, USA. [3]Laboratory of Atomic and Solid State Physics, Department of Physics, Clark Hall, Cornell University, Ithaca, New York 14853-2501, USA. [4]CNR–Consiglio Nazionale delle Ricerche, IENI, Via R. Cozzi 53, 20125 Milano, Italy. [5]ISI Foundation, Via Alassio 11/c, 10126 Torino, Italy.

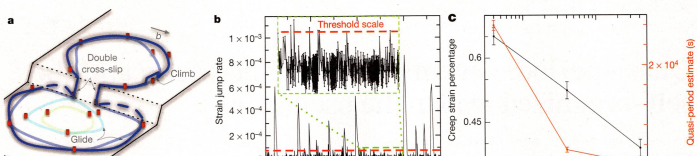

Figure 1 | Dislocation motion and several slow relaxation processes during the waiting intervals between avalanches. **a**, Diagram of typical unit dislocation motions. Lighter to darker indicates time evolution. Under stress, a dislocation loop nucleates and grows until it gets pinned on its slip plane, which is a common and fast glide-slip burst unit process. Then, a screw dislocation segment undergoes double cross-slip to a parallel slip plane, bypassing glide barriers. Finally, the dislocation glides and ultimately, may climb. These unit processes underlie the dislocation ensemble dynamics (not shown). **b**, Strain jump rate time series of a nickel sample at a strain rate of 10^{-4} s^{-1}. The avalanche phenomenon not only involves fast and violent scale-invariant bursts[24], but also long waiting times[3] between glide events. During those times, slow relaxation events happen that are typically hard to experimentally distinguish due to the external noise levels (inset). **c**, Black data points show the estimated strain percentage accumulated in slow relaxation events (generally called 'creep'), with the threshold set by the event size distribution (Fig. 2): this percentage (relaxation strain/total final strain) strongly increases as the rate decreases. Experimental noise contributes to the relaxation strain measured. Red data points show that a non-trivial quasi-period (see Fig. 2) of avalanche behaviour emerges and increases dramatically as the nominal rate decreases. Error bars indicate the size of systematic variability due to thresholding.

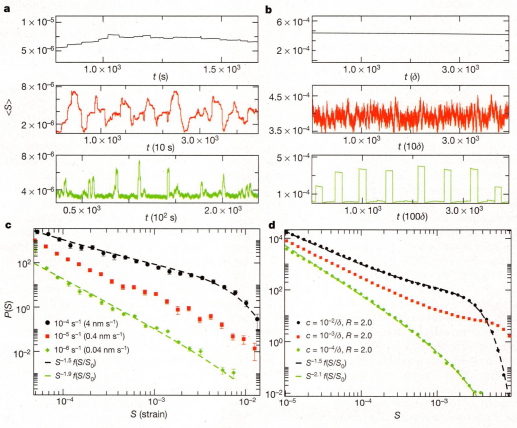

Figure 2 | Comparison between microplasticity experiments and theoretical modelling. **a**, Average avalanche size in 400-s windows versus time for different strain rates (decreasing top to bottom: 10^{-4}, 10^{-5}, 10^{-6} s^{-1}, corresponding to respective velocities of the microcrystal top surfaces of 4, 0.4, 0.04 nm s^{-1}). Time axes are rescaled by the nominal strain rate, aligning the 'strain scales'. Quasi-periodic avalanche behaviour emerges as the nominal strain rate decreases. The period is similar in 'strain scale'—a key prediction of our theory. **b**, Stick-slip oscillations observed experimentally in **a** show typical characteristics of the model of equation (1) (using 400δ-long averaging windows). The relaxation rate is fixed ($R = 2$) and the strain-rate is varied (by modifying c: top to bottom; $10^{-2}/\delta$, $10^{-3}/\delta$, $10^{-4}/\delta$), following the experiments. The unit of strain is 2×10^{-6} and the fast timescale $\delta = 0.5$ s. We show the actual avalanche events without the distortion that appears due to the strain coming from slow relaxation; this difference gives the overall scale mismatch of **a** and **b**. **c**, The probability distribution $P(S)$ is shown. There is a marked increase in the critical exponent for the size of the displacement jumps as the strain rate decreases. The highest (10^{-4}) and lowest (10^{-6}) strain rates are fitted to power laws $S^{-1.5}f(S/S_0)$ and $S^{-2.1}f(S/S_0)$, respectively. The key shows strain rate and corresponding velocity for data points. **d**, In the model of equation (1), the variation of the rate c shows similar behaviour to that observed in **c**, with exponent drift from $\sim$1.5 (ref. 8) to $\sim$2.1, with fitting error $\sim$0.2, consistent with the discussion in the text and with fitting cut-off functional forms $f(S/S_0)$ that are discussed in Methods.

series over a fixed window of 400 s and then rescale the time axis to display comparable strain evolution, very clear (Fig. 2a) oscillatory-like behaviour emerges at the $10^{-6}\,s^{-1}$ rate. The emergent period displays a strong dependence on the strain rate, while its magnitude reaches ~8 h (for $10^{-6}\,s^{-1}$), consistently much larger than the length we chose for the fixed window averaging (Fig. 1c). The novel behaviour is also reflected within statistical distributions of S: these show power-law behaviour ($P(S) \propto S^{-\tau}$) for all studied strain rates ($10^{-4}\,s^{-1}$, $10^{-5}\,s^{-1}$, $10^{-6}\,s^{-1}$), while the value of the power law exponent τ drifts from ~1.5 (consistent with refs 7 and 25) to a higher, unexpected value of ~2.0 for the slowest strain rate (Fig. 2c). Analogous behaviour is observed for the avalanche durations T and their correlation with the sizes.

Our explanation of the experimental data builds on the model framework of dislocations moving through a disordered landscape of forest dislocations, on a single slip plane under shear stress. This is a successful picture for avalanches during stage I plasticity[10,11,25] that strongly relies on well-understood models of 2+1-dimensional interface depinning[12]. We construct a minimal generalization via an added relaxation term, (I):

$$\frac{d\phi(r)}{dt} = \overbrace{D\left(\frac{\sigma(r)}{\mu}\right)^{n}\Theta(\sigma(r))}^{(I)} + \overbrace{\frac{1}{\mu\varepsilon}(\sigma(r)-\sigma_i(r))\Theta(\sigma(r)-\sigma_i(r))}^{(II)} \quad (1)$$

Here r denotes the location on the slip plane, t is time, Θ is the Heaviside step function, μ is the shear modulus of the system, $\varepsilon \ll 1$ is a dimensionless constant that controls the timescale separation of the two processes (I) and (II), n is the stress exponent dependent on the slow relaxation mechanism, σ is the local applied stress and σ_i denotes random stress barriers to glide slip. The basic slip variable of the system ϕ is the y–x component (Burgers vector along x) of the plastic distortion tensor when only infinite dislocations along z on x–z slip planes are considered[10]. Part (I) of equation (1) denotes the coarse-grained relaxation of edge dislocations, with rate D at fixed temperature. Only positive slip motion is considered to simplify our simulations, and we have shown that our conclusions are qualitatively independent of such assumptions (see Supplementary Information). With D we define an effective rate of thermally activated processes that lead to slow relaxation. We set the exponent $n = 1$ but our conclusions do not qualitatively depend upon it. The applied stress is the x–y component of the stress tensor:

$$\sigma(r) = \sigma_{ext} + \sigma_{int}(r) + \sigma_{hard}(r) = Mct + \int d^2r' K(r-r')\phi(r') - k\phi(r) \quad (2)$$

where σ_{ext} is the external stress with c the stress increase rate, σ_{int} is the dislocation local stress, σ_{hard} is the local stress due to dislocation hardening with k a phenomenological hardening parameter, and r' is defined on the slip plane.

We consider a stress-controlled test in a stationary plastic regime ($\sigma_{ext} \equiv Mct$)[26], where M is a machine stiffness, and c has strain-rate units. The relative timescales of the relaxation and stress rate are controlled by the dimensionless parameter $R \equiv D/c$. Term (II) of equation (1) describes the fast glide process which drives the avalanche dynamics. Hardening is phenomenologically represented via a coefficient k that controls the distance from the depinning critical point. For clarity, we separate the relevant timescales by considering $\varepsilon \ll 1$, leading to infinitely fast avalanches compared to the slow relaxations. Finally, σ_{int} contains the appropriate interaction kernel K for single slip straight edge dislocations[10] and σ_i denotes the uncorrelated local pinning potential due to dislocation forests. We find that our main qualitative conclusions are independent of the kernel, and thus are equally applicable to other models of avalanches in plasticity. If we were considering the model of ref. 11 where mixed dislocations are included, we would modify our definitions by using a single x–y slip plane, assume ϕ to be the x–y tensor component, and only apply the z–x component of the stress.

The model of equations (1) and (2) is solved by explicit integration on a two-dimensional grid: for no relaxation ($D = 0$), the avalanches display statistics consistent with the predictions of the mean-field theory of interface depinning[2,8]. As D increases, both the critical exponent τ for strain jump sizes S ($P(S) \propto S^{-\tau}$) and the critical exponent α for event durations T ($P(T) \propto T^{-\alpha}$) increase substantially. In the context of mean-field theory, somewhat similar behaviour takes place when the driving rate c is increased[22], leading to avalanche overlap and exponents decreasing below the mean-field values; we study the case where $c \to 0$, keeping R fixed (and >1) where the exponents increase above their mean-field values.

The increase of the exponents is accompanied by a quasi-periodic behaviour, with intermittent but regularly spaced large slip events (Fig. 2b), keeping in mind that the term quasi-periodic is unrelated to the formal definition of quasiperiodic functions. If one considers the average avalanche size in a window, similar to the experimental study but without strain from relaxation included, it is clear that the $D = 0$ flat-in-time profile is replaced by strongly oscillating profiles in the presence of slow relaxation ($D > 0$). The average avalanche size ($D = 0$) is inversely related to the hardening coefficient k, $k \propto <S>^{-1}$. Thus, there is a distribution of hardening coefficients being effectively sampled, reflecting local heterogeneity. We assume that such a distribution $g(k')$ biases the integration, over all possible hardenings k', of the size probability distribution of the $D = 0$ model, leading to the observed dynamically integrated size distribution. That is, a curve in Fig. 2d may be obtained as:

$$P_{int}(S) = \int_0^\infty g(k')P(S,k')dk' \quad (3)$$

For the case of interest we have $P_{int}(S) = S^{-2}P(S/S_0)$, where S_0 is the cutoff of the size distribution, yielding a higher effective size-exponent $\tilde{\tau} \equiv 2$ for slow strain rates. It is worth noting that in this picture, the largest events have a non-trivial scaling behaviour (see Supplementary Information).

The profound effects of slow rate processes within our dislocation model and the comparison with experiments forces us to ask if our findings are general. To make analytical progress towards an answer, we consider the slip susceptibility ρ, the multiplier giving the net number of local slips triggered by a single slip. Here, $\langle\rho\rangle$ is proportional to the hardening coefficient, $\langle\rho\rangle \propto 1 - k$. In traditional mean-field interface depinning models[1], this is the 'distance' of the system from the critical depinning point and is saturated to a fixed point value after short-time transients. When $\rho \ll 1$, the system is far from critical, whereas the system is near critical when $\rho \approx 1$. Numerical solutions to equation (1) verify that the additional relaxation process affects ρ in an unusual way. When an avalanche with size S_t takes place, ρ instantaneously decreases proportionally to S_t, whereas it increases linearly between avalanches. We suggest that the basic physical mechanism behind the behaviour of equation (1) (with $c \to 0$ but R fixed) is given by the behaviour of the slip susceptibility ρ, whose basic characteristics can be described by a Markov process:

$$\rho_{t+1} - \rho_t \equiv \Delta\rho_t = c_d\left(1 - \frac{S_t}{\bar{S}}\right) \quad (4)$$

where S_t is mean-field $P(S_t) = NS_t^{-3/2}\exp(-S_t/S_0)$; here N is a normalization factor, $S_0 = a/(1-\rho_t)^2$ (ref. 1) and the step c_d can be thought as being proportional to R. The traditional avalanche mean-field behaviour is described by the $c_d \to 0$ fixed point (analogous to higher experimental strain rates). The size of the avalanche at time t, S_t, is a stochastic variable which mimics the avalanche dynamics of

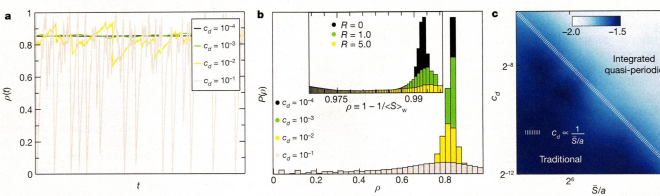

Figure 3 | The avalanche oscillator mechanism and stochastic modelling of the slip susceptibility. a, As the rate c_d increases (key), for $\bar{S} = 0.1$, large noise causes $\rho(t)$ of equation (4) to oscillate between $\rho \approx 1$ and small ρ, causing larger exponents. **b**, The probability distribution of ρ. As c_d increases (stronger relaxation, slower strain rate), any ρ becomes equiprobable. In the inset, we use $\langle S\rangle_{50}$ calculated for equation (1), averaged with a running window of size 50δ. The simulations of equation (1) have the same parameters as in Fig. 2. The histograms, shown in the appropriate scale ($1 - 1/\langle S\rangle = \rho$ for the kernel used) shows qualitatively similar flattening behaviour as equation (4). **c**, The novel regime ('integrated quasi-periodic') with large ρ fluctuations is separated from the traditional regime $\rho \approx \rho_0$. The line $c_d \propto 1/\bar{S}$ shown, as described in the text. $\bar{\tau}$ was calculated using equation (3) at equidistant points with a final Gaussian interpolation for the colour background.

equation (1). When $c_d \ll 1$, ρ increases in small steps towards the fixed point (Fig. 3a) given by $\rho_0 = 1 - (\sqrt{\pi a/2\bar{S}})$ with average size $\bar{S}$ (a being the minimum accessible size).

However, there is a finite probability of a large avalanche which takes the system far from the fixed point, with $\Delta\rho_f$ large and negative. If $\delta\bar{S} = S_s - \bar{S}$, then $\Delta\rho_f = -c_d\delta\bar{S}/\bar{S} \approx -1$ indicates the emergence of a novel quasi-periodic behaviour (Fig. 1b) showing large negative jumps in ρ with rare avalanches whose sizes S_f are much larger than $\bar{S}$. ρ performs a Sisyphean task, constantly ascending towards the original critical point ρ_0 before the sharp descent after a large rare avalanche. In this way, the distribution of ρ effectively flattens (Fig. 3b) as c_d increases (low experimental strain rates), leading to larger integrated exponents (equation (3)). Consistently, the analogous distribution for equation (1) flattens as R increases (Fig. 3b, inset). The rare $\delta\bar{S}$ events scale with $S_0 \propto 4\bar{S}^2/(\pi a)$ and qualitatively, there is a transition when $c_d \approx a\pi/(4\bar{S}) \approx 1/(\bar{S}\sqrt{a})$ (Fig. 3c). We call a system undergoing this qualitative behaviour an 'avalanche oscillator', based on its strong resemblance to the case of relaxation limit cycle oscillations near a singular Hopf bifurcation with stochastic perturbations[27].

Single microcrystals display a rich collection of novel mechanical behaviours: together with size effects[15] and the emergence of avalanche slip events[6,7], the importance of often-neglected slow processes on intermittency has now come to light. The presented experiments at the microscale now force us to reconsider our understanding of the macroscopic world, such as disordered solids and earthquake faults[28–30]. Our general theory proposes that whenever avalanches compete with other slow coexisting processes to minimize the local internal stress, the dynamics will give rise to the self-organized avalanche oscillator.

METHODS SUMMARY

The experimental measurements were performed using the methodology described earlier[15,16]. The data are taken at time resolutions of 5, 50 and 500 Hz for different samples. The nominal strain rates (in s^{-1}) were 10^{-4}, 10^{-5} and 10^{-6}, with corresponding average platen velocities of 4, 0.4 and 0.04 nm s^{-1}, given the dimensions of the microcrystals. The experimental time series were filtered using Wiener filtering methods optimized for studying avalanches[23]. In the simulations of equation (1), Euler time stepping is used to evolve the differential equation on an $L \times L$ grid. During an avalanche, the stress is not increased and the relaxation term (1) does not participate in the evolution. During the avalanche process, we evolve the system by using cellular automata rules: when the total local stress crosses its σ_t threshold, the associated local slip ϕ increases randomly with a normal distribution of mean 1 and variance 1. The assumption of strict positivity in the local slip is used for simulation efficiency purposes, without affecting our conclusions. In the stress of equation (1), we have also added a term for regularizing purposes that slightly smooths the slip profiles. It takes the form $\alpha\nabla^2\phi$ with very small $\alpha = 0.05$. In our simulations, we used a flat distribution ranged in (0,1] for the quenched disorder $\sigma_t(r)$, following a typical protocol. The kernel $K(r)$ has a continuum Fourier representation $\bar{K}(k) = -Ck_x^2k_y^2/(k_x^2 + k_y^2)^2$, where we set $C = 1$ for clarity in our analysis. In the simulations of equation (4), the stochastic equation was solved using random variables that follow the required power-law distribution with exponential cut-off, generated with standard rejection methods. During the numerical solution of equation (4), ρ can jump above 1, a regime we do not consider (see Supplementary Information).

Full Methods and any associated references are available in the online version of the paper.

Received 24 February; accepted 5 September 2012.

1. Fisher, D. S. Collective transport in random media: from superconductors to earthquakes. *Phys. Rep.* **301,** 113–150 (1998).
2. Sethna, J., Dahmen, K. & Myers, C. Crackling noise. *Nature* **410,** 242–250 (2001).
3. Le Doussal, P. & Wiese, K. J. Driven particle in a random landscape: disorder correlator, avalanche distribution, and extreme value statistics of records. *Phys. Rev. E* **79,** 051105 (2009).
4. Ben-Zion, Y. Collective behavior of earthquakes and faults: continuum-discrete transitions, progressive evolutionary changes and different dynamic regimes. *Rev. Geophys.* **46,** RG4006 (2008).
5. Cottrell, A. H. *Dislocations and Plastic Flow in Metals* (Clarendon, 1953).
6. Miguel, M. C., Vespignani, A., Zapperi, S., Weiss, J. & Grasso, J.-R. Intermittent dislocation flow in viscoplastic deformation. *Nature* **410,** 667–671 (2001).
7. Dimiduk, D. M., Woodward, C., LeSar, R. & Uchic, M. D. Scale-free intermittent flow in crystal plasticity. *Science* **312,** 1188–1190 (2006).
8. Zaiser, M. Scale invariance in plastic flow of crystalline solids. *Adv. Phys.* **55,** 185–245 (2006).
9. Jagla, E. A. Realistic spatial and temporal earthquake distributions in a modified Olami-Feder-Christensen model. *Phys. Rev. E* **81,** 046117 (2010).
10. Zaiser, M. & Moretti, P. Fluctuation phenomena in crystal plasticity—a continuum model. *J. Stat. Mech.* **2005,** P08004 (2005).
11. Koslowski, M., LeSar, R. & Thomson, R. Avalanches and scaling in plastic deformation. *Phys. Rev. Lett.* **93,** 125502 (2004).
12. Kardar, M. Nonequilibrium dynamics of interfaces and lines. *Phys. Rep.* **301,** 85–112 (1998).
13. Becker, R. & Orowan, E. Uber sprunghafte Dehnung von Zinkkristallen. *Z. Phys.* **79,** 566–572 (1932).
14. Weiss, J. *et al.* Evidence for universal intermittent crystal plasticity from acoustic emission and high-resolution extensometry experiments. *Phys. Rev. B* **76,** 224110 (2007).
15. Uchic, M. D., Dimiduk, D. M. & Shade, P. A. Plasticity of micrometer-scale single crystals in compression. *Annu. Rev. Mater. Res.* **39,** 361–386 (2009).
16. Dimiduk, D. M., Uchic, M. D., Rao, S. I., Woodward, C. & Parthasarathy, T. A. Overview of experiments on microcrystal plasticity in FCC-derivative materials: selected challenges for modelling and simulation of plasticity. *Model. Simul. Mater. Sci. Eng.* **15,** 135–146 (2007).
17. Lebyodkin, M., Dunin-Barkowskii, L., Bréchet, Y., Estrin, Y. & Kubin, L. P. Spatio-temporal dynamics of the Portevin–Le Chatelier effect: experiment and modelling. *Acta Mater.* **48,** 2529–2541 (2000).
18. Kubin, L. P. *et al.* in *Dislocations in Solids* (eds Nabarro, F. R. N. & Duesberry, M. S.) Ch. 57, 103–188 (North Holland, 2002).
19. Bharathi, M. S., Lebyodkin, M., Ananthakrishna, G., Fressengeas, C. & Kubin, L. P. The hidden order behind jerky flow. *Acta Mater.* **50,** 2813–2824 (2002).

20. Lebyodkin, M. A. *et al.* On the similarity of plastic flow processes during smooth and jerky flow: statistical analysis. *Acta Mater.* **60,** 3729–3740 (2012).
21. Fisher, D. S., Dahmen, K., Ramanathan, S. & Ben-Zion, Y. Statistics of earthquakes in simple models of heterogeneous faults. *Phys. Rev. Lett.* **78,** 4885–4888 (1997).
22. Papanikolaou, S. *et al.* Universality beyond power laws and the average avalanche shape. *Nature Phys.* **7,** 316–320 (2011).
23. Kassner, M. & Perez-Prado, M.-T. *Fundamentals of Creep in Metals and Alloys* (Elsevier, 2004).
24. Rao, S. I. *et al.* Activated states for cross-slip at screw dislocation intersections in face-centered cubic nickel and copper via atomistic simulation. *Acta Mater.* **58,** 5547–5557 (2010).
25. Csikor, F. F., Motz, C., Weygand, D., Zaiser, M. & Zapperi, S. Dislocation avalanches, strain bursts, and the problem of plastic forming at the micrometer scale. *Science* **318,** 251–254 (2007).
26. Zaiser, M. & Nikitas, N. Slip avalanches in crystal plasticity: scaling of the avalanche cut-off. *J. Stat. Mech.* **2007,** P04013 (2007).
27. Muratov, C. & Vanden-Eijnden, E. Noise-induced mixed-mode oscillations in a relaxation oscillator near the onset of a limit cycle. *Chaos* **18,** 015111 (2008).
28. Rogers, G. & Dragert, H. Episodic tremor and slip on the Cascadia subduction zone: the chatter of silent slip. *Science* **300,** 1942–1943 (2003).
29. Salerno, K. M., Maloney, C. E. & Robbins, M. O. Avalanches in strained amorphous solids: does inertia destroy critical behavior? Preprint at http://arxiv.org/abs/1204.5965 (2012).
30. Dahmen, K. A., Ben-Zion, Y. & Uhl, J. T. A simple analytic theory for the statistics of avalanches in sheared granular materials. *Nature Phys.* **7,** 554–557 (2011).

Supplementary Information is available in the online version of the paper.

Acknowledgements We thank J. Guckenheimer, C. L. Henley, E. A. Jagla, E. Nadgorny, C. O'Hern, R. Thorne, D. Trinkle, E. van der Giessen and V. Vitelli for discussions. We acknowledge support from DTRA 1-10-1-0021 (S.P.), DOE-BES DE-FG02-07ER-46393 (S.P., W.C. and J.P.S.), the Air Force Office of Scientific Research (D. Stargel) and the Materials and Manufacturing Directorate (D.M.D., C.F.W. and M.D.U.) and the ComplexityNet pilot project LOCAT (S.Z.).

Author Contributions D.M.D., M.D.U. and C.F.W. designed and performed the experiments. S.P., D.M.D. and C.F.W. performed the experimental data analysis. S.P., W.C., J.P.S. and S.Z. developed the theoretical modelling, performed the numerical simulations and carried out the data analysis. S.P. wrote the first draft of the manuscript and then all authors contributed equally to improve the manuscript.

Author Information Reprints and permissions information is available at www.nature.com/reprints. The authors declare no competing financial interests. Readers are welcome to comment on the online version of the paper. Correspondence and requests for materials should be addressed to S.P. (stefanos.papanikolaou@yale.edu).

LETTER

doi:10.1038/nature11569

Forming all-carbon quaternary stereogenic centres in acyclic systems from alkynes

Yury Minko[1], Morgane Pasco[1], Lukas Lercher[1], Mark Botoshansky[2] & Ilan Marek[1]

The formation of all-carbon quaternary stereocentres in acyclic systems is one of the most difficult contemporary challenges in modern synthetic organic chemistry[1,2]. Particularly challenging is the preparation of all-carbon quaternary stereocentres in aldol adducts[3]; this difficulty is problematic because the aldol reaction represents one of the most valuable chemical transformations in organic synthesis[4]. The main problem that limits the formation of these stereocentres is the absence of an efficient method of preparing stereodefined trisubstituted enolates in acyclic systems[5–8]. Here we describe a different approach that involves the formation of two new stereogenic centres—including the all-carbon quaternary one—via a combined carbometalation–oxidation reaction of an organocuprate to give a stereodefined trisubstituted enolate. We use this method to generate a series of aldol and Mannich products from ynamides with excellent diastereomeric and enantiomeric ratios and moderate yields.

In the past few decades, stereoselective synthesis has played a crucial role in organic chemistry, leading to the rapid development of myriad widely used synthetic transformations. One of the remaining significant challenges in this field is the development of strategies for the enantioselective creation of carbon atoms bonded to four different carbon substituents[1], particularly in acyclic systems[2]. Several attractive methods based on asymmetric catalysis have therefore been developed in recent years[2]. However, the current limitation of all of these asymmetric approaches is that they combine only two components, resulting in the formation of a single carbon–carbon bond in the critical step. Consequently, attention has focused on how to synthesize quaternary stereocentres efficiently, in a minimum number of steps, with optimum convergence, with as little as possible functional group transformation, little or no by-products and maximum atom-efficiency[9]. Simply put, we need to accomplish more with less[10], making use of new reactions or concepts[11]. The number of steps in the synthesis is of paramount importance[12]. This challenging goal of step economy can be achieved by using reactions that allow a great increase in complexity, or through one-pot operations that string together many steps that collectively achieve the same high complexity increase[13]. This last approach is indeed generally beyond our reach, particularly when addressing challenging issues such as the creation of all-carbon quaternary stereocentres in acyclic systems[14].

For the past few years, we have concentrated our efforts on the creation of such quaternary stereocentres. We found that acyclic homoallylic alcohols possessing the desired all-carbon quaternary stereocentre could be formed with excellent diastereomeric and enantiomeric ratios from simple alkynes, through successive *in situ* synthetic transformations with important stereochemical implications[15–17]. We turned our attention to reactions that form aldol products, as they represent one of the most versatile carbon–carbon bond forming processes available to synthetic chemists[4], and the formation of all-carbon quaternary stereogenic centres at the α-position to carbonyl groups remains elusive and has been the focus of only four independent studies, first in racemic[18,19] and then in enantiomerically enriched forms[5,20]. A different approach that avoids the issues associated with enolate geometry is the use of silyl ketene imines that successfully led to aldol surrogates[21]. In all of these examples[5,18–21], only a single carbon–carbon bond is formed in the reaction sequence between two components, and as discussed earlier, issues of efficiency and convergence have to be addressed. Although aldol adducts could be formed, easy and efficient access to stereodefined trisubstituted enolates (**1** in Fig. 1) as reactive intermediates could drastically increase the scope of this chemistry. Indeed, enolates are involved in a multitude of powerful applications in asymmetric organic synthesis, but the generation of fully substituted acyclic enolates in geometrically defined form requires resident chirality on the enolizable carbon centre (Fig. 1). The *E*/*Z* selectivity of these trisubstituted enolates is therefore determined either by the stereochemistry and geometry of the starting bicyclic lactam (path A in Fig. 1)[5], by the configuration of the diastereomerically pure α-methylbutyramide (path B)[6], or by a matched combination of the chirality of the ester substrates and lithium amide bases (path C)[7,8].

Our initial approach to tackling the problem of formation of aldol adducts possessing a quaternary stereocentre was based on the concept we developed for the formation of stereodefined homoallylic alcohols through a combined carbometalation—zinc homologation—allylation reaction, followed by acidic hydrolysis of the resulting enamides[3]. Despite the success of chiral oxazolidinone imides (Evans' method)[22] for the incorporation of adjacent stereocentres in aldol reactions, the asymmetric construction of all-carbon quaternary carbon stereocentres is hampered, as discussed previously, by the lack of *E*/*Z* selectivity in the enolization reactions of acyclic oxazolidinone imides (**2** in Fig. 2). However, owing to the attractiveness of these auxiliaries, we reasoned that the selective formation of trisubstituted enolates **1** from oxazolidinone-based chiral auxiliaries would constitute the best approach to solve the problem of formation of all-carbon quaternary

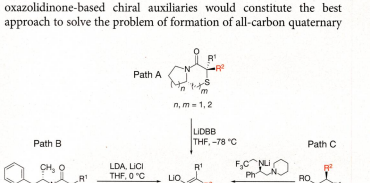

Figure 1 | General strategies for the formation of stereodefined enolates. Synthesis of geometrically defined trisubstituted enolate **1** requires substrates possessing a stereodefined enolizable sp^3 carbon centre, such as bicyclic thioglycolate lactams (path A), diastereomerically pure methyl-α-ethyl disubstituted pseudoephedrine amides (path B), or structurally matched enantiomers of the ester and chiral amide base (path C).

[1]The Mallat Family Laboratory of Organic Chemistry, Schulich Faculty of Chemistry, and the Lise Meitner-Minerva Center for Computational Quantum Chemistry, Technion-Israel Institute of Technology, Haifa 32000, Israel. [2]Laboratory for X-ray Analysis, Technion-Israel Institute of Technology, Haifa 32000, Israel.

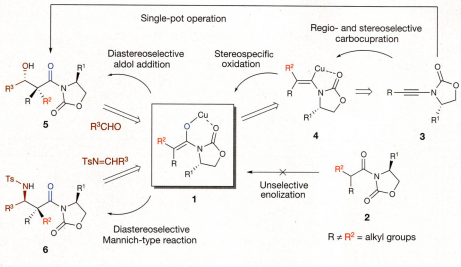

Figure 2 | Proposed approach. The applicability of the aldol reaction is limited by the lack of selective enolization of α,α-disubstituted carbonyl compound **2**, which results in a mixture of diastereomeric products. Here we propose an alternative retrosynthetic analysis for the formation of aldol-type products **5** and Mannich-type adducts **6**. It would consist of a carbocupration reaction of ynamide **3** yielding the vinyl copper species **4**. Then, subsequent stereospecific oxidation should lead to the metal-enolate **1** *in situ*, which reacts with an aldehyde to form the aldol adduct **5**. Use of the ynamide possessing the Evans oxazolidinone as a chiral auxiliary should control the absolute stereochemistry. Moreover, the synthetic use of stereodefined trisubstituted enolate could be easily extended to the addition to a large variety of electrophiles such as imines for the creation of various quaternary stereocentres.

centres in not only aldol reactions, but also for reactions with different electrophiles. So, the real challenge is to prepare such species through the concomitant formation of several bonds in a single-pot operation from simple alkynes.

As we have recently reported the regioselective carbocupration of ynamides **3** (ref. 23; easily obtained by a coupling reaction between an alkyne and the oxazolidinone)[24], the formation of stereodefined enolates **1** could logically result from an oxidation reaction of the resulting vinyl copper species **4**, as shown in Fig. 2. However, when traces of oxygen are present, instantaneous degradation (that is, dimerization) of organocopper species **4** through single-electron transfer to dioxygen is observed[25]. So oxidation of organocopper requires a different approach, meaning a different mechanistic oxidation pathway. On the basis of our recent work on zinc homologation of vinyl copper with zinc carbenoid[15,16], we thought that oxenoid species (oxo-analogues of carbenoids) would be good candidates[26–28].

Here we describe the development and study of reactions that meet these challenges and enable this long-sought synthetic strategy. The feasibility of this approach was initially checked by reacting vinyl copper **4Cu** (Fig. 3, method A, R = *n*-Bu), easily obtained by carbocupration of ynamide **3** (R = *n*-Bu)[23], with oxenoid *t*-BuOOLi (see Supplementary Information) at low temperature. We found that the oxidation reaction proceeds very cleanly to give the corresponding imides **2** after protonation with alcohol in good yields, as shown in entries 1 and 2 in Table 1. We assume that this successful transformation results from a 1,2-metalate rearrangement[13], via the initial formation of a heterocuprate **7**, leading to the copper enolate **1** (Fig. 3).

To get information on the stereochemistry of the oxidation reaction, copper enolate **1** was trapped with triethylchlorosilane. A single geometrical isomer was obtained for silyl enol ether **8** (Fig. 3) and the stereochemistry was determined by X-ray analysis. The oxidation reaction indeed proceeds with preservation of the stereochemistry of

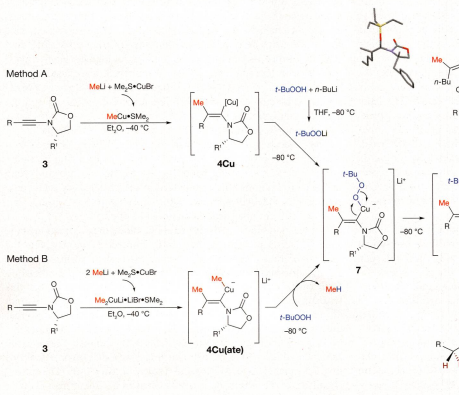

Figure 3 | Combined carbometalation-oxidation sequence. Method A describes the addition of oxenoid *t*-BuOOLi to the vinyl copper **4Cu** to give the heterocuprate **7**. After 1,2-metalate rearrangement, copper enolate **1** was formed and could be trapped as silylenol ether **8**. Addition of a protic source leads to the secondary imide **2**. Method B describes the addition of an organocuprate to the ynamide **3** to give the dissymmetric cuprate **4Cu(ate)**. Addition of *t*-BuOOH to the reaction mixture leads to deprotonation of the peroxide by the more basic organometallic species (that is, alkyl group Me) with formation of **7**. The same chemical pathway then proceeds to give the copper enolate **1**. The oxidation proceeds with a complete preservation of the stereochemical information resulting from the syn-carbometalation, as determined by the single isomer of the trisubstituted enol silyl ether **8** (the X-ray crystal structure of **8** is shown as a stick model).

Table 1 | One-pot formation of imides 2 from ynamides 3

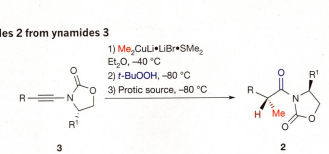

3 2

Entry	R	R1	Ynamide	Method	Protic source	Product	d.r.*	Yield† (%)
1	Bu	Bn	**3a**	A	*i*-PrOH	**2a**	79:21	50
2	Hex	Bn	**3b**	A	*i*-PrOH	**2b**	87:13	45
3	Bu	Bn	**3a**	B	*i*-PrOH	**2a**	86:14	61
4	Bu	Bn	**3a**	B	H_2O	**2a**	85:15	64
5	Bu	Bn	**3a**	B		**2a**	87:13	52
6	Bu	Bn	**3a**	B	$Me_2N(CH_2)_2OH$	**2a**	90:10	61
7	Bu	Bn	**3a**	B	$EtNH(CH_2)_2OH$	**2a**	93:7	64
8	Hex	Bn	**3b**	B	$EtNH(CH_2)_2OH$	**2b**	90:10	50
9	Hex	*i*-Pr	**3f**	B	$EtNH(CH_2)_2OH$	**2f**	92:8	62
10	$i\text{-PrCO}_2(CH_2)_2$	Bn	**3c**	B	$EtNH(CH_2)_2OH$	**2c**	90:10	48
11	$AdCO_2(CH_2)_3$	Bn	**3d**	B	$EtNH(CH_2)_2OH$	**2d**	93:7	49
12	$TIPSO(CH_2)_3$	Bn	**3e**	B	$EtNH(CH_2)_2OH$	**2e**	92:8	58

Methods A and B are given in Fig. 3. Bu, butyl; hex, hexyl; Bn, benzyl; Pr, propyl; Ad, adamantyl; TIPSO, tri-isopropylsilyl ether.
* Diastereomeric ratios determined by ^{1}H-NMR spectroscopy and by HPLC analysis.
† Isolated yields after column chromatography (based on **3**).

the double bond. The diastereomeric ratio of **2** clearly needs to be improved, but we wanted first to develop an experimentally simpler approach to the formation of the copper enolate **1**. Indeed, the original method (method A; Fig. 3) requires the preparation of *t*-BuOOLi in a separate reaction vessel at low temperature, followed by a subsequent transfer into the vinyl copper species solution at −80 °C. To achieve this goal, we developed a new method (method B; Fig. 3) in which the carbocupration reaction was performed with an organocuprate ($Me_2CuLi•Me_2S$ from 2 equiv. of MeLi and 1 equiv. of $CuBr•Me_2S$) instead of the previously used organocopper ($MeCu•Me_2S$). To this organocuprate was added 1 equiv. of ynamide **3**; only one of the two alkyl groups was regio- and stereoselectively added to the triple bond, to give the dissymmetric organocuprate species **4Cu(ate)**. As an alkyl organometallic species is more basic than a vinyl metal species, the addition of *t*-BuOOH should lead to an *in situ* deprotonation of the peroxide by the Me group present on the copper, with liberation of MeH and concomitant formation of the heterocuprate **7**. The latter would undergo a 1,2-metalate rearrangement to give the same copper-enolate **1** that would finally react with an electrophile (for example, protonolysis). Following this new protocol (method B), better yields and improved diastereomeric ratios were obtained, as described in Table 1 (compare entries 1 and 3). Now that an easy, safe and reproducible protocol was set, we decided to further improve the diastereomeric ratio, and various protic sources were tested for the hydrolysis of the copper enolate **1**, as described in Table 1.

Addition of water or phenol possessing bulky groups in *ortho*-positions did not improve the diastereomeric ratio (Table 1, entries 4 and 5 respectively). On the other hand, addition of amino alcohols such as *N*-dimethylaminoethanol (Table 1, entry 6) or, even better, *N*-ethylaminoethanol (Table 1, entry 7), give higher ratios in similar yields. If a different oxazolidinone-based chiral auxiliary is used ($R^1 = i$-Pr), ratios and yields are comparable (Table 1, compare entries 8 and 9). Our combined sequence was then applied to various functionalized ynamides (**3c**–**e**), possessing ester (Table 1, entries 10 and 11) or silyl ether groups (Table 1, entry 12) that led to adducts with good diastereoselectivities albeit with lower yields in some cases (but based on the starting ynamide after three consecutive chemical steps). The absolute configuration of the major isomer was determined by chemical correlation with authentic samples for **2a** and **2b** after transformation into the corresponding carboxylic acids (see Supplementary Information).

Importantly, when trisubstituted enolate **1a** was slowly warmed to room temperature over a period of one hour and stirred at this temperature for one additional hour followed by hydrolysis with *N*-ethylamínoethanol at low temperature, the adduct **2a** was obtained with a similar diastereomeric ratio. Therefore, enolate **1** shows remarkable stereochemical stability and no observable isomerization.

Finally, we turned our attention to the development and study of aldol and Mannich-type adducts to validate this long-sought synthetic strategy. The sequence is based on our previously optimized protocol, as described in Fig. 4 and Table 2. Accordingly, the aldol reaction using the previously described conditions (Me_2CuLi, *t*-BuOOH and R^3CHO), proceeds smoothly to give the aldol adducts **5a**–**f** in good overall yields (based on the starting ynamides **3**) and diastereomeric ratios (Table 2, entries 1–6). The major diastereoisomer was easily separated by simple column chromatography on silica gel and the absolute configuration of the major isomer was determined by X-ray crystallographic analysis of **5a** (Supplementary Information).

The stereochemistry of the major isomer can be rationalized by a Zimmerman–Traxler transition state (a six-membered ring transition state adopting a chair conformation, Fig. 4 at top right). The benzyl group of the oxazolidinone shields one face in the chelated six-membered ring, and the aldehyde approaches the enolate *anti* to this group, with its R^3 substituent in a pseudo-equatorial position.

The reaction sequence described above allows the preparation of the aldol adducts **5** possessing the oxazolidinone chiral moiety, with the creation of three new bonds and two new stereogenic centres, including the all-carbon quaternary stereocentre, in a single-pot procedure from easily accessible ynamide **3**. It is important to note that this transformation can be scaled up to larger quantities (that is, 5 mmol of **3**) without erosion of the diastereomeric ratios and yields, and that the experimental conditions are mild enough to avoid retroaldol reactions. The addition of imines to the stereodefined enolate **1** leads to the Mannich adducts **6a**–**c** with similar impressive diastereomeric ratios in good isolated yields (Fig. 4 and Table 2, entries 7–9). The stereochemistry of the adduct **6a** is consistent with a Zimmerman–Traxler transition state with approach of the imine from the back face of the

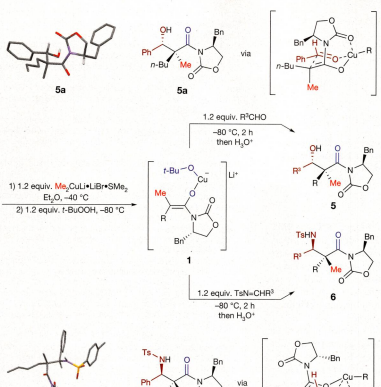

Figure 4 | Application to the aldol and Mannich reactions. Shown is a one-pot reaction *en route* to aldol and Mannich adducts (**5** and **6** respectively) possessing the all-carbon quaternary stereocentre through a combined carbometalation of **3**–oxidation–addition of electrophiles. Stick models show X-ray crystal structure determination of the absolute configuration of the major isomer **5a** and **6a** (see Table 2, entries 1 and 7, respectively). A mechanistic explanation of the reaction is as follows. An enolate species **1**, formed by reaction of **4Cu(ate)** with the *t*-BuOOH followed by 1,2-metalate rearrangement, reacts with the aldehyde via a six-membered transition state adopting a chair-like conformation. The oxazolidinone intramolecularly chelates the copper atom, and thus a second pseudo-heterocycle is formed, with one face shielded by the benzyl group. The aldehyde approaches the enolate moiety *anti* to this group with its R^3 substituent in a pseudo-equatorial position. When *N*-sulphonyl imines are added to the stereodefined enolate **1**, the Mannich adduct **6** is formed through a chair-like transition state where the sulphonylimine adopts a *Z*-configuration *anti* to the bulky substituent of the oxazolidinone.

bulky benzyl group of the oxazolidinone. As the barrier of planar inversion of *N*-sulphonyl imines (*E* to *Z*) is low, steric factors may account for the formation of the *Z*-isomer in the six-membered transition state[29]. Cleavage of the oxazolidinone moiety of **5** could be performed using standard and reliable high-yielding transformations (with recovery of the oxazolidinone-based chiral auxiliaries, see Supplementary Information) and the aldehyde **11a** can be obtained diastereomerically and enantiomerically pure, as shown in Fig. 5.

These results demonstrate that alternative approaches to the preparation of all-carbon quaternary stereocentres and more particularly to the formation of aldol and Mannich adducts can be designed from simple alkynes through the concomitant formation of several new bonds in a single-pot operation. This study illustrates that even the most challenging problems can be efficiently addressed when new and powerful synthetic tools are provided. Owing to its versatility, our approach will surely find a large number of applications for the transformation of heterosubstituted alkynes into stereodefined trisubstituted enolates that may subsequently react with a large variety of electrophiles, leading to a new and general approach to the formation of quaternary all-carbon stereocentres[30]. This study could be extended to include other auxiliaries and, more importantly, achiral groups for the development of catalytic strategies.

Table 2 | One-pot formation of products possessing the all-carbon quaternary stereocentre from ynamides

Entry	R	R^3	Ynamide	Product	d.r.*	Yield† (%)
1	Bu	Ph	**3a**	**5a**	93:2:4:1	50
2	Bu	*p*-BrC_6H_4	**3a**	**5b**	90:2:5:3	52
3	Bu	*p*-MeC_6H_4	**3a**	**5c**	90:1:4:5	54
4	Hex	Ph	**3b**	**5d**	94:1:2:3	54
5	Bu	*p*-$MeOCOC_6H_4$	**3a**	**5e**	93:3:1:3	50
6	Bu	2-Naphthyl	**3a**	**5f**	95:2:2:1	62
7	Bu	Ph	**3a**	**6a**	93:5:2:0	50
8	Bu	*p*-MeC_6H_4	**3a**	**6b**	94:3:2:1	58
9	Bu	*p*-BrC_6H_4	**3a**	**6c**	94:5:1:0	45

5a–f, aldols; **6a–c**, Mannich products.
* Diastereomeric ratios determined by ^{1}H-NMR spectroscopy for the four possible diastereomers.
† Isolated yields after column chromatography (based on **3**).

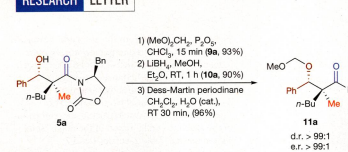

Figure 5 | Cleavage of the auxiliaries. Transformation of the aldol adduct **5a** into **11a** after subsequent protection (step 1)-cleavage (step 2) and oxidation (step 3) reactions. Dess-Martin periodinane is an oxidant. RT, room temperature; d.r., diastereomeric ratio; e.r., enantiomeric ratio.

METHODS SUMMARY

General procedure for the one-pot formation of aldol adduct 5a. CuBr•DMS complex (1.20 mmol, 1.2 equiv.) was placed into a flame-dried three-necked round-bottomed flask equipped with a magnetic stirring bar and connected to an argon line. Dry diethyl ether (8.0 ml) was added, and the system was cooled to −50 °C. A solution of methyllithium (1.60 M in diethyl ether, 2.40 mmol, 2.4 equiv.) was added dropwise, and the reaction mixture was allowed to warm to −40 °C and stirred for 30 min at this temperature to form a solution of lithium dimethylcuprate complex. The reaction mixture was cooled to −50 °C, and a solution of the starting alkynyl carbamate **3** (1.00 mmol, 1.0 equiv.) in 1.5 ml of diethyl ether was added dropwise. The reaction mixture was allowed to warm to −40 °C and stirred at this temperature for 1.5 h (monitored by thin-layer chromatography (TLC) using 20% ethyl acetate in hexane as eluent) to form a pale-yellow clear solution of vinylcuprate. Upon completion, the reaction mixture was cooled to −90 °C, and a solution of *t*-butylhydroperoxide in nonane (1.20 mmol, 1.2 equiv.) was added in one fast injection using a syringe. The resulting reaction mixture was allowed to warm up slowly to −80 °C, and stirred at the indicated temperature for 1 h to form a green-brown opaque solution. Upon completion of the oxidation step, freshly purified aldehyde was added at −80 °C to the reaction mixture and was allowed to stir for additional 1.5 h keeping the temperature at −80 °C. The reaction was quenched with an aqueous saturated solution of NH_4Cl and allowed to warm up to room temperature. Phases were separated, and the aqueous phase was extracted three times with diethyl ether (15 ml). The combined organic phases were dried over anhydrous Na_2SO_4, filtered, and concentrated under reduced pressure. Purification was accomplished by silica gel flash column chromatography (gradient of solvents 15–30% of diethyl ether in hexane, TLC analysis using 1:1 diethyl ether–hexane).

General procedure for the one-pot formation of Mannich adduct 6a. The preparation of lithium dimethyl cuprate complex followed by the carbometallation and oxidation were performed according to the developed general procedure described above. Upon completion of the oxidation step, 1.2 equiv. of tosylimine (0.6 M solution in dry THF) were added to the reaction mixture at −80 °C. The reaction mixture was allowed to stir for additional 2 h keeping the temperature at −80 °C (progress monitored by TLC using 8:2 hexane–ethyl acetate as an eluent). The reaction was quenched with an aqueous saturated solution of NH_4Cl and allowed to warm up to the ambient temperature. Phases were separated, and the aqueous phase was extracted three times with diethyl ether (15 ml). The combined organic phases were dried over anhydrous Na_2SO_4, filtered, and concentrated under reduced pressure. Purification was accomplished by silica gel flash column chromatography (10% of ethyl acetate in hexane, TLC analysis using 8:2 hexane–ethyl acetate).

Received 20 May; accepted 6 September 2012.

1. Hawner, C. & Alexakis, A. Metal-catalyzed asymmetric conjugate addition reaction: formation of quaternary stereocenters. *Chem. Commun.* **46,** 7295–7306 (2010).
2. Das, J. P. & Marek, I. Enantioselective synthesis of all-carbon quaternary stereogenic centers in acyclic systems. *Chem. Commun.* **47,** 4593–4623 (2011).
3. Das, J. P., Chechik, H. & Marek, I. A unique approach to aldol products for the creation of all-carbon quaternary stereocentres. *Nature Chem.* **1,** 128–132 (2009).
4. Carreira, E. M. in *Modern Carbonyl Chemistry* (ed. Otera, J.) Ch. 8 227–248 (Wiley-VCH, 2001).
5. Manthorpe, J. M. & Gleason, J. L. Stereoselective generation of *E*- and *Z*-disubstituted amide enolates. Reductive enolate formation from bicyclic thioglycolate lactams. *J. Am. Chem. Soc.* **123,** 2091–2092 (2001).
6. Kummer, D. A., Chain, W. J., Morales, M. R., Quiroga, O. & Myers, A. G. Stereocontrolled alkylative construction of quaternary carbon centers. *J. Am. Chem. Soc.* **130,** 13231–13233 (2008).
7. Qin, Y.-C., Stivala, C. E. & Zakarian, A. Acyclic stereocontrol in the Ireland-Claisen rearrangement of α-branched esters. *Angew. Chem. Int. Edn* **46,** 7466–7469 (2007).
8. Gu, Z., Herrmann, A. T., Stivala, C. E. & Zakarian, A. Stereoselective construction of adjacent quaternary chiral centers by the Ireland-Claisen rearrangement: stereoselection with esters of cyclic alcohols. *Synlett* 1717–1722 (2010).
9. Newhouse, T., Baran, P. S. & Hoffmann, R. W. The economies of synthesis. *Chem. Soc. Rev.* **38,** 3010–3021 (2009).
10. Baran, P. S., Maimone, T. J. & Richter, J. M. Total synthesis of marine natural products without using protecting groups. *Nature* **446,** 404–408 (2007).
11. Seebach, D. Organic synthesis — where now? *Angew. Chem. Int. Edn Engl.* **29,** 1320–1367 (1990).
12. Wender, P. A. & Miller, B. L. Synthesis at the molecular frontier. *Nature* **460,** 197–201 (2009).
13. Scott, H. K. & Aggarwal, V. K. Highly enantioselective synthesis of tertiary boronic esters and their stereospecific conversion to other functional groups and quaternary stereocentres. *Chem. Eur. J.* **17,** 13124–13132 (2011).
14. Marek, I. A shift in retrosynthetic paradigm. *Chem. Eur. J.* **14,** 7460–7468 (2008).
15. Sklute, G. & Marek, I. Multicomponent approach for the creation of chiral quaternary centers in the carbonyl allylation reactions. *J. Am. Chem. Soc.* **128,** 4642–4649 (2006).
16. Dutta, B., Gilboa, N. & Marek, I. Highly diastereoselective preparation of homoallylic alcohols containing two contiguous quaternary stereocenters in acyclic systems from simple terminal alkynes. *J. Am. Chem. Soc.* **132,** 5588–5589 (2010).
17. Gilboa, N., Wang, H., Houk, K. N. & Marek, I. Axial preferences in allylation via the Zimmerman-Traxler transition state. *Chem. Eur. J.* **17,** 8000–8004 (2011).
18. Yamago, S., Machii, D. & Nakamura, E. Simple diastereoselectivity of the aldol reaction of persubstituted enolates. Stereoselective construction of quaternary centers. *J. Org. Chem.* **56,** 2098–2106 (1991).
19. Häner, R., Laube, T. & Seebach, D. Regio- and diastereoselective preparation of aldols from α-branched ketone enolates generated from BHT ester enolates and organolithium reagents: in-situ generation and trapping of ketenes from ester enolates. *J. Am. Chem. Soc.* **107,** 5396–5403 (1985).
20. Mase, N., Tanaka, F. & Barbas, C. F. III. Synthesis of β-hydroxyaldehydes with stereogenic quaternary carbon centers by direct organocatalytic asymmetric aldol reactions. *Angew. Chem. Int. Edn* **43,** 2420–2423 (2004).
21. Denmark, S. E., Wilson, T. W., Burk, M. T. & Heemstra, J. R. Jr. Enantioselective construction of quaternary stereogenic centers by the Lewis base catalyzed additions of silyl imines to aldehydes. *J. Am. Chem. Soc.* **129,** 14864–14865 (2007).
22. Evans, D. A., Bartroli, J. & Shih, T. L. Enantioselective aldol condensations. Erythro-selective chiral aldol condensations via boron enolates. *J. Am. Chem. Soc.* **103,** 2127–2129 (1981).
23. Chechik-Lankin, H. Livshin, S. & Marek, I. Regiocontrolled carbometalation reactions of ynamides. *Synlett* 2239–2241 (2005).
24. Evano, G., Coste, A. & Jouvin, K. Ynamides: versatile tools in organic synthesis. *Angew. Chem. Int. Edn* **49,** 2840–2859 (2010).
25. Wendlandt, A. E., Suess, A. M. & Stahl, S. S. Copper-catalyzed aerobic oxidative C-H functionalizations: trends and mechanistic insights. *Angew. Chem. Int. Edn* **50,** 11062–11087 (2011).
26. Panek, E. J., Kaiser, L. R. & Whitesides, G. M. Vinylic radicals are intermediates in the oxidation of vinylic lithium reagents to lithium enolates by dioxygen, but not by lithium tert-butyl peroxide. *J. Am. Chem. Soc.* **99,** 3708–3713 (1977).
27. Zhang, D. & Ready, J. M. Tandem carbocupration/oxygenation of terminal alkynes. *Org. Lett.* **7,** 5681–5683 (2005).
28. DeBergh, J. R., Spivey, K. M. & Ready, J. M. Preparation of substituted enol derivatives from terminal alkynes and their synthetic utility. *J. Am. Chem. Soc.* **130,** 7828–7829 (2008).
29. Tiong, E. A. & Gleason, J. L. Stereoselective formation of α-quaternary stereocenters in Mannich reaction. *Org. Lett.* **11,** 1725–1728 (2009).
30. Stivala, C. E. & Zakarian, A. Total synthesis of (+)-pinnatoxin A. *J. Am. Chem. Soc.* **130,** 3774–3776 (2008).

Supplementary Information is available in the online version of the paper.

Acknowledgements This research was supported by the Israel Science Foundation administrated by the Israel Academy of Sciences and Humanities (140/12), and by the Fund for Promotion of Research at the Technion. L.L. thanks the Bayer-Stiftung for financial support. I.M. is holder of the Sir Michael and Lady Sobell Academic Chair.

Author Contributions Y.M., M.P. and L.L. planned, conducted and analysed experiments. I.M. conceived and directed the project and wrote the manuscript with contributions from Y.M. and M.P. X-ray structures were resolved by M.B. All authors contributed to discussions.

Author Information Crystallographic data have been deposited with the Cambridge Crystallographic Data Centre, accession numbers CCDC 881250 (**8**), CCDC 881248 (**5a**) and CCDC 881249 (**6a**). Reprints and permissions information is available at www.nature.com/reprints. The authors declare no competing financial interests. Readers are welcome to comment on the online version of the paper. Correspondence and requests for materials should be addressed to I.M. (chilanm@tx.technion.ac.il).

LETTER

doi:10.1038/nature11528

Recent changes to the Gulf Stream causing widespread gas hydrate destabilization

Benjamin J. Phrampus[1] & Matthew J. Hornbach[1]

The Gulf Stream is an ocean current that modulates climate in the Northern Hemisphere by transporting warm waters from the Gulf of Mexico into the North Atlantic and Arctic oceans[1,2]. A changing Gulf Stream has the potential to thaw and convert hundreds of gigatonnes of frozen methane hydrate trapped below the sea floor into methane gas, increasing the risk of slope failure and methane release[3–9]. How the Gulf Stream changes with time and what effect these changes have on methane hydrate stability is unclear. Here, using seismic data combined with thermal models, we show that recent changes in intermediate-depth ocean temperature associated with the Gulf Stream are rapidly destabilizing methane hydrate along a broad swathe of the North American margin. The area of active hydrate destabilization covers at least 10,000 square kilometres of the United States eastern margin, and occurs in a region prone to kilometre-scale slope failures. Previous hypothetical studies[3,5] postulated that an increase of five degrees Celsius in intermediate-depth ocean temperatures could release enough methane to explain extreme global warming events like the Palaeocene–Eocene thermal maximum (PETM) and trigger widespread ocean acidification[7]. Our analysis suggests that changes in Gulf Stream flow or temperature within the past 5,000 years or so are warming the western North Atlantic margin by up to eight degrees Celsius and are now triggering the destabilization of 2.5 gigatonnes of methane hydrate (about 0.2 per cent of that required to cause the PETM). This destabilization extends along hundreds of kilometres of the margin and may continue for centuries. It is unlikely that the western North Atlantic margin is the only area experiencing changing ocean currents[10–12]; our estimate of 2.5 gigatonnes of destabilizing methane hydrate may therefore represent only a fraction of the methane hydrate currently destabilizing globally. The transport from ocean to atmosphere of any methane released—and thus its impact on climate—remains uncertain.

Methane hydrate, a solid consisting of methane and water, is stable at high pressures and low temperatures. Owing to a positive thermal gradient in the Earth, methane hydrate exists only within the first few hundred metres of sediments in deep marine settings, below which methane gas and liquid water are stable[13]. Methane hydrates represent one of the largest reservoirs of organic carbon on Earth[6,13,14]. Studies speculate that destabilization of methane hydrates could inject significant quantities of methane into the ocean and possibly the atmosphere, leading to spikes in atmospheric carbon levels[4,6,8].

The base of hydrate stability can sometimes be detected directly in seismic data via bottom-simulating reflectors (BSRs) that appear as strong, negative-polarity, high-impedance seismic reflections caused by free gas at the base of the phase boundary[15,16] (Fig. 1b). Hydrate formation is strongly dependent on temperature, and because of this, the base of the hydrate stability zone, as indicated by BSRs, is used for estimating subsurface temperature[17].

Warming waters in the Gulf Stream can potentially destabilize methane hydrate[3]. Additionally, slight changes in the Gulf Stream flow direction can also destabilize methane hydrate by introducing warm waters to regions previously exposed only to cold bottom-water currents. The Gulf Stream consists of anomalously warm water at depths as great as 1,000 metres below sea level (m.b.s.l.; Fig. 2a). In regions where the Gulf Stream is absent, ocean temperatures are markedly colder at intermediate water depths (300–1,000 m.b.s.l.; Fig. 2a).

Although much is known about the current state of the Gulf Stream, relatively little is known about the evolution of the Gulf Stream before

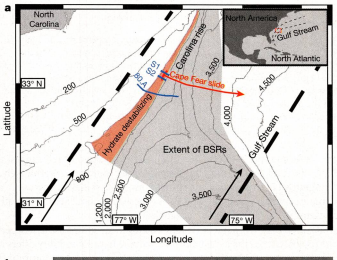

Figure 1 | Gas hydrates below the Gulf Stream in the western North Atlantic. a, Study area, shown boxed in the map-view inset, where the location of the Gulf Stream is also shown (dashed black lines), flowing along the western edge of the North Atlantic margin[1,2]. In the main figure, the grey area denotes where BSRs exist below the sea floor[21]; the pink area is where methane hydrate is destabilizing owing to recent changes in ocean temperature; and the approximate location of the Gulf stream is between the two solid black arrows. **b**, Multi-channel seismic line 80-A is one of several seismic lines in the region showing clear BSRs shoaling westward along the edge of the continental margin[20]. The rectangle indicated in white is shown magnified in the inset. Inset, the gas hydrate phase boundary (that is, BSR) shows as a strong, negative polarity reflector (black arrows) that behaves erratically with depth beneath sea-floor less than ~1,000 m.b.s.l.

[1]Huffington Department of Earth Sciences, Southern Methodist University, Dallas, Texas 75275, USA.

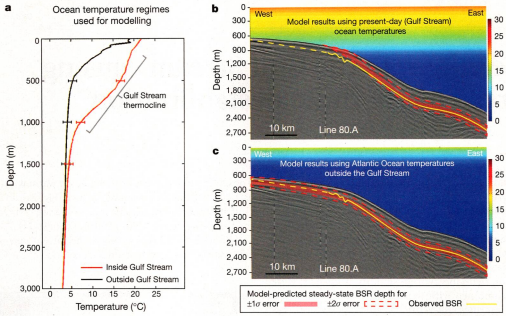

Figure 2 | Evidence for recent changes in ocean temperature and hydrate destabilization. a, Two different ocean temperature regimes exist in the western North Atlantic, with Gulf Stream temperatures as much as 8 ± 1.1 °C (1σ error) warmer at intermediate water depths than ocean temperatures outside the Gulf Stream. Seismic line 80.A was acquired within the Gulf Stream, yet the predicted BSR depth using present day (Gulf Stream) ocean temperatures is shallower than observed BSR depths for sea-floor depths less than ~1,000 m.b.s.l. (**b**). Comparison between observed and predicted BSR depths for the two ocean temperature regimes indicate cold, non-Gulf Stream intermediate ocean temperatures produce a much better fit to observed BSR depths (**c**). This implies recent ocean warming or northwest intrusion of the Gulf Stream along the Carolina rise and the onset of methane hydrate destabilization along the margin. This observation is widespread (Supplementary Information). Dashed yellow lines indicate where the BSR is inferred but difficult to identify clearly in seismic data.

the Holocene epoch. Lynch-Stieglitz *et al.*[1,2] and Lund *et al.*[18] suggest a lower-flux, cooler Gulf Stream during cooler climates. Alternatively, Winguth *et al.*[3], using computer simulations, suggest that during warmer climates, warm ocean temperatures like those of the Gulf Stream prevail, resulting in methane hydrate destabilization.

Where ocean temperature is well-constrained, comparison between the predicted and the actual base of methane hydrate stability offers a valuable means of identifying recent changes in ocean temperature and sub-sea-floor temperature. Here we analyse the stability of methane hydrates along the Carolina rise off the east coast of North America using active-source seismic reflection data, with the goal of characterizing hydrate stability below the Gulf Stream. The Carolina rise is a region where both the Gulf Stream and methane hydrate stability are well-constrained[1,16,19–21] (Fig. 1). Seismic data show clearly observable BSRs imaged continuously below the sea floor at water depths of 800–4,000 m.b.s.l. throughout the region[21,22] (Fig. 1b, Supplementary Information). At water depths shallower than ~1,000 m.b.s.l., the BSR shoals owing to lower hydrostatic pressures and warmer ocean temperatures, resulting in a vertically thinner hydrate stability zone within the sediments (Fig. 1b).

By comparing the predicted base of the hydrate stability zone using current hydrological and geological conditions with the observed base of the hydrate stability zone, we determine if differences exist between the observed and predicted temperature regime. Results show that at depths greater than ~1,000 m.b.s.l., the model-predicted BSR matches observed BSR depths in seismic data (Fig. 2b). At shallower depths, however, model predictions diverge from observations, with the observed BSR consistently deeper than model predictions. Even after accounting for end-member uncertainty (to 2σ), the observed BSR is deeper than model predictions (Fig. 2b).

Many phenomena might explain the difference between observed and predicted BSR depths, including changing sea level, gas composition, fluid flow, variable sedimentation rates, changes in heat flow, seismic velocity model errors, and variations in ocean temperature. Changing sea level affects hydrate stability by altering the hydrostatic pressure regime; however, sea level in the early Holocene was lower, resulting in lower pressure and shallower BSRs. Holocene changes in sea level cannot therefore explain the anomalously deep BSRs observed today. A consistent increase in the contribution of thermogenic gas along the margin could also cause the phase boundary to deepen; however, geochemical measurements indicate natural gas concentrations are consistently 99% methane across the region[19,23,24]. Fluid flow, by transporting heat more efficiently via advection, can have a significant effect on temperature; however, the anomalously deep hydrate stability zone observed along the edge of the margin requires downward flow, which is inconsistent with regional fluid models[25]. Rapid sedimentation can also result in anomalously cool shallow sediment temperatures[26]. However, sedimentation in this region has not exceeded 30 m Myr^{-1} since the Pleistocene epoch, and modelling indicates that the regional sedimentation rate is too low to explain the discrepancy between observed and predicted BSR depth[23,26]. Lateral variations in heat production can also vary heat flow and temperature. Previous studies across this region suggest no significant variations in heat flow or radiogenic material across the site[19,20,22]. Indeed, an average heat flow of 19 mW m^{-2} is necessary to explain the anomalously deep BSR at the margin edge. This is a factor of two below regional observations[20]. Finally, anomalously high seismic velocities used to create the seismic depth section could also result in anomalously deep BSRs. The seismic velocities necessary to offset observed BSR depths to model predictions are physically unreasonable[16]; a compression-wave velocity averaging less than 250 m s^{-1} in sediments above the BSR is needed to explain the discrepancy. This leaves ocean temperature variations as the last plausible explanation for the discrepancy between the observed and predicted BSR. Specifically, if ocean temperatures recently warmed at intermediate water depths, it would take time for heat to propagate downward. Before thermal equilibration, the observed BSR would therefore be cooler and appear anomalously deep compared to model predictions.

To test whether cooler intermediate-depth ocean temperatures in the recent past might explain the discrepancy between the observed

and predicted depth of methane hydrate stability along the Carolina rise, we re-ran the heat-flow model but removed the warming effects of the Gulf Stream. Instead, we apply as our top boundary condition a mid-Atlantic temperature–depth profile acquired outside the Gulf Stream (Fig. 2a). Model results show a remarkably good fit between observed and predicted BSR depth for all depths (Fig. 2c).

Warming of the intermediate-depth ocean within the Holocene provides a simple explanation for the discrepancy between the observed and predicted base of the methane hydrate phase boundary (Fig. 3). The analysis implies that the Gulf Stream was cooler, lower flux, or recently diverted northwest during the Holocene, consistent with previous studies[1,2,10,18]. The result also implies that recent changes in ocean temperature are causing contemporary destabilization of methane hydrates along the North American margin.

Analysis of BSRs in other regional seismic data suggests that recent ocean bottom warming is ubiquitous along the Carolina rise. In addition to line 80.A, we analysed two other published seismic lines acquired in the Gulf Stream along the North Atlantic margin that show clearly identifiable BSRs[22] (Supplementary Information). Both lines are located more than 40–50 km away from line 80.A, yet results from all three seismic lines are identical. Specifically, analysis of all three seismic lines suggests that BSRs located below sea-floor depths shallower than ~1,000 m.b.s.l. are unstable along the Carolina rise, and that recent intermediate ocean temperature warming is widespread along the margin just east of North Carolina.

Other studies support the idea that shifting ocean currents and significant (>1 °C) Holocene ocean temperature changes occur in this region[10–12]. During the twentieth century, the most significant measured sea surface temperature warming in the North Atlantic Ocean occurred above the Carolina rise[10]. Ocean surface warming above the Carolina rise has been attributed[10] to either a northwest shift in the Gulf Stream flow direction or a warming Gulf Stream, as we suggest. Analysis of ocean drilling data also indicates recent (Holocene) changes in the Deep Western Boundary Current along the edge of this margin[11].

Extrapolating our observations across the area where the Gulf Stream and known methane hydrate deposits exist, we place first-order constraints on the area of hydrate destabilization (Fig. 1). Our analysis suggests that we are observing the onset of methane hydrate destabilization along a ~300-km span of the North American margin that will continue for centuries unless the Gulf Stream shifts southward or intermediate ocean temperatures cool several degrees[1,2,16,21] (Fig. 3). We estimate that hydrates are currently destabilizing within a volume of $\sim 7.5 \times 10^{11}$ m^3. Assuming an average porosity of 60% in the shallow sediments where hydrates are destabilizing, hydrate filling 5% of the pore space, and 123 kg of methane per cubic metre of hydrate, we estimate that ~2.5 Gt of methane—or ~0.2% of that necessary to explain the PETM—are currently destabilizing beneath a sea-floor area of ~10,000 km^2 off the US eastern seaboard[9]. If continuing hydrate destabilization triggers slope failure at this site, the amount of methane released could be an order of magnitude greater[16]. Hydrate destabilization, by converting solid methane hydrate into methane gas and water, can elevate pore fluid pressure along the slope edge, reducing slope stability in areas prone to frequent, potentially tsunamigenic slope failure[4,5,7,16]. It is perhaps no coincidence that the upper headwall of the Cape Fear slide, the largest submarine slide complex along the western North Atlantic margin, resides within the area of active hydrate destabilization (Fig. 1).

Recent shifts in Gulf Stream flow or temperature provide a simple yet powerful mechanism for contemporary methane hydrate dissociation and carbon release. The analysis presented here provides a method for constraining Holocene changes in intermediate-depth ocean temperatures and also demonstrates that slight deviations in ocean currents have a profound impact on margin stability and the ocean carbon budget. It is unlikely that the western North Atlantic margin is the only area experiencing widespread hydrate destabilization due to changing ocean currents. Recent studies have suggested that similar ocean temperature shifts may occur both in the Arctic Ocean[7,27,28] and globally along subtropical western boundary currents[12]. Our estimate of 2.5 Gt of destabilizing methane hydrate may therefore represent only a fraction of the methane hydrate currently destabilizing globally.

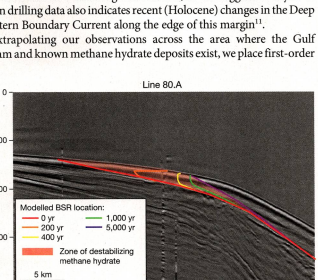

Figure 3 | Timing methane hydrate dissociation along the western Atlantic margin. To place first-order constraints on the timing of ocean temperature warming and methane hydrate dissociation along line 80.A, we run a time dependent diffusive heat-flow forward model in which we start initially with our steady-state cold ocean temperature model result (Fig. 2c), but instantaneously change the ocean temperature boundary condition to present day (Gulf Stream) values. The resulting forward model shows evolution of hydrate stability and BSR depth through time. Each coloured line represents a model-predicted BSR location in the future. These results indicate that dissociation will continue for the next several thousand years if no change in ocean temperature occurs. The pink zone represents the total area of destabilizing methane hydrate.

METHODS SUMMARY

To test whether methane hydrates below the Carolina rise are stable and temperatures are in steady state, we developed a 2D finite difference diffusive heat-flow model, discretized into 20 m (vertical) × 50 m (horizontal) cells, that accounts for conductivity, temperature, bathymetry and depth along depth-converted seismic line 80.A[29,30]. To constrain ocean temperature with depth, we average nine conductivity–temperature–depth (CTD) measurements near the site (Fig. 2a). We estimate heat flow at this site using the method outlined in ref. 17 that calculates heat flow from deep-water (>2,000 m.b.s.l.) BSRs located below the Gulf Stream thermocline. For thermal conductivity, we use a value of 1 W m^{-1} K^{-1}, consistent with regional measurements[19,20,23]. We calculate an average heat flow of 40.7 ± 4.6 mW m^{-2} (2σ), consistent with regional conductive heat-flow measurements and borehole thermal data collected near this site[19,20,23].

With conductivity, sea-floor temperature, sea-floor shape and heat flow constrained, we calculate the 2D steady-state temperature distribution within the marine sediments using a finite-difference diffusive heat flow approach. We calculate thermal diffusivity assuming constant thermal conductivity of 1 W m^{-1} K^{-1}, an average bulk density of 1,700 kg m^{-3}, and a specific heat capacity of 2,500 J K^{-1} kg^{-1}, consistent with drilling results[19,20,23]. We hold heat flow constant with time at the bottom boundary and sea-floor temperature constant with time and variable with depth, consistent with CTD values. We estimate temperature uncertainty by integrating end-member uncertainty values into the model. We calculate the base of the hydrate stability zone and location of the BSR by integrating heat flow results with the CSMGem hydrate stability program[24] assuming hydrostatic conditions and a constant salinity of 34.9‰, as measured across the region[23].

Full Methods and any associated references are available in the online version of the paper.

Received 25 May; accepted 20 August 2012.

1. Lynch-Stieglitz, J., Curry, W. & Slowey, N. Weaker Gulf Stream in the Florida Straits during the Last Glacial Maximum. *Nature* **402**, 644–648 (1999).

2. Lynch-Stieglitz, J., Schmidt, M. W. & Curry, W. Evidence from the Florida Straits for Younger Dryas ocean circulation changes. *Paleoceanography* **26**, PA1205, http://dx.doi.org/abs/10.1029/2010PA002032 (2011).
3. Winguth, A., Shellito, C., Shields, C. & Winguth, C. Climate response at the Paleocene-Eocene Thermal Maximum to greenhouse gas forcing — a model study with CCSM3. *J. Clim.* **23,** 2562–2584 (2010).
4. Dickens, G. R. The potential volume of oceanic methane hydrates with variable external conditions. *Org. Geochem.* **32**, 1179–1193 (2001).
5. Hornbach, M. J., Saffer, D. M. & Holbrook, W. S. Critically pressured free-gas reservoirs below gas-hydrate provinces. *Nature* **427,** 142–144 (2004).
6. Kennett, J. P., Cannariato, K. G., Hendy, I. L. & Behl, R. J. *Methane Hydrates in Quaternary Climate Change: The Clathrate Gun Hypothesis* (Spec. Publ. Ser. Vol. 54, American Geophysical Union, 2003).
7. Biastoch, A. *et al.* Rising Arctic Ocean temperatures cause gas hydrate destabilization and ocean acidification. *Geophys. Res. Lett.* **38,** L08602, http://dx.doi.org/abs/10.1029/2011GL047222 (2011).
8. Archer, D. *et al.* The importance of ocean temperature to global biogeochemistry. *Earth Planet. Sci. Lett.* **222**, 333–348 (2004).
9. Flemings, B. P., Liu, X. & Winters, W. J. Critical pressure and multiphase flow in Blake Ridge gas hydrates. *Geology* **31,** 1057–1060 (2003).
10. Deser, C. & Blackmon, M. L. Surface climate variations over the North Atlantic Ocean during winter: 1900–1989. *J. Clim.* **6,** 1743–1753 (1993).
11. Evans, H. K., Hall, I. R., Bianchi, G. G. & Oppo, D. W. Intermediate water links to Deep Western Boundary Current variability in the subtropical NW Atlantic during marine isotope stages 5 and 4. *Paleoceanography* **22**, PA3209, http://dx.doi.org/abs/10.1029/2006PA001409 (2007).
12. Wu, L. *et al.* Enhanced warming over the global subtropical western boundary currents. *Nature Clim. Change* **2,** 161–166 (2012).
13. Kvenvolden, K. A. Gas hydrates: geological perspective and global change. *Rev. Geophys.* **31,** 173–187 (1993).
14. Milton, D. J. in *The Future Supply of Nature-Made Gas* (ed. Meyer, R. F.) 927–943 (Technical Reports, Pergamon, 1976).
15. Shipley, T. H. *et al.* Seismic evidence for widespread possible gas hydrate horizons on continental slopes and rises. *Bull. Am. Assoc. Petrol. Geol.* **63,** 2204–2213 (1979).
16. Holbrook, W. S., Hoskins, H., Wood, W. T., Stephen, R. A. & Lizarralde, D. Methane hydrate and free gas on the Blake Ridge from vertical seismic profiling. *Science* **273,** 1840–1843 (1996).
17. Yamano, M., Uyeda, S., Aoki, Y. & Shipley, T. H. Estimates of heat flow derived from gas hydrates. *Geology* **10,** 339–343 (1982).
18. Lund, D., Lynch-Stieglitz, J. & Curry, W. Gulf Stream density structure and transport during the past millennium. *Nature* **444,** 601–604 (2006).
19. Ruppel, C. D. Anomalously cold temperatures observed at the base of the gas hydrate stability zone on the US Atlantic passive margin. *Geology* **25,** 699–702 (1997).
20. Ruppel, C. D., Von Herzen, R. P. & Bonneville, A. Heat flux through an old (~175 Ma) passive margin: offshore southeastern United States. *J. Geophys. Res.* **100** (B10), 20037–20057 (1995).
21. Dillon, W. P., Lee, M. W., Fehlhaber, K. & Coleman, D. F. Gas hydrates on the Atlantic margin of the United States — controls on concentration. *US Geol. Surv. Prof. Pap.* **1570,** 313–330 (1993).
22. Carpenter, G. Coincident sediment slump/clathrate complexes on the U.S. Atlantic continental slope. *Geo-Mar. Lett.* **1,** 29–32 (1981).
23. Paull, C. K., Matsumoto, R. & Wallace, P. J. Gas hydrate sampling on the Blake Ridge and Carolina Rise. *Proc. ODP Init. Rep.* **164,** 5–12, http://dx.doi.org/10.2973/odp.proc.ir.164.1996 (1996).
24. Sloan, E. D. & Koh, C. A. *Clathrate Hydrates of Natural Gases* 3rd edn (CRC Press, 2008).
25. Dugan, B. & Fleming, P. B. Overpressure and fluid flow in the New Jersey continental slope: implications for slope failures and cold seeps. *Science* **289,** 288–291 (2000).
26. Hutchison, I. The effects of sedimentation and compaction on oceanic heat flow. *Geophys. J. R. Astron. Soc.* **82**, 439–459 (1985).
27. Westbrook, G. K. *et al.* Escape of methane gas from the seabed along the West Spitsbergen continental margin. *Geophys. Res. Lett.* **36,** L15608, http://dx.doi.org/abs/10.1029/2009GL039191 (2009).
28. Rajan, A. Mienert, J. & Bünz, S. Acoustic evidence for a gas migration and release system in Arctic glaciated continental margins offshore NW-Svalbard. *Mar. Petrol. Geol.* **32**, 36–49 (2012).
29. Bryan, G. M., Markl, R. G. & Sheridan, R. E. IPOD site survey in the Blake-Bahamas Basin. *Mar. Geol.* **35,** 43–63 (1980).
30. Mackenzie, K. V. Discussion of seawater sound-speed determinations. *J. Acoust. Soc. Am.* **70,** 801–806 (1981).

Supplementary Information is available in the online version of the paper.

Acknowledgements We thank L. Gahagan and the UTIG Marine Seismic Data Center for providing access to seismic line 80.A.

Author Contributions B.J.P. performed all experimental work integrating seismic lines and CTD temperature data into 2D thermal models and the hydrate stability model. M.J.H. conceived the work and developed and tested the prototype 2D models. Both authors worked together to refine the model, analyse data, interpret results, write the manuscript and create the figures.

Author Information Reprints and permissions information is available at www.nature.com/reprints. The authors declare no competing financial interests. Readers are welcome to comment on the online version of the paper. Correspondence and requests for materials should be addressed to B.J.P. (bphrampus@mail.smu.edu).

LETTER

doi:10.1038/nature11506

The origin of the terrestrial noble-gas signature

Svyatoslav S. Shcheka[1] & Hans Keppler[1]

In the atmospheres of Earth and Mars, xenon is strongly depleted relative to argon, when compared to the abundances in chondritic meteorites[1,2]. The origin of this depletion is poorly understood[3–13]. Here we show that more than one weight per cent of argon may be dissolved in $MgSiO_3$ perovskite, the most abundant phase of Earth's lower mantle, whereas the xenon solubility in $MgSiO_3$ perovskite is orders of magnitude lower. We therefore suggest that crystallization of perovskite from a magma ocean in the very early stages of Earth's history concentrated argon in the lower mantle. After most of the primordial atmosphere had been lost, degassing of the lower mantle replenished argon and krypton, but not xenon, in the atmosphere. Our model implies that the depletion of xenon relative to argon indicates that perovskite crystallized from a magma ocean in the early history of Earth and perhaps also Mars.

The relative abundance of noble gases in Earth's atmosphere is largely controlled by the early evolution of our planet. Most of the argon in Earth's atmosphere is the isotope ^{40}Ar, which is a radioactive decay product of ^{40}K. However, the abundances of 'primordial' (non-radiogenic) noble-gas isotopes also differ among the Sun, the terrestrial planets and chondritic meteorites[1,2]. Both chondritic meteorites and terrestrial planets are strongly depleted in the light noble gases helium and neon compared to the Sun. This feature can readily be explained by the loss of light noble gases to space in a relatively weak gravitational field. However, compared to chondrites, which are believed to be similar to the material from which the terrestrial planets formed, xenon is strongly depleted on Earth and Mars relative to argon and krypton. This depletion cannot be explained by loss to space, because xenon, the heaviest of all noble gases, should be least affected by this process.

Therefore, a number of alternative hypotheses has been proposed to account for the 'missing xenon'. One class of models assumes that xenon is present on Earth in its expected chondritic ratio relative to argon and krypton and that the xenon is hidden in some near-surface reservoir, such as glacier ices, clathrates, sediments or silicates[3–6]. However, such a xenon-rich reservoir has never been found in nature. Another class of models has suggested that xenon may be concentrated in Earth's core, either in solid solution with iron or possibly as a separate phase[7,8]. Recent experiments, however, did not find any evidence for dissolution of xenon in iron at core pressures, although the full range of pressures and temperature relevant to core formation has not yet been explored[9]. A third class of models explains the terrestrial noble-gas abundance by a combination of hydrodynamic escape to space and mantle degassing, but these models do not provide a simple physical explanation for the depletion of xenon relative to argon in the atmosphere either[2,10]. Alternative hypotheses include the delivery of volatiles to Earth by comets that may be depleted in xenon[11] or the preferential loss of xenon to space owing to its low ionization potential[12,13].

The lower mantle is the largest reservoir on Earth, with a mass exceeding 50% of the mass of the entire planet. Surprisingly, the potential role of the lower mantle in producing the terrestrial noble-gas signature has never been investigated. We have therefore studied the solubility of noble gases (argon, krypton, and xenon) in $MgSiO_3$ perovskite, the major phase of the lower mantle. Although it is widely believed that noble gases are very poorly soluble in upper-mantle minerals[14], there are structural considerations suggesting that this may be different for the perovskite phase. $MgSiO_3$ perovskite may contain abundant oxygen vacancies[15–21]. These oxygen vacancies may occur charge-balanced by Si vacancies at low silica activity, such as in equilibrium with the ferropericlase (Mg,Fe)O phase in the lower mantle. The substitution of Al^{3+} for Si^{4+} may also produce oxygen vacancies. Given that the atomic radius of argon is not far away from the ionic radius of the O^{2-} ion, oxygen vacancies in perovskite may provide suitable storage sites for noble-gas atoms of appropriate radius.

Experimental results on noble-gas solubility in $MgSiO_3$ perovskite are compiled in Supplementary Table 1. The experiments with argon yielded $MgSiO_3$ perovskite with up to more than 1 wt% of argon, whereas the xenon solubility was nearly 300 parts per million (p.p.m.), even if excess xenon was clearly present during the experiment (Fig. 1a). Data for krypton overlap with the argon data, but tend to be somewhat lower. The high argon concentrations are a characteristic property of the perovskite phase. This can clearly be seen in Fig. 1b, which shows a sample in which argon-saturated $MgSiO_3$ majorite (with garnet structure) coexists with $MgSiO_3$ perovskite. No argon is found in the majorite (detection limit 150 p.p.m.), while the coexisting perovskite contains about 3,000 p.p.m. of argon. In some samples argon solubility is so high that the distribution can be visualized by X-ray mapping (Fig. 1c and d), although the instability of perovskite under the electron beam limits the quality of the images that may be obtained. Again, these maps show that the high argon solubility is restricted to the perovskite phase. In the course of this study, numerous phases were produced by accident because the experiments did not reach the perovskite stability field. In none of these phases, which included $MgSiO_3$ ilmenite, SiO_2 stishovite, Mg_2SiO_4 ringwoodite, and MgO periclase was any argon ever detected. Careful study of the perovskite samples by scanning and transmission electron microscopy did not reveal any impurities or foreign phases, such as gas bubbles, that may account for the observed argon content. We therefore conclude that the argon must be incorporated into the crystal lattice of the perovskite phase. This is consistent with some preliminary single-crystal X-ray diffraction data. The Ar-bearing perovskite shows some additional, weak reflections that are consistent with the symmetry of the phase, but do not occur in argon-free samples. Subtle, but systematic differences in reflection intensity were also observed. A detailed structure refinement was not possible owing to the large width of the X-ray reflections. However, the broadening of the reflections ($0.5^\circ\,\Omega$ half width as opposed to 0.07° for pure $MgSiO_3$ perovskite; MoK_α radiation) indicates some internal strain that itself is suggestive of argon being incorporated in the crystal lattice of the perovskite. Moreover, in some samples, high argon contents appear to correlate with low Si/Mg ratios. This is consistent with argon being incorporated in oxygen vacancies, which are charge-balanced by Si vacancies.

If argon primarily substitutes for oxygen vacancies in perovskite, the low solubility of xenon is probably related to the size mismatch between xenon and the oxygen vacancies. The atomic radius of argon (1.64 Å; ref. 22) is close to the radius of O^{2-} (1.28–1.4 Å), but xenon with an atomic radius of 1.96 Å is probably too large to fit into an oxygen vacancy. Our data therefore suggest that noble gases of suitable atomic radius can easily be incorporated in minerals that have appropriate vacancies. Such vacancies exist in lower-mantle perovskite[15–21], but

[1]Bayerisches Geoinstitut, Universität Bayreuth, 95440 Bayreuth, Germany.

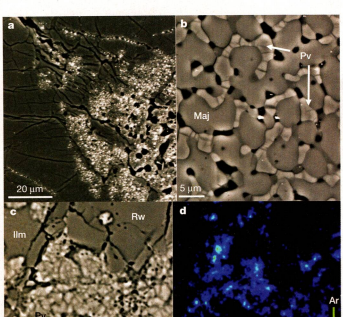

Figure 1 | Scanning electron microscope images of $MgSiO_3$ perovskite samples saturated with noble gases. a, Perovskite crystallized in the presence of excess xenon. The bright spots in the image are xenon-filled bubbles in perovskite below the sample surface. However, in those parts of the perovskite crystals that are far away from bubbles, no xenon can be detected, implying very low xenon solubility (<100 p.p.m.). **b**, Argon-saturated sample with perovskite (Pv, arrows) coexisting with $MgSiO_3$ majorite (garnet structure, Maj). Dark spots are holes previously filled by argon gas. No argon can be detected in majorite (detection limit 150 p.p.m.), but the perovskite contains 3,000 p.p.m. of argon. **c**, Another sample, containing perovskite (lighter areas) coexisting with Mg_2SiO_4 ringwoodite (Rw, dark) and $MgSiO_3$ ilmenite (Ilm, dark). **d**, X-ray map of argon distribution in the same sample as shown in **c**. Argon is only found in the perovskite phase. The concentration scale shown corresponds to the range from 0 (blue) to approximately 0.8 wt% (green) of Ar.

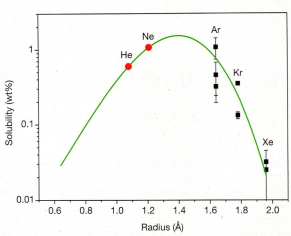

Figure 2 | A lattice-strain model[29] of noble-gas solubility in $MgSiO_3$ perovskite. The fit is based on Ar, Kr and Xe solubility data for 25 GPa at 1,600 °C to 1,800 °C. Estimated values for the solubilities of He and Ne are also shown. Fit parameters are the effective Young's modulus E_m = 35 GPa; radius of the oxygen site r_1 = 1.4 Å, and strain-free solubility c_0 = 1.53 wt%. Noble-gas radii are from ref. 22. Error bars are one standard deviation. For further details, see Supplementary Information.

not in the minerals of the upper mantle; the behaviour of noble gases in the lower mantle therefore fundamentally differs from that observed in upper-mantle minerals. Noble-gas solubilities in silicate perovskite observed in this study reach the level of weight per cent, implying that these phases are actually a new kind of noble-gas compound. The dependence of noble-gas solubility on the size of the noble gas atom can be well described by a lattice strain model (Fig. 2). The model predicts that helium and particularly neon should also be highly soluble in perovskite.

The idea that noble gases are quite soluble in some minerals with appropriate vacancies is supported by an observation that was accidentally made during the course of this study. In an attempt to obtain better single crystals of perovskite for X-ray diffraction studies, some experiments were carried out with K_2CO_3 as the fluxing agent added to the starting material. In these experiments, a K-bearing phase was observed that also dissolved up to 0.5 wt% of argon (Fig. 3). Further investigations showed that this phase had been previously described as 'phase X'. Structure refinements of phase X (ref. 23) suggest that it always contains vacancies on the K site, with a general formula of $K_{2-x}Mg_2Si_2O_7H_x$. Given that the ionic radius of K^+ is almost identical to the radius of Ar, the high argon solubility observed in this phase is not surprising. Another observation in these experiments is that the argon solubility in perovskite coexisting with phase X is low. This may be due to preferred partitioning of Ar into phase X or to high silica activity, because in some of these experiments SiO_2 stishovite was detected as a separate phase. The perovskite in these experiments is therefore silica-saturated and no vacancies on the Si^{4+} and O^{2-} sites are expected.

Our results offer a simple explanation for the depletion of xenon relative to argon observed in Earth's atmosphere. Very early in Earth's history, our planet was probably completely molten[24]. This magma ocean probably coexisted with an early atmosphere containing volatiles released upon melting of chondritic materials as well as possibly some component of the nebular gas from which the Sun had formed[25]. Crystallization of perovskite from this magma ocean would then have concentrated argon and krypton, but much less xenon in the lower mantle. At the same time, most of the primary atmosphere was lost by hydrodynamic escape due to high surface temperatures, intense ultraviolet radiation from the early Sun and meteorite impacts[2,10]. The signature of mass-dependent fractionation due to hydrodynamic escape can still be seen today in the relative abundance of xenon isotopes in Earth's atmosphere[2]. After solidification of the magma ocean, mantle convection transported material from the lower mantle close to Earth's surface, where degassing occurred that replenished Earth's atmosphere in primordial argon and krypton, but much less in xenon. Evidence for this process may have been recently observed[12], as atmospheric xenon trapped in 3.5-billion-year-old fluid inclusions appears to be intermediate in isotopic composition between modern atmospheric and chondritic xenon. This could imply continued degassing of the lower mantle in the Archaean era.

Recent simulations[26] suggest significant radial mixing in the Solar System during the late stages of accretion, so that volatile-rich material from the outer parts of the Solar System was incorporated into the growing Earth. We therefore assume that most of the terrestrial volatiles were supplied by chondritic material in the main stage of accretion. During the crystallization of the magma ocean, most volatiles were enriched in the residual melt, so that at the latest stages of crystallization, the saturation point for volatiles may have been reached. This probably happened in the lower mantle, because water solubility in the lower-mantle minerals is exceedingly small[27]. If the noble gases mix nearly ideally with the other gases in the residual gas phase, the mineral/fluid partition coefficients of the noble gases will be proportional to the measured solubilities. This means that the ratios of Xe:Kr:Ar dissolved in lower-mantle perovskite will correspond to the original ratio of these gases multiplied by factors of 0.027:0.32:1, the latter being the ratio of the solubilities of Xe, Kr, and Ar in perovskite as derived from the fit in Fig. 2.

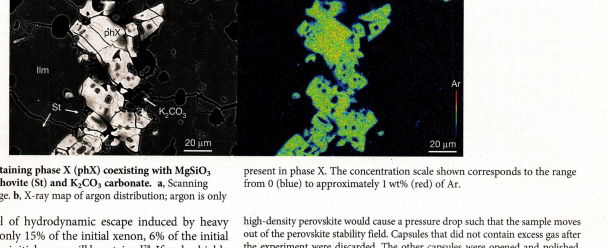

Figure 3 | A sample containing phase X (phX) coexisting with $MgSiO_3$ ilmenite (Ilm), SiO_2 stishovite (St) and K_2CO_3 carbonate. a, Scanning electron microscope image. **b**, X-ray map of argon distribution; argon is only present in phase X. The concentration scale shown corresponds to the range from 0 (blue) to approximately 1 wt% (red) of Ar.

A numerical model of hydrodynamic escape induced by heavy impacts suggests that only 15% of the initial xenon, 6% of the initial krypton and 0.8% of the initial argon will be retained[28]. If such a highly fractionated residual component is mixed with noble gases outgassed from the lower mantle, such that the present-day xenon is one-third a residual and two-thirds an outgassed component, the resulting ratio of Xe:Kr:Ar in the atmosphere would be 0.041:0.32:1, relative to the primordial ratios of these gases. The predicted depletion of xenon relative to krypton and argon is in good agreement with observation. Moreover, the present-day xenon would contain a third of a heavily fractionated component, in agreement with the observed mass-dependent fractionation of xenon isotopes. However, atmospheric krypton and argon would have nearly primordial isotopic composition, containing only a trace of fractionated gas (1.7% for Kr and 0.07% for Ar), in agreement with the essentially chondritic ratios of argon and krypton isotopes in Earth's atmosphere. The only shortcoming of this model is that it predicts a small (factor of three) fractionation between argon and krypton. However, this fractionation may disappear with increasing pressure in the lower mantle (see Supplementary Information). Both argon and krypton are very compressible, which could change their atomic radii in the deeper part of the lower mantle such that no relative fractionation occurs. The precise ratio of the two noble-gas components invoked in this model essentially depends on the degree of xenon isotope fractionation induced by hydrodynamic escape, which itself is a function of assumed bulk atmospheric composition, shock temperature and other parameters[28]. Additional processes may be required to explain the relative depletion of the heaviest isotopes of xenon[2].

The 'planetary' noble-gas pattern with a depletion of xenon relative to argon is also seen on Mars[2]. This may seem surprising, because the mantle of Mars probably contains only a thin layer of silicate perovskite. However, the present atmosphere of Mars is much thinner than on Earth and accordingly, a much smaller degree of mantle degassing may be sufficient to produce the characteristic depletion of xenon relative to argon. Moreover, the xenon isotopes on Mars show no mass-dependent fractionation, which in our model would imply that the primordial atmosphere had been lost completely, in line with the low gravitational field of Mars. We therefore suggest that the depletion of xenon relative to argon is diagnostic for the fractionation of perovskite from a magma ocean in the early history of a planet.

METHODS SUMMARY

Experiments on noble gas solubility in $MgSiO_3$ perovskite were carried out in a multi-anvil apparatus. $MgSiO_3$ glass containing small amounts (<1 wt%) of Al_2O_3 was loaded together with 40–80 bar of argon or xenon into platinum capsules using a special gas-loading device. These capsules were first run at 10 GPa and 1,200 °C for one hour to crystallize $MgSiO_3$ enstatite from the glass. The capsules were then recovered and re-run without opening at 25 GPa and 1,600–1,800 °C for one hour to convert the enstatite into perovskite. This two-stage procedure is necessary because in a one-stage run, the conversion of low-density glass into high-density perovskite would cause a pressure drop such that the sample moves out of the perovskite stability field. Capsules that did not contain excess gas after the experiment were discarded. The other capsules were opened and polished. Phases were identified by Raman spectroscopy and chemical compositions were measured by electron microprobe (major elements and Ar; JEOL JXA-8200) and laser-ablation inductively coupled plasma mass spectrometry (ICP-MS) (Kr and Xe; Elan DRC-e quadrupole mass spectrometer attached to a Geolas M 193-nm ArF Excimer Laser system). Noble-gas-saturated glasses were used as standards for Ar, Kr and Xe.

Full Methods and any associated references are available in the online version of the paper.

Received 31 May; accepted 8 August 2012.
Published online 10 October 2012.

1. Anders, E. & Owen, T. Mars and Earth—origin and abundance of volatiles. *Science* **198,** 453–465 (1977).
2. Pepin, R. O. & Porcelli, D. Origin of noble gases in the terrestrial planets. *Rev. Mineral. Geochem.* **47,** 191–246 (2002).
3. Matsuda, J. & Matsubara, K. Noble gases in silica and their implication for the terrestrial missing Xe. *Geophys. Res. Lett.* **16,** 81–84 (1989).
4. Sanloup, C. *et al.* Retention of xenon in quartz and Earth's missing xenon. *Science* **310,** 1174–1177 (2005).
5. Sill, G. T. & Wilkening, L. L. Ice clathrate as a possible source of atmospheres of terrestrial planets. *Icarus* **33,** 13–22 (1978).
6. Wacker, J. F. & Anders, E. Trapping of xenon in ice—implications for the origin of the Earth's noble gases. *Geochim. Cosmochim. Acta* **48,** 2373–2380 (1984).
7. Jephcoat, A. P. Rare-gas solids in the Earth's deep interior. *Nature* **393,** 355–358 (1998).
8. Lee, K. K. M. & Steinle-Neumann, G. High-pressure alloying of iron and xenon: "missing" Xe in the Earth's core? *J. Geophys. Res.* **111,** B02202 (2006).
9. Nishio-Hamane, D., Yagi, T., Sata, N., Fujita, T. & Okada, T. No reactions observed in Xe-Fe system even at Earth core pressures. *Geophys. Res. Lett.* **37,** L04302 (2010).
10. Pepin, R. O. On the origin and early evolution of terrestrial planet atmospheres and meteoritic volatiles. *Icarus* **92,** 2–79 (1991).
11. Dauphas, M. The dual origin of the terrestrial atmosphere. *Icarus* **165,** 326–339 (2003).
12. Pujol, M., Marty, B. & Burgess, R. Chondritic-like xenon trapped in Archean rocks: a possible signature of the ancient atmosphere. *Earth Planet. Sci. Lett.* **308,** 298–306 (2011).
13. Marty, B. The origins and concentrations of water, carbon, nitrogen and noble gases on Earth. *Earth Planet. Sci. Lett.* **313–314,** 56–66 (2012).
14. Heber, V. S., Brooker, R. A., Kelley, S. P. & Wood, B. J. Crystal-melt partitioning of noble gases (helium, neon, argon, krypton, and xenon) for olivine and clinopyroxene. *Geochim. Cosmochim. Acta* **71,** 1041–1061 (2007).
15. Kojitani, H., Katsura, T. & Akaogi, M. Aluminum substitution mechanisms in perovskite-type $MgSiO_3$: an investigation by Rietveld analysis. *Phys. Chem. Mineral.* **34,** 257–267 (2007).
16. Lauterbach, S., McCammon, C. A., van Aken, P., Langenhorst, F. & Seifert, F. Mossbauer and ELNES spectroscopy of $(Mg,Fe)(Si,Al)O_3$ perovskite: a highly oxidised component of the lower mantle. *Contrib. Mineral. Petrol.* **138,** 17–26 (2000).
17. McCammon, C. A. Perovskite as a possible sink for ferric iron in the lower mantle. *Nature* **387,** 694–696 (1997).
18. Navrotsky, A. Mantle geochemistry—a lesson from ceramics. *Science* **284,** 1788–1789 (1999).
19. Navrotsky, A. *et al.* Aluminum in magnesium silicate perovskite: formation, structure, and energetics of magnesium-rich defect solid solutions. *J. Geophys. Res.* **108,** 2330 (2003).
20. Stashans, A., Piedra, L. & Briceno, T. Fundamental and excited states of F-type centres in $MgSiO_3$ perovskite. *Physica B* **405,** 4350–4354 (2010).
21. Stebbins, J. F. *et al.* Aluminum substitution in stishovite and $MgSiO_3$ perovskite: high-resolution ^{27}Al NMR. *Am. Mineral.* **91,** 337–343 (2006).

22. Zhang, Y. X. & Xu, Z. J. Atomic radii of noble gas elements in condensed phases. *Am. Mineral.* **80,** 670–675 (1995).
23. Yang, H. X., Konzett, J. & Prewitt, C. T. Crystal structure of phase X, a high pressure alkali-rich hydrous silicate and its anhydrous equivalent. *Am. Mineral.* **86,** 1483–1488 (2001).
24. Greenwood, R. C., Franchi, I. A., Jambon, A. & Buchanan, P. C. Widespread magma oceans on asteroidal bodies in the early Solar System. *Nature* **435,** 916–918 (2005).
25. Porcelli, D., Woolum, D. & Cassen, P. Deep Earth rare gases: initial inventories, capture from the solar nebula, and losses during moon formation. *Earth Planet. Sci. Lett.* **193,** 237–251 (2001).
26. Morbidelli, A. *et al.* Source regions and timescales for the delivery of water to the Earth. *Meteorit. Planet. Sci.* **35,** 1309–1320 (2000).
27. Bolfan-Casanova, N., Keppler, H. & Rubie, D. C. Water partitioning at the 660 km discontinuity and evidence for very low water solubility in magnesium silicate perovskite. *Geophys. Res. Lett.* **30,** 1905 (2003).
28. Pepin, R. O. Evolution of Earth's noble gases: consequences of assuming hydrodynamic loss driven by giant impact. *Icarus* **126,** 148–156 (1997).
29. Brooker, R. A. *et al.* The 'zero charge' partitioning behaviour of noble gases during mantle melting. *Nature* **423,** 738–741 (2003).

Supplementary Information is available in the online version of the paper.

Acknowledgements This work was supported by the German Science Foundation (DFG, SPP 1236). We thank A. Audetat for measurements of Kr and Xe by laser-ablation ICP-MS, N. Miyajima for help with TEM studies of the samples and T. Boffa-Ballaran for preliminary X-ray data of Ar-bearing perovskite.

Author Contributions S.S.S. carried out all experiments and chemical analyses reported in this paper. H.K. suggested this study. Both authors wrote the manuscript together.

Author Information Reprints and permissions information is available at www.nature.com/reprints. The authors declare no competing financial interests. Readers are welcome to comment on the online version of the paper. Correspondence and requests for materials should be addressed to S.S.S. (svyatoslav.shcheka@uni-bayreuth.de).

LETTER

doi:10.1038/nature11510

Epistasis as the primary factor in molecular evolution

Michael S. Breen[1], Carsten Kemena[1], Peter K. Vlasov[1], Cedric Notredame[1] & Fyodor A. Kondrashov[1,2]

The main forces directing long-term molecular evolution remain obscure. A sizable fraction of amino-acid substitutions seem to be fixed by positive selection[1–4], but it is unclear to what degree long-term protein evolution is constrained by epistasis, that is, instances when substitutions that are accepted in one genotype are deleterious in another. Here we obtain a quantitative estimate of the prevalence of epistasis in long-term protein evolution by relating data on amino-acid usage in 14 organelle proteins and 2 nuclear-encoded proteins to their rates of short-term evolution. We studied multiple alignments of at least 1,000 orthologues for each of these 16 proteins from species from a diverse phylogenetic background and found that an average site contained approximately eight different amino acids. Thus, without epistasis an average site should accept two-fifths of all possible amino acids, and the average rate of amino-acid substitutions should therefore be about three-fifths lower than the rate of neutral evolution. However, we found that the measured rate of amino-acid substitution in recent evolution is 20 times lower than the rate of neutral evolution and an order of magnitude lower than that expected in the absence of epistasis. These data indicate that epistasis is pervasive throughout protein evolution: about 90 per cent of all amino-acid substitutions have a neutral or beneficial impact only in the genetic backgrounds in which they occur, and must therefore be deleterious in a different background of other species. Our findings show that most amino-acid substitutions have different fitness effects in different species and that epistasis provides the primary conceptual framework to describe the tempo and mode of long-term protein evolution.

The study of the factors determining the tempo and mode of molecular evolution continues to be at the forefront of evolutionary biology. Since the inception of the neutral theory[5], many studies of the rate of molecular evolution have focused on the relative role of selection versus genetic drift in the fixation of amino-acid substitutions[6]. It now seems certain that both of these factors, selection and genetic drift, contribute to a substantial fraction of all amino-acid substitutions in the course of evolution[1–4]. However, the neutral-versus-selective debate on the nature of molecular evolution has primarily focused on the short-term effects of substitutions that may not provide the framework necessary to understand the differences between the functional and selective effects of amino-acid substitutions that accumulate in the course of long-term evolution.

An amino-acid substitution that is neutral or beneficial in one genetic context may be deleterious in another[7–11]. Such a situation, when the fitness effect of one allele state depends on the allele states at other loci, is called epistasis[9,10]. Both the neutral and selective theories of protein evolution provide an accurate framework for understanding long-term protein evolution only if amino-acid states in different genetic contexts have the same effect on fitness, that is, if epistasis is rare. In the absence of epistasis, when the fitness effects of all amino-acid states are independent of one another, substitutions in different species are expected to have similar effects on fitness except in cases where these substitutions enable differences in adaptation to environmental conditions. In that case, if an amino-acid state were found in one species in a protein sequence that is not directly involved in environmental adaptation, such as a housekeeping protein, then the same amino-acid state should be acceptable in an orthologous site in a different species. However, if epistasis is common then amino-acid substitutions that were beneficial or neutral in one species should often be deleterious in another. Therefore, unravelling the extent and basis of epistasis may be crucial to understanding differences in protein sequences between species and long-term protein evolution[2–15]. At present, studies of the differences in the fitness of substitutions in different genetic contexts consider specific genes or events[1,1,16–24], and it is unknown what fraction of amino-acid substitutions that occur in one species would also be acceptable in another species if they were to occur in orthologous sites (but see ref. 11). Here we develop an approach to quantifying the impact of epistasis in protein evolution and show that the fitness effects of most amino-acid substitutions must depend on the genetic context in which they occur.

We obtained sequence data for some of the most widely sequenced genes for organelle and nuclear-encoded proteins. The choice of genes selected for this study was dictated by four considerations: the availability of at least 1,000 unique orthologous sequences from different species; a well-defined, conserved housekeeping function; the absence or a low rate of gene duplication; and conserved sequence with few insertions and deletions (indels), leading to an unequivocal multiple alignment of the orthologous sequences. Our final data set included orthologous sequences from Metazoa, including 13 mitochondrial genes and 2 nuclear genes, and the large subunit of ribulose 1,5-bisphosphate carboxylase–oxygenase (Rubisco) encoded by the *rbcL* gene in chloroplast genomes of Viridiplantae. The number of unique sequences from different species ranged between 949 and 13,912, with proteins encoded in the organelles having more sequences in the alignment (Table 1). The sequences were aligned using a version of the T-Coffee algorithm[25] adapted to align large data sets of up to 100,000 sequences (Methods). For each of these alignments, we calculated the amino-acid usage (u), defined as the number of different amino acids observed per site (Table 1). We found that the average usage across all genes in our data set was ~9, meaning that in the course of long-term evolution an average site accepted approximately half of all possible amino acids. The distribution of u reveals few invariant sites (those where a single amino acid was observed), indicating that the high usage was not caused by an average of invariant and extremely variable sites (Supplementary Fig. 1).

Amino-acid usage can be used to predict the expected short-term rates of protein evolution without epistasis. Without epistasis, an amino-acid state observed in one species should also be acceptable in the orthologous site of another species. Therefore, substitutions in a protein sequence leading to amino-acid states observed in orthologous sites should not be inhibited by negative selection. For example, if one-half of amino acids were accepted in a protein sequence in the long term then, in a non-epistatic model, the same fraction of amino acids should be acceptable to this protein in the course of short-term evolution. This prediction can be expressed in terms of the ratio of the per-site rates of non-synonymous and synonymous evolution[6] (dN/dS): if on average ~0.5 of all amino acids were found per site then the expected non-epistatic dN/dS ratio between two closely related orthologues of this gene should be ~0.5 (Methods).

[1]Bioinformatics and Genomics Programme, Centre for Genomic Regulation and Universitat Pompeu Fabra, 88 Dr Aiguader, Barcelona 08003, Spain. [2]Institució Catalana de Recerca i Estudis Avançats (ICREA), 23 Passeig Lluís Companys, Barcelona 08010, Spain.

Table 1 | Amino-acid usage, frequency of non-fixed states and rates of evolution

Gene	Number of species with non-redundant sequences	Average amino-acid usage	Frequency of non-fixed state (p)	Average amino-acid usage after Poisson correction	Expected, non-epistatic dN/dS ratio from Poisson correction	Observed average dN/dS ratio	Fraction of epistatic evolution
ATP6	3,021	9.83	5.41×10^{-4}	9.39	0.44	0.056	0.87
ATP8	1,244	12.82	8.24×10^{-4}	11.61	0.56	0.224	0.60
COX1	4,450	6.87	7.13×10^{-4}	6.33	0.28	0.015	0.95
COX2	4,204	9.70	7.64×10^{-4}	9.12	0.43	0.025	0.94
COX3	2,191	9.43	2.00×10^{-4}	7.15	0.32	0.036	0.89
CYTB	7,954	10.70	1.17×10^{-3}	10.68	0.51	0.039	0.92
ND1	2,056	9.76	4.99×10^{-4}	8.41	0.39	0.040	0.90
ND2	5,963	10.67	1.64×10^{-3}	10.66	0.51	0.067	0.87
ND3	2,852	10.54	6.8×10^{-4}	10.24	0.49	0.069	0.86
ND4	2,041	10.08	5.31×10^{-4}	9.00	0.42	0.045	0.89
ND4L	1,785	11.85	4.97×10^{-4}	10.24	0.49	0.076	0.84
ND5	949	8.97	4.07×10^{-4}	7.10	0.32	0.057	0.82
ND6	1,015	11.28	2.88×10^{-4}	8.97	0.42	0.073	0.83
EEF1A1	1,743	3.81	5.31×10^{-4}	3.05	0.11	0.020	0.82
H3.2	1,228	5.18	8.97×10^{-4}	3.59	0.14	0.037	0.74
rbcL	13,912	8.65	1.39×10^{-3}	8.65	0.40	0.072	0.82

Under the simplifying assumption that at a site in a large multiple alignment all permissible amino-acid states are equally likely to be observed at least once, dN/dS should be equal to $(u-1)/19$, where 19 is the number of possible substitutions possible at a site. However, to apply amino-acid usage as a measure for estimating the expected non-epistatic dN/dS value, it is necessary to take into account potential biases that are inherent to usage. Specifically, u is sensitive to erroneous inclusions of rare amino-acid states because an amino acid that is found only once at a site in an alignment makes the same contribution to the measure as an amino acid that is found thousands of times. Indeed, the majority of the observed amino-acid states in our alignments are rare (Supplementary Fig. 2), which at first glance seems to suggest that sequencing errors or deleterious polymorphisms had a large influence on u. However, the frequency distribution of fixed amino-acid states is also expected to follow an exponential decay function. On a realistic phylogeny with many species, the majority of evolutionary time is found in recent branches, and many amino-acid states are therefore expected to be rare because they would have evolved recently (Supplementary Fig. 3). Thus, a majority of fixed events are also expected to be rare as a direct consequence of the phylogenetic nature of evolution and, therefore, a sophisticated method to take into account the impact of rare erroneous states is required.

There are three potential sources of error in our estimate of amino-acid usage: alignment errors, sequencing errors and sequence polymorphisms. The latter two we treat as a single confounding factor of non-fixed amino-acid states. We used different approaches to deal with potential alignment errors and the contribution of non-fixed states. To minimize the effect of misaligned sequences, we post-processed the alignments by removing the sequences most likely to be misaligned. In a progressive alignment procedure, such as the one used here, mistakes usually arise through inaccurate indel accumulation. We therefore recursively removed the sequences inducing the largest fraction of indels and realigned the remaining sequences (Supplementary Table 1). We found that the resulting alignments contained few indels, and different alignment methods yielded virtually identical amino-acid usage measures (Supplementary Table 2). Thus, we do not expect alignment errors to contribute to the usage measure of our data set.

Next we used a probabilistic approach to estimate the contribution of non-fixed amino-acid states to the amino-acid usage measure. First we estimated the probability of occurrence of a non-fixed state at one site in one sequence, p, by calculating the divergence of sequences from the same species (Supplementary Methods). This approach combines the estimate of the frequency of occurrence of sequencing errors and segregating polymorphisms into one measure. Using multiple sequences from the same species from a large subset of those species that were used in the original multiple alignment (Supplementary Table 3), we estimated the amino-acid diversity of non-fixed states, π_a, in the same manner as the commonly used nucleotide diversity measure. From π_a we then estimated p as $\pi_a/6$, where 6 is the average number of non-synonymous mutations per codon (Methods). We found that p was generally small, with $0.0002 < p < 0.007$ across the genes in our data set (Table 1). We then calculated the probability of multiple occurrences of the same non-fixed state at one site in the multiple alignment using the Poisson approximation of a binomial distribution. The probability that a non-fixed state with probability of occurrence p is observed k times in an alignment of N sequences is $m = (pN)^k e^{-pN}/k!$. The probability that an amino-acid state is observed at least once out of k times in a fixed rather than non-fixed state is $r = 1 - m$. Thus, at each site the amino-acid usage measure that takes into account the probability that some of the states were non-fixed is $\sum_{i=1}^{u} r_i$, where i is the amino-acid state and u is the amino-acid usage at that site. By applying this approach to our data, we obtained the amino-acid usage corrected for the contribution of non-fixed states. This was slightly smaller than the uncorrected amino-acid usage (Table 1), indicating that the impact of non-fixed states is small. Two different approaches, one probabilistic and one empirical, confirm the low impact of non-fixed states on our measurement of amino-acid usage (Supplementary Tables 4 and 5).

Our data show that a site in a protein can, on average, accept about eight different amino acids in different species over the course of long-term evolution. This estimate is undoubtedly a lower bound owing to the restricted phylogenetic breadth and quantity of sequences included in the alignment. In our data, u tends to plateau as the number of sequences included in the alignment is increased; however, the actual plateau of this function is apparently beyond the number of sequences that were available for our study (Supplementary Fig. 4), confirming our estimate of u as a lower bound. The non-epistatic model predicts that an amino acid that is acceptable to one species should be acceptable to another, such that the expected non-epistatic dN/dS value of orthologues from the same alignment should equal $(u-1)/19$; in our case, for amino-acid usage of eight, the expected dN/dS value is 7/19, or ~0.37. We compared this prediction with the observed dN/dS ratio estimated for each of the 16 genes in our data set using many of the species present in the multiple alignment (Supplementary Table 6). On average, the observed dN/dS ratio was about seven times smaller than that predicted by the non-epistatic model (Table 1).

The $(u-1)/19$ approximation is a crude estimate of the expected dN/dS value because it relies on the assumption that in the multiple alignment all permissible amino acids are equally likely to be observed. However, some amino-acid states may be more than one mutational step away from a sequence in which dN/dS is measured, and such states should therefore not be taken into account when comparing the expected non-epistatic dN/dS ratio with the observed ratio for this particular sequence. We thus estimated the expected dN/dS value using only those amino-acid states that are one mutational step away

from the sequence for which dN/dS was measured. We estimated the non-epistatic dN/dS ratio for these sequences as the average of u_m/n_m across all sites, where n_m is the total number of possible amino-acid states one mutational step away from the state in a given site and u_m is the number of such states observed in the entire alignment. The u_m/n_m measure of epistatic evolution was larger than that predicted by our crude measure $(u-1)/19$, resulting in a difference between the expected non-epistatic dN/dS value and the observed value of more than one order of magnitude (Table 2). The higher expected dN/dS value in this case can be explained to be the result of closely related sequences exploring only a limited part of the sequence space[13] or by the physicochemical similarity of amino acids that are located in the mutational vicinity in the genetic code.

The large difference between the dN/dS value predicted on the basis of amino-acid usage and that observed across a large fraction of the same sequences (Supplementary Table 6) indicates that the vast majority of amino-acid states are acceptable in a species- or clade-specific manner. There are two ways to explain this pattern. First, most amino-acid substitutions may have been subject to positive selection for an environmental adaptation specific to the environment of a particular species. Thus, an amino acid that was beneficial to one species because of a specific environmental adaptation may be detrimental to a species that does not live in the same environment. The second explanation is that the fitness of most amino-acid substitutions could have depended on the genetic context, or internal cellular environment, of the species in which the substitution occurs, such that a substitution beneficial in one background would be expected to be detrimental in a different background. In other words, epistatic interactions are the norm and not the exception when we consider amino-acid substitutions in protein sequences. Two considerations indicate that widespread epistasis is the most likely explanation for the observed data. First, the McDonald–Kreitman test[1] showed that positive selection was not common in the evolution of the proteins in our data set (Table 3), as would have been expected if the majority of substitutions conferred an environmental adaptation. Second, the nature of the functions of the proteins considered here, especially that of mitochondrial proteins, implies that interaction with the external environment was limited. Additionally, numerous examples of genetic interactions within proteins, through structural interactions within the same molecule[8–11,16–20,26] or interaction of cellular components[21–24,27–30], support the hypothesis that epistatic interactions may affect a large majority of all amino-acid substitutions.

We identify epistasis as a powerful factor affecting long-term protein evolution and one that must necessarily be invoked to explain why the vast majority of amino-acid substitutions that occur in one species cannot occur in another regardless of whether or not positive selection plays the dominant role in the course of fixation of amino-acid substitutions in specific genetic contexts. An epistatic perspective of molecular evolution leads to the formulation of several fundamental questions, in addition to the largely unanswered questions posed by John Maynard Smith in 1970 (ref. 12). First, given a specific site, substitutions in how many other sites in the same gene or in the entire genome could change the strength of selection associated with substitutions at this site? Second, out of the entire network of pairwise epistatic interactions between sites across the genome, are there many non-overlapping epistatic subnetworks or are most sites interconnected within the entire network of epistatic interactions? Third, what is the ratio of intergenic to intragenic epistatic interactions? Fourth, what is the molecular basis of epistatic interactions within the genome? Finally, pervasive epistasis in long-term protein evolution raises the possibility that similar epistatic interactions may be prevalent in short-term evolution[20,21] and that situations when a polymorphism is benign or beneficial to one individual but deleterious to another individual within the same population may be more common than is thought at present.

Table 2 | Fraction of epistatic evolution measured by u_m/n_m

Gene	Number of species with dN/dS estimate	Average expected non-epistatic dN/dS ratio estimated by u_m/n_m	Observed average dN/dS ratio	Average fraction of epistatic evolution (s.d.)
ATP6	1,300	0.77	0.056	0.93 (0.063)
ATP8	781	0.52	0.224	0.57 (0.303)
COX1	1,123	0.81	0.015	0.98 (0.027)
COX2	1,214	0.81	0.025	0.97 (0.029)
COX3	622	0.81	0.036	0.96 (0.038)
CYTB	3,992	0.84	0.039	0.95 (0.034)
ND1	569	0.81	0.040	0.95 (0.039)
ND2	3,210	0.79	0.067	0.92 (0.042)
ND3	989	0.69	0.069	0.90 (0.069)
ND4	510	0.83	0.045	0.95 (0.033)
ND4L	441	0.65	0.076	0.88 (0.121)
ND5	370	0.87	0.057	0.93 (0.033)
ND6	406	0.70	0.073	0.90 (0.098)
EEF1A1	1,343	0.77	0.020	0.97 (0.018)
H3.2	670	0.72	0.037	0.95 (0.090)
rbcL	13,546	0.88	0.072	0.92 (0.093)

Table 3 | McDonald–Kreitman test on select species for each gene

Gene	Average s using polymorphisms with >1% frequency in the population	Average s using polymorphisms with >5% frequency in the population	Number of species with polymorphism and divergence data
ATP6	−0.7 (0.06)	−0.4 (0.08)	52
ATP8	−0.1 (0.16)	−0.1 (0.15)	18
COX1	−0.8 (0.08)	−0.8 (0.08)	25
COX2	−0.7 (0.06)	−0.4 (0.09)	54
COX3	−0.5 (0.18)	−0.6 (0.17)	13
CYTB	−0.8 (0.02)	−0.4 (0.04)	255
ND1	−0.6 (0.15)	−0.5 (0.18)	16
ND2	−0.6 (0.06)	−0.4 (0.06)	77
ND3	−0.4 (0.09)	−0.3 (0.09)	38
ND4	−0.6 (0.11)	−0.6 (0.09)	22
ND4L	−0.6 (0.11)	−0.4 (0.12)	20
ND5	−0.6 (0.17)	−0.7 (0.16)	9
ND6	−0.4 (0.12)	−0.5 (0.11)	25
EEF1A1	NA	NA	NA
H3.2	−1.0 (0.04)	−1.0 (0.03)	11
rbcL	−0.3 (0.70)	−1.0 (0.00)	2

The propensity for positive selection, s, was estimated as $1-(D_n/D_s)/(P_n/P_s)$, where D_n and P_n correspond to the number of synonymous fixed differences and polymorphisms, respectively, and D_s and P_s are the corresponding values for non-synonymous substitutions and polymorphisms. A negative s value indicates that there were fewer non-synonymous substitutions in evolution than expected given the number of non-synonymous polymorphisms. Deleterious polymorphisms with a frequency >5% are expected to be rare, and the presented data therefore suggest a minor role for positive selection in the evolution of these proteins. The reported values represent averages for all species with polymorphism data, with s.e.m. shown in parentheses. Such data were not available (NA) for one gene in our data set.

METHODS SUMMARY

Orthologous sequences for 15 genes from Metazoa and 1 from Viridiplantae were aligned using an adapted version of the T-Coffee multiple-sequence aligner. Each sequence was encoded as a 20^3-vector where each component was the frequency of amino-acid words of size 3. The vectors were clustered in 200 groups using the k-means algorithm. Each resulting group containing fewer than 200 sequences was aligned with the default T-Coffee algorithm, and larger clusters were further divided by reapplying the k-means algorithm. The resulting alignments were treated as profiles and realigned using the multiple-profile alignment procedure supported by the default T-Coffee algorithm. A small subset of sequences, ~14% on average across genes, contributed a substantial fraction of gaps to the alignment and were removed. Amino-acid usage was measured as the number of different amino-acid states across all sites in the final multiple alignment of orthologues. We used pairwise sequence comparisons to estimate dN/dS values across genes with the codeml program in the PAML package for all pairwise comparisons in the data set with $0.05 < dS < 0.5$. We then averaged the dN/dS estimates across all species with $dS < 0.5$ and then averaged the dN/dS values across such clusters.

Full Methods and any associated references are available in the online version of the paper.

Received 6 March; accepted 14 August 2012.
Published online 14 October 2012.

1. McDonald, J. H. & Kreitman, M. Adaptive protein evolution at the Adh locus in *Drosophila*. *Nature* **351,** 652–654 (1991).

2. Andolfatto, P. Adaptive evolution of non-coding DNA in *Drosophila*. *Nature* **437,** 1149–1152 (2005).
3. Charlesworth, J. & Eyre-Walker, A. The rate of adaptive evolution in enteric bacteria. *Mol. Biol. Evol.* **23,** 1348–1356 (2006).
4. Boyko, A. R. *et al.* Assessing the evolutionary impact of amino acid mutations in the human genome. *PLoS Genet.* **4,** e1000083 (2008).
5. Kimura, M. Evolutionary rate at the molecular level. *Nature* **217,** 624–626 (1968).
6. Li, W. H. *Molecular Evolution* 419–429 (Sinauer, 1997).
7. Kimura, M. The role of compensatory neutral mutations in molecular evolution. *J. Genet.* **64,** 7–19 (1985).
8. Weinreich, D. M., Watson, R. A. & Chao, L. Sign epistasis and genetic constraint on evolutionary trajectories. *Evolution* **59,** 1165–1174 (2005).
9. Lehner, B. Molecular mechanisms of epistasis within and between genes. *Trends Genet.* **27,** 323–331 (2011).
10. de Visser, J. A., Cooper, T. F. & Elena, S. F. The causes of epistasis. *Proc. R. Soc. Lond. B* **278,** 3617–3624 (2011).
11. Kondrashov, A. S., Sunyaev, S. & Kondrashov, F. A. Dobzhansky-Muller incompatibilities in protein evolution. *Proc. Natl Acad. Sci. USA* **99,** 14878–14883 (2002).
12. Maynard Smith, J. Natural selection and the concept of a protein space. *Nature* **225,** 563–564 (1970).
13. Fitch, W. M. & Markowitz, E. An improved method for determining codon variability in a gene and its application to the rate of fixation of mutations in evolution. *Biochem. Genet.* **4,** 579–593 (1970).
14. Gillespie, J. H. Natural selection and the molecular clock. *Mol. Biol. Evol.* **3,** 138–155 (1986).
15. Povolotskaya, I. S. & Kondrashov, F. A. Sequence space and the ongoing expansion of the protein universe. *Nature* **465,** 922–926 (2010).
16. Poon, A. F. & Chao, L. Functional origins of fitness effect-sizes of compensatory mutations in the DNA bacteriophage phiX174. *Evolution* **60,** 2032–2043 (2006).
17. Bridgham, J. T., Ortlund, E. A. & Thornton, J. W. An epistatic ratchet constrains the direction of glucocorticoid receptor evolution. *Nature* **461,** 515–519 (2009).
18. Meer, M. V., Kondrashov, A. S., Artzy-Randrup, Y. & Kondrashov, F. A. Compensatory evolution in mitochondrial tRNAs navigates valleys of low fitness. *Nature* **464,** 279–282 (2010).
19. Costanzo, M. S. & Hartl, D. L. The evolutionary landscape of antifolate resistance in Plasmodium falciparum. *J. Genet.* **90,** 187–190 (2011).
20. Salverda, M. L. *et al.* Initial mutations direct alternative pathways of protein evolution. *PLoS Genet.* **7,** e1001321 (2011).
21. Woods, R. J. *et al.* Second-order selection for evolvability in a large *Escherichia coli* population. *Science* **331,** 1433–1436 (2011).
22. Osada, N. & Akashi, H. Mitochondrial-nuclear interactions and accelerated compensatory evolution: evidence from the primate cytochrome C oxidase complex. *Mol. Biol. Evol.* **29,** 337–346 (2012).
23. Kvitek, D. J. & Sherlock, G. Reciprocal sign epistasis between frequently experimentally evolved adaptive mutations causes a rugged fitness landscape. *PLoS Genet.* **7,** e1002056 (2011).
24. Silva, R. F. *et al.* Pervasive sign epistasis between conjugative plasmids and drug-resistance chromosomal mutations. *PLoS Genet.* **7,** e1002181 (2011).
25. Notredame, C., Higgins, D. G. & Heringa, J. T-Coffee: a novel method for fast and accurate multiple sequence alignment. *J. Mol. Biol.* **302,** 205–217 (2000).
26. Lunzer, M., Golding, G. B. & Dean, A. M. Pervasive cryptic epistasis in molecular evolution. *PLoS Genet.* **6,** e1001162 (2010).
27. Costanzo, M. *et al.* The genetic landscape of a cell. *Science* **327,** 425–431 (2010).
28. Tokuriki, N. & Tawfik, D. S. Chaperonin overexpression promotes genetic variation and enzyme evolution. *Nature* **459,** 668–673 (2009).
29. Poelwijk, F. J., de Vos, M. G. & Tans, S. J. Tradeoffs and optimality in the evolution of gene regulation. *Cell* **146,** 462–470 (2011).
30. Burga, A. Olivia Casanueva, M. & Lehner, B. Predicting mutation outcome from early stochastic variation in genetic interaction partners. *Nature* **480,** 250–253 (2011).

Supplementary Information is available in the online version of the paper.

Acknowledgements The work was supported by Plan Nacional grants from the Spanish Ministry of Science and Innovation, to F.A.K. and C.N.. C.K. was supported by the European Union FP7 project Quantomics (KBBE2A222664). F.A.K. is a European Molecular Biology Organization Young Investigator and Howard Hughes Medical Institute International Early Career Scientist. We thank B. Lehner and T. Warnecke for input and a critical reading of the manuscript.

Author Contributions M.S.B., C.K., P.K.V. and F.A.K. participated in obtaining and quality-testing the data; C.K. and C.N. participated in the design of the alignment algorithm; and F.A.K. designed the study and wrote the manuscript with the participation of all authors.

Author Information Reprints and permissions information is available at www.nature.com/reprints. The authors declare no competing financial interests. Readers are welcome to comment on the online version of the paper. Correspondence and requests for materials should be addressed to F.A.K. (fyodor.kondrashov@crg.es).

LETTER

doi:10.1038/nature11429

Phosphorylation of NLRC4 is critical for inflammasome activation

Yan Qu[1]*, Shahram Misaghi[2]*, Anita Izrael-Tomasevic[3], Kim Newton[1], Laurie L. Gilmour[4], Mohamed Lamkanfi[5,6], Salina Louie[2], Nobuhiko Kayagaki[1], Jinfeng Liu[7], László Kömüves[8], James E. Cupp[4], David Arnott[3], Denise Monack[9] & Vishva M. Dixit[1]

NLRC4 is a cytosolic member of the NOD-like receptor family that is expressed in innate immune cells. It senses indirectly bacterial flagellin and type III secretion systems, and responds by assembling an inflammasome complex that promotes caspase-1 activation and pyroptosis[1–6]. Here we use knock-in mice expressing NLRC4 with a carboxy-terminal 3×Flag tag to identify phosphorylation of NLRC4 on a single, evolutionarily conserved residue, Ser 533, following infection of macrophages with *Salmonella enterica* serovar Typhimurium (also known as *Salmonella typhimurium*). Western blotting with a NLRC4 phospho-Ser 533 antibody confirmed that this post-translational modification occurs only in the presence of stimuli known to engage NLRC4 and not the related protein NLRP3 or AIM2. *Nlrc4*$^{-/-}$ macrophages reconstituted with NLRC4 mutant S533A, unlike those reconstituted with wild-type NLRC4, did not activate caspase-1 and pyroptosis in response to *S. typhimurium*, indicating that S533 phosphorylation is critical for NLRC4 inflammasome function. Conversely, phosphomimetic NLRC4 S533D caused rapid macrophage pyroptosis without infection. Biochemical purification of the NLRC4-phosphorylating activity and a screen of kinase inhibitors identified PRKCD (PKCδ) as a candidate NLRC4 kinase. Recombinant PKCδ phosphorylated NLRC4 S533 *in vitro*, immunodepletion of PKCδ from macrophage lysates blocked NLRC4 S533 phosphorylation *in vitro*, and *Prkcd*$^{-/-}$ macrophages exhibited greatly attenuated caspase-1 activation and IL-1β secretion specifically in response to *S. typhimurium*. Phosphorylation-defective NLRC4 S533A failed to recruit procaspase-1 and did not assemble inflammasome specks[7] during *S. typhimurium* infection, so phosphorylation of NLRC4 S533 probably drives conformational changes necessary for NLRC4 inflammasome activity and host innate immunity.

NLRC4 is activated as part of the innate immune response to a range of intracellular bacteria, including *S. typhimurium* and *Legionella pneumophila*[8]. To explore the details of NLRC4 activation, we created *Nlrc4*$^{F/F}$ knock-in mice expressing NLRC4 with a C-terminal 3×Flag tag (Supplementary Fig. 1a, b). The 3×Flag tag did not compromise NLRC4 function because *Nlrc4*$^{F/F}$ bone-marrow-derived macrophages (BMDMs), unlike *Nlrc4*$^{-/-}$ BMDMs, processed caspase-1 and secreted IL-1β like their wild-type counterparts following infection with *S. typhimurium* or transfection with purified *S. typhimurium* flagellin (Supplementary Fig. 1c). *Nlrc4*$^{F/F}$ BMDMs also exhibited normal IL-1β secretion in response to ATP and double-stranded DNA (dsDNA; Supplementary Fig. 1c), stimuli that engage not NLRC4, but NLRP3 and AIM2, respectively[9–12]. Mass spectrometry of NLRC4–3×Flag affinity purified from *Nlrc4*$^{F/F}$ BMDMs identified a single amino acid, Ser 533, as being phosphorylated after infection with *S. typhimurium* (Fig. 1a and Supplementary Fig. 2a). Peptides containing phosphorylated Ser 533 represented nearly a quarter of all Ser 533-containing peptides (Fig. 1b). Located between the NACHT domain and C-terminal leucine rich repeats (LRRs; Fig. 1a), Ser 533 is conserved in mammals (Fig. 1c). Western blotting with a phospho-Ser 533 NLRC4 antibody (Supplementary Fig. 2b) after immunoprecipitation of NLRC4–3×Flag confirmed phosphorylation of Ser 533 in BMDMs infected with *S. typhimurium*. Significantly, Ser 533 phosphorylation coincided with NLRC4-dependent processing of caspase-1 and IL-1β (Fig. 1d).

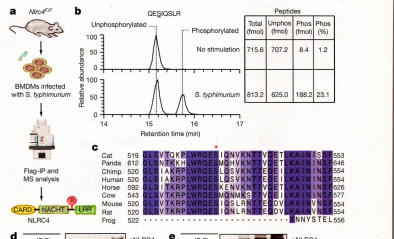

Figure 1 | NLRC4 Ser 533 is phosphorylated in response to *S. typhimurium*. **a**, Mass spectrometry (MS) of NLRC4–3×Flag from BMDMs infected with *S. typhimurium* identified phosphorylation at Ser 533. **b**, Quantification of NLRC4 phosphopeptide QEpSIQSLR and its unphosphorylated counterpart. **c**, Alignment of NLRC4 orthologues. The depth of purple shading indicates the degree of residue conservation. Asterisk, mouse Ser 533. **d**–**f**, Western blot (WB) analysis of *Nlrc4*$^{F/F}$ BMDMs and their culture medium after infection with *S. typhimurium* (**d**), *L. pneumophila* (**e**) or transfection with flagellin (**f**). NLRC4–3×Flag was immunoprecipitated (IP) before western blot. Data are representative of three independent experiments.

[1]Department of Physiological Chemistry, Genentech Inc., 1 DNA Way, South San Francisco, California 94080, USA. [2]Department of Early Stage Cell Culture, Genentech Inc., 1 DNA Way, South San Francisco, California 94080, USA. [3]Department of Protein Chemistry, Genentech Inc., 1 DNA Way, South San Francisco, California 94080, USA. [4]Department of Immunology, Genentech Inc., 1 DNA Way, South San Francisco, California 94080, USA. [5]Department of Medical Protein Research, VIB, B-9000 Ghent, Belgium. [6]Department of Biochemistry, Ghent University, B-9000 Ghent, Belgium. [7]Department of Bioinformatics and Computational BiologyGenentech Inc., 1 DNA Way, South San Francisco, California 94080, USA. [8]Department of Pathology, Genentech Inc., 1 DNA Way, South San Francisco, California 94080, USA. [9]Department of Microbiology and Immunology, Stanford School of Medicine, California 94305, USA.
*These authors contributed equally to this work.

Next we determined whether BMDMs phosphorylated NLRC4 Ser 533 in response to other NLRC4-activating stimuli. *L. pneumophila* infection (Fig. 1e) and transfection with purified *S. typhimurium* flagellin (Fig. 1f) both triggered NLRC4 Ser 533 phosphorylation that coincided with caspase-1 processing. In contrast, robust Ser 533 phosphorylation was not detected in LPS-primed BMDMs treated with ATP, nigericin or dsDNA (Fig. 2a), indicating that NLRC4 Ser 533 phosphorylation is specific to NLRC4-activating stimuli and not a general consequence of caspase-1 activation. In keeping with the latter notion, caspase-1 inhibitor Ac-YVAD-fmk decreased self-processing of caspase-1 in BMDMs infected with *S. typhimurium*, but did not reduce NLRC4 Ser 533 phosphorylation (Fig. 2b). To delineate whether flagellin is essential for NLRC4 Ser 533 phosphorylation after *S. typhimurium* infection, we infected BMDMs with *S. typhimurium* Δ*flgB*, which lacks flagellin, but has an intact type III secretion system (T3SS)[4]. Whereas BMDMs infected with the Δ*flgB* mutant yielded less NLRC4 phospho-Ser 533 than cells infected with wild-type bacteria (SL1344 or 12023), no NLRC4 phospho-Ser 533 was detected when BMDMs were infected with a Δ*prgJ* mutant, which lacks essential components of the SPI1 T3SS, or a Δ*sipB* mutant, which lacks the virulence factor known to induce apoptosis and caspase-1 activation[4,13] (Fig. 2c). These data indicate that phosphorylation of NLRC4 Ser 533 probably reflects both flagellin and T3SS recognition.

We investigated whether NLRC4 Ser 533 phosphorylation is required for inflammasome function by reconstituting immortalized macrophage progenitors[14] from *Nlrc4*$^{-/-}$ mice with wild-type NLRC4 or NLRC4 mutant S533A. Independent clonal progenitor populations were established that expressed comparable amounts of NLRC4 after differentiation into macrophages (Supplementary Fig. 3a). *Nlrc4*$^{-/-}$ cells reconstituted with wild-type NLRC4 processed caspase-1 (Fig. 2d), secreted IL-1β (Fig. 2e) and underwent pyroptosis (Fig. 2f) upon infection with *S. typhimurium*. In contrast, *Nlrc4*$^{-/-}$ cells reconstituted with NLRC4 S533A behaved like *Nlrc4*$^{-/-}$ cells, neither cleaving caspase-1 nor secreting IL-1β, and demonstrating improved cell viability (Fig. 2d–f). Similar results were obtained when the reconstituted macrophages were infected with *L. pneumophila* (Fig. 2d). Importantly, the NLRC4 S533A macrophages resembled wild-type NLRC4 reconstituted macrophages in their ability to secrete IL-6 after *S. typhimurium* infection (Supplementary Fig. 3b), and IL-1β when treated with lipopolysaccharide (LPS)/ATP or LPS/dsDNA (Fig. 2e), indicating that they have a specific defect in NLRC4-dependent caspase-1 activation.

Inflammasome components tend to aggregate and kill cells when overexpressed[15] so another assay for inflammasome function is whether reconstituted inflammasome components can be expressed stably. The retroviral vector used to reconstitute NLRC4 expression in *Nlrc4*$^{-/-}$ immortalized progenitors also expressed green fluorescent protein (GFP), which allowed us to monitor the frequency of transduced cells. GFP^{+} progenitor cells transduced with empty vector, wild-type NLRC4, NLRC4 S533A or phosphomimetic mutant NLRC4 S533D accounted for 82–93% of live cells at 3 days after infection (Supplementary Table 1). GFP^{+} cells were sorted, grown for a further 15 days, and then subjected to single-cell sorting. At this later time, GFP^{+} cells reconstituted with wild-type NLRC4 represented <10% of live cells in the culture, whereas 38% of cells in cultures receiving NLRC4 S533A virus remained GFP^{+}. These results imply that NLRC4 S533A is less deleterious to macrophage progenitors than wild-type NLRC4, which is consistent with phosphorylation of Ser 533

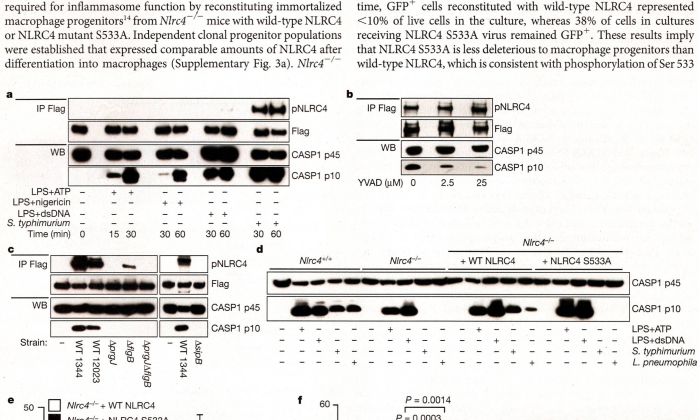

Figure 2 | NLRC4 Ser 533 phosphorylation is essential for NLRC4-dependent caspase-1 processing. **a**–**c**, *Nlrc4*^{FLAG} BMDMs infected with *S. typhimurium* SL1344 for 4 h, except where indicated (**a**, **c**). **b**, YVAD-fmk was added 30 min before infection. **d**–**f**, *Nlrc4*$^{-/-}$ progenitors were immortalized with ER-Hoxb8 and reconstituted with wild-type or S533A NLRC4. Clonal populations were differentiated into macrophages for bacterial infection for 4 h, or treatment with LPS/ATP or LPS/transfected dsDNA for 30 min. **e**, **f**, IL-1β (**e**) or LDH (**f**) release is the mean ± s.d. of three independent experiments. *P* values determined by two-tailed *t*-test. All immunoblots show cells plus their culture medium.

being important for inflammasome function. Further supporting this notion, cells transduced with phosphomimetic mutant NRLC4 S533D comprised <1% GFP^+ cells after 15 days and we were unsuccessful at isolating a stable, clonal progenitor line. In sum, our data indicate that phosphorylation of NLRC4 on Ser 533 is critical for NLRC4 inflammasome activation.

We sought the kinase responsible for phosphorylating NLRC4 Ser 533 in fractionated *Nlrc4*$^{+/+}$ BMDM cytosolic extracts (Supplementary Fig. 4a). Fractions that phosphorylated Ser 533 of NLRC4–3×Flag *in vitro* were fractionated further and then analysed by mass spectrometry (Supplementary Fig. 4b). PKCδ and PAK2 were identified as candidate NLRC4 kinases (Supplementary Table 2), but only immunodepletion of PKCδ from *Nlrc4*$^{+/+}$ BMDM lysates reduced phosphorylation of NLRC4–3×Flag Ser 533 *in vitro* (Fig. 3a, b). In addition, recombinant PKCδ phosphorylated NLRC4 Ser 533 *in vitro* (Fig. 3c). Consistent with, but not proving NLRC4 S533 phosphorylation by PKCδ, the non-selective PKC inhibitors staurosporine[16] and K-252a[17] reduced S533 phosphorylation in *Nlrc4*$^{F/F}$ BMDMs infected with *S. typhimurium* (Fig. 3d). Also implicating PKCδ involvement, phosphorylation of PKCδ Tyr 311, which is a modification induced by PMA and certain other stimuli[18], increased in BMDMs infected with *S. typhimurium* (Supplementary Fig. 4c).

Initially we explored whether PKCδ activity is important for inflammasome activation using rottlerin, which often is used as a PKC inhibitor but can also have other activities[19]. Rottlerin blocked NLRC4 S533 phosphorylation, caspase-1 and IL-1β processing, and pyroptosis in BMDMs infected with *S. typhimurium*, and this did not seem to be due to impaired uptake of the bacteria (Supplementary Fig. 5a–c). Experiments with *Prkcd*$^{-/-}$ macrophages lacking PKCδ, however, provided more compelling evidence of a role for PKCδ in activation of the NLRC4 inflammasome. Specifically, *Prkcd*$^{-/-}$ BMDMs showed markedly less caspase-1 activation and IL-β processing than *Prkcd*$^{+/+}$ BMDMs after infection with *S. typhimurium* (Fig. 3e). This defect in caspase-1 activation and IL-1β release was not observed when the *Prkcd*$^{-/-}$ BMDMs were stimulated with ATP or dsDNA (Fig. 3f), consistent with a specific requirement for PKCδ in NLRC4-dependent caspase-1 activation. The caspase-1 and IL-1β processing that does occur in *Prkcd*$^{-/-}$ cells infected with *S. typhimurium* suggests the existence of a compensatory mechanism of NLRC4 activation, albeit a less efficient one. This residual inflammasome activity probably explains why *S. typhimurium*-induced pyroptosis is not reduced significantly in *Prkcd*$^{-/-}$ BMDMs (Supplementary Fig. 6c).

We have shown previously by immunofluorescence microscopy that endogenous apoptosis-associated speck-like protein containing a caspase recruitment domain (ASC) forms a single focus in primary BMDMs infected with *S. typhimurium*[7]. This focus co-localizes with active caspase-1 and its formation correlates with IL-1β processing and release. We obtained similar results with macrophages differentiated from *Nlrc4*$^{+/+}$ immortalized macrophage progenitors or *Nlrc4*$^{-/-}$ cells reconstituted with wild-type NLRC4 (Fig. 4a, b). Approximately 30% of infected cells displayed a bright ASC focus that co-stained for the processed caspase-1 p10 subunit at 3 h after infection. In contrast, both *Nlrc4*$^{-/-}$ macrophages and *Nlrc4*$^{-/-}$ cells reconstituted with NLRC4 S533A did not form foci containing ASC and caspase-1 (Fig. 4a, b). These data are consistent with NLRC4 Ser 533 phosphorylation being essential for procaspase-1 recruitment to the NLRC4 inflammasome complex. Consistent with PKCδ contributing to NLRC4 inflammasome activation, fewer *Prkcd*$^{-/-}$ BMDMs contained an ASC focus when compared to wild-type BMDMs (Supplementary Fig. 6a, b), despite equivalent uptake of the bacteria (Supplementary Fig. 6d).

Next we examined NLRC4 protein interactions by immunoprecipitating wild-type NLRC4 or NLRC4 S533A from macrophages before and after *S. typhimurium* infection (Fig. 4c). *Nlrc4*$^{F/F}$ BMDMs were grown in the presence of the pan-caspase inhibitor zVAD-fmk to limit cell death, and then a reversible cross-linker was used to stabilize protein complexes for immunoprecipitation. These conditions were essential to detect the association of endogenous NLRC4–3×Flag with endogenous ASC and pro-caspase-1 at 2 and 3 h after infection. Neither interaction was detected in uninfected BMDMs, consistent with *S. typhimurium* inducing NLRC4 inflammasome assembly. Remarkably, PKCδ also co-precipitated with NLRC4–3×Flag from infected cells, but not uninfected cells, providing further biochemical evidence of its participation in the NLRC4 inflammasome. We did not culture reconstituted *Nlrc4*$^{-/-}$ macrophages expressing NLRC4 S533A in zVAD-fmk because the cells are resistant to *S. typhimurium*-induced pyroptosis (Fig. 2f). Unfortunately, *Nlrc4*$^{-/-}$ macrophages reconstituted with wild-type NLRC4 did not tolerate culture in zVAD-fmk and could not be analysed in parallel. Given that anti-Flag antibodies detect NLRC4–3×Flag more readily than S533A NLRC4–1×Flag, we used a lot more of the immunoprecipitated NLRC4 S533A in western blots to favour complex detection. Despite this bias, we failed to detect any interaction of NLRC4 S533A with pro-caspase-1, ASC or PKCδ after *S. typhimurium* infection (Fig. 4c). These data indicate that phosphorylation of NLRC4 S533 is critical for inflammasome assembly.

It has been shown that specific NLR family, apoptosis inhibitory proteins (NAIPs) engage NLRC4 after interacting directly with flagellin or T3SS components such as PrgJ[5,6]. Our data indicate that phosphorylation of NLRC4 Ser 533 by kinases such as PKCδ represents another important step in the formation of a fully functional inflammasome (Fig. 4d). It will be interesting to learn whether phosphorylation regulates the related NLRP3 inflammasome, which is mutated in chronic inflammatory autoimmune syndrome[20].

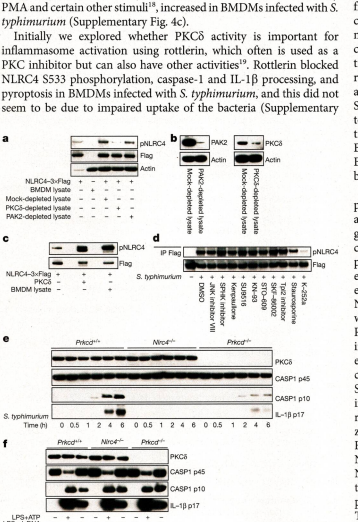

Figure 3 | PKCδ phosphorylates NLRC4 Ser 533 after *S. typhimurium* infection. **a**–**c**, *In vitro* kinase assays using NLRC4–3×Flag from *Nlrc4*$^{F/F}$ BMDMs and *Nlrc4*$^{+/+}$ BMDM lysates (**a**) or recombinant PKCδ (**c**). Western blots (**b**) indicate PKCδ or PAK2 immunodepletion in **a**. **d**, NLRC4 Ser 533 phosphorylation (pNLRC4) after *Nlrc4*$^{F/F}$ BMDMs were cultured with 5 μM inhibitor or dimethylsulphoxide (DMSO) vehicle for 30 min before and during *S. typhimurium* infection for 3 h. **e**, **f**, BMDMs infected with *S. typhimurium* (multiplicity of infection 5) (**e**), or primed with LPS and then treated with ATP or transfected dsDNA for 30 min (**f**). Cells plus medium were immunoblotted.

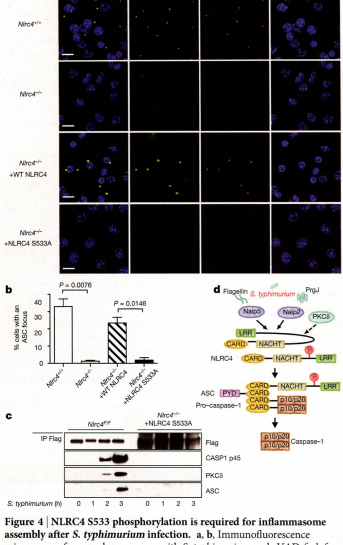

Figure 4 | NLRC4 S533 phosphorylation is required for inflammasome assembly after *S. typhimurium* infection. **a**, **b**, Immunofluorescence microscopy of macrophages grown with *S. typhimurium* and zVAD-fmk for 3 h. Bars, 10 μm (**a**). The percentage of cells containing an ASC focus ± s.d. was determined from three independent experiments (**b**). *P* values determined by two-tailed *t*-test. **c**, $Nlrc4^{F/F}$ BMDMs and $Nlrc4^{-/-}$ NLRC4 S533A reconstituted macrophages were infected with *S. typhimurium* and NLRC4 immunoprecipitated after cross-linking. **d**, Model for NLRC4 activation. NAIPs recognizing specific bacterial ligands and phosphorylation of NLRC4 Ser 533 between the NACHT and LRR motifs together promote NLRC4 inflammasome activation.

METHODS SUMMARY

Mice. $Nlrc4^{F/F}$ mice were generated from C57BL/6 ES cells containing a 3×Flag sequence knocked into exon 9 of *Nlrc4* ahead of its translation termination codon (Supplementary Fig. 1a). Gene Bridges engineered the targeting construct. The Genentech Institutional Animal Care and Use Committee approved all mouse protocols.

Mass spectrometry. $Nlrc4^{F/F}$ BMDMs were infected with *S. typhimurium* for 4 h. Immunoprecipitations with anti-Flag agarose were performed on BMDM lysate and culture medium. Proteins eluted with 3×Flag peptide were resolved by SDS–PAGE, and bands corresponding to NLRC4 were excised, reduced, alkylated and digested *in situ* with trypsin or chymotrypsin as described previously[21]. Extracted peptides were analysed by ultra high-pressure, reverse-phase chromatography (nanoAcquity; Waters Corp.) electrospray ionization tandem mass spectrometry (LTQ-Orbitrap; ThermoFisher Scientific) in a 'top-8' data-dependent experiment[22]. Tandem mass spectra were searched against a database of mouse proteins using the Mascot program (Matrix Science Ltd). Hits were filtered to a false discovery rate of <1% and spectra of putative phosphopeptides validated by inspection. Phosphopeptide QEpSIQSLR and its unphosphorylated counterpart were quantified by isotope dilution using stable-isotope-labelled synthetic peptides (Cell Signaling Technology) spiked into tryptic digests of NLRC4–3×Flag and analysed by LC-orbitrap mass spectrometry.

Crosslinking. BMDMs were cultured with 30 μM zVAD-fmk for 30 min and then infected with *S. typhimurium* in the continued presence of 30 μM zVAD-fmk. A cleavable imidoester crosslinker DTBP (dimethyl 3,3′-dithiobispropionimidate-2 HCl) was added to cultures 30 min before cell lysis. Cell extracts were obtained by addition of 100 mM Tris pH 8.0 and 1% Triton X-100. NLRC4 was immunoprecipitated with anti-Flag agarose overnight.

Full Methods and any associated references are available in the online version of the paper.

Received 30 January; accepted 24 July 2012.
Published online 12 August 2012.

1. Mariathasan, S. *et al.* Differential activation of the inflammasome by caspase-1 adaptors ASC and Ipaf. *Nature* **430,** 213–218 (2004).
2. Miao, E. A. *et al.* Cytoplasmic flagellin activates caspase-1 and secretion of interleukin 1β via Ipaf. *Nature Immunol.* **7,** 569–575 (2006).
3. Franchi, L. *et al.* Cytosolic flagellin requires Ipaf for activation of caspase-1 and interleukin 1β in *Salmonella*-infected macrophages. *Nature Immunol.* **7,** 576–582 (2006).
4. Miao, E. A. *et al.* Innate immune detection of the type III secretion apparatus through the NLRC4 inflammasome. *Proc. Natl Acad. Sci. USA* **107,** 3076–3080 (2010).
5. Kofoed, E. M. & Vance, R. E. Innate immune recognition of bacterial ligands by NAIPs determines inflammasome specificity. *Nature* **477,** 592–595 (2011).
6. Zhao, Y. *et al.* The NLRC4 inflammasome receptors for bacterial flagellin and type III secretion apparatus. *Nature* **477,** 596–600 (2011).
7. Broz, P. *et al.* Redundant roles for inflammasomes receptors NLRP3 and NLRC4 in host defense against *Salmonella*. *J. Exp. Med.* **207,** 1745–1755 (2010).
8. Amer, A. *et al.* Regulation of *Legionella* phagosome maturation and infection through flagellin and host Ipaf. *J. Biol. Chem.* **281,** 35217–35223 (2006).
9. Mariathasan, S. *et al.* Cryopyrin activates the inflammasome in response to toxins and ATP. *Nature* **440,** 228–232 (2006).
10. Rathinam, V. A. *et al.* The AIM2 inflammasome is essential for host defense against cytosolic bacteria and DNA viruses. *Nature Immunol.* **11,** 395–402 (2010).
11. Fernandes-Alnemri, T. *et al.* The AIM2 inflammasome is critical for innate immunity to *Francisella tularensis*. *Nature Immunol.* **11,** 385–393 (2010).
12. Jones, J. W. *et al.* Absent in melanoma 2 is required for innate immune recognition of *Francisella tularensis*. *Proc. Natl Acad. Sci. USA* **107,** 9771–9776 (2010).
13. Hersh, D. *et al.* The *Salmonella* invasin SipB induces macrophage apoptosis by binding to caspase-1. *Proc. Natl Acad. Sci. USA* **96,** 2396–2401 (1999).
14. Wang, G. G. *et al.* Quantitative production of macrophages or neutrophils *ex vivo* using conditional Hoxb8. *Nature Methods* **3,** 287–293 (2006).
15. Poyet, J. L. *et al.* Identification of Ipaf, a human caspase-1-activating protein related to Apaf-1. *J. Biol. Chem.* **276,** 28309–28313 (2001).
16. Wolf, M. & Baggiolini, M. The protein kinase inhibitor staurosporine, like phorbol esters, induces the association of protein kinase C with membranes. *Biochem. Biophys. Res. Commun.* **154,** 1273–1279 (1988).
17. Mizuno, K., Saido, T. C., Ohno, S., Tamaoki, T. & Suzuki, K. Staurosporine-related compounds, K252a and UCN-01, inhibit both cPKC and nPKC. *FEBS Lett.* **330,** 114–116 (1993).
18. Steinberg, S. F. Structural basis of protein kinase C isoform function. *Physiol. Rev.* **88,** 1341–1378 (2008).
19. Soltoff, S. P. Rottlerin: an inappropriate and ineffective inhibitor of PKCδ. *Trends Pharmacol. Sci.* **28,** 453–458 (2007).
20. Agostini, L. *et al.* NALP3 forms an IL-1β-processing inflammasome with increased activity in Muckle-Wells autoinflammatory disorder. *Immunity* **20,** 319–325 (2004).
21. Vendel, A. C. *et al.* B and T lymphocyte attenuator regulates B cell receptor signaling by targeting Syk and BLNK. *J. Immunol.* **182,** 1509–1517 (2009).
22. Castellana, N. E. *et al.* Resurrection of a clinical antibody: template proteogenomic de novo proteomic sequencing and reverse engineering of an anti-lymphotoxin-α antibody. *Proteomics* **11,** 395–405 (2011).

Supplementary Information is available in the online version of the paper.

Acknowledgements We thank P. Broz, A. Paler Martinez, M. Roose-Girma, X. Rairdan, C. Kung, V. Asghari and S. Mukund for technical support, and K. O'Rourke for editorial assistance.

Author Contributions Y.Q., S.M., A.J.-T., D.A., L.L.G., J.E.C., L.K. and S.L. designed and conducted experiments; K.N. generated the $Nlrc4^{F/F}$ mice; J.L. performed bioinformatics analyses; M.L., N.K. and D.M. discussed the study; Y.Q., K.N. and V.M.D. wrote the manuscript.

Author Information Reprints and permissions information is available at www.nature.com/reprints. The authors declare competing financial interests: details are available in the online version of the paper. Readers are welcome to comment on the online version of the paper. Correspondence and requests for materials should be addressed to V.M.D. (dixit@gene.com).

LETTER

doi:10.1038/nature11530

BATF–JUN is critical for IRF4–mediated transcription in T cells

Peng Li[1]*, Rosanne Spolski[1]*, Wei Liao[1], Lu Wang[1], Theresa L. Murphy[2], Kenneth M. Murphy[2,3] & Warren J. Leonard[1]

Interferon regulatory factor 4 (IRF4) is an IRF family transcription factor with critical roles in lymphoid development and in regulating the immune response[1,2]. IRF4 binds DNA weakly owing to a carboxy-terminal auto-inhibitory domain, but cooperative binding with factors such as PU.1 or SPIB in B cells increases binding affinity[3], allowing IRF4 to regulate genes containing ETS–IRF composite elements (EICEs; 5′-GGAAnnGAAA-3′)[1]. Here we show that in mouse CD4$^+$ T cells, where PU.1/SPIB expression is low, and in B cells, where PU.1 is well expressed, IRF4 unexpectedly can cooperate with activator protein-1 (AP1) complexes to bind to AP1–IRF4 composite (5′-TGAnTCA/GAAA-3′) motifs that we denote as AP1–IRF composite elements (AICEs). Moreover, BATF–JUN family protein complexes cooperate with IRF4 in binding to AICEs in pre-activated CD4$^+$ T cells stimulated with IL-21 and in T$_H$17 differentiated cells. Importantly, BATF binding was diminished in *Irf4*$^{-/-}$ T cells and IRF4 binding was diminished in *Batf*$^{-/-}$ T cells, consistent with functional cooperation between these factors. Moreover, we show that AP1 and IRF complexes cooperatively promote transcription of the *Il10* gene, which is expressed in T$_H$17 cells and potently regulated by IL-21. These findings reveal that IRF4 can signal via complexes containing ETS or AP1 motifs depending on the cellular context, thus indicating new approaches for modulating IRF4-dependent transcription.

There are nine mammalian interferon regulatory factor (IRF) family members, IRF1 to IRF9[1], that collectively have broad actions within and beyond the immune system[2]. IRFs were identified on the basis of their induction by type I interferons (IFN-α/β), and some IRFs are induced by Toll-like receptors and other pattern-recognition receptors[1,2]. IRF4 expression is restricted to the immune system and is induced in T cells by T-cell receptor stimulation[4,5]. IRFs contain an amino-terminal DNA-binding domain that recognizes 5′-GAAAnnGAAA-3′ motifs, but IRF4 only weakly binds DNA due to its carboxy-terminal auto-inhibitory domain[3]. In B cells, PU.1 or the related factor SPIB relieves auto-inhibition to increase binding affinity, allowing IRF4 to regulate genes expressing composite 5′-GGAAnnGAAA-3′ ETS–IRF consensus motif elements (EICEs)[3,6], including κ and λ immunoglobulin light chain genes. Whereas PU.1 binds directly to EICEs, efficient IRF4 binding requires phosphorylated, DNA-bound PU.1[1,2]. IRF4 also acts in T cells[7], contributing to development of multiple T$_H$ cell subsets[2], with defective T$_H$1[8], T$_H$2[8–11], T$_H$9[12] and T$_H$17[13] differentiation in its absence. Using genome-wide chromatin immunoprecipitation coupled to DNA sequencing (ChIP-Seq), we previously demonstrated that IRF4 cooperates with STAT3 to control IL-21-induced *Prdm1* expression and that these factors globally regulate IL-21-mediated gene expression[14]. Moreover, we found that IRF4 expression is required for normal STAT3 binding *in vivo* and for development of an additional T-cell effector population, namely Tfh cells[14].

As anticipated, analysis of IRF4 ChIP-Seq peaks from B cell libraries we previously generated[14] identified EICEs as the top motif (Fig. 1a, b). In contrast, EICEs were not readily identified in IRF4 ChIP-Seq libraries from activated T cells (Fig. 1c, d) or T$_H$17 cells (Fig. 1e), consistent with T cells expressing much less PU.1 than B cells (Fig. 1f and Supplementary Fig. 1). Instead, examination of the top 1,000 peaks (sorted by *P* values) from libraries from pre-activated T cells, unstimulated or stimulated with IL-21, or from T$_H$17 cells, unexpectedly revealed that the top IRF4 ChIP-Seq motifs were activator protein-1 (AP1) 5′-TGA[G/C]TCA-3′ motifs (Fig. 1c–e). IRF8, which like IRF4 also interacts with PU.1[6], bound to some

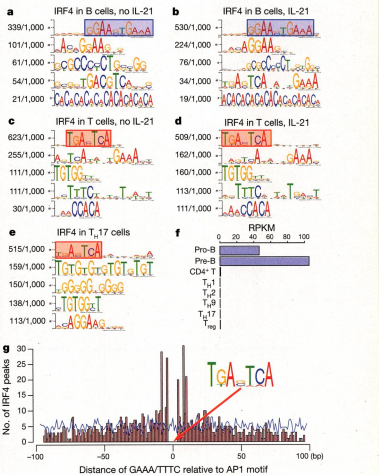

Figure 1 | Preferential IRF4 binding to AP1 motifs in T cells. a–e, IRF4 motifs in B cells not stimulated (**a**) or stimulated (**b**) with IL-21, in pre-activated T cells not stimulated (**c**) or stimulated (**d**) with IL-21 for 1 h, or in T$_H$17 cells (**e**). **f**, *Sfpi1*/PU.1 mRNA expression in the indicated populations based on RNA-Seq. **g**, 5′-TTTC/GAAA-3′ motif distribution relative to the 5′-TGAnTCA-3′ AP1 motif in 1000 sequences with strong IRF4 binding, and the number of IRF4 ChIP-Seq peaks at each spacing. The blue line shows the 5′-TTTC/GAAA-3′ distribution in 1000 random sequences; motif frequency was approximately 0.5%.

[1]Laboratory of Molecular Immunology and Immunology Center, National Heart, Lung, and Blood Institute, National Institutes of Health, Bethesda, Maryland 20892-1674, USA. [2]Department of Pathology and Immunology, Washington University School of Medicine, St Louis, Missouri 63110, USA. [3]Howard Hughes Medical Institute, Washington University School of Medicine, St Louis, Missouri 63110, USA. *These authors contributed equally to this work.

AP1-containing sites but dominantly bound to canonical IRF motifs with tandem GAAA motifs (5′-GAAA[C/G][T/A]GAAA[G/C]-3′) (Supplementary Fig. 2a, b). To elucidate the IRF4–AP1 interaction, we examined whether IRF4 GAAA/TTTC core motifs were associated with AP1 sites, and within IRF4 ChIP-Seq peaks, we found enrichment of these motifs adjacent to or five base pairs away (four intervening base pairs) from AP1 sites (Fig. 1g and Supplementary Fig. 3), in contrast to their overall random distribution (Fig. 1g, blue line), indicating binding cooperativity for AP1 and IRF4. We denote these AP1–IRF4 composite elements as AICEs.

Of 14,838 IRF4 ChIP-Seq peaks, 5,304 bound within genes annotated by RefSeq (Fig. 2a), and analysis of our published Affymetrix array data sets[14] revealed that 2,356 of these genes were regulated by IL-21 at 1, 6 or 24 h (Fig. 2b). RNA-Seq analysis revealed markedly lower expression of some of these genes, including *Prdm1* and *Il10*, in IL-21-stimulated *Irf4*$^{-/-}$ than in wild-type T cells (Fig. 2c), underscoring the importance of IRF4 for their expression. To characterize the IRF4-binding complex in T cells, we analysed ChIP-Seq libraries from T_H17-differentiated cells and IL-21-stimulated pre-activated T cells, focusing on JUN family proteins and BATF, which can heterodimerize with JUN proteins to bind to AP1 motifs and is critical for T_H17 differentiation[15–17], a process promoted by IL-21[18–20]. In T_H17 cells, approximately 54% (11,693 out of 21,775) of the IRF4 binding sites overlapped with BATF binding sites, and approximately 65% of the BATF sites overlapped with IRF4, indicating substantial co-localization of these factors (Fig. 2d). As expected, the dominant binding motif for BATF was an AP1 motif (5′-TGA[G/C]TCA-3′) (Supplementary Fig. 4), and IRF4, BATF and JUN family proteins co-localized by ChIP-Seq (Fig. 2d and Supplementary Fig. 5a, b). The specificity of these data was indicated by essentially absent ChIP-Seq peaks in the IgG control as well as with anti-IRF4 in *Irf4*$^{-/-}$ cells or anti-BATF in *Batf*$^{-/-}$ cells (Fig. 2e). ChIP-Seq peaks for STAT3 also globally co-localized with IRF4 (Supplementary Fig. 5c), including at the *Prdm1* region previously studied[14] and in the *Il21* promoter and *Il17a* 3′ region (Fig. 2e). Interestingly, approximately 50% of genes (1,167 out of 2,356) with co-localization of these transcription factors in T_H17 cells were also induced by IL-21 in activated CD4$^+$ T cells. STAT3 binds to GAS motifs rather than AP1 motifs, but its co-localization at AP1 motifs might be explained by the ability of STAT3 to physically associate with JUN[21].

To investigate potential cooperative binding between IRF4 and AP1 complexes, we identified strong IRF4 binding sites containing a 5′-GAAA-3′ motif adjacent to or 5 bp away from the AP1 motif (a preferred spacing in Fig. 1g; Supplementary Table 1 lists genes with these sites). We selected sites in the *Il10*, *Ikzf2* (which encodes Helios) and *Ctla4* genes and confirmed co-localization of IRF4, STAT3, BATF and JUN by ChIP-Seq (Fig. 2f). The *Il10* gene, which is expressed in IL-21-stimulated CD4$^+$ T cells, CD8$^+$ T cells and polarized T_H17 cells[22,23], contained two IRF4 binding sites with associated AP1 motifs (Fig. 2f). We performed electrophoretic mobility shift assays (EMSAs) with T_H17 nuclear extracts and a probe corresponding to the conserved noncoding sequence, CNS9, located approximately 9.1 kilobases 5′ of the *Il10* transcription start site (Fig. 3a, *Il10* peak 1), which is known to be an *Il10* regulatory element[24]. A strong complex formed, but it was

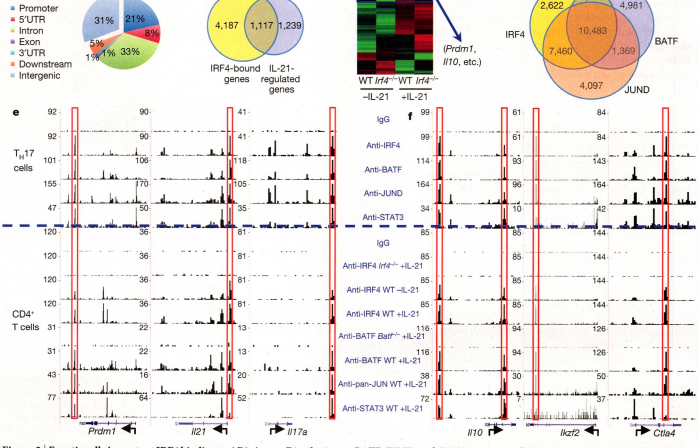

Figure 2 | Functionally important IRF4 binding to AP1 sites. a, Distribution of IRF4 ChIP-Seq peaks. UTR, untranslated region. **b**, Venn diagram of genes bound by IRF4 and regulated by IL-21. **c**, Heat map of 130 genes regulated in pre-activated CD4$^+$ T cells after 1 h stimulation with IL-21. WT, wild type. **d**, IRF4, BATF, and JUND binding in T_H17 cells. **e**, **f**, ChIP-Seq data for IRF4, BATF, JUND, and STAT3 in T_H17 cells (upper 5 rows) or IRF4, BATF, pan-JUN, and STAT3 in CD4$^+$ T cells (lower 6 rows) treated with IL-21, in *Prdm1*, *Il21*, and *Il17a* (**e**) or *Il10*, *Ikzf2*, and *Ctla4* (**f**) genes. RPKM, reads per kilobase per million reads. Gene orientations are indicated.

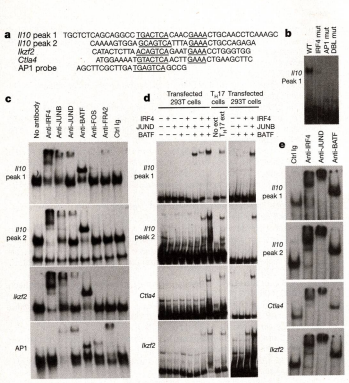

Figure 3 | Cooperative IRF4/BATF/JUN binding. a, Probes for IRF4 ChIP-Seq peaks in *Il10*, *Ikzf2*, and *Ctla4*, and an AP1 probe; AP1–IRF motifs are underlined. The AP1 probe is from ref. 15. **b**, EMSA with *Il10* peak1 probe (WT or IRF, AP1, or IRF4/AP1 double mutants) and T_H17 nuclear extracts. **c**, EMSAs using *Il10* peak1, *Il10* peak2, *Ikzf2*, or AP1 probes and T_H17 nuclear extracts; supershifting was performed as indicated. Ctrl Ig, control immunoglobulin. **d**, EMSAs using nuclear extracts from 293T cells transfected with indicated cDNAs; T_H17 extract vs. no extract are also shown (10^{th} vs. 9^{th} lane). **e**, EMSAs with nuclear extracts from 293T cells transfected with IRF4, JUND, and BATF; supershifting was with anti-IRF4, anti-JUND, or anti-BATF. EMSA were performed at least 3 times.

reduced when the 5′-GAAA-3′ motif was mutated and abolished when the AP1 motif was mutated (Fig. 3b). Supershifting with antibodies revealed that IRF4, JUNB, JUND and BATF were components of the complex (Fig. 3c); these factors also bound to *Il10* peak 2 and *Ikzf2* probes (Fig. 3c). As expected, no shift was seen when nuclear extracts were omitted (Supplementary Fig. 6). Antibodies to FOS and FRA2 had a minor effect on the *Il10* peak 1 and no effect on the *Il10* peak 2 and *Ikzf2* complexes (Fig. 3c). In contrast, an AP1 consensus probe complex was not supershifted by anti-IRF4 but was supershifted by antibodies against BATF, FOS and FRA2 (Fig. 3c). We next studied binding to the *Il10* peak 1 IRF4 motif in B cells, T_H2 cells and T_H9 cells, which all express *Il10*. B-cell nuclear extracts formed a complex supershifted by antibodies against IRF4, BATF and JUNB, but not PU.1 (Supplementary Fig. 7a), even though anti-PU.1 antibody supershifted a complex formed with an EICE probe from the immunoglobulin λ light chain enhancer (Supplementary Fig. 7b). Thus, EICEs were the most common IRF4-containing complexes in B cells (Fig. 1 a, b), but IRF4/AP1 AICEs also formed in these cells (Fig. 1b). Although T_H2 and T_H9 polarized cells were reported to express PU.1 protein[25,26], RNA-Seq analysis showed little PU.1 messenger RNA in these cells (Fig. 1f), and EMSAs showed IRF4–BATF–JUNB interactions but no PU.1-binding activity (Supplementary Fig. 7c). To determine whether IRF4 and BATF–JUN proteins cooperatively bound to DNA, we used nuclear extracts from 293T cells transfected with various combinations of IRF4, BATF and JUNB or JUND and performed EMSAs with *Il10*, *Ctla4* and *Ikzf2* probes. Little if any binding activity was observed with extracts from 293T cells expressing IRF4, JUND or BATF alone, certain pairwise combinations showed some binding, but strong binding was seen with extracts containing all three proteins, indicating cooperative binding to these sites (Fig. 3d, left); this was also observed when JUNB was substituted for JUND (Fig. 3d, right). Cooperative binding was indicated by slower mobility, particularly of the *Il10* peak 1 probe (Fig. 3d). Although mobility changes for other probes were less evident, even on 4% or 7% gels (not shown), supershifting experiments confirmed that IRF4, JUND and BATF were present in complexes formed with each probe (Fig. 3e).

To examine the functional significance of the *Il10* IRF4 motif, we first analysed *Il10* mRNA expression in *Irf4*$^{-/-}$ T cells and found much lower *Il10* mRNA in response to IL-21, anti-CD3 + anti-CD28, or IL-21 + anti-CD3 + anti-CD28 than was observed in wild-type cells ($P < 0.02$ at both time points; Fig. 4a). Correspondingly, *Il10* luciferase reporter activity was potently induced by IL-21 or anti-CD3 + anti-CD28, and more so by IL-21 + anti-CD3 + anti-CD28, but expression was diminished when the GAAA IRF4 motif or associated AP1 site was mutated ($P < 0.02$; Fig. 4b). Moreover, IRF4, JUNB, JUND and BATF

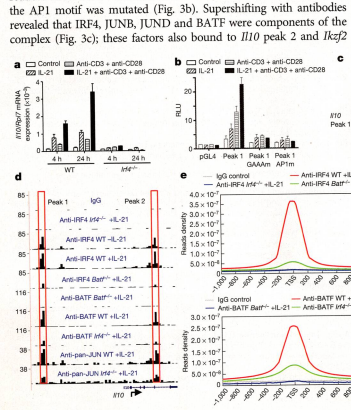

Figure 4 | Cooperative action of IRF4, BATF, and JUN. a, *Il10* mRNA expression relative to *Rpl7* in WT or *Irf4*$^{-/-}$ T cells pre-activated and treated as indicated for 4 or 24 h. ($n = 3$; mean ± s.d.). **b**, WT or mutant *Il10* reporter constructs transfected into pre-activated T cells and treated as indicated for 7 h ($n = 3$; mean ± S.D.). RLU, relative light units. **c**, EMSA with *Il10* peak1 probe and nuclear extracts from WT or *Irf4*$^{-/-}$ pre-activated CD4$^+$ T cells stimulated with IL-21 for 4 h. Supershifting antibodies are indicated. EMSA was performed twice. **d**, IRF4, BATF, and pan-JUN ChIP-Seq data from WT or *Irf4*$^{-/-}$ T cells pre-activated and stimulated with IL-21 at the *Il10* gene. **e**, IRF4 binding in WT vs. *Batf*$^{-/-}$ cells (upper) and BATF binding in WT vs. *Irf4*$^{-/-}$ cells (lower). TSS, transcription start site. **f**, As in **d**, except at *Il17ra*.

each bound to a wild-type probe spanning this region, but binding was diminished when $Irf4^{-/-}$ nuclear extracts were used (Fig. 4c). Moreover, in ChIP-Seq experiments, there was markedly decreased binding of IRF4 in $Batf^{-/-}$ T cells and of BATF and JUN in $Irf4^{-/-}$ T cells (Fig. 4d) at the *Il10* locus but also globally (Fig. 4e), including for example at the *Il17a* gene (Fig. 4f), consistent with defective *Il17a* expression and T_H17 differentiation in $Irf4^{-/-}$[13] and $Batf^{-/-}$[15] T cells. These results indicate cooperative binding and transcriptional activation by IRF4 and BATF–JUN family proteins.

IRF4 is a pleiotropic IRF family transcription factor with broad immunological actions. Its critical role in regulating immunoglobulin genes involves functional cooperation with the largely B-cell-restricted factor PU.1. We now demonstrate that in T cells, where PU.1 expression is low, IRF4 instead functionally cooperates with AP1 family proteins to act via AICEs, with functional cooperation with BATF and JUN family proteins in pre-activated T cells stimulated with IL-21 as well as in T_H2, T_H9 and T_H17 polarized cells. Interestingly, a number of genes we selected for analysis (*Il10*, *Ctla4*, *Il17a*, *Prdm1* and *Ikzf2*) were functionally grouped in a study of T_H2 inhibitory effector cells during chronic inflammation as preferentially expressed in IL-10$^+$ versus IL-10$^-$ cells[27]; it will be interesting to determine whether IRF4/AP1-dependent gene expression helps to explain these observations. Although IRF4 and BATF cooperatively bound in the context of AICEs, it was unclear if they associated in the absence of these sites. In T cells, we could co-precipitate BATF and JUN (Supplementary Fig. 8), but we only co-precipitated IRF4 and JUN in a single experiment and could not co-precipitate BATF and IRF4. Thus, if a direct interaction occurs, it may be relatively weak, but the marked decrease of BATF binding in $Irf4^{-/-}$ and of IRF4 in $Batf^{-/-}$ cells (Fig. 4) indicates cooperative binding to AICEs. This binding is dependent on the BATF leucine zipper domain[28]. The ability of IRF4 to act via two types of complexes, PU.1–IRF4 EICEs in B cells and AP1–IRF4 AICEs in T cells and to some degree in B cells, highlights mechanisms for IRF4-mediated transcriptional activation. The identification of the IRF4–AP1 connection suggests new approaches may be employed to selectively target certain actions of IRF4, potentially allowing ways to manipulate the immune response in a cell-type-restricted fashion.

METHODS SUMMARY

T and B cells were cultured in standard medium. Cells were pre-activated with anti-CD3 + anti-CD28 for 3 days, rested overnight and stimulated with IL-21 for 1 h (ChIP-Seq) or 4 h (EMSAs). T_H17 polarization was performed by standard methods and unlike CD4$^+$ T cells, T_H17 polarized cells were not stimulated with IL-21. WT, $Batf^{-/-}$ and $Irf4^{-/-}$ mice were 6-8 weeks old C57BL/6 background mice of mixed gender. All experiments with mice were performed under protocols approved by the NHLBI Animal Care and Use Committee, and followed NIH guidelines for use of animals in intramural research. ChIP-Seq[14,29] and RNA-Seq[30] experiments were performed as previously described. ChIP-Seq and RNA-Seq libraries are summarized in Supplementary Table 2; details of binding site identification and motif analysis are in the online methods. For reporter assays, activated T cells were electroporated with reporter plasmid and pRLTK, and dual luciferase assays performed. For EMSAs, nuclear extracts[14] were bound to ^{32}P-labelled probes. For supershifts, extracts were pre-incubated with indicated antibodies, before analysis on 5% polyacrylamide gels.

Full Methods and any associated references are available in the online version of the paper.

Received 21 May; accepted 29 August 2012.
Published online 19 September 2012.

1. Taniguchi, T., Ogasawara, K., Takaoka, A. & Tanaka, N. IRF family of transcription factors as regulators of host defense. *Annu. Rev. Immunol.* **19,** 623–655 (2001).
2. Lohoff, M. & Mak, T. W. Roles of interferon-regulatory factors in T-helper-cell differentiation. *Nature Rev. Immunol.* **5,** 125–135 (2005).
3. Brass, A. L., Kehrli, E., Eisenbeis, C. F., Storb, U. & Singh, H. Pip, a lymphoid-restricted IRF, contains a regulatory domain that is important for autoinhibition and ternary complex formation with the Ets factor PU.1. *Genes Dev.* **10,** 2335–2347 (1996).
4. Grossman, A. *et al.* Cloning of human lymphocyte-specific interferon regulatory factor (hLSIRF/hIRF4) and mapping of the gene to 6p23–p25. *Genomics* **37,** 229–233 (1996).
5. Grumont, R. J. & Gerondakis, S. Rel induces interferon regulatory factor 4 (*IRF-4*) expression in lymphocytes: modulation of interferon-regulated gene expression by Rel/nuclear factor κB. *J. Exp. Med.* **191,** 1281–1292 (2000).
6. Escalante, C. R. *et al.* Crystal structure of PU.1/IRF-4/DNA ternary complex. *Mol. Cell* **10,** 1097–1105 (2002).
7. Pernis, A. B. The role of IRF-4 in B and T cell activation and differentiation. *J. Interferon Cytokine Res.* **22,** 111–120 (2002).
8. Lohoff, M. *et al.* Dysregulated T helper cell differentiation in the absence of interferon regulatory factor 4. *Proc. Natl Acad. Sci. USA* **99,** 11808–11812 (2002).
9. Tominaga, N. *et al.* Development of T_H1 and not T_H2 immune responses in mice lacking IFN-regulatory factor-4. *Int. Immunol.* **15,** 1–10 (2003).
10. Rengarajan, J. *et al.* Interferon regulatory factor 4 (IRF4) interacts with NFATc2 to modulate interleukin 4 gene expression. *J. Exp. Med.* **195,** 1003–1012 (2002).
11. Hu, C. M., Jang, S. Y., Fanzo, J. C. & Pernis, A. B. Modulation of T cell cytokine production by interferon regulatory factor-4. *J. Biol. Chem.* **277,** 49238–49246 (2002).
12. Staudt, V. *et al.* Interferon-regulatory factor 4 is essential for the developmental program of T helper 9 cells. *Immunity* **33,** 192–202 (2010).
13. Brüstle, A. *et al.* The development of inflammatory T_H-17 cells requires interferon-regulatory factor 4. *Nature Immunol.* **8,** 958–966 (2007).
14. Kwon, H. *et al.* Analysis of interleukin-21-induced *Prdm1* gene regulation reveals functional cooperation of STAT3 and IRF4 transcription factors. *Immunity* **31,** 941–952 (2009).
15. Schraml, B. U. *et al.* The AP-1 transcription factor *Batf* controls T_H17 differentiation. *Nature* **460,** 405–409 (2009).
16. Echlin, D. R., Tae, H. J., Mitin, N. & Taparowsky, E. J. B-ATF functions as a negative regulator of AP-1 mediated transcription and blocks cellular transformation by Ras and Fos. *Oncogene* **19,** 1752–1763 (2000).
17. Dorsey, M. J. *et al.* B-ATF: a novel human bZIP protein that associates with members of the AP-1 transcription factor family. *Oncogene* **11,** 2255–2265 (1995).
18. Korn, T. *et al.* IL-21 initiates an alternative pathway to induce proinflammatory T_H17 cells. *Nature* **448,** 484–487 (2007).
19. Nurieva, R. *et al.* Essential autocrine regulation by IL-21 in the generation of inflammatory T cells. *Nature* **448,** 480–483 (2007).
20. Zhou, L. *et al.* IL-6 programs T_H-17 cell differentiation by promoting sequential engagement of the IL-21 and IL-23 pathways. *Nature Immunol.* **8,** 967–974 (2007).
21. Zhang, X., Wrzeszczynska, M. H., Horb, M. E., Heath, C. M. & Darnell, J. E. Jr. Interacting regions in Stat3 and c-Jun that participate in cooperative transcriptional activation. *Mol. Cell. Biol.* **19,** 7138–7146 (1999).
22. Spolski, R., Kim, H. P., Zhu, W., Levy, D. E. & Leonard, W. J. IL-21 mediates suppressive effects via its induction of IL-10. *J. Immunol.* **182,** 2859–2867 (2009).
23. Pot, C. *et al.* Cutting edge: IL-27 induces the transcription factor c-Maf, cytokine IL-21, and the costimulatory receptor ICOS that coordinately act together to promote differentiation of IL-10-producing Tr1 cells. *J. Immunol.* **183,** 797–801 (2009).
24. Lee, C. G. *et al.* A distal *cis*-regulatory element, CNS-9, controls NFAT1 and IRF4-mediated IL-10 gene activation in T helper cells. *Mol. Immunol.* **46,** 613–621 (2009).
25. Chang, H. C. *et al.* PU.1 expression delineates heterogeneity in primary Th2 cells. *Immunity* **22,** 693–703 (2005).
26. Chang, H. C. *et al.* The transcription factor PU.1 is required for the development of IL-9-producing T cells and allergic inflammation. *Nature Immunol.* **11,** 527–534 (2010).
27. Altin, J. A., Goodnow, C. C. & Cook, M. C. IL-10$^+$ CTLA-4$^+$ Th2 inhibitory cells form in a Foxp3-independent, IL-2-dependent manner from Th2 effectors during chronic inflammation. *J. Immunol.* **188,** 5478–5488 (2012).
28. Tussiwand, R. *et al.* Compensatory dendritic cell development mediated by BATF-IRF interactions. *Nature* http://dx.doi.org/10.1038/nature11531 (19 September 2012).
29. Liao, W., Lin, J. X., Wang, L., Li, P. & Leonard, W. J. Modulation of cytokine receptors by IL-2 broadly regulates differentiation into helper T cell lineages. *Nature Immunol.* **12,** 551–559 (2011).
30. Lin, J. X. *et al.* Critical role of STAT5 transcription factor tetramerization for cytokine responses and normal immune function. *Immunity* **36,** 586–599 (2012).

Supplementary Information is available in the online version of the paper.

Acknowledgements This work was supported by the Division of Intramural Research, National Heart, Lung, and Blood Institute, NIH (P.L., R.S., W.L., L.W. and W.J.L.) and the Howard Hughes Medical Institute (T.L.M. and K.M.M.). We thank J.-X. Lin for valuable suggestions, critical comments and RNA-Seq data for pro-B/pre-B-enriched populations. We thank J. Zhu and Y. Wakabayashi, NHLBI DNA Sequencing Core, for excellent services, K. Ozato and Y. Hiroaki, NICHD, for *Irf4*$^{-/-}$ mice, and J. Thierry-Mieg and D. Thierry-Mieg, NCBI, for early analysis of ChIP-Seq data from ref. 14.

Author Contributions P.L. designed experiments, analysed data and wrote the paper. R.S. designed and performed experiments, analysed data and wrote the paper. W.L. and L.W. designed and performed experiments and analysed data. T.L.M. and K.M.M. provided reagents and made suggestions. W.J.L. designed experiments, analysed data and wrote the paper.

Author Information Data sets (ChIP-Seq and RNA-Seq data) have been deposited in the Gene Expression Omnibus (GSE39756). Reprints and permissions information is available at www.nature.com/reprints. The authors declare competing financial interests: details are available in the online version of the paper. Readers are welcome to comment on the online version of the paper. Correspondence and requests for materials should be addressed to P.L. (lip3@nhlbi.nih.gov) or W.J.L. (wjl@helix.nih.gov.).

LETTER

doi:10.1038/nature11452

Mitochondrial defect drives non-autonomous tumour progression through Hippo signalling in *Drosophila*

Shizue Ohsawa[1], Yoshitaka Sato[1], Masato Enomoto[1], Mai Nakamura[1], Aya Betsumiya[1] & Tatsushi Igaki[1,2]

Mitochondrial respiratory function is frequently impaired in human cancers[1–4]. However, the mechanisms by which mitochondrial dysfunction contributes to tumour progression remain elusive. Here we show in *Drosophila* imaginal epithelium that defects in mitochondrial function potently induce tumour progression of surrounding tissue in conjunction with oncogenic Ras. Our data show that Ras activation and mitochondrial dysfunction cooperatively stimulate production of reactive oxygen species, which causes activation of c-Jun amino (N)-terminal kinase (JNK) signalling. JNK cooperates with oncogenic Ras to inactivate the Hippo pathway, leading to upregulation of its targets Unpaired (an interleukin-6 homologue) and Wingless (a Wnt homologue). Mitochondrial dysfunction in Ras-activated cells further cooperates with Ras signalling in neighbouring cells with normal mitochondrial function, causing benign tumours to exhibit metastatic behaviour. Our findings provide a mechanistic basis for interclonal tumour progression driven by mitochondrial dysfunction and oncogenic Ras.

Cell–cell interactions between oncogenic cells and surrounding normal cells in the tumour microenvironment play crucial roles in cancer progression[5]. To study the genetic basis of tumour progression through cell–cell communications, we performed a genetic screen in *Drosophila* to identify mutations that cause oncogenic Ras^{V12}-expressing cells to induce non-autonomous growth of surrounding tissue. Clones of cells expressing Ras^{V12} overgrow and develop into benign tumours in the eye imaginal epithelium (Fig. 1e)[6]. Using the MARCM technique[7], we introduced further homozygous mutations in GFP-labelled Ras^{V12}-expressing clones and screened for those that triggered non-autonomous growth (*nag*) (Supplementary Fig. 1a). We isolated *nag* mutations that resulted in enlarged larval eye discs (Fig. 1f and Supplementary Fig. 2a) and subsequent overgrown 'folded-eyes' in the adult (Fig. 1b). These *nag* mutations did not promote autonomous growth (Fig. 1a–f and Supplementary Fig. 2b), indicating that the mutant clones stimulated growth in the surrounding tissue (Supplementary Fig. 2a, c). Indeed, increased cell proliferation was evident in wild-type tissue adjacent to $Ras^{V12}/nag^{-/-}$ clones (Fig. 1g). The non-autonomous overgrowth was not caused by *nag* mutations alone (Fig. 1d, e and Supplementary Figs 1j, k and 2o).

Analysis of *nag* mutations identified lesions in a series of genes required for mitochondrial respiratory function: either genes encoding components of the mitochondrial respiratory complexes or mitochondrial ribosomal proteins (Supplementary Fig. 1l, m). Mutations in different components of the mitochondrial respiratory system, including *Pdsw* (*nag-19*, a component of complex I)[8], *mRpL4* (*nag-24*, a mitochondrial ribosomal protein)[8] and *CoVa* (a component of complex IV)[8], cooperated with Ras^{V12} to induce indistinguishable non-autonomous overgrowth (Fig. 1b and Supplementary Figs 1b–i and 2). These results show that impairments of the mitochondrial respiratory chain in Ras-activated cells trigger overgrowth of surrounding tissue.

It has been reported that dying cells stimulate 'compensatory proliferation' of their surrounding cells[9]. However, we found that neither mitochondrial mutations themselves nor in combination with Ras^{V12} caused cell death (Supplementary Fig. 3c–f). Furthermore, blocking caspase activity by baculoviral p35, which enhances compensatory proliferation, did not cause mitochondrial mutant clones to induce non-autonomous overgrowth (Supplementary Fig. 3a, b). These results indicate that the non-autonomous overgrowth is not caused by compensatory proliferation but by specific cooperation between Ras activation and mitochondrial dysfunction.

To dissect the mechanism underlying the non-autonomous overgrowth, we conducted a secondary genetic screen to identify dominant modifiers of the *nag* phenotype. Using a series of chromosomal deficiencies, we introduced heterozygous genomic deletions in flies bearing $Ras^{V12}/CG9140^{nag\text{-}28-/-}$ clones (CG9140 encodes a component of complex I). We found that one of the strong dominant suppressors of *nag*, *Df(3R)H-B79*, uncovered *Stat92E*, a component of the JAK/STAT pathway (Supplementary Fig. 4a, b, o). The *Drosophila* JAK/STAT pathway is activated by binding of its ligand Unpaired (Upd) to its receptor Domeless (Dome), thereby activating the transcription factor Stat92E, which stimulates cell proliferation[10]. Heterozygosity for either *Stat92E* or *dome* in animals bearing Ras^{V12}-expressing clones with mitochondrial mutations ($Ras^{V12}/mito^{-/-}$) notably suppressed non-autonomous overgrowth (Fig. 1h, i and Supplementary Fig. 4c–h, l, m, p–u). In addition, reducing *upd* expression suppressed the *nag* phenotype (Fig. 1j and Supplementary Fig. 4i, j, n, v, w). Furthermore, although neither Ras activation nor mitochondrial dysfunction induced Upd expression, combination of these two alterations notably upregulated Upd (Fig. 1l–n and Supplementary Figs 5a–c, e, f and 6a–c). These data indicate that $Ras^{V12}/mito^{-/-}$ clones cause non-autonomous overgrowth through the Upd-JAK/STAT pathway.

It has been reported that *upd* expression is induced by either JNK signalling or Notch signalling[11–14]. We found that blocking JNK in $Ras^{V12}/mito^{-/-}$ clones by a dominant-negative form of the *Drosophila* JNK Bsk (Bsk^{DN}) abolished Upd induction (Fig. 1o and Supplementary Figs 5d–f and 6d) and notably suppressed non-autonomous overgrowth (Fig. 1k and Supplementary Fig. 7). In addition, although Ras activation or mitochondrial dysfunction caused only low-level expression of the *puc-lacZ* JNK activity reporter[15], combination of Ras activation and mitochondrial dysfunction cooperatively activated JNK signalling (Fig. 1p and Supplementary Fig. 8). On the other hand, reducing Notch activity did not affect the overgrowth (data not shown). These data show that $Ras^{V12}/mito^{-/-}$ clones cooperatively activate JNK signalling, which causes Upd induction.

We next examined the mechanism of JNK activation in $Ras^{V12}/mito^{-/-}$ clones. Mitochondrial malfunction is often associated with reactive oxygen species production, which activates intracellular stress signalling such as JNK signalling[16]. Interestingly, although neither Ras activation nor mitochondrial dysfunction ($Pdsw^{-/-}$ or $CoVa^{-/-}$) caused oxidative stress, the combination of these two alterations strongly induced oxidative stress (Fig. 2a–c and Supplementary Fig. 9a, b), as visualized by the gstD–green fluorescent protein (GFP) reporter[17]. In addition, staining with dihydroethidium (DHE), a fluorescent probe for superoxide anion (O_2^-), showed that $Ras^{V12}/Pdsw^{-/-}$

[1]Division of Genetics, Kobe University Graduate School of Medicine, 7-5-1 Kusunoki-cho, Chuo-ku, Kobe 650-0017, Japan. [2]PRESTO, Japan Science and Technology Agency (JST), 4-1-8 Honcho Kawaguchi, Saitama 332-0012, Japan.

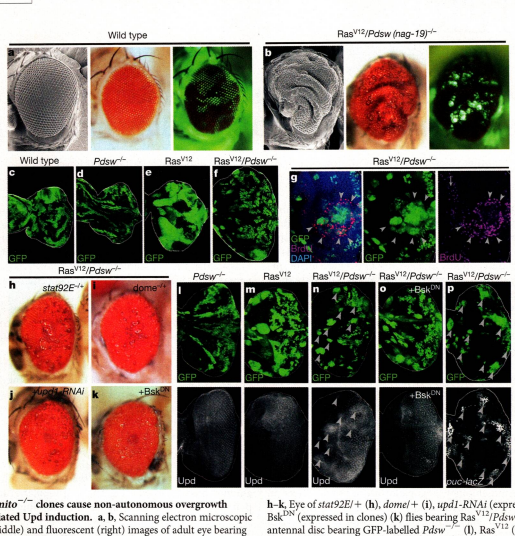

Figure 1 | Ras^{V12}/*mito*$^{-/-}$ clones cause non-autonomous overgrowth through JNK-mediated Upd induction. **a**, **b**, Scanning electron microscopic (left), light level (middle) and fluorescent (right) images of adult eye bearing GFP-labelled wild-type (**a**) or Ras^{V12}/*Pdsw*$^{nag-19-/-}$ (**b**) clones. **c**–**f**, Eye-antennal disc bearing GFP-labelled wild-type (**c**), *Pdsw*$^{-/-}$ (**d**), Ras^{V12} (**e**) or Ras^{V12}/*Pdsw*$^{-/-}$ (**f**) clones. **g**, 5-Bromodeoxyuridine (BrdU) labelling in eye-antennal disc bearing GFP-labelled Ras^{V12}/*Pdsw*$^{-/-}$ clones. Normal BrdU incorporation in the second mitotic wave is indicated (**g**, right panel, arrow). **h**–**k**, Eye of *stat92E*/+ (**h**), *dome*/+ (**i**), *upd1-RNAi* (expressed in clones) (**j**) or Bsk^{DN} (expressed in clones) (**k**) flies bearing Ras^{V12}/*Pdsw*$^{-/-}$ clones. **l**–**o**, Eye-antennal disc bearing GFP-labelled *Pdsw*$^{-/-}$ (**l**), Ras^{V12} (**m**), Ras^{V12}/*Pdsw*$^{-/-}$ (**n**) or Ras^{V12}/*Pdsw*$^{-/-}$ + Bsk^{DN} (**o**) clones stained with anti-Upd. Arrowheads indicate representative clones upregulating Upd. **p**, GFP-labelled Ras^{V12}/*Pdsw*$^{-/-}$ clones were induced in *puc-LacZ*/+ eye-antennal disc and stained with anti-β-gal. Arrowheads indicate representative clones activating JNK.

clones cooperatively induced O_2^- production (Fig. 2d–f). Notably, blocking oxidative stress by glutathione peroxidase (GPx)[18] in mutant clones abrogated JNK activation (Fig. 2h, compare with Fig. 1p) as well as the non-autonomous overgrowth (Fig. 2i and Supplementary Fig. 9e, h, j). On the other hand, blocking JNK in Ras^{V12}/*mito*$^{-/-}$ clones had no effect on the oxidative stress (Fig. 2g and Supplementary Fig. 9c). These results indicate that oxidative stress is the upstream trigger for JNK activation in Ras^{V12}/*mito*$^{-/-}$ clones.

Intriguingly, we found that Ras^{V12}/*CoVa*$^{-/-}$ clones did not produce O_2^-, despite the strong induction of oxidative stress (Supplementary Fig. 9b, d). This is consistent with previous observations that O_2^- was induced by defects in complex I *Pdsw* but not by defects in complex IV *CoVa*[19]. These observations raised the possibility that Ras^{V12}/*CoVa*$^{-/-}$ clones produce H_2O_2, whereas Ras^{V12}/*Pdsw*$^{-/-}$ clones produce O_2^- (Supplementary Fig. 9m). Indeed, reducing O_2^- by superoxide dismutase (SOD) in Ras^{V12}/*Pdsw*$^{-/-}$ clones, but not in Ras^{V12}/*CoVa*$^{-/-}$ clones, suppressed non-autonomous overgrowth (Fig. 2j and Supplementary Fig. 9f, i, k). Furthermore, reducing H_2O_2 in Ras^{V12}/*CoVa*$^{-/-}$ clones by Catalase suppressed the non-autonomous overgrowth (Supplementary Fig. 9g, l). Consistent with these results, another fluorescent reactive oxygen species indicator, H_2DCFDA, which can detect H_2O_2, strongly labelled Ras^{V12}/*CoVa*$^{-/-}$ clones (Supplementary Fig. 9n–p). These data indicate that Ras activation in cells with impaired mitochondrial respiratory function triggers oxidative stress through production of either O_2^- or H_2O_2, which activates JNK.

Our genetic data establish that JNK activation in Ras^{V12}/*mito*$^{-/-}$ clones is necessary to cause *nag* phenotype. However, JNK activation is not sufficient, as clones of cells solely activating JNK signalling (for example, by overexpression of the *Drosophila* tumour-necrosis factor Eiger) do not cause non-autonomous overgrowth[6] (Fig. 3a), indicating that Ras^{V12}/*mito*$^{-/-}$ clones must induce an additional downstream effect(s) essential for the induction of *nag*. Interestingly, we found that co-activation of JNK and Ras signalling caused Upd induction (Fig. 3b), which is mediated through the Hippo pathway (see below). The Hippo pathway is an evolutionarily conserved kinase cascade that negatively regulates tissue growth by phosphorylating and inhibiting the transcriptional co-activator Yorkie (Yki). Inactivation of the Hippo pathway reduces Yki phosphorylation, which results in induction of its target genes[20]. Recent studies have shown that *upd* is a target of Yki[14,21–23] and Yki activity is mediated by JNK signalling during intestinal regeneration[14,24]. Interestingly, co-activation of JNK and Ras signalling upregulated Yki target genes such as *diap1* and *cyclin E*, whereas neither JNK nor Ras activation alone did not (Fig. 3d–f and Supplementary Fig. 10a–c). Similarly, the combination of Ras activation and mitochondrial dysfunction caused upregulation of Yki targets *expanded* (*ex*), *diap1* and *cyclin E* (Fig. 3j–l and Supplementary Fig. 10e–h, m). Furthermore, forced activation of the Hippo kinase cascade

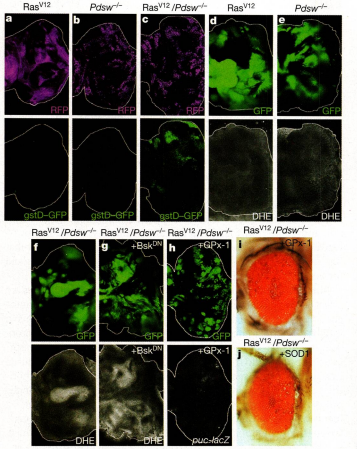

Figure 2 | JNK signalling is activated by oxidative stress in Ras^{V12}/*mito*$^{-/-}$ clones. **a**–**c**, Red fluorescent protein (RFP)-labelled Ras^{V12} (**a**), *Pdsw*$^{-/-}$ (**b**) or Ras^{V12}/*Pdsw*$^{-/-}$ (**c**) clones were induced in *gstD–GFP/+* eye-antennal disc. **d**–**g**, Eye-antennal disc bearing GFP-labelled Ras^{V12} (**d**), *Pdsw*$^{-/-}$ (**e**), Ras^{V12}/*Pdsw*$^{-/-}$ (**f**) or Ras^{V12}/*Pdsw*$^{-/-}$ + Bsk^{DN} (**g**) clones was incubated with DHE for 5 min. A slight increase in production of reactive oxygen species was observed when incubated for 10 min (data not shown)[19]. **h**, GFP-labelled Ras^{V12}/*Pdsw*$^{-/-}$ + GPx-1 clones were induced in *puc-LacZ/+* eye-antennal disc and stained with anti-β-gal. **i**, **j**, Adult eye bearing Ras^{V12}/*Pdsw*$^{-/-}$ + GPx-1 (**i**) or Ras^{V12}/*Pdsw*$^{-/-}$ + SOD1 (**j**) clones.

by Warts (Wts, a Yki kinase) or Hippo (Hpo, a Wts kinase), which inhibits Yki activity, as well as reducing *yki* expression by *yki* RNA interference (RNAi), blocked the induction of *upd*, *diap1* and *cyclin E* both in Ras/JNK-activating clones (Fig. 3c, g and Supplementary Fig. 10d) and Ras^{V12}/*mito*$^{-/-}$ clones (Fig. 3i, o and Supplementary Fig. 10i–l, n–p) and suppressed the non-autonomous overgrowth (Fig. 3p and Supplementary Fig. 11a, b, e, g, h). We also found that the expression of a secreted growth factor Wingless (Wg), another target of Yki[20], was notably upregulated in Ras^{V12}/*mito*$^{-/-}$ clones through Hippo signalling (Fig. 3m, o and Supplementary Fig. 10p). Furthermore, reducing *wg* expression in Ras^{V12}/*mito*$^{-/-}$ clones suppressed the non-autonomous overgrowth (Supplementary Fig. 11c, d, i, j). Notably, combined expression of *upd-RNAi* and *wg-RNAi* in Ras^{V12}/*mito*$^{-/-}$ clones almost completely suppressed *nag* phenotype (Fig. 3q and Supplementary Fig. 11f), indicating that induction of these factors through Hippo signalling is responsible for the non-autonomous overgrowth. Blocking JNK signalling in Ras^{V12}/*mito*$^{-/-}$ clones abolished the upregulation of all Yki target genes (Supplementary Fig. 12a–d). These data establish that JNK activation in Ras^{V12}/*mito*$^{-/-}$ clones cooperates with Ras signalling to inactivate the Hippo pathway, leading to induction of Yki targets *upd* and *wg*, which causes overgrowth of surrounding tissue.

In human cancers, oncogenic cooperation occurs in a context of clonal evolution where somatic mutations in mitochondrial DNA

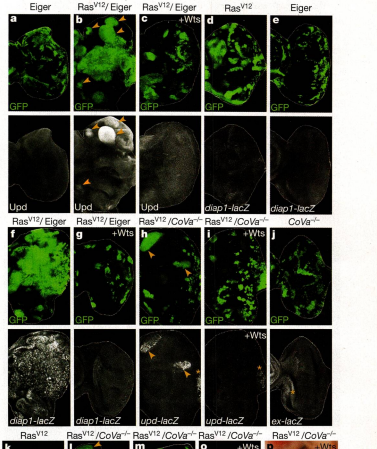

Figure 3 | Co-activation of JNK and Ras signalling causes upregulation of Upd and Wg through Hippo pathway inactivation. **a**–**c**, Eye-antennal disc bearing GFP-labelled Eiger (**a**), Ras^{V12}/Eiger (**b**) or Ras^{V12}/Eiger + Wts (**c**) was stained with anti-Upd. Arrowheads indicate representative clones upregulating Upd (**b**). **d**–**g**, GFP-labelled Ras^{V12} (**d**), Eiger (**e**), Ras^{V12}/Eiger (**f**) or Ras^{V12}/Eiger + Wts (**g**) clones were induced in *diap1-lacZ/+* eye-antennal disc and stained with anti-β-gal. Endogenous *diap1-lacZ* expression is weakly observed in the region posterior to the morphogenetic furrow. **h**, **i**, GFP-labelled Ras^{V12}/*CoVa*$^{-/-}$ (**h**) or Ras^{V12}/*CoVa*$^{-/-}$ + Wts (**i**) clones were induced in *upd-lacZ/+* eye-antennal disc and stained with anti-β-gal. Endogenous *upd-lacZ* expression is indicated (**h**, **i**, bottom panels, asterisks). **j**–**l**, GFP-labelled *CoVa*$^{-/-}$ (**j**), Ras^{V12} (**k**) or Ras^{V12}/*CoVa*$^{-/-}$ (**l**) clones were induced in *expanded-lacZ/+* eye-antennal disc and stained with anti-β-gal. Endogenous *expanded-lacZ* expression is indicated (**j**–**l**, bottom panels, asterisks). **m**, **o**, Eye-antennal disc bearing GFP-labelled Ras^{V12}/*CoVa*$^{-/-}$ (**m**) or Ras^{V12}/*CoVa*$^{-/-}$ + Wts (**o**) clones was stained with anti-Wg. Endogenous expression domains of Wg are indicated (**m**, **o**, bottom panels, asterisks). **p**, **q**, Adult eye bearing Ras^{V12}/*CoVa*$^{-/-}$ + Wts (**p**) or Ras^{V12}/*Pdsw*$^{-/-}$ + *upd1-RNAi* + *wg-RNAi* (**q**) clones.

(mtDNA) or nuclear mitochondrial genes occur in a clone of cells within a developing tumour. Strikingly, when such situation was genetically created by inducing Ras^{V12}/*mito*$^{-/-}$ clones surrounded

by Ras^{V12}-expressing tissue, the tumour cells not only overproliferated but also exhibited invasive behaviour; the tumour cells migrated out of eye-antennal discs and invaded adjacent tissues such as brain hemispheres and ventral nerve cord (Fig. 4b, d and Supplementary Fig. 13c), whereas tissues entirely composed of Ras^{V12} cells never displayed such invasive behaviour (Fig. 4a, c)[25]. The invading tumour cells were mostly Ras^{V12} cells with normal mitochondrial function, as $Ras^{V12}/mito^{-/-}$ clones surrounded by Ras^{V12} clones grew very poorly (Supplementary Fig. 13a, b). The invasive behaviour was strongly blocked by reducing *stat92E* gene dosage (Fig. 4e, f). Thus, the invasive growth is most probably due to Upd-JAK/STAT signalling[25], although Wg may also contribute to the proliferation and/or invasion. Together, these observations show that clones of cells with impaired mitochondrial function arising inside Ras-activated benign overgrowths promote tumour progression of neighbouring Ras-activated tissue (Fig. 4g).

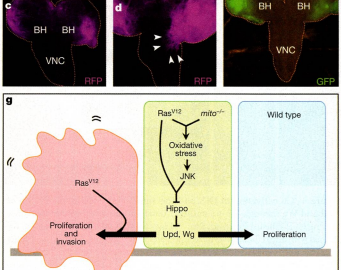

Figure 4 | $Ras^{V12}/mito^{-/-}$ clones drive tumour progression of surrounding tumours. **a**, **b**, Lateral view of larval cephalic complex with eye-antennal discs entirely expressing Ras^{V12} and GFP (**a**) or Ras^{V12} and GFP simultaneously bearing GFP-labelled $Ras^{V12}/Pdsw^{-/-}$ clones (**b**). **c**, **d**, Dorsal view of dissected larval central nervous system from animal with eye-antennal discs entirely expressing Ras^{V12} and RFP simultaneously bearing either RFP-labelled Ras^{V12} (**c**) or RFP-labelled $Ras^{V12}/mRpL4^{-/-}$ (**d**) clones. **e**, **f**, Dorsal view of dissected larval central nervous system from animal with eye-antennal discs entirely expressing Ras^{V12} and GFP simultaneously bearing GFP-labelled $Ras^{V12}/Pdsw^{-/-}$ clones. The *stat92E* gene is heterozygous in **f**. Arrowheads in **b**, **d**, **e** indicate eye-antennal cells invading the ventral nerve cord. **g**, A model for non-autonomous tumour progression by Ras activation and mitochondrial dysfunction.

Although it has been extensively studied how Ras signalling stimulates cell-autonomous proliferation and thereby contributes to cancers[26], our findings uncover a non-cell-autonomous oncogenic role of Ras in cooperation with mitochondrial dysfunction. Intriguingly, a similar non-autonomous overgrowth is caused by co-expression of constitutively activated (CA) Hep (a JNK kinase) and Raf (a downstream effector of Ras)[27]. However, Raf^{CA}/Hep^{CA} clones cause massive cell death[27], and blocking cell death by p35 in Hep^{CA} clones is sufficient to cause non-autonomous overgrowth (data not shown), indicating that, although interesting cooperation, the Raf^{CA}/Hep^{CA}-induced non-autonomous overgrowth could be simply caused by compensatory proliferation. Thus, the non-autonomous tumour progression mechanism is specifically triggered by mitochondrial dysfunction in Ras-activated cells. Mutations in mitochondrial respiratory complexes cause cell cycle arrest[8,19,28], which could explain why inactivation of the Hippo pathway in $Ras^{V12}/mito^{-/-}$ clones does not promote cell-autonomous proliferation. Intriguingly, we found that E-cadherin and Discs-large are downregulated in these clones (data not shown), raising the possibility that $Ras^{V12}/mito^{-/-}$ clones disrupt the epithelial integrity, which could further contribute to Hippo pathway inactivation[29].

Mitochondrial number and oxidative phosphorylation activities are often downregulated in many cancers[4]. The high rates of the mitochondrial malfunctions in cancers are caused by somatic mutations in mtDNA[1–3], which encode components of mitochondrial respiratory complexes. Our genetic data in *Drosophila* not only provide a mechanistic insight into tumour progression driven by mitochondrial dysfunction but also support Warburg's hypothesis that mitochondrial defects play an active role in the aetiology of cancer. Strikingly, mtDNA mutations were frequently identified in pancreatic cancers[3], a highly aggressive cancer that mostly bears (~90%) Ras mutations[26]. Given the evolutionary conservation of the pathways examined, similar cooperative mechanisms could have a role in human cancers.

METHODS SUMMARY

Clones of mutant cells were generated in eye-antennal discs as described[6]. Detailed genotypes of the experimental individuals are described in Supplementary Information. The following antibodies and dyes were used: anti-Upd (D. Harrison), anti-Cyclin E (T. Orr-Weaver and H. Richardson), anti-cleaved caspase-3 (Cell Signaling), anti-β-gal (Sigma), anti-Wg (DSHB), anti-cleaved PARP (Cell Signaling), anti-phospho-JNK G9 (Cell Signaling), anti-BrdU BMG 6H8 (Roche), DHE (Invitrogen) and CM-H_2DCFDA (Invitrogen).

Full Methods and any associated references are available in the online version of the paper.

Received 9 February; accepted 30 July 2012.
Published online 30 September 2012.

1. Brandon, M., Baldi, P. & Wallace, D. C. Mitochondrial mutations in cancer. *Oncogene* **25,** 4647–4662 (2006).
2. Carew, J. S. & Huang, P. Mitochondrial defects in cancer. *Mol. Cancer* **1,** 9 (2002).
3. Madica-Napolitano, J. S., Kulawiec, M. & Singh, K. K. Mitochondria and human cancer. *Curr. Mol. Med.* **7,** 121–131 (2007).
4. Pedersen, P. L. Tumor mitochondria and the bioenergetics of cancer cells. *Prog. Exp. Tumor Res.* **22,** 190–274 (1978).
5. Bissell, M. J. & Hines, W. C. Why don't we get more cancer? A proposed role of the microenvironment in restraining cancer progression. *Nature Med.* **17,** 320–329 (2011).
6. Igaki, T., Pagliarini, R. A. & Xu, T. Loss of cell polarity drives tumor growth and invasion through JNK activation in *Drosophila*. *Curr. Biol.* **16,** 1139–1146 (2006).
7. Lee, T. & Luo, L. Mosaic analysis with a repressible cell marker for studies of gene function in neuronal morphogenesis. *Neuron* **22,** 451–461 (1999).
8. Mandal, S., Guptan, P., Owusu-Ansah, E. & Banerjee, U. Mitochondrial regulation of cell cycle progression during development as revealed by the tenured mutation in *Drosophila*. *Dev. Cell* **9,** 843–854 (2005).
9. Morata, G., Shlevkov, E. & Perez-Garijo, A. Mitogenic signaling from apoptotic cells in *Drosophila*. *Dev. Growth Differ.* **53,** 168–176 (2011).
10. Hou, S. X., Zheng, Z., Chen, X. & Perrimon, N. The Jak/STAT pathway in model organisms: emerging roles in cell movement. *Dev. Cell* **3,** 765–778 (2002).
11. Giebel, B. & Wodarz, A. Tumor suppressors: control of signaling by endocytosis. *Curr. Biol.* **16,** R91–R92 (2006).
12. Jiang, H. *et al.* Cytokine/Jak/Stat signaling mediates regeneration and homeostasis in the *Drosophila* midgut. *Cell* **137,** 1343–1355 (2009).

13. Pastor-Pareja, J. C. & Wu, M. and Xu, T. An innate immune response of blood cells to tumors and tissue damage in *Drosophila*. *Dis. Model. Mech.* **1,** 144–154 (2008).
14. Staley, B. K. & Irvine, K. D. Warts and Yorkie mediate intestinal regeneration by influencing stem cell proliferation. *Curr. Biol.* **20,** 1580–1587 (2010).
15. Martin-Blanco, E. *et al.* puckered encodes a phosphatase that mediates a feedback loop regulating JNK activity during dorsal closure in *Drosophila*. *Genes Dev.* **12,** 557–570 (1998).
16. Shen, H. M. & Liu, Z. G. JNK signaling pathway is a key modulator in cell death mediated by reactive oxygen and nitrogen species. *Free Radic. Biol. Med.* **40,** 928–939 (2006).
17. Sykiotis, G. P. & Bohmann, D. Keap1/Nrf2 signaling regulates oxidative stress tolerance and lifespan in *Drosophila*. *Dev. Cell* **14,** 76–85 (2008).
18. Finkel, T. & Holbrook, N. J. Oxidants, oxidative stress and the biology of ageing. *Nature* **408,** 239–247 (2000).
19. Owusu-Ansah, E., Yavari, A., Mandal, S. & Banerjee, U. Distinct mitochondrial retrograde signals control the G1-S cell cycle checkpoint. *Nature Genet.* **40,** 356–361 (2008).
20. Pan, D. The hippo signaling pathway in development and cancer. *Dev. Cell* **19,** 491–505 (2010).
21. Karpowicz, P., Perez, J. & Perrimon, N. The Hippo tumor suppressor pathway regulates intestinal stem cell regeneration. *Development* **137,** 4135–4145 (2010).
22. Ren, F. *et al.* Hippo signaling regulates *Drosophila* intestine stem cell proliferation through multiple pathways. *Proc. Natl Acad. Sci. USA* **107,** 21064–21069 (2010).
23. Shaw, R. L. *et al.* The Hippo pathway regulates intestinal stem cell proliferation during *Drosophila* adult midgut regeneration. *Development* **137,** 4147–4158 (2010).
24. Sun, G. & Irvine, K. D. Regulation of Hippo signaling by Jun kinase signaling during compensatory cell proliferation and regeneration, and in neoplastic tumors. *Dev. Biol.* **350,** 139–151 (2011).
25. Wu, M., Pastor-Pareja, J. C. & Xu, T. Interaction between Ras(V12) and scribbled clones induces tumour growth and invasion. *Nature* **463,** 545–548 (2010).
26. Downward, J. Targeting RAS signalling pathways in cancer therapy. *Nature Rev. Cancer* **3,** 11–22 (2003).
27. Uhlirova, M., Jasper, H. & Bohmann, D. Non-cell-autonomous induction of tissue overgrowth by JNK/Ras cooperation in a *Drosophila* tumor model. *Proc. Natl Acad. Sci. USA* **102,** 13123–13128 (2005).
28. Frei, C., Galloni, M., Hafen, E. & Edgar, B. A. The *Drosophila* mitochondrial ribosomal protein mRpL12 is required for Cyclin D/Cdk4-driven growth. *EMBO J.* **24,** 623–634 (2005).
29. Doggett, K., Grusche, F. A., Richardson, H. E. & Brumby, A. M. Loss of the *Drosophila* cell polarity regulator Scribbled promotes epithelial tissue overgrowth and cooperation with oncogenic Ras-Raf through impaired Hippo pathway signaling. *BMC Dev. Biol.* **11,** 57 (2011).

Supplementary Information is available in the online version of the paper.

Acknowledgements We thank J. Pastor-Pareja and M. Miura for comments on the manuscript; T. Sawada and K. Takino for technical support; D. Harrison, T. Orr-Weaver and H. Richardson for antibodies; T. Adachi-Yamada, U. Banerjee, D. Bohmann, F. Missirlis, M. Miura, H. Sun, T. Xu, Y. Hiromi, the Bloomington Stock Center, the Vienna *Drosophila* RNAi Center, the National Institute of Genetics Stock Center and the *Drosophila* Genetic Resource Center for fly stocks. We also thank T. Xu for encouragement. This work was supported in part by grants from the Ministry of Education, Culture, Sports, Science and Technology (MEXT) to S.O., M.E. and T.I, a Grant-in-Aid for Scientific Research on Innovative Areas from the MEXT to S.O. and T.I., the Japan Society for the Promotion of Science for Young Scientists to S.O. and M.E., the Japan Science and Technology Agency to T.I., the G-COE program for Global Center for Education and Research in Integrative Membrane Biology to S.O. and T.I.,the Fumi Yamamura Memorial Foundation for Female Natural Scientists to S.O, the Tomizawa Jun-ichi & Keiko Fund of the Molecular Biology Society of Japan for Young Scientists to S.O., the Takeda Science Foundation to S.O. and T.I., the Astellas Foundation for Research on Metabolic Disorders to T.I., the Kanae Foundation for the Promotion of Medical Science to T.I., the Senri Life Science Foundation to T.I. and a Human Frontier Science Program Career Development Award to T.I.

Author Contributions S.O., Y.S., M.E. and T.I. designed the research, S.O., Y.S., M.E., M.N., A.B. and T.I. performed experiments, S.O., Y.S., M.E. and T.I. analysed the data, and S.O. and T.I. wrote the manuscript.

Author Information Reprints and permissions information is available at www.nature.com/reprints. The authors declare no competing financial interests. Readers are welcome to comment on the online version of the paper. Correspondence and requests for materials should be addressed to T.I. (igaki@med.kobe-u.ac.jp).

LETTER

doi:10.1038/nature11494

Black mamba venom peptides target acid-sensing ion channels to abolish pain

Sylvie Diochot[1,2,3]*, Anne Baron[1,2,3]*, Miguel Salinas[1,2,3], Dominique Douguet[1,2], Sabine Scarzello[1,2]†, Anne-Sophie Dabert-Gay[1,2], Delphine Debayle[1,2], Valérie Friend[1,2,3], Abdelkrim Alloui[4,5], Michel Lazdunski[1,2] & Eric Lingueglia[1,2,3]

Polypeptide toxins have played a central part in understanding physiological and physiopathological functions of ion channels[1,2]. In the field of pain, they led to important advances in basic research[3–6] and even to clinical applications[7,8]. Acid-sensing ion channels (ASICs) are generally considered principal players in the pain pathway[9], including in humans[10]. A snake toxin activating peripheral ASICs in nociceptive neurons has been recently shown to evoke pain[11]. Here we show that a new class of three-finger peptides from another snake, the black mamba, is able to abolish pain through inhibition of ASICs expressed either in central or peripheral neurons. These peptides, which we call mambalgins, are not toxic in mice but show a potent analgesic effect upon central and peripheral injection that can be as strong as morphine. This effect is, however, resistant to naloxone, and mambalgins cause much less tolerance than morphine and no respiratory distress. Pharmacological inhibition by mambalgins combined with the use of knockdown and knockout animals indicates that blockade of heteromeric channels made of ASIC1a and ASIC2a subunits in central neurons and of ASIC1b-containing channels in nociceptors is involved in the analgesic effect of mambalgins. These findings identify new potential therapeutic targets for pain and introduce natural peptides that block them to produce a potent analgesia.

In a screen to discover new blockers of ASIC channels from animal venoms, we identified the venom of black mamba (*Dendroaspis polylepis polylepis*) as a potent and reversible inhibitor of the ASIC1a channel expressed in *Xenopus* oocytes (Fig. 1a). After purification, two active fractions were collected (Supplementary Fig. 1a, b). A partial amino-acid sequence was used to clone by degenerated PCR the corresponding complementary DNA (cDNA) from lyophilized venom (Supplementary Fig. 1c). Two isopeptides were identified and named mambalgin-1 and mambalgin-2. They are composed of 57 amino acids with eight cysteine residues, and only differ by one residue at position 4 (Supplementary Fig. 1d).

Mambalgins belong to the family of three-finger toxins[12] (Supplementary Fig. 1d, e). They have no sequence homology with either PcTx1 or APETx2, two toxins that we previously identified to target ASIC channels[13,14]. A three-dimensional model of mambalgin-1 has been established from a pool of five templates with known structures (Supplementary Fig. 1e), which shows a triple-stranded and short double-stranded antiparallel β-sheets connecting loops II and III, and loop I, respectively, the three loops emerging from the core of the toxin like fingers from a palm (Fig. 1b). The model structure presents a concave face commonly found in neurotoxins and is stabilized by four disulphide bonds with a pattern identical to that observed in the crystal structure template (Cys 1–Cys 3, Cys 2–Cys 4, Cys 5–Cys 6 and Cys 7–Cys 8; Fig. 1b and Supplementary Fig. 1f). Mambalgins show a strong positive electrostatic potential that may contribute to binding to negatively charged ASIC channels (Fig. 1c).

Mambalgins have the unique property of being potent, rapid and reversible inhibitors of recombinant homomeric ASIC1a and heteromeric ASIC1a + ASIC2a or ASIC1a + ASIC2b channels, that is, all the ASIC channel subtypes expressed in the central nervous system[15–18], with a similar potency for both isopeptides and IC_{50} values (the toxin concentration half-maximally inhibiting the current) of 55 nM, 246 nM and 61 nM, respectively (Fig. 1d). Mambalgins also inhibit human ASIC channels (Supplementary Fig. 2a). The peptides inhibit ASIC1b and ASIC1a + ASIC1b channels that are specific of sensory neurons[19] with IC_{50} values of 192 nM and 72 nM, respectively (Fig. 1e). Mambalgins, which bind to the closed and/or inactivated state of the channels (Supplementary Fig. 2b), modify the affinity for protons ($pH_{0.5act}$ shifted from 6.35 ± 0.04 to 5.58 ± 0.02, and $pH_{0.5inact}$ shifted from 7.10 ± 0.01 to 7.17 ± 0.01, $n = 4$, $P < 0.001$ and $n = 5$, $P < 0.05$, respectively; Fig. 1f) and act as gating modifier toxins. They potently inhibit native ASIC currents in spinal cord, hippocampal and sensory neurons (Fig. 1g, h and Supplementary Fig. 3). In central spinal cord neurons, mambalgin-1 (674 nM) decreased ASIC current amplitude to 13.0 ± 2.0% ($n = 14$) of the control (Fig. 1g) and reduced the excitability in response to acidic pH without unspecific effect on basal neuronal excitability (resting potential) or on the threshold and the shape of evoked or spontaneous action potentials and on spontaneous post-synaptic currents (Supplementary Fig. 4). Mambalgins had no effect on ASIC2a, ASIC3, ASIC1a + ASIC3 and ASIC1b + ASIC3 channels, as well as on TRPV1, P2X2, 5-HT_{3A}, Nav1.8, Cav3.2 and Kv1.2 channels (Supplementary Figs 5 and 6).

Most three-finger toxins, such as α-neurotoxins that block nicotinic acetylcholine receptors[20], evoke neurotoxic effects in animals. This is not the case of mambalgins, which do not produce motor dysfunction (Supplementary Fig. 7), apathy, flaccid paralysis, convulsions or death upon central injections (intrathecal or intracerebroventricular) in mice, but instead induce analgesic effects against acute and inflammatory pain (Fig. 2) that can be as strong as morphine but resistant to naloxone, with much less tolerance (Fig. 3a) and no respiratory distress (Fig. 3b). In the tail-flick and paw-flick tests, intrathecal injection of mambalgin-1 (or mambalgin-2) increased the latency for the tail and paw withdrawal reflex from 8.8 ± 0.4 s and 8.0 ± 0.8 s to 23.2 ± 1.3 s and 19.8 ± 1.6 s, respectively, 7 min after injection ($n = 15$–22, $P < 0.001$) (Fig. 2a, b). The effects were completely lost in ASIC1a knockout mice (Fig. 2a, b), demonstrating the essential implication of ASIC1a-containing channels. The key involvement of ASIC channels present in central neurons in the analgesic effect of mambalgins was confirmed using intracerebroventricular injections of the peptides (Supplementary Fig. 8). Mambalgin-1 also suppressed inflammatory heat hyperalgesia and produced a strong analgesia evaluated in the paw-flick test after intraplantar injection of carrageenan (Fig. 2c), and drastically decreased acute (phase I) and inflammatory (phase II) pain assessed in the formalin test (Fig. 2d), with a potency similar to

[1]CNRS, Institut de Pharmacologie Moléculaire et Cellulaire, UMR 7275, 06560 Valbonne, France. [2]Université de Nice-Sophia Antipolis, 06560 Valbonne, France. [3]LabEx Ion Channel Science and Therapeutics, 06560 Valbonne, France. [4]Clermont Université, Université d'Auvergne, NEURO-DOL, BP 10448, F-63000 Clermont-Ferrand, France. [5]Inserm U1107, F-63001 Clermont-Ferrand, France. †Present address: IRCAN, CNRS UMR 7284, Inserm U1081, UNS, 06107 Nice, France.
*These authors contributed equally to this work.

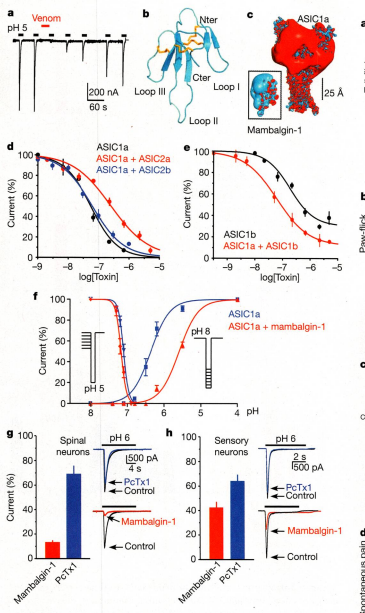

Figure 1 | Mambalgins represent a new class of three-finger toxins targeting ASIC channels. **a**, Black mamba venom (0.1 mg ml^{-1}) reversibly inhibits rat ASIC1a current expressed in *Xenopus* oocytes. **b**, Three-dimensional model of mambalgin-1 (disulphide bridges in yellow). **c**, Electrostatic properties of mambalgin-1 and human ASIC1a channel (on the basis of the three-dimensional structure of chicken ASIC1a[20]) with positive and negative isosurfaces in blue and red, respectively. **d**, **e**, Inhibition of rat ASIC channels expressed in COS-7 cells ($n = 4$–15; peptides applied before the pH drop as in **a**). Hill coefficients of 0.7–1 suggest a 1:1 stoichiometry between mambalgins and channels. **f**, Effect of mambalgin-1 on the pH-dependent activation and inactivation of ASIC1a current recorded in *Xenopus* oocytes (protocol shown in inset). **g**, **h**, Inhibition of native ASIC currents in dorsal spinal cord neurons (**g**) and DRG neurons (**h**) by mambalgin-1 (674 nM) and PcTx1 (20 nM), $n = 14$–34. Right panels: effect of mambalgin-1 on neurons expressing no PcTx1-sensitive current. ($V_h = -60$ mV in **a**, **d**, **e** and -50 mV in **f**–**h**.) Mean ± s.e.m.

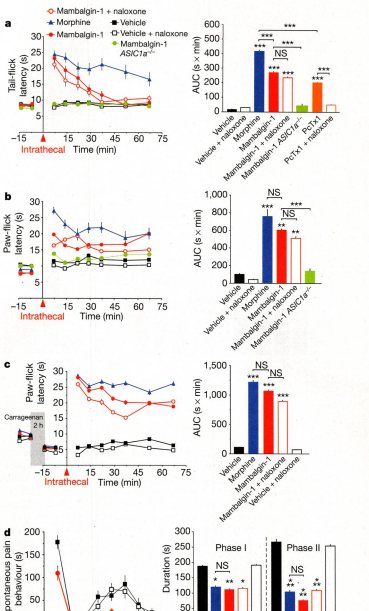

Figure 2 | Intrathecal injections of mambalgin-1 exert potent naloxone-resistant and ASIC1a-dependent analgesia in mice. **a**, **b**, Effects on acute thermal pain (46 °C) determined using tail-immersion ($n = 13$–22) and paw-immersion (**b**, $n = 5$–15) tests showing a large increase in response latencies, which is lost in *ASIC1a*$^{-/-}$ mice. **c**, Effects on inflammatory hyperalgesia induced by intraplantar carrageenan (grey bar) ($n = 8$–16). Right panels in **a**–**c**: area under curve (AUC, s × min) calculated from each mouse. **d**, Effects on first (0–10 min) and second (10–45 min) phase of formalin-induced spontaneous pain behaviour ($n = 11$–20). Naloxone was injected subcutaneously 10 min before the peptide. Comparisons are versus vehicle unless specified. Mean ± s.e.m. ***$P < 0.001$; **$P < 0.01$; *$P < 0.05$; NS, $P > 0.05$.

morphine (Fig. 2c, d). These effects were not significantly decreased by naloxone.

Mambalgins, unlike the spider peptide PcTx1 (refs 5, 14), inhibit not only homomeric ASIC1a channels but also heteromeric ASIC1a + ASIC2 channels, which are abundantly expressed in central neurons[15–17,21,22]. This led us to analyse the participation of ASIC2 in central analgesia evoked by mambalgins. Intrathecal injections of short interfering RNA (siRNA) to silence either ASIC2 (both variants a and b) or ASIC2a (Supplementary Fig. 9) induced an analgesia that was partly (ASIC2) or fully (ASIC2a) resistant to naloxone (Fig. 3c). In the presence of naloxone, central injection of mambalgin-1 in these knockdown mice had a decreased effect (Fig. 3d), consistent with a contribution of ASIC2a in the pain suppressing effect of the peptide. Compensation by homomeric ASIC1a channels[15,16], which are also

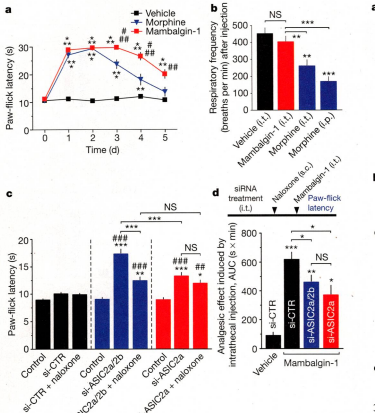

Figure 3 | The central analgesic effect of mambalgin-1 shows reduced tolerance compared with morphine, no respiratory depression and involves the ASIC2a subunit. **a**, Repeated intrathecal injections of mambalgin-1 induce less tolerance than morphine at concentrations giving the same analgesic efficacy ($n = 10$, comparison with vehicle (*) or morphine (#)). **b**, Mambalgin-1 (i.t., intrathecal) induces no respiratory depression unlike morphine (i.t., intrathecal or i.p., intraperitoneal), 0.01 and 0.4 mg per mouse, respectively; $n = 4$–7, comparison with vehicle unless specified). **c**, Paw-flick latency before (control) and after treatment with non-specific siRNA (si-CTR, $n = 24$), siRNA against ASIC2a and ASIC2b (si-ASIC2a/2b, $n = 27$), or siRNA against ASIC2a (si-ASIC2a, $n = 19$) with or without naloxone. Comparison with si-CTR (#) or untreated control (*), unless specified. **d**, Paw-flick area under curve calculated after intrathecal injection of mambalgin-1 or vehicle in siRNA-treated mice ($n = 5$–27; protocol shown in inset above; s.c., subcutaneous). Comparison with mice injected with vehicle after treatment by si-CTR, unless specified. Mean ± s.e.m. ***or ###, $P < 0.001$; ** or ##, $P < 0.01$; * $P < 0.05$; NS, $P > 0.05$.

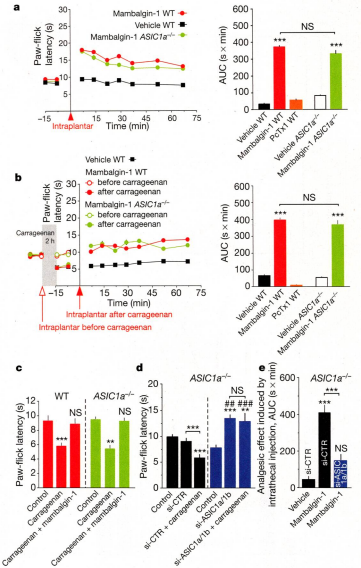

Figure 4 | Intraplantar injections of mambalgin-1 evoke peripheral analgesic effects through ASIC1b-containing channels. **a**, Effects of mambalgin-1 on acute thermal pain (46 °C) in wild-type (WT) and *ASIC1a*$^{-/-}$ mice ($n = 10$–23). **b**, Effects of mambalgin-1 on carrageenan-induced hyperalgesia when injected before (open symbols) or 2 h after (filled symbols) carrageenan ($n = 7$–20). Right panels: area under curve (after carrageenan in **b**). Comparison with vehicle unless specified. **c**, Mambalgin-1 prevents inflammatory hyperalgesia when co-injected with carrageenan ($n = 7$–20, comparison with control). **d**, Paw-flick latency before (control) and after treatment with si-CTR ($n = 13$) or siRNA against ASIC1a and ASIC1b (si-ASIC1a/1b, $n = 10$) in *ASIC1a*$^{-/-}$ mice upon normal and inflammatory conditions. Comparison with si-CTR (#) or untreated control (*), unless specified. **e**, Paw-flick area under curve calculated after injection of mambalgin-1 or vehicle in siRNA-treated *ASIC1a*$^{-/-}$ mice ($n = 7$–11). Comparison with mice injected with vehicle after treatment by si-CTR, unless specified. Mean ± s.e.m. *** or ###, $P < 0.001$; ** or ##, $P < 0.01$.

blocked by mambalgin-1, as well as incomplete *in vivo* knockdown (Supplementary Fig. 9) account for the residual analgesic effect that is observed.

Because mambalgins are able to target different ASIC channel subtypes expressed in nociceptors, we tested their peripheral effect after intraplantar injections. Mambalgin-1 (unlike PcTx1) has a significant analgesic effect on acute heat pain (Fig. 4a) and reverts or prevents inflammatory hyperalgesia (Fig. 4b, c). However, this effect is clearly different from the previously described effect of central (intrathecal) injection of the peptide because it is still present in ASIC1a knockout mice (Fig. 4a–c) contrary to the central effect (Fig. 2a, b). If ASIC1a is not involved, what are then the mechanisms that support the peripheral effect of mambalgins? ASIC1b is specifically expressed in nociceptors[19,25] but its role in pain is not known. A functional expression of ASIC1b-containing channels in dorsal root ganglion (DRG) neurons is demonstrated by the effect of mambalgin-1, which blocks both ASIC1a and ASIC1b, and has more potent effects than PcTx1, which only blocks ASIC1a channels (Fig. 1h). Moreover, silencing of the ASIC1b subunit in nociceptors of ASIC1a knockout mice (that is, where only ASIC1b is present; Supplementary Fig. 9) mimicked the analgesic effect of peripheral injection of mambalgin-1 on both acute pain and inflammatory hyperalgesia, and largely decreased the effect of subsequent intraplantar injection of the peptide (Fig. 4d, e), supporting the specific participation of ASIC1b in the peripheral effect of mambalgin-1.

Our results indicate that mambalgins have analgesic effects by targeting both primary nociceptors and central neurons, but through different ASIC subtypes (Supplementary Fig. 12). After demonstrating the important role of ASIC3 in peripheral pain and sensory perception

in the skin[3,4,24], we now show that ASIC1b, but not ASIC1a, is important for cutaneous nociception and inflammatory hyperalgesia. In the central nervous system, injections of mambalgins evoke a naloxone-insensitive analgesia through an opioid-independent pain pathway involving ASIC1a + ASIC2a channels. Central injections of PcTx1, instead, evoke a naloxone-sensitive analgesia through its specific action on homomeric ASIC1a[5], and probably heteromeric ASIC1a + ASIC2b channels (Fig. 3c and ref. 22). In addition, mambalgins, unlike PcTx1 (ref. 5), maintain a potent analgesia in mice deficient for the preproenkephalin gene (Supplementary Fig. 10). These results taken together indicate that different pathways involving different subtypes of ASIC channels can lead to different types of central analgesia (opioid-sensitive or insensitive) (Supplementary Fig. 12). They also indicate that despite their capacity *in vitro* to inhibit homomeric ASIC1a and heteromeric ASIC1a + ASIC2b channels, *in vivo*, mambalgin central analgesic action is mainly targeted to neurons expressing ASIC1a + ASIC2a channels (Supplementary Fig. 11).

It is essential to understand pain better to develop new analgesics[25,26]. The black mamba peptides discovered here have the potential to address both of these aims. They show a potent role for different ASIC channel subtypes in both the central and peripheral pain pathways, providing promising new targets for therapeutic interventions against pain, and they are themselves powerful, naturally occurring, analgesic peptides of potential therapeutic value.

METHODS SUMMARY

Mambalgins were purified from *Dendroaspis polylepis polylepis* venom (Latoxan) using cation exchange and reverse phase chromatography steps. The molecular mass and peptide sequence were determined by Edman degradatation and/or tandem mass spectrometry sequencing, and used to design primers for cloning the full-length mambalgin-1 cDNA from venom. The three-dimensional structure was modelled from five templates of three-finger snake toxins. Recordings of recombinant ASIC currents were done after expression in *Xenopus laevis* oocytes[14] and COS-7 cells, and patch-clamp recordings of native ASIC currents were obtained from primary cultures of mouse dorsal spinal cord neurons[16], hippocampal neurons and rat DRG neurons. Pain behaviour experiments were performed in C57BL/6J mice after intrathecal (or intracerebroventricular) injection of mambalgins (10 μl at 34 μM), PcTx1 (10 μl at 10 μM) or morphine (Cooper, 10 μl at 3.1 mM), in the absence or in the presence of naloxone (Fluka, 2 mg kg^{-1}), and after intraplantar injection of mambalgins (10 μl at 34 μM) and PcTx1 (10 μl at 10 μM). The effects of mambalgins on acute pain were also tested in *ASIC1a*$^{-/-}$ (ref. 27) and *Penk1*$^{-/-}$ (ref. 28) mice. Inflammation was evoked by intraplantar 2% carrageenan (Sigma) or 2% formalin. *In vivo* ASIC1 and ASIC2 gene silencing experiments were performed by repeated intrathecal injections (2 μg per mouse twice a day for 3 days) of siRNAs targeting ASIC1a + b, ASIC2a + b or only ASIC2a, mixed with i-Fect (Neuromics) as previously described[4].

Full Methods and any associated references are available in the online version of the paper.

Received 21 December 2011; accepted 7 August 2012.
Published online 3 October 2012.

1. Lewis, R. J. & Garcia, M. L. Therapeutic potential of venom peptides. *Nature Rev. Drug Discov.* **2,** 790–802 (2003).
2. Terlau, H. & Olivera, B. M. Conus venoms: a rich source of novel ion channel-targeted peptides. *Physiol. Rev.* **84,** 41–68 (2004).
3. Deval, E. *et al.* Acid-sensing ion channels in postoperative pain. *J. Neurosci.* **31,** 6059–6066 (2011).
4. Deval, E. *et al.* ASIC3, a sensor of acidic and primary inflammatory pain. *EMBO J.* **27,** 3047–3055 (2008).
5. Mazzuca, M. *et al.* A tarantula peptide against pain via ASIC1a channels and opioid mechanisms. *Nature Neurosci.* **10,** 943–945 (2007).
6. Vanegas, H. & Schaible, H. Effects of antagonists to high-threshold calcium channels upon spinal mechanisms of pain, hyperalgesia and allodynia. *Pain* **85,** 9–18 (2000).
7. Schmidtko, A., Lotsch, J., Freynhagen, R. & Geisslinger, G. Ziconotide for treatment of severe chronic pain. *Lancet* **375,** 1569–1577 (2010).
8. Malmberg, A. B. & Yaksh, T. L. Effect of continuous intrathecal infusion of omega-conopeptides, N-type calcium-channel blockers, on behavior and antinociception in the formalin and hot-plate tests in rats. *Pain* **60,** 83–90 (1995).
9. Deval, E. *et al.* Acid-sensing ion channels (ASICs): pharmacology and implication in pain. *Pharmacol. Ther.* **128,** 549–558 (2010).
10. Jones, N. G., Slater, R., Cadiou, H., McNaughton, P. & McMahon, S. B. Acid-induced pain and its modulation in humans. *J. Neurosci.* **24,** 10974–10979 (2004).
11. Bohlen, C. J. *et al.* A heteromeric Texas coral snake toxin targets acid-sensing ion channels to produce pain. *Nature* **479,** 410–414 (2011).
12. Kini, R. M. & Doley, R. Structure, function and evolution of three-finger toxins: mini proteins with multiple targets. *Toxicon* **56,** 855–867 (2010).
13. Diochot, S. *et al.* A new sea anemone peptide, APETx2, inhibits ASIC3, a major acid-sensitive channel in sensory neurons. *EMBO J.* **23,** 1516–1525 (2004).
14. Escoubas, P. *et al.* Isolation of a tarantula toxin specific for a class of proton-gated Na^+ channels. *J. Biol. Chem.* **275,** 25116–25121 (2000).
15. Askwith, C. C., Wemmie, J. A., Price, M. P., Rokhlina, T. & Welsh, M. J. Acid-sensing ion channel 2 (ASIC2) modulates ASIC1 H^+-activated currents in hippocampal neurons. *J. Biol. Chem.* **279,** 18296–18305 (2004).
16. Baron, A., Voilley, N., Lazdunski, M. & Lingueglia, E. Acid sensing ion channels in dorsal spinal cord neurons. *J. Neurosci.* **28,** 1498–1508 (2008).
17. Lingueglia, E. *et al.* A modulatory subunit of acid sensing ion channels in brain and dorsal root ganglion cells. *J. Biol. Chem.* **272,** 29778–29783 (1997).
18. Waldmann, R., Champigny, G., Bassilana, F., Heurteaux, C. & Lazdunski, M. A proton-gated cation channel involved in acid-sensing. *Nature* **386,** 173–177 (1997).
19. Chen, C. C., England, S., Akopian, A. N. & Wood, J. N. A sensory neuron-specific, proton-gated ion channel. *Proc. Natl Acad. Sci. USA* **95,** 10240–10245 (1998).
20. Tsetlin, V. Snake venom alpha-neurotoxins and other 'three-finger' proteins. *Eur. J. Biochem.* **264,** 281–286 (1999).
21. Baron, A., Waldmann, R. & Lazdunski, M. ASIC-like, proton-activated currents in rat hippocampal neurons. *J. Physiol. (Lond.)* **539,** 485–494 (2002).
22. Sherwood, T. W., Lee, K. G., Gormley, M. G. & Askwith, C. C. Heteromeric acid-sensing ion channels (ASICs) composed of ASIC2b and ASIC1a display novel channel properties and contribute to acidosis-induced neuronal death. *J. Neurosci.* **31,** 9723–9734 (2011).
23. Bassler, E. L., Ngo-Anh, T. J., Geisler, H. S., Ruppersberg, J. P. & Grunder, S. Molecular and functional characterization of acid-sensing ion channel (ASIC) 1b. *J. Biol. Chem.* **276,** 33782–33787 (2001).
24. Fromy, B., Lingueglia, E., Sigaudo-Roussel, D., Saumet, J. L. & Lazdunski, M. Asic3 is a neuronal mechanosensor for pressure-induced vasodilation that protects against pressure ulcers. *Nature Med.* **18,** 1205–1207 (2012).
25. Basbaum, A. I., Bautista, D. M., Scherrer, G. & Julius, D. Cellular and molecular mechanisms of pain. *Cell* **139,** 267–284 (2009).
26. Woolf, C. J. Overcoming obstacles to developing new analgesics. *Nature Med.* **16,** 1241–1247 (2010).
27. Wemmie, J. A. *et al.* The acid-activated ion channel ASIC contributes to synaptic plasticity, learning, and memory. *Neuron* **34,** 463–477 (2002).
28. Konig, M. *et al.* Pain responses, anxiety and aggression in mice deficient in pre-proenkephalin. *Nature* **383,** 535–538 (1996).
29. Jasti, J., Furukawa, H., Gonzales, E. B. & Gouaux, E. Structure of acid-sensing ion channel 1 at 1.9 A resolution and low pH. *Nature* **449,** 316–323 (2007).

Supplementary Information is available in the online version of the paper.

Acknowledgements We are grateful to M. P. Price and M. J. Welsh for their gift of the *ASIC1a*$^{-/-}$ mice, to A. Zimmer for providing the *Penk1*$^{-/-}$ mice, to H. Schweitz and L. Beress for their gift of pre-purified peptide fractions of black mamba venom, to J. Noël for cultures of hippocampal neurons and comments, to E. Deval, P. Inquimbert, A. Delaunay and M. Christin for discussions, to C. Heurteaux and N. Blondeau for help with stereotaxic injections, to A. Lazzari for support with plethysmography, to V. Thieffin, N. Leroudier, S. Boulakirba, T. Lemaire, C. Karoutchi and G. Marrane for technical assistance, and to C. Chevance for secretarial assistance. We thank E. Bourinet, F. Rassendren and M. B. Emerit for providing the Cav3.2, P2X2 and 5-HT3A cDNAs, respectively. This work was supported by the Fondation pour la Recherche Medicale, the Association Française contre les Myopathies and the Agence Nationale de la Recherche. Part of this work has been supported by EMMAservice under European Union contract Grant Agreement number 227490 of the EC FP7 Capacities Specific Programme.

Author Contributions S.D. and A.B. conducted a large part of the experiments including the screening and high-performance liquid chromatography purification of mambalgins (S.D.) and pain experiments, analysed the data and participated to the preparation of the manuscript. M.S. conducted the cloning of mambalgin cDNA and electrophysiological experiments. D. Douguet realized the three-dimensional modelling. S.S., A.-S.D.-G. and D. Debaye performed the mass spectrometry experiments and the amino-acid sequencing. V.F. performed validation of the siRNAs and provided technical support. A.A. was associated with pain behaviour experiments. M.L. contributed to initial aspects of the work and participated in the final preparation of the manuscript. E.L. supervised the project and participated in data analysis and manuscript preparation.

Author Information Mambalgin-1 cDNA and mambalgin-1 and -2 protein sequences have been deposited in GenBank and UniProt Knowledgebase under accession numbers JX428743, B3EWQ5 and B3EWQ4, respectively. Reprints and permissions information is available at www.nature.com/reprints. The authors declare competing financial interests: details accompany the online version of the paper. Readers are welcome to comment on the online version of the paper. Correspondence and requests for materials should be addressed to A.B. (baron@ipmc.cnrs.fr) or E.L. (lingueglia@ipmc.cnrs.fr).

LETTER

doi:10.1038/nature11503

Structure-based prediction of protein–protein interactions on a genome-wide scale

Qiangfeng Cliff Zhang[1,2,3]*, Donald Petrey[1,2,3]*, Lei Deng[2,3,4], Li Qiang[5], Yu Shi[6], Chan Aye Thu[2], Brygida Bisikirska[3], Celine Lefebvre[3,7], Domenico Accili[5], Tony Hunter[6], Tom Maniatis[2], Andrea Califano[2,3,7,8] & Barry Honig[1,2,3]

The genome-wide identification of pairs of interacting proteins is an important step in the elucidation of cell regulatory mechanisms[1,2]. Much of our present knowledge derives from high-throughput techniques such as the yeast two-hybrid assay and affinity purification[3], as well as from manual curation of experiments on individual systems[4]. A variety of computational approaches based, for example, on sequence homology, gene co-expression and phylogenetic profiles, have also been developed for the genome-wide inference of protein–protein interactions (PPIs)[5,6]. Yet comparative studies suggest that the development of accurate and complete repertoires of PPIs is still in its early stages[7–9]. Here we show that three-dimensional structural information can be used to predict PPIs with an accuracy and coverage that are superior to predictions based on non-structural evidence. Moreover, an algorithm, termed PrePPI, which combines structural information with other functional clues, is comparable in accuracy to high-throughput experiments, yielding over 30,000 high-confidence interactions for yeast and over 300,000 for human. Experimental tests of a number of predictions demonstrate the ability of the PrePPI algorithm to identify unexpected PPIs of considerable biological interest. The surprising effectiveness of three-dimensional structural information can be attributed to the use of homology models combined with the exploitation of both close and remote geometric relationships between proteins.

Until now, structural information has had relatively little impact in constructing protein–protein interactomes, primarily because there is a marked difference between the number of proteins with known sequences and those with an experimentally known structure. For example, as of early 2010, the Protein Data Bank (PDB) provided structures for ~600 of the total complement of ~6,500 yeast proteins (~10%), whereas the structural coverage of protein–protein complexes is even more sparse, with only about 300 structures available out of the approximately 75,000 PPIs (<0.5%) recorded in publically available databases. However, ~3,600 additional yeast proteins have homology models in either the ModBase[10] or SkyBase[11] databases. Moreover, there were about 37,000 protein–protein complexes derived from multiple organisms in the PDB and Protein Quaternary Structure[12] (PQS) databases, which might be used as 'templates' to model PPIs. Clearly, if structure is to be useful on a large scale, it is essential that modelling of individual proteins and of complexes be exploited.

A number of studies have used structurally characterized complexes as templates to construct models of the complexes that might be formed between proteins that have been classified as having sequence and/or structural relationships to the proteins in the template[13–15]. We searched more broadly for templates, using geometric relationships between groups of secondary structure elements as revealed by structural alignment, independently of how they are classified. It has been demonstrated that even distantly related proteins often use regions of their surface with similar arrangements of secondary structure elements to bind to other proteins[16–18], suggesting the possibility of considerably expanding the number of putative PPIs that can be identified. It is likely that further expansion can be achieved if interactions involving unstructured regions of proteins are taken into account, but these are not considered in this work.

Our approach to the prediction of PPIs is embodied in an algorithm we have named PrePPI (predicting protein–protein interactions), which combines structural and non-structural interaction clues using Bayesian statistics (see Fig. 1 and Methods for details). The structural component of PrePPI involves a number of steps. Briefly, given a pair of query proteins (QA and QB), we first use sequence alignment to identify structural representatives (MA and MB) that correspond to either their experimentally determined structures or to homology models. We then use structural alignment to find both close and remote structural neighbours (NA_1 and NB_1) of MA and MB (an average of ~1,500 neighbours are found for each structure). Whenever two (for example, NA_1 and NB_1) of the over 2 million pairs of neighbours of MA and MB form a complex reported in the PDB, this defines a template for modelling the interaction of QA and QB. Models of the complex are created by superimposing the representative structures on their corresponding structural neighbours in the template (that is, MA on NA_1 and MB on NB_1). This procedure produces about 550 million 'interaction models' for about 2.4 million PPIs involving about 3,900 yeast proteins, and about 12 billion models for about 36 million PPIs involving about 13,000 human proteins. Note that an interaction model is based on structure-based sequence alignments of query proteins to their individual templates (Supplementary Fig. 1) and that we do not construct a three-dimensional model of each complex because the scoring of so many individual complexes would be prohibitively time consuming using standard energy functions (for example, as used in docking[19]).

Once an interaction model has been created, it is evaluated using a combination of five empirical scores that measure properties derived from alignments of the individual monomers to their templates (Supplementary Fig. 1). The first score, SIM, depends on the structural similarity between models of the two query proteins (that is, MA and MB) and those in the template complex (that is, NA_1 and NB_1). The next two scores determine whether the interface in the template complex actually exists in the model. They are calculated as SIZ, the number, and COV, the fraction, of interacting residue pairs in the template (for example, NA_1–NB_1) that align to some pair of residues in the model (MA–MB). The final two scores reflect whether the residues that appear in the model interface have properties consistent with those that mediate known PPIs (for example, residue type, evolutionary conservation, or statistical propensity to be in protein–protein interfaces). This information is obtained from three publically available servers that predict interfacial residues based on the sequence and structure of the

[1]Howard Hughes Medical Institute, Columbia University, New York, New York 10032, USA. [2]Department of Biochemistry and Molecular Biophysics, Columbia University, New York, New York 10032, USA. [3]Center for Computational Biology and Bioinformatics, Columbia Initiative in Systems Biology, Columbia University, New York, New York 10032, USA. [4]Department of Computer Science and Technology, Tongji University, Shanghai 201804, China. [5]Naomi Berrie Diabetes Center, Department of Medicine, College of Physicians & Surgeons of Columbia University, New York, New York 10032, USA. [6]Molecular and Cell Biology Laboratory, The Salk Institute for Biological Studies, La Jolla, California 92037, USA. [7]Institute of Cancer Genetics, Columbia University, New York, New York 10032, USA. [8]Department of Biomedical Informatics, Columbia University, New York, New York 10032, USA.
*These authors contributed equally to this work.

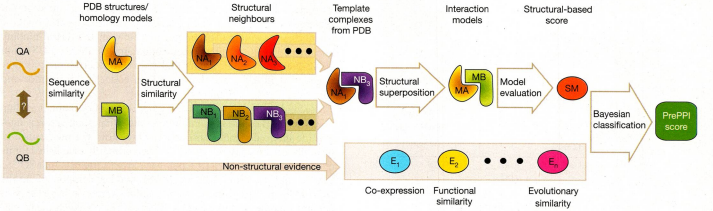

Figure 1 | Predicting protein–protein interactions using PrePPI. Given a pair of query proteins that potentially interact (QA, QB), representative structures for the individual subunits (MA, MB) are taken from the PDB, where available, or from homology model databases. For each subunit we find both close and remote structural neighbours. A 'template' for the interaction exists whenever a PDB or PQS structure contains a pair of interacting chains (for example, NA_1–NB_3) that are structural neighbours of MA and MB, respectively. A model is constructed by superposing the individual subunits, MA and MB, on their corresponding structural neighbours, NA_1 and NB_3. We assign five empirical-structure-based scores to each interaction model (Supplementary Fig. 1) and then calculate a likelihood for each model to represent a true interaction by combining these scores using a Bayesian network (Supplementary Fig. 2) trained on the HC and the N interaction reference sets. We finally combine the structure-derived score (SM) with non-structural evidence associated with the query proteins (for example, co-expression, functional similarity) using a naive Bayesian classifier.

individual subunits of the model[20–22]. These scores are calculated as OS, which is identical to SIZ but with the additional requirement that both residues in an interacting pair of the template align to predicted interfacial residues in MA and MB, and OL_n the number of template interfacial residues that align to predicted interfacial residues in MA and MB. We note that although the interaction models produced by our procedure can reveal the approximate locations of potential interfaces, they will not, in general, be accurate at atomic resolution.

The five empirical scores are combined using a Bayesian network (Supplementary Fig. 2) to yield a likelihood ratio (LR) that a candidate protein–protein complex represents a true interaction (see Methods). The network is trained on positive and negative 'gold standard' reference data sets. Similar to two recent studies[23,24], we combine interaction data from multiple databases to ensure a broad coverage of true interactions. We divide these sets into high-confidence (HC) and low-confidence (LC) subsets (Supplementary Table 1); the HC sets contain 11,851 yeast interactions and 7,409 human interactions that have more than one publication supporting their existence; interactions with only one supporting publication compose the LC set. All potential PPIs in a given genome not in the HC plus LC set form the negative (N) reference set. Using the Bayesian network classifier trained on the yeast HC set, we select the best interaction model with the highest LR for each PPI.

To assess quantitatively the performance of structural modelling (SM), we compared it with a number of non-structural clues previously used to infer PPIs[24–26]: (1) essentiality of the proteins in the interacting pair; (2) co-expression level; (3) gene ontology (GO) functional similarity; (4) Munich Information Centre for Protein Sequences (MIPS) functional similarity; and (5) phylogenetic profile similarity. We used the same algorithms or data for clues 1–4 as previously described[25] but developed our own phylogenetic profile algorithm (for details, see Methods and Supplementary Table 2). Briefly, a phylogenetic profile was constructed for every protein using a set of completely resolved proteomes as references. Because interacting proteins tend to co-evolve, proteins with similar profiles are predicted to interact.

As shown in Supplementary Figs 3 and 4, SM yields comparable performance to other clues over the entire range of false positive rate (FPR) values but is considerably more effective at low FPRs (for example, FPR ≤0.1%). This is critical as, owing to the huge number of negative interactions, only very low FPR rates can produce a small enough number of false positives to be used effectively in practice. At low FPRs, SM by itself outperforms even the naive Bayesian classifiers that combine all non-structure-based clues (NS). Looking specifically at the thousands of high-confidence SM predictions in the LC and the N sets with an LR score >600 (a value used in ref. 25 and corresponding in our study to a FPR of ~0.1%; see Methods), about 70% and 50%, respectively, share GO biological terms at, or more specific than, the sixth level of the GO hierarchy, suggesting that many of these interactions are real (Supplementary Fig. 5).

As mentioned earlier, PrePPI combines structural and non-structural clues using a naive Bayesian network[24–26]. Supplementary Fig. 4 shows that the performance of PrePPI is superior to that obtained from structural and non-structural evidence alone, implying that the two sources of information are largely complementary. This point can be clearly seen in the Venn diagrams of high-confidence (LR >600) predictions shown in Supplementary Fig. 6. It is evident from the figure that combining structural and non-structural clues yields many more high-confidence predictions and identifies more interactions in the HC set than either source of information alone. As an independent test of PrePPI, we assessed its performance against one of the challenges in the 2009 Dialogue for Reverse Engineering Assessments and Methods (DREAM) workshop specifically aimed at PPI predictions[27]. As discussed in Supplementary Table 3, PrePPI outperformed all other methods for cases where structural information is available.

We compared the performance of PrePPI to that of high-throughput experiments (Supplementary Table 4) using data provided in a detailed comparison of different high-throughput techniques reported previously[23]. We used the data sets in ref. 23 to define true positives, and compiled a new negative reference set that consists of protein pairs in which each protein is annotated as localized to a different cellular compartment (see Supplementary Fig. 7 and Methods). This was essential for comparison to experimental assays because, as constructed, our N set excludes data compiled from high-throughput experiments, and hence the FPR for experimental assays is artificially zero (see also related discussion in supplementary information in ref. 23).

As can be seen in the receiver operating characteristic (ROC) curves reported in Fig. 2a and Supplementary Fig. 8, PrePPI performance is generally comparable, although somewhat better overall, than high-throughput methods for most data sets that were tested. Figure 2b shows a Venn diagram in which the PrePPI data set is based on an LR cutoff of 600 (FPR ≈ 0.1%). Results for other LRs and additional reference sets are shown in Supplementary Fig. 9. As can be seen, many of the interactions inferred by PrePPI are different from those identified

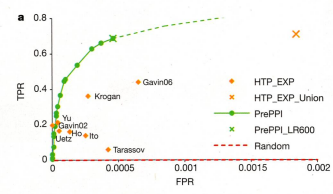

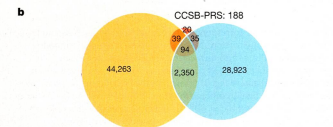

Figure 2 | ROC curve and Venn diagram for PrePPI predictions and high-throughput experiments in yeast. a, ROC curve. TPR, true positive rate. **b**, Venn diagram. The CCSB-PRS positive reference interaction set is defined in ref. 23 and described in Methods. High-throughput experiments are labelled with the first author of the relevant publication (Supplementary Table 4). The number of interactions in each set is given after the set label in the Venn diagram.

by high-throughput assays. Methods that combine both approaches may thus prove to be highly effective in expanding the coverage of PPIs.

At an LR cutoff of 600, PrePPI predicts 31,402 high-confidence interactions for yeast and 317,813 interactions for human. These, as well as predictions with lower LR scores, are available in a database from the PrePPI website (http://bhapp.c2b2.columbia.edu/PrePPI/). As a further validation of PrePPI we tested its performance on the approximately 24,000 new interactions involving human proteins that were added to public databases after August 2010 (Supplementary Table 5). Among these interactions, 1,644 are predicted by PrePPI to have an LR >600 (based on a Bayesian classifier derived from pre-2009 data on yeast), so that they essentially correspond to experimental validation of true predictions.

Specific experimental validation of 19 individual PrePPI predictions, using co-immunoprecipitation assays, was carried out in four separate laboratories, leading to confirmation of 15 of these interactions (Supplementary Figs 10–14 and Supplementary Table 6). Specifically, the investigators in each laboratory queried the PrePPI database for previously uncharacterized interactions involving proteins of interest and that, as much as possible, had relatively high SM and PrePPI scores (see Supplementary Table 6 for more information).

One set of predictions involves potential PPIs formed between the nuclear receptor peroxisome proliferator-activated receptor γ (PPAR-γ) and other transcription factors. PPAR-γ has a pivotal role in regulating glucose and lipid metabolism, the inflammatory response and tumorigenesis, and is known to heterodimerize with retinoid X receptors (RXRs) and to recruit cofactors to regulate target gene transcription. PrePPI predicts high-confidence interactions between PPAR-γ and the transcription factors LXR-β (also known as NR1H2), PAX7, PDX1, NKX2-2 and HHEX (Supplementary Table 6). Except for HHEX, all of the interactions were validated (Supplementary Fig. 10). The predicted interaction with nuclear receptor LXR-β might have been expected based on the ability of these proteins to heterodimerize through their ligand-binding domains. Nevertheless, this specific interaction had not previously been characterized and suggests a so far unrecognized convergence of signalling and metabolic pathways regulated by these two nuclear receptors. The interaction between the ligand-binding domain of PPAR-γ and the homeodomains of PAX7, PDX1 and NKX2-2 are new observations that require further studies, as they suggest that PPAR-γ may have a role in endocrine progenitor and pancreatic β-cell development.

A second set of examples involves suppressor of cytokine signalling (SOCS3), an SH2-domain-containing protein that negatively regulates cytokine-induced signal transduction. Until now, the mechanism of the inhibitory function of SOCS3 has been primarily established for its involvement in the JAK/STAT pathway. PrePPI predicts that SOCS3 forms complexes with GRB2 and RAF1, two key components in the RAS/MAPK pathway, and these interactions were confirmed experimentally (Supplementary Fig. 11A, B). PrePPI also predicts the formation of a complex between SOCS3 and BTK, a cytoplasmic tyrosine kinase important in B-lymphocyte development, differentiation and signalling, and this interaction was also validated (Supplementary Fig. 11C). The SOCS3–GRB2 interaction is predicted to be mediated by their SH2 domains, whereas the SOCS3 interaction with BTK is predicted to be mediated by an SH2–SH3 domain interaction. Analysis of the predicted binding preferences of SH2 domains as well as results on other protein families indicate that the PrePPI scoring function accounts, at least in part, for the binding preference of closely related protein domains (Supplementary Fig. 15, see also later).

A third group of novel observations involves the identification of kinases that interact with the clustered protocadherin proteins (protocadherin α, β and γ (PCDH-α, -β and -γ)). The PCDHs have six cadherin-like extracellular domains, and unique cytoplasmic domains. They assemble into large complexes at the cell surface, and associate with a variety of proteins, including signalling adaptors, kinases and phosphatases. Analysis of potential PCDH-kinase PPIs confirmed published interactions between PCDH-α and -γ with the tyrosine kinase RET, and predicted interactions with ROR2, VEGFR2 and ABL1 (Supplementary Table 6 and Supplementary Fig. 12; experiments done in mice). PrePPI predicts that these PPIs are mediated by the extracellular cadherin domains and immunoglobulin (Ig) domains, a result that was confirmed experimentally (Supplementary Fig. 12A–D). A hydrophobic residue, Phe 64, of the ROR2 Ig domain is predicted to be in the centre of the interface it forms with PCDH-α4. Mutating this Phe to an Ala, a smaller hydrophobic residue, has no detectable effect on binding, whereas mutating it to charged residues considerably weakens the interaction (Supplementary Fig. 12B, C). These results suggest that, in addition to predicting binary interactions, PrePPI has the potential to reveal novel and unsuspected interfaces.

The fourth group of experiments was carried out with the goal of identifying new components of large protein–protein complexes. We validated two previously uncharacterized interactions between the special AT-rich sequence-binding protein SATB2 and the Emerin 'proteome' complex 32, and one involving the pre-mRNA-processing factor PRPF19 and the centromere chromatin complex (Supplementary Fig. 13). It is important to emphasize that each of the PPIs detected must be confirmed through appropriate *in vivo* experiments. Taken together, however, these findings suggest that PrePPI has sufficient accuracy and sensitivity to provide a wealth of novel hypotheses that can drive biological discovery.

The accuracy and range of applicability of PrePPI, and the crucial role of structural modelling, were unanticipated, but should not come as a complete surprise. Most protein complexes in the PDB have structural neighbours that share binding properties[17], and protein interface space may well be close to 'complete' in terms of the packing orientations of secondary structure elements[18]. Moreover, these elements can be identified with geometric alignment methods[17,28], a fact that has been exploited in the approach introduced here. Although the information required to predict whether two proteins interact appears to be present in the PDB, the question has been how to mine the data.

Three key elements are responsible for the success of structural modelling and PrePPI. The first is the marked expansion in the number of interactions that can be modelled, owing to the use of both homology models and remote structural relationships. About 8,600 PDB structures but more than 31,000 models are found as representatives of at least one domain of ~14,100 human proteins. If we had only used experimentally determined structures in our analysis, a total of only ~2.5 million human PPIs (versus 36 million when homology models are used) could have been modelled. Similarly, had we limited ourselves to structural neighbours taken from the same Structural Classification of Proteins (SCOP) fold, only ~225 thousand interactions could have been modelled, as opposed to 36 million.

As might be expected, predictions based on structural modelling that use only PDB structures or close structural neighbours are more likely to recover known interactions (defined by their presence in databases) than those that only use homology models or remote structural relationships (Supplementary Fig. 16). However, the latter, on their own, yield a marked expansion in the total number of interaction models and, consequently, many more high-confidence predictions and known interactions. Most importantly, in the calculation of the PrePPI score, the huge number of low-confidence structural interaction models led to an even greater expansion in high-confidence predictions when combined with functional, evolutionary and other sources of evidence (Supplementary Fig. 16).

The second key element in our strategy is the efficiency of our scoring scheme for interaction models, which allows us to evaluate an extremely large number of models while still discriminating among closely related family members. Discrimination among complexes involving members of the same protein family—that is, specificity—is obtained from the properties of the predicted interface, for example, the statistical propensity of certain amino acids to appear in interfaces[20,21] (and, additionally, from non-structural clues; for example, are the two proteins co-expressed). As examples, our analysis of the SH2 and GTPase families shows that the structural modelling (and PrePPI scores) for these closely related proteins produce a wide range of LRs, with the higher LRs associated with a higher probability of being a known interaction (Supplementary Fig. 15).

The third element responsible for the success of PrePPI is the Bayesian evidence integration method that allows independent and possibly weak interaction clues to be combined to make reliable predictions and to improve prediction specificity (Supplementary Figs 15 and 16).

Figure 3 provides two examples of the use of remote structural relationships and homology models. In Fig. 3a, an HC set interaction of serine/threonine-protein kinase D1 (PRKD1) and protein kinase C-ε (PRKCE) is recovered by structural modelling using a complex of two proteins in the ubiquitin pathway (not kinases) as template. Note that PRKD1 and PRKCE are not sequence homologues of the two corresponding ubiquitin pathway proteins and are classified as belonging to different SCOP folds. However, the interaction model has a significant SM score (LR = 130) arising from both local structural similarity and a conserved interface. Figure 3b describes a prediction of an LC set interaction between the elongation factor 1-δ (EEF1D) and the von Hippel–Lindau tumour suppressor (VHL) using the same template as that used in Fig. 3a. Again, there is no sequence relationship between the target and the template proteins, and they are classified into different folds. Nevertheless, the interaction model has an LR of 70. We note that the EEF1D and VHL were found to interact using mass spectroscopy[29] and by co-immunoprecipitation experiments reported here (Supplementary Fig. 14).

The exploitation of homology models and of remote structural relationships implies that each new structure that is determined experimentally can be used to detect large numbers of new functional relationships, even if the protein in question is of only limited biological interest on its own. In this regard, our approach has benefitted from structural genomics initiatives, which produced a large increase in the coverage of sequence families that did not have structural representatives[30]. We note that PrePPI appears in many cases to offer a viable alternative to high-throughput experiments yielding, in addition to a likelihood of a given interaction, a model (albeit a crude one) of the domains and residues that form the relevant protein–protein interface. This should in turn facilitate the generation of experimentally testable hypotheses as to the presence of a true physical interaction. In conclusion, our study suggests the ability to add a structural 'face' for a large number of PPIs, and that structural biology can have an important role in molecular systems biology.

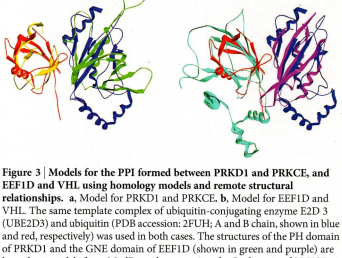

Figure 3 | Models for the PPI formed between PRKD1 and PRKCE, and EEF1D and VHL using homology models and remote structural relationships. a, Model for PRKD1 and PRKCE. **b**, Model for EEF1D and VHL. The same template complex of ubiquitin-conjugating enzyme E2D 3 (UBE2D3) and ubiquitin (PDB accession: 2FUH; A and B chain, shown in blue and red, respectively) was used in both cases. The structures of the PH domain of PRKD1 and the GNE domain of EEF1D (shown in green and purple) are homology models from ModBase; the structure of a C1 domain of PRKCE (yellow) is a homology model from SkyBase; the structure of VHL (cyan) is from PDB (accession 1LM8; V chain). In each case, the relevant homology models are structurally superimposed on one of the two templates in the UBE2D3–ubiquitin complex.

METHODS SUMMARY

Details of the PrePPI algorithm, protein datasets, and experimental validations are available in Methods.

Full Methods and any associated references are available in the online version of the paper.

Received 29 June 2011; accepted 10 August 2012.
Published online 30 September 2012.

1. Bonetta, L. Protein–protein interactions: interactome under construction. *Nature* **468,** 851–854 (2010).
2. Vidal, M., Cusick, M. E. & Barabasi, A. L. Interactome networks and human disease. *Cell* **144,** 986–998 (2011).
3. Shoemaker, B. A. & Panchenko, A. R. Deciphering protein–protein interactions. Part I. Experimental techniques and databases. *PLOS Comput. Biol.* **3,** e42 (2007).
4. Reguly, T. *et al.* Comprehensive curation and analysis of global interaction networks in *Saccharomyces cerevisiae*. *J. Biol.* **5,** 11 (2006).
5. Shoemaker, B. A. & Panchenko, A. R. Deciphering protein–protein interactions. Part II. Computational methods to predict protein and domain interaction partners. *PLOS Comput. Biol.* **3,** e43 (2007).
6. Salwinski, L. & Eisenberg, D. Computational methods of analysis of protein–protein interactions. *Curr. Opin. Struct. Biol.* **13,** 377–382 (2003).
7. von Mering, C. *et al.* Comparative assessment of large-scale data sets of protein–protein interactions. *Nature* **417,** 399–403 (2002).
8. Braun, P. *et al.* An experimentally derived confidence score for binary protein–protein interactions. *Nature Methods* **6,** 91–97 (2009).
9. Deane, C. M., Salwinski, L., Xenarios, I. & Eisenberg, D. Protein interactions: two methods for assessment of the reliability of high throughput observations. *Mol. Cell. Proteomics* **1,** 349–356 (2002).
10. Pieper, U. *et al.* MODBASE: a database of annotated comparative protein structure models and associated resources. *Nucleic Acids Res.* **34,** D291–D295 (2006).
11. Mirkovic, N., Li, Z., Parnassa, A. & Murray, D. Strategies for high-throughput comparative modeling: applications to leverage analysis in structural genomics and protein family organization. *Proteins* **66,** 766–777 (2007).
12. Henrick, K. & Thornton, J. M. PQS: a protein quaternary structure file server. *Trends Biochem. Sci.* **23,** 358–361 (1998).

13. Aloy, P. & Russell, R. B. Interrogating protein interaction networks through structural biology. *Proc. Natl Acad. Sci. USA* **99,** 5896–5901 (2002).
14. Lu, L., Lu, H. & Skolnick, J. MULTIPROSPECTOR: an algorithm for the prediction of protein–protein interactions by multimeric threading. *Proteins* **49,** 350–364 (2002).
15. Davis, F. P. *et al.* Protein complex compositions predicted by structural similarity. *Nucleic Acids Res.* **34,** 2943–2952 (2006).
16. Tuncbag, N., Gursoy, A., Guney, E., Nussinov, R. & Keskin, O. Architectures and functional coverage of protein–protein interfaces. *J. Mol. Biol.* **381,** 785–802 (2008).
17. Zhang, Q. C., Petrey, D., Norel, R. & Honig, B. H. Protein interface conservation across structure space. *Proc. Natl Acad. Sci. USA* **107,** 10896–10901 (2010).
18. Gao, M. & Skolnick, J. Structural space of protein–protein interfaces is degenerate, close to complete, and highly connected. *Proc. Natl Acad. Sci. USA* **107,** 22517–22522 (2010).
19. Wass, M. N., Fuentes, G., Pons, C., Pazos, F. & Valencia, A. Towards the prediction of protein interaction partners using physical docking. *Mol. Syst. Biol.* **7,** 469 (2011).
20. Chen, H. L. & Zhou, H. X. Prediction of interface residues in protein–protein complexes by a consensus neural network method: test against NMR data. *Proteins* **61,** 21–35 (2005).
21. Liang, S., Zhang, C., Liu, S. & Zhou, Y. Protein binding site prediction using an empirical scoring function. *Nucleic Acids Res.* **34,** 3698–3707 (2006).
22. Zhang, Q. C. *et al.* PrePUs: a web server for predicting protein interfaces using structural neighbors. *Nucleic Acids Res.* **39,** 283–287 (2011).
23. Yu, H. *et al.* High-quality binary protein interaction map of the yeast interactome network. *Science* **322,** 104–110 (2008).
24. Lefebvre, C. *et al.* A human B-cell interactome identifies MYB and FOXM1 as master regulators of proliferation in germinal centers. *Mol. Syst. Biol.* **6,** 377 (2010).
25. Jansen, R. *et al.* A Bayesian networks approach for predicting protein–protein interactions from genomic data. *Science* **302,** 449–453 (2003).
26. von Mering, C. *et al.* STRING: known and predicted protein–protein associations, integrated and transferred across organisms. *Nucleic Acids Res.* **33,** D433–D437 (2005).
27. Stolovitzky, G., Prill, R. J. & Califano, A. Lessons from the DREAM2 challenges. *Ann. NY Acad. Sci.* **1158,** 159–195 (2009).
28. Keskin, O., Nussinov, R. & Gursoy, A. PRISM: protein–protein interaction prediction by structural matching. *Methods Mol. Biol.* **484,** 505–521 (2008).
29. Ewing, R. M. *et al.* Large-scale mapping of human protein–protein interactions by mass spectrometry. *Mol. Syst. Biol.* **3,** 89 (2007).
30. Levitt, M. Nature of the protein universe. *Proc. Natl Acad. Sci. USA* **106,** 11079–11084 (2009).

Supplementary Information is available in the online version of the paper.

Acknowledgements This work is supported by National Institutes of Health grants GM030518 and GM094597 (B.H.), CA121852 (A.C. and B.H.), DK057539 (D.A.), CA082683 (T.H.), R01NS043915 (T.M.). L.D. thanks the China Scholarship Council scholarship 2010626059. We thank U. Pieper from A. Sali's laboratory for help with ModBase, and H. Lee for help with SkyBase.

Author Contributions Q.C.Z., D.P., A.C. and B.H. designed the research; Q.C.Z. performed the computational work; Q.C.Z., D.P., A.C. and B.H. analysed the data; L.D. set up the PrePPI web server, L.Q., Y.S., C.A.T. and B.B. performed co-immunoprecipitation studies, Q.C.Z., D.P., A.C. and B.H. wrote the paper including text from C.L., D.A., T.H. and T.M.

Author Information Reprints and permissions information is available at www.nature.com/reprints. The authors declare no competing financial interests. Readers are welcome to comment on the online version of the paper. Correspondence and requests for materials should be addressed to A.C. (califano@c2b2.columbia.edu) or B.H. (bh6@columbia.edu).

LETTER

doi:10.1038/nature11496

Clonal allelic predetermination of immunoglobulin-κ rearrangement

Margarit Farago[1]*, Chaggai Rosenbluh[1]*, Maya Tevlin[1]†*, Shira Fraenkel[1], Sharon Schlesinger[1], Hagit Masika[1], Masha Gouzman[1], Grace Teng[2], David Schatz[2,3], Yoach Rais[4], Jacob H. Hanna[4], Alexander Mildner[5], Steffen Jung[5], Gustavo Mostoslavsky[6], Howard Cedar[1] & Yehudit Bergman[1]

Although most genes are expressed biallelically, a number of key genomic sites—including immune and olfactory receptor regions—are controlled monoallelically in a stochastic manner, with some cells expressing the maternal allele and others the paternal allele in the target tissue[1,2]. Very little is known about how this phenomenon is regulated and programmed during development. Here, using mouse immunoglobulin-κ (*Igκ*) as a model system, we demonstrate that although individual haematopoietic stem cells are characterized by allelic plasticity, early lymphoid lineage cells become committed to the choice of a single allele, and this decision is then stably maintained in a clonal manner that predetermines monoallelic rearrangement in B cells. This is accompanied at the molecular level by underlying allelic changes in asynchronous replication timing patterns at the κ locus. These experiments may serve to define a new concept of stem cell plasticity.

The κ locus undergoes monoallelic rearrangement in B cells. To study the developmental programming of this allelic exclusion event, we used mice carrying a normal murine constant region (mCκ) on one allele and a human constant region (hCκ) on the other[3], or *Mus musculus*/*Mus castaneous* hybrid mice (C57BL/6/*M. castaneous* (B6/Cast)), and isolated interleukin-7 (IL-7)-dependent pre-B cell clones (Supplementary Figs 1 and 2) from fetal liver. Although pre-B cells themselves have not yet undergone rearrangement at this locus, a number of different studies have suggested that they may already be programmed to direct the process of κ rearrangement that occurs after differentiation[4,5]. To test this hypothesis, we transferred these single-cell pre-B clones to medium lacking IL-7, thereby inducing them to undergo rearrangement (Supplementary Fig. 2c), as occurs in normal B cells[6]. Using specific mCκ and hCκ polymerase chain reaction (PCR) primers (Supplementary Table 1) to pick up the RNA products of rearranged loci, we were able to measure independently the extent of recombination for each allele (Fig. 1a). Notably, even though the original pool of pre-B cells was capable of recombining both alleles equally, individual single-cell clones were found to undergo rearrangement almost exclusively on a single allele. Clone 7, for example, was mainly able to rearrange the hCκ allele, whereas clone 10 had the alternative phenotype, with all rearrangements apparently occurring on the mCκ allele.

To test whether this is also true under normal conditions *in vivo*, we used the same hCκ/mCκ pre-B-cell clones to reconstitute the B-cell compartment of severe combined immunodeficiency (SCID) mice, and then isolated $B220^+$ splenic cells 3 weeks after the original injection. In mice reconstituted with clone 7, we found that almost 100% of the rearrangement events occurred on the hCκ allele. In contrast, *in vivo* B cells derived from clone 10 predominantly expressed mCκ (Fig. 1b), and similar allele-specific results were also obtained using pre-B-cell clones from B6/Cast hybrid mice for reconstitution (Fig. 1c). These experiments show that allelic choice is clonally maintained in pre-B cells, and that this ultimately restricts the selection of alleles for recombination in all derivative B cells.

We next attempted to understand the molecular basis for this phenomenon by examining chromatin structure. Allele-specific chromatin immunoprecipitation (ChIP) analysis on pre-B-cell clone 7 indicated that acetylated histone 3 (H3ac) is preferentially enriched on the hCκ allele, consistent with our findings that this same allele is the one preferred for rearrangement after differentiation. Reciprocally, it is the alternative mCκ allele that is highly enriched in clone 10 (Fig. 2a). To explore allelic differences at other sites along the κ locus, we generated additional pre-B-cell clones from B6/Cast hybrid mice, and these revealed a similar allelic pattern of histone acetylation. Furthermore, analysis of these cells demonstrated that the same open allele is also marked with trimethylated histone 3 lysine 4 (H3K4me3) over the Jκ domain (Fig. 2b, c, Supplementary Fig. 3 and Supplementary Table 2).

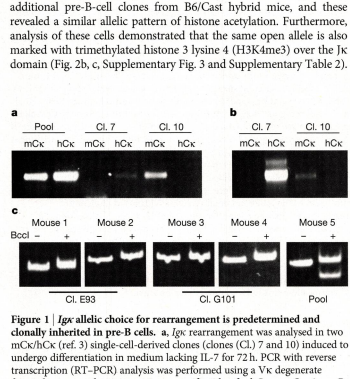

Figure 1 | *Igκ* allelic choice for rearrangement is predetermined and clonally inherited in pre-B cells. a, *Igκ* rearrangement was analysed in two mCκ/hCκ (ref. 3) single-cell-derived clones (clones (Cl.) 7 and 10) induced to undergo differentiation in medium lacking IL-7 for 72 h. PCR with reverse transcription (RT–PCR) analysis was performed using a Vκ degenerate forward primer and a reverse primer, specific either for hCκ or mCκ. A pre-B-cell pool was used as a control. **b**, **c**, Cells (10^7) from hCκ/mCκ (**b**) or B6/Cast (**c**) single-cell-derived pre-B-cell clones were used to reconstitute the B-cell compartment of SCID mice. As a control, SCID mice were injected with pools of pre-B cells. RT–PCR was performed on RNA derived from $B220^+$ splenic cells 3–4 weeks after reconstitution. The allelic nature of the each rearrangement product was analysed using either allele-specific primers (hCκ/mCκ) or an allele-specific restriction site, BclI, which only recognized the Cast allele (B6/Cast).

[1]Department of Developmental Biology and Cancer Research, Institute for Medical Research Israel–Canada, Hebrew University Medical School, POB 12272, Ein Kerem, Jerusalem 91120, Israel. [2]Department of Immunobiology, Yale University School of Medicine, 300 Cedar Street, PO Box 208011, New Haven, Connecticut 06520, USA. [3]Howard Hughes Medical Institute, Yale University School of Medicine, 300 Cedar Street, New Haven, Connecticut 06520, USA. [4]Department of Molecular Genetics, Weizmann Institute of Science, Rehovot 76100, Israel. [5]Department of Immunology, Weizmann Institute of Science, Rehovot 76100, Israel. [6]Department of Medicine, Center for Regenerative Medicine (CReM), Boston University School of Medicine, 650 Albany Street, Suite 513, Boston, Massachusetts 02118, USA. †Present address: Laboratory of Developmental Genetics, Rockefeller University, 1230 York Avenue, New York, New York 10065, USA.
*These authors contributed equally to this work.

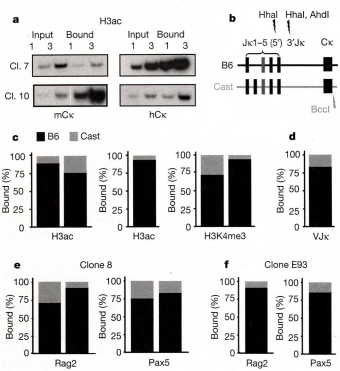

Figure 2 | *Igκ*-allele-specific ChIP analyses in pre-B cells. **a**, ChIP analysis with anti-H3Ac on chromatin derived from pre-B-cell clones 7 and 10 (hCκ/mCκ). Precipitated DNA was amplified through semi-quantitative PCR using primers specific for either hCκ or mCκ. Data from input and bound fractions were obtained using two concentrations of DNA (onefold and threefold). **b**, Schematic view of the κ locus in pre-B-cell clones from B6/Cast F1 mice. Allele-specific restriction sites generated by single-nucleotide polymorphisms (SNPs) between the two alleles were used to distinguish between them; HhaI and AhdI recognize only the B6 allele, whereas BccI recognizes the Cast allele. **c**, ChIP analysis on chromatin derived from a B6/Cast single-cell-derived pre-B clone (clone 8) using antibodies to H3ac or H3K4me3. Preferential enrichment (as indicated) was determined by digesting the chromatin input and bound fractions with HhaI or BccI (shown in **b**) or by direct sequencing. Quantification of results is shown in the histograms. The bars of the histograms represent measurements of gel densitometry (left) or direct sequencing (20 molecules of the input and bound fractions) (right). **d**, Preferential rearrangement of one allele after removal of IL-7 from the medium (60 molecules were sequenced). **e**, **f**, Preferential enrichment of Rag2 or Pax5 in clone 8 (**e**) and E93 (**f**) was determined by amplifying the 3′ Jκ region followed by digesting the input and bound chromatin fractions with the indicated restriction enzymes (**e**, left columns, and **f**), or by sequencing (**e**, right columns, 20 molecules were sequenced from the input and bound fractions). Quantification of results is shown in the histograms.

In all cases, the acetylated allele seems to be the preferred target for rearrangement (Fig. 2d).

Recombination itself is carried out by the proteins Rag1 and Rag2, and previous results demonstrated that Rag2 is already bound to the Jκ region in pre-B cells[7]. With this in mind, we did a ChIP analysis on chromatin from individual clones and used either restriction enzymes or sequence analysis to distinguish between the two alleles. Notably, we found that Rag2 always binds preferentially to the acetylated allele (Fig. 2e, f and Supplementary Fig. 4), perhaps because of its inherent ability to specifically identify nucleosomes labelled with H3K4me3 (refs 8, 9). In keeping with this idea, the same open allele was also preferentially marked with Pax5 (Fig. 2e, f), a protein that binds to well-characterized *cis*-acting elements known to be required for demethylation and rearrangement[10,11]. Taken together, these experiments demonstrate that the κ alleles are clonally maintained in a fixed differential configuration in pre-B cells, with one allele specifically opened and primed for rearrangement.

Because these chromatin marks seem to be maintained differentially on essentially identical alleles over many cell generations, it appears that there must be some basic underlying feature that directs this process. DNA replication timing is an important domain-wide epigenetic mark that is correlated with gene expression. Early replicating DNA is closely linked with gene transcription, whereas late replication is associated with gene repression. Furthermore, many monoallelically expressed genes are known to replicate asynchronously[12]. It has been proposed that this property can be clonally transmitted and thus serve as a form of epigenetic memory in proliferating somatic cells[13].

Even though the rearranged allele in B cells is always early replicating[2], there is as yet no direct proof that the presence of this mark in pre-B cells can predict which allele will be the first to undergo recombination after differentiation. To address this question, we carried out replication time analysis on a number of individual pre-B-cell clones by pulsing with bromodeoxyuridine (BrdU), fractionating S-phase cells, and then isolating the BrdU DNA for gene-specific real-time PCR[2] (Fig. 3). In clone 7, we found that the hCκ allele replicates earlier than the mouse allele, whereas in clone 10 it is the mCκ allele that replicates early. These results show that there is a one-to-one correlation between allele-specific early replication, histone acetylation, and the predisposition to undergo rearrangement after differentiation to B cells.

It has been demonstrated that replication timing itself strongly influences the repackaging of chromatin after DNA synthesis, with deacetylated histones being assembled onto DNA that replicates in late S phase, whereas early replicating DNA is differentially repackaged with nucleosomes containing acetylated histones[14–16]. It is thus not difficult to imagine how asynchronous replication itself may cause the two κ alleles to be in different configurations within the same cell. Furthermore, as domain-wide replication timing is itself controlled by histone acetylation at origin modules[17], this same mechanism may also explain how differential replication can be autonomously maintained over many cell generations[18].

The κ locus replicates asynchronously in embryonic stem (ES) cells, and this same pattern is also observed in a wide range of different somatic cell types[2,15]. Because in some pre-B-cell clones the paternal κ allele replicates early whereas in others it replicates late, it is clear that there must be a stage in development at which these patterns become clonally fixed. To trace this process, we first analysed the κ locus for clonal asynchronous replication in ES cells. This was accomplished by growing cells carrying the Rosa26 marker on one allele of chromosome 6 and using fluorescence *in situ* hybridization (FISH) probes to identify this locus[19]. A polyclonal population of ES cells shows that in 50% of nuclei the early κ allele is associated with the Rosa26 marker, whereas the other 50% show the same allele replicating late. Notably,

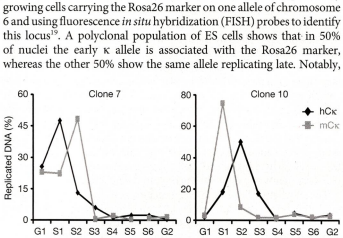

Figure 3 | Asynchronous *Igκ* replication. Replication timing was analysed by cell-cycle fractionation of BrdU-labelled clones 7 and 10 (see Methods). The κ locus was amplified by PCR using specific primers for hCκ (black) or mCκ (grey). PCR analysis of a control region (mouse globin) showed a completely synchronous replication pattern (data not shown). Graphs represent quantification of gel panels shown below.

all single-cell-derived ES subclones show this same bimodal pattern (Supplementary Table 3 and Supplementary Fig. 5), indicating that although the κ locus always replicates asynchronously in these cells, the replication-time mode for each allele is not maintained in a clonal manner, as opposed to fibroblasts (Supplementary Table 3). This same form of allelic plasticity in ES cells has also been observed for the X chromosome[20], as well as other monoallelic loci[21].

On the basis of this idea, we next tried to determine when during B-cell development the clonal choice of allele is established at the functional level. To this end, early haematopoietic stem cells (HSCs) from the hCκ/mCκ hybrid mice were isolated, infected with a lentiviral vector that integrates stochastically at numerous sites in the genome[22],

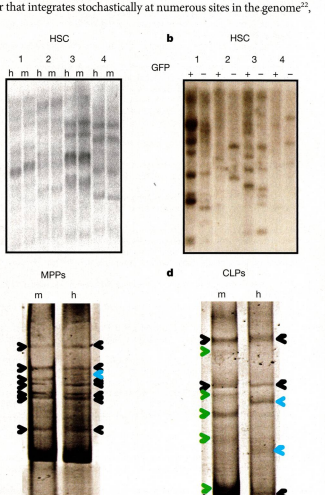

Figure 4 | Establishment of *Igκ* allelic choice. **a**, HSCs were isolated from hCκ/mCκ mouse bone marrow and infected with lentiviral vector expressing GFP. SCID mice were reconstituted with GFP-expressing cells, spleens were extracted 2–3 months later, and hCκ- and mCκ-expressing B cells were separated by FACS. DNA was digested with BamHI and subjected to Southern blot analyses using a fragment recognizing the WPRE element in the lentiviral construct as a radioactive probe. **b**, SCID mice were reconstituted with DS-Red-infected HSCs extracted from $GFP^{+/-}$ female mice in which the GFP construct has been inserted into the X chromosome. Splenic B cells were sorted for GFP^+ and GFP^- cells and viral integration sites were analysed as in **a**. **c**, **d**, MPPs (**c**) or CLPs (**d**) were isolated from the bone marrow of hCκ/mCκ mice and treated as in **a**. SCID mice were reconstituted with GFP-expressing cells and FACS-sorted splenic hCκ- and mCκ-expressing B cells were analysed for viral integration using linear-amplification-mediated PCR (LAM-PCR)[30]. **c**, **d**, Integration identical in hCκ- and mCκ-expressing cells is indicated by black arrows; integration specific for mCκ is indicated by green arrows; and integration specific for hCκ is indicated by blue arrows.

and then used to reconstitute the immune system in SCID mice. After 3 months, B cells were isolated from the spleen and subjected to fluorescence-activated cell sorting (FACS) to separate cells that express hCκ from those that express mCκ. DNA was isolated from these two cell fractions, and subjected to Southern blot analysis to identify viral integration sites (Fig. 4a and Supplementary Fig. 6a). This analysis showed that hCκ and mCκ cells have identical integration-site patterns, indicating that individual HSCs do not have a fixed predetermined allelic pattern at the κ locus, but rather seem to maintain the potential to choose either allele.

As an internal control for these experiments, we reconstituted SCID mice with virally infected HSCs from female animals containing a GFP expression marker on one of their X chromosomes[23] and then isolated splenic B cells. Because this reporter gene is on the X chromosome, we could separate out GFP^+ and GFP^- B-cell populations. Both fractions showed distinct viral integration patterns (Fig. 4b and Supplementary Fig. 6b). Thus, whereas the allelic choice of X chromosome is already set up in adult HSCs, presumably as a result of a commitment made during early development, the κ locus retains plasticity in these same cells.

We next carried out similar tracing experiments on multipotent progenitors (MPPs) and, in this case also, individual cells were able to choose either allele (Fig. 4c and Supplementary Fig. 6c). In contrast, hCκ and mCκ cell populations derived from common lymphoid precursors (CLPs) showed a mixed pattern, with some integration bands coming from cells that were already committed to one particular κ allele, whereas other bands were seen in both hCκ and mCκ expressers, and were thus representative of cells that had not yet made a commitment (Fig. 4d and Supplementary Fig. 6d). As expected, pro-B cells had already chosen a fixed allele (Supplementary Fig. 7), consistent with our observations that histone acetylation, H3K4 methylation and Rag2 allelic binding are already set up in a clonal manner at this stage of development (Supplementary Fig. 8).

We next asked whether the transition from plasticity to commitment at the functional level is also associated with underlying changes at the epigenetic level. To this end, we isolated HSCs, MPPs and CLPs from mice carrying a large deletion on one allele of the *Tcrb* gene[24], and cultured them to generate single-cell subclones. Using double-label FISH on interphase nuclei, we analysed asynchronous replication timing with a κ-specific probe, and allele specificity by probing the *Tcrb* locus in these same cells. In HSCs and MPPs, the κ locus was found to replicate asynchronously, with either allele being the early one in each subclone (Table 1 and Supplementary Fig. 9), indicating that allele specificity is constantly switching in cells at these early stages of

Table 1 | Asynchronous replication clonality during haematopoiesis.

	Cκ	
Clone	Paternal	Maternal
HSC B10	25	23
HSC C9	23	21
HSC F10	17	19
HSC H5	23	22
HSC H10	24	22
MPP B6	25	27
MPP E8	26	23
MPP F2	24	22
MPP G1	21	21
MPP H11	23	25
CLP B5	21	3
CLP C3	10	8
CLP E6	6	24
CLP E11	32	4
CLP G6	32	7
CLP H6	33	7
CLP H10	22	19

HSC, MPP and CLP single-cell clones originating from mice carrying a large deletion on the *Tcrb* paternal allele gene were assayed by FISH for asynchronous DNA replication by counting the number of Cκ single/doubles, using the Cκ and *Tcrb* probes. The number of paternal early or maternal early nuclei was determined by reference to a *Tcrb* probe.

haematopoiesis. Although several CLP subclones showed this same behaviour (CLP C3 and H10), others revealed a clonal pattern with either the paternal or maternal allele replicating early in every cell (Table 1). These clones have made a molecular commitment to one particular allele. Interestingly, FISH analysis of additional asynchronous markers on the same chromosome showed a pattern parallel to that of the κ locus (Supplementary Table 4), suggesting that both plasticity and selection of alleles operates on a chromosome-wide level.

The establishment of random asynchronous replication seems to take place in three steps during normal development. In the pre-implantation embryo, the patterns present in the gametes are erased so that these loci replicate synchronously. Asynchronous replication in the developing organism is only initiated at about the time of implantation[2,25], and experiments in ES cells suggest that these patterns are not clonally maintained at this stage (Supplementary Table 3). Rather, these cells must be constantly switching their alleles between early and late replication after each cell division. Finally, allele-specific replication becomes clonally fixed in differentiated somatic cells, generating a mixed population containing some clones that always choose the maternal allele to replicate early, with others replicating the paternal allele early (Table 1). This occurs as a chromosome-wide primary event, independent of allele-specific expression[2,13,26] (Supplementary Table 4).

This transition from the switching state to the clonally inherited state has never been studied at the functional level, to our knowledge. Our results on the κ locus show that this domain replicates in a switchable manner in HSCs, but becomes clonally fixed at the time of lymphoid commitment. Notably, we have shown that the pattern of replication can predict the choice of allele for rearrangement, both in pro-B- and pre-B-cell clones. Before this, HSCs and MPPs still retain the ability to generate clonal populations that can chose either the maternal or paternal allele for rearrangement. This suggests that these adult stem cells not only have the potential to differentiate into multiple lineages, but also to maintain the plasticity required to switch between alleles. It thus appears that HSCs themselves are derived from precursor populations tracing back to the original ES cell, and that they probably retain allelic plasticity throughout this process. These results indicate that the ability to generate allelic diversity is still present in adult stem cells, explaining how the entire B lineage compartment can be generated from a single stem cell[27]. Therefore, it seems that allelic plasticity is a common feature of stem cells regardless of their developmental potency.

Taken together, our experiments indicate that chromatin has a *cis*-acting role in organizing stable regulatory signals on the DNA that can direct subsequent allelic choice during B-lineage differentiation. This structural organization is consistent with the overall logic of haematopoiesis. As opposed to the developmental kinetics of stem cells involved in organ formation during embryogenesis, the dynamic generation of blood cells in the adult seems to be designed in a manner that allows each sub-branch of the system to operate autonomously to enable a steady supply of each cell type according to its own needs. It may be for this reason that the network is built with so many different semi-stable intermediate stages programmed for specific tasks, and it is likely that epigenetic pre-marking is what makes this entire system possible[28]. Our studies fit into this plan by showing that allelic choice is also programmed in a similar manner.

METHODS SUMMARY

Pro-B- and pre-B-cell clones were prepared from fetal liver harvested at 11.5–13.5 days post-coitum (d.p.c.) from hybrid hCκ/mCκ or B6/Cast mice. Cells were grown on an ST2 feeder layer in medium containing IL-7 (ref. 6). After 10–14 days of IL-7-mediated positive selection, cells were plated on 96-well plates in limiting dilutions to generate single-cell-derived pre-B- or pro-B-cell clones. ChIP was carried out as previously described[8,29]. IL7-dependent pre-B-cell clones were analysed for their replication timing by S-phase fractionation, as previously described[2]. HSCs, MPPs and CLPs isolated from LN3 ($V\beta1^{NT/+}$) mice[24] were FACS sorted (using cell surface markers) and single-cell cloned in 96-well plates by limiting dilution. FISH analysis was performed as previously described[2]. FACS-sorted pro-B cells, CLPs, MPPs and HSCs were purified from bone marrow of hCκ/mCκ mice and were infected with lentiviral vectors expressing GFP[22]. B cells were FACS sorted either for the expression of hCκ or mCκ, or for GFP^+ and GFP^- subpopulations. Viral insertion site patterns were detected either by Southern blot analysis or by LAM-PCR, as previously described[30].

Full Methods and any associated references are available in the online version of the paper.

Received 27 July 2011; accepted 9 August 2012.
Published online 30 September 2012.

1. Chess, A., Simon, I., Cedar, H. & Axel, R. Allelic inactivation regulates olfactory receptor gene expression. *Cell* **78,** 823–834 (1994).
2. Mostoslavsky, R. *et al.* Asynchronous replication and allelic exclusion in the immune system. *Nature* **414,** 221–225 (2001).
3. Casellas, R. *et al.* Contribution of receptor editing to the antibody repertoire. *Science* **291,** 1541–1544 (2001).
4. Goldmit, M. *et al.* Epigenetic ontogeny of the *Igκ* locus during B cell development. *Nature Immunol.* **6,** 198–203 (2005).
5. Fitzsimmons, S. P., Bernstein, R. M., Max, E. E., Skok, J. A. & Shapiro, M. A. Dynamic changes in accessibility, nuclear positioning, recombination, and transcription at the *Igκ* locus. *J. Immunol.* **179,** 5264–5273 (2007).
6. Rolink, A., Kudo, A., Karasuyama, H., Kikuchi, Y. & Melchers, F. Long-term proliferating early pre-B cell lines and clones with the potential to develop to surface Ig-positive, mitogen reactive B cells *in vitro* and *in vivo*. *EMBO J.* **10,** 327–336 (1991).
7. Ji, Y. *et al.* The *in vivo* pattern of binding of RAG1 and RAG2 to antigen receptor loci. *Cell* **141,** 419–431 (2010).
8. Matthews, A. G. *et al.* RAG2 PHD finger couples histone H3 lysine 4 trimethylation with V(D)J recombination. *Nature* **450,** 1106–1110 (2007).
9. Liu, Y., Subrahmanyam, R., Chakraborty, T., Sen, R. & Desiderio, S. A plant homeodomain in RAG-2 that binds hypermethylated lysine 4 of histone H3 is necessary for efficient antigen-receptor-gene rearrangement. *Immunity* **27,** 561–571 (2007).
10. Medvedovic, J., Ebert, A., Tagoh, H. & Busslinger, M. Pax5: a master regulator of B cell development and leukemogenesis. *Adv. Immunol.* **111,** 179–206 (2011).
11. Ramírez, J., Lukin, K. & Hagman, J. From hematopoietic progenitors to B cells: mechanisms of lineage restriction and commitment. *Curr. Opin. Immunol.* **22,** 177–184 (2010).
12. Goren, A. & Cedar, H. Replicating by the clock. *Nature Rev. Mol. Cell Biol.* **4,** 25–32 (2003).
13. Singh, N. *et al.* Coordination of the random asynchronous replication of autosomal loci. *Nature Genet.* **33,** 339–341 (2003).
14. Rountree, M. R., Bachman, K. E. & Baylin, S. B. DNMT1 binds HDAC2 and a new co-repressor, DMAP1, to form a complex at replication foci. *Nature Genet.* **25,** 269–277 (2000).
15. Zhang, J., Feng, X., Hashimshony, T., Keshet, I. & Cedar, H. Establishment of transcriptional competence in early and late S-phase. *Nature* **420,** 198–202 (2002).
16. Lande-Diner, L., Zhang, J. & Cedar, H. Shifts in replication timing actively affect histone acetylation during nucleosome reassembly. *Mol. Cell* **34,** 767–774 (2009).
17. Goren, A., Tabib, A., Hecht, M. & Cedar, H. DNA replication timing of the human β-globin domain is controlled by histone modification at the origin. *Genes Dev.* **22,** 1319–1324 (2008).
18. Lande-Diner, L. & Cedar, H. Silence of the genes—mechanisms of long term repression. *Nature Rev. Genet.* **6,** 648–654 (2005).
19. Frommer, F. *et al.* Tolerance without clonal expansion: self-antigen-expressing B cells program self-reactive T cells for future deletion. *J. Immunol.* **181,** 5748–5759 (2008).
20. Gribnau, J., Luikenhuis, S., Hochedlinger, K., Monkhorst, K. & Jaenisch, R. X chromosome choice occurs independently of asynchronous replication timing. *J. Cell Biol.* **168,** 365–373 (2005).
21. Alexander, M. K. *et al.* Differences between homologous alleles of olfactory receptor genes require the polycomb group protein Eed. *J. Cell Biol.* **179,** 269–276 (2007).
22. Mostoslavsky, G. *et al.* Efficiency of transduction of highly purified murine hematopoietic stem cells by lentiviral and oncoretroviral vectors under conditions of minimal *in vitro* manipulation. *Mol. Ther.* **11,** 932–940 (2005).
23. Ikawa, M., Yamada, S., Nakanishi, T. & Okabe, M. Green fluorescent protein (GFP) as a vital marker in mammals. *Curr. Top. Dev. Biol.* **44,** 1–20 (1999).
24. Serwold, T., Hochedlinger, K., Inlay, M. A., Jaenisch, R. & Weissman, I. L. Early TCR expression and aberrant T cell development in mice with endogenous prerearranged T cell receptor genes. *J. Immunol.* **179,** 928–938 (2007).
25. Simon, I. *et al.* Asynchronous replication of imprinted genes is established in the gametes and maintained during development. *Nature* **401,** 929–932 (1999).
26. Gimelbrant, A. A., Ensminger, A. W., Qi, P., Zucker, J. & Chess, A. Monoallelic expression and asynchronous replication of p120 catenin in mouse and human cells. *J. Biol. Chem.* **280,** 1354–1359 (2005).
27. Lemischka, I. R., Raulet, D. H. & Mulligan, R. C. Developmental potential and dynamic behavior of hematopoietic stem cells. *Cell* **45,** 917–927 (1986).
28. Cedar, H. & Bergman, Y. Epigenetics of hematopoietic cell development. *Nature Rev. Immunol.* **11,** 478–488 (2011).
29. Epsztejn-Litman, S. *et al. De novo* DNA methylation promoted by G9a prevents reprogramming of embryonically silenced genes. *Nature Struct. Mol. Biol.* **15,** 1176–1183 (2008).
30. Schmidt, M. *et al.* High-resolution insertion-site analysis by linear amplification-mediated PCR (LAM-PCR). *Nature Methods* **4,** 1051–1057 (2007).

Supplementary Information is available in the online version of the paper.

Acknowledgements We thank M. Nussenzweig for providing the $Igx^{m/m}$ mice, A. Waisman for providing the IiMOG-marked ES cells, A. G. Fisher and V. Azuara for guiding us through the replication timing analysis by S-phase fractionation assay, M. Inlay for coaching us on the purification and culturing of MPPs and CLPs, A. Wutz for providing some of the single-cell clones, Y. Smith for image analysis and L. Dempsey for sharing ideas. This work was supported by research grants from the Israel Academy of Sciences (H.C., Y.B.), National Institutes of Health (Y.B.), the Israel Cancer Research Foundation (H.C., Y.B.), the European Community 5th Framework Quality of Life Program (Y.B.), Lew Sanders (H.C.) and Norton Herrick (H.C.).

Author Contributions M.F. and C.R. designed the experiments, did the research, interpreted the results and assisted in writing the manuscript; M.T. initiated the allelic ChIP and DNA replication analyses; S.F. performed the allelic V_JK rearrangement in B6/Cast clones; S.S. studied asynchronous replication in ES cells; H.M. studied asynchronous replication in HSCs, MPPs and CLPs; G.T. and D.S. helped with Rag2 ChIP assays; Y.R. and J.H.H. generated the LN3 ($Vβ1^{NT/+}$) mice from the appropriate ES cells; M.G., A.M. and S.J. designed and helped with the MPP and CLP reconstitution, and FACS experiments; G.M. designed and helped with the HSCs, pro-B, MPP and CLP reconstitution experiments; and H.C. and Y.B. directed the study and wrote the manuscript.

Author Information Reprints and permissions information is available at www.nature.com/reprints. The authors declare no competing financial interests. Readers are welcome to comment on the online version of the paper. Correspondence and requests for materials should be addressed to H.C. (cedar@mail.huji.ac.il) or Y.B. (Yehudit.Bergman@huji.ac.il).

LETTER

doi:10.1038/nature11448

Crystal structure of the multidrug transporter P-glycoprotein from *Caenorhabditis elegans*

Mi Sun Jin[1], Michael L. Oldham[2], Qiuju Zhang[2] & Jue Chen[1,2]

P-glycoprotein (P-gp) is an ATP-binding cassette transporter that confers multidrug resistance in cancer cells[1,2]. It also affects the absorption, distribution and clearance of cancer-unrelated drugs and xenobiotics. For these reasons, the structure and function of P-gp have been studied extensively for decades[3]. Here we present biochemical characterization of P-gp from *Caenorhabditis elegans* and its crystal structure at a resolution of 3.4 ångströms. We find that the apparent affinities of P-gp for anticancer drugs actinomycin D and paclitaxel are approximately 4,000 and 100 times higher, respectively, in the membrane bilayer than in detergent. This affinity enhancement highlights the importance of membrane partitioning when a drug accesses the transporter in the membrane[4]. Furthermore, the transporter in the crystal structure opens its drug pathway at the level of the membrane's inner leaflet. In the helices flanking the opening to the membrane, we observe extended loops that may mediate drug binding, function as hinges to gate the pathway or both. We also find that the interface between the transmembrane and nucleotide-binding domains, which couples ATP hydrolysis to transport, contains a ball-and-socket joint and salt bridges similar to the ATP-binding cassette importers[5], suggesting that ATP-binding cassette exporters and importers may use similar mechanisms to achieve alternating access for transport. Finally, a model of human P-gp derived from the structure of *C. elegans* P-gp not only is compatible with decades of biochemical analysis[6–12], but also helps to explain perplexing functional data regarding the Phe335Ala mutant[13,14]. These results increase our understanding of the structure and function of this important molecule.

P-glycoprotein uses the energy from ATP hydrolysis to pump substrates across the cell membrane. Drug transport depends on ATP hydrolysis[15,16], and the ATPase activity of P-gp is stimulated by the transported drugs[17–19]. *Caenorhabditis elegans* P-gp is 46% identical to human P-gp. To ensure that this level of sequence identity translates into functional similarity, we tested whether overexpression of *C. elegans* P-gp confers cellular resistance to cytotoxic drugs known to be transported by human P-gp. Two potent anticancer drugs, actinomycin D and paclitaxel (Taxol) kill *Spodoptera frugiperda* (Sf9) cells at concentrations greater than 0.1 μM (Fig. 1a). In comparison, cells infected by recombinant baculoviruses carrying the *C. elegans* P-gp gene are resistant to these drugs in concentrations more than 1,000-fold higher (Fig. 1a and Supplementary Fig. 1a). Using detergent-purified protein, we measured whether substrates of human P-gp also stimulate the ATPase activity of *C. elegans* P-gp. Among the 30 compounds we screened, actinomycin D, paclitaxel, progesterone, dipyridamole, and valinomycin increased the ATPase activity of *C. elegans* P-gp more than fivefold (Fig. 1b and Supplementary Fig. 1b). As expected for an ATP-binding cassette (ABC) transporter, both the basal and drug-stimulated levels of ATPase activity are inhibited by vanadate (Fig. 1b). The ATPase activity plotted as a function of drug concentration shows the characteristic biphasic response: with increasing drug concentration, ATPase activity increases to a maximum value and then decreases (Fig. 1c). This behaviour has been studied extensively with human P-gp[20,21]. Like the P-glycoproteins identified in other species[22], the substrate profile of *C. elegans* P-gp only partly overlaps with that of human P-gp. Nevertheless, the similarities between their amino-acid sequences and functional properties suggest that the structure of *C. elegans* P-gp would be a reasonable starting point for a mechanistic understanding of how human P-gp functions as a multidrug pump.

P-glycoprotein is a single polypeptide with two homologous halves, each containing a transmembrane domain (TMD) and a cytoplasmic nucleotide-binding domain (NBD) (Fig. 2a). Crystals of *C. elegans* P-gp were obtained in the absence of nucleotides and transport substrates. The structure was determined at a resolution of 3.4 Å and the amino-acid assignments were confirmed by 34 selenium-labelled methionines and three mercury-labelled cysteines (Supplementary Fig. 2 and Supplementary Table 1).

Compared with the crystal structure of mouse P-gp determined at a resolution of 3.8 Å (ref. 23), that of *C. elegans* P-gp shows a similar

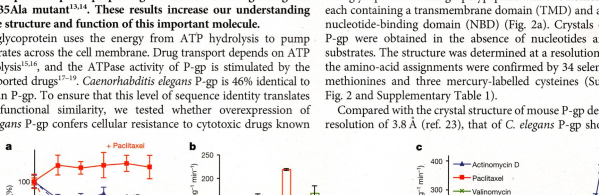

Figure 1 | *Caenorhabditis elegans* P-gp is a multidrug transporter. **a**, Cytotoxicity assay. *Spodoptera frugiperda* Sf9 cells expressing P-gp were cultured with various concentrations of actinomycin D (ActD, blue line) or paclitaxel (red line). Uninfected cells were cultured in the presence of the same drugs as controls (dashed lines). **b**, ATPase activity in the presence and absence of 1 mM orthovanadate. **c**, ATPase activity as a function of substrate concentration. The protein concentration was kept at 0.15 μM for all measurements. Data points represent the means and standard deviations of triplicate measurements from the same preparation.

[1]Department of Biological Sciences, Purdue University, Indiana 47907, USA. [2]Howard Hughes Medical Institute, West Lafayette, Indiana 47907, USA.

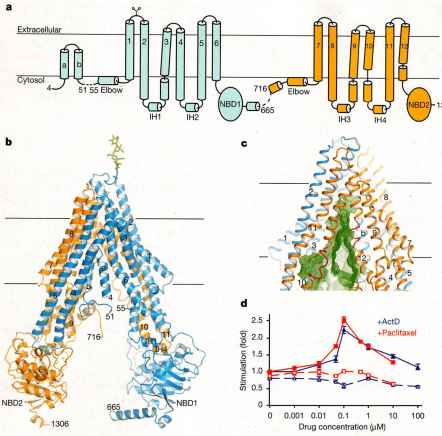

Figure 2 | The molecular architecture of P-gp. **a**, Secondary structure. **b**, Ribbon presentation. **c**, The transmembrane cavity (green mesh) open to the cytosol and continuous with the membrane inner leaflet. The loops in TM10 and TM12 are coloured red. **d**, Drug-stimulated ATPase activities in isolated membranes. The differences measured in the absence and presence of vanadate (1 mM) are plotted. Membranes from untransfected cells were used as controls (dashed lines). The data points show the means and standard deviations of three determinations from the same preparation. These results have been reproduced using different protein preparations.

inward-facing conformation (that is, one open to the cytoplasm), with a larger degree of separation between the two NBDs (Fig. 2b and Supplementary Fig. 3). Superposition of the transmembrane helices individually shows that sequence assignments of six comparable helices (TM1, TM2, TM6, TM7, TM8 and TM11) agree well. The two structures have different conformations in TM9, TM10 and TM12 and these helices thus cannot easily be compared. Helices TM3, TM4 and TM5, which can be compared, show important differences due to register shifts in model building (Supplementary Figs 4–6). As we will discuss later, these corrections in the structure are relevant to the identification of drug-interacting amino acids and an accurate definition of the NBD–TMD interface.

In the crystal structure, the drug transport pathway is open to the cytoplasmic surface and is continuous with the membrane inner leaflet (Fig. 2c). Thus, in principle, drugs could gain access to the transport pathway from the aqueous phase as well as the membrane. It has been proposed that P-gp interacts with drugs from the inner leaflet of the membrane instead of the cytoplasm[4] (the 'hydrophobic vacuum' model). On the basis of this hypothesis, P-gp would be expected to be more sensitive to drug stimulation in membranes than in detergents, because most P-gp substrates are highly concentrated in the membrane, with partition coefficients ranging from 100 to 10,000 (ref. 24). In detergents, 400 μM actinomycin D or 10 μM paclitaxel was required to obtain the maximum ATPase activity of purified P-gp (Fig. 1c). The addition of lipid molecules does not change the apparent drug affinities. Using membranes from yeast cells overexpressing *C. elegans* P-gp, we showed that both drugs stimulate the ATPase activities at a concentration of 0.1 μM (Fig. 2d), which is a 4,000-fold increase in sensitivity for actinomycin D and a 100-fold increase for paclitaxel. The degree of stimulation was lower when using the membrane sample than when using purified P-gp in detergent, probably owing to baseline activity of other cellular ATPases in the yeast cell membranes. We note that the dependence on drug concentration of ATPase stimulation in membranes matches well the concentration dependence observed in the cell protection assay (Figs 1a and 2d). The shift in drug sensitivity in membranes supports the hypothesis that drugs enter the transporter through the membrane's inner leaflet. Such a mechanism, whereby transport depends on an elevated local drug concentration due to membrane partitioning, also implies that the intrinsic affinity of drugs for the transporter itself is low, consistent with the ability of P-gp to transport many different compounds.

The structure of *C. elegans* P-gp presents an interesting variation on the theme of membrane access, in that only one lateral opening is patent (Fig. 2c). An amino-terminal helical hairpin is inserted into the other lateral opening observed in the bacterial exporter MsbA (ref. 25) and mouse P-gp[23] between TM4 and TM6 (Fig. 2b). A truncation mutant devoid of the helical hairpin functions similarly to the full-length protein in a cytotoxic assay (Supplementary Fig. 7a) but has a reduced maximum level of stimulation in an ATPase activity assay (Supplementary Fig. 7b). The dependence on drug concentration, however, is unaltered for the truncation mutant (Supplementary Fig. 7b).

Another notable feature of *C. elegans* P-gp is a discontinuity of helices TM10 and TM12 lining the lateral opening (Fig. 2c). We can think of two possible reasons why the helical secondary structure gives rise to more-disordered loop structures in this region. The first is that a breakdown of secondary structure creates a greater number of possible interactions between protein atoms and drugs entering the pathway. In other transporters where discontinuous transmembrane helices have been observed, the loops inside the membrane have been shown to bind substrates[26]. Thus, loops flanking the lateral opening could assist drug recognition and entry. The second possible reason is that these loop regions could function as flexible hinges to gate the pathway, mediate conformational changes associated with drug transport or both.

The NBD–TMD interface is important in ABC transporters because it transmits conformational changes associated with ATP hydrolysis to substrate translocation. In all ABC importers for which structures have been determined, the TMD is connected to the NBD through a 'ball-and-socket' joint[5]. This joint consists of a cytoplasmic helix from the TMD known as the coupling helix or EAA loop (the ball), which docks into a cleft on the NBD surface (the socket) (Fig. 3a). A similar

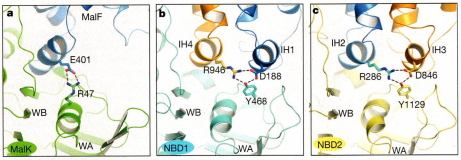

Figure 3 | Interactions between the TMDs and NBDs. a, NBD–TMD interface of the maltose importer. MalF is the transmembrane subunit and MalK is the NBD. Glu 401 is the conserved glutamate residue in the EAA loop. **b**, **c**, NBD1–TMD (**b**) and NBD2–TMD (**c**) interfaces in P-gp. Dash lines indicate the conserved salt bridges and hydrogen bonds. WA, Walker A motif; WB, Walker B motif.

structural feature is observed in P-gp, in which intracellular helices IH2 and IH4 on the TMDs resemble the coupling helices and engage the same surface of the NBDs (Fig. 3b, c). In addition to the ball-and-socket joint, ABC exporters, including P-gp, have an additional set of interactions in which IH1 and IH3 also interact with the NBDs, creating a more extensive interaction surface between the TMDs and the NBDs (Fig. 3b, c). The importance of this interface in P-gp to both structure and function is underscored by the high degree of amino-acid conservation, which approaches 80% identity between *C. elegans* and human P-gp (Supplementary Figs 8 and 9).

Multiple crystal structures of the maltose importer show that the transition between different structures is accompanied by rotations of the EAA loop inside the cleft[27]. Salt bridge interactions seem to be central to tethering a pivot point in these conformational changes; elimination of the salt bridges by double mutations results in a defective transporter and dissociation of the MalK subunit[28]. For the NBD1–TMD interface in P-gp, three highly conserved residues, Arg 946 (IH4), Asp 188 (IH1) and Tyr 468 (NBD1), are engaged in a network of salt bridge interactions (Fig. 3b). The same atomic interactions are also observed in the NBD2–TMD interface, involving residues Arg 286 (IH2), Asp 846 (IH3) and Tyr 1129 (NBD2) (Fig. 3c). It is likely that these interactions in P-gp have a role similar to the salt bridge interactions in importers such as the maltose transporter.

To assist structural and functional analysis of human P-gp, we generated a homology model of human P-gp based on the structure of the *C. elegans* P-gp determined in this study. The modelled structure is consistent with a large body of biochemical and biophysical data on human P-gp (Fig. 4 and Supplementary Fig. 10). For example, pairs of residues in the TMDs shown by cysteine mutagenesis to form disulphide bonds[6,7] are located in close proximity to each other (Fig. 4b, c). The NBD–TMD interfaces are consistent with data showing that Ala 266 in TMD1 is in close proximity to Phe 1086 in NBD2[29] and that cysteines introduced at positions 443 and 474 in NBD1 crosslink with residues 909 and 905 in TMD2, respectively[12] (Fig. 4d, e). Residues protected by drug substrates from inhibition by thiol-reactive analogues are suggested to form the drug-binding region[8–11]. In the modelled structure, 17 of the 19 residues are distributed on the surface of the drug-translocation pathway (Fig. 4f). Most of these residues are non-polar, consistent with the hydrophobic nature of the substrates. In contrast, the 17 residues that were not protected by substrate, and therefore are presumed to be not involved in drug binding[11], are scattered throughout the TMDs (Fig. 4f). Previously, the orientations of TM3, TM4 and TM5 with respect to the drug-translocation pathway predicted by arginine-scanning mutagenesis were incompatible with the crystal structure of mouse P-gp[30]. On correction of amino-acid registry (Supplementary Figs 5 and 6), these biochemical data are now consistent with the homology-modelled human P-gp (Supplementary Fig. 10).

The atomic structure of P-gp offers insights into functional data that otherwise are difficult to explain. For example, mutants that enhance

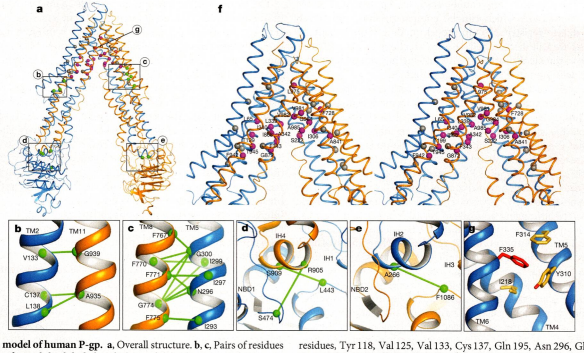

Figure 4 | A model of human P-gp. a, Overall structure. **b**, **c**, Pairs of residues in TMDs that formed disulphide bonds (green line) when mutated to cysteines[6,7]. **d**, **e**, Pairs of residues at the NBD–TMD interfaces that were crosslinked[12,29]. **f**, Stereo view of the drug transport pathway. Drug-interacting residues[8–11] are labelled and shown as magenta balls. The non-protected residues, Tyr 118, Val 125, Val 133, Cys 137, Gln 195, Asn 296, Gly 300, Tyr 310, Phe 314, Ala 729, Phe 759, Ser 766, Gly 774, Asn 842, Ala 871, Ser 943 and Phe 957, are shown in grey[31]. **g**, Phe 335 in TM6 (red) interacts with residues in TM4 and TM5 (yellow sticks), thereby stabilizing the inward-facing conformation.

drug-stimulated ATPase activity often show stronger resistance to the same drug, probably owing to an increased affinity for the drug. However, this correlation does not hold for the Phe335Ala mutant, which has a higher ATPase activity but confers lower or similar drug resistance[13,14]. The structure shows that Phe 335 is located at the apex of the drug transport pathway, making van der Waals interactions with Tyr 310 and Phe 314 in TM5, and Ile 218 in TM4 (Fig. 4a, g). These contacts will be broken in the outward-facing conformation, in which the transport pathway has to be continuous with the extracellular side of the membrane[25]. Mutating the phenylalanine to alanine, if doing so destabilized the inward-facing conformation, would facilitate the transition to the outward-facing conformation and thus give rise to higher basal and drug-stimulated ATPase activities. In this description, the Phe335Ala mutant would be reminiscent of mutants identified in the maltose transporter that allow constitutive ATP hydrolysis in the absence of the binding protein[27].

The structure of *C. elegans* P-gp provides an accurate model with which to interpret decades of functional and biochemical data on P-gp. The functional data complement the crystal structure to support a picture in which P-gp uses the energy from ATP hydrolysis to expel lipophilic molecules from the inner leaflet of the membrane. Many details of this molecule, such as how substrate binding activates the ATPase activity, how ATP hydrolysis is coupled to substrate flipping and how multiple substrates are recognized by a single transporter, remain to be elucidated.

METHODS SUMMARY

The gene encoding *C. elegans* P-gp was synthesized and optimized for expression in yeast and insect cells (Bio Basic Inc.). Native protein was expressed in *Pichia pastoris* strain SMD1163 and selenomethionine-substituted protein was expressed in Hi5 cells. The cytotoxicity assays were performed using baculovirus-infected *S. frugiperda* Sf9 cells and the ATP/NADH coupled assays were carried out at 25 °C. Crystals were obtained at 4 °C by the vapour diffusion method. Diffraction data were collected at the Advanced Photon System at Argonne National Laboratory. The initial phase was obtained by molecular replacement (PHASER, CCP4) using separate domains of Sav1866 and mouse P-gp structures as search models. The molecular replacement phase was combined with single-wavelength anomalous dispersion phasing (PHASEREP, CCP4) to identify selenomethionine-substituted residues and mercury-labelled cysteines. The model was built in COOT and refined using CNS and REFMAC5. The human P-gp model was generated using MODELLER (http://salilab.org/modeller/about_modeller.html).

Full Methods and any associated references are available in the online version of the paper.

Received 3 March; accepted 27 July 2012.
Published online 23 September 2012.

1. Juliano, R. L. & Ling, V. A surface glycoprotein modulating drug permeability in Chinese hamster ovary cell mutants. *Biochim. Biophys. Acta* **455,** 152–162 (1976).
2. Ueda, K. *et al.* The mdr1 gene, responsible for multidrug-resistance, codes for P-glycoprotein. *Biochem. Biophys. Res. Commun.* **141,** 956–962 (1986).
3. Sharom, F. J. The P-glycoprotein multidrug transporter. *Essays Biochem.* **50,** 161–178 (2011).
4. Higgins, C. F. & Gottesman, M. M. Is the multidrug transporter a flippase? *Trends Biochem. Sci.* **17,** 18–21 (1992).
5. Oldham, M. L., Davidson, A. L. & Chen, J. Structural insights into ABC transporter mechanism. *Curr. Opin. Struct. Biol.* **18,** 726–733 (2008).
6. Loo, T. W., Bartlett, M. C. & Clarke, D. M. Val133 and Cys137 in transmembrane segment 2 are close to Arg935 and Gly939 in transmembrane segment 11 of human P-glycoprotein. *J. Biol. Chem.* **279,** 18232–18238 (2004).
7. Loo, T. W., Bartlett, M. C. & Clarke, D. M. Disulfide cross-linking analysis shows that transmembrane segments 5 and 8 of human P-glycoprotein are close together on the cytoplasmic side of the membrane. *J. Biol. Chem.* **279,** 7692–7697 (2004).
8. Loo, T. W., Bartlett, M. C. & Clarke, D. M. Transmembrane segment 1 of human P-glycoprotein contributes to the drug-binding pocket. *Biochem. J.* **396,** 537–545 (2006).
9. Loo, T. W., Bartlett, M. C. & Clarke, D. M. Transmembrane segment 7 of human P-glycoprotein forms part of the drug-binding pocket. *Biochem. J.* **399,** 351–359 (2006).
10. Loo, T. W., Bartlett, M. C. & Clarke, D. M. Suppressor mutations in the transmembrane segments of P-glycoprotein promote maturation of processing mutants and disrupt a subset of drug-binding sites. *J. Biol. Chem.* **282,** 32043–32052 (2007).
11. Loo, T. W. & Clarke, D. M. Do drug substrates enter the common drug-binding pocket of P-glycoprotein through "gates"? *Biochem. Biophys. Res. Commun.* **329,** 419–422 (2005).
12. Zolnerciks, J. K., Wooding, C. & Linton, K. J. Evidence for a Sav1866-like architecture for the human multidrug transporter P-glycoprotein. *FASEB J.* **21,** 3937–3948 (2007).
13. Loo, T. W. & Clarke, D. M. Functional consequences of phenylalanine mutations in the predicted transmembrane domain of P-glycoprotein. *J. Biol. Chem.* **268,** 19965–19972 (1993).
14. Loo, T. W. & Clarke, D. M. Rapid purification of human P-glycoprotein mutants expressed transiently in HEK 293 cells by nickel-chelate chromatography and characterization of their drug-stimulated ATPase activities. *J. Biol. Chem.* **270,** 21449–21452 (1995).
15. Azzaria, M., Schurr, E. & Gros, P. Discrete mutations introduced in the predicted nucleotide-binding sites of the mdr1 gene abolish its ability to confer multidrug resistance. *Mol. Cell. Biol.* **9,** 5289–5297 (1989).
16. Hamada, H. & Tsuruo, T. Purification of the 170- to 180-kilodalton membrane glycoprotein associated with multidrug resistance. 170- to 180-kilodalton membrane glycoprotein is an ATPase. *J. Biol. Chem.* **263,** 1454–1458 (1988).
17. Al-Shawi, M. K. & Senior, A. E. Characterization of the adenosine triphosphatase activity of Chinese hamster P-glycoprotein. *J. Biol. Chem.* **268,** 4197–4206 (1993).
18. Ambudkar, S. V. Drug-stimulatable ATPase activity in crude membranes of human MDR1-transfected mammalian cells. *Methods Enzymol.* **292,** 504–514 (1998).
19. Sarkadi, B., Price, E. M., Boucher, R. C., Germann, U. A. & Scarborough, G. A. Expression of the human multidrug resistance cDNA in insect cells generates a high activity drug-stimulated membrane ATPase. *J. Biol. Chem.* **267,** 4854–4858 (1992).
20. Al-Shawi, M. K., Polar, M. K., Omote, H. & Figler, R. A. Transition state analysis of the coupling of drug transport to ATP hydrolysis by P-glycoprotein. *J. Biol. Chem.* **278,** 52629–52640 (2003).
21. Litman, T., Zeuthen, T., Skovsgaard, T. & Stein, W. D. Structure-activity relationships of P-glycoprotein interacting drugs: kinetic characterization of their effects on ATPase activity. *Biochim. Biophys. Acta* **1361,** 159–168 (1997).
22. Ambudkar, S. V., Kim, I.-W. & Booth-Genthe, C. Relationship between drugs and functional activity of various mammalian P-glycoproteins (ABCB1). *Mini Rev. Med. Chem.* **8,** 193–200 (2008).
23. Aller, S. G. *et al.* Structure of P-glycoprotein reveals a molecular basis for poly-specific drug binding. *Science* **323,** 1718–1722 (2009).
24. Gatlik-Landwojtowicz, E., Aanismaa, P. & Seelig, A. Quantification and characterization of P-glycoprotein-substrate interactions. *Biochemistry* **45,** 3020–3032 (2006).
25. Ward, A., Reyes, C. L., Yu, J., Roth, C. B. & Chang, G. Flexibility in the ABC transporter MsbA: alternating access with a twist. *Proc. Natl Acad. Sci. USA* **104,** 19005–19010 (2007).
26. Screpanti, E. & Hunte, C. Discontinuous membrane helices in transport proteins and their correlation with function. *J. Struct. Biol.* **159,** 261–267 (2007).
27. Khare, D., Oldham, M. L., Orelle, C., Davidson, A. L. & Chen, J. Alternating access in maltose transporter mediated by rigid-body rotations. *Mol. Cell* **33,** 528–536 (2009).
28. Mourez, M., Hofnung, M. & Dassa, E. Subunit interactions in ABC transporters: a conserved sequence in hydrophobic membrane proteins of periplasmic permeases defines an important site of interaction with the ATPase subunits. *EMBO J.* **16,** 3066–3077 (1997).
29. Loo, T. W., Bartlett, M. C. & Clarke, D. M. Processing mutations disrupt interactions between the nucleotide binding and transmembrane domains of P-glycoprotein and the cystic fibrosis transmembrane conductance regulator (CFTR). *J. Biol. Chem.* **283,** 28190–28197 (2008).
30. Loo, T. W., Bartlett, M. C. & Clarke, D. M. Identification of residues in the drug translocation pathway of the human multidrug resistance P-glycoprotein by arginine mutagenesis. *J. Biol. Chem.* **284,** 24074–24087 (2009).

Supplementary Information is available in the online version of the paper.

Acknowledgements We thank the beamline staff of the GM/CA CAT at the Advanced Photon System for assistance with data collection, Y.-K. Cho for assistance with protein purification and A. Davidson for comments on the manuscript. We also thank the MacKinnon laboratory for reagents and advice on the *P. pastoris* expression system. This work was supported by Howard Hughes Medical Institute (J.C.), Purdue Center for Cancer Research (NCI CCSG CA23168), and postdoctoral fellowships from the National Research Foundation of Korea and the International Human Frontier Science Program (M.S.J.).

Author Contributions All authors helped design the study and analysed the data. M.S.J. and M.L.O. determined the crystal structure. M.S.J. and Q.Z. performed the biochemical experiments. M.S.J., M.L.O. and J.C. wrote the manuscript.

Author Information Coordinates and structure factors have been deposited in the Protein Data Bank under accession number 4F4C. Reprints and permissions information is available at www.nature.com/reprints. The authors declare no competing financial interests. Readers are welcome to comment on the online version of the paper. Correspondence and requests for materials should be addressed to J.C. (chenjue@purdue.edu).

CORRECTIONS & AMENDMENTS

CORRIGENDUM

doi:10.1038/nature11235

Corrigendum: Neutralizing antibodies derived from the B cells of 1918 influenza pandemic survivors

Xiaocong Yu, Tshidi Tsibane, Patricia A. McGraw, Frances S. House, Christopher J. Keefer, Mark D. Hicar, Terrence M. Tumpey, Claudia Pappas, Lucy A. Perrone, Osvaldo Martinez, James Stevens, Ian A. Wilson, Patricia V. Aguilar, Eric L. Altschuler, Christopher F. Basler & James E. Crowe Jr

Nature **455,** 532–536 (2008); doi:10.1038/nature07231

In this Letter, the heavy-chain sequence of 1F1 was in error and has been corrected in GenBank (EU169674.2). Also, the 1947 virus tested that was not inhibited by 1F1 should have been designated A/USA/L3/1947(H1N1) rather than A/Fort Monmouth/1/1947(H1N1). In addition, 1F1 exhibits HAI activity of 1.3 $\mu g\,ml^{-1}$ (not undetectable) against A/Fort Monmouth/1/1947 virus. These errors do not affect our main conclusions. These errors have been corrected in the HTML and PDF of the original paper (particularly Table 1 and Fig. 1) and in the original Supplementary Information.

CORRIGENDUM

doi:10.1038/nature11644

Corrigendum: RNA sequencing of pancreatic circulating tumour cells implicates WNT signalling in metastasis

Min Yu, David T. Ting, Shannon L. Stott, Ben S. Wittner, Fatih Ozsolak, Suchismita Paul, Jordan C. Ciciliano, Malgorzata E. Smas, Daniel Winokur, Anna J. Gilman, Matthew J. Ulman, Kristina Xega, Gianmarco Contino, Brinda Alagesan, Brian W. Brannigan, Patrice M. Milos, David P. Ryan, Lecia V. Sequist, Nabeel Bardeesy, Sridhar Ramaswamy, Mehmet Toner, Shyamala Maheswaran & Daniel A. Haber

Nature **487,** 510–513 (2012); doi:10.1038/nature11217

In this Letter, we omitted the following accession information. The digital gene expression matrix and the Helicos single-molecule sequence data from which it was derived are available at the NCBI GEO database with accession number GSE40176. A total of 44 samples were uploaded including 12 mouse and 32 human samples. Paired RNA sequencing data for epithelial cell adhesion molecule (EPCAM) and control immunoglobulin circulating tumour cell (CTC)-Chips from two pancreatic cancer mice, four human healthy donors, and 12 human metastatic pancreatic cancer patients are included in this data set.

CORRIGENDUM

doi:10.1038/nature11645

Corrigendum: High-performance bulk thermoelectrics with all-scale hierarchical architectures

Kanishka Biswas, Jiaqing He, Ivan D. Blum, Chun-I Wu, Timothy P. Hogan, David N. Seidman, Vinayak P. Dravid & Mercouri G. Kanatzidis

Nature **489,** 414–418 (2012); doi:10.1038/nature11439

In this Letter, the units of thermal conductivity on the *y*-axes of Fig. 2d and e should be $W\,m^{-1}\,K^{-1}$ and the *y*-axis label of Fig. 3d should be 'Count (%)'. Figures 2 and 3 of the original paper have been corrected online.

Product Focus: Biochemistry

Assaying Ahead

Biochemical Services and Instruments

As the understanding of the complexity of human biology increases, so does the need for experiments that analyze larger swaths of data. A number of different technologies have matured into commercial services and instruments that can handle greater throughput.

Mass Spectrometry Services

High-throughput screens against enzyme targets typically utilize antibodies, fluorescence or radiological labels, which can interfere with enzyme activity and place unwanted restrictions on assay parameters. Surface plasmon resonance, impedance, mass spectrometry, and other label-free technologies are appealing because they do not suffer from these limitations. Yet, these methods are typically low-throughput. A few recent iterations of label-free technologies address the throughput-limiting bottlenecks.

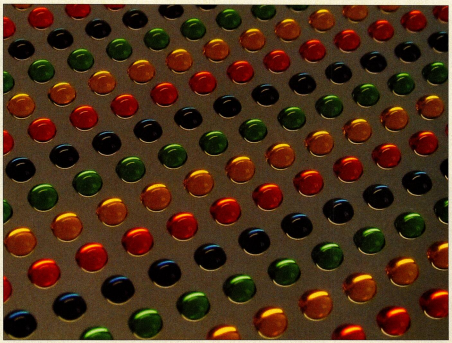

SAMDI Tech's biochip for high-through mass spectrometry

One such approach for high-throughput mass spectrometry, available as a service from **SAMDI Tech**, can eliminate the use of labels and allow up to 30,000 assays per day.

"The key is our highly efficient sample preparation method for mass spectrometry," says Michael Scholle, Director of Technology and Operations at SAMDI Tech.

The approach uses self-assembled monolayers (SAMs) of alkanethiolates on gold. Some SAMs contain tags that capture substrates (typically small molecules, peptides, proteins, or nucleic acids). The substrates are captured onto high density SAMDI 384 or 1536-spot biochips, rinsed to remove salts and other components, and then analyzed by matrix-assisted laser desorption/ionization time-of-flight (MALDI TOF) mass spectrometry.

Originally developed by Professor Milan Mrksich at the University of Chicago, the SAMDI method can identify the products, yields, and rates of reactions involving kinases, proteases, glycosyltransferases, methyltransferases, and many other enzymes. Since the method uses mass spectrometry, multiple enzymatic events or products can be monitored simultaneously.

"We can screen for new modifications and monitor methylation, ubiquitination, and acetylation in the same assay. We use a universal format for all assays of interest to our drug discovery clients," Scholle says.

Substrate discovery is also an option, in which peptide libraries are immobilized in a grid pattern, subjected to a solid-phase enzymatic reaction, and sequentially read by MALDI TOF to produce a heat map of an enzyme's kinetic activity for hundreds of substrates in one pass.

Scholle notes this option helps provide an accelerated path for developing a high-throughput screening program. "We can identify an optimal peptide substrate, determine the biochemical properties of the enzyme on that substrate, and then feed that into a high-throughput screen."

Another application of mass spectrometry is

Material compiled by Harris D. McKinney, Inc.

hdm
Life Science Marketing
www.harrisdmckinney.com
nature@harrisdmckinney.com

Product Focus: Biochemistry

identifying the components of a mixture of proteins.

One company is employing this technique with a **Whole Proteome Screening** service. **ITSI-Biosciences** uses validated sample preparation protocols and high performance mass spectrometers to generate a global map of both simple and complex protein samples. The service includes full sample preparation and accepts a variety of raw samples from protein isolates, gel-bands, and tissues to cell lysates, serum, and plasma. Using nano-LC/MS/MS, along with the MudPIT protein identification process for very complex samples, ITSI-Biosciences is able to provide full protein annotation and gene ontology classification within 48 hours. The generation of fully annotated datasets allows researchers to quickly identify proteins in a sample and the relevance of multiple disease pathways.

The service is ideal for biomarker research, contaminant identification, purity verification, and characterization of antibodies and recombinant proteins.

Next-Gen Bisulfite Sequencing

Methylation patterns have garnered significant interest and attention in the oncology field for being implicated in the development of many cancer types.

The most common method used to detect methylation status is Sanger-based bisulfite sequencing. While this approach provides single base pair resolution, it requires cloning of amplicons. In order to understand population variance and achieve statistically significant data, multiple clones must be sequenced—a time consuming process that is limited by the number of colonies (8 to 10) that can be cloned and sequenced in a given experiment.

Companies mentioned in this Product Focus

Active Motif	www.activemotif.com
BMG LABTECH	www.bmglabtech.com
ITSI-Biosciences	www.itsibio.com
SAMDI Tech	www.samditech.com

BMG LABTECH's NEPHELOstar Plus laser-based nephelometer

Active Motif's **Targeted Next-Gen Bisulfite Sequencing Service** has the ability to multiplex several amplicons from multiple bisulfite-converted DNA samples in a single next-gen sequencing reaction. Using Illumina's next generation sequencing platform, 100 to 10,000 times more data is generated for each cytosine, which enables more robust analyses. This methodology also permits direct sequencing using longer amplicons and eliminates cloning biases. Active Motif's services are provided as end-to-end assays and include bisulfite conversion, primer design and testing, PCR amplification, library preparation, DNA sequencing, and data analysis.

"The real power of this technique is that the extraordinarily high number of sequence reads accurately reflects the variance in the population. The ability to eliminate cloning biases and to multiplex samples and amplicons is an added bonus," said Brian Egan, Ph.D., Product Manger at Active Motif.

Solubility Determination

The solubility of a compound is a key determinant of its potential for therapeutic applications. Thus, solubility is assessed early in the discovery process.

One of the most effective methods for measuring solubility is the use of light scattering. The practice of nephelometry is one method that measures light scattered by particles suspended in a solution, the intensity of which is a function of concentration.

BMG LABTECH developed the first laser-based nephelometer that measures light-scattering in a microplate based environment, which helps meet the high-throughput demands of drug discovery programs. The **NEPHELOstar Plus** detects insoluble particles in liquid samples by measuring forward-scattered light and can be used for compound solubility screening, microbial cell growth kinetics, antibody-antigen interaction, immunoprecipitation, and polymerization monitoring.

With its wide dynamic range, NEPHELOstar Plus also offers microbiology laboratories a more precise measure of cellular growth. Options to adjust the intensity and beam diameter of the laser light enables more accurate readings of colored or turbid solutions. The flexible beam diameter also allows for measurements in 24, 48, 96, and 384-well microplate formats. ■

"This article was compiled by Harris D. McKinney, Inc. and submitted to Nature. It has not been written by or reviewed by the Nature editorial team and Nature takes no responsibility for the accuracy or otherwise of the information provided. Submit press releases for consideration to productfocus@nature.com with the topic in the subject line."

nature podcast
science... wherever you are.
nature.com/nature/podcast
nature publishing group
npg

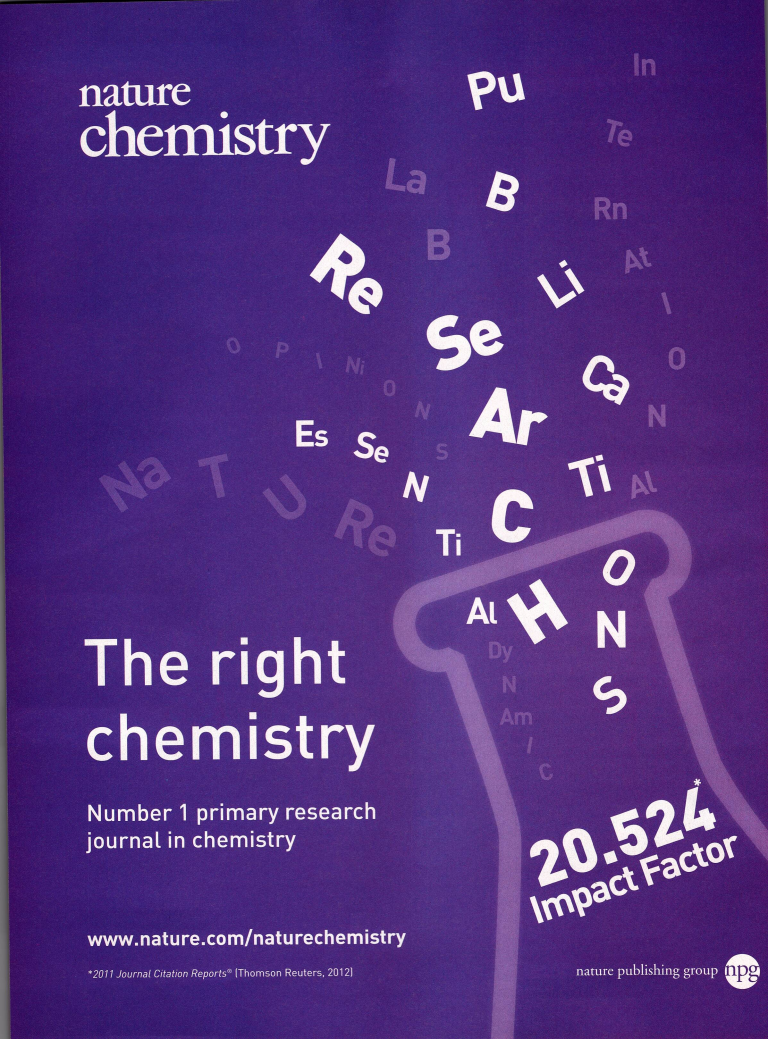
nature
chemistry
The right
chemistry
Number 1 primary research
journal in chemistry
www.nature.com/naturechemistry
*2011 Journal Citation Reports® (Thomson Reuters, 2012)
20.524*
Impact Factor
nature publishing group
npg

CAREERS

EMERGING NATIONS Opportunities in academia for mobile researchers **p.573**

EUROPE Research council issues strategy for tackling misconduct **p.573**

NATUREJOBS For the latest career listings and advice **www.naturejobs.com**

OCEAN/CORBIS

WORK EXPERIENCE

Stepping stones

Internships can help scientist job seekers to get a head start on the competition.

BY AMANDA MASCARELLI

In late 2009, Mark Brown was at the end of a six-year postdoctoral position in parasitology at the University of California, Los Angeles. Having completed a PhD in molecular and cellular pharmacology, he was primed for a position in academia. But he hungered to move into industry. "I really wanted to take what I'd learned and apply it, and I felt that academia really didn't offer me that option whereas industry did," says Brown.

But the economy was in trouble and industry jobs in research and development were disappearing. Prospects looked grim. Brown learned about the Postdoc Professional Masters (PPM) at the Keck Graduate Institute of Applied Life Sciences in Claremont, California, one of the growing number of programmes that aim to provide practical, hands-on business savvy to graduates with PhDs and medical doctorates who want to enter the biosciences industry (see *Nature* **469,** 569; 2011).

Before he started the course, Brown was keenly aware that he faced stiff competition from more-experienced job seekers. "It was going to be a hurdle to make that jump," he says. "I did have a lot of technical skills, but I felt I didn't have the experience that industry might want." The two-semester PPM programme encourages students to participate in industry-sponsored internships, and Brown landed a placement with Claremont BioSolutions, a small company that develops research tools for scientists, based in Upland, California. The internship taught him about marketing strategies, developing a product and the culture of a start-up company. After Brown graduated from Keck in 2010, Claremont BioSolutions hired him as a senior scientist.

US researchers trained on the academic track are increasingly pursuing job opportunities outside academia. The US National Science Foundation's 2010 Survey of Earned Doctorates found that only just over half of new, employed US PhD recipients across all fields hold research positions at academic institutions.

Yet conventional science and engineering PhD programmes in the United States don't always provide the practical experiences and skills needed to make a transition to industry. The flagging economy and increased competition for fewer jobs has made preparation for the job market even more crucial. Internships — whether offered as part of a graduate degree or pursued independently — can provide necessary skills, look good on a CV and offer a taste of the world outside academia.

More and more young US scientists are pursuing internships and cross-training opportunities that will give them an edge. Outside the United States, they are already common: in Germany, for example, internships and applied industry experience are often integral to graduate training (see 'Part of the package'). Many employers and educational institutions in the United Kingdom recognize the value of internships or placements for graduate students, notes Janet Metcalfe, head of Vitae, a research-career advisory organization in Cambridge, UK.

NOT-SO-ACADEMIC HURDLES

Internships take various guises. But they generally last from two to six months, often over the summer. Graduate or postgraduate interns are usually paid salaries comparable to graduate stipends and postdoc wages.

Academic programmes are increasingly enabling students to gain practical work experience through fellowships, interdisciplinary collaborations, traineeships and other forms of professional development. And internships may be directly related to a student's research, or serve as segues to opportunities in areas such as communications, venture capital, law, clinical-trial management or intellectual property.

But even as awareness grows about non-academic tracks, many institutions and faculty members have not adjusted. Graduate advisers might not support internships that take time away from the student's primary research — grant money is limited, and PhDs already take a long time to complete. Doctoral programmes, especially in the life sciences, don't typically encourage internships, says Jung Choi, director of the bioinformatics master's programme at the Georgia Institute of Technology in ▶

nature

A key thread in your scientific career

Whether in print, online or mobile, *Nature* is always at the forefront of science and is your forum to read, watch, listen and engage with key research, news and opinion.

How will you access the next landmark discovery?

NATURE.COM/NATURE

nature publishing group npg

Atlanta. "There are all kinds of disincentives for both faculty and students," he adds.

Sudipto Guha, a chemical-engineering PhD student at the University of Illinois at Urbana-Champaign, found that there was little precedent among his peers for seeking an internship. "It's a rare case that you would find an adviser who would let you do an internship in graduate school," he says. Yet Guha struck lucky: his adviser did support him, helping him to seek out opportunities and putting him in touch with companies. Guha networked aggressively, introducing himself to company representatives regardless of whether their firm offered a formal internship programme. This summer, he completed an internship at Brady Corporation in Milwaukee, Wisconsin, which develops identification solutions such as barcode labels and safety markings.

ALL IN THE PLAN

Some US institutions have formally recognized the need for internships and other practical experience. In 2008, after collecting survey results suggesting that many students were interested in opportunities outside academia but lacked confidence in how to pursue them, the school of medicine at the University of California, San Francisco (UCSF), teamed up with other UCSF basic and biomedical science graduate departments to launch the Graduate Student Internships for Career Exploration Program (GSICE).

"Our strategy was to convey the realities of where our graduate students are going in terms of careers, what our graduate students are interested in, and to remember that UCSF has the responsibility to train our students for fulfilling careers," says Alexandra Schnoes, GSICE coordinator and one of two people who spearheaded the effort. Between January and March each year, students complete a series of workshops designed to help them to pinpoint the career choices most suitable for them. They can then pursue internships either during their graduate programmes (after passing the programmes' qualifying exams and receiving approval from their advisers) or immediately after finishing.

Bethann Hromatka, one of the first graduate students to benefit from the internship programme, parlayed her placement into a full-time job. By the end of her PhD in biomedical sciences at UCSF, Hromatka knew that she was not interested in a postdoc or academia in general. "I was getting burnt out on the bench," she recalls. "In my last year I had that conversation with my adviser, and at the end of the day she understood." In 2011, after defending her PhD, she wrapped up her lab work on a Sunday evening. The next morning, she began a two-month internship at 23andMe, a personal-genetics start-up based in Mountain View, California. Hromatka's internship consisted mainly of researching and writing genetic health reports for the company's website — and last November, 23andMe hired her as a full-time health-content scientist, with the same core responsibilities.

S. PARS

"We don't define success in an internship as meaning they get a job in that field."
Terri O'Brien

For those, like Hromatka, who have grown weary of bench work, internships can provide inroads into various career paths outside research and development. The University of North Carolina at Chapel Hill offers internships across disciplines.

That is part of a tradition of practical science-career planning in Germany. At the Technical University of Munich, for example, international internships are mandatory for all doctoral candidates and are backed with financial support from the university. The emphasis is on training for careers both inside and outside academia, says Ernst Rank, director of the institution's graduate school. He points to surveys showing that some 80% of PhD students in Germany do not end up in academic positions. "Not one of our PhD students who graduates from our university would consider him or herself failed if they don't make an academic career," says Rank. **A.M.**

GERMANY

Part of the package

Some US institutions are only now starting to incorporate non-academic career paths into graduate training, but at many German institutions, that emphasis is integral to doctoral training. In the past decade, such efforts have received an extra boost.

In 2005, the government launched the German Excellence Initiative to support new strategies for research and graduate training (see *Nature* **487,** 519–521; 2012). It invested around €2.1 billion (US$2.8 billion) in the programme's first five years, and has now renewed it with another €2.5 billion for the next five years. Both phases have funded 'research clusters' and graduate schools at select institutions to foster international collaborations and

a technology-transfer internship that gives graduate students and postdocs the opportunity to learn about intellectual property, patent filings, licence agreements and technology commercialization through eight-month internships in the university's Office of Technology Development. Interns commit 8–12 hours per week to the training programme, which is carried out during the academic year, alongside the students' main research.

Cato Research, a clinical-research organization in Durham, North Carolina, runs a fellows programme offering doctoral students a one-year, full-time internship in clinical research and drug development. It acts as a sort of alternative postdoc and is becoming a popular choice, says Patrick Brandt, director of the office of science, training and diversity at the University of North Carolina, noting that in the past two years, an increasing number of students have come to him asking about fellowships in clinical-trial management.

At Stanford University School of Medicine in California, an internship programme for life-sciences PhD students is set to begin in 2013. Career-centre advisers will help students to seek out 10-week placements in fields such as biopharmaceuticals, venture capital and finance, consulting, law and journalism.

Internships don't usually lead directly to full-time jobs at the host company or internship site, says Terri O'Brien, associate dean for research strategy at the UCSF school of medicine. GSICE coordinators warn their students not to expect an immediate job offer, but they also point out that internships greatly improve the overall odds of landing a job. On the basis of preliminary data, the coordinators have found that more than 90% of their students who have done an internship successfully move onto their chosen career path after graduation, compared with 60% of those who have not. But most important are the insights into potential career tracks — and the confidence to pursue them. "We don't define success in an internship as meaning they get a job in that field," says O'Brien. "They may go through the GSICE programme's career assessment and training and realize they want another field. We're really trying to impact the career-decision process and the point at which it happens."

ANOTHER DEGREE?

Pursuing a further degree may help students to build the practical experience needed to move into industry or other non-academic career paths. This is the explicit purpose of the Professional Science Master's (PSM) and PPM programmes. Increasingly popular, these degrees generally involve up to two years of academic training and a professional component such as an internship or other type of cross-training opportunity in business, communications or regulatory affairs. The effect is "dramatic", says James Sterling, vice-president for academic affairs at Keck. "PSM graduates have a foot in the door at these companies," he says, noting that each year, some interns do go on to get jobs at the same firm. Sterling says that 95% of graduates from Keck's PSM and PPM programmes find employment in industry within eight months of graduation — although sample sizes are small for the PPM, which is much newer. Keck PSM graduates usually have starting salaries of about US$70,000, and Keck PPM graduates about $80,000.

"Professional Science Master's graduates have a foot in the door at companies."
James Sterling

"The internship definitely sharpened my focus," says Neha Gupta, a bioinformatics analyst at the J. Craig Venter Institute in Rockville, Maryland, who earned a PSM in bioinformatics at the Georgia Institute of Technology in 2010 and did an internship at Merck Research Laboratories in Rahway, New Jersey, the same year. "I wasn't sure before if I wanted to go into a PhD programme or get a job. But after the internship I decided I definitely wanted to work in industry first," she says. The Venter institute hired Gupta last year.

Internships and other unconventional training opportunities complement, rather than detract from, students' research, says Richard Linton, National Science Foundation dean-in-residence at the Council of Graduate Schools in Washington DC, a national organization that promotes graduate education and research. Students who build industry connections will often create valuable collaborations, bring new expertise to their academic labs and gain access to facilities that reinforce their projects, he says. "Data suggest that these non-traditional tracks actually elevate student productivity and give them more motivation to complete their degrees and move forward into careers," says Linton. "There's much evidence that this is an enhancement, not a barrier, to degree completion." ■

Amanda Mascarelli *is a freelance writer based in Denver, Colorado.*

CLARIFICATION

In the article 'Turbulent times' (*Nature* **488**, 685–688; 2012), we referred to research conducted by Ruth Müller. The work was done while she was at the Department of Social Studies of Science at the University of Vienna, in a team headed by Ulrike Felt.

EMERGING NATIONS

Scientists wanted

Researchers are in demand in east Asia, Latin America and southern Africa — regions not considered traditional scientific powerhouses — where doctoral-degree holders tend to leave academia for government or the private sector, says a report. *CODOC — Cooperation on Doctoral Education Between Africa, Asia, Latin America and Europe*, published on 4 October by the European University Association (EUA) in Brussels, examined international collaboration across fields at universities to assess efforts to build research capacity. It documents ample international collaboration at universities in east Asia and an increasing number in Brazil and Mexico, but notes the need for more research investment in southern Africa to expand such efforts. Thomas Jørgensen, head of the EUA's council for doctoral education and author of the report, says that increasing collaboration hasn't made it any easier to retain academic faculty members at universities in the three emerging regions. But early-career scientists who are willing to leave their home countries can find posts that match their research specialities, he says. "The need for early-stage researchers is desperately there," adds Jørgensen.

EUROPE

Misconduct policy

The European Research Council (ERC) has issued a strategy for identifying and addressing scientific misconduct — the first such policy on the European level. Under the strategy, released on 9 October, host institutions are responsible for detecting, investigating and adjudicating on suspected breaches of research integrity or misconduct by ERC-funded researchers or applicants for ERC grants. But the research council, based in Brussels, will also take action once institutions confirm cases of misconduct or questionable research practices: among other steps, it may notify the European Commission and the commission's anti-fraud office, hold a hearing, suspend or terminate grants or refuse further grant proposals. Since the ERC was launched in 2007, it has issued some 3,000 grants and handled between 10 and 20 allegations of misconduct, says ERC vice-president Pavel Exner. On 17 October, the InterAcademy Council in Amsterdam and the InterAcademy Panel in Trieste, Italy, released *Responsible Conduct in the Global Research Enterprise: A Policy Report* to promote research integrity.

CAMBRIDGE RESEARCH INSTITUTE

PhD Studentships

The Cambridge Research Institute is a joint venture between Cancer Research UK and the University of Cambridge. It opened in 2007 and has excellent state-of-the-art facilities. Research ranges from basic cancer biology and computational biology through to translational research and clinical application.

Graduate students play a pivotal role in the continuing success of our research programme and gaining a studentship in the Institute is an excellent opportunity to start a research career in an environment committed to training outstanding cancer research scientists of the future.

We seek highly motivated and talented students to enter our PhD programme in October 2013. All of our students gain their degrees from the University of Cambridge and have access to the wide range of talks and courses to be found across the University.

No nationality restrictions apply to Cancer Research UK funded studentships.

Applications are invited from recent graduates or final year undergraduates who hold or expect to gain a first/upper second class degree (or equivalent) in a relevant subject from any recognised university worldwide. You may apply for a maximum of 3 projects.

Please clearly state in your cover letter which projects you are applying for.

A Cancer Research UK studentship includes full funding for University and College fees and in addition, a stipend of £19,000 per annum.

Applications must be made online via the following website:
http://www.cancerresearchuk.org/about-us/jobs

The closing date for applications is 30th November 2012.

The Institute offers projects in the following areas:

James Brenton - Genomic drivers of intratumoural heterogeneity

Kevin Brindle - A novel approach to imaging cell surface glycans in cancer

or

Kevin Brindle - Monitoring tumour responses to treatment using hyperpolarized magnetic resonance imaging

Fanni Gergely - The role of the centrosome in genome stability

Florian Markowetz - Breast Cancer Systems Biology

Masashi Narita - High-order chromatin architecture and gene regulation in senescence

Duncan Odom - Linking tissue-specific genetic regulation and epigenetics to cancer evolution

UNIVERSITY OF CAMBRIDGE

CANCER RESEARCH UK

Cancer Research UK is a registered charity in England and Wales (1089464), Scotland (SC041666) and the Isle of Man (1103).
Registered company in England and Wales (4325234) and the Isle of Man (5713F).

U229650R

MRC National Institute for Medical Research

MRC National Institute for Medical Research (NIMR)

2013 PhD Studentships

NIMR has been at the forefront of international excellence in basic biomedical research for more than 80 years and its scientists, including students, have contributed to the prevention and improved treatment of many serious diseases and increased understanding of human health

We are looking for exceptional students to join our four year PhD programme commencing in September 2013

NIMR offers projects in the following areas:

Infections and Immunity, Genetics and Development, Neurosciences, Structural Biology

Successful students will receive an annual tax-free stipend of £20,000, and payment of their tuition fees (eligibility requirements apply)

Details on each of the projects, eligibility requirements and how to apply can be found at
http://www.nimr.mrc.ac.uk/phd

The closing date for applications is 28th November 2012
Interviews will be held16th-17th January 2013
Enquiries: student@nimr.mrc.ac.uk

The NIMR will become part of the new Francis Crick Institute opening in 2015

CANCER RESEARCH UK
London Research Institute

London Research Institute

Four Year PhD Studentships
Clare Hall & Lincoln's Inn Fields

The London Research Institute (LRI) invites outstanding final year undergraduates or recent graduates with backgrounds in biological or medical sciences, physics, chemistry, maths and/or computer science to apply for four year PhD studentships to start in September 2013.

The LRI has an international reputation for research into the basic biology of cancer. Our well-resourced research labs with state-of-the-art equipment and technologies are based at Lincoln's Inn Fields (Central London) and Clare Hall (just north of London). Our students benefit from challenging research projects, a comprehensive PhD programme and the facilities of University College London, where they are registered.

Applicants should hold or expect to gain a first/upper second class honours degree or equivalent in a relevant subject and have some research experience. Successful applicants will be awarded a non-taxable annual stipend of £21,000 plus payment of tuition fees.

Applications must be made online via our website:
http://www.london-research-institute.org.uk/phd/

Application closing date: Thursday 15th November 2012
Interviews: 20-22 Jan 2013 (Clare Hall);
23-25 Jan 2013 (Lincoln's Inn Fields)

The LRI will become part of the new Francis Crick Institute opening in 2015

U228961

Technical University of Denmark DTU

Start your career with a PhD education of international standard

– and create superior technology and welfare for the benefit of society

Leading international research

Technical University of Denmark (DTU) is one of the best technical universities in Europe and has some of the best research facilities in the world. This leading position must be maintained by continually attracting the best Researchers and Students from all over the world. Today DTU has 5,000 employees, including 1,200 PhD Students.

Research Career

At DTU, we have internationally Elite Researchers within many areas of research. As a PhD student, you become part of an exciting academic environment and will participate in a group of talented, experienced, and dedicated colleagues. Traveling, guest lectures and conferences will be a natural part of your working day.

As PhD student at DTU, you will be prepared to compete for a career at a high international level. It is of great importance, that our PhD program is of international standing and we focus on making our study and research environment attractive for PhD students.

Jobs

We are constantly looking for PhD students in many different areas of research. On career.dtu.dk you can learn more about DTU, and find currently available jobs. You can also create a job agent and get updated information when there is a job in your particular area of interest. You are always welcome to contact us, if you have questions.

DTU is a technical university providing internationally leading research, education, innovation and public service. Our staff of 5,000 advance science and technology to create innovative solutions that meet the demands of society; and our 7,000 students are educated to address the technological challenges of the future. DTU is an independent academic university collaborating globally with business, industry, government, and public agencies.

SCIENCE AND TECHNOLOGY AT A GLOBAL SCALE – SET THE STANDARDS FOR THE FUTURE

See our PhD-programmes at dtu.dk/phd

W229933R

cambridge cancer centre

UNIVERSITY OF CAMBRIDGE

Cambridge Cancer Centre PhD Studentships

The Cambridge Cancer Centre is an umbrella organisation incorporating clinical and basic science departments of the University of Cambridge and their affiliated research institutes (e.g. Cancer Research UK Cambridge Research Institute, MRC Cancer Cell Unit, Gurdon Institute). The Centre encourages interdisciplinary and collaborative research across all disciplines, and covers an exciting and remarkably broad range of approaches to cancer research.

Applications are invited for PhD studentships in cancer studies throughout the Cambridge Cancer Centre. No nationality restrictions apply to these studentships. The studentships are funded by Cancer Research UK and the MRC Laboratory of Molecular Biology, and include fees (University and College) and a stipend (£19,000 per annum), together with an allowance for research costs.

The Centre offers the following eight projects of which four will be funded:

Chromosome translocations and other genome rearrangements in oesophageal adenocarcinoma
Paul Edwards (Department of Pathology and Hutchison/MRC Research Centre) and Rebecca Fitzgerald (MRC Cancer Cell Unit)

Characterization of the effect of loss of fumarate hydratase on signal transduction and regulation in renal cancer using a systems biology approach
Christian Frezza (MRC Cancer Cell Unit), Julio Saez-Rodriguez (European Bioinformatics Institute) and Kathryn Lilley (Department of Biochemistry)

Mechanism of fascin in filopodia formation
Jennifer Gallop (Gurdon Institute and Department of Biochemistry) and Nick Brown (Gurdon Institute and Department of Physiology, Development and Neuroscience)

Single-cell analysis of stable isotope-labelled DNA for probing proliferative heterogeneity of tumours *in vivo*
Michelle Oyen (Department of Engineering) and Robert Busch (Department of Medicine)

Manipulation of cell cycle-dependent regulation of proneural protein activity for differentiation therapy in glioblastomas
Anna Philpott (Department of Oncology and Hutchison/MRC Research Centre), Colin Watts (Brain Repair Centre) and Ben Simons (Department of Physics)

What is the defective differentiation programme of ALK and N-Myc driven neuroblastoma?
Suzanne Turner and Heike Laman (Department of Pathology) and Gerard Evan (Department of Biochemistry)

Oncogene-induced remodelling of cellular networks: a systems approach using optogenetics and next-generation microscopy
Ashok Venkitaraman and Alessandro Esposito (MRC Cancer Cell Unit)

Structural biology of autophagy in cancer
Roger Williams (MRC Laboratory of Molecular Biology)

The detailed project descriptions can be found on the Cambridge Cancer Centre website (www.cancer.cam.ac.uk). Applicants should submit their application as one pdf file (cover letter followed by CV with the names and e-mail addresses of two academic referees) in the format: surname_firstname.pdf to CambridgeCancerCentre@cancer.org.uk by **30 November 2012**. Successful applicants will be invited for interview in the week of 14 January 2013.

U229949R

Radcliffe Department of Medicine

UNIVERSITY OF OXFORD

4 year PhD Scholars Programme in Medical Sciences

- **Fully funded**
- **College and University fees paid**
- **Stipend of £18,000/annum**
- **A 4 year full time research project in a single laboratory**

The Radcliffe Department of Medicine is committed to training the next generation of scientists in biological and clinical sciences through its graduate programme in the University of Oxford. The Department's PhD Scholars Programme is open to **outstanding candidates** of any nationality, without restriction.

The Radcliffe Department of Medicine at the University of Oxford is a large multi-disciplinary Department that links high quality basic biological science with medical applications.

The department has internationally renowned programmes in a broad spectrum of sciences related to medicine, including:

- Cardiovascular Medicine
- Diabetes, Endocrinology & Metabolism
- Epidemiology & Clinical Trials
- Haematology & Pathology
- Immunology
- Regenerative Medicine & Stem Cells
- Acute Stroke

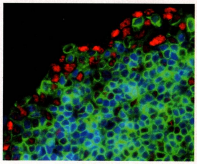

Further details on the application process and the wide range of projects available can be found at: www.rdm.ox.ac.uk/rdm-scholarships.

The closing date for applications is 4th January 2013; interviews will take place on 23rd & 24th January; offers will be made in early February.

NUFFIELD DEPARTMENT of MEDICINE

UNIVERSITY OF OXFORD

IMAGES BY DR BEN DAVIES & PROF XIN LU

The Nuffield Department of Medicine Four-year PhD Prize Studentships

The Nuffield Department of Medicine at the University of Oxford hosts one of the largest groupings of Biomedical Researchers in the university sector. The last RAE rated it at the highest level in both **basic science and clinical research** across a wide range of fields. The Department has internationally renowned programmes in the following themes: **cancer biology, physiology, cellular & molecular biology, clinical trials & epidemiology, genetics & genomics, immunology & infectious disease, protein science & structural biology, and tropical medicine & global health**. The Department is committed to training the next generation of scientists in biological and clinical sciences through its graduate programme at the University of Oxford.

MAGDALEN TOWER FROM THE BOTANICAL GARDENS

The four-year PhD Prize Studentships are our flagship fully funded awards, which are open to **outstanding candidates** of any nationality, without restriction. Support for the programme comes from a variety of sources including the University of Oxford, the Ludwig Institute for Cancer Research, Medical Research Council and Clarendon Fund. In 2013 we expect to make at least twenty awards to students of the highest calibre. Students are full members of the University of Oxford and receive a stipend of £18,000/annum. In exceptional circumstances, additional awards may be made. These awards allow students to focus on research in a single laboratory for the full four years.

More details on the application process and the wide range of projects are available on the NDM website. Individual supervisors can also be contacted by email about their projects. The **closing date for applications is 4 January 2013**. Interviews will take place on 23 and 24 January 2013.

To find out more visit our website: www.ndm.ox.ac.uk/prizestudentships

U228454R

MEDICAL SCIENCES Graduate School

Oxford University Medical Sciences Graduate School

UNIVERSITY OF OXFORD

Applications are invited from outstanding students for PhD and other graduate programmes in Medical Sciences.

Why Oxford?

- Oxford continues to be rated the top University in the world in medical sciences.*
- A wide range of PhD programmes are available to suit any potential applicant.
- Generous full funding packages are available for all programmes and for applicants of all nationalities.

Find out more about the options available and how to apply at the Medical Sciences Graduate School website [www.medsci.ox.ac.uk/graduateschool]

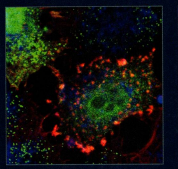
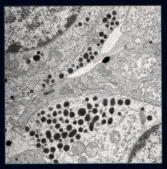

* http://www.timeshighereducation.co.uk/world-university-rankings/2012-13/subject-ranking/subject/clinical-pre-clinical-health

U229888R

CAMPUS VISIT DAY November 24, 2012

CALL FOR PhD STUDENTS

The Graduate School at IST Austria invites applicants from all countries to its PhD program. IST Austria is a new institution located on the outskirts of Vienna dedicated to cutting-edge basic research in the natural sciences and related disciplines. The language at the Institute and the Graduate School is English.

The PhD program combines advanced coursework and research, with a focus on Biology, Computer Science, Mathematics, Physics, Neuroscience, and interdisciplinary areas. IST Austria offers internationally competitive PhD salaries supporting 4–5 years of study. Applicants must hold either a BS or MS degree or equivalent.

The Institute offers PhD students positions in the following fields:

Biology | Computer Science | Mathematics | Physics | Neuroscience

For a list of faculty members please visit www.ist.ac.at. For further information and access to the online application please consult www.ist.ac.at/gradschool. For inquiries, please contact gradschool@ist.ac.at. For students wishing to enter the program in the fall of 2013, the deadline for applications is January 15, 2013.

IST Austria is committed to Equality and Diversity.

IST AUSTRIA
Institute of Science and Technology

W229894R

Postdoc and research **opportunities** in Brazil

Fifty percent of all science created in Brazil is produced in the State of São Paulo. The state hosts three of the most important Latin American universities: USP, UNICAMP and UNESP. Other universities and 19 research institutes are also located in São Paulo, among them the renowned Instituto Tecnológico de Aeronáutica (ITA), Instituto Nacional de Pesquisas Espaciais (INPE) and Laboratório Nacional de Luz Síncrotron, besides most of Brazilian Industrial P&D.

The São Paulo Research Foundation (FAPESP), one of the leading Brazilian agencies dedicated to the support of research, has ongoing programs and support mechanisms to bring researchers from abroad to excellence centers in São Paulo.

The **Young Investigators Awards** is part of FAPESP's strategy to strengthen the State research institutions, favoring the creation of new research groups. See more about it at www.fapesp.br/yia.

FAPESP **Post-Doctoral Scholarship** is aimed at distinguished researchers with a recent doctorate degree and a successful research track record. The scholarship enables the development of research within higher education and research institutions in São Paulo. Postdoc scholarships are available when calls for applications are issued internationally, or as individual scholarships requested on demand.

In the first case, positions are advertised at **www.fapesp.br/oportunidades/en** and candidates are selected through international competition. In the second, the proposal must represent an addition to a pre-existent research group and should be developed in association with faculty in higher education and research institutions in São Paulo. More information at **www.fapesp.br/en/postdoc**.

FAPESP 50 YEARS

FAPESP

www.fapesp.br/en

NW226526R

Sir William Dunn School of Pathology

University of Oxford

www.path.ox.ac.uk

4 YEAR PRIZE PhD STUDENTSHIPS

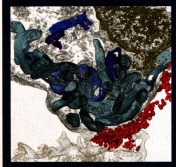

Outstanding and motivated students are sought for up to eight highly prestigious **Four Year Departmental Prize PhD** studentships in this internationally renowned research department. Funded by the MRC, EP Abraham Research Fund, the Clarendon Fund and Colleges, they provide full support for up to 4 years with an enhanced stipend of ~ £15,500 per annum. Applications are open to all nationalities. Projects are available in **cancer, molecular microbiology, cell biology, immunology, and molecular biology.** Project details and information on how to apply are available at http://www.path.ox.ac.uk. The application deadline is **4th January 2013.** Interviews will take place from 23rd-25th January 2013.

The University is an equal opportunities employer.

U229304R

UCL RESEARCH DEPARTMENT OF CELL AND DEVELOPMENTAL BIOLOGY

UCL

Wellcome Trust 4-year PhD Programme in Developmental and Stem Cell Biology at UCL/NIMR

This programme offers a unique environment with one of the largest and strongest concentrations of high quality developmental and stem cell biologists anywhere in the world, including a large list of supervisors and projects throughout UCL, its related teaching hospitals and specialist centres and the National Institute for Medical Research. Located in Bloomsbury, in the heart of London, the programme also offers an excellent opportunity to join in the professional and social life of this vibrant city.

The four-year structure comprises three lab rotations and a taught component in the first year, providing the basis for an informed choice and an excellent platform for progression in the research project in years 2-4.

Funding and eligibility:

All applicants will be required to satisfy standard UCL academic and English language entry criteria, including a minimum upper-second class (2.1) honours degree (or overseas equivalent) in a relevant subject.

The studentship covers a maintenance stipend of £22,278 per annum (2013-14 rate) and tuition fees paid in full at the home/EU rate. International (non-EU) students are also welcome to apply – an opportunity exists for additional funding to cover the difference between overseas and home/EU rates.

How to apply:

For all details of the application procedure, please visit the programme website: http://www.ucl.ac.uk/cdb/students/PhD

Applications for entry in September 2013 to be received by Thursday 3 January 2013. Interviews will be held in late January/early February 2013.

wellcome trust

U229941R

CHARITÉ
UNIVERSITÄTSMEDIZIN BERLIN

NEUROCURE
Cluster of Excellence

Neurosciences in Berlin – International PhD Fellowships

The NeuroCure Excellence Cluster invites applications for its PhD program starting in 2013

NeuroCure is an inter-institutional research network based at the Charité - Universitätsmedizin Berlin, the Humboldt-Universität zu Berlin and the Freie Universität Berlin, with its partners, the Max Delbrück Center for Molecular Medicine Berlin-Buch (MDC), the Leibniz-Institut für Molekulare Pharmakologie (FMP) and the Deutsche Rheuma-Forschungszentrum Berlin (DRFZ).

With over 45 internationally recognized research groups, NeuroCure offers outstanding interdisciplinary training and research opportunities for national and international scientists from a wide range of academic backgrounds.

Fellowships are available in the following subject areas:

- Molecular mechanisms of nervous system development and function
- Mechanisms of neural damage and cellular age
- Endogenous brain protection
- Nervous system regeneration
- Crosstalk between nervous and immune system
- Developmental disturbances
- Synaptic plasticity

For more details on subject areas and participating research groups go to: **http://www.neurocure.de/en**

How to apply: Send a full CV, two academic references and a personal statement of your interest in this program to **neurocure-phd@charite.de**.

Closing date for applications is 7 January 2013. Short-listed applicants will be invited to a Skype interview in February; the final interview will take place in March 2013.

W229980R

KING'S College LONDON

MRC Centre for Developmental Neurobiology

Four year MRes/PhD programme – intake 2013

MRC Centre for Developmental Neurobiology, Guy's Campus, KCL

Outstanding research training will be provided at the internationally recognised MRC Centre for Developmental Neurobiology, utilising state-of-the-art techniques in various model systems. Applications are welcomed from a wide range of academic backgrounds: from molecular and cellular biology, embryology, developmental biology, electrophysiology, computational neuroscience to the physical and mathematical sciences.

- **Year 1 - MRes:** three lab rotations, a taught course, seminars and workshops run by leading experts
- **Year 2-4 - PhD:** an original research project, transferable skills, seminars and conferences

Projects are available with the following group leaders:

Paula Alexandre	Mechanisms of self-renewal and neuronal differentiation
Laura Andreae	Synaptogenesis and neurodevelopmental disorders
Esther Bell	Molecular mechanisms of neural induction
Eric Blanc	Development of software for *Drosophila* climbing assay
Juan Burrone	Synaptic physiology and plasticity
QueeLim Ch'ng	Neuroendocrine regulation of *C. elegans* physiology
David Chambers	Patterning and specification of cranial motor neurons
Jon Clarke	Morphogenesis and neurogenesis in the zebrafish CNS
Uwe Drescher	Molecular analysis of the development of neural circuits
Manolis Fanto	Neuron-glia interactions in neurodegeneration in *Drosophila*
Caroline Formstone	Neuron migration and Planar Cell Polarity signalling
Phillip Gordon-Weeks	Cytoskeletal dynamics and growth cone pathfinding
Anthony Graham	The neural crest and neurogenic placodes
Matthew Grubb	Activity-dependent control of neuronal excitability
Sarah Guthrie	Motor neuron development and diseases
Robert Hindges	Synaptic specificity in the vertebrate visual system
Corinne Houart	Signalling centres in control of forebrain complexity
Tara Keck	Mechanisms of structural plasticity
Clemens Kiecker	Specification and neurogenesis in the vertebrate forebrain
Camilla Larsen	Patterning of sub-regions in the *Drosophila* brain
Ivo Lieberam	ES cell-based models of neuromuscular circuits
Ivor Mason	Signalling mechanisms in brain development
Martin Meyer	Development and function of the zebrafish visual system
Setsuko Sahara	Differentiation of neural progenitors in the cortex
Rita Sousa-Nunes	Neural stem cell transformation and cancer
Guy Tear	Molecular mechanisms of axon guidance in *Drosophila*
Ian Thompson	Development of the vertebrate visual system
Darren Williams	Dendrite development in *Drosophila*
Richard Wingate	Neuron migration and evolution of the cerebellum

For more details go to www.kcl.ac.uk/depsta/biomedical/mrc/phd.php

MRC eligibility criteria:
http://www.mrc.ac.uk/Fundingopportunities/Applicanthandbook/Studenthips/Eligibility/index.htm

Candidates should have or expect at least an upper second class degree. Closing date for applications is 4th January 2013. To apply email a full CV, the names and contact details of two academic referees and personal statement of your interest in this programme to Ms Stefania Boscolo at stefania.boscolo@kcl.ac.uk.

NB Additional funding for the Centre's 4-year MRes/PhD Programme (plus individual 4-year PhD projects) is available through a competitive KCL Health Schools Studentships Programme. Details available at www.kcl.ac.uk/studentships; closing date 26th November 2012.

Applications through *both* routes are strongly encouraged.

U229826R

---

the Beatson institute for cancer research

Graduate Studentships

Cell Biology of Cancer

The Beatson Institute for Cancer Research is core-funded by Cancer Research UK and provides a dynamic, supportive and well-resourced environment for its scientists in parkland on the edge of Glasgow. Our research groups are working in two key areas: cell metabolism and survival; and cell migration.

We are looking for students with a very good degree in Life Sciences and an aptitude for experimental work who are highly committed to pursuing a career in cancer research. The Beatson has an excellent reputation and success record in training its graduate students. Students, whilst being trained at the Institute working within our research groups, will matriculate with the University of Glasgow.

Projects are available in the following groups in 2013:

Kurt Anderson Tumour Cell Migration

Karen Blyth Transgenic Models of Cancer

Eyal Gottlieb Apoptosis and Tumour Metabolism

Danny Huang Ubiquitin Signalling

Robert Insall Cell Migration and Chemotaxis

Laura Machesky Migration, Invasion and Metastasis

Mike Olson Molecular Cell Biology

Kevin Ryan Tumour Cell Death

Owen Sansom Colorectal Cancer and Wnt Signalling

Marcos Vidal Drosophila Approaches to Cancer

Studentships are funded for four years, starting in October 2013. The annual stipend will be £19,000. Further information and details of how to apply can be found on our website www.beatson.gla.ac.uk.

Closing date: 16th November 2012.

CANCER RESEARCH UK

Scottish charity no SC006106

U229826R

International PhD Programme

INTERNATIONAL MAX PLANCK RESEARCH SCHOOL UFAST

Ultrafast Imaging & Structural Dynamics

- Cutting-edge research
- Internationally renowned research institutions
- Excellent research conditions
- Advanced training
- Language: English
- No tuition fees
- fellowships/ fully-funded

We seek highly motivated graduates world-wide with an MSc or equivalent in Physics, Chemistry, or Biochemistry.

Apply by 31st January
www.imprs-ufast.de

W229861R

Initial Training Network of the European Commission **FP7-PEOPLE-2012-ITN** no. 317013

NK CELL-BASED ANTI-CANCER IMMUNOTHERAPIES
11 PhD students
2 post-doctoral fellows

Within a newly formed ITN we are searching for 11 PhD students and 2 postdoctoral fellows* interested in the native immune response of natural killer cells to herpes viruses and tumors and the development of leukemia therapies. Candidates should have a solid basis in molecular medicine, cell biology, immunology, gene technology and/or bioinformatics. 1-2 positions will be available in each of the individual partner laboratories:

- **Erhard Hofer,** Medical University of Vienna*
- **James di Santo,** Institute Pasteur, Paris
- **Ofer Mandelboim,** Hebrew University, Jerusalem
- **Miguel Lopez-Botet,** Universitat Pompeu Fabra, Barcelona
- **Thomas Schlitt,** King's College London
- **Amit Nathwani/Stephen Beck,** University College London
- **Ulrike Koehl,** Medical University of Hannover
- **Volker Huppert,** Miltenyi Biotec, Bergisch Gladbach
- **Dirk Groenewegen,** Glycostem Therapeutics, Nijmegen
- **Eugene Zhukovsky,** Affimed Therapeutics AG, Heidelberg*

The training program pursued will include research training in the individual laboratories with regular exchange between the laboratories and 6 Summer/Winter Schools including workshops and training courses in bioinformatics at EBI, priority rights at EPA and biotech business at WU Vienna. Fellowships will run for 3 (PhD students) or 2 years (post-docs) and start between October 2012 and September 2013.

Applications including CV, publication list (if available), and addresses of two referees should be sent to Prof. E. Hofer, Medical University of Vienna, under the E-mail address:
sandra.schulz@meduniwien.ac.at

Recruitment will start in November, so early application will be an advantage. Candidates are required to undertake trans-national mobility.

W229900R

naturejobs

European Head Office, London naturejobs@nature.com
The Macmillan Building, 4 Crinan Street, London N1 9XW, UK
Tel: +44 (0) 20 7843 4961 Fax: +44 (0) 20 7843 4996

Global Head:
Nils Moeller,+44 (0) 20 7843 4953 n.moeller@nature.com
Southwest UK/RoW:
Emma Hare, +44 (0) 20 7843 4944 e.hare@nature.com
Northeast UK/Ireland:
Matthew Ward, +44 (0) 20 7014 4059 m.ward@nature.com
France/Switzerland/Belgium:
Julie Aramburu, +44 (0) 20 7843 4994 j.aramburu@nature.com
Scandinavia/Spain/Portugal/Italy:
Megan Ball, +44 (0) 20 7843 4973 m.ball@nature.com
North Germany/The Netherlands/Eastern Europe:
Kristin Doelling, +44 (0) 20 7843 4970 k.doelling@nature.com
South Germany/Austria:
Maria Kubalova, +44 (0) 20 7014 4084 m.kubalova@nature.com
Natureevents:
Matthew Clare, +44 (0) 20 7014 4015 m.clare@nature.com
Business Development Manager, Middle East:
Jon Giuliani, +44 (0) 20 7843 4922 j.giuliani@nature.com

USA Head Office, New York naturejobs@us.nature.com
75 Varick Street, 9th Floor, New York, NY 10013-1917
Tel: +1 800 989 7718 Fax: +1 800 989 7103

US Sales Manager:
Ken Finnegan, +1 212 726 9248 k.finnegan@us.nature.com

Japan Head Office, Tokyo
Chiyoda Building, 2-37 Ichigayatamachi, Shinjuku-ku, Tokyo 162-0843
Tel: +81 3 3267 8751, Fax: +81 3 3267 8746

Asia-Pacific Sales & Business Development Manager:
Yuki Fujiwara, +81-3-3267-8765 y.fujiwara@natureasia.com
Business Development Manager, Greater China/Singapore:
Gloria To, +852 2811 7181 g.to@natureasia.com

India
3a, 4th Floor, DLF Corporate Park, Gurgaon, 122 002, India
Advertisement Sales:
Vikas Chawla, +91 1242881057 v.chawla@nature.com

MRC | Biostatistics Unit

Cambridge, UK

Group Leader
MRC Biostatistics Unit
Salary: Competitive

The MRC Biostatistics Unit, one of Europe's leading biostatistics research institutions, is seeking a Group Leader to develop an independent scientific programme, investigating statistical method for the analysis of high throughput data in biomedicine, for example next generation sequencing data or other high resolution data used to investigate complex diseases.

Candidates should have a PhD and will have completed a period of postdoctoral training or equivalent, with an excellent track record, and show outstanding potential for independent research. The successful candidate will lead a small team and resources will be available.

This appointment will be made at either Programme Leader or Programme Leader-track level, depending on achievements and experience. Candidates for Programme Leader position should have a strong international track record of relevant independent research and a proven ability to lead a research team, pursuing original approaches to long-term research goals. A Programme Leader-track appointment will be made for those who demonstrate the potential to develop into Programme Leaders within six years. Salaries are competitive (Programme Leader-track **£35,935-£48,000** per annum; Programme Leader **£45,213-£70,000** per annum).

The Biostatistics Unit provides an excellent environment for research. Core-funding by the Medical Research Council provides long-term support for ambitious projects, while administrative duties are minimal and no teaching is required. Appointment at either level will be made with the resources for one postdoctoral appointment to support the developing programme.

This position will remain open until it is filled; applications received by end of 28th November 2012 will be given priority.

Informal enquiries can be addressed to Sylvia Richardson (sylvia.richardson@mrc-bsu.cam.ac.uk).

Applications should include a covering letter and full CV, an outline of current research interests (1 page) and a proposal for future research (up to 2 pages), along with the names and addresses of three professional referees who have agreed to be contacted prior to interview. Applications are handled by the RCUK Shared Services Centre; to apply please visit our job board at http://www.topcareer.jobs/Vacancy/irc69850_2431.aspx If you are unable to apply online please contact us on 01793 867003 quoting reference IRC69850.This position is subject to pre-employment screening.

For further information about the MRC visit http://www.mrc.ac.uk/

Medical Research Council is an Equal Opportunities Employer

U229965R

THE LANCET

Senior Editor—*The Lancet*

The Lancet, one of the world's most respected medical journals, seeks a Senior Editor to join its team of physicians and scientists at the weekly journal. In this role, you will take part in peer review and selection of primary research articles and review material. There will also be opportunities to be involved in other aspects of the journal's varied work such as commissioning and writing.

In addition to your medical (MD) or postdoctoral (PhD) qualification, you should ideally have research experience and a wide-ranging interest in all aspects of medicine. Previous editorial experience would be a considerable asset. Your writing skills will be first class and you will have a clear view of what our largely clinical readership seeks. This is a full-time permanent position based in our London (Camden) office; possible location in our New York office will be considered.

www.elsevier.com/careers

ELSEVIER

To find out more, you can telephone Dr Sabine Kleinert on (+44) (0)207 424 4933. To apply, please send your full CV, together with a covering letter, stating your current salary details and why you feel you are suitable for the job, to sabine.kleinert@lancet.com. The closing date is Nov 30.

U229892R

www.elsevier.com/careers

Part of the Reed Elsevier Group plc

UNIVERSITY OF CAMBRIDGE

A world of opportunities

www.cam.ac.uk/jobs/

The GlaxoSmithKline Professorship of Microbial Pathogenesis

The Board of Electors to the GlaxoSmithKline Professorship in Microbial Pathogenesis invite applications from appropriately qualified candidates working in the broad area of microbial pathogenesis, including those with an interest in diseases of importance to Global Health. The Professorship is based in the Department of Medicine in the School of Clinical Medicine which has a strategic focus on infection and immunity.

This is a senior Professorship in the Clinical School and will provide leadership in developing infectious disease and microbiological research in the University and, where appropriate, facilitate its development within the UK. If appropriate, the Professor could assume a senior role in driving Global Health Research in Cambridge. For appropriate candidates an association with the Wellcome Trust Sanger Institute may be negotiable.

Salary will be on the academic Professorial scale at a point commensurate with seniority and experience. The appointment of a clinically qualified applicant is also possible, in which case the salary scale will be aligned to the NHS consultant scale.

Further information is available at: www.admin.cam.ac.uk/offices/academic/secretary/professorships/ or contact the Academic Secretary, University Offices, The Old Schools, Cambridge, CB2 1TT, (email: ibise@admin.cam.ac.uk), to whom a letter of application should be sent, together with details of current and future research plans, a curriculum vitae, a publications list and form CHRIS/6 (parts 1 and 3 only with details of two referees) so as to reach him no later than 16 November 2012.

Informal enquiries may be made to Professor KGC Smith, Department of Medicine, Level 5, Box 156, Addenbrooke's Hospital, Cambridge CB2 2QQ (email: kgcs2@cam.ac.uk).

The University is committed to Equality of Opportunity.

U229971F

Imperial College London

Imperial College Healthcare NHS
NHS Trust

Renal and Vascular Inflammation – basic science to clinical translation

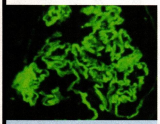

Imperial College London is making a major investment in research connecting Immunology, Inflammation and Matrix Biology related to glomerular and vascular inflammatory diseases. We plan to make a number of senior clinical and non-clinical academic appointments in line with existing preclinical and clinical strengths, and to develop a world-leading portfolio of translational research in collaboration with Imperial College Healthcare NHS Trust, which includes the largest Renal and Transplantation Centre in Europe. Existing well-funded research within the Faculty of Medicine focuses on autoimmunity, renal inflammation and scarring, and vascular inflammation.

We are especially interested to hear from both clinical and non-clinical academics with a track record of high quality publications. We seek to develop a multi-disciplinary group with interfaces between:

- Autoimmunity
- Glomerulonephritis and diabetic nephropathy
- Pathophysiology of vasculitis
- Matrix and cell biology
- Cytokine/chemokine biology
- Innate immunity
- Renal and vascular imaging (preclinical and clinical)
- Development of novel therapy

However these fields are not exclusive or exhaustive and we will be pleased to consider those with other relevant interests.

The level of appointment (Professor, Reader, Senior Lecturer or Lecturer) and the generous supporting package will be determined according to experience. Thus, appointments will be individually negotiated and job descriptions appropriately tailored.

Imperial College London provides an outstanding multidisciplinary environment in basic, clinical and translational research and this is a unique career opportunity for individuals with the vision, leadership ability and ambition to be among the best in the field. Interested individuals are encouraged to make informal enquiries to Joanna Thompson (Tel: 0208 383 3935; email: joanna.thompson@imperial.ac.uk)

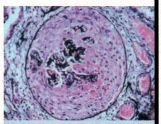

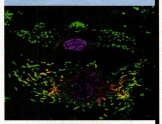

Committed to equality and valuing diversity. We are also an Athena Bronze SWAN Award winner, a Stonewall Diversity Champion and a Two Ticks Employer.

Stonewall DIVERSITY CHAMPION

U229975R

"The Center for Biotechnology has been partnering with NatureJobs on special events and programs utilizing several of their innovative services. Working with their representatives has been a pleasure. They took time to meet with us and develop a service package strategically targeted towards our needs. One of the most useful services was their third party email. It allowed us to reach a wider audience that might not have known about us in the past. NatureJobs is an invaluable resource for any organization and we look forward to continuing our partnership with them in the future."

Kate Posnanski
Center for Biotechnology
Stony Brook University, New York

naturejobs

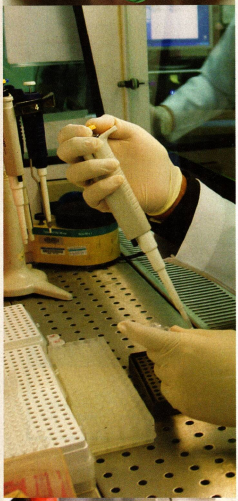

VIVARIUM
RESEARCH FACILITY

The state-of-the-art animal Research Facilities at King Abdullah International Medical Research Center are designed according to international standards to ensure the safety and humane care of research animals. Three vivariums will be inaugurated this summer in Riyadh, Dammam and Al Hassa, respectively. The animal Research Vivarium in Riyadh covers a vast 7500 square meters and offers a unique research environment that combines housing, laboratories, imaging and surgery suites located in the same area. It comprises pathogen-free housing areas equipped with the newest individualized environmental cages that can hold up to 60,000 rodents. Likewise, automated animal housing and hygienic equipments are provided for rabbits, dogs, and sheep to warrant the highest possible care. Unique to the Gulf region, the facility also accommodates aquatic animals such as Zebrafish and Xenopus. The Vivarium Research Facility provides a complete range of equipment for recombinant DNA research, and Transgenesis, together with the latest generation of Optical Imaging, Positron Emission Tomography and Magnetic Resonance Imaging. Each vivarium is staffed with highly qualified veterinarians to ensure proper handling, care and use of animals in scientific research and education in accordance with the highest scientific, humane and ethical principles. Further, each Vivarium Research Facility is open for international accreditation and regular monitoring by the Institutional Animal Care and Use Committee.

* Saudi Arabia's Population : 28.08 million

* The largest spender on healthcare in the GCC with investments totaling $24.2bn last year, according to Frost & Sullivan

* Government plans to spend $373 billion between 2010 and 2014 on social development and infrastructure projects to advance economic development

* Set to be 6th richest economy in the World in terms of GDP per capita by 2050, according to a forecast by Citibank

* The largest free economic market in the Middle East, holding 25% of the total gross national Arab income

King Abdullah International Medical Research Center

Today's Question. Tomorrow's Answer

We are an international translational health science research institution that believes in creating a knowledge-based society through our channel of extraordinary human talent.

www.kaimrc.med.sa
research1@ngha.med.sa

RW228607R

南方科技大学

SOUTH UNIVERSITY OF SCIENCE AND TECHNOLOGY OF CHINA

Faculty Positions at South University of Science and Technology of China(SUSTC)

SUSTC is a public institution funded by the municipality of Shenzhen, a special economic zone city in southern China. The University receives full financial support from the municipality. Set on five hundred acres of wooded landscape in the picturesque Nanshan (South Mountain) area, SUSTC offers an idyllic environment suitable for learning and scholarship. SUSTC promotes academic freedom, engages in basic and problem-solving research of lasting impact to benefit society and mankind, and strives to become one of the best research universities in the world.

Academic Disciplines:

SUSTC has a broad range of academic disciplines, covering natural science, engineering and some newly emerging inter-disciplines. All disciplines are open to applicants. The university especially encourages research that requires a multi-disciplinary and non-traditional approach. Successful applicants are expected to lead or establish new research directions at SUSTC.

Positions:

SUSTC invites applications and nominations from outstanding scholars of all nationalities for faculty positions at all ranks with full-time arrangements. Full-time positions include leading professor, chair professor, professor, associate professor, assistant professor, and PostDoc.

Qualifications & Responsibilities:

Applicants should have a doctoral degree in a relevant research field with outstanding communication skills and a proven record of research excellence.

Responsibilities include teaching undergraduate and graduate courses, developing and sustaining externally funded research programs, graduate student supervision, and professional/institutional services.

Recruiting Positions at:

- Leading Professor
  Applicants should have a Ph.D. degree with extensive research and teaching experience. Applicants should be internationally recognized as holding a leading position in important areas of research.
- Chair Professor
  Applicants should have a Ph.D. degree with extensive research and teaching experience. Applicants should possess a large number of internationally recognized research accomplishments.
- Professor
  Applicants should have a Ph.D. degree with extensive research and teaching experience. Applicants should have made a number of important contributions in research.
- Associate Professor
  Applicants should have a Ph.D. degree. Applicants should have made a few important contributions in research.
- Assistant Professor
  Applicants should have a Ph.D. degree. Applicants should possess evidence that demonstrates the ability in performing high quality research.

Salaries and Benefits:

The University offers competitive salaries and start-up packages. Benefits include housing, medical insurances, pensions, etc.

Contact Us:

Qualified applicants are invited to send a job intention letter and a curriculum vitae to: **hiring@sustc.edu.cn.**

Mailing Address:
Human Resources Department,
South University of Science and Technology of China
No.1088, Xueyuan Blvd, Xili, Nanshan, Shenzhen, China Zip Code: 518055

Telephone: +86-755- 86249985, 86249969

Relevant Links:

South University of Science and Technology of China: http://www.sustc.edu.cn/

JP221489R

Westfalian Wilhelms-University Muenster, Germany

The Medical Faculty of the Westfalian Wilhelms-University (Westfälische Wilhelms-Universität) Muenster offers a position of a

University Professur (Full Professor; W3) for Molecular Biology

at the Center for Molecular Biology of Inflammation (ZMBE), which comprises five institutes (Cell Biology, Infectiology, Medical Biochemistry, Molecular Biology and Molecular Virology) and associated junior research groups. The ZMBE is a joint institution of the Faculties of Medicine, Chemistry/Pharmacy and Biology.

The future holder of the position must fully represent the subject with regard to research and teaching and should have an internationally recognized research profile in molecular and cellular life sciences. She/He is expected to establish an independent research program, to closely interact with the existing research groups at the ZMBE (http://zmbe.uni-muenster.de) and to cooperate with research programs of the university, in particular the Interdisciplinary Clinical Research Center (IZKF), the „Sonderforschungsbereich" (SFB) 629 (Molecular cell dynamics: intracellular and cellular movements), the SFB 656 (Molecular cardio-vascular imaging), the SFB 1009 (Breaking Barriers), the Max Planck Institute of Molecular Biomedicine and the interfaculty research center „Cells in Motion" (www.cells-in-motion.de). The successful candidate will be the director of the Institute for Molecular Biology.

Prerequisite for the application are scientific achievements as a Junior Professor, from a postdoctoral lecture qualification (habilitation), as a research scientist at a school of higher education/university, non-university institute, industry, administration, or other fields of society within or outside Germany.

Applications of women are specifically invited. In the case of equal qualification, competence and specific achievements, women will be considered on preferential terms within the framework of the legal possibilities. Handicapped candidates with equivalent qualifications will be given preference.

Documents supporting the application, including CV, structured catalogue of publications, acquired third-party funding, teaching concept and reprints of the five most important publications should be submitted to the **Dean of the Faculty of Medicine, University of Muenster, Albert-Schweitzer-Campus 1, Gebaeude D3, 48129 Muenster, Germany,** by **06.12.2012.**
References: http://campus.uni-muenster.de

W229977R

Bringing jobseekers and recruiters together.

Academic • Industry • Government

Search now at **naturejobs.com**

naturejobs
making science work

Technical Fellow, Research Scientist

CVRx, Inc. is currently seeking a Technical Fellow, Research Scientist, at our office in Minneapolis, Minnesota. The primary duty of the Technical Fellow, Research Scientist is to conduct research projects associated with innovative approaches to baroreflex activation therapy. This position requires a Ph.D. or equivalent in Biomedical Engineering, Physiology, or related field and five(5) years of experience which includes five(5) years of demonstrated ability with each of the following:

1) Conducting research projects associated with developing innovative approaches to baroreflex activation therapy;
2) Utilizing experience in renal and pulmonary physiology to develop methods of studying changes in blood pressure, vascular stiffness and cardiac properties as a result of therapy;
3) Clinical and/or basic science research of vascular health and heart disease/failure;
4) Presenting research at professional conferences and publishing research results in peer-reviewed scientific journals; and
5) Presenting data and interfacing with physicians and research coordinators at clinical sites. The position also requires travel at a minimum of 50%.

Experience may have been gained prior to, concurrent with, or following completion of a PhD degree program. Employer will accept any suitable combination of education or experience. To apply send resume to resume@cvrx.com

NW229836R

Fall 2012

California Institute of Technology

Cellular, Developmental, or Regulatory Biology

The California Institute of Technology invites applications for a tenure-track professorial position in the Division of Biology. The successful applicant is expected to develop an innovative research program aimed at deciphering the molecular mechanisms that underlie biological phenomena at the level of molecules, cells, or organisms, and to be committed to high quality teaching. Preference will be given to candidates at the Assistant Professor level; however, consideration will also be given to more senior applicants. Initial appointments at the assistant professor level are for four years, and are contingent upon completion of the Ph.D. degree.

Please submit on-line application at http://biology.caltech.edu/Positions and include a brief cover letter, curriculum vitae, relevant publications, and a description of proposed research. Instructions will be given for submission of letters of reference when you apply on-line. Application deadline is December 15, 2012.

The California Institute of Technology is an Equal Opportunity/Affirmative Action Employer. Women, minorities, veterans, and disabled persons are encouraged to apply.

NW229830R

Fall 2012

California Institute of Technology

Faculty Positions in Neuroscience

The California Institute of Technology invites applications for tenure-track professorial positions in the Division of Biology. Positions in **Systems Neuroscience** are open to investigators studying the neural mechanisms and circuit properties that underlie behavior. Positions in **Cellular and Molecular Neuroscience** are aimed at applicants whose research programs concern molecular and/or cellular aspects of physiology, behavior, or neural development. Successful applicants are expected to develop innovative research programs and should also have a commitment to undergraduate teaching. Preference will be given to candidates at the Assistant Professor level; however, consideration will also be given to more senior applicants. Initial appointments at the assistant professor level are for four years, and are contingent upon completion of the Ph.D. degree.

Please submit on-line application at http://biology.caltech.edu/Positions and include a brief cover letter, curriculum vitae, relevant publications, and a description of proposed research. Instructions will be given for submission of letters of reference when you apply on-line. Application deadline is December 15, 2012.

The California Institute of Technology is an Equal Opportunity/Affirmative Action Employer. Women, minorities, veterans, and disabled persons are encouraged to apply.

NW229828R

Cary Institute of Ecosystem Studies

Disease Ecologist
– Open Rank

The Cary Institute of Ecosystem Studies in Millbrook, NY seeks a Disease Ecologist to join the scientific staff at the level of Assistant, Associate, or Senior Scientist. We seek an empirical or theoretical ecologist whose research focuses on the ecology of human disease in the context of environmental change. Position is 12-month, full time, 100% research. Applicants must have a PhD; postdoctoral experience preferred.

The Cary Institute is an independent, not-for-profit research and education institution in the Hudson River Valley of New York, dedicated to providing the science behind environmental solutions. The permanent scientific staff, numbering ~16, conducts research on freshwater ecology, biogeochemistry, urban ecology, invasive species, climate change, ecological literacy, and disease ecology.

Please submit in pdf format a CV, brief statement of research interests, up to five publications, and three letters of recommendation to: Human Resources, Cary Institute of Ecosystem Studies, Job Ref. 12019-CE, to jobs@caryinstitute.org

Review of applications begins December 3, 2012.

EOE/AAD/Min/Fem/Vet/Disab

NW229834R

---

nature

Chief News Editor, London

Nature, the international weekly journal of science, seeks a Chief News Editor to head its global news operation. With 15 staff reporters and a network of freelance correspondents, *Nature* produces daily online coverage and weekly print stories about all fields of research, the scientific community, policy, funding, and science and society.

The Chief News Editor plans coverage, commissions and edits stories, and works with art, production, and other *Nature* editors to deliver unique, high-impact journalism aimed at an audience of working scientists.

We seek a science journalist with extensive reporting and editing experience and a demonstrated interest in science policy and funding as well as in research findings. Management skills are essential, as is the ability to thrive under pressure.

This position is offered on a full-time, permanent basis and is based in our London office.

Applicants should submit a CV and a covering letter explaining their interest in the post to vacancy **NPG/112/12** on http://jobs.macmillan.com.

Closing Date: 5th November 2012

nature publishing group npg

IN229584R

30 Career Positions as Research Associate

Karolinska Institutet announces funding for 30 Research Associates within:

- Medical Sciences
- Cancer
- Cell and Tumor Biology
- Clinical Microbiology
- Epidemiology/Biostatistics
- Immunogenetics
- Immunology
- Infection Biology
- Neuroscience

W229861R

Application deadline
November 15th 2012
ki.se/job

Karolinska Institutet

The Faculty of Biology at the Albert-Ludwigs-University Freiburg (Germany) invites applications for a

Junior Professorship (W1) in Microbiology

We are looking for candidates with an outstanding scientific reputation in the field of organismic microbiology and/or ecology of prokaryotes using modern experimental approaches. Close interactions and cooperations with the research groups of the faculty as well as with the various local collaborative research centers (SFB 592 and 746; FRISYS; ZBSA) and Graduate Schools would be appreciated. For further information please visit the homepage of the faculty at www.bio.uni-freiburg.de

In teaching, the candidate is expected to contribute to the curricula in Microbiology of the B.Sc., M.Sc. and teacher training program in Biology, with a focus on organismic microbiology.

The successful candidate will have completed his/her doctoral studies with distinction, followed by an international postdoctoral phase. Formal employment conditions are based on § 51 Landeshochschulgesetz. The appointment is limited to four years with the possibility of extension for another two years after evaluation.

Deadline for applications is November 30th, 2012. Complete applications along with all pertinent documents including a teaching record (exclusively in electronic form; e-mail: dekanat@biologie.uni-freiburg.de) should be addressed to the Dean of the Faculty of Biology, Schänzlestr. 1, D-79104 Freiburg.

The University of Freiburg is an equal opportunity employer. Applications of women are strongly encouraged. Handicapped candidates with equivalent qualifications will be given preference.

W229903R

ETH

Eidgenössische Technische Hochschule Zürich
Swiss Federal Institute of Technology Zurich

Assistant Professor of Structural Biology / Biophysics

The Department of Biology (www.biol.ethz.ch) at ETH Zurich invites applications for above-mentioned assistant professorship.

The successful candidate is expected to study the molecular mechanisms of biological reactions and to build an innovative and internationally competitive research program within the Institute of Molecular Biology and Biophysics (www.mol.biol.ethz.ch), which provides an excellent scientific environment and access to state-of-the-art equipment. The search is not limited to a specific research field or technology, but we are specifically encouraging candidates with expertise in methods complementary to those already used at the Institute, e.g. single particle cryo-electron microscopy or single molecule spectroscopy. For electron microscopy, transmission electron microscopes (including a FEI Tecnai G2 F20 cryo and a Titan Krios) are available within the Electron Microscopy Center of ETH Zurich. The new professor will be expected to teach undergraduate level courses (German or English) and graduate level courses (English) for students of the Department of Biology, and to actively contribute to an interactive, scientific environment at ETH Zurich.

This assistant professorship has been established to promote the careers of younger scientists. The initial appointment is for four years with the possibility of renewal for an additional two-year period.

Your application should include your curriculum vitae, a list of publications, the names of at least three referees, and a short overview of your research interests. The letter of application should be addressed **to the President of ETH Zurich, Prof. Dr. Ralph Eichler. The closing date for applications is 31 December 2012.** ETH Zurich is an equal opportunity and affirmative action employer. In order to increase the number of women in leading academic positions, we specifically encourage women to apply. ETH Zurich is further responsive to the needs of dual career couples and qualifies as a family friendly employer.
Please apply online at **www.facultyaffairs.ethz.ch.**

W229517R

---

nature jobs

Need help with your career?
Ask the Expert on **naturejobs.com**

- **Browse past Q&A**
- **Get professional advice**
- **Email your questions**

Ask the Expert is located in the **Career Toolkit** section of **naturejobs.com**

EMBO

excellence in life sciences

EMBO Young Investigators are some of Europe's best young group leaders selected for the high quality of their research. They form a prestigious scientific network.

PhD students and postdocs working in EMBO Young Investigator laboratories benefit from EMBO training opportunities, networking events and laboratory exchanges.

Apply directly to the EMBO Young Investigator. Find contact information on website:

www.embo.org
/programmes/yip/vacancies.html

Apply for PhD or postdoc positions in EMBO Young Investigator laboratories

Robert ARKOWITZ
PhD and Postdoc Yeast cell biology **Nice** FR

Richard BENTON
PhD Neurogenetics **Lausanne** CH

Eugene BEREZIKOV
Postdoc Stem cells, regeneration & ageing **Groningen** NL

Anne BERTOLOTTI
Postdoc Misfolded proteins **Cambridge** UK

Janusz BUJNICKI
Postdocs RNA structural biology/ bioinformatics **Warsaw** PL

Dirk BUMANN
Postdoc Infection biology **Basel** CH

Rut CARBALLIDO-LOPEZ
Postdocs Bacterial cytoskeleton **Jouy-en-Josas** (Paris) FR

Fernando CASARES
PhD Gene regulatory networks **Seville** ES

Barbara CONRADT
PhD Regulation of apoptosis **Martinsried** (Munich) DE

Fabrizio D'ADDA DI FAGAGNA
Postdoc ncRNA & the DNA damage response **Milan** IT

Jiří DAMBORSKÝ
Postdocs Enzymatic catalysis **Brno** CZ

Daniel DAVIS
Postdoc Immunology **London / Manchester** UK

Jan-Willem DE GIER
PhD Engineering *E.coli* for protein production **Stockholm** SE

Miguel Ángel DEL POZO
Postdoc Caveolae in membrane tension & trafficking **Madrid** ES

Cory DUNN
Postdoc Mitochondrial dysfunction **Istanbul** TR

Andrzej DZIEMBOWSKI
Postdoc RNA metabolism **Warsaw** PL

Oliver EINSLE
Postdoc Bacterial metabolic pathways **Freiburg** DE

Johan ELF
Postdoc Super-resolution live-cell imaging **Uppsala** SE

Ebru ERBAY
Postdoc Signal transduction & atherosclerosis **Ankara** TR

Óscar FERNÁNDEZ-CAPETILLO
PhD DNA repair **Madrid** ES

Luísa FIGUEIREDO
Other Bioinformatician **Lisbon** PT

François FUKS
PhD and Postdoc Epigenetics & cancer **Brussels** BE

Jesús GIL
Postdoc Regulators of senescence & reprogramming **London** UK

Acaimo GONZÁLEZ-REYES
PhD Developmental biology **Seville** ES

Monica GOTTA
PhD and Postdoc Spindle positioning/cell polarity **Geneva** CH

Devrim GÖZÜAÇIK
Postdoc Tissue engineering **Istanbul** TR

László HOMOLYA
Postdoc ABC transporters **Budapest** HU

Torben Heick JENSEN
PhDs Regulation of RNA **Aarhus** DK

Luca JOVINE
Postdocs Structural biology **Huddinge** (Stockholm) SE

Henrik KAESSMANN
Postdoc Functional evolutionary genomics **Lausanne** CH

Claudia KÖHLER
Postdocs Epigenetic control of cell fate **Uppsala** SE

David KOMANDER
Postdocs The ubiquitin system **Cambridge** UK

Ben LEHNER
Postdoc Biology of individuals **Barcelona** ES

Esben LORENTZEN
PhD Structural biology of the cilium **Martinsried** (Munich) DE

Tom LÜDDE
PhD Molecular cancer research **Aachen** DE

Sophie MARTIN
PhD and Postdocs Cell polarity/cell cycle regulation **Lausanne** CH

Irene MIGUEL-ALIAGA
Postdoc Brain–gut interactions **London** UK

Eric MISKA
Postdoc Cancer cell biology **Cambridge** UK

Nurhan ÖZLÜ
Postdoc Proteomics and cell biology **Istanbul** TR

Antoine PETERS
PhD Mammalian germ cell biology **Basel** CH

Markus RALSER
Postdoc Systems biology **Cambridge** UK

Ziv REICH
Postdoc Photosynthetic machineries **Rehovot** IL

Beatriz RICO
Postdocs Neural circuits **Alicante** ES

Iris SALECKER
PhD Targeting axons to a synaptic layer **London** UK

Frédéric SAUDOU
Postdoc Cellular and molecular neurobiology **Orsay** (Paris) FR

Joan SEOANE
Postdoc Glioblastoma genesis & progression **Barcelona** ES

Eric SO
Postdoc Stem cell and cancer epigenetics **London** UK

Anne SPANG
PhDs Molecular transport processes **Basel** CH

Kvido STŘÍŠOVSKÝ
Postdoc Intramembrane proteases **Prague** CZ

Luca TAMAGNONE
Other Mouse models of cancer **Candiolo** (Turin) IT

Nicolas TAPON
Postdocs Control of tissue size **London** UK

Nektarios TAVERNARAKIS
PhDs Biology of ageing **Heraklion,** Crete GR

Tambet TEESALU
PhD Cancer therapeutics **Tartu** EE

Pascal THÉROND
Postdoc Cell and developmental biology **Nice** FR

Barry THOMPSON
Postdoc Epithelial biology **London** UK

Helle ULRICH
PhD and Postdocs Ubiquitin, SUMO and genome stability **Mainz** DE

Bartosz WILCZYŃSKI
Postdoc Computational biology **Warsaw** PL

Daniel WILSON
PhD Biochemistry and structural biology **Munich** DE

Bojan ZAGROVIC
Postdoc Protein–RNA interactions **Vienna** AT

Alena ZÍKOVÁ
Postdoc Functional biology of protists **Ceske Budejovice** CZ

Pascale ZIMMERMANN
Postdoc Cancer biology **Marseille** FR

a nature conference

University of Miami, International Union of Biochemistry and Molecular Biology, Nature Publishing Group and Scripps Florida present:

Miami 2013 Winter Symposium: The Molecular Basis of Metabolism and Nutrition

Join leaders in the field to discuss advances in our molecular understanding of obesity, calorie restriction, diabetes, ageing and the microbiome as they relate to human nutrition.

February 10-13, 2013
JW Marriott Marquis Miami
Miami, FL, USA

SYMPOSIUM AWARDEES

Feodor Lynen Lectures
Ana Maria Cuervo (Albert Einstein College of Medicine, USA)
Leonard Guarente (Massachusetts Institute of Technology, USA)
David Sabatini (Whitehead Institute for Biomedical Research, USA)

Distinguished Service Award
Bruce Spiegelman (Harvard University, USA)

Special Achievement Awards
Lewis Cantley (Harvard University, USA)

IUBMB Jubilee Lecture
Michael Karin (University of California, San Diego, USA)

CONFIRMED SPEAKERS:

Arthur Agatston
Fredrik Bäckhed
Anne Brunet
Tom Burris
John Cleveland
Miguel Constância
Ronald DePinho
Richard Flavell
Stanley Hazen
Jules Hirsch
Randal Kaufman
Salvador Moncada
Deborah Muoio
Chris Newgard
Jared Rutter
Reuben Shaw
Matthew Vander Heiden
Douglas Wallace
Robert Waterland

For more information and to register visit:
www.nature.com/natureconferences/miami/mws2013

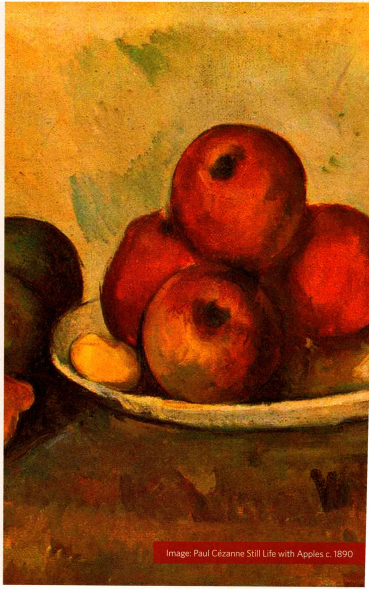

Image: Paul Cézanne Still Life with Apples c. 1890

UNIVERSITY OF MIAMI
MILLER SCHOOL of MEDICINE

SCRIPPS FLORIDA
THE SCRIPPS RESEARCH INSTITUTE

IUBMB

South Dakota State University

Geographic Information Science Center of Excellence

The Geographic Information Science Center of Excellence (GIScCE) seeks a person with research experience and teaching interests focused on remote sensing science and applications that enable understanding of the rates, causes, and consequences of land cover land use change. This 12-month position is funded by state funds and carries a workload of 80% research, 10% teaching, and 10% service. Responsibilities include securing externally funded research grants, recruiting and mentoring doctoral students and post-doctoral researchers, and delivering one graduate course per year. Minimum qualifications include an earned Ph.D. degree in an appropriate field with a background in remote sensing; minimum of five years' experience conducting externally funded research; scholarly activity, including collaborative research and peer-reviewed publications as first author; and a demonstrated ability to communicate effectively.

A diverse portfolio of sponsored research, demonstrated excellence in mentoring students, demonstrated leadership in professional service are desired qualifications. For questions on the position, contact the search committee chair, Dr. David Roy via email at David.Roy@sdstate.edu.

Application deadline is December 21, 2012. To view a full position description and to apply, visit https://yourfuture.sdbor.edu/applicants/Central?quickFind=56621 and click on "apply for this posting". For questions on the electronic employment process, contact SDSU Human Resources at (605) 688-4128. SDSU is an AA/EEO employer.

NW229909R

"Based on the huge response to our adverts in *Naturejobs* we have hired many excellent candidates annually. We highly appreciate the kind and professional support of the *Nature* team."

Karin Osibow,
Program Administrator,
Medical University of Graz, Austria

naturejobs

UNIVERSITY OF OXFORD

www.ox.ac.uk/jobs

Postdoctoral Research Assistant x3

Grade 7.1 - 7.4: £29,249 - £31,948 p.a.

School of Geography and the Environment

Applications are invited for three Postdoctoral Research Assistants on a fixed-term contract for 3 years, to conduct studies of plant traits, leaf physiology and forest structure along tropical forest elevation gradients, with a particular focus on a study transect in SE Peru.

Two posts (with a focus on Peru) are funded by the UK Natural Environment Research Council and will be part of a large on-going multi-partner research project working on the impacts of climate change in the eastern Andean slopes and nearby lowland Amazon (www.andesconservation.org). The third post is funded by the European Research Council, and will take a pan-tropical perspective, including sites in Peru, Australia and possibly other major tropical forest elevation transects.

The positions will be based in the Ecosystems Group of the Environmental Change Institute (http://www.eci.ox.ac.uk/research/ecodynamics/index.php) and led by Professor Yadvinder Malhi. The posts are available from December 2012 or as soon as possible thereafter. The successful candidates will have a PhD in a quantitative environmental science and a demonstrated ability to conduct advanced analyses and produce scientific publications.

For informal enquiries, please contact Professor Yadvinder Malhi (yadvinder.malhi@ouce.ox.ac.uk). For further details and to apply, please visit the following

https://www.recruit.ox.ac.uk/pls/hrisliverecruit/erq_jobspec_version_4.jobspec?p_id=105199

https://www.recruit.ox.ac.uk/pls/hrisliverecruit/erq_jobspec_version_4.jobspec?p_id=105202

https://www.recruit.ox.ac.uk/pls/hrisliverecruit/erq_jobspec_version_4.jobspec?p_id=105203

The closing date is 12 noon on 21 November 2012.

Committed to equality and valuing diversity

U229983R

Don't miss the intoxicatingly good job opportunities in *Nature* each week and on naturejobs.com

naturejobs

REPROGRAPHICS: CC Media Group, London EC1V 8AR UK and **The Charlesworth Group,** Wakefield, UK.
PRINTED BY: William Gibbons & Sons Ltd, UK; **Publishers Press**, Lebanon Junction, Ky, USA and **Obun Printing Co. Inc,** Tokyo, Japan

GLASS FUTURE

A time to reflect.

BY DEBORAH WALKER

The waitress seems reluctant to come over, pretending not to see us, even though I've tried to catch her eye several times. We'd ordered our omelettes 40 minutes ago. How long does it take to crack a few eggs into a hot pan?

"Do you think she's post-human?" I whisper to my husband. She looks too good to be real.

Caleb glances over. "Maybe. She's very pretty, but mods are so subtle, it's difficult to see who's human and who's not."

I wonder what such an attractive looking woman is doing working in a low-rent place like this, a greasy-spoon cafe in a habitat on the edge of Rhea.

We'd booked into the habitat's motel last night. It reeked of overenthusiastic, grandiose plans for the future that would never come true. At dinner, I'd watched the motel's guests. I knew them, their small-time liaisons and their wild plans. They didn't want much, just enough to be able to turn up on their home habitat and impress the ones who stayed behind, impress the ones who said they'd never amount to anything. They all ended up here, or someplace like it, scrabbling for success, trying to make a splash in an over-crowded system. This was a place for people who'd never escape the gravity well of their own failures.

It was a sad place to end a marriage.

"Is she ever going to come over?" I ask.

Caleb says: "I see that we *will* get the omelettes. They'll be … disappointing."

I smile. Caleb has a sense of humour about his gift. Even now, when he knows what I'm about to do, he still keeps cracking jokes.

I take a deep breath and say: "I want a divorce." I wait a moment to see if he's going to make things easier on me. He doesn't say anything. I don't blame him. "I'm so sorry, Caleb."

"So am I." He stares out of the window. "We're on opposite sides of the reflection, Alice. You knew that when you married me."

I look at his reflection in the metal glass window. Caleb was a designer baby. A person designed for space. The multiple copies of his genome in each cell protect him against ionizing radiation. But modding is always erratic. There's no way to predict how changes to the genome will affect the body — or the mind. Multiple-genome people, like Caleb, develop unusual connections in their brains. Precognition. They remember their future. And all of them are unable to pass the mirror test. They can see their reflections, but they can't recognize themselves. Caleb hasn't got the self-awareness that most human babies develop at 18 months. That used to fascinate me, that lack of self. It seemed so strange, so exotic; now I find it sad. When love turns to pity, it's time to end the relationship. Caleb didn't deserve my pity.

I look beyond Caleb's reflection to the habitat's garden. Gardens don't thrive in space. The light collected from the solar foils and retransmitted to the plants is wrong. Earth plants either wither and die or they go wild. The habitat's garden was overgrown and mutated. Swathes of honeysuckle, with enormous monstrous blooms, smothered everything. "It's a pretty lousy garden."

"All these mutants should be cut away," says Caleb. "I'm designing Zen gardens for the Oort habitats, swirls of pebbles, low maintenance." A heartbeat later, he says: "Why do you want a divorce, Alice?"

He was going to make me say everything. "I've met somebody else, while you were working on the Oort Cloud project." Caleb's an architect, very much in demand in the ongoing push of colonization.

"Did you?" The note of surprise in his voice is convincing. Caleb's good at pretending to be something other than what he is. Every moment he swims in the seas of his future. Even when he met me, he must have known that one day we'd be here. Poor Caleb.

No wonder most precogs end up in hospital, overburdened by the nature of their gifts, or more specifically, overwhelmed by the fact that they're unable to change anything they see. "And you love him?"

"I do. I'm going to move in with him. I'm sorry, Caleb."

"I know."

The waitress comes over. She places two plates of greasy omelette on the table. She looks at Caleb, her violet eyes widening in recognition. Caleb's famous. There aren't too many functioning precogs in the system. Every now and again, someone will put out a documentary about him, usually spurious, about how he's refusing to use his precognition to help people. It doesn't work like that. The future's set. No amount of foreknowledge will change anything.

"Thank you," I say, trying to dismiss her. Just because I don't want him, doesn't mean that I want anybody else to have him.

The waitress lingers at a nearby table, straightening the place settings, wondering how she can attract him, thinking that a knowledge of her future might bring her an advantage — just like I did when I met Caleb. She's looking for her future, wanting to use Caleb, not realizing that the only thing we, on this side of the mirror, will ever have are reflections.

"We'll keep in touch, Caleb," I say.

"No, we won't. Goodbye, Alice." He leaves the table, walks over to the waitress. He says something that makes her laugh.

I walk out of the cafe, stepping into my future, my unseen and unknowable future, without him. ■

➲ NATURE.COM
Follow Futures:
@NatureFutures
go.nature.com/mtoodm

Deborah Walker *grew up in the most English town in the country, but she soon high-tailed it down to London where she now lives with her partner and two young children.*

JACEY

7,000 Human Proteins Made from Human Cells.

More Assays! Better Assays!

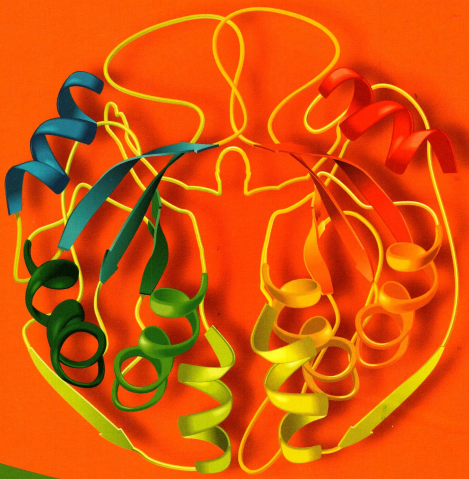

The Largest Collection of Mammalian Cell-Derived Proteins

- Protein functional studies
- Compound screening
- Immunogens for antibody production
- Assay standards: ELISA, Mass Spec, and more
- Bulk production available

Human MTOR protein activity verified in a kinase assay

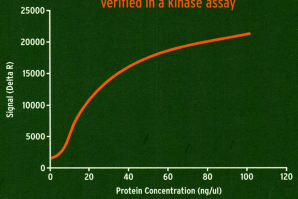

origene.com/protein

ORIGENE
Your Gene Company

More translational and predictive animal models.

Plot your pathway for breakthroughs in neuroscience with knockout rat models from SAGE® Labs.

Biosynaptic.

Advancements in neuroscience are yours to discover with targeted knockout rats from SAGE Labs. Our comprehensive suite of rat models can help move your neuroscience research forward. Map your next breakthrough with smarter rat models for studying neurodegenerative, mood, and affective disorders, including seven new models of autism.

SAGE® LABS
Sigma Advanced Genetic Engineering

Explore our collection of knockout rat models
sageresearchmodels.com

©2012 Sigma-Aldrich Co. LLC. All rights reserved. SIGMA and SIGMA-ALDRICH are trademarks of Sigma-Aldrich Co. LLC, registered in the US and other countries. SAGE is a registered trademark of Sigma-Aldrich Co. LLC. Where bio begins is a trademark of Sigma-Aldrich Co. LLC.